Genomic Editing as a Therapeutic Approach to Congenital Adrenal Hyperplasia

Lara Graves

The Children's Medical Research Institute

Faculty of Medicine and Health

The University of Sydney

A thesis submitted to fulfil requirements for the degree of Doctor of Philosophy

2024

This research reported in this thesis was supported by the award of a Research Training Program scholarship to the PhD Candidate

Declaration

This is to certify that to the best of my knowledge the content of this thesis is my own work, except where specifically indicated in the text. This thesis has not been submitted for any degree or other purposes.

I certify that the intellectual content of this thesis is the product of my own work and that all the assistance received in preparing this thesis and sources have been acknowledged.

Lara Graves

Acknowledgements

I would like to thank my supervisors Prof Ian Alexander, A/Prof Sam Ginn and Clinical A/Prof Shubha Srinivasan for their support and mentorship throughout this PhD. As a clinician, it has been a steep learning curve, starting with being shown how to use a pipette back in March 2020 to now producing this thesis. I am grateful that Prof Chris Cowell suggested I discuss PhD opportunities with Prof Alexander, and that he took me under his wing as a mentor, despite me not knowing a thing about gene therapy when I started. I appreciated Prof Alexander's excitement with my bringing endocrinology to his liver lab, and his enthusiasm for my ideas. I particularly appreciated his inspiring mentorship and high level of skill in grant and manuscript writing. Thank you to A/Prof Ginn for her patience in teaching me how to be a scientist. Thank you to A/Prof Srinivasan for her support and encouragement with my career trajectory.

I want to thank all members of the Gene Therapy Research Unit for their patience teaching me lab techniques and answering my questions. I want to particularly thank Sharntie Christina, my fellow PhD student who not only built the computer on which this thesis was written but helped me almost every step of the way in the first year, as I found my feet in the lab. Thank you to Dr Sharon Cunningham, A/Prof Grant Logan, Cindy Zhu, Eva van Dijk and Caitlin Lucas who all helped me in various ways. Thank you to Dr Kate Mullany for your moral support as we (the two clinicians) muddled our way through the lab work in those early days. Thank you to Margot Latham for your support with grant applications, and other logistical challenges. Thank you to Lakshmy Viswanath for all your help, particularly with the digital PCR.

From the Translational Vectorology Research Unit, I would like to thank Marti Cabanes-Creus, Adrian Westhaus and Matthieu Droyer for their help with the vectorology component of this thesis, particularly the AAV testing kit and associated protocols.

I want to thank Vanessa Scott and the rest of the team in the Bioresources Facility at CMRI for their expertise and assistance with the H-2aw18 mouse model. Their gentle and consistent care contributed to the improvement in the survival rate of this fragile model.

At The Children's Hospital at Westmead, I would like to thank Dr Sundar Koyyalamudi from the Endocrinology Mass Spec Lab and Tiffany Wotton from Newborn Screening for generously finding the time to analyse my research samples and providing me with the incredible phenotypic data I have presented in this thesis. I would like to thank Peter Barclay, Pharmacy, for helping me with the practicalities of creating customised corticosterone/fludrocortisone injectable solutions for the mouse model.

In the greater Children's Medical Research Institute community, I would like to thank Hilary Knowles, Embryology Unit, for her assistance with the preparation of the adrenal glands for single cell RNA sequencing, particularly as they were the most difficult tissue she had worked with. Thank you to Nader Aryamanesh, Embryology, for the huge amount of work he put into my bioinformatics pipeline and data.

Further afield, I give my thanks to Prof Gary Hammer and Typhanie Dumontet from the Hammer Laboratory, University of Michigan for their advice, particularly around the practicalities of harvesting and imaging murine adrenals. I look forward to meeting them,

eventually, in person. I would like to thank Prof Pierre Bougnères, Inserm, French Institute of Health and Medical Research, for his advice on the mouse model.

I would especially like to thank Prof David Handelsman, Andrology Research Laboratory, ANZAC Research Institute for his never-ending encouragement and support throughout my PhD. He helped me brainstorm ideas, introduced me to experts in the field and always gave wise advice.

Abstract

Genome editing technology has reached a critical point where potentially curative treatments for a range of monogenic disorders are within reach. Monogenic adrenal disorders are underrepresented in gene therapy research, despite congenital adrenal hyperplasia (CAH) caused by 21 hydroxylase deficiency occurring in approximately 1 in 15000 live births. Current management for CAH involves corticosteroid treatment at pituitary axis-suppressing doses. Fluctuation from under- to over-treatment is common and expected, and results in adverse outcomes including adrenal crisis, virilisation of female patients (hirsutism, clitoromegaly, disordered menstruation), precocious puberty, short stature, hypertension, cushingoid side effects and impacts on mental health.

Adeno-associated virus (AAV) is one of the most promising gene therapy vectors available. A key advantage of this vector is the capsid serotype confers tissue tropism and recombinant vector genomes utilising the AAV2 inverted terminal repeats can be packaged into multiple different capsids, a process known as pseudoserotyping. This allows specific tissues to be targeted in a preferential manner. However, a limitation of this vector is that it persists predominantly as an episome, with low rates of integration, and is lost with cellular replication. Gene editing technology exploiting the CRISPR/Cas9 system has the potential to overcome this limitation. However, the adrenal cortex entirely renews itself from a population of stem and progenitor cells in the periphery of the gland. Therefore, in order to develop a robust and durable gene therapy for monogenic

adrenocortical disorders, the stem/progenitor cells must be the target for any genome editing strategy.

This thesis explored the possibility of using recombinant AAV (rAAV) technology to treat CAH. There were three distinct facets that were examined: rAAV-mediated delivery of adrenocortical enzymes to the liver for extra-adrenal expression, exploration of capsid tropism for direct targeting of specific populations of adrenocortical cells and specific editing of the *Cyp21a1* locus *in vivo*. The first component was to explore a potential strategy to overcome the biological properties of the adrenal cortex that limit the use of gene addition therapy. The liver is a relatively stable organ in adults and rAAV is highly tropic for the liver. Ectopic adrenal enzyme expression in the liver successfully improved the phenotype in the mouse model, however, it did not completely normalise the steroid hormone profile. Therefore, adrenal cortex targeting gene therapy is warranted. Capsid tropism for the murine adrenal gland had not previously been studied and so this comprised the second component of this thesis. Multiple capsids were identified that provided more efficient gene delivery and expression to the murine adrenal cortex than the commonly used capsid in murine adrenal gene therapy studies, AAVRh10. The difficulty with targeting the adrenocortical progenitor cells is that this population has not been adequately described or reliably identified. In an attempt to overcome some of the obstacles associated with identifying adrenocortical progenitors, single-cell RNA sequencing technology was used to examine the cell populations that make up the murine adrenal cortex and to identify potential adrenocortical progenitor cells. In addition, the transcriptomes of the wild-type and 21-hydroxylase deficient adrenal glands were compared. Third and finally, a strategy was developed to edit the mutant murine *Cyp21a1* locus *in vivo* using homology-independent targeted integration. The editing strategy

developed improved the biochemical phenotype and proved that the locus is amenable to editing. The reagents could be repackaged into an appropriate capsid targeting the adrenocortical progenitor population once that is determined.

This thesis sets the foundation for overcoming the biological properties of the adrenal cortex that renders standard rAAV gene therapy for CAH unsuitable, through delivering adrenocortical genes to a stable organ outside the adrenal, developing strategies to determine capsid tropism for the adrenocortical cells and successfully editing the *Cyp21a1* locus with biological effect.

Peer-reviewed manuscripts

Publications arising from this thesis

Graves, LE, van Dijk, EB, Zhu, E, Koyyalamudi, S, Wotton, T, Sung, D, Srinivasan, S, Ginn, SL, and Alexander, IE. AAV-delivered hepato-adrenal cooperativity in steroidogenesis: implications for gene therapy for congenital adrenal hyperplasia. *Molecular Therapies Methods & Clinical Development.* 2024;32(2): 101232. DOI: 10.1016/j.omtm.2024.101232

Graves, LE, Torpy, DJ, Coates, PT, Alexander, IE, Bornstein, S and Clarke, B, Future directions for adrenal insufficiency: cellular transplantation and genetic therapies, *The Journal of Clinical Endocrinology and Metabolism*. 2023;108(6):1273-1289. DOI: 10.1210/clinem/dgac751

Other publications associated with this thesis

Graves LE, Horton A, Alexander IE, and Srinivasan, S. Gene Therapy for Paediatric Homozygous Familial Hypercholesterolaemia. *Heart Lung and Circulation* 2023;32(7):769-779. DOI: 10.1016/j.hlc.2023.01.017.

Conference abstracts and awards

Graves, LE, van Dijk, E, Srinivasan, S, Ginn, S and Alexander, IE. Recombinant AAV-mediated delivery of CRISPR/Cas9 to the adrenal gland in the development of a gene editing approach for congenital adrenal hyperplasia. Free Papers Session presented at: *Australia and New Zealand Society for Paediatric Endocrinology and Diabetes Annual Scientific Meeting*; 2023 Nov 19-22, Mornington Peninsula, VIC.
Awarded best oral presentation

Graves, LE, Aryamanesh, N, Srinivasan, S, Ginn, S and Alexander, IE. Comparing the single cell transcriptome of wild-type and 21-hydroxylase deficient murine adrenal glands [Abstract FC13.4], Free Communication Session presented at: 11th International Meeting in Pediatric Endocrinology (IMPE); 2023 Mar 4-7, Buenos Aires, Argentina, *Hormone Research in Paediatrics*, 2023;96(suppl2):48. Doi: 10.1159/000529083. Available from: https://www.karger.com/Article/Abstract/529083.
Awarded best oral presentation in Adrenals and HPA axis

Graves, LE, Koyyalamudi, S, Wotton, T, Srinivasan, S, Ginn, S and Alexander, IE. Recombinant AAV-mediated liver-targeted dual adrenal enzyme gene delivery in a model for congenital adrenal hyperplasia, Free Papers Session presented at: *Australasian Paediatric Endocrine Group Annual Scientific Meeting (jointly with ESA, SRB & NZSE)*; 2022 Nov 13-16, Christchurch, New Zealand.
Awarded best oral presentation

Graves, LE, Aryamanesh, N, Srinivasan, S, Ginn, S and Alexander, IE. Mapping the single cell transcriptome of murine adrenal glands, Speed Poster Session presented at: *Australasian Paediatric Endocrine Group Annual Scientific Meeting (jointly with ESA, SRB & NZSE)*; 2022 Nov 13-16, Christchurch, New Zealand.

Graves, LE, Koyyalamudi, S, Wotton, T, Srinivasan, S, Ginn, S and Alexander, IE. The liver as a site for rAAV-induced ectopic adrenocortical enzyme expression [Abstract FC5.3], Free Communication session presented at: 60th Annual Meeting of the European Society for Paediatric Endocrinology (ESPE), Rome, Italy, *Hormone Research in Paediatrics* 2022;95(suppl 2):40. doi: 10.1159/000525606 Available from: https://www.karger.com/Article/Abstract/525606

Graves, LE, Koyyalamudi, S, Wotton, T, Srinivasan, S, Ginn, S and Alexander, IE. Inducing ectopic 21-hydroxylase expression in a mouse model for congenital adrenal hyperplasia through hepatocyte-targeting gene addition, Emerging Investigators Session presented at: *Australasian Paediatric Endocrine Group Annual Scientific Meeting*; 2021 Nov 22-23; Virtual Event.
Awarded Emerging Investigator of the Year

Graves, LE, Cabanes Creus, M, Westhaus, A, Srinivasan, S, Lisowski, L, Ginn, S, and Alexander, IE. Adeno-associated virus tropism for the murine adrenal gland, Free Papers Session presented at: *Australasian Paediatric Endocrine Group Annual Scientific Meeting*; 2021 Nov 22-23; Virtual Event.
Awarded best oral presentation

Graves, LE, Scott, V, Koyyalamudi, S, Wotton, T, Srinivasan, S, Ginn, S and Alexander, IE. Determining phenotype and improving survival of 21-hydroxylase deficient mice, Speed Poster Session presented at: *Australasian Paediatric Endocrine Group Annual Scientific Meeting*; 2021 Nov 22-23; Virtual Event

Authorship attribution statement

Excerpts from Chapter 1 of this thesis are published as:
Graves, LE, Torpy, DJ, Coates, PT, Alexander, IE, Bornstein, S and Clarke, B, Future directions for adrenal insufficiency: cellular transplantation and genetic therapies, *The Journal of Clinical Endocrinology and Metabolism*. 2023;108(6):1273-1289.

and

Graves LE, Horton A, Alexander IE, and Srinivasan, S. Gene Therapy for Paediatric Homozygous Familial Hypercholesterolaemia. *Heart Lung and Circulation* 2023;32(7):769-779.
The included excerpts, figures and tables from these narrative reviews were written or created by the candidate and documented in the preface of chapter 1.

Chapter 4.1 of this thesis is published as:
Graves, LE, van Dijk, EB, Zhu, E, Koyyalamudi, S, Wotton, T, Sung, D, Srinivasan, S, Ginn, SL, and Alexander, IE. AAV-delivered hepato-adrenal cooperativity in steroidogenesis: implications for gene therapy for congenital adrenal hyperplasia. *Molecular Therapy Methods & Clinical Development.* 2024;32(2): 101232.
The candidate co-designed the study with SLG and IEA, produced the vectors, performed the study, analysed the data, created the figures, and wrote the manuscript.

The work presented in this thesis is the candidate's own unless otherwise stated specifically in the text.

Attest to the Authorship Attribution Statement

Student

I attest to the authorship attribution statement above.

Dr Lara Graves

Supervisor

As supervisor for the candidature upon which this thesis is based, I can confirm that the authorship attribution statements above are correct.

Prof Ian Alexander

Grants and scholarships supporting this thesis

Research Grants

European Society for Paediatric Endocrinology/International Fund for Congenital Adrenal Hyperplasia (ESPE/IFCAH) Research Grant 2022, €150 000 (AU$210 000)
Alexander, I.E., **Graves, L.E.,** Ginn, S., "Genomic editing as a therapeutic approach to congenital adrenal hyperplasia"

APEG/Pfizer Industry Research Grant 2019, AU$60 000
Graves, L. E., "Genomic editing as a therapeutic approach to congenital adrenal hyperplasia"

Scholarships

Australian Government Research Training Program Scholarship, University of Sydney, 2020-2022

Yass Memorial Scholarship, Children's Medical Research Institute, 2020-2024

Travel Grants

Early/Mid-Career Researcher (EMCR) Conference Travel Award 2023, Children's Medical Research Institute, to attend ANZSPED ASM 2023

ESPE/IMPE 2023 Travel Grant, 11th International Meeting of Paediatric Endocrinology, Buenos Aires, Argentina

ESPE 2022 Travel Grant, European Society of Paediatric Endocrinology ASM, Rome, Italy

Abbreviations

11ketoDHT	11keto-dihydrotestosterone
11ßHSD1	11ß-hydroxysteroid dehydrogenase type 1
11ßHSD2	11ß-hydroxysteroid dehydrogenase type 2
17OH	17α hydroxylase
17OHP	17-hydroxyprogesterone
17ßHSD1	17ß-hydroxysteroid dehydrogenase type 1
17ßHSD3	17ß-hydroxysteroid dehydrogenase type 3
17ßHSD5	17ß-hydroxysteroid dehydrogenase type 5
17ßHSD6	17ß-hydroxysteroid dehydrogenase type 6
3ßHSD2	3ß-hydroxysteroid dehydrogenase type 2
5αRed1	5α-reductase type 1
5αRed2	5α-reductase type 2
AAV	adeno-associated virus
ACTH	Adrenocorticotropic hormone
ADA	adenosine deaminase
AKR1C2	3α-hydroxysteroid dehydrogenase type 3
AKR1C3	17ß-hydroxysteroid dehydrogenase type 5
AKR1C4	3α-hydroxysteroid dehydrogenase type 1
ApoE	apolipoprotein E
bGH	bovine growth hormone
bp	base pairs
CAH	congenital adrenal hyperplasia
CAR	Chimeric Antigen Receptor
Cas	CRISPR associated protein
Cas9	CRISPR associated protein 9
cDNA	complementary DNA
CMRI	Children's Medical Resesarch Institute
CMV	cytomegalovirus
CRISPR	clustered regularly interspaced short palindromic repeats
CYP	cytochrome P450
CYP11A1	Cholesterol side-chain cleavage enzyme
CYP11B1	11ß-hydroxylase
CYP11B2	human aldosterone synthase
Cyp11b2	murine aldosterone synthase
CYP17A1	human 17α-hydroxylase/17,20 lyase
Cyp17a1	murine 17α-hydroxylase/17,20 lyase
CYP19A1	Aromatase
Cyp21a1	murine 21-hydroxylase
CYP21A1P	human 21-hydroxylase pseudogene
CYP21A2	human 21-hydroxylase
Cyp21a2-ps	murine 21-hydroxylase pseudoegene

DAPI	4′,6-Diamidine-2′-phenylindole dihydrochloride
DAX1	dosage-sensitive sex reversal, adrenal hypoplasia critical region, on chromosome X, gene 1
ddPCR	digital droplet polymerase chain reaction
DHEA	Dehydroepiandrosterone
DHEAS	Dehydroepiandrosterone sulfate
DHT	dihydrotestosterone
DMEM	Dulbecco's Modified Eagle's Medium
DMSO	Dimethylsulphoxide
DNA	deoxyribonucleic acid
dNTP	deoxyribonucleotide triphosphate
dPCR	digital polymerase chain reaction
ds	double-stranded
DSB	double-stranded breaks
DTT	Dithiothreitol
e.g.	for example
EDTA	Ethylenediaminetetraacetic acid
EDTA	Ethylenediaminetetraacetic acid
ELISA	Enzyme linked immunosorbent assay
FBS	foetal bovine serum
g	relative centrifugal force
GFP	green florescent protein
GLI	glioma-associated oncogene homolog
GLI1	GLI family zinc finger 1
gRNA	guide RNA
GTRU	Gene Therapy Research Unit
hAAT	human alpha 1-antitrypsin promoter
HDL	high-density lipoprotein
HDR	homology-directed repair
HEK	human embryonic kidney
HEPES	4-(2-hydroxyethyl)-1-piperazineethanesulfonic acid
HGMD	human genome mutation database
HITI	homology-independent targeted integration
HLA	Human leukocyte antigen
HSD	hydroxysteroid dehydrogenase
HSD11B1	11ß-hydroxysteroid dehydrogenase type 1
HSD11B2	11ß-hydroxysteroid dehydrogenase type 2
HSD17B1	17ß-hydroxysteroid dehydrogenase type 1
HSD17B3	17ß-hydroxysteroid dehydrogenase type 3
HSD17B6	17ß-hydroxysteroid dehydrogenase type 6
HSD3B2	3ß-hydroxysteroid dehydrogenase type 2
IHC	immunohistochemistry
IMDM	Iscove's Modified Dulbecco's Medium
indels	insertions/deletions

ITR	Inverted terminal repeat
IV	intravenous
kb	kilobases
LB	lysogeny broth
LDL	low-density lipoprotein
LDLR	LDL receptor
LNP	lipid nanoparticle
Mc2r	Melanocortin 2 receptor
MHC	Major histocompatibility complex
mRNA	messenger RNA
NADPH	Nicotinamide adenine dinucleotide phosphate
NCBI	National Center for Biotechnology Information
NGS	next generation sequencing
NHEJ	non-homologous end joining
NHP	non-human primate
OCT	Optimal Cutting Temperature
OTC	ornithine transcarbamylase
P450aro	Aromatase
P450c11AS	Aldosterone synthase
P450c11ß	11ß-hydroxylase
P450c17	17α-hydroxylase/17,20 lyase
P450c21	21-hydroxylase
P450scc	Cholesterol side-chain cleavage enzyme
pA	poly-adenylation tail
PAM	protospacer adjacent motif
PBS	Phosphate-buffered saline
PCR	polymerase chain reaction
PEG	Polyethylene glycol
PFA	paraformaldehyde
PITCh	precise integration into target chromosome
POR	P450-oxidoreductase
qPCR	quantitative polymerase chain reaction
rAAV	recombinant adeno-associated virus
Ren1	Renin
RNA	ribonucleic acid
rpm	revolutions per minute
RSPO3	R-spondin 3
SaCas9	Staphylococcus aureus Cas9
SATI	single homology arm donor mediated intron-targeting integration
SCID	severe combined immunodeficiency
SCID-X1	severe combined immunodeficiency X1 disease
scRNA seq	single-cell RNA sequencing
SD	standard deviation
SF1	steroidogenic factor 1

SHH	sonic hedgehog
SRD5A1	5α-reductase type 1
SRD5A2	5α-reductase type 2
ss	single-stranded
STAR	Steroidogenic acute regulatory protein
TALEN	transcription activator-like effector nuclease
TAZ	transcriptional coactivator with the PDZ-binding motif
TBE	Tris-Borate-EDTA
Tbp	TATA-box binding protein
TE	Tris-EDTA
Tris	Trisaminomethane
TVRU	Translational Vectorology Research Unit
U6	RNA polymerase III promoter
UMAP	Uniform Manifold Approximation and Projection
vcn	vector copy number
vg	vector genomes
vgc	vector genome copies
VGEF	Vector Genome Engineering Facility
VP	viral protein
WIMR	The Westmead Institute for Medical Research
WT1	Wilms tumour protein homolog 1
WPRE	Woodchuck Hepatitis Virus Posttranscriptional Regulatory Element
YAP	Yes-associated protein
zF	zona fasciculata
ZFN	zinc-finger nuclease
zG	zona glomerulosa
zR	zona reticularis

Table of Contents

Chapter 2: Materials and Methods

Chapter 5: Towards determining rAAV capsid tropism for the adrenocortical progenitor cells

Chapter 6: A genomic editing approach to congenital adrenal hyperplasia

List of Figures

List of Tables

Chapter 1

Gene Therapy and Congenital Adrenal Hyperplasia

1.1 Preface

The candidate published two first author narrative reviews during the candidature (Appendix). Sections of Chapter 1 that have been reproduced from those publications were written by the candidate and are listed below:

Graves, LE, Torpy, DJ, Coates, PT, Alexander, IE, Bornstein, S and Clarke, B, Future directions for adrenal insufficiency: cellular transplantation and genetic therapies, *The Journal of Clinical Endocrinology and Metabolism*. 2023;108(6):1273-1289. DOI: 10.1210/clinem/dgac751

Excerpts from this manuscript contributed to sections 1.5, 1.5.2, 1.5.2.1, 1.6.1, 1.6.1.1, 1.6.1.2, 1.6.1.3, 1.6.2, Figure 1-1 and Table 1-4.

Graves, LE, Horton, A, Alexander, IE, and Srinivasan, S, Gene therapy for paediatric homozygous familial hypercholesterolaemia, *Heart, Lung and Circulation*. 2023;32(7):769-779. DOI: 10.1016/j.hlc.2023.01.017

Excerpts from this manuscript contributed to sections 1.5.2.1, 1.5.3, 1.5.3.1, 1.5.3.2 and Figures 1-10 and 1-11.

1.2 Introduction

Gene therapy technology has reached a critical point where potential curative treatments for monogenic disorders are within reach. Congenital adrenal hyperplasia (CAH) is an autosomal recessive monogenic endocrine disorder caused in >95% of instances by a deficiency of the 21-hydroxylase enzyme. It can lead to devastating consequences, including death. This disease is characterised by elevated androgen levels, ambiguous genitalia in newborn females, post-natal virilisation in both males and females and in severe cases may lead to salt wasting crises and death at any life stage from birth. Current standard management involves corticosteroid replacement therapy which is fraught with inaccuracy and does not completely mimic the physiological profile. Undoubtedly, there is a need for a better treatment. Recent progress in genomic therapies and genome editing technology have put a potential viable alternative within reach. While the biology of the adrenal cortex obviates standard recombinant adeno-associated virus (rAAV) gene delivery, a potential alternative is to use rAAV to deliver adrenal enzyme genes to stable organs outside of the adrenal gland to ameliorate the phenotype. To further exploit rAAV technology, capsid specificity for the adrenocortical progenitor cells needs to be established. Single cell transcriptomic techniques could be key in the identification of these rare cell populations. CRISPR/Cas9-based gene editing technology could then be used to repair the mutant 21-hydroxylase gene in target progenitor cells of the adrenal cortex by homology independent targeted integration, which is a powerful new genome editing strategy. By combining these strategies and unravelling adrenal biology, the future could hold robust, durable gene therapy that provides a cure for this devastating disease.

1.3 Adrenal glands

The adrenals are a pair of endocrine glands that derive their name from their anatomical location superior to the kidneys. They were first formally described as a separate entity from the perinephric fat in 1564 by Bartolomeo Eustachio in his book *Opuscola Anatomica.*[1] Multiple anatomists from the 1600s and 1700s described them as hollow organs containing "black bile"; this was most likely autolysed medulla.[1] In 1805 Georges Cuvier determined that the adrenal gland was solid, and that it was divided into what would be later named as the cortex and medulla in 1836.[2, 3] They remained simply an anatomical curiosity until Thomas Addison first described adrenal insufficiency in the mid-1800s.[4] Their importance in the sustainment of life was established by Brown-Sequard who demonstrated in 1856 that adrenalectomy was fatal in dogs.[1]

1.3.1 Blood supply

The adrenal glands are supplied by several small arteries that arise from the renal and phrenic arteries and aorta. Some variants include supply from the ovarian and left spermatic arteries. Arterial blood enters the periphery of the cortex, and then drains towards the medulla. The left adrenal vein drains into the left renal vein and the right adrenal vein drains directly into the vena cava.[5] The adrenal gland has high blood flow relative to organ size[6] and fenestrated endothelium,[7] which makes it an ideal candidate to target with gene therapy.

1.3.2 Embryology

The adrenal cortex and medulla have distinct embryological origins. The adrenocortical cells derive from the mesoderm, and the medulla from the ectoderm.[8] The gonadal ridge develops on the mesonephros at about 5 weeks following conception, and this gives rise to both the adrenocortical and gonadal cells.[9] The adrenogonadal primordium separates and the adrenocortical cells migrate into the retroperitoneum where they are invaded by sympathetic neural cells during weeks 7-8 which ultimately give rise to the adrenal medulla. The zones of the foetal adrenal cortex differ from that of the adult adrenal cortex. The outer foetal cortex produces glucocorticoids and mineralocorticoids and is known as the "definitive" zone.[10] There is a large "foetal" zone deep to this that produces steroid precursors, particularly androgens, for placental steroidogenesis.[10] The neonatal adrenal glands are very large, representing 0.5% of total body weight at birth, whereas they only represent 0.0175% of body weight in an adult.[5]

1.3.3 Zonation

The foetal adrenal cortex is divided into the outer definitive zone and inner foetal zone. The foetal zone is present at birth, and this large zone involutes over the first year of age. The remaining definitive zone becomes the outer two adult cortical zones.[10] The adult adrenal cortex is divided into three zones (Figure 1-1):

- the zona glomerulosa which is the most peripheral zone, just deep to the capsule and produces mineralocorticoids.[11] It is characterised by the expression of *CYP11B2*. This zone makes up 10% of the cortex.
- The middle and largest zone is the zona fasciculata and makes up ~75% of the cortex. It produces glucocorticoids and is characterised by the expression of *CYP11B1*.

- In the primate adrenal gland, the zona reticularis is next to the medulla and contributes 10% to the adult adrenal cortex. It produces adrenal androgens and is characterised by expression of *CYP17A1,* although this gene is also expressed in the zona fasciculata to facilitate cortisol rather than corticosterone production.

The zona glomerulosa and fasciculata are not completely differentiated from the combined definitive zone until 3 years of age. The zona reticularis appears during a process known as adrenarche, and starts to appear from around age 4 years, but is not fully differentiated until about 15 years of age.[5, 12] The murine adrenal gland does not express *Cyp17a1,* does not have a zone reticularis and does not produce androgens or cortisol: the major glucocorticoid produced by the murine zona fasciculata is corticosterone.[13, 14] Therefore, a murine model of adrenal disease will not have abnormalities of androgen production. In the application of a murine model for gene therapy in the adrenal gland the lack of hyperandrogenism must be considered and elevation of progesterone could be considered a surrogate marker for hyperandrogenism.

1.3.4 Adrenocortical cellular migration and turnover

Since the 1930s it has been known that the adrenal cortex can regenerate itself when only the capsule remains,[15, 16] from a population of cells located in the capsule or in the subcapsular region.[17] Cells from the peripheral layers proliferate and migrate centripetally until they reach the cortico-medullary junction where they apoptose.[18] The cells differentiate into steroidogenic cells in the zona glomerulosa, and during migration, undergo lineage conversion and populate the deeper zones.[19] Adrenocortical cellular proliferation is less well characterised in the human than in the mouse, however cell proliferation is also thought to originate from the periphery of the gland in humans, with

the presence of Ki67 staining (a marker for cell proliferation) scattered through the peripheral cortex.[20]

There are multiple populations of long-lived stem and progenitor cells in the adult adrenal capsule and cortex. As there is no clear consensus in the definitions, in this chapter "stem" refers to the quiescent, long-term retained, multipotent cells that do not express steroidogenic factor 1 (SF1) and "progenitor" cells are those that are actively dividing, with the capacity to differentiate and express SF1+ and sonic hedgehog (SHH).[21] SF1+ embryonic adrenocortical cells give rise to SF1– somatic stem cells that reside as a thin layer in the adrenal capsule.[22] Within the capsule are populations of cells that variously express Wilms tumour protein homolog 1 (WT1), GLI family zinc finger 1 (GLI1), R-spondin 3 (RSPO3), Yes-associated protein (YAP) and transcriptional coactivator with the PDZ-binding motif (TAZ), and Nestin.[23] Cells expressing GLI1+ are the largest population of capsular cells and they give rise to cortical SF1+ progenitor and SF1+ differentiated steroidogenic cells of the zona glomerulosa.[22, 24]

Peripheral progenitor cells of the subcapsular zona glomerulosa are characterised by nuclear beta-catenin, SF1+ and SHH+ expression and lack *CYP11B2* expression.[19, 24] It is unconfirmed whether these cells are long-term retained.[21] SF1+ SHH+ progenitor cells of the zona glomerulosa differentiate into CYP11B2+ steroidogenic cells that produce aldosterone, and then they migrate and undergo lineage conversion to become CYP11B1+ steroidogenic cells of the zona fasciculata that produce corticosterone in the mouse or cortisol in the human (Figure 1-1).[19, 23]

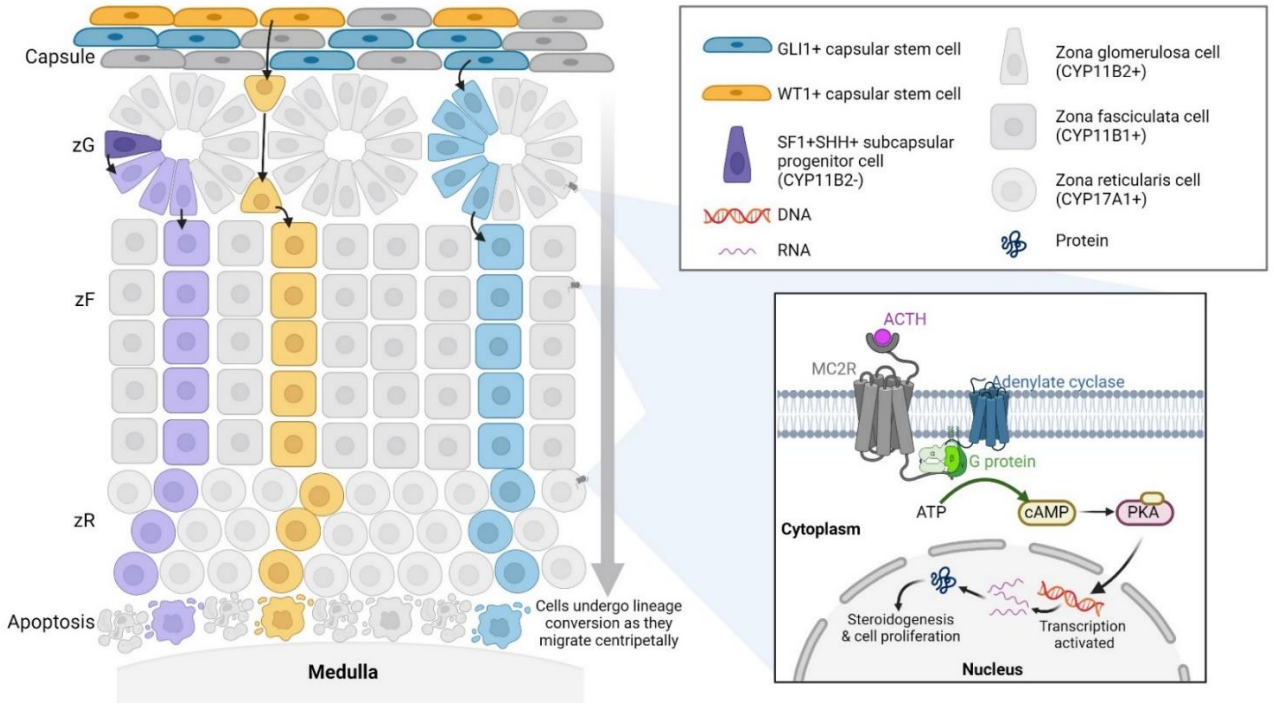

Figure 1-1 Migration and lineage conversion of adrenocortical cells.

The subcapsular adrenal cortex contains stem cells expressing GLI1 which respond to paracrine signals of the Hedgehog pathway, crucial in adrenal differentiation. WT1 expressing cells produce WT1 to initiate SF1 expression to initiate the adrenal cell steroidogenic pathway, requiring activation of the cyclic AMP pathway stimulated by circulating pituitary ACTH for effective steroidogenesis and negatively regulate the Wnt-β-catenin pathway. High Wnt pathway activity keeps adrenal cells in a zG state, reducing Wnt activity has a mitogenic effect. The MC2R (ACTH) receptor is expressed following SF-1 action as are steroidogenic genes; ACTH stimulates expression of most adrenal transcription factors and acts through the cAMP/protein kinase A (PKA) pathway. The three adrenal layers differentially express steroidogenic pathways to produce a predominance of aldosterone (zG, CYP11B2+), cortisol (zF, CYP11B1+) and adrenal androgens, DHEA and androstenedione (zR, CYP17A1+). Adrenal cells migrate centripetally to reach an apoptotic state at the corticomedullary junction. Abbreviations: Glioma associated oncogene homolog, GLI1; Wilms tumour 1, WT1; Steroidogenic factor 1, SF1; adrenocorticotropin, ACTH; zona glomerulosa, zG; zona fasciculata, zF; dehydroepiandrostenedione, DHEA; zona reticularis, zR. Created with BioRender.com. Reproduced from Graves, et al 2023.[25]

The multiple populations of multipotent adrenal stem and progenitor cells are recruited depending on the physiological or pathophysiological requirement.[23, 26] Subcapsular SHH+, SF1+ progenitor cells give rise to virtually all cortical cells.[23] The capsular multipotent stem cells are recruited in response to severe stress, but their contribution to the cortex during homeostasis is small.[21] The capsular SF1– stem cells also significantly contribute to cell renewal in the adult female mouse adrenal cortex but have an insignificant role in the adult male.[27] Male adrenocortical cell renewal relies on SHH+, SF1+ subcapsular progenitor cells.[24, 27] Recruitment of the GLI1+, SF1- capsular stem cells is inhibited in the presence of androgens in both male and female mice.[27] Capsular cells expressing WT1+ may be recruited in the context of supraphysiological demand.[28] Nestin+ cells are scattered in the capsule and throughout the cortex and have the ability to differentiate into steroidogenic cells, particularly during times of stress.[29, 30] With this constant rate of cell turnover, and renewal, the mouse adrenocortical cells are almost entirely replaced in 200 days.[31] This renewal process appears to be faster in female mice than male (3 months vs 9 months).[27]

In addition to providing a source of cell renewal, these stem/progenitor cell populations provide paracrine signalling pathways which have a major role in the determination of adrenocortical zonation.[23] Subcapsular progenitor cells secrete Shh ligands which act on the capsular stem cells, and capsular cells provide Wnt signalling which is required for the maintenance of subcapsular progenitors and differentiated glomerular cells.[26] Cells expressing DAX1 (*NR0B1*) may also have an important role in maintaining the progenitor pool.[32]

1.3.5 Adrenal steroids

In the 1920s and 30s mixed bovine adrenal extracts (known as "cortin") were used to treat refractory Addisonian cases.[33] Following this, many of the known adrenal steroids were isolated during the 1930s by Reichstein and Kendall,[34, 35] who were both then awarded the Nobel Prizes for Medicine in 1950.[36] All steroid hormones are synthesised from cholesterol; in humans most of this cholesterol comes from dietary-derived low-density lipoproteins (LDLs) in the plasma via the LDL receptor (LDLR).[37] In contrast, rodent adrenal steroidogenesis derives cholesterol from high-density lipoproteins (HDLs) which is taken up by the scavenger receptor B1 (*SRB1*), a minor pathway in humans,[38] Cholesterol may also be synthesised *de novo* by the adrenocortical endoplasmic reticulum.[38] ACTH can stimulate the LDLR uptake of LDL which is either stored or converted to free cholesterol and immediately used for steroid synthesis.[39] Free cholesterol is first transported to the outer mitochondrial membrane, and then the StAR enzyme (encoded by *STAR*) facilitates cholesterol to move from the outer mitochondrial membrane to the inner mitochondrial membrane for steroidogenesis.[38]

Steroids are lipophilic. Therefore, they cannot be stored in vesicles, and must be synthesized as needed. The traditional view of steroid action is that of regulating gene transcription. The genomic action of steroids is well established[40, 41] whereby the steroid hormone binds to the relevant receptor and the steroid-receptor complex then modulates gene transcription. However, steroids can also bind to cell surface receptors for fast action that is independent of gene transcription.[42]

1.3.5.1 Steroidogenesis and canonical androgen synthesis

There are six cytochrome P450 (CYP) enzymes that play a major role in steroidogenesis. The cholesterol side chain cleavage enzyme (P450scc, encoded by *CYP11A1*), 11ß-hydroxylase (P450c11ß, encoded by *CYP11B1*) and aldosterone synthase (P450c11AS, *CYP11B2*) are mitochondrial, while the remainder are microsomal: 17-hydroxylase (P450c17, *CYP17A1*), 21-hydroxylase (P450c21, *CYP21A2*) and aromatase (P450aro, *CYP19A1*)[38]. Together with the hydroxysteroid dehydrogenases (HSDs) these enzymes catalyse the production of corticosteroids (Figure 1-2, Table 1-1). 17ß-hydroxysteroid dehydrogenase type 3 (17ßHSD3, *HSD17B3*) is predominantly expressed in the testis for testosterone production, and there are small amounts of 17ß-hydroxysteroid dehydrogenase type 5 (17ßHSD5, *AKR1C3*) expressed in the zona reticularis of the primate adrenal for testosterone production, however androstenedione is the predominant adrenal androgen. Testosterone is reduced to the more potent dihydrotestosterone (DHT) in the genital skin by 5α-reductase (5αRed2, *SRD5A2*).

Table 1-1 Enzymes involved in steroidogenesis.

Enzyme	Protein abbreviation	Human Gene	Murine Ortholog
Steroidogenic acute regulatory protein	StAR	*STAR*	*Star*
P450-oxidoreductase	POR	*POR*	*Por*
Cholesterol side-chain cleavage enzyme	P450scc	*CYP11A1*	*Cyp11a1*
11ß-hydroxylase	P450c11ß	*CYP11B1*	*Cyp11b1*
Aldosterone synthase	P450c11AS	*CYP11B2*	*Cyp11b2*
21-hydroxylase	P450c21	*CYP21A2*	*Cyp21a1*
17α-hydroxylase/17,20 lyase	P450c17	*CYP17A1*	*Cyp17a1*
Aromatase	P450aro	*CYP19A1*	*Cyp19a1*
11ß-hydroxysteroid dehydrogenase type 1	11ßHSD1	*HSD11B1*	*Hsd11b1*
11ß-hydroxysteroid dehydrogenase type 2	11ßHSD2	*HSD11B2*	*Hsd11b2*
17ß-hydroxysteroid dehydrogenase type 1	17ßHSD1	*HSD17B1*	*Hsd17b1*
17ß-hydroxysteroid dehydrogenase type 3	17ßHSD3	*HSD17B3*	*Hsd17b3*
17ß-hydroxysteroid dehydrogenase type 6	17ßHSD6 / RoDH	*HSD17B6*	*Hsd17b6*
3ß-hydroxysteroid dehydrogenase type 1	3ßHSD1	*HSD3B1*	*Hsd3b1*
3ß-hydroxysteroid dehydrogenase type 2	3ßHSD2	*HSD3B2*	
3α-hydroxysteroid dehydrogenase type 3	AKR1C2	*AKR1C2*	*Akr1c21*
17ß-hydroxysteroid dehydrogenase type 5	AKR1C3 / 17ßHSD5	*AKR1C3*	*Akr1c18*
3α-hydroxysteroid dehydrogenase type 1	AKR1C4	*AKR1C4*	*Akr1c6*
5α-reductase type 1	5αRed1	*SRD5A1*	*Srd5a1*
5α-reductase type 2	5αRed2	*SRD5A2*	*Srd5a2*
Cytochrome b_5	b_5	*CYB5A*	*Cyb5a*

Note the 21-hydroxylase pseudogene is non-functional, and not included in the table. In the human it is encoded by *CYP21A1-P* and in the mouse by *Cyp21a2-ps*.

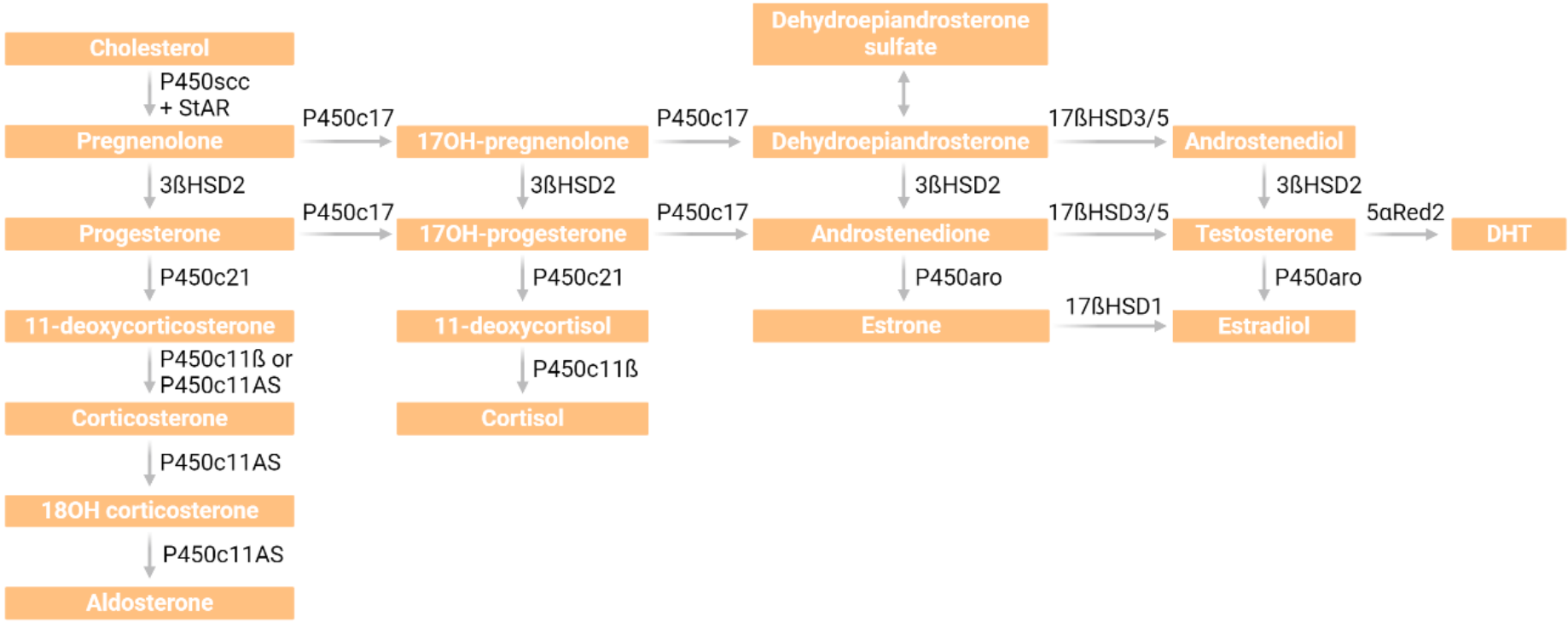

Figure 1-2 Steroidogenesis in humans.

The major glucocorticoid is cortisol, produced in the zona fasciculata by the expression of *CYP11B1*. The major adrenal androgen is androstenedione. P450-oxidoreductase (POR) is required for the reactions catalysed by all cytochrome P450 enzymes. For P450c17 to have 17,20 lyase activity (for conversion of 17OH-Preg and 17OHP to DHEA and androstenedione, respectively), it requires cytochrome b_5. Adapted from Miller and Auchus, 2011.[38]

The murine adrenal cortex does not express *Cyp17a1*, and thus the major glucocorticoid in mice is corticosterone (Figure 1-3). The murine adrenal gland does not produce androgens.

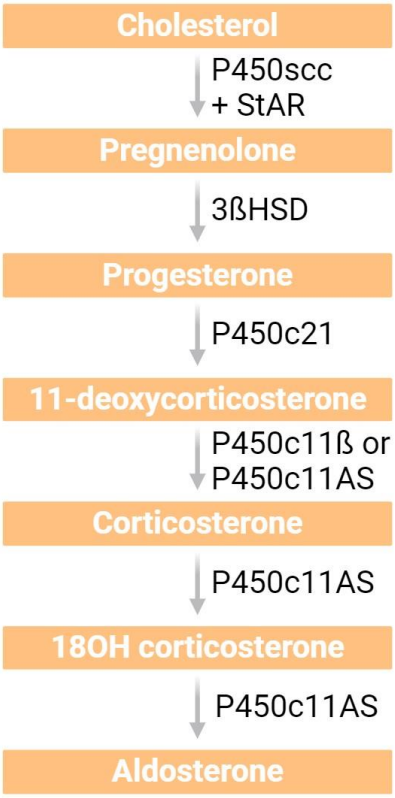

Figure 1-3 Murine adrenal gland steroidogenesis.
Cyp11b2 is expressed in the zona glomerulosa to produce aldosterone. As *Cyp17a1* is not expressed in the adrenal cortex, *Cyp11b1*, expressed in the zona fasciculata, produces corticosterone as the major glucocorticoid in mice. *Cyp17a1* is expressed in the murine gonads for sex steroid synthesis (pathway not shown).

1.3.5.2 Androgen backdoor pathway

The canonical androgen pathway involves the production of testosterone from DHEA and androstenedione in the testes and the zona reticularis of adrenal glands.[38] The more potent form of testosterone, 5α-dihydrotestosterone (DHT) is produced by 5α-reductase acting on testosterone. In the backdoor pathway, DHT is synthesised without the DHEA/androstenedione/testosterone intermediaries (Figure 1-4). A pathway that converted 17OHP to androstanediol which then circulated and was converted to DHT peripherally, without the intermediate step involving testosterone production, was first discovered in the Tammar wallaby in the early 2000s.[43] This pathway has been shown to be present in humans and contributes to male foetal sexual differentiation pathways.[44] The backdoor intermediaries have been mostly found in the placenta, liver and adrenal, rather than the testis.[44] The significance of this pathway is that it can be activated in hyperandrogenic conditions such as CAH, even in the absence of measurably elevated testosterone.

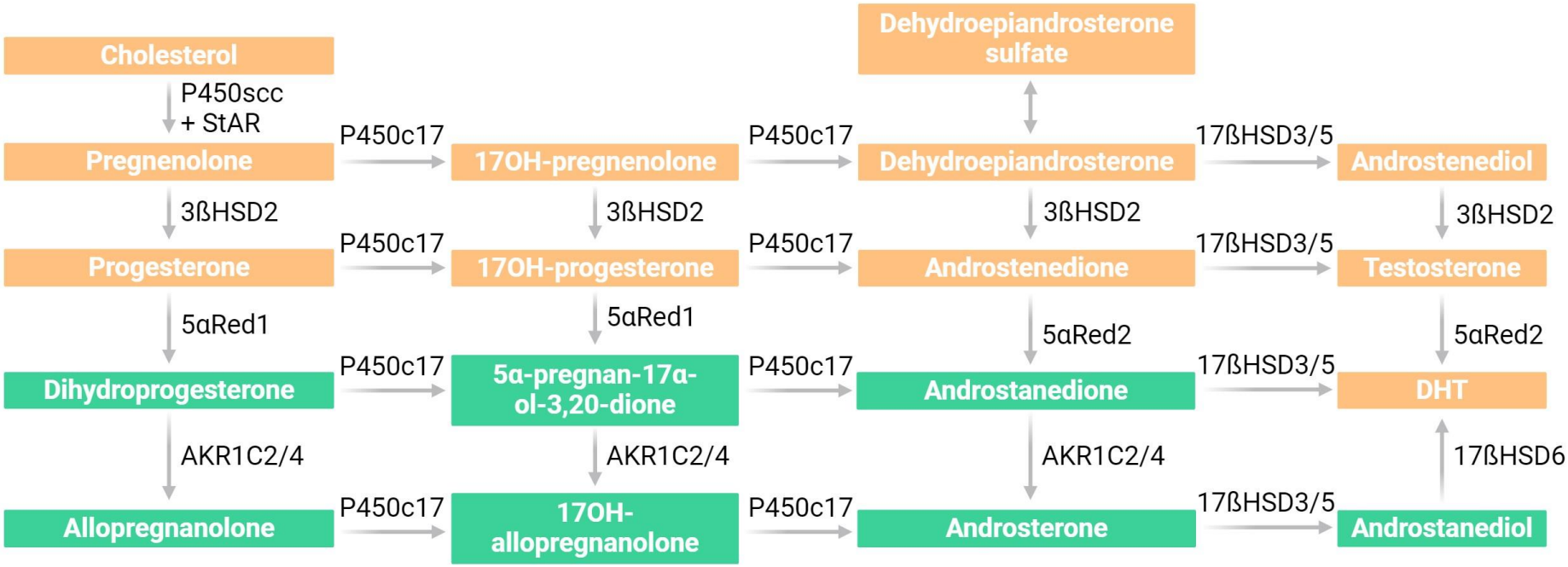

Figure 1-4 Backdoor androgen pathway (green).

The 3α-oxidation of androstanediol is probably performed by 17ßHSD6 but this has not been confirmed. Similarly, the identity of the enzyme that is involved in the 3α-reduction of dihydroprogesterone to allopregnanolone and 5α-prenan-17α-ol-3,20-dione to 17OH-allopregnanolone has not been confirmed but suspected to be AKR1C2 and/or 4. Adapted from Miller and Auchus, 2019.[45]

1.3.5.2.1 11-Oxygenated androgens

11-ketotestosterone and 11-ketodihydrotestosterone (11-ketoDHT) can both bind and activate the androgen receptor with similar efficacy as testosterone and DHT, respectively.[46, 47] 11-hydroxyandrostenedione and 11-hydroxytestosterone may be produced in the adrenal gland by P450c11ß where they are converted to the active 11-ketotestosterone and 11-ketoDHT peripherally (Figure 1-5). There are additional parallel pathways not shown in the figure, but they do not lead to other active androgens.[48] These keto-androgens contribute to the androgen excess seen in P450c21 deficiency,[49] where P45011ß is likely to be upregulated in response to the lack of P450c21. They are also associated with premature adrenarche and polycystic ovarian syndrome.[48] There is a possible pathway between the C11-oxygenated androgen pathway and the backdoor androgen pathway that has been demonstrated through *in vitro* studies: progesterone or 17OHP are 11ß-hydroxylated by P450c11ß and then converted to 11-ketoDHT. It is thought that P450c11ß only acts on 17OHP and progesterone in the absence of P450c21, and so is postulated to be a contributory pathway to hyperandrogenism in CAH.[50]

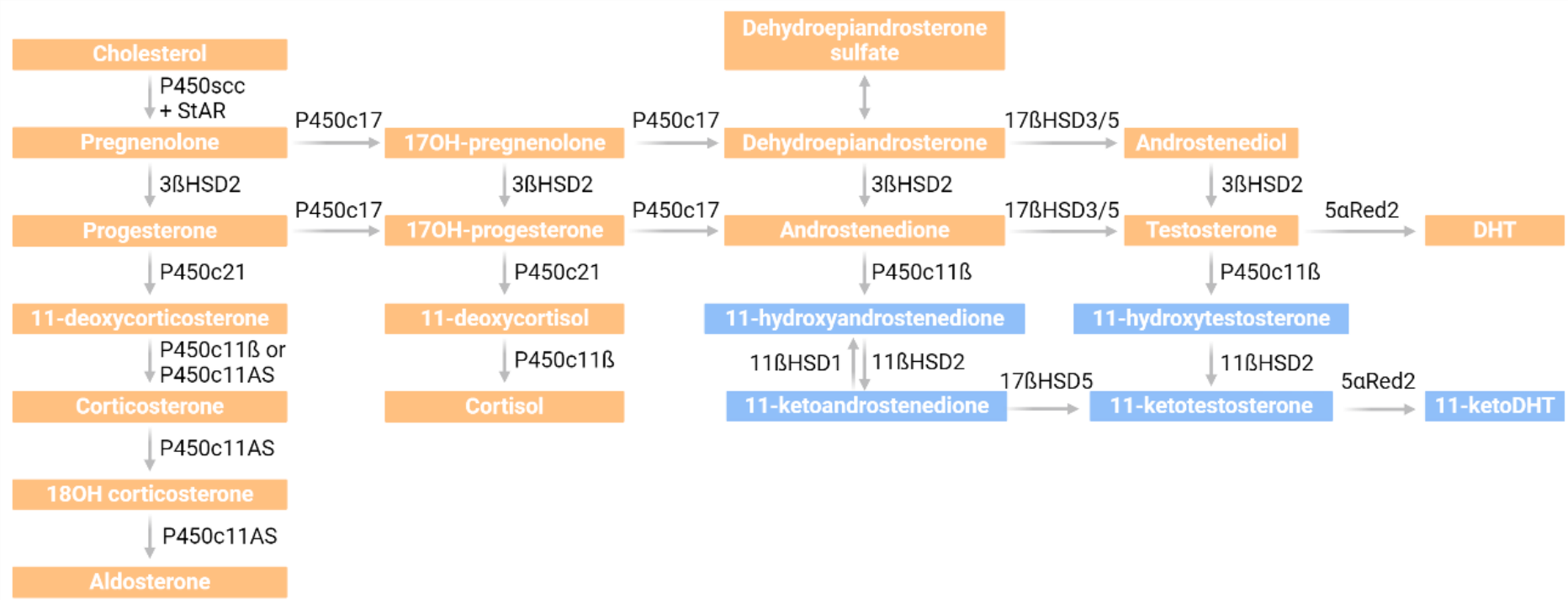

Figure 1-5 11-Oxygenated androgen production (simplified) (blue).

11-hydroxyandrostenedione and a small amount of 11-hydroxytestosterone is produced in the adrenal gland by 11-beta hydroxylase from androstenedione and testosterone respectively. This is converted by peripheral tissue (eg kidney, adipose) HSD11B2 to 11-ketoandrostenedione and 11-ketotestosterone. 11-ketoandrostenedione may also be converted to 11-ketotestosterone, which has similar activity as testosterone. This can then be further activated by 5α reductase to 11-ketoDHT. Adapted from Naamneh et al, 2022.[48]

1.4 Congenital adrenal hyperplasia

Congenital adrenal hyperplasia (CAH) refers to a group of seven monogenic adrenal disorders, caused by mutations in genes coding for enzymes in the adrenal steroidogenic pathway: *CYP21A2*, *CYP11B1*, *CYP17A1*, *HSD3B2*, *STAR*, *CYP11A1*, and *POR*.[51] In approximately 95% of cases, CAH is caused by mutations in *CYP21A2* resulting in 21-hydroxylase deficiency, and this autosomal recessive disorder affects approximately one in 15,000 livebirths.[52] Cytochrome P450 enzymes are located in endoplasmic reticulum or mitochondrial membranes. 21-hydroxylase, along with all microsomal cytochrome P450 enzymes, requires a flavoprotein POR which transfers electrons from NADPH to the enzymes.[53]

1.4.1 Non-21-hydroxylase deficient CAH

1.4.1.1 Lipoid congenital adrenal hyperplasia – StAR deficiency

Lipoid CAH is extremely rare, with an unknown incidence (ORPHA90790) and with most cases reported in Korean, Japanese and Palestinian populations.[54] As StAR is required for the regulation of transport of cholesterol from the outer to inner mitochondrial membrane, reduced StAR activity results in deficiency of all steroid hormones. Lipid droplets accumulate in the adrenal gland and may be seen on autopsy, giving rise to the name of this condition. In addition to the inability to produce steroids, lipid accumulation is toxic.[51] Severely affected infants present with adrenal crisis. There will be female external genitalia in both 46XX and 46XY infants.[54] A milder form exists, with some residual StAR activity with wide variation in phenotype.[55]

1.4.1.2 Cholesterol side-chain cleavage enzyme deficiency

The cholesterol side-chain cleavage enzyme (P450scc) is the first step in steroidogenesis. Pathogenic variants in *CYP11A1* present identically to lipoid CAH, however the adrenal glands and gonads are atrophic.[56] Distinguishing this from lipoid CAH requires molecular genetic testing. P450scc deficiency is considered rare with a prevalence of less than 1 in 1,000,000 (ORPHA168558),[51, 57] however recent genomic investigation of a large cohort of children with primary adrenal insufficiency has suggested that it may be more common than previously thought.[58]

1.4.1.3 3ß-hydroxysteroid dehydrogenase deficiency

HSD3B2 encodes 3ß-hydroxysteroid dehydrogenase type 2 (3ßHSD2) which is expressed in the adrenals and gonads. Deficiency of 3ßHSD2 results in reduced aldosterone, cortisol and androstenedione. Increased DHEA (produced by P450c17) can be converted to testosterone by 3-beta hydroxysteroid dehydrogenase type 1 (3ßHSD1, *HSD3B1*) which is expressed in the placenta or other peripheral sites.[51] Infants will present with salt-wasting adrenal crisis due to insufficient mineralocorticoid and glucocorticoid production. 46XY infants may be under-virilised whereas some 46XX infants may have virilisation.[51] 3ßHSD2 deficiency is rare, with an estimated prevalence of less than 1 in 1 000 000 (ORPHA90791).

1.4.1.4 17α-hydroxylase/17,20-lyase deficiency

For androgen production, *CYP17A1* encodes for an enzyme that has both 17-alpha hydroxylase (17OH) and 17,20-lyase activities (P450c17) and is required for the conversion of pregnenolone to 17-OH-pregnenolone and progesterone to 17-OH-progesterone (17OHP), and the subsequent conversion to DHEA and androstenedione,

respectively. Therefore, P450c17 deficiency impairs both adrenal and gonadal sex steroid production, resulting in absence of puberty and low cortisol.[51] Elevated ACTH results in increased deoxycorticosterone and corticosterone. Deoxycorticosterone has mineralocorticoid activity resulting in hypertension, hypernatremia and hypokalaemia while corticosterone has glucocorticoid activity and prevents adrenal crisis even in the presence of inadequate cortisol production. 46XY infants will have female external genitalia and both 46XY and 46XX children usually present in adolescence with absence of secondary sex characteristics, hypergonadotrophic hypogonadism and hypertension with low renin.[51] P450c17 deficiency is rare with an estimated prevalence of 1 to 9 in 1 000 000 (ORPHA90793), but there is increased frequency among Brazilians.[59]

1.4.1.5 P450 oxidoreductase deficiency

Cytochrome P450 enzymes depend on POR activity for electron transport in the endoplasmic reticulum, including P450c17, P450c21 and P450aro, as well as other P450 enzymes outside of the adrenal cortex. There is a wide range in the presentation of POR deficiency based on residual POR activity. It includes women with a PCOS-like phenotype, men with androgen deficiency as well as ambiguous genitalia in both 46XX and 46XY infants.[51, 60] Pre-natal virilisation occurs due to either insufficient placental aromatisation of testosterone or production of androgens via the alternative pathway. Post-natally, there is sex steroid deficiency. There may also be skeletal dysplasia due to extra-adrenal P450 enzymes being affected.[61] Mineralocorticoid production is sufficient and glucocorticoid production is variable. POR deficiency is rare with an unknown prevalence (ORPHA95699).

1.4.1.6 11ß-hydroxylase deficiency

CYP11B1 is expressed in the zona fasciculata (P450c11ß) and catalyses the conversion of 11-deoxycortisol and 11-deoxycorticosterone to cortisol and corticosterone, respectively. Deficiency of this enzyme results in inadequate cortisol and corticosterone synthesis, and resultant increased androgens and precursors. Infants with P450c11ß deficiency present similarly to those with P450c21 deficiency with androgen excess and adrenal crisis, however they do not have salt-wasting.[62] Importantly, deoxycorticosterone has weak mineralocorticoid activity and elevated levels can suppress the renin-angiotensin system, resulting in hypertension, hypernatraemia and hypokalaemia despite low serum aldosterone (despite normal aldosterone synthesis capabilities).[63] Mineralocorticoid excess tends to present in the first few months of life after neonatal renal mineralocorticoid resistance wanes. P450c11ß deficiency is the second most common form of CAH, thought to cause 5-8% of cases.[64, 65] It has an estimated prevalence of 1 in 100 000 to 1 in 300 000 with a higher prevalence (1 in 5000 to 1 in 7000) in Jewish Moroccans.[64, 66, 67]

1.4.2 Other monogenic adrenocortical disorders

While these conditions are not considered congenital adrenal hyperplasia, they can present similarly to CAH in the newborn period, and a gene therapy strategy that targets one adrenocortical gene could be re-designed and re-purposed to treat other monogenic adrenal cortex disorders.

1.4.2.1 Aldosterone synthase deficiency

Aldosterone synthase (P450c11AS) is required for the final steps in the production of aldosterone, namely conversion of deoxycorticosterone to aldosterone. Mutations in the *CYP11B2* gene lead to mineralocorticoid deficiency with salt-wasting in the urine, renal potassium retention resulting in hyponatraemia and hypokalaemia, and markedly elevated plasma renin activity and hypotension. Severely affected infants may present with vomiting, dehydration and shock. Milder forms can present later with failure to thrive. Electrolyte abnormalities tend to stabilise by mid childhood.[68] Aldosterone synthase deficiency is a rare disorder with unknown prevalence (ORPHA427).

1.4.2.2 Congenital adrenal hypoplasia

This condition is also known as adrenal hypoplasia congenita. The X-linked form is caused by pathogenic variants of the *NR0B1* gene and results in absence or minimal development of the definitive zone of the foetal adrenal gland. Severely affected boys present with salt-wasting crisis in infancy due to mineralocorticoid and glucocorticoid deficiency.[38] Deletions in *NR0B1* can be part of a contiguous gene deletion syndrome that may variably involve an X-linked mental retardation locus, glycerol kinase deficiency locus, ornithine transcarbamylase deficiency or Duchenne muscular dystrophy.[69, 70] An autosomal form may be related to variants in *NR5A1*.[38] The prevalence is unknown, and estimates vary widely from 1 in 140 000 to 1 in 1.2 million.[70]

1.4.3 21-hydroxylase deficiency

Deficiency of 21-hydroxylase (P450c21) is the most common form of CAH and for simplicity from here onwards the term “CAH” will refer to this form. The P450c21

enzyme is located in the adrenal cortical cell cytoplasm, with the N-terminal integrated into the membrane of the endoplasmic reticulum.[71, 72]

1.4.3.1 Genetics

The gene for P450c21, *CYP21A2 (*previously *CYP21B)*, contains 10 exons spanning 3 kb and is located on the short arm of chromosome 6 in the human leukocyte antigen (HLA, also major histocompatibility complex MHC) class III region (Figure 1-6).[73] The segment of the MHC class III region that contains the *C4* and *CYP21A* gene cluster is considered the most complex region of the human genome.[74-77] There are at least 14 distinct transcripts in the 140 kb region, and this includes genes that overlap and genes within genes.[78, 79] The RP-C4-CYP21-TNX (RCCX) module is a ~30 kb region that contains 4 genes in close association: serine/threonine kinase 19 (*STK19*, previously *RP*), complement component 4 (*C4*), 21-hydroxylase (*CYP21*), and tenascin-X (*TNX*).[80] This module is usually in duplicate (69% of Europeans) but may also be found as monomodular (17%) or trimodular (14%) copy number variants.[81] Duplication of the complement 4 gene conferred an evolutionary advantage in immunological function as both genes remain active in primates, allowing variety in the complement C4 protein through differences in gene size, gene number and nucleotide polymorphisms.[82]

While both the *C4* genes retain biological activity, the remaining duplicated genes have one or more pseudogenes. There is a homologous 21-hydroxylase pseudogene (*CYP21A1P;* previously *CYP21A*) that shares 98% and 96% homology in the exonic and intronic regions respectively.[73] The human pseudogene has at least 15 mutations along the length of the gene that render it non-functional.[83] Significantly, an 8-base deletion in codons 110-112 (exon 3) results in a frameshift and, subsequently, a stop codon at codon

130.[73] Downstream in *CYP21A1P* there are two further mutations including a cluster of four point mutations in codons 234-239 and a nonsense mutation in codon 318.[84]

The CYP21 locus most likely duplicated by non-homologous recombination[74] possibly after mammalian speciation as some mammals do not possess two genes,[85] although others suggest that the duplication may have occurred prior to 90 million years ago in a proto-mammalian synapsid ancestor and some mammal species have since eliminated the duplication.[82] However, duplication may have arisen independently in primates and rodents as the duplication borders vary.[74] In rodents, *Cyp21a2-ps* was inactivated rather than *Cyp21a1*.[74] In humans, inactivation of the *CYP21A1P* pseudogene is thought to have occurred 6 million years ago after our primate ancestors diverged from orangutan and gorilla ancestors but it is unclear whether this occurred prior[86] or subsequent[87] to the split between chimpanzees and humans, as both possess the 8 bp deletion that renders the pseudogene non-functional.[88]

The *CYP21A2* gene is 30 kb downstream from *CYP21A1P* and meiotic recombination events are common due to the high degree of homology between *CYP21A2* and *CYP21A1P*.[73, 84, 89-91] *CYP21A1P* lies between genes encoding the fourth serum complement components *C4A* and *C4B*, and the *C4B* gene lies between *CYP21A1P* and *CYP21A2*.[91] Due to the high homology and tandem-repeat organisation of the genes, pathogenic variants due to misalignment of chromosomes causing unequal crossover and gene conversion events are common, causing the majority of *CYP21A2* mutations.[92-95] There are over 350 known variants in *CYP21A2* listed in the Human Gene Mutation Database (HGMD, http://www.hgmd.cf.ac.uk)[96] spanning all 10 exons.

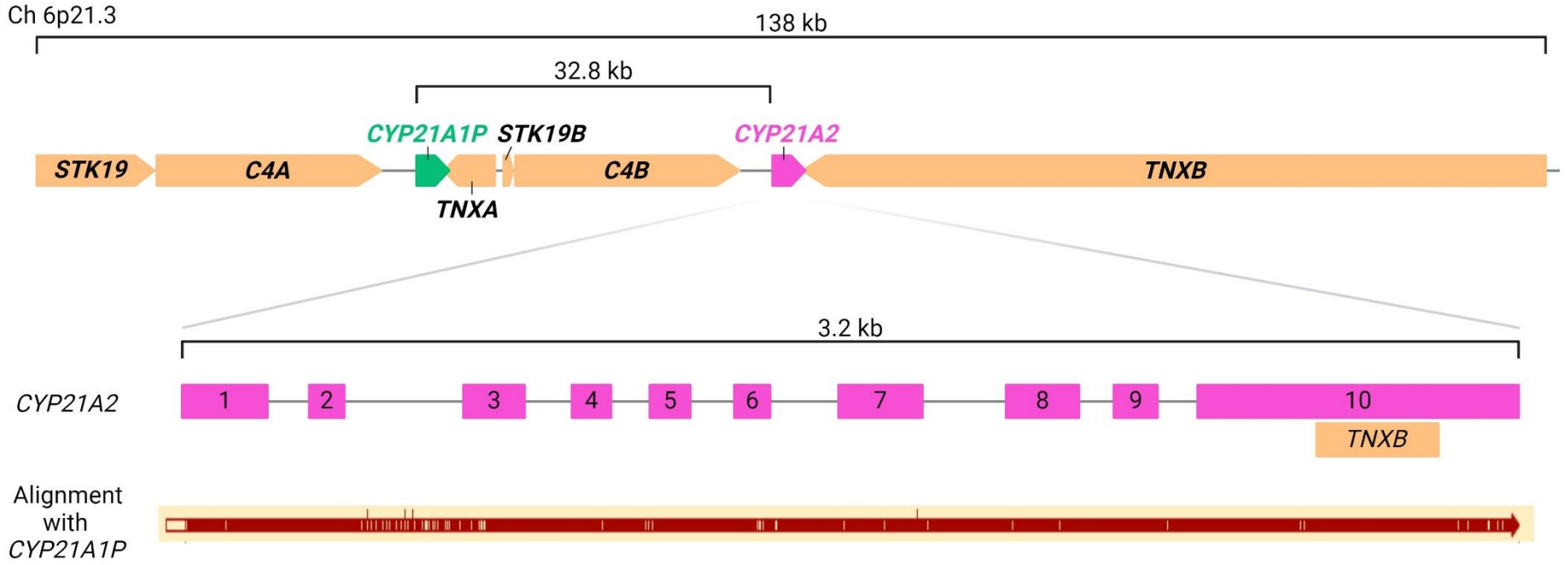

Figure 1-6 *CYP21A2* region on chromosome 6.

A 138 kb region of from the short arm of chromosome 6 is shown (NCBI Accession number NC_000006). There is a tandem arrangement of *C4A*, *CYP21A1P*, *C4B* and *CYP21A2*. The *CYP21A2* gene is 32.8 kb downstream from the *CYP21A1P* pseudogene. The *CYP21A2* locus is 3.2 kb and the cDNA is 2 kb. Alignment with the *CYP21A1P* pseudogene is shown .

1.4.3.2 Biochemistry

Pathogenic variants in the *CYP21A2* gene which lead to defective 21-hydroxylation result in a reduction in the synthesis of life-sustaining adrenocortical hormones: cortisol (glucocorticoid) and aldosterone (mineralocorticoid). There is accumulation of upstream precursor steroid hormones such as 17-OHP which are shunted into the P450c17 pathway, leading to increased levels of adrenal androgens via the canonical androgen pathway, the backdoor androgen pathway and through production of 11-oxygenated androgens (Figure 1-7).[51, 97, 98] The lack of cortisol leads to stimulation of the adrenal cortex by adrenocorticotropic hormone (ACTH) and thus to further androgen production. Excess 17OHP may also be converted to 21-deoxycortisol by P450c11ß, which has been suggested to be a better marker of P450c21 deficiency than 17OHP.[99, 100]

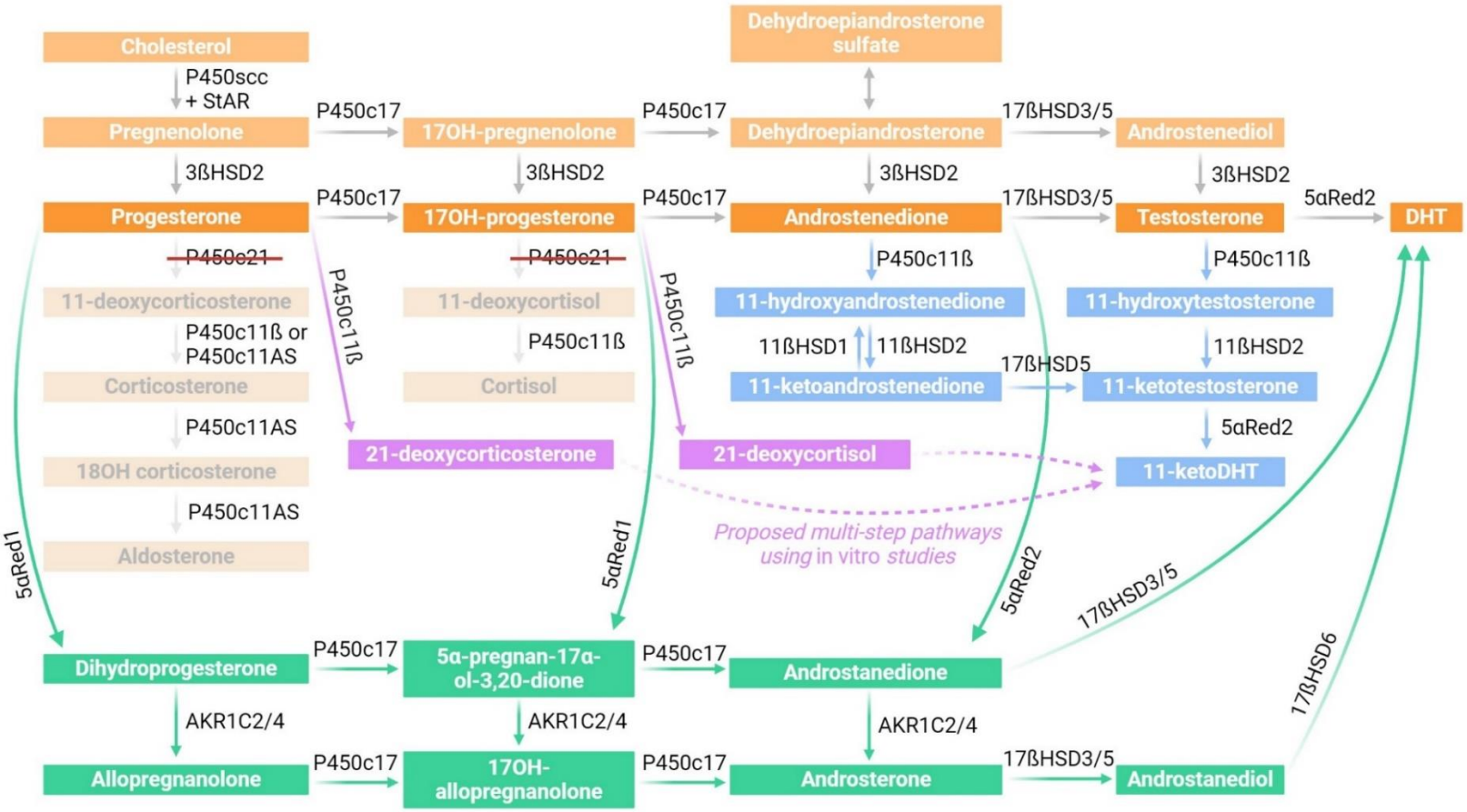

Figure 1-7 Steroidogenesis in P450c21 deficiency.

As 11-deoxycorticosterone and 11-deoxycortisol cannot be produced in adequate amounts (pale orange), there is a buildup of the precursors (progesterone and 17OHP) which are then shunted along the canonical androgen pathway via P450c17 (dark orange). Furthermore, there is enhanced activation of the backdoor pathway (green) and 11-oxygenated androgen pathway (blue), further exacerbating the hyperandrogenic state. 21-deoxycorticosterone and 21-deoxycortisol may be produced by P450c11ß as specific markers of P450c21 deficiency (purple) and have been proposed to enter the C11-oxygenated androgen pathway.

1.4.3.3 Phenotypes

There is a spectrum of disease severity. Phenotypically, CAH can be divided into classical and non-classical forms, with the classical form further divided into salt-wasting and simple virilising. Although the phenotypes are defined as such, it is a continuous spectrum based on residual enzyme activity. While aldosterone deficiency is not generally clinically significant in simple virilising and non-classical CAH, there is some degree of aldosterone deficiency in all phenotypes.[101]

Most patients have compound heterozygosity, and the phenotype tends to correlate with the less severely affected allele. While there is some genotype-phenotype correlation, particularly with severe or mild disease, the phenotype in patients with genetic variants that are associated with intermediate disease may be harder to predict, even within families.[90, 102]

1.4.3.3.1 Classical sat-wasting CAH

Complete inactivation of the P450c21 enzyme results in classical salt-wasting CAH, which is the most severe phenotype. Aldosterone and cortisol are unable to be produced in sufficient quantities to sustain life. Due to elevated androgens *in utero*, 46XX infants may be born with virilised genitalia and CAH may be detected and treatment commenced prior to a salt-wasting crisis. Virilised genitalia may be permanent. Normal male genitalia are present in 46XY infants and in some 46XX infants the virilisation is subtle. If CAH is not suspected and detected shortly after birth, classical salt-wasting disease will present in the first couple of weeks of life with a severe adrenal crisis: hyponatraemia, hyperkalaemia, elevated renin and hypovolaemic shock.[103, 104] This can be fatal. Infants may also have a history of vomiting, lethargy, and failure to thrive.

1.4.3.3.2 Simple virilising CAH

With greater than 2% P450c21 function, patients can produce enough aldosterone to avoid severe salt-wasting crises but have inadequate cortisol for all functions and produce excessive androgens. This is known as the simple virilising phenotype.[104, 105] Female infants may have evidence of virilised genitalia at birth. Either sex may present with hypocortisolaemia or as toddlers or children with early pubic hair development and increased growth velocity with tall stature.[51, 105] They will have advanced bone age, and if untreated their final height may be compromised due to early closure of their growth plates.

1.4.3.3.3 Non-classical CAH

Enzyme activity between 10-75% causes the non-classical form which is the mildest of the three phenotypes, where enough cortisol is produced for maintenance of homeostasis however there is not enough to suppress ACTH secretion and may lead to elevated androgens.[106] Individuals with non-classical CAH may be relatively asymptomatic or may have evidence of hyperandrogenism with early pubic hair development in children of either sex and hirsutism, oligomenorrhoea and anovulation in female adults.[104, 105] The signs and symptoms can be similar to polycystic ovarian syndrome in women.

As 2% residual enzyme function confers protection from severe salt-wasting, it is plausible that delivering the wild-type *CYP21A2* gene to a small number of cells in severe salt-wasting CAH could improve the phenotype to simple-virilising CAH, or even non-classical CAH.

1.4.3.4 Historical context of congenital adrenal hyperplasia

Almost 200 years have passed since the probable first case of presumed CAH was described in *The Lancet* in 1833: a 62-year-old "man" died following an episode of cholera and autopsy revealed a penis with hypospadias, ovaries, fallopian tubes and a uterus, however the adrenal glands were not mentioned.[107] More than 30 years later the best-described early case of CAH was reported by the forensic pathologist Luigi De Crecchio in *Sopra un Caso di Apparenze Virili in una Donna* (*A Case Report of Masculine Appearance in a Woman*) in 1865.[108] A published translation shows that in this report he described the autopsy of a person who lived as a man (he was recorded as female on his birth certificate, however this was changed at age 4 years), and had a phallus, no testes, internal female genital structures and enlarged adrenal glands and the description of his death could be consistent with an adrenal crisis.[109] It is likely that the subject of this report had simple virilising congenital adrenal hyperplasia as he survived until age 44 years. The first report of familial, salt-wasting CAH, where infants with "hermaphroditism" developed wasting, followed by death within a few weeks of life, came from 1886 when John Phillips described four infant siblings with ambiguous genitalia who died in circumstances consistent with a salt-wasting crisis.[110] He performed an autopsy on the last sibling and found normal female internal genitalia (the infant was designated male in life) and enlarged "suprarenal capsules". Dr Phillips believed that the cause in the first case was triggered by the mother being "badly frightened by a runaway horse in her third month of pregnancy", and the remaining three cases were due to her anxiety regarding the recurrence of hermaphroditism, on a background of family predisposition due to "hernial or other weakness present in one of the parents", in this case the father. He also drew the conclusion that there is a "distinct tendency towards bearing hermaphrodites may be developed in a mother who has already borne one of that class".[110] While this

history strongly suggests a hereditary basis for CAH, the possibility of inheritance was disputed in the 1950s. Some of this confusion arose due to the proximity of the adrenal glands to the kidney and the difficulty in distinguishing adrenocortical cancers (which may also cause virilisation) from cancers of renal origin, and it was thought that renal cancers arose from abnormal adrenal gland tissue, including hyperplastic glands.[1]

Despite the medical community's awareness of CAH since the late 19th century, the pathogenesis remained poorly understood, and treatment with glucocorticoids was not attempted until more than 8 decades later in the mid-20th century.[111-113] The administration of corticosterone to cases of the "adrenogenital syndrome", the earlier name for a number of disorders that included CAH, was associated with a reduction of 17-ketosteroid excretion in urine (17-ketosteroids include adrenal androgens such as androstenedione and dehydroepiandrosterone and their metabolites), onset of menarche or improved menstrual regularity, commencement of breast development, reduction in acne, and reduced skin pigmentation.[111, 112] One of these studies also showed that there is an increased steroid requirement during times of stress.[112] Prior to this, treatment with ACTH and exogenous androgens or partial adrenalectomy had failed.[111, 112] Five years after CAH was successfully treated with glucocorticoid, it was first demonstrated that there was deficient synthesis of cortisol ("Compound F") in virilising CAH due to defective 21-hydroxylation.[114] The enzyme blockage was found to be between 17-hydroxyprogesterone and cortisol, with deficiency of 11-hydroxylase unlikely due to minimal excretion of 21-hydroxylated steroids upstream from 11ß-hydroxylation (e.g. 17-hydroxy-11-deoxycorticosterone).[114] In 1985 the genetic basis for P450c21 deficiency was determined to be due to pathogenic variants in the *21-OHase "B"* gene (now known as *CYP21A2*) and not the other *21-OHase "A"* gene (*CYP21A1P*).[115] While our

understanding of the pathogenesis of this disease has improved, we have not come very far in terms of treatment for CAH since the mid-20th century and continue to treat this condition with glucocorticoid, mineralocorticoid, and salt (see Section 1.4.3.6).[52]

1.4.3.5 Newborn screening

Failure to diagnose classical CAH in the early neonatal period can lead to life-threatening adrenal crisis in infants, incorrect male gender assignment in virilised females or other complications in childhood which have been discussed previously. A screening tool using heel prick capillary blood collected on filter paper (similar to other newborn screening tests) to measure 17OHP was developed in 1977.[116] Following this, the first CAH pilot newborn screening program was commenced in 1977 in Alaska after a very high incidence (1:1481 live births) of P450c21 deficiency was found in the indigenous Alaskan population.[117, 118] CAH has been on the newborn screening test in New Zealand since 1984.[119] By 2015, CAH was on a newborn screening program for all states in the US, parts of Canada, 19/48 European countries, 9/20 Latin American countries (an additional 5 countries offer CAH newborn screening in the private sector), and 6/24 countries in the Asia-Pacific region (Japan, South Korea, New Zealand, Palau, Philippines, and Taiwan).[120] After a pilot study in Australia,[121] P450c21 deficient CAH was added to the myriad of newborn screening tests in New South Wales for babies born from the 1st of May 2018.[122] Other Australian states have followed but newborn screening for CAH is not yet universal in Australia. As a result of newborn screening, it is possible to diagnose infants prior to their first salt-losing crisis and to, therefore, treat earlier, reducing morbidity and mortality.[52] Due to the presence of the highly homologous pseudogene, *CYP21A1P*, mutations are unable to be reliably detected in *CYP21A2* with next generation sequencing.[123] For this reason and because CAH is now screened for in

Newborn Screening, The Australian Reproductive Carrier Screening Project (Mackenzie's Mission[124]; ClinicalTrials.gov Identifier: NCT04157595) did not include P450c21 deficiency and, therefore, it is unlikely that the most common cause of CAH will be part of any future parent carrier screening program (E. Kirk, personal communication, 2020). Since implementation of the NSW Newborn screening program in May 2018 until April 2020, over 200 000 newborns were screened, and classical salt wasting CAH was detected at an incidence of 1: 22 551.[122]

1.4.3.6 Treatment and impact

While early diagnosis and treatment are imperative in saving the lives of infants born with the severe form of this condition, treatment is far from perfect, and little has changed since it was first introduced in the 1950s.[111, 112, 125] Current standard management is fraught with inaccuracy as there is no perfect biochemical test to monitor therapy. Classic CAH is treated with glucocorticoids with or without mineralocorticoids, depending on the phenotype and management choices. Glucocorticoids are required to replace cortisol deficiency and a supraphysiological glucocorticoid dosage is required to suppress androgen production. Too little hydrocortisone can result in adrenal crisis, virilisation of female patients (hirsutism, clitoromegaly, disordered menstruation), precocious puberty, and short stature; too much hydrocortisone can result in short stature, hypertension, and cushingoid side effects.[51, 52, 95, 126] Mineralocorticoids are required in salt-wasting forms. Infants have mineralocorticoid resistance and, therefore, high doses are needed for the first months of life.[127] If increasing sensitivity is not recognised, infants may become hypertensive when the dose is weaned too slowly. Infants may also require salt supplementation. Although not required for maintenance of salt homeostasis, mineralocorticoid supplementation may also be used in simple virilising forms to treat

relative aldosterone deficiency which allows reduction in the glucocorticoid dose and improves final height.[128]

Patients on daily glucocorticoid treatment or those with a suboptimal response to ACTH stimulation testing must receive increased glucocorticoid dosing during times of stress (e.g. illness, injury, surgery) to avoid adrenal crisis.[52] The burden of treatment involves taking medication up to three to four times per day, and increased doses at times of stress (illness, surgery, and trauma). The distribution of these doses is controversial, and replacement is not completely physiological. In the paediatric population, there is the addition of care giver burden and disruption to the parents' daily life.[129] Even with good adherence to treatment, patients are shorter than the general population, have fertility issues, develop hypertension, may have obesity, are at risk of low bone mineral density and have been shown to have a poorer quality of life.[126, 130-132] They may also be more prone to attention-deficit hyperactivity disorder, anxiety and depression.[133, 134] In some cases, suppression of hyperandrogenism is so challenging that bilateral adrenalectomy may be considered, resulting in absolute adrenal hormone deficiency.[135] Furthermore, patients with CAH have a shortened life expectancy compared with the general population with both adrenal crisis and all-cause mortality contributory.[136]

As current standard management is far from perfect, alternative and adjunctive treatment options have been explored, including subcutaneous hydrocortisone pumps and modified release once-daily hydrocortisone.[137-141] Neither of these alternatives is ideal as pump management is complex and the modified release hydrocortisone is not superior to standard management.[142, 143] Adjunctive treatment to reduce androgen excess have been trialled in small groups of patients. The enzyme P450c17 converts steroid precursors to

DHEA and androstenedione which in turn may be converted to other adrenal androgens (Figure 1-2). Abiraterone acetate inhibits P450c17,[144] and has been trialled in women with poorly controlled CAH resulting in normalisation of androstenedione levels.[145] However, abiraterone acetate will inhibit gonadal steroid production and therefore should only be used in pre-pubertal children, women on effective contraception/hormone replacement therapy or men who receive exogenous testosterone replacement.[142] Other strategies to reduce androgen excess include reducing ACTH production. A selective corticotropin-releasing hormone receptor type 1 agonist was trialled in addition to standard therapy and was able to reduce morning ACTH and lower serum 17OHP in a small trial of eight women with classic CAH.[146]

Treatment for CAH has changed minimally since it was first applied in the 1950s, despite being far from a perfect remedy. Alternative treatments have been explored but are not superior to standard corticosteroid treatment. Gene therapy is a potentially viable alternative treatment by increasing the P450c21 expression and, thereby, overcoming the deficiency.

1.5 Gene therapy

Gene therapy technology has advanced to a point where potential curative treatments are realistic and enticing possibilities for monogenic adrenal disorders such as CAH. Gene therapy approaches correct, prevent, or alleviate disease by replacing (gene addition) or repairing (gene editing) genes carrying pathogenic variants. Therapeutic options include naked DNA, synthetic oligonucleotides, viral vectors, and lipid nanoparticles (LNP). Potential gene therapy complications include acute toxicity from infusion of foreign

material (e.g., viral particles), cellular and humoral immune responses against the transduced cells and the therapeutic gene product respectively, and insertional mutagenesis.[147]

1.5.1 History of gene therapy

Gene therapy research has origins in bacterial work from the early 20th century. The ability for bacterial cells to take up cell-modifying material at the time called the "transforming principle" from the environment (transformation) was discovered in the 1920s.[148] Bacterial transformation is exploited in the production of gene therapy whereby engineered plasmids are taken up by bacteria, and subsequently the plasmid-containing bacteria is grown. Thus the plasmid is reproduced by the bacterial genetic replication machinery. The "transforming principle" was determined to be DNA, not protein as was previously thought, by Oswald Avery and colleagues in the 1940s.[149] Two other methods for transferring DNA between bacterial cells were discovered in the 1940s and 1950s and include conjugation (mating)[150] and transduction.[151] Transduction was discovered by Norton Zinder and colleagues, and occurs when a bacteriophage (virus) transfers genetic material from one bacterium to another and is one of the mechanisms by which bacteria may acquire antibiotic resistance.[151] Transduction is not limited to bacterial cells, and this concept underpins gene therapy whereby a viral vector introduces foreign genetic material into a eukaryotic cell. The rescue of a genetic defect through the transfer of foreign DNA was demonstrated in the 1960s and was the first time that gene transfer was shown to be potentially heritable.[152] Shortly thereafter, it was shown that stable inheritance occurred through the integration of foreign DNA into the host chromosome.[153]

It was postulated as early as the 1960s that viral gene transfer could possibly be exploited as a genetic therapy, particularly for disease due to enzymatic defects.[154-156] Following initial proof-of-concept for virus-mediated gene transfer in plants,[157] an attempt at a human gene therapy trial was made in the 1970s, prior to the development of recombinant DNA technology.[158, 159] The Shope rabbit papilloma virus was known to induce arginase in rabbits and was able to induce arginase in skin fibroblasts from humans with arginase deficiency.[158] Following the *in vitro* study, three siblings with arginase deficiency were injected intravenously with purified Shope virus, however there was no change in serum arginine.[159] The trial was inherently flawed, as the virus had degraded in storage and was no longer infective.[159, 160] The first approved gene transfer study was undertaken in 1989. A γ-retroviral vector was used to tag lymphocytes *ex vivo* which were then returned to the patient.[161] The first trial using a therapeutic gene was conducted in the 1990s where autologous T cells were genetically modified *ex vivo* and then engrafted back into two infant patients with severe combined immunodeficiency (SCID) due to adenosine deaminase (ADA) deficiency.[162] While gene expression persisted, the therapeutic effect was not significant.[163] Hundreds of trials were commenced in the 1990s. However, there was concern raised in the Orkin-Motulsky report in 1995 regarding the lack of scientific understanding of the viral vectors and their interactions with hosts: there was a recommendation that funding be targeted towards basic research.[164] This heralded a devastating outcome where in 1999 a participant in a gene therapy trial for ornithine transcarbamylase deficiency, Jesse Gelsinger, died from multiorgan failure 4 days after administration of an adenovirus vector.[165-167] Yet, the first successful gene therapy trial in humans was published in 2000, using a retroviral vector in patients with severe combined immunodeficiency X1 disease (SCID-X1).[168] Shortly thereafter, risk of insertional mutagenesis was reported in a mouse model using a retroviral vector,[169] and

in 2003 pre-malignant cellular proliferation was reported in two patients from the SCID-X1 trial in 2000.[170] Subsequently, several further reports showed a risk of insertional mutagenesis following gene therapy in humans,[171-174] and approval for gene therapy trials declined.[175, 176] Despite these setbacks, the field of gene therapy persevered[177] and as the technology has improved, the number of trials has exploded.[178] A deepening understanding of the science behind gene therapy, improvements in safety and advancements in efficiency of gene transfer have led to considerable progress in the field of genetic therapies.[179]

While the technology for genetic therapeutics has entered a new era, clinical translation remains a major barrier. There has been a steady rise in the number of clinical trials for human gene therapy, however the majority of these are in early stages of development. From 1989-2004 over 900 clinical trials in gene therapy had been approved,[175] increasing to 1300 by 2007.[180] By 2012, there were over 1800 clinical trials that had been approved worldwide.[181] By the end of 2017, 2597 gene therapy clinical trials had been approved worldwide.[182] Despite this exponential growth in clinical trials, by December 2023, only 30 gene therapies were available commercially in the world.[178] In addition, there were 18 approved non-coronavirus related RNA therapies.[178] The commercial gene therapies released to the end of 2023 are summarised (Table 1-2).

Table 1-2 Commercially available gene therapies.

Name	Gene therapy description	Indication	First Approved	Note
Gendicine (recombinant p53 gene)	Recombinant adenoviral vector expressing p53, rAd-53	Head and neck cancer	2004	Considered the first commercially available gene therapy
Oncorine (E1B/E3 deficient adenovirus)	Recombinant human Adenovirus type 5 injection, H101	Nasopharyngeal carcinoma. Head and neck cancer	2005	
Rexin-G (mutant cyclin-G1 gene)	Retroviral-dnG1	Soft tissue sarcoma and osteosarcoma	2006	
Neovasculgen (Cambiogenplasmid)	Plasmid-VEGF	Peripheral vascular disease and limb ischaemia	2011	
Glybera (Alipogene tiparvovec)	Recombinant adeno-associated virus (rAAV) vector: rAAV1-LPL	Familial lipoprotein lipase deficiency	2012	First rAAV gene therapy approved. Withdrawn from market due to lack of demand and expensive production
Imlygic (Talimogene laherparepvec)	Genetically modified oncolytic viral therapy medicine: HSV1-GM-CSF	Melanoma	2015	
Zalmoxis	Allogenic T cells with retroviral-δLNGFR/HSV1-TK	Restoring immune system after haematopoietic stem-cell transplant	2016	Was initially conditionally approved pending phase III studies, however trial

				suspected as no benefit to survival[183]
Strimvelis	Autologous CD34+ cells transduced with retroviral-ADA	Severe combined immunodeficiency due to adenosine deaminase deficiency	2016	First *ex vivo* corrective gene therapy to achieve approval[184]
Kymriah (Tisagenlecleucel)	chimeric antigen receptor (CAR) T cell immunotherapy: lentiviral-CD19 applied to patient's T cells *ex vivo*	Relapsed B cell acute lymphoblastic leukaemia (paediatric patients up to 25 years of age)	2017	
Luxturna (Voretigene neparvovec)	rAAV2-PRE65	Bi-allelic RPE65 associated retinal dystrophy	2017	
Yescarta (Axicabtagene ciloleucel)	CAR T cell immunotherapy: retroviral-CD19	Relapsed or refractory large B cell lymphoma (adult patients)	2017	
Invossa	Human allogenic chondrocytes transduced with retroviral-TGF-β1	Moderate knee osteoarthritis	2017	Withdrawn in 2019[183]
Collategene (Beperminogene perplasmid)	Naked plasmid-HGF	Critical limb ischaemia	2019	
Zolgensma (Onasemnogene abeparvovec)	rAAV9-SMN1	Spinal muscular atrophy with biallelic mutation in *SMN 1* gene (paediatric patients)	2019	
Zynteglo (Betibeglogene autotemcel)	Haematopoietic stem cells transduced with lentiviral-β-globin vector	Transfusion dependant β-thalassemia (patients over 12 years of age)	2019	

Tecartus (Brexucabtagene autoleucel)	CAR T cell immunotherapy: retroviral-CD19	Relapsed or refractory mantle cell lymphoma (adult patients)[185]	2020	
Libmeldy (Atidarsagene autotemcel)	Autologous CD34+ cells transduced with lentiviral vector encoding *ARSA* gene	Metachromic leukodystrophy	2020	
Breyanzi (Lisocabtagene maraleucel)	CAR T cell immunotherapy	Diffuse large B-cell lymphoma; follicular lymphoma	2021	
Abecma (Idecabtagene vicleucel)	CAR T cell immunotherapy targeting B-cell maturation antigen	Multiple myeloma	2021	
Delytact (Teserpaturev)	Recombinant Herpes simplex 1 virus	Malignant glioma	2021	
Relma-cel (Relmacabtagen autoleucel)	CAR T cell immunotherapy	Diffuse large B-cell lymphoma; follicular lymphoma	2021	
Skysona (Elivaldogene autotemcel)	Autologous CD34+ cells transduced with lentiviral vector encoding *ABCD1* gene	Early cerebral adrenoleukodystrophy (CALD)	2021	
Carvykti (Ciltacabtagene autoleucel)	CAR T cell immunotherapy targeting B-cell maturation antigen	Multiple myeloma	2022	
Upstaza (Eladocagene exuparvovec)	rAAV2-AADC	Aromatic L amino acid decarboxylase (AADC) deficiency	2022	
Roctavian (Valoctocogene roxaparvovec)	rAAV5-F8	Haemophilia A	2022	

Hemgenix (Etranacogene dezaparvovec)	rAAV-F9	Haemophilia B	2022	
Adstiladrin (Nadofaragene firadenovec)	Adenoviral vector encoding IFN alpha2b gene	Bladder cancer	2022	
Elevidys (Delandistrogene moxeparvovec)	rAAVRh74 micro dystrophin transgene	Duchenne muscular dystrophy	2023	
Vyjuvek (Beremagene geperpavec)	HSV1 vector delivering *COL7A1*	Dystrophic epidermolysis bullosa	2023	Topically applied to wounds. Redosable.
Fucaso (Equecabtagene autoleucel)	CAR T cell immunotherapy anti-B cell maturation antigen	Multiple myeloma	2023	
Casgevy (Exagamglogene autotemcel)	Electroporation of patient's CD34+ haemtopoetic stem cells to introduce CRISPR/Cas9 complex. Disrupts *BCL11A* expression which induces foetal haemoglobin expression	Sickle cell anaemia; thalassaemia	2023	First approved CRISPR-based therapy
Inaticabtagene autoleucel	CAR T cell	Acute lymphocytic leukaemia	2023	
Lyfgenia (Lovotibeglogene autotemcel)	Lentiviral vector delivering modified b-globin (T87Q).	Sickle cell anaemia	2023	

Adapted from Ma et al (2020)[186], Evans (2019)[183] and ASGCT quarterly report Q4 (2023).[178]

The first gene therapy recognised to be commercially available was Gendicine (Shenzhen SiBiono GeneTech, China) for the treatment of head and neck squamous cell carcinoma which was approved in China in 2003.[160] In the European Union, the first clinically approved gene therapy was Glybera (uniQure, Netherlands) in 2012, which utilised an AAV vector designed to express lipoprotein lipase in the muscle for treatment of lipoprotein lipase deficiency.[187] Glybera was withdrawn from the market due to high cost of production and low utilisation.[186] The first American AAV-based gene therapy Luxturna (Spark Therapeutics, USA) was approved in 2017 for treatment of a form of retinal dystrophy caused by RPE65 deficiency.[182] Zolgensma (AveXis, USA) is another commercially available AAV-based gene therapy that treats spinal muscular atrophy and has been shown to have advantages over Spinraza (BioGen),[188] an oligonucleotide drug which requires repeated intrathecal injections.[189] The exponential growth in gene therapy clinical trials and paucity of commercially available gene therapies alludes to the presence of challenges faced in the commercialisation of ultra-expensive bespoke therapies for ultra-rare conditions.

1.5.1.1 Challenges in commercial sustainability

In the process of therapeutic development and implementation, there are hurdles at every step, and many of these barriers are more difficult to surmount for ultra-rare diseases. Gene therapies are extraordinarily cost intense, in both the research and development phases and during commercial manufacture. Regulatory processes may also be cost-prohibitive. If a disease is rare and the intervention is mutation-specific, regulatory compliance may be required for each individual disease variant, rather than batching the treatment as one – limiting the utilisation of bespoke products. The inherent rarity of these conditions means that the market size may not provide opportunity for cost recuperation. The health economic burden must also be considered: a million-dollar transformative

treatment that results in an individual reaching adulthood and entering the workforce with little or no disability where previously the condition would have resulted in early death has great health economic benefit. In comparison, it is more difficult to assess whether a partially effective treatment that may still leave considerable disability results in less overall cost to the healthcare system than going without advanced therapeutic treatment. In addition, the complexity of treatment administration must be considered. In *ex vivo* gene therapy, cells are harvested from an individual, purified, treated with the therapeutic product and reintroduced to the patient, who may have been required to undergo myeloablation or other conditioning therapy. This means that the centres that are able to administer this treatment are limited to those with facilities that can fulfill each step in the treatment pathway. This in turn limits the scalability of treatment delivery, and patients may need to travel long distances to receive treatment.

Strimvelis, the first *ex vivo* gene therapy to gain regulatory approval,[184] exemplifies the challenges faced by advanced therapeutics for ultra-rare diseases. Strimvelis treats adenosine deaminase deficient severe combined immune deficiency (ADA-SCID), a rare autosomal recessive disease with an estimated incidence of 1 in 200 000 to 1 000 000 (ORPHA 277). The therapy was developed at the San Raffaele Telethon Institute for Gene Therapy in Milan, Italy in the early 2000s. It utilises a gammaretroviral vector encoding human *ADA* cDNA that transduces autologous CD34+ cells for the treatment of patients with ADA-SCID who cannot have an allogenic stem cell transplant due to unavailability of a suitable donor.[190-193] The transduced cells that are able to produce adequate quantities of ADA are conferred with a survival advantage over the untransduced cells, without the need for complete myeloablation. The development of this therapy was funded by the Italian Telethon Foundation (Fondazione Telethon), a

charity that supports research for rare genetic diseases.[190] A partnership between the Telethon Foundation, San Raffaele Hospital, and GlaxoSmithKline (GSK) in 2010 provided the network of resources and infrastructure required to complete the commercialisation of Strimvelis, and it was licenced in 2016.[184, 194] However, in 2018 GSK sold their portfolio of gene therapies, including Strimvelis, to Orchard Therapeutics,[195] and by 2022, Orchard had determined Strimvelis was not economically viable and discontinued the program.[196] The licence was transferred back to the Telethon Foundation, which was the first time that a non-profit organisation has taken on the responsibility of distributing a gene therapy product, and Strimvelis remains available to patients through the San Raffaele Hospital in Milan, Italy.[196] These events demonstrate the difficulty in recuperating costs of highly expensive therapies with limited market size: two commercial biomedical companies attempted and failed. However, the licencing the product to a not-for-profit organisation is an innovation solution and may future-proof the continual availability of advanced therapeutics to patients with ultra-rare conditions.

Glybera is another example of the challenges faced in the commercialisation of expensive therapies for ultra-rare conditions. It is an AAV1 vector that encodes the gene *LPL* with a naturally occurring gain-of-function mutation for treatment of lipoprotein lipase deficiency,[197] and was the first gene therapy to reach market.[187] Lipoprotein lipase deficiency is a rare monogenic disorder affecting 1 to 9 in 1 000 000 (ORPHA 309015) that causes dyslipidaemia and recurrent pancreatitis. While Glybera shown to reduce incidence and severity of pancreatitis, it did not improve dyslipidaemia[198] and it was removed from market in October 2017, 5 years after it was approved for use in the European Union.[199] Treatment with this therapy was approximately $1 million per person,[200] and coupled with the rarity of the disease it treated, was not commercially

sustainable.[199, 201] Moreover, long-term data has since shown that the clinical efficacy was not sustained.[202] The fate of Glybera serves as a cautionary tale in the development of high cost treatments for ultrarare diseases, where the treatment is only partially effective and the small patient population may not provide opportunity for recouperation of development costs. Therefore, biotechnology companies must include health economic considerations in their gene therapy development programs, including robust scientific merit and justification that the high cost of production will fulfil and imperative unmet need.

Traditional pharmaceutical development pipelines may not be appropriate to gene therapy due to the aforementioned challenges and alternative models are required. Collaboration between academic institutions and industry can facilitate efficient streamlining of the transition of therapy from bench to bedside. Additionally, innovating funding models such as public-private partnerships, crowdfunding, and venture philanthropy can help mitigate the financial risks associated with gene therapy development and may permit investment into less commercially viable therapeutic areas.

1.5.2 Vectorology

The major challenge for gene therapy is delivery. *Ex vivo* gene therapy has been explored in tissues that can be genetically manipulated in culture and then engrafted into the patient, but this approach has limited application in the adrenal cortex.[203] For *in vivo* gene delivery, viral vectors are currently the most capable delivery approach: by 2021 89% of genetic therapeutics in development used viral vectors, and recombinant adeno-associated virus (rAAV) was the leading viral vector for gene delivery.[204, 205] Non-viral approaches involving lipid nanoparticle (LNP) and RNA technology are developing rapidly and will

increasingly complement the power of viral vector-mediated gene transfer. Vectorology exploits the natural ability of a virus to introduce its own genome into a host cell, where the viral genes are removed and replaced with therapeutic genetic cargo, eliminating the ability for viral replication and infection: only the ability to deliver genetic cargo to cells remains. Common viruses that have been exploited for use in gene therapy are summarised (Table 1-3).

A number of viral vectors have been used in gene therapy to package therapeutic machinery.[147, 160] Simple retroviruses and lentivirus will integrate into the host genome, whereas herpes simplex virus and adenovirus are less likely to integrate. While adeno-associated virus (AAV) genomes are generally episomal, random chromosomal integration can occur.[206, 207] Retroviruses tend to establish a chronic infection however there is a risk of complications such as malignancy and immunodeficiency. Lentiviral vectors are a complex form of retrovirus and can infect non-dividing cells and can carry large gene cassettes (<8 kb).[179] They also integrate preferentially into the coding region of genes.[179] Lentivirus does not have specific tissue tropism and intravenous administration will lead to widespread delivery. To target an organ of interest it must be directly administered to that organ. In most haematopoietic stem cell applications, lentivirus is the vector of choice, and it is usually delivered to cells *ex vivo*.[179] Herpesvirus vectors can persist in humans and have a capacity for a large therapeutic cassette, however entry into cells is complex which limits their application.[147] Adenoviruses are efficient vectors for gene transfer; however, can lead to inflammatory and immune responses.[165] In the past, adenoviral vectors were the most commonly used, however their popularity is decreasing.[178, 182] AAV is from the genera *Dependovirus* which is part of the *Parvoviridae* family.[208] AAV was discovered in the 1960s and has no confirmed disease

associated with it.[209, 210] AAV is predominantly non-integrating, using episomal DNA transfer and without the use of editing strategies, AAV gene delivery is limited to stable, non-dividing cell populations.[179]

Table 1-3 Viral vectors used in gene therapy.

Virus type	Coating	Genome	Mechanism	Note	Limitations	Use in vector-based gene therapies in development[204]
Simple retrovirus	Lipid-enveloped	ss RNA	Retro-transcribed into linear ds DNA and integrated into host cell chromatin. Transduction requires target cell to undergo mitosis shortly after viral entry.[147]	Chronic infection.	Target cells must undergo mitosis after viral entry. EG lymphocytes and haematopoetic progenitors.[147] Latent disease eg malignancy (insertional mutagenesis)[171, 174]	7.5%
Lentivirus (complex retrovirus)	Lipid-enveloped	ss RNA	Target cell actively transports pre-intergration complex into nucleus. Transduction of non-dividing cells possible.[147] Integration into host genome.[211]	Long term transgene expression.[212]	Packaging capacity <8kb[179]	30%
Herpes simplex virus		ds DNA	Large capacity >30kb.[147] By deleting the genes for replication, HSV can mimic the latent state without reactivation.[213] Episomal.	Persistent latent state	Complex attachment and entry into cells[147]. Episomal, lost after cellular division[213].	3.7%
Adenovirus	Capsid	ds DNA	Episomal and generally not integrated into host genome. Split into two for gene therapy: helper virus contains	Inflammatory response	Episomal, lost after cellular division. Intravenous injection	13%

			genes for replication. Therapeutic vector contains ITRS, gene of interest and packaging signals.[147] Large capacity up to 35kb. High efficiency of transduction and able to transduce nondividing cells.[182]		generally goes to liver, but direct injection into organs is possible[147].	
Adeno-associated virus (parvovirus)	Capsid	ds DNA	Require helper virus for infection (eg adenovirus or herpesvirus). Episomal OR random chromosomal integration. Will transduce non-dividing cells.[147]	No proven human disease.[205] Emerging evidence that AAV2 may be associated with paediatric acute hepatitis.[214-217]	Packaging capacity <5kb[147]. Neutralising antibodies if readministered.	42%
Other (including poxivirus)						3.8%

Abbreviations: ss, single-stranded; ds, double-stranded; HSV, herpes-simplex virus.

1.5.2.1 Adeno-associated virus

There has been a decline in the use of retroviral and adenovirus vectors in favour of recombinant adeno-associated viral (rAAV) and lentiviral vector-based therapy.[182, 205] Viral vectors were used in 89% of gene therapies in development, and of these, rAAV was the leading vector used for *in vivo* gene delivery.[204] AAV is a small dependent parvovirus[208] that has not been proven to cause disease in humans and in non-dividing cells is a stable vector for gene transfer *in vivo*.[218, 219] Risk of adverse events increases with very high doses of rAAV which are often utilised when targeting organs outside of the liver, and in 2020 four children who received some of the highest human doses of rAAV as part of a trial for treatment of X-linked myotubular myopathy passed away after developing severe hepatobiliary disease as a result of the rAAV treatment.[220, 221] Adverse events that have been associated with rAAV therapy include liver toxicity,[222, 223] thrombotic microangiopathy[224] and dorsal root ganglion toxicity.[221]

The structural components of wild-type AAV include an icosahedral protein capsid and a single stranded DNA genome that is 4.68 kb in size (Figure 1-8). The capsid has three viral protein subunits VP1, VP2 and VP3.[208] Flanking the AAV genome are inverted terminal repeats (ITRs) which are T shaped structures that serve as the primers for DNA replication. Two main genes exist in the AAV genome: *rep*, and *cap*, located between the ITRs. The *rep* gene encodes proteins required for viral replication. There is no DNA polymerase or single-stranded DNA (ssDNA) binding protein in the AAV and thus these must be supplied by a helper virus[208] such as adenovirus or herpes simplex virus.[225] Similarly, the *cap* gene encodes the three subunits of the capsid in open reading frame one (VP1, VP2 and VP3). Open reading frame two of the *cap* gene encodes the assembly-activating protein (AAP), required for assembly of AAV.[226, 227] There is a third gene

known as *X* that is in the 3' end of the genome, within the *cap* sequence, and codes for a protein that has a supportive function in genome replication.[228] AAV generally exists in a predominantly extrachromosomal state, although in some instances it may integrate into the genome to establish latency.[229] In the absence of a helper virus, AAV establishes latency by integration into a specific site called AAVS1 on human chromosome 19.[230] Integration at AAVS1 is *rep*-mediated,[231] and therefore should not occur with vectors that as they do not encode *rep*, although inefficient vector integration events may occur elsewhere in the genome.[232]

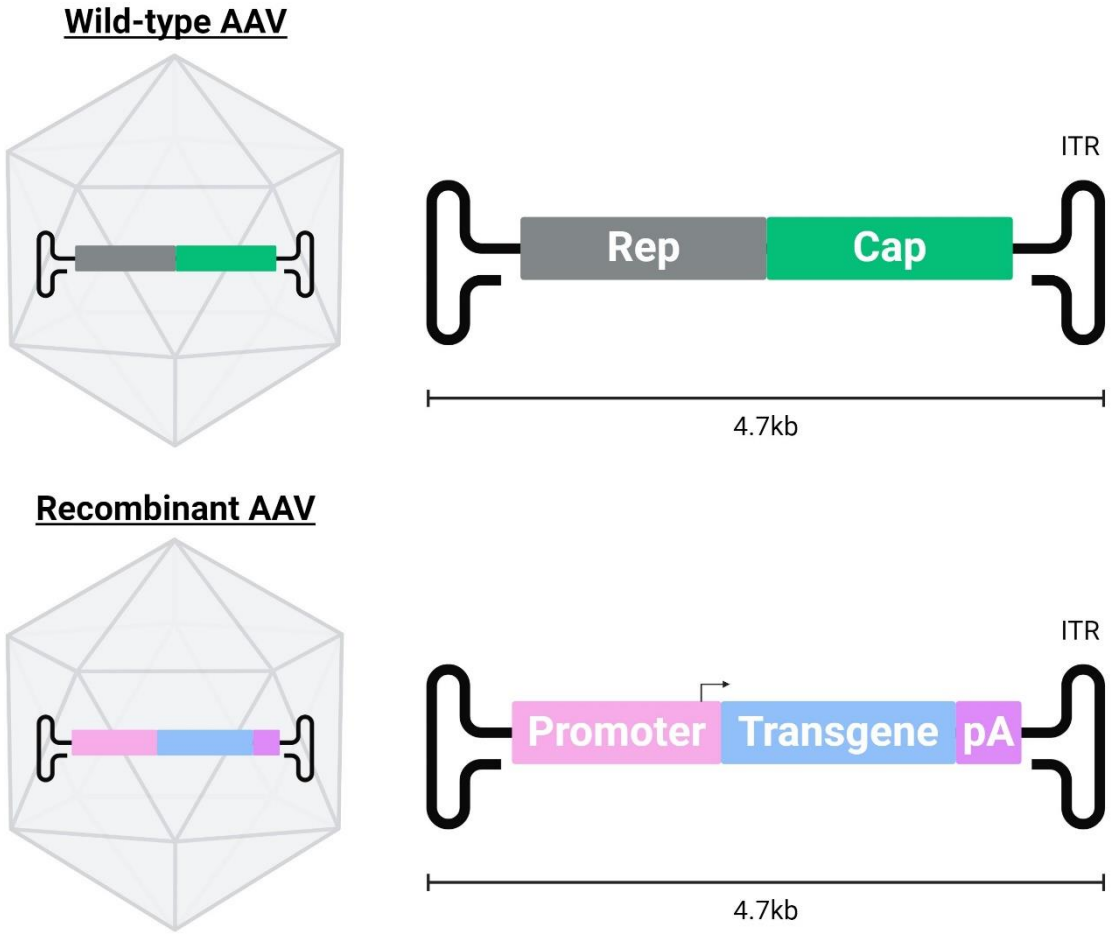

Figure 1-8 Adeno-associated virus structure.
Wild-type AAV genome consists of two genes, *Rep* and *Cap*. In recombinant AAV, the wild-type genome has been removed and replaced with a transgene and other regulator elements. Abbreviations: AAV, adeno-associated virus; ITR, inverted terminal repeats; pA, polyadenylation tail.

Recombinant AAV vectors have had most of their native genetic sequence removed, leaving only inverted terminal repeats (ITRs) which contain the *cis*-acting elements critical for rescue and replication from proviral plasmids and packaging of the recombinant genomic during vector production.[205, 233, 234] Instead, the therapeutic cassette which, depending on the specific application, commonly includes the gene of interest and various regulatory genes such as promoter-enhancers and polyadenylation signals, may be cloned in its place. By removing the wild-type genome, the packaging capacity is maximised, and reduces the immunogenicity and cytotoxicity.[205] The capacity of an AAV vector is approximately 4.5 kb.[235]

While AAV is less immunogenic than adenovirus, neutralising antibodies will develop. As current immunomodulatory technology stands, rAAV treatment can currently only be administered once as subsequent development of neutralising antibodies renders further doses ineffective; pre-existing naturally acquired wild-type AAV antibodies also preclude treatment.[236, 237] Some of the strategies undergoing investigation to permit immune tolerance include immune suppressive agents,[238] engineering antibody resistance in capsids,[239] and AAV-specific plasmaphoresis.[240] Capsid engineering is thought to have the most promise in addressing this fundamental challenge.[241]

A crucial advantage of rAAV over other vector types is that the rAAV2 genome can be cross-packaged into the capsid (protein shell) of numerous types of AAV, known as pseudo-serotyping. The capsid serotype determines the type of cells the vector enters and the efficiency with which the genetic material is delivered (efficiency of transduction).[242, 243] With appropriate capsid selection, parenteral administration of targeted treatment is

possible. Specific tissues may be targeted by naturally occurring AAV serotypes or AAV capsids that have been optimised.[243] AAV capsids may be altered to change tissue tropism and allow transduction of cells that would not normally be targeted by AAV. Capsid development utilises both discovery of naturally occurring novel AAV in both humans and animals and by engineering novel capsids through structure-guided design or directed evolution.[205] A limitation of AAV capsids in non-human species is that they may have less efficient transduction in human cells and this can only be established empirically.[205, 244] Directed evolution is a method to create new AAV vectors which overcomes insufficient knowledge of AAV molecular mechanisms.[245] This utilises procedures such as multiple rounds of selection *in vitro* (recovering capsids from tissue of interest and then readministering), generating novel variants through error-prone PCR, by generation of chimeric capsids at random (capsid shuffling) or a combination of these methods.[205, 246-248] However, there are species differences in the response to AAV serotypes which have implications for preclinical experimental design. Specific tissue tropism and efficiency of cellular transduction in one species do not reliably predict the same tropism and efficiency in another species.[244, 248] Immunological responses to various AAV serotypes may differ between different animal models and between animal models and humans.[249-251] Furthermore, dose calculations based on animal models may not be appropriate for humans.[252] As a result of species differences, animal models may not be the most reliable way to explore capsid tropism and AAV action. In preclinical disease modelling it may, therefore, be necessary to explore experimental AAV therapeutics either in animal models that have been engrafted with human cells[248] or through the utilisation of donated human tissue and organs, otherwise unsuitable for transplantation, maintained on perfusion circuits *ex situ*.[253]

To produce recombinant AAV vectors, multiple plasmids are required: the gene of interest/transgene between two ITRs *in cis* (that is, on the same plasmid); the *rep* and *cap* sequences without the ITRs supplied *in trans* (separate plasmid), and a helper virus, such as adenovirus in *trans* (Figure 1-9).[208, 234, 254, 255] These are used to transduce cell cultures which then produce the packaged recombinant AAV vector containing the gene of interest. To utilise genome editing technology that supplies a donor template and the tissue specificity of modified AAV capsids, two vectors are required: one, encoding the gene of interest packaged in the capsid of choice, and a second vector usually with the same capsid carrying user-defined programmable nuclease technology. The small packaging capacity of AAV means that when using a large gene of interest, these are unable to be packaged in the same unit. By administration of a vector containing the editing machinery and another vector containing the gene of interest, each packaged in capsids with specific tissue tropism, gene editing can be administered in a highly targeted fashion.

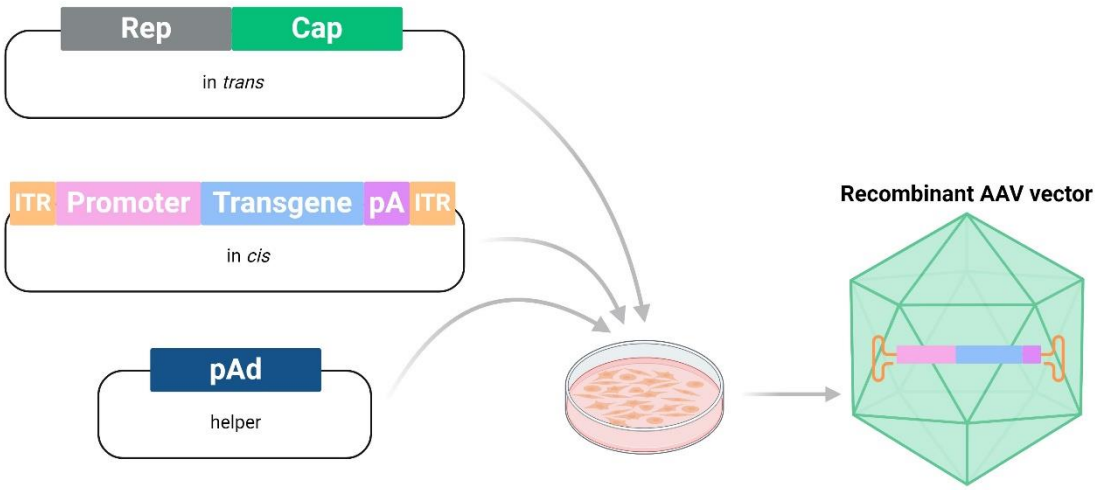

Figure 1-9 Producing rAAV vectors.
To produce a recombinant AAV vector, the transgene is provided in *cis* and the Rep and Cap genes are supplied in *trans*. A helper virus is required, as the plasmids are replication incompetent. Abbreviations: ITR, inverted terminal repeats; pA, polyadenylation tail; pAd, adenovirus plasmid; AAV, adeno-associated virus.

One caveat with the use of rAAV is that the vector genomes are predominantly extra-chromosomal (episomal) and are lost in actively dividing cells such as during paediatric organ growth or in organs with rapid cellular turnover throughout life.[219, 256] This may be overcome by stable, precise integration of genetic change into the host genome at a specific locus by the utilisation of genome editing techniques.

1.5.3 Genomic editing

Much of the early work in gene therapy utilised viral vectors for gene transfer. A limitation of gene addition using rAAV is that generally the transgene is not predictably or efficiently integrated into the host cell's genome in its entirety and may be lost at the time of cellular replication.[219] This is particularly important in the paediatric population where rapid growth through cell division is taking place,[257] but cells of many organs continually turnover during the human life span, such as in the adrenal cortex. Genomic editing offers the potential to repair a native locus, retaining physiological gene expression with minimal risk of mutagenesis as the native endogenous enhancer-promoter elements are utilised. Various technological platforms based on programmable nucleases have been employed in order to enable loci-specific genomic editing including meganucleases, zinc-finger nucleases, and transcription activator-like effector nucleases.[258, 259] These strategies have largely been superseded by the clustered regularly interspaced short palindromic repeat-associated nuclease Cas (CRISPR/Cas). CRISPR/Cas9 is a bacterial defence system and was found to be capable of being manipulated to target a DNA site of interest using short RNA guide sequences, a process which is far simpler than its predecessors in gene editing technologies.[260, 261] Genome editing approaches are poised to supplant gene addition approaches with rapid progress

in CRISPR/Cas9-based gene editing technology.[203] With gene editing strategies, the transgene is stably integrated into the host genome and will be passed on to daughter cells following cellular replication.

1.5.3.1 CRISPR/Cas9

The CRISPR/Cas system and its potential in programmable genome editing was described by Doudna and Charpentier in 2012[261] resulting in a Nobel Prize for the authors in 2020.[262] The CRISPR/Cas system facilitates RNA-guided double-stranded DNA cleavage with Cas proteins and originates as an immune defence mechanism for bacteria against viruses and plasmids.[261, 263, 264] Shortly after its potential in genome editing was considered, the CRISPR/Cas ability to facilitate genome engineering in mammalian cells was demonstrated.[265] Target recognition of the Cas9 protein requires the guide RNA and upstream protospacer-adjacent motif (PAM).[260] The RNA guide strand pairs with the homologous site in the host genome, unzipping the nucleotides and allowing Cas9 to cut the DNA. When exploited for genome editing, the double stranded DNA cleavage occurs simultaneously in the host genome and the donor DNA template, creating blunt ends for repair.[266] To repair the native locus, a DNA repair template is provided and is used by the host's DNA repair mechanisms to repair the cut site and simultaneously introduce a site-specific modification into the host genome.[267] CRISPR/Cas9 has the advantages of ease of customisation, high targeting efficiency and may be used to target multiple sites simultaneously.[265]

1.5.3.2 DNA repair mechanisms

By inducing targeted DNA double-strand breaks (DSBs), pre-existing cellular DNA repair pathways are activated which repair the break and at the same time integrate site-

specific modification into the host genome.[267] DNA repair mechanisms include non-homologous end joining (NHEJ) or homology-directed repair (HDR) where the donor template has homology to the target site (Figure 1-10).[265, 268, 269] Ligation of DNA ends through NHEJ is error-prone and may cause small insertions or deletions (indels) at the break site which can be exploited to disrupt pathogenic sequences.[270] In the absence of a donor template, NHEJ can be used to introduce indels which disrupt the function of a gene resulting in gene silencing. HDR can be used to repair a pathogenic variant at either the endogenous locus or another region of the genome that is considered safe from insertional mutagenesis or disruption of resident gene function.[271] HDR repair is limited to actively dividing cells.[272]

HDR requires a unique set of reagents for each group of variants and risks eliminating residual function in a hypomorphic allele as not all double stranded DNA breaks will undergo repair.[271, 272] Homology-independent targeted integration (HITI) overcomes the limitations of HDR limitation by using NHEJ and allows robust DNA modification in both dividing and non-dividing cells (Figure 1-11).[273]

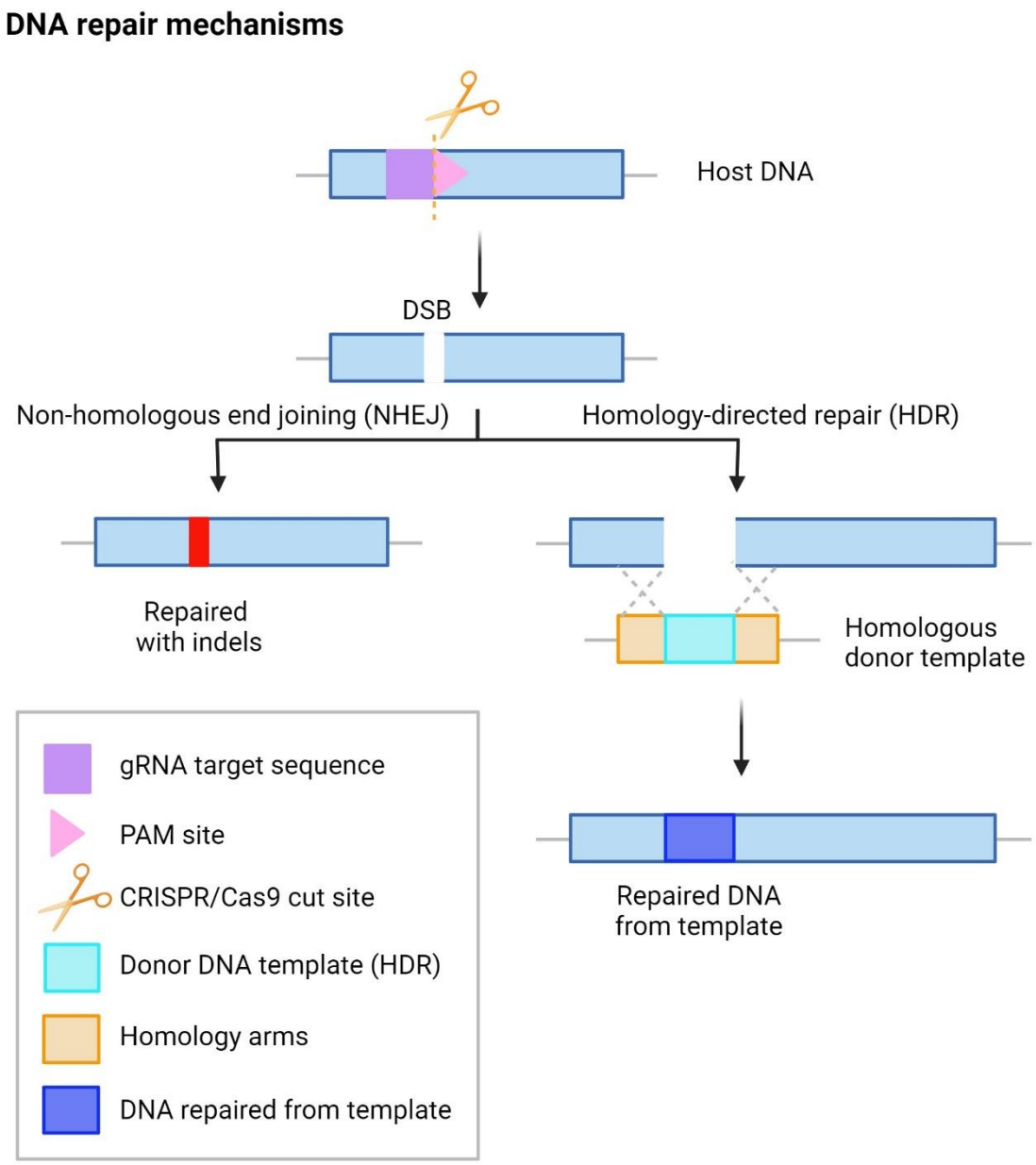

Figure 1-10 DNA repair mechanisms.
CRISPR/Cas9 introduces a double stranded break in DNA at a protospacer adjacent motif (PAM) site and is directed there using guide RNA. Repairing the cut with non-homologous end-joining (NHEJ) is error prone and can result in small insertions and deletions (indels). Homology-directed repair (HDR) is more reliable as the cut site is repairs using a template with homology arms, however it is limited to actively dividing cells, risks knocking down a hypomorphic allele if repair does not occur and a separate set of reagents is required for each group of variants. Figure adapted from Ginn et al 2021[274] and reproduced from Graves et al 2023.[275]

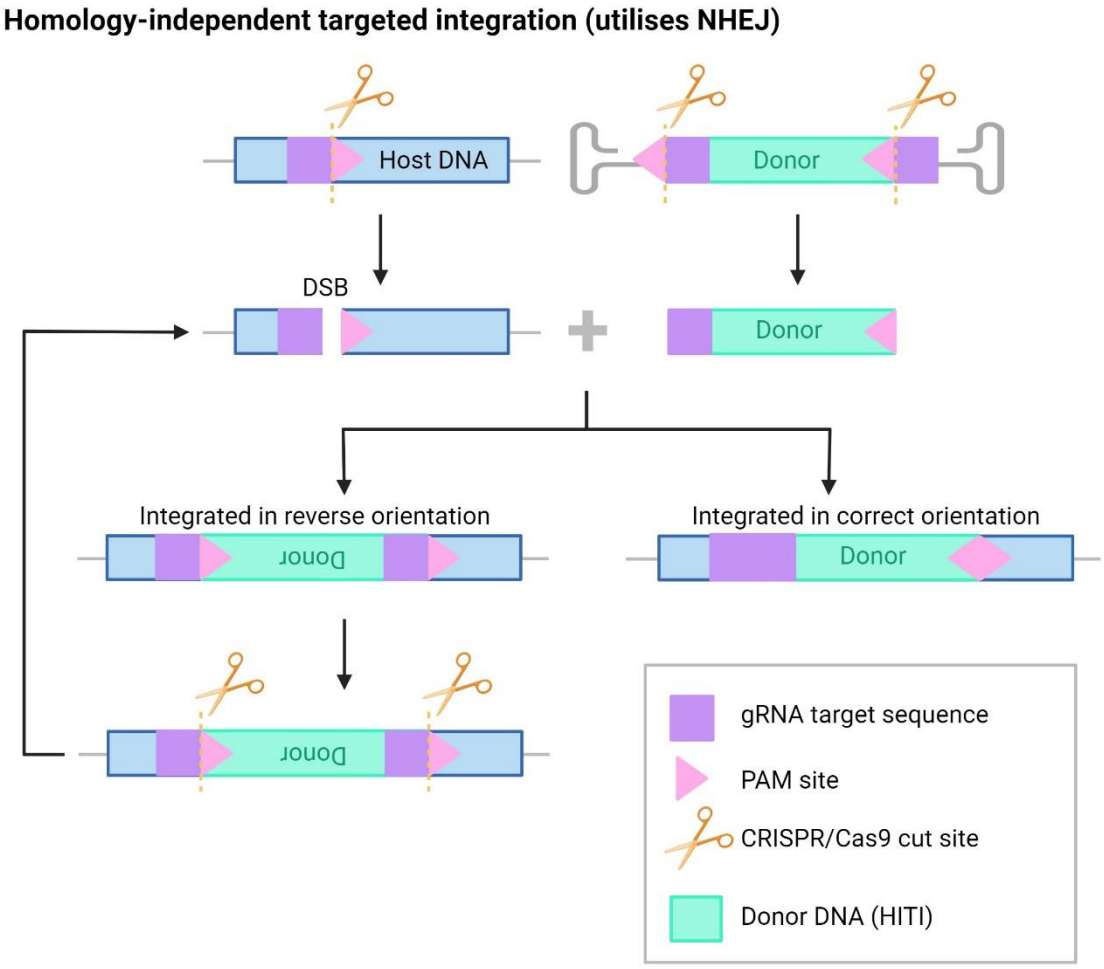

Figure 1-11 Homology-independent targeted integration (utilises NHEJ).
Homology-independent targeted integration (HITI) is not limited to the cell cycle as it utilises NHEJ, and the entire wild-type cDNA can be integrated under a native promoter, refunctioning the locus with a single cassette. The donor sequence is integrated into the host DNA at the cut site. If the donor sequence is integrated in the reverse orientation, the guide sequence and PAM sites realign, and further double stranded breaks occur until the template is integrated in the correct orientation. Figure adapted from Ginn et al 2021[274] and reproduced from Graves et al 2023.[275]

Guide RNA within the CRISPR/Cas9 complex ensures the host DNA is precisely cleaved between the guide sequence and the PAM site. Similarly, CRISPR/Cas9 creates DSB in the donor DNA. Using NHEJ, the donor sequence is the integrated into the host DNA, between the guide sequence and the PAM site. If the donor sequence is integrated in the reverse orientation, the guide sequence and PAM sites re-align, and CRISPR/Cas9 will cleave the donor sequence out again. If the donor sequence is integrated in the correct position, the guide sequence and PAM sites do not align, and no further cuts occur.[266] NHEJ is the major repair pathway in mammalian cells and therefore editing using this technique will occur at a relatively high frequency.[270] However, this may be limited by the formation of undesirable indels. HDR strategies are precise however they are reliant on the target cell undergoing mitosis and occurs at lower frequencies.

Other editing strategies include single homology arm donor mediated intron-targeting integration (SATI) which is a combination of HDR and NHEJ,[276] precise integration into target chromosome (PITCh) which can be used in non-dividing cells using micro-homology-mediated end-joining.[277, 278] The efficiency of an editing technique is dependent on the DNA repair process used. Editing techniques which do not induce a break in the DNA include base editing which introduces precise point mutations[279] and prime editing which allows targeted insertion, deletion or replacement of a single nucleotide through the delivery of RNA reagents, without the need for a repair template.[280] However, these strategies are not generalisable to all causative mutations in CAH.

By utilising robust editing technology with efficient DNA repair in the right target cell, a durable therapeutic effect may be expected.

1.6 Gene therapy and the adrenal cortex

1.6.1 Gene therapy studies for CAH to date

Gene therapy for CAH is conceptually appealing, however there is a paucity of adrenocortical gene therapy studies (Table 1-4). All studies thus far have utilised a gene addition strategy, and none has proven durability beyond the adrenocortical cellular turnover period.

Table 1-4 Published adrenocortical gene therapy studies to date.

Year	Species	Vector and delivery	Outcome – phenotype	Outcome – molecular
1999 [281]	Mouse	Adenovirus with human *CYP21A2* cDNA Intra-adrenal	Improvement in adrenal cortex ultrastructure 7 days after treatment. Plasma corticosterone increased to wild-type levels by days 7-14, but declining over next 40 days.	Highest mRNA expression day 2-7 then gradual decline. *In vitro* 21-hydroxylase activity in adrenals harvested from treated mice increased from undetectable to levels found in wild-type mice 2-7 days after treatment.
2016 [282]	Mouse	Retrovirus with murine *Cyp21a1* cDNA Tail fibroblasts transduced *in vitro* and then implanted subcutaneously	Statistically insignificant reduction of serum progesterone/deoxycorticosterone ratio at 4 weeks in 4/6 mice (increase in 2/6) 4 weeks after treatment	
2016 [282]	Mouse	AAV2 with murine *Cyp21a1* cDNA intramuscular	Statistically insignificant reduction in serum progesterone/deoxycorticosterone ratio at 4 weeks after treatment. Single mouse monitored to 7 months where serum progesterone/deoxycorticosterone remained low.	*Cyp21a1* weak expression in thigh muscle, heart and liver.
2017 [283]	Mouse	AAVrh10 with human *CYP21A2* cDNA intravenous	Increased body mass after treatment. Reduced urine progesterone by 5 weeks, for at least 15 weeks.	*CYP21A2* expression detected in adrenals and weakly in heart. Improved expression of *renin, Mc2r, Prkar2a, Sf1, Star, Cyp17a1* and *Cyp11b2* genes.

2018 [284]	Mouse	AAVrh10 with human *CYP21A2* cDNA Intravenous	Serum progesterone and ACTH normalised to wild-type levels from 2-8 weeks, and then increased to pre-injection levels by 32 weeks.	*CYP21A2* expression was highest at 2 weeks then waned over time to 32 weeks. Liver had substantial *CYP21A2* expression at 32 weeks. *CYP21A2* expression also waned over a similar time period in immunodeficient mice, indicating loss of transgene was not due to immune responses to the vector/transgene.
2022 [285]	Mouse	AAV9 with human *CYP11B1* cDNA Intra-adrenal	Statistically significant improvement but not normalisation in serum deoxycorticosterone-to-corticosterone ratio, 4 weeks after treatment. Two mice were monitored to 4 and 5 months post-treatment with persistence of effect, although the ratio started to increase again from 2 months post-treatment.	*Cyp11a1* expression in the adrenal was increased in the vector treated *Cyp11b1* knockout mice compared to wild-type. Even with vector treatment, *Cyp11b1* expression in the adrenal was markedly lower than wild-type.

Studies published 1999-2018 used the same 21-hydroxylase deficient mouse model C57BL/10SnSlc-H-2aw18, which develops elevated progesterone rather than 17OHP as the murine adrenal lacks *Cyp17a1* expression [286]. The 2022 study created a mouse model for 11-beta hydroxylase deficiency by knocking down *Cyp11b1* function using CRISPR/Cas9, which developed elevated deoxycorticosterone [285]. The 21-hydroxylase gene is expressed as *CYP21A2* for human origin, *Cyp21a1* for murine. The 11 beta hydroxylase gene is expressed as *CYP11B1* for human and *Cyp11b1* for murine. Reproduced from Graves et al, 2023.[25]

1.6.1.1 Murine studies

The 21-hydroxylase deficient mouse model (C57BL/10SnSlc-H-2<aw18>; *Cyp21a1*$^{-/-}$) used in pre-clinical adrenocortical gene therapy studies, has elevated progesterone levels rather than 17-hydroxyprogesterone, due to lack of 17-hydroxylase expression in the murine adrenal.[286, 287] The first attempt at gene therapy for CAH was in 1999 where an adenovirus vector containing human *CYP21A2* was directly injected into the adrenal glands of *Cyp21a1*$^{-/-}$ mice and resulted in improvement in adrenal morphology and increased plasma corticosterone. The effect was brief, and corticosterone concentrations declined over 40 days.[281] Wild-type adenovirus infection and adenoviral-mediated gene transfer may interfere with adrenocortical function as adenoviral vectors are more pro-inflammatory than rAAV, with vigorous stimulation of the innate immune response.[288] Furthermore, intra-adrenal injections are invasive, with a high mortality rate in the mouse model,[289] and less invasive parenteral injection is desirable.

Transduction of adrenocortical cells using a systemic intravenous injection of human *CYP21A2* packaged in an AAVrh10 capsid in male and female *Cyp21a1*$^{-/-}$ mice reduced urine progesterone for at least 15 weeks, and improved the expression of *Mc2r*, *Sf1*, *Star*, *Cyp17a1* and *Cyp11b2* in the adrenal and *Ren1* in the kidney.[283] Despite very low vector genome copies (vgc), a measurement of vector-derived DNA in the host tissue, in the mouse adrenals at 15 weeks (0.13 +/- 0.09 vgc per cell), the therapeutic effect was still present.[283] A subsequent rAAV gene therapy study used female mice alone, which have a more rapid adrenocortical cellular turnover than males.[27] It was demonstrated that the effect from intravenous administration of their AAVRh10-*CYP21A2* vector on serum progesterone was transient, lasting only 8 weeks.[284] Perhaps the durability of effect seen in some studies is due to the use of male animal subjects with slower adrenocortical

turnover or transduction of stable cells outside of the adrenal cortex. The use of a ubiquitous promoter means that it is plausible that the transgene could be expressed by any cell that is transduced including in extra-adrenal sites, such as liver and muscle, hence it is difficult to ascertain if the study results were exclusively due to adrenal 21-hydroxylase expression.

One way to overcome rapid adrenocortical cellular turnover is the use of stable extra-adrenal tissue to gain 21-hydroxylation function.[290] Two strategies have been tested using *Cyp21a1*$^{-/-}$ mice: the first strategy was to auto-transplant primary tail fibroblasts transduced *in vitro* with an AAV2 vector containing murine *Cyp21a1* into subcutaneous tissue, and the second strategy was to inject rAAV2-*Cyp21a1* vector directly into thigh muscle. Due to small numbers of mice used, neither strategy produced statistically significant results, however in both, there was a trend to reduced progesterone levels during the 4-week study period, indicating extra-adrenal 21-hydroxylation may be possible.[282] A single mouse was studied for 7 months and there was a durable effect after intramuscular vector administration.[282] Although the vector was injected intramuscularly, vector DNA was detected in liver and cardiac muscle indicating that the extra-adrenal 21-hydroxylation may not have been from the thigh muscles alone. Despite initial indicators of success with ectopic expression, in a later study by the same group, they moved away from intramuscular administration. A mouse model for 11-beta hydroxylase deficiency was created using CRISPR/Cas9 to knock down *Cyp11b1* function, and these mice were subsequently treated with unilateral intra-adrenal injection of a rAAV vector containing human *CYP11B1* with a ubiquitous promoter packaged in either AAV2 or AAV9.[285] Statistically significant reduction in the serum deoxycorticosterone-to-corticosterone was achieved using the AAV9 capsid serotype from 4 weeks post treatment (n=4) and

persisted up to 5 months after treatment (n=1). There was no effect using the AAV2 serotype.[285] Why AAV9 and AAV2 serotypes were chosen is unclear, as the AAVRh10 serotype transduces adrenocortical cells more efficiently than AAV9.[284] Moreover, the applicability to the human clinical context is unclear, as an invasive delivery strategy which is undesirable was used despite previous studies showing effective delivery of vector to the adrenal using intravenous administration.[283, 284]

There have also been early gene therapy studies aiming to introduce expression of suicide genes in adrenocortical tumours. Using a herpes simplex virus vector, a *CYP11B1* promoter was found to be specific in targeting adrenal tissue,[291] although *CYP11B1* is only expressed in the zona fasciculata and not in the zona glomerulosa.

While in the following study the adrenal was not the target organ, adrenal cell genomes have previously been shown to have been edited. Adrenoleukodystrophy is a genetic condition due to a mutation in the *ABCD1* gene which results in multi-organ pathology. A pre-clinical genomic editing study used rAAV9 to deliver editing machinery in a mouse model for adrenoleukodystrophy at a dose of 1×10^{12} vg/mouse (total vector which included both the CRISPR/Cas9 vector and the donor vector, but the ratio of each vector was not described). Serotype rAAV9 was chosen for the ability to transduce both the central nervous system and the liver. AAV9-CRISPR/Cas9 delivered systemically resulted in 7% indels in the liver and 1% indels in the adrenal gland, but indels were not detected in other organs. The HITI cassette was detectably integrated in the adrenal gland. Using two rAAV9 vectors to deliver CRISPR/Cas9 and a HITI repair cassette systemically, the *ABCD1* gene was edited in both the liver and adrenal.[292] While this study

is the first to demonstrate *in vivo* editing of the murine adrenal, adrenal editing was not its main goal and the study did not account for the adrenocortical turnover.

1.6.1.2 Non-human primate studies

While there are no published studies using non-human primates (NHP) for adrenocortical gene therapy, preliminary data have been presented at scientific meetings. To determine the most effective rAAV capsid serotype for gene delivery, NHP were administered *CYP21A2* cDNA packaged in either AAV1, AAV5 or AAV6, and these were given intra-adrenally or intravenously (International Patent no. WO 2019/143803 A1).[293] *CYP21A2* cDNA packaged in capsid serotype AAV5 resulted in the highest vector presence (determined by vgc) in the adrenals from both administration methods, and subsequent studies used this capsid serotype. Why these three specific serotypes were initially chosen is unclear, as capsid technology has evolved such that unique capsid serotypes have been developed that can target relatively specific cell populations with high tropism and there are now innumerable capsids available with the rapid expansion of the capsid engineering field.[294-296] NHP (21-hydroxylase sufficient) received rAAV5-*CYP21A2* with a ubiquitous promoter.[297] Vector DNA in the adrenal tissue waned over time. Two animals were studied to 24 weeks, one male and one female. While the sex of these animals was not specified, one had a low vector copy count at 24 weeks (3vgc/cell) and one had a relatively higher count (13vgc/cell). There was more vector DNA and higher transgene expression in the liver than the adrenal, which is expected when using rAAV5 with a ubiquitous promoter, as most AAV serotypes target hepatocytes. The adult liver is a relatively stable organ and episomal gene therapy will persist, unlike the growing paediatric liver.[257, 298, 299]

1.6.1.3 Human clinical trial

A phase I/II human clinical trial is now underway where adult patients with 21-hydroxylase deficiency are administered an intravenous infusion of a rAAV5-*CYP21A2* with a ubiquitous promoter (NCT04783181). The first human subject was treated in early 2022 and by January 2024 a total of seven adults had been treated, with one treated subject reportedly improving their serum cortisol from 105 nmol/L to 235 nmol/L.[300] Results of this study are not yet available. While it is expected that this rAAV therapy will have some effect, the duration of effect is uncertain, and there is some hesitancy regarding the potential prematurity of this trial.[143] If a durable effect is seen, it could be related to extra-adrenal transduction and expression of 21-hydroxylase, and it will be difficult to ascertain the source of 21-hydroxylation in human subjects.

1.6.2 Adrenocortical biology hinders standard AAV-based gene therapy

Thus far, no adrenocortical targeting gene therapy has shown durability of effect beyond the cellular turnover period. Episomal gene therapy used in the adrenal cortex will be transient due to the adrenocortical cellular turnover as the vector DNA will not replicate during cell division. Furthermore, differentiated adrenocortical cells apoptose without significant cellular replication and thus even the *CYP21A2* locus was directly repaired in differentiated cells this would only provide a transient effect. To overcome this, the genome of the adrenal progenitor cells must be repaired, to ensure daughter cells maintain the correction. CRISPR/Cas is one technological platform that could achieve this.[260, 265] There are several editing techniques with various applications including homology directed repair (HDR),[271] homology-independent targeted integration (HITI),[273] single homology arm donor mediated intro-targeting integration (SATI),[266] precise integration

into target chromosome (PITCh),[278, 301] and non-CRISPR based strategies including base editing[302] and prime editing.[280] The major limitation is that the progenitor cells have not yet been adequately defined and without accurate methods to identify these cell populations it is difficult to establish which rAAV serotypes (if any) can deliver editing machinery to adrenal progenitor cells with any certainty.

The 21-hydroxylase pseudogene (*CYP21A1P* in the human and *Cyp21a2-ps* in the mouse) creates an added complication due to high homology with the active gene, with 98% exonic and 96% intronic homology.[73] As a result, the target protospacer adjacent motif (PAM) sequence chosen as the cut site in a CRISPR/Cas strategy must not also cause a double stranded break in the pseudogene. As the *CYP21A2* gene at 6p21.3 is within 30 kb of *CYP21A1P*,[136] a cut in both sites could induce a large deletion and/or genomic rearrangements. Therefore, potential PAM sites are limited to those that are unique to *CYP21A2*. There are over 300 known variants in *CYP21A2* listed in the Human Gene Mutation Database (HGMD, http://www.hgmd.cf.ac.uk) spanning all 10 exons. Therefore, the editing strategy chosen is important: HDR is limited to actively dividing cells, has relatively low editing efficiency and requires a unique set of reagents for each group of variants.[271, 272] Furthermore, not all double stranded breaks induced will undergo repair and risks eliminating any residual function of a hypomorphic allele if the strand break is exonic. These limitations can be overcome by using the HITI strategy which is dependent on DNA repair by NHEJ.[273] The *CYP21A2* open reading frame is approximately 1.5 kb,[89] compatible with packaging into the rAAV genome backbone which has a capacity of 4.7 kb. With HITI, a strategy could be developed whereby a double stranded DNA break is induced deep in a non-coding sequence such as an intron and the entire wild-type *CYP21A2* open reading frame is integrated downstream of the

endogenous *CYP21A2* promoter, treating all pathogenic variants that occur distal to the insertion site. Alternatively, mutations upstream of the insertion site could also be treated by introducing termination of the upstream cistron and expressing the entire wild-type *CYP21A2* cDNA for example from a downstream cistron using an internal ribosome entry site.

Although the adrenal cortex shares properties such as high relative blood flow and fenestrated vascular endothelium with the liver that make it highly amenable to gene delivery,[6, 7, 303] the predilection of rAAV to transduce hepatocytes is a challenge in adrenal-targeting gene therapy. Without liver de-targeting, much higher doses of vector may be required to ensure adequate amounts reach the adrenal cortex. This entails a greater risk of AAV-associated adverse events such as liver toxicity,[222, 223] thrombotic microangiopathy[224] and dorsal root ganglion toxicity[221].

AAV vectors used in parenterally administered adrenocortical gene therapy have used the capsids AAVrh10[283, 284] and AAV9[284] in mice, AAV5 and AAV8 in rats,[304] and AAV5 in cynomolgus monkeys.[297] However, none of these studies has proven tropism for the adrenocortical progenitor cells through either anatomical demonstration of transduction of the capsule or subcapsular zona glomerulosa, or integration into the progenitor cell genome through durability of effect beyond adrenocortical cell renewal. While lentiviral vector systems may have the capacity for stable integration in adrenocortical stem/progenitor cells, this system is limited by the need to administer the therapy directly to the adrenal cortex through a surgical procedure (with 88% fatality when attempted in a mouse model[289]) as systemic delivery results in a generalised cellular transduction, increasing the risk of off target effects. Thus, AAV is the delivery system of choice as

administration can be parenteral while delivering cellular specificity. Identification of the progenitor population, however, is required for further technological development in this area. Furthermore, the liver sequesters a substantial fraction of systemically delivered vector which is a challenge in adrenal-targeting gene therapy. Liver de-targeting is required to allow lower doses of vector to be used and still ensure adequate amounts reach the adrenal cortex. If high doses are required, there is a greater risk of adverse events such as liver toxicity,[222, 223] thrombotic microangiopathy[224] and dorsal root ganglion toxicity.[221]

1.7 Adrenal cortex single cell transcriptome

Single cell RNA sequencing is a relatively new technology that allows individual cell transcriptomic pattern detection in a dissociated tissue sample. This technology provides new insights into the complexity of biological tissues by the identification and characterisation of RNA expression at a single cell resolution. It can be used to identify heterogeneity between single cells in the same tissue and isolate rare cell populations.[305] A small number of studies have examined the single cell transcriptomic pattern in the murine or human adrenal cortex[306-310] and more have examined the medullary compartment. This technology may be applied to identification of subpopulations within a single tissue. During a study examining the transcriptional effect of chronic stress exposure on the hypothalamic-pituitary-adrenal axis, a new subpopulation of adrenocortical cells involved in stress response were found that expressed *Abcb1b*+.[306] Following chronic stress, the adrenal glands became larger and underwent distinct cellular population changes including increased zona fasciculata cells and decreased zona glomerulosa cells.[306] The zona fasciculata cells are responsible for corticosterone production in the mouse, the major glucocorticoid involved in the stress response.

Furthermore, after exposure to chronic stress, a large number of genes were down regulated in the adrenal, whereas chronic stress induced gene upregulation in the hypothalamus and pituitary.[306] The subpopulation of expanded zona fasciculata cells expressed *Abcb1b*, *Sbsn* and *Srd5a2*. In humans, ABCB1 is also upregulated in Cushing syndrome adrenal samples.[306]

It is important to note that there are sex differences in the adrenal cortex and this was demonstrated with increased expression of *IGKC, IGHG4 IGLC2*, and *IGHG1* in a human female adrenal sample compared with the male.[307] This group also found variations in gene expression between left and right human adrenals with the right side having higher CYP11B2 expression compared to the left, indicating a possible variation in aldosterone production between the glands.[307]

Single cell transcriptomic analysis has been applied to the developing adrenal gland, and while the primordial cortex was identified and analysed at different pre-natal timepoints, the focus of the study was on the developing adrenal medulla.[308]

A subpopulation of cells expressing *RSPO3, COL1A2, NR2F2* and *ID1* were identified to be located within and just deep to the adrenal capsule.[309] *RSPO3* and *COL1A2* are markers for the adrenal capsule. *NR2F2* is expressed by adrenal capsular cells as well as stromal, endothelial and smooth muscle cells.[27, 311] The same cells also expressed *ID1*[309] which is a known marker of various mesenchymal stem cells.[312] This cluster is postulated to include capsular adrenocortical stem cells which have not previously been identified in single cell RNA sequencing. While *Nr2f2* expression has been demonstrated in the

murine adrenal capsular cells,[27] this is the first time NR2F2+ stem cells have been identified in adult human adrenal glands.[309]

The elusive progenitor cell population has not yet been reliably identified by any method. However, some gene expression pattern is known: these cells express *SHH, NR5A1* and *CTNNB1*.[23] Single cell transcriptomic analysis could be a potential methodology that allows the identification of this cell population. By combining this technology with high-throughput barcoded rAAV capsid libraries, rAAV capsid serotypes that transduce specific cell populations could be identified.[313]

1.8 Conclusion

CAH is a potentially devastating disease, and current therapies are inadequate. Genome therapy has the potential to provide a robust curative treatment for CAH, although current limits in knowledge of the adrenal progenitor cell system preclude its use as a durable treatment. There are no published attempts to target the adrenocortical stem or progenitor population in genetic therapy for monogenic adrenal disorders, nor have genome editing strategies been attempted in the adrenal cortex.

By using robust gene editing machinery with CRISPR/Cas9 and exploiting AAV capsid technology with specificity to target adrenal progenitor cells, it may be possible to integrate the transgene stably into the genome of the adrenocortical progenitor cells, providing permanent correction of P450c21 function, and other monogenic adrenal cortex disorders. A future dominated by genome therapy is within sight and it is imperative that endocrinologists gain a deep understanding of this technology to further exploit its full potential.

1.9 Hypothesis and Aims

Hypothesis 1: That the limitations imposed by adrenocortical cellular turnover can be overcome by an AAV-based gene therapy that delivers adrenocortical enzyme DNA to a population of cells external to the adrenal gland. As, in the presence of 21-hydroxylase deficiency, the steroid precursor (progesterone in mice, 17OHP in humans) is elevated in the systemic circulation, such that it will be available to all organs.

Aim 1: To develop a gene therapy approach to treat congenital adrenal hyperplasia which overcomes the intrinsic limitations of the adrenal cortical cellular turnover by delivering adrenocortical gene expression extra-adrenally.

Hypothesis 2: That rAAV with tropism for the adrenal cortex is discoverable from the large repository of rAAV capsids that have been identified or engineered, and that adrenocortical progenitor cells can be identified on single cell RNA sequencing using the expression pattern Nr5a1+, Shh+, Ctnnb1+, Cyp11b2-, Cyp11b1- when cells with a low number of expressed genes are not excluded from analysis.

Aim 2: To develop a strategy to determine capsid tropism for the adrenal cortex.

Part A. To determine the optimal rAAV capsid serotype from a defined set of known serotypes for gene delivery to the adrenal gland.

Part B. To compare the single cell transcriptome of wild-type and 21-hydroxylase deficient mouse adrenal glands and to identify potential progenitor cell populations.

Hypothesis 3: That the adrenal cortex is amenable to rAAV-mediated delivery of editing machinery in order to correct the mutant *Cyp21a1* locus due to its high blood flow relative to organ size[6] and fenestrated endothelium[7]. While this technique would likely be transient unless the capsid was able to transduce the progenitors in addition to the differentiated cells, it could potentially demonstrate one strategy to edit the adrenal cortex which could then be re-packaged into an appropriate capsid once discovered.

Aim 3: To stably integrate new genetic material into the 21-hydroxylase locus in 21-hydroxylase deficient mice using a homology-independent-targeted integration genomic editing strategy.

This thesis sets the foundation for overcoming the biological properties of the adrenal cortex that renders standard rAAV gene therapy for CAH unsuitable, through delivering adrenocortical genes to a stable organ outside the adrenal, developing strategies to determine capsid tropism for the adrenocortical cells and successfully editing the *Cyp21a1* locus with biological effect.

1.10 References

1. Miller WL and White PC. History of Adrenal Research: From Ancient Anatomy to Contemporary Molecular Biology. *Endocr Rev* 2023; 44: 70-116. 2022/08/11. DOI: 10.1210/endrev/bnac019.
2. Cuvier G. *Lecons d'Anatomie Comparée, Tome III*. Paris: Recueillies et Publiés par L Duvernoy, 1805.
3. Nagel N. Über die Struktur der Nebennieren. *Arch Anat Phys Wiss Med* 1836: 365-383.
4. Addison T. On the constitutional and local effects of disease of the supura-renal capsules. *Highley, London* 1855.
5. Miller WL. The Adrenal Cortex and its Disorders. *Brook's Clinical Pediatric Endocrinology*. 2009, pp.283-326.
6. Sapirstein LA and Goldman H. Adrenal blood flow in the albino rat. *Am J Physiol* 1959; 196: 159-162. 1959/01/01. DOI: 10.1152/ajplegacy.1958.196.1.159.
7. Ryan US, Ryan JW, Smith DS, et al. Fenestrated endothelium of the adrenal gland: freeze-fracture studies. *Tissue Cell* 1975; 7: 181-190. 1975/01/01. DOI: 10.1016/s0040-8166(75)80015-2.
8. Gruenwald P. Embryonic and postnatal development of the adrenal cortex, particularly the zona glomerulosa and accessory nodules. *Anat Rec* 1946; 95: 391-421. 1946/08/01. DOI: 10.1002/ar.1090950404.
9. Hanley NA, Hagan DM, Clement-Jones M, et al. SRY, SOX9, and DAX1 expression patterns during human sex determination and gonadal development. *Mech Dev* 2000; 91: 403-407. 2000/03/08. DOI: 10.1016/s0925-4773(99)00307-x.
10. Zubair M, Parker KL and Morohashi K. Developmental links between the fetal and adult zones of the adrenal cortex revealed by lineage tracing. *Mol Cell Biol* 2008; 28: 7030-7040. 2008/09/24. DOI: 10.1128/MCB.00900-08.
11. Xing Y, Lerario AM, Rainey W, et al. Development of adrenal cortex zonation. *Endocrinol Metab Clin North Am* 2015; 44: 243-274. 2015/06/04. DOI: 10.1016/j.ecl.2015.02.001.
12. Rosenfield RL. Normal and Premature Adrenarche. *Endocr Rev* 2021; 42: 783-814. 2021/04/01. DOI: 10.1210/endrev/bnab009.
13. van Weerden WM, Bierings HG, van Steenbrugge GJ, et al. Adrenal glands of mouse and rat do not synthesize androgens. *Life Sci* 1992; 50: 857-861. 1992/01/01. DOI: 10.1016/0024-3205(92)90204-3.
14. Le Goascogne C, Sananes N, Gouezou M, et al. Immunoreactive cytochrome P-450(17 alpha) in rat and guinea-pig gonads, adrenal glands and brain. *J Reprod Fertil* 1991; 93: 609-622. 1991/11/01. DOI: 10.1530/jrf.0.0930609.
15. Ingle DJ and Higgins GM. Autotransplantation and Regeneration of the Adrenal Gland. *Endocrinology* 1938; 22: 458-464. DOI: 10.1210/endo-22-4-458.
16. Greep RO and Deane HW. Histological, cytochemical and physiological observations on the regeneration of the rat's adrenal gland following enucleation. *Endocrinology* 1949; 45: 42-56. 1949/07/01. DOI: 10.1210/endo-45-1-42.
17. Zwemer RL, Wotton RM and Norkus MG. A study of corticoadrenal cells. *The Anatomical Record* 1938; 72: 249-263. DOI: 10.1002/ar.1090720210.
18. Chang SP, Morrison HD, Nilsson F, et al. Cell proliferation, movement and differentiation during maintenance of the adult mouse adrenal cortex. *PLoS One* 2013; 8: e81865. 2013/12/11. DOI: 10.1371/journal.pone.0081865.
19. Freedman BD, Kempna PB, Carlone DL, et al. Adrenocortical zonation results from lineage conversion of differentiated zona glomerulosa cells. *Dev Cell* 2013; 26: 666-673. 2013/09/17. DOI: 10.1016/j.devcel.2013.07.016.
20. Bruning JC, Gautam D, Burks DJ, et al. Role of brain insulin receptor in control of body weight and reproduction. *Science* 2000; 289: 2122-2125. 2000/09/23. DOI: 10.1126/science.289.5487.2122.
21. Hammer GD and Basham KJ. Stem cell function and plasticity in the normal physiology of the adrenal cortex. *Mol Cell Endocrinol* 2021; 519: 111043. 2020/10/16. DOI: 10.1016/j.mce.2020.111043.
22. Wood MA, Acharya A, Finco I, et al. Fetal adrenal capsular cells serve as progenitor cells for steroidogenic and stromal adrenocortical cell lineages in M. musculus. *Development* 2013; 140: 4522-4532. 2013/10/18. DOI: 10.1242/dev.092775.
23. Finco I, Mohan DR, Hammer GD, et al. Regulation of stem and progenitor cells in the adrenal cortex. *Curr Opin Endocr Metab Res* 2019; 8: 66-71. 2020/04/08. DOI: 10.1016/j.coemr.2019.07.009.
24. King P, Paul A and Laufer E. Shh signaling regulates adrenocortical development and identifies progenitors of steroidogenic lineages. *Proc Natl Acad Sci U S A* 2009; 106: 21185-21190. 2009/12/04. DOI: 10.1073/pnas.0909471106.

25. Graves LE, Torpy DJ, Coates PT, et al. Future Directions for Adrenal Insufficiency: Cellular Transplantation and Genetic Therapies. *J Clin Endocrinol Metab* 2023; 108: 1273-1289. 2023/01/08. DOI: 10.1210/clinem/dgac751.
26. Walczak EM and Hammer GD. Regulation of the adrenocortical stem cell niche: implications for disease. *Nat Rev Endocrinol* 2015; 11: 14-28. 2014/10/08. DOI: 10.1038/nrendo.2014.166.
27. Grabek A, Dolfi B, Klein B, et al. The Adult Adrenal Cortex Undergoes Rapid Tissue Renewal in a Sex-Specific Manner. *Cell Stem Cell* 2019; 25: 290-296 e292. 2019/05/21. DOI: 10.1016/j.stem.2019.04.012.
28. Mathieu M, Drelon C, Rodriguez S, et al. Steroidogenic differentiation and PKA signaling are programmed by histone methyltransferase EZH2 in the adrenal cortex. *Proc Natl Acad Sci U S A* 2018; 115: E12265-E12274. 2018/12/14. DOI: 10.1073/pnas.1809185115.
29. Steenblock C, Rubin de Celis MF, Delgadillo Silva LF, et al. Isolation and characterization of adrenocortical progenitors involved in the adaptation to stress. *Proc Natl Acad Sci U S A* 2018; 115: 12997-13002. 2018/12/06. DOI: 10.1073/pnas.1814072115.
30. Balyura M, Gelfgat E, Steenblock C, et al. Expression of progenitor markers is associated with the functionality of a bioartificial adrenal cortex. *PLoS One* 2018; 13: e0194643. 2018/03/30. DOI: 10.1371/journal.pone.0194643.
31. Kataoka Y, Ikehara Y and Hattori T. Cell proliferation and renewal of mouse adrenal cortex. *J Anat* 1996; 188 (Pt 2): 375-381. 1996/04/01.
32. Scheys JO, Heaton JH and Hammer GD. Evidence of adrenal failure in aging Dax1-deficient mice. *Endocrinology* 2011; 152: 3430-3439. 2011/07/08. DOI: 10.1210/en.2010-0986.
33. Rowntree LG, Greene CH, Swingle WW, et al. The Treatment of Patients with Addison's Disease with the "Cortical Hormone" of Swingle and Pfiffner. *Science* 1930; 72: 482-483. 1930/11/07. DOI: 10.1126/science.72.1871.482.
34. Steiger M and Reichstein T. Desoxy-cortico-steron (21-Oxy-progesteron) aus Δ5-3-Oxy-ätio-cholensäure. *Helv Chim Acta* 1937; 20: 1164-1179.
35. Kendall EC. *Isolation in Crystalline Form of the Hormone Essential to Life from the Suprarenal Cortex: Its Chemical Nature & Physiologic Properties*. Mayo Foundation, 1934.
36. Schumacher J. [The Nobel prize winners in physiology and medicine, 1901-50]. *Munch Med Wochenschr* 1951; 93: 1149-1154. 1951/06/08.
37. Gwynne JT and Strauss JF, 3rd. The role of lipoproteins in steroidogenesis and cholesterol metabolism in steroidogenic glands. *Endocr Rev* 1982; 3: 299-329. 1982/01/01. DOI: 10.1210/edrv-3-3-299.
38. Miller WL and Auchus RJ. The molecular biology, biochemistry, and physiology of human steroidogenesis and its disorders. *Endocr Rev* 2011; 32: 81-151. 2010/11/06. DOI: 10.1210/er.2010-0013.
39. Brown MS, Kovanen PT and Goldstein JL. Receptor-mediated uptake of lipoprotein-cholesterol and its utilization for steroid synthesis in the adrenal cortex. *Recent Prog Horm Res* 1979; 35: 215-257. 1979/01/01. DOI: 10.1016/b978-0-12-571135-7.50009-6.
40. Beato M, Arnemann J, Chalepakis G, et al. Gene regulation by steroid hormones. *J Steroid Biochem* 1987; 27: 9-14. 1987/01/01. DOI: 10.1016/0022-4731(87)90288-3.
41. Spanjaard RA and Chin WW. Reconstitution of ligand-mediated glucocorticoid receptor activity by trans-acting functional domains. *Mol Endocrinol* 1993; 7: 12-16. 1993/01/01. DOI: 10.1210/mend.7.1.8446102.
42. Brann DW, Hendry LB and Mahesh VB. Emerging diversities in the mechanism of action of steroid hormones. *J Steroid Biochem Mol Biol* 1995; 52: 113-133. 1995/02/01. DOI: 10.1016/0960-0760(94)00160-n.
43. Wilson JD, Auchus RJ, Leihy MW, et al. 5alpha-androstane-3alpha,17beta-diol is formed in tammar wallaby pouch young testes by a pathway involving 5alpha-pregnane-3alpha,17alpha-diol-20-one as a key intermediate. *Endocrinology* 2003; 144: 575-580. 2003/01/23. DOI: 10.1210/en.2002-220721.
44. O'Shaughnessy PJ, Antignac JP, Le Bizec B, et al. Alternative (backdoor) androgen production and masculinization in the human fetus. *PLoS Biol* 2019; 17: e3000002. 2019/02/15. DOI: 10.1371/journal.pbio.3000002.
45. Miller WL and Auchus RJ. The "backdoor pathway" of androgen synthesis in human male sexual development. *PLoS Biol* 2019; 17: e3000198. 2019/04/04. DOI: 10.1371/journal.pbio.3000198.
46. Storbeck KH, Bloem LM, Africander D, et al. 11beta-Hydroxydihydrotestosterone and 11-ketodihydrotestosterone, novel C19 steroids with androgenic activity: a putative role in castration resistant prostate cancer? *Mol Cell Endocrinol* 2013; 377: 135-146. 2013/07/17. DOI: 10.1016/j.mce.2013.07.006.
47. Rege J, Nakamura Y, Satoh F, et al. Liquid chromatography-tandem mass spectrometry analysis of human adrenal vein 19-carbon steroids before and after ACTH stimulation. *J Clin Endocrinol Metab* 2013; 98: 1182-1188. 2013/02/07. DOI: 10.1210/jc.2012-2912.

48. Naamneh Elzenaty R, du Toit T and Fluck CE. Basics of androgen synthesis and action. *Best Pract Res Clin Endocrinol Metab* 2022; 36: 101665. 2022/05/21. DOI: 10.1016/j.beem.2022.101665.
49. Turcu AF, Nanba AT, Chomic R, et al. Adrenal-derived 11-oxygenated 19-carbon steroids are the dominant androgens in classic 21-hydroxylase deficiency. *Eur J Endocrinol* 2016; 174: 601-609. 2016/02/13. DOI: 10.1530/EJE-15-1181.
50. Barnard L, Gent R, van Rooyen D, et al. Adrenal C11-oxy C(21) steroids contribute to the C11-oxy C(19) steroid pool via the backdoor pathway in the biosynthesis and metabolism of 21-deoxycortisol and 21-deoxycortisone. *J Steroid Biochem Mol Biol* 2017; 174: 86-95. 2017/08/05. DOI: 10.1016/j.jsbmb.2017.07.034.
51. El-Maouche D, Arlt W and Merke DP. Congenital adrenal hyperplasia. *Lancet* 2017; 390: 2194-2210. 2017/06/04. DOI: 10.1016/S0140-6736(17)31431-9.
52. Speiser PW, Arlt W, Auchus RJ, et al. Congenital Adrenal Hyperplasia Due to Steroid 21-Hydroxylase Deficiency: An Endocrine Society Clinical Practice Guideline. *J Clin Endocrinol Metab* 2018; 103: 4043-4088. 2018/10/03. DOI: 10.1210/jc.2018-01865.
53. Miller WL. Minireview: regulation of steroidogenesis by electron transfer. *Endocrinology* 2005; 146: 2544-2550. 2005/03/19. DOI: 10.1210/en.2005-0096.
54. Bose HS, Sugawara T, Strauss JF, 3rd, et al. The pathophysiology and genetics of congenital lipoid adrenal hyperplasia. *N Engl J Med* 1996; 335: 1870-1878. 1996/12/19. DOI: 10.1056/NEJM199612193352503.
55. Baker BY, Lin L, Kim CJ, et al. Nonclassic congenital lipoid adrenal hyperplasia: a new disorder of the steroidogenic acute regulatory protein with very late presentation and normal male genitalia. *J Clin Endocrinol Metab* 2006; 91: 4781-4785. 2006/09/14. DOI: 10.1210/jc.2006-1565.
56. Miller WL. Disorders in the initial steps of steroid hormone synthesis. *J Steroid Biochem Mol Biol* 2017; 165: 18-37. 2016/03/10. DOI: 10.1016/j.jsbmb.2016.03.009.
57. Guran T, Buonocore F, Saka N, et al. Rare Causes of Primary Adrenal Insufficiency: Genetic and Clinical Characterization of a Large Nationwide Cohort. *J Clin Endocrinol Metab* 2016; 101: 284-292. 2015/11/03. DOI: 10.1210/jc.2015-3250.
58. Maharaj A, Buonocore F, Meimaridou E, et al. Predicted Benign and Synonymous Variants in CYP11A1 Cause Primary Adrenal Insufficiency Through Missplicing. *J Endocr Soc* 2019; 3: 201-221. 2019/01/09. DOI: 10.1210/js.2018-00130.
59. Costa-Santos M, Kater CE, Auchus RJ, et al. Two prevalent CYP17 mutations and genotype-phenotype correlations in 24 Brazilian patients with 17-hydroxylase deficiency. *J Clin Endocrinol Metab* 2004; 89: 49-60. 2004/01/13. DOI: 10.1210/jc.2003-031021.
60. Krone N, Reisch N, Idkowiak J, et al. Genotype-phenotype analysis in congenital adrenal hyperplasia due to P450 oxidoreductase deficiency. *J Clin Endocrinol Metab* 2012; 97: E257-267. 2011/12/14. DOI: 10.1210/jc.2011-0640.
61. Fluck CE, Tajima T, Pandey AV, et al. Mutant P450 oxidoreductase causes disordered steroidogenesis with and without Antley-Bixler syndrome. *Nat Genet* 2004; 36: 228-230. 2004/02/06. DOI: 10.1038/ng1300.
62. White PC, Curnow KM and Pascoe L. Disorders of steroid 11 beta-hydroxylase isozymes. *Endocr Rev* 1994; 15: 421-438. 1994/08/01. DOI: 10.1210/edrv-15-4-421.
63. White PC. Congenital adrenal hyperplasia owing to 11beta-hydroxylase deficiency. *Adv Exp Med Biol* 2011; 707: 7-8. 2011/06/22. DOI: 10.1007/978-1-4419-8002-1_2.
64. Werder EA, Siebenmann RE, Knorr-Murset G, et al. The incidence of congenital adrenal hyperplasia in Switzerland--a survey of patients born in 1960 to 1974. *Helv Paediatr Acta* 1980; 35: 5-11. 1980/03/01.
65. Curnow KM, Slutsker L, Vitek J, et al. Mutations in the CYP11B1 gene causing congenital adrenal hyperplasia and hypertension cluster in exons 6, 7, and 8. *Proc Natl Acad Sci U S A* 1993; 90: 4552-4556. 1993/05/15. DOI: 10.1073/pnas.90.10.4552.
66. Zachmann M, Tassinari D and Prader A. Clinical and biochemical variability of congenital adrenal hyperplasia due to 11 beta-hydroxylase deficiency. A study of 25 patients. *J Clin Endocrinol Metab* 1983; 56: 222-229. 1983/02/01. DOI: 10.1210/jcem-56-2-222.
67. Rosler A, Leiberman E and Cohen T. High frequency of congenital adrenal hyperplasia (classic 11 beta-hydroxylase deficiency) among Jews from Morocco. *Am J Med Genet* 1992; 42: 827-834. 1992/04/01. DOI: 10.1002/ajmg.1320420617.
68. White PC. Aldosterone synthase deficiency and related disorders. *Mol Cell Endocrinol* 2004; 217: 81-87. 2004/05/12. DOI: 10.1016/j.mce.2003.10.013.
69. Phelan JK and McCabe ER. Mutations in NR0B1 (DAX1) and NR5A1 (SF1) responsible for adrenal hypoplasia congenita. *Hum Mutat* 2001; 18: 472-487. 2001/12/19. DOI: 10.1002/humu.1225.

70. Lin L, Gu WX, Ozisik G, et al. Analysis of DAX1 (NR0B1) and steroidogenic factor-1 (NR5A1) in children and adults with primary adrenal failure: ten years' experience. *J Clin Endocrinol Metab* 2006; 91: 3048-3054. 2006/05/11. DOI: 10.1210/jc.2006-0603.
71. Lajic S, Nikoshkov A, Holst M, et al. Effects of missense mutations and deletions on membrane anchoring and enzyme function of human steroid 21-hydroxylase (P450c21). *Biochem Biophys Res Commun* 1999; 257: 384-390. 1999/04/13. DOI: 10.1006/bbrc.1999.0482.
72. Hu MC, Hsu LC, Hsu NC, et al. Function and membrane topology of wild-type and mutated cytochrome P-450c21. *Biochem J* 1996; 316 (Pt 1): 325-329. 1996/05/15. DOI: 10.1042/bj3160325.
73. White PC, New MI and Dupont B. Structure of human steroid 21-hydroxylase genes. *Proc Natl Acad Sci U S A* 1986; 83: 5111-5115. 1986/07/01. DOI: 10.1073/pnas.83.14.5111.
74. Gitelman SE, Bristow J and Miller WL. Mechanism and consequences of the duplication of the human C4/P450c21/gene X locus. *Mol Cell Biol* 1992; 12: 2124-2134. 1992/05/01. DOI: 10.1128/mcb.12.5.2124-2134.1992.
75. Yu CY. Molecular genetics of the human MHC complement gene cluster. *Exp Clin Immunogenet* 1998; 15: 213-230. 1999/03/11. DOI: 10.1159/000019075.
76. Mungall AJ, Palmer SA, Sims SK, et al. The DNA sequence and analysis of human chromosome 6. *Nature* 2003; 425: 805-811. 2003/10/24. DOI: 10.1038/nature02055.
77. Milner CM and Campbell RD. Genetic organization of the human MHC class III region. *Front Biosci* 2001; 6: D914-926. 2001/08/07. DOI: 10.2741/milner.
78. Shen L, Wu LC, Sanlioglu S, et al. Structure and genetics of the partially duplicated gene RP located immediately upstream of the complement C4A and the C4B genes in the HLA class III region. Molecular cloning, exon-intron structure, composite retroposon, and breakpoint of gene duplication. *J Biol Chem* 1994; 269: 8466-8476. 1994/03/18.
79. Tee MK, Babalola GO, Aza-Blanc P, et al. A promoter within intron 35 of the human C4A gene initiates abundant adrenal-specific transcription of a 1 kb RNA: location of a cryptic CYP21 promoter element? *Hum Mol Genet* 1995; 4: 2109-2116. 1995/11/01. DOI: 10.1093/hmg/4.11.2109.
80. Horton R, Wilming L, Rand V, et al. Gene map of the extended human MHC. *Nat Rev Genet* 2004; 5: 889-899. 2004/12/02. DOI: 10.1038/nrg1489.
81. Blanchong CA, Zhou B, Rupert KL, et al. Deficiencies of human complement component C4A and C4B and heterozygosity in length variants of RP-C4-CYP21-TNX (RCCX) modules in caucasians. The load of RCCX genetic diversity on major histocompatibility complex-associated disease. *J Exp Med* 2000; 191: 2183-2196. 2000/06/22. DOI: 10.1084/jem.191.12.2183.
82. Banlaki Z, Szabo JA, Szilagyi A, et al. Intraspecific evolution of human RCCX copy number variation traced by haplotypes of the CYP21A2 gene. *Genome Biol Evol* 2013; 5: 98-112. 2012/12/18. DOI: 10.1093/gbe/evs121.
83. Narasimhan ML and Khattab A. Genetics of congenital adrenal hyperplasia and genotype-phenotype correlation. *Fertil Steril* 2019; 111: 24-29. 2019/01/07. DOI: 10.1016/j.fertnstert.2018.11.007.
84. White PC, Vitek A, Dupont B, et al. Characterization of frequent deletions causing steroid 21-hydroxylase deficiency. *Proc Natl Acad Sci U S A* 1988; 85: 4436-4440. 1988/06/01. DOI: 10.1073/pnas.85.12.4436.
85. Geffrotin C, Chardon P, de Andres-Cara DF, et al. The swine steroid 21-hydroxylase gene (CYP21): cloning and mapping within the swine leucocyte antigen complex. *Anim Genet* 1990; 21: 1-13. 1990/01/01. DOI: 10.1111/j.1365-2052.1990.tb03202.x.
86. Kawaguchi H, O'HUigin C and Klein J. Evolutionary origin of mutations in the primate cytochrome P450c21 gene. *Am J Hum Genet* 1992; 50: 766-780. 1992/04/01.
87. Kawashima A and Satta Y. Substrate-dependent evolution of cytochrome P450: rapid turnover of the detoxification-type and conservation of the biosynthesis-type. *PLoS One* 2014; 9: e100059. 2014/07/01. DOI: 10.1371/journal.pone.0100059.
88. Kawaguchi H, Golubic M, Figueroa F, et al. Organization of the chimpanzee C4-CYP21 region: implications for the evolution of human genes. *Eur J Immunol* 1990; 20: 739-745. 1990/04/01. DOI: 10.1002/eji.1830200405.
89. Higashi Y, Yoshioka H, Yamane M, et al. Complete nucleotide sequence of two steroid 21-hydroxylase genes tandemly arranged in human chromosome: a pseudogene and a genuine gene. *Proc Natl Acad Sci U S A* 1986; 83: 2841-2845. 1986/05/01. DOI: 10.1073/pnas.83.9.2841.
90. Finkielstain GP, Chen W, Mehta SP, et al. Comprehensive genetic analysis of 182 unrelated families with congenital adrenal hyperplasia due to 21-hydroxylase deficiency. *J Clin Endocrinol Metab* 2011; 96: E161-172. 2010/10/12. DOI: 10.1210/jc.2010-0319.
91. Carroll MC, Campbell RD and Porter RR. Mapping of steroid 21-hydroxylase genes adjacent to complement component C4 genes in HLA, the major histocompatibility complex in man. *Proc Natl Acad Sci U S A* 1985; 82: 521-525. 1985/01/01. DOI: 10.1073/pnas.82.2.521.

92. Higashi Y, Tanae A, Inoue H, et al. Evidence for frequent gene conversion in the steroid 21-hydroxylase P-450(C21) gene: implications for steroid 21-hydroxylase deficiency. *Am J Hum Genet* 1988; 42: 17-25. 1988/01/01.
93. Wedell A and Luthman H. Steroid 21-hydroxylase (P450c21): a new allele and spread of mutations through the pseudogene. *Hum Genet* 1993; 91: 236-240. 1993/04/01. DOI: 10.1007/BF00218263.
94. Werkmeister JW, New MI, Dupont B, et al. Frequent deletion and duplication of the steroid 21-hydroxylase genes. *Am J Hum Genet* 1986; 39: 461-469. 1986/10/01.
95. Yau M, Khattab A, Yuen T, et al. Congenital Adrenal Hyperplasia. In: Feingold KR, Anawalt B, Blackman MR, et al. (eds) *Endotext*. South Dartmouth (MA): MDText.com, Inc, 2000.
96. Stenson PD, Mort M, Ball EV, et al. The Human Gene Mutation Database (HGMD((R))): optimizing its use in a clinical diagnostic or research setting. *Hum Genet* 2020; 139: 1197-1207. 2020/07/01. DOI: 10.1007/s00439-020-02199-3.
97. Turcu AF and Auchus RJ. Clinical significance of 11-oxygenated androgens. *Curr Opin Endocrinol Diabetes Obes* 2017; 24: 252-259. 2017/02/25. DOI: 10.1097/MED.0000000000000334.
98. Kamrath C, Hochberg Z, Hartmann MF, et al. Increased activation of the alternative "backdoor" pathway in patients with 21-hydroxylase deficiency: evidence from urinary steroid hormone analysis. *J Clin Endocrinol Metab* 2012; 97: E367-375. 2011/12/16. DOI: 10.1210/jc.2011-1997.
99. Jailer JW, Gold JJ, Vande Wiele R, et al. 17alpha-hydroxyprogesterone and 21-desoxyhydrocortisone; their metabolism and possible role in congenital adrenal virilism. *J Clin Invest* 1955; 34: 1639-1646. 1955/11/01. DOI: 10.1172/JCI103217.
100. Miller WL. Congenital Adrenal Hyperplasia: Time to Replace 17OHP with 21-Deoxycortisol. *Horm Res Paediatr* 2019; 91: 416-420. 2019/08/27. DOI: 10.1159/000501396.
101. Nimkarn S, Lin-Su K, Berglind N, et al. Aldosterone-to-renin ratio as a marker for disease severity in 21-hydroxylase deficiency congenital adrenal hyperplasia. *J Clin Endocrinol Metab* 2007; 92: 137-142. 2006/10/13. DOI: 10.1210/jc.2006-0964.
102. Krone N, Braun A, Roscher AA, et al. Predicting phenotype in steroid 21-hydroxylase deficiency? Comprehensive genotyping in 155 unrelated, well defined patients from southern Germany. *J Clin Endocrinol Metab* 2000; 85: 1059-1065. 2000/03/17. DOI: 10.1210/jcem.85.3.6441.
103. Concolino P and Costella A. Congenital Adrenal Hyperplasia (CAH) due to 21-Hydroxylase Deficiency: A Comprehensive Focus on 233 Pathogenic Variants of CYP21A2 Gene. *Mol Diagn Ther* 2018; 22: 261-280. 2018/02/17. DOI: 10.1007/s40291-018-0319-y.
104. White PC and Speiser PW. Congenital adrenal hyperplasia due to 21-hydroxylase deficiency. *Endocr Rev* 2000; 21: 245-291. 2000/06/17. DOI: 10.1210/edrv.21.3.0398.
105. Krone N and Arlt W. Genetics of congenital adrenal hyperplasia. *Best Pract Res Clin Endocrinol Metab* 2009; 23: 181-192. 2009/06/09. DOI: 10.1016/j.beem.2008.10.014.
106. New MI, Abraham M, Gonzalez B, et al. Genotype-phenotype correlation in 1,507 families with congenital adrenal hyperplasia owing to 21-hydroxylase deficiency. *Proc Natl Acad Sci U S A* 2013; 110: 2611-2616. 2013/01/30. DOI: 10.1073/pnas.1300057110.
107. Anonymous. Extraordinary Case of Hermaphrodism. *The Lancet* 1833; 20: 60-62. DOI: 10.1016/s0140-6736(02)93770-0.
108. de Crecchio L. Sopra un caso di apparenze virili in una donna. *Il Morgagni* 1865; 7: 151-189.
109. Delle Piane L, Rinaudo PF and Miller WL. 150 years of congenital adrenal hyperplasia: translation and commentary of De Crecchio's classic paper from 1865. *Endocrinology* 2015; 156: 1210-1217. 2015/01/31. DOI: 10.1210/en.2014-1879.
110. Phillips J. Four cases of spurious hermaphroditism in one family. *Trans Obstet Soc Lond* 1886 (1887); 28: 158-168.
111. Bartter FC, Albright F, Forbes AP, et al. The effects of adrenocorticotropic hormone and cortisone in the adrenogenital syndrome associated with congenital adrenal hyperplasia: an attempt to explain and correct its disordered hormonal pattern. *J Clin Invest* 1951; 30: 237-251. 1951/03/01. DOI: 10.1172/JCI102438.
112. Wilkins L, Lewis RA, Klein R, et al. Treatment of congenital adrenal hyperplasia with cortisone. *J Clin Endocrinol Metab* 1951; 11: 1-25. 1951/01/01. DOI: 10.1210/jcem-11-1-1.
113. Wilkins L, Lewis RA, Klein R, et al. The suppression of androgen secretion by cortisone in a case of congenital adrenal hyperplasia. *Bull Johns Hopkins Hosp* 1950; 86: 249-252. 1950/04/01.
114. Eberlein WR and Bongiovanni AM. Partial characterization of urinary adrenocortical steroids in adrenal hyperplasia. *J Clin Invest* 1955; 34: 1337-1343. 1955/08/01. DOI: 10.1172/JCI103181.
115. White PC, Grossberger D, Onufer BJ, et al. Two genes encoding steroid 21-hydroxylase are located near the genes encoding the fourth component of complement in man. *Proc Natl Acad Sci U S A* 1985; 82: 1089-1093. 1985/02/01. DOI: 10.1073/pnas.82.4.1089.

116. Pang S, Hotchkiss J, Drash AL, et al. Microfilter paper method for 17 alpha-hydroxyprogesterone radioimmunoassay: its application for rapid screening for congenital adrenal hyperplasia. *J Clin Endocrinol Metab* 1977; 45: 1003-1008. 1977/11/01. DOI: 10.1210/jcem-45-5-1003.
117. Hirschfeld AJ and Fleshman JK. An unusually high incidence of salt-losing congenital adrenal hyperplasia in the Alaskan Eskimo. *J Pediatr* 1969; 75: 492-494. 1969/09/01. DOI: 10.1016/s0022-3476(69)80280-5.
118. Pang S, Murphey W, Levine LS, et al. A pilot newborn screening for congenital adrenal hyperplasia in Alaska. *J Clin Endocrinol Metab* 1982; 55: 413-420. 1982/09/01. DOI: 10.1210/jcem-55-3-413.
119. Cutfield WS and Webster D. Newborn screening for congenital adrenal hyperplasia in New Zealand. *J Pediatr* 1995; 126: 118-121. 1995/01/01. DOI: 10.1016/s0022-3476(95)70513-9.
120. Therrell BL, Padilla CD, Loeber JG, et al. Current status of newborn screening worldwide: 2015. *Semin Perinatol* 2015; 39: 171-187. 2015/05/17. DOI: 10.1053/j.semperi.2015.03.002.
121. Gleeson HK, Wiley V, Wilcken B, et al. Two-year pilot study of newborn screening for congenital adrenal hyperplasia in New South Wales compared with nationwide case surveillance in Australia. *J Paediatr Child Health* 2008; 44: 554-559. 2008/11/18. DOI: 10.1111/j.1440-1754.2008.01383.x.
122. Lai F, Srinivasan S and Wiley V. Evaluation of a Two-Tier Screening Pathway for Congenital Adrenal Hyperplasia in the New South Wales Newborn Screening Programme. *Int J Neonatal Screen* 2020; 6: 63. 2020/10/30. DOI: 10.3390/ijns6030063.
123. Ludwig K, Lai F, Wiley V, et al. Genotyping in patients with congenital adrenal hyperplasia by sequencing of newborn bloodspot samples. *J Pediatr Endocrinol Metab* 2023; 36: 966-973. 2023/09/20. DOI: 10.1515/jpem-2023-0044.
124. Archibald AD, McClaren BJ, Caruana J, et al. The Australian Reproductive Genetic Carrier Screening Project (Mackenzie's Mission): Design and Implementation. *J Pers Med* 2022; 12: 1781. 2022/12/30. DOI: 10.3390/jpm12111781.
125. Bornstein SR, Allolio B, Arlt W, et al. Diagnosis and Treatment of Primary Adrenal Insufficiency: An Endocrine Society Clinical Practice Guideline. *J Clin Endocrinol Metab* 2016; 101: 364-389. 2016/01/14. DOI: 10.1210/jc.2015-1710.
126. Bachelot A, Plu-Bureau G, Thibaud E, et al. Long-term outcome of patients with congenital adrenal hyperplasia due to 21-hydroxylase deficiency. *Horm Res* 2007; 67: 268-276. 2006/12/16. DOI: 10.1159/000098017.
127. Martinerie L, Pussard E, Foix-L'Helias L, et al. Physiological partial aldosterone resistance in human newborns. *Pediatr Res* 2009; 66: 323-328. 2009/06/23. DOI: 10.1203/PDR.0b013e3181b1bbec.
128. Muthusamy K, Elamin MB, Smushkin G, et al. Clinical review: Adult height in patients with congenital adrenal hyperplasia: a systematic review and metaanalysis. *J Clin Endocrinol Metab* 2010; 95: 4161-4172. 2010/09/09. DOI: 10.1210/jc.2009-2616.
129. Halper A, Hooke MC, Gonzalez-Bolanos MT, et al. Health-related quality of life in children with congenital adrenal hyperplasia. *Health Qual Life Outcomes* 2017; 15: 194. 2017/10/08. DOI: 10.1186/s12955-017-0769-7.
130. Gilban DL, Alves Junior PA and Beserra IC. Health related quality of life of children and adolescents with congenital adrenal hyperplasia in Brazil. *Health Qual Life Outcomes* 2014; 12: 107. 2014/08/15. DOI: 10.1186/s12955-014-0107-2.
131. Yau M, Vogiatzi M, Lewkowitz-Shpuntoff A, et al. Health-Related Quality of Life in Children with Congenital Adrenal Hyperplasia. *Horm Res Paediatr* 2015; 84: 165-171. 2015/08/19. DOI: 10.1159/000435855.
132. Fleming L, Van Riper M and Knafl K. Management of Childhood Congenital Adrenal Hyperplasia-An Integrative Review of the Literature. *J Pediatr Health Care* 2017; 31: 560-577. 2017/04/19. DOI: 10.1016/j.pedhc.2017.02.004.
133. Idris AN, Chandran V, Syed Zakaria SZ, et al. Behavioural outcome in children with congenital adrenal hyperplasia: experience of a single centre. *Int J Endocrinol* 2014; 2014: 483718. 2014/05/07. DOI: 10.1155/2014/483718.
134. Engberg H, Butwicka A, Nordenstrom A, et al. Congenital adrenal hyperplasia and risk for psychiatric disorders in girls and women born between 1915 and 2010: A total population study. *Psychoneuroendocrinology* 2015; 60: 195-205. 2015/07/18. DOI: 10.1016/j.psyneuen.2015.06.017.
135. MacKay D, Nordenstrom A and Falhammar H. Bilateral Adrenalectomy in Congenital Adrenal Hyperplasia: A Systematic Review and Meta-Analysis. *J Clin Endocrinol Metab* 2018; 103: 1767-1778. 2018/03/20. DOI: 10.1210/jc.2018-00217.
136. Claahsen-van der Grinten HL, Speiser PW, Ahmed SF, et al. Congenital Adrenal Hyperplasia-Current Insights in Pathophysiology, Diagnostics, and Management. *Endocr Rev* 2022; 43: 91-159. 2021/05/08. DOI: 10.1210/endrev/bnab016.

137. Nella AA, Mallappa A, Perritt AF, et al. A Phase 2 Study of Continuous Subcutaneous Hydrocortisone Infusion in Adults With Congenital Adrenal Hyperplasia. *J Clin Endocrinol Metab* 2016; 101: 4690-4698. 2016/09/30. DOI: 10.1210/jc.2016-1916.
138. Mallappa A, Nella AA, Sinaii N, et al. Long-term use of continuous subcutaneous hydrocortisone infusion therapy in patients with congenital adrenal hyperplasia. *Clin Endocrinol (Oxf)* 2018; 89: 399-407. 2018/07/14. DOI: 10.1111/cen.13813.
139. Mortensen ML, Ornstrup MJ and Gravholt CH. Patients with Hypocortisolism Treated with Continuous Subcutaneous Hydrocortisone Infusion (CSHI): An Option for Poorly Controlled Patients. *Int J Endocrinol* 2023; 2023: 5315059. 2023/03/31. DOI: 10.1155/2023/5315059.
140. Mallappa A, Sinaii N, Kumar P, et al. A phase 2 study of Chronocort, a modified-release formulation of hydrocortisone, in the treatment of adults with classic congenital adrenal hyperplasia. *J Clin Endocrinol Metab* 2015; 100: 1137-1145. 2014/12/17. DOI: 10.1210/jc.2014-3809.
141. Jones CM, Mallappa A, Reisch N, et al. Modified-Release and Conventional Glucocorticoids and Diurnal Androgen Excretion in Congenital Adrenal Hyperplasia. *J Clin Endocrinol Metab* 2017; 102: 1797-1806. 2016/11/16. DOI: 10.1210/jc.2016-2855.
142. Speiser PW. Emerging medical therapies for congenital adrenal hyperplasia. *F1000Res* 2019; 8: 363. 2019/04/16. DOI: 10.12688/f1000research.17778.1.
143. White PC. Emerging treatment for congenital adrenal hyperplasia. *Curr Opin Endocrinol Diabetes Obes* 2022; 29: 271-276. 2022/03/15. DOI: 10.1097/MED.0000000000000723.
144. Garrido M, Peng HM, Yoshimoto FK, et al. A-ring modified steroidal azoles retaining similar potent and slowly reversible CYP17A1 inhibition as abiraterone. *J Steroid Biochem Mol Biol* 2014; 143: 1-10. 2014/02/11. DOI: 10.1016/j.jsbmb.2014.01.013.
145. Auchus RJ, Buschur EO, Chang AY, et al. Abiraterone acetate to lower androgens in women with classic 21-hydroxylase deficiency. *J Clin Endocrinol Metab* 2014; 99: 2763-2770. 2014/05/02. DOI: 10.1210/jc.2014-1258.
146. Turcu AF, Spencer-Segal JL, Farber RH, et al. Single-Dose Study of a Corticotropin-Releasing Factor Receptor-1 Antagonist in Women With 21-Hydroxylase Deficiency. *J Clin Endocrinol Metab* 2016; 101: 1174-1180. 2016/01/12. DOI: 10.1210/jc.2015-3574.
147. Kay MA, Glorioso JC and Naldini L. Viral vectors for gene therapy: the art of turning infectious agents into vehicles of therapeutics. *Nat Med* 2001; 7: 33-40. 2001/01/03. DOI: 10.1038/83324.
148. Griffith F. The Significance of Pneumococcal Types. *J Hyg (Lond)* 1928; 27: 113-159. 1928/01/01. DOI: 10.1017/s0022172400031879.
149. Avery OT, Macleod CM and McCarty M. Studies on the Chemical Nature of the Substance Inducing Transformation of Pneumococcal Types : Induction of Transformation by a Desoxyribonucleic Acid Fraction Isolated from Pneumococcus Type Iii. *J Exp Med* 1944; 79: 137-158. 1944/02/01. DOI: 10.1084/jem.79.2.137.
150. Tatum EL and Lederberg J. Gene Recombination in the Bacterium Escherichia coli. *J Bacteriol* 1947; 53: 673-684. 1947/06/01. DOI: 10.1128/jb.53.6.673-684.1947.
151. Zinder ND and Lederberg J. Genetic exchange in Salmonella. *J Bacteriol* 1952; 64: 679-699. 1952/11/01. DOI: 10.1128/jb.64.5.679-699.1952.
152. Szybalska EH and Szybalski W. Genetics of human cell line. IV. DNA-mediated heritable transformation of a biochemical trait. *Proc Natl Acad Sci U S A* 1962; 48: 2026-2034. 1962/12/15. DOI: 10.1073/pnas.48.12.2026.
153. Sambrook J, Westphal H, Srinivasan PR, et al. The integrated state of viral DNA in SV40-transformed cells. *Proc Natl Acad Sci U S A* 1968; 60: 1288-1295. 1968/08/01. DOI: 10.1073/pnas.60.4.1288.
154. Tatum EL. Molecular biology, nucleic acids, and the future of medicine. *Perspect Biol Med* 1966; 10: 19-32. 1966/01/01. DOI: 10.1353/pbm.1966.0027.
155. Lederberg J. Molecular biology, eugenics and euphenics. *Nature* 1963; 198: 428-429. 1963/05/04. DOI: 10.1038/198428a0.
156. Nirenberg MW. Will society be prepared? *Science* 1967; 157: 633. 1967/08/11. DOI: 10.1126/science.157.3789.633.
157. Rogers S and Pfuderer P. Use of viruses as carriers of added genetic information. *Nature* 1968; 219: 749-751. 1968/08/17. DOI: 10.1038/219749a0.
158. Rogers S, Lowenthal A, Terheggen HG, et al. Induction of arginase activity with the Shope papilloma virus in tissue culture cells from an argininemic patient. *J Exp Med* 1973; 137: 1091-1096. 1973/04/01. DOI: 10.1084/jem.137.4.1091.
159. Terheggen HG, Lowenthal A, Lavinha F, et al. Unsuccessful trial of gene replacement in arginase deficiency. *Z Kinderheilkd* 1975; 119: 1-3. 1975/01/01. DOI: 10.1007/BF00464689.

160. Wirth T, Parker N and Yla-Herttuala S. History of gene therapy. *Gene* 2013; 525: 162-169. 2013/04/27. DOI: 10.1016/j.gene.2013.03.137.
161. Rosenberg SA, Aebersold P, Cornetta K, et al. Gene transfer into humans--immunotherapy of patients with advanced melanoma, using tumor-infiltrating lymphocytes modified by retroviral gene transduction. *N Engl J Med* 1990; 323: 570-578. 1990/08/30. DOI: 10.1056/NEJM199008303230904.
162. Blaese RM, Culver KW, Miller AD, et al. T lymphocyte-directed gene therapy for ADA- SCID: initial trial results after 4 years. *Science* 1995; 270: 475-480. 1995/10/20. DOI: 10.1126/science.270.5235.475.
163. Kohn DB, Hershfield MS, Carbonaro D, et al. T lymphocytes with a normal ADA gene accumulate after transplantation of transduced autologous umbilical cord blood CD34+ cells in ADA-deficient SCID neonates. *Nat Med* 1998; 4: 775-780. 1998/07/14. DOI: 10.1038/nm0798-775.
164. Orkin SH and Motulsky AG. *Report and Recommendations of the Panel to Assess the NIH Investment in Research on Gene Therapy*. December 7 1995. Bethesda, MD: National Institutes of Health.
165. Stolberg SG. The biotech death of Jesse Gelsinger. *N Y Times Mag* 1999: 136-140, 149-150. 2001/10/20.
166. Marshall E. Gene therapy death prompts review of adenovirus vector. *Science* 1999; 286: 2244-2245. 2000/01/15. DOI: 10.1126/science.286.5448.2244.
167. Raper SE, Chirmule N, Lee FS, et al. Fatal systemic inflammatory response syndrome in a ornithine transcarbamylase deficient patient following adenoviral gene transfer. *Mol Genet Metab* 2003; 80: 148-158. 2003/10/22. DOI: 10.1016/j.ymgme.2003.08.016.
168. Cavazzana-Calvo M, Hacein-Bey S, de Saint Basile G, et al. Gene therapy of human severe combined immunodeficiency (SCID)-X1 disease. *Science* 2000; 288: 669-672. 2000/04/28. DOI: 10.1126/science.288.5466.669.
169. Li Z, Dullmann J, Schiedlmeier B, et al. Murine leukemia induced by retroviral gene marking. *Science* 2002; 296: 497. 2002/04/20. DOI: 10.1126/science.1068893.
170. Hacein-Bey-Abina S, Von Kalle C, Schmidt M, et al. LMO2-associated clonal T cell proliferation in two patients after gene therapy for SCID-X1. *Science* 2003; 302: 415-419. 2003/10/18. DOI: 10.1126/science.1088547.
171. Check E. Gene therapy put on hold as third child develops cancer. *Nature* 2005; 433: 561. 2005/02/11. DOI: 10.1038/433561a.
172. Hacein-Bey-Abina S, Garrigue A, Wang GP, et al. Insertional oncogenesis in 4 patients after retrovirus-mediated gene therapy of SCID-X1. *J Clin Invest* 2008; 118: 3132-3142. 2008/08/09. DOI: 10.1172/JCI35700.
173. Howe SJ, Mansour MR, Schwarzwaelder K, et al. Insertional mutagenesis combined with acquired somatic mutations causes leukemogenesis following gene therapy of SCID-X1 patients. *J Clin Invest* 2008; 118: 3143-3150. 2008/08/09. DOI: 10.1172/JCI35798.
174. Hacein-Bey-Abina S, von Kalle C, Schmidt M, et al. A serious adverse event after successful gene therapy for X-linked severe combined immunodeficiency. *N Engl J Med* 2003; 348: 255-256. 2003/01/17. DOI: 10.1056/NEJM200301163480314.
175. Edelstein ML, Abedi MR, Wixon J, et al. Gene therapy clinical trials worldwide 1989-2004-an overview. *J Gene Med* 2004; 6: 597-602. 2004/06/02. DOI: 10.1002/jgm.619.
176. Check E. Harmful potential of viral vectors fuels doubts over gene therapy. *Nature* 2003; 423: 573-574. 2003/06/06. DOI: 10.1038/423573a.
177. Kohn DB and Gansbacher B. Letter to the editors of Nature from the American Society of Gene Therapy (ASGT) and the European Society of Gene Therapy (ESGT). *J Gene Med* 2003; 5: 641. 2003/06/26. DOI: 10.1002/jgm.446.
178. ASGCT and Citeline. *Gene, Cell, + RNA Therapy Landscape Report: Q4 2023 Quarterly Data Report*. 2023.
179. Dunbar CE, High KA, Joung JK, et al. Gene therapy comes of age. *Science* 2018; 359: eaan4672. 2018/01/13. DOI: 10.1126/science.aan4672.
180. Edelstein ML, Abedi MR and Wixon J. Gene therapy clinical trials worldwide to 2007--an update. *J Gene Med* 2007; 9: 833-842. 2007/08/28. DOI: 10.1002/jgm.1100.
181. Ginn SL, Alexander IE, Edelstein ML, et al. Gene therapy clinical trials worldwide to 2012 - an update. *J Gene Med* 2013; 15: 65-77. 2013/01/29. DOI: 10.1002/jgm.2698.
182. Ginn SL, Amaya AK, Alexander IE, et al. Gene therapy clinical trials worldwide to 2017: An update. *J Gene Med* 2018; 20: e3015. 2018/03/27. DOI: 10.1002/jgm.3015.
183. Evans CH. The vicissitudes of gene therapy. *Bone Joint Res* 2019; 8: 469-471. 2019/11/16. DOI: 10.1302/2046-3758.810.BJR-2019-0265.

184. Aiuti A, Roncarolo MG and Naldini L. Gene therapy for ADA-SCID, the first marketing approval of an ex vivo gene therapy in Europe: paving the road for the next generation of advanced therapy medicinal products. *EMBO Mol Med* 2017; 9: 737-740. 2017/04/12. DOI: 10.15252/emmm.201707573.
185. Wang M, Munoz J, Goy A, et al. KTE-X19 CAR T-Cell Therapy in Relapsed or Refractory Mantle-Cell Lymphoma. *N Engl J Med* 2020; 382: 1331-1342. 2020/04/04. DOI: 10.1056/NEJMoa1914347.
186. Ma CC, Wang ZL, Xu T, et al. The approved gene therapy drugs worldwide: from 1998 to 2019. *Biotechnol Adv* 2020; 40: 107502. 2019/12/31. DOI: 10.1016/j.biotechadv.2019.107502.
187. Yla-Herttuala S. Endgame: glybera finally recommended for approval as the first gene therapy drug in the European union. *Mol Ther* 2012; 20: 1831-1832. 2012/10/02. DOI: 10.1038/mt.2012.194.
188. Dabbous O, Maru B, Jansen JP, et al. Survival, Motor Function, and Motor Milestones: Comparison of AVXS-101 Relative to Nusinersen for the Treatment of Infants with Spinal Muscular Atrophy Type 1. *Adv Ther* 2019; 36: 1164-1176. 2019/03/18. DOI: 10.1007/s12325-019-00923-8.
189. Luu KT, Norris DA, Gunawan R, et al. Population Pharmacokinetics of Nusinersen in the Cerebral Spinal Fluid and Plasma of Pediatric Patients With Spinal Muscular Atrophy Following Intrathecal Administrations. *J Clin Pharmacol* 2017; 57: 1031-1041. 2017/04/04. DOI: 10.1002/jcph.884.
190. Aiuti A, Slavin S, Aker M, et al. Correction of ADA-SCID by stem cell gene therapy combined with nonmyeloablative conditioning. *Science* 2002; 296: 2410-2413. 2002/06/29. DOI: 10.1126/science.1070104.
191. Aiuti A, Cassani B, Andolfi G, et al. Multilineage hematopoietic reconstitution without clonal selection in ADA-SCID patients treated with stem cell gene therapy. *J Clin Invest* 2007; 117: 2233-2240. 2007/08/03. DOI: 10.1172/JCI31666.
192. Aiuti A, Cattaneo F, Galimberti S, et al. Gene therapy for immunodeficiency due to adenosine deaminase deficiency. *N Engl J Med* 2009; 360: 447-458. 2009/01/31. DOI: 10.1056/NEJMoa0805817.
193. Cicalese MP, Ferrua F, Castagnaro L, et al. Update on the safety and efficacy of retroviral gene therapy for immunodeficiency due to adenosine deaminase deficiency. *Blood* 2016; 128: 45-54. 2016/05/01. DOI: 10.1182/blood-2016-01-688226.
194. Monaco L and Faccio L. Patient-driven search for rare disease therapies: the Fondazione Telethon success story and the strategy leading to Strimvelis. *EMBO Mol Med* 2017; 9: 289-292. DOI: 10.15252/emmm.201607293.
195. GSK signs strategic agreement to transfer rare disease gene therapy portfolio to Orchard Therapeutics. London, UK2018.
196. Valsecchi MC. Rescue of an orphan drug points to a new model for therapies for rare diseases. *Nature Italy* 2023. DOI: 10.1038/d43978-023-00145-1.
197. Burnett JR and Hooper AJ. Alipogene tiparvovec, an adeno-associated virus encoding the Ser(447)X variant of the human lipoprotein lipase gene for the treatment of patients with lipoprotein lipase deficiency. *Curr Opin Mol Ther* 2009; 11: 681-691. 2010/01/15.
198. Gaudet D, Methot J, Dery S, et al. Efficacy and long-term safety of alipogene tiparvovec (AAV1-LPLS447X) gene therapy for lipoprotein lipase deficiency: an open-label trial. *Gene Ther* 2013; 20: 361-369. 2012/06/22. DOI: 10.1038/gt.2012.43.
199. Warner E. Goodbye Glybera! The World's First Gene Therapy will be Withdrawn, https://www.labiotech.eu/trends-news/uniqure-glybera-marketing-withdrawn/ (2017, accessed 6th October 2024).
200. Morrison C. $1-million price tag set for Glybera gene therapy. *Nat Biotechnol* 2015; 33: 217-218. 2015/03/10. DOI: 10.1038/nbt0315-217.
201. uniQure Announces It Will Not Seek Marketing Authorization Renewal for Glybera in Europe. 2017.
202. Chebli J, Forest F, Gaudet I, et al. 15-year retrospective analysis of Glybera (alipogene tiparvovec) gene replacement therapy for lipoprotein lipase deficiency. *Atherosclerosis* 2024; 395: 118433. DOI: 10.1016/j.atherosclerosis.2024.118433.
203. Wilson RC and Gilbert LA. The Promise and Challenge of In Vivo Delivery for Genome Therapeutics. *ACS Chem Biol* 2018; 13: 376-382. 2017/10/12. DOI: 10.1021/acschembio.7b00680.
204. Barrett D, Nguyen-Jatkoe L, Foss-Campbell B, et al. *Gene, Cell, & RNA Therapy Landscape, Q2 2021 Quarterly Data Report*. 2021.
205. Wang D, Tai PWL and Gao G. Adeno-associated virus vector as a platform for gene therapy delivery. *Nat Rev Drug Discov* 2019; 18: 358-378. 2019/02/03. DOI: 10.1038/s41573-019-0012-9.
206. Deyle DR and Russell DW. Adeno-associated virus vector integration. *Curr Opin Mol Ther* 2009; 11: 442-447. 2009/08/04.
207. Kaeppel C, Beattie SG, Fronza R, et al. A largely random AAV integration profile after LPLD gene therapy. *Nat Med* 2013; 19: 889-891. 2013/06/19. DOI: 10.1038/nm.3230.

208. Berns KI and Parrish CR. Parvoviridae. In: Fields BN, Knipe DM and Howley PM (eds) *Fields Virology*. 6th ed. Philadelphia: Wolters Kluwer Health/Lippincott Williams & Wilkins, 2013.
209. Atchison RW, Casto BC and Hammon WM. Adenovirus-Associated Defective Virus Particles. *Science* 1965; 149: 754-756. 1965/08/13. DOI: 10.1126/science.149.3685.754.
210. Blacklow NR, Hoggan MD and Rowe WP. Isolation of adenovirus-associated viruses from man. *Proc Natl Acad Sci U S A* 1967; 58: 1410-1415. 1967/10/01. DOI: 10.1073/pnas.58.4.1410.
211. Milone MC and O'Doherty U. Clinical use of lentiviral vectors. *Leukemia* 2018; 32: 1529-1541. 2018/04/15. DOI: 10.1038/s41375-018-0106-0.
212. Cockrell AS and Kafri T. Gene delivery by lentivirus vectors. *Mol Biotechnol* 2007; 36: 184-204. 2007/09/18. DOI: 10.1007/s12033-007-0010-8.
213. Miyagawa Y, Marino P, Verlengia G, et al. Herpes simplex viral-vector design for efficient transduction of nonneuronal cells without cytotoxicity. *Proc Natl Acad Sci U S A* 2015; 112: E1632-1641. 2015/03/17. DOI: 10.1073/pnas.1423556112.
214. Gates S, Andreani J, Dewar R, et al. Postpandemic rebound of adeno-associated virus type 2 (AAV2) infections temporally associated with an outbreak of unexplained severe acute hepatitis in children in the United Kingdom. *J Med Virol* 2023; 95: e28921. 2023/07/05. DOI: 10.1002/jmv.28921.
215. Mitchell MM, Leng Y, Boppana S, et al. Signatures of AAV-2 immunity are enriched in children with severe acute hepatitis of unknown etiology. *Sci Transl Med* 2023; 15: eadh9917. 2023/07/26. DOI: 10.1126/scitranslmed.adh9917.
216. Servellita V, Sotomayor Gonzalez A, Lamson DM, et al. Adeno-associated virus type 2 in US children with acute severe hepatitis. *Nature* 2023; 617: 574-580. 2023/03/31. DOI: 10.1038/s41586-023-05949-1.
217. Ho A, Orton R, Tayler R, et al. Adeno-associated virus 2 infection in children with non-A-E hepatitis. *Nature* 2023; 617: 555-563. 2023/03/31. DOI: 10.1038/s41586-023-05948-2.
218. Buning H and Srivastava A. Capsid Modifications for Targeting and Improving the Efficacy of AAV Vectors. *Mol Ther Methods Clin Dev* 2019; 12: 248-265. 2019/03/01. DOI: 10.1016/j.omtm.2019.01.008.
219. Alexander IE, Cunningham SC, Logan GJ, et al. Potential of AAV vectors in the treatment of metabolic disease. *Gene Ther* 2008; 15: 831-839. 2008/04/11. DOI: 10.1038/gt.2008.64.
220. Paulk NK. Gene Therapy: It's Time to Talk about High-Dose AAV. *Genet Eng Biotechnol News* 2020; 40: 14-16. DOI: 10.1089/gen.40.09.04.
221. Mullard A. Gene therapy community grapples with toxicity issues, as pipeline matures. *Nat Rev Drug Discov* 2021; 20: 804-805. 2021/10/03. DOI: 10.1038/d41573-021-00164-x.
222. Hinderer C, Katz N, Buza EL, et al. Severe Toxicity in Nonhuman Primates and Piglets Following High-Dose Intravenous Administration of an Adeno-Associated Virus Vector Expressing Human SMN. *Hum Gene Ther* 2018; 29: 285-298. 2018/01/31. DOI: 10.1089/hum.2018.015.
223. Taha EA, Lee J and Hotta A. Delivery of CRISPR-Cas tools for in vivo genome editing therapy: Trends and challenges. *J Control Release* 2022; 342: 345-361. 2022/01/14. DOI: 10.1016/j.jconrel.2022.01.013.
224. Chand DH, Zaidman C, Arya K, et al. Thrombotic Microangiopathy Following Onasemnogene Abeparvovec for Spinal Muscular Atrophy: A Case Series. *J Pediatr* 2021; 231: 265-268. 2020/12/02. DOI: 10.1016/j.jpeds.2020.11.054.
225. Muzyczka N. Use of adeno-associated virus as a general transduction vector for mammalian cells. *Curr Top Microbiol Immunol* 1992; 158: 97-129. 1992/01/01. DOI: 10.1007/978-3-642-75608-5_5.
226. Sonntag F, Schmidt K and Kleinschmidt JA. A viral assembly factor promotes AAV2 capsid formation in the nucleolus. *Proc Natl Acad Sci U S A* 2010; 107: 10220-10225. 2010/05/19. DOI: 10.1073/pnas.1001673107.
227. Sonntag F, Kother K, Schmidt K, et al. The assembly-activating protein promotes capsid assembly of different adeno-associated virus serotypes. *J Virol* 2011; 85: 12686-12697. 2011/09/16. DOI: 10.1128/JVI.05359-11.
228. Cao M, You H and Hermonat PL. The X gene of adeno-associated virus 2 (AAV2) is involved in viral DNA replication. *PLoS One* 2014; 9: e104596. 2014/08/16. DOI: 10.1371/journal.pone.0104596.
229. Song S, Lu Y, Choi YK, et al. DNA-dependent PK inhibits adeno-associated virus DNA integration. *Proc Natl Acad Sci U S A* 2004; 101: 2112-2116. 2004/02/10. DOI: 10.1073/pnas.0307833100.
230. Kotin RM, Menninger JC, Ward DC, et al. Mapping and direct visualization of a region-specific viral DNA integration site on chromosome 19q13-qter. *Genomics* 1991; 10: 831-834. 1991/07/01. DOI: 10.1016/0888-7543(91)90470-y.
231. Weitzman MD, Kyostio SR, Kotin RM, et al. Adeno-associated virus (AAV) Rep proteins mediate complex formation between AAV DNA and its integration site in human DNA. *Proc Natl Acad Sci U S A* 1994; 91: 5808-5812. 1994/06/21. DOI: 10.1073/pnas.91.13.5808.

232. Smith RH. Adeno-associated virus integration: virus versus vector. *Gene Ther* 2008; 15: 817-822. 2008/04/11. DOI: 10.1038/gt.2008.55.
233. Wilmott P, Lisowski L, Alexander IE, et al. A User's Guide to the Inverted Terminal Repeats of Adeno-Associated Virus. *Hum Gene Ther Methods* 2019; 30: 206-213. 2019/11/23. DOI: 10.1089/hgtb.2019.276.
234. Samulski RJ, Berns KI, Tan M, et al. Cloning of adeno-associated virus into pBR322: rescue of intact virus from the recombinant plasmid in human cells. *Proc Natl Acad Sci U S A* 1982; 79: 2077-2081. 1982/03/01. DOI: 10.1073/pnas.79.6.2077.
235. Grieger JC and Samulski RJ. Packaging capacity of adeno-associated virus serotypes: impact of larger genomes on infectivity and postentry steps. *J Virol* 2005; 79: 9933-9944. 2005/07/15. DOI: 10.1128/JVI.79.15.9933-9944.2005.
236. Boutin S, Monteilhet V, Veron P, et al. Prevalence of serum IgG and neutralizing factors against adeno-associated virus (AAV) types 1, 2, 5, 6, 8, and 9 in the healthy population: implications for gene therapy using AAV vectors. *Hum Gene Ther* 2010; 21: 704-712. 2010/01/26. DOI: 10.1089/hum.2009.182.
237. Li A, Tanner MR, Lee CM, et al. AAV-CRISPR Gene Editing Is Negated by Pre-existing Immunity to Cas9. *Mol Ther* 2020; 28: 1432-1441. 2020/04/30. DOI: 10.1016/j.ymthe.2020.04.017.
238. Mueller C, Berry JD, McKenna-Yasek DM, et al. SOD1 Suppression with Adeno-Associated Virus and MicroRNA in Familial ALS. *N Engl J Med* 2020; 383: 151-158. 2020/07/09. DOI: 10.1056/NEJMoa2005056.
239. Selot R, Arumugam S, Mary B, et al. Optimized AAV rh.10 Vectors That Partially Evade Neutralizing Antibodies during Hepatic Gene Transfer. *Front Pharmacol* 2017; 8: 441. 2017/08/05. DOI: 10.3389/fphar.2017.00441.
240. Salas D, Kwikkers KL, Zabaleta N, et al. Immunoadsorption enables successful rAAV5-mediated repeated hepatic gene delivery in nonhuman primates. *Blood Adv* 2019; 3: 2632-2641. 2019/09/11. DOI: 10.1182/bloodadvances.2019000380.
241. Li X, Wei X, Lin J, et al. A versatile toolkit for overcoming AAV immunity. *Front Immunol* 2022; 13: 991832. 2022/09/20. DOI: 10.3389/fimmu.2022.991832.
242. Rabinowitz JE, Rolling F, Li C, et al. Cross-packaging of a single adeno-associated virus (AAV) type 2 vector genome into multiple AAV serotypes enables transduction with broad specificity. *J Virol* 2002; 76: 791-801. 2001/12/26. DOI: 10.1128/jvi.76.2.791-801.2002.
243. Zhong L, Li B, Mah CS, et al. Next generation of adeno-associated virus 2 vectors: point mutations in tyrosines lead to high-efficiency transduction at lower doses. *Proc Natl Acad Sci U S A* 2008; 105: 7827-7832. 2008/05/31. DOI: 10.1073/pnas.0802866105.
244. Wang L, Bell P, Somanathan S, et al. Comparative Study of Liver Gene Transfer With AAV Vectors Based on Natural and Engineered AAV Capsids. *Mol Ther* 2015; 23: 1877-1887. 2015/09/29. DOI: 10.1038/mt.2015.179.
245. Maheshri N, Koerber JT, Kaspar BK, et al. Directed evolution of adeno-associated virus yields enhanced gene delivery vectors. *Nat Biotechnol* 2006; 24: 198-204. 2006/01/24. DOI: 10.1038/nbt1182.
246. Paulk NK, Pekrun K, Zhu E, et al. Bioengineered AAV Capsids with Combined High Human Liver Transduction In Vivo and Unique Humoral Seroreactivity. *Mol Ther* 2018; 26: 289-303. 2017/10/23. DOI: 10.1016/j.ymthe.2017.09.021.
247. Deverman BE, Pravdo PL, Simpson BP, et al. Cre-dependent selection yields AAV variants for widespread gene transfer to the adult brain. *Nat Biotechnol* 2016; 34: 204-209. 2016/02/02. DOI: 10.1038/nbt.3440.
248. Lisowski L, Dane AP, Chu K, et al. Selection and evaluation of clinically relevant AAV variants in a xenograft liver model. *Nature* 2014; 506: 382-386. 2014/01/07. DOI: 10.1038/nature12875.
249. Jiang H, Couto LB, Patarroyo-White S, et al. Effects of transient immunosuppression on adenoassociated, virus-mediated, liver-directed gene transfer in rhesus macaques and implications for human gene therapy. *Blood* 2006; 108: 3321-3328. 2006/07/27. DOI: 10.1182/blood-2006-04-017913.
250. Manno CS, Pierce GF, Arruda VR, et al. Successful transduction of liver in hemophilia by AAV-Factor IX and limitations imposed by the host immune response. *Nat Med* 2006; 12: 342-347. 2006/02/14. DOI: 10.1038/nm1358.
251. Nietupski JB, Hurlbut GD, Ziegler RJ, et al. Systemic administration of AAV8-alpha-galactosidase A induces humoral tolerance in nonhuman primates despite low hepatic expression. *Mol Ther* 2011; 19: 1999-2011. 2011/06/30. DOI: 10.1038/mt.2011.119.
252. Kay MA, Manno CS, Ragni MV, et al. Evidence for gene transfer and expression of factor IX in haemophilia B patients treated with an AAV vector. *Nat Genet* 2000; 24: 257-261. 2000/03/04. DOI: 10.1038/73464.

253. Cabanes-Creus M, Liao SHY, Gale Navarro R, et al. Harnessing whole human liver ex situ normothermic perfusion for preclinical AAV vector evaluation. *Nat Commun* 2024; 15: 1876. 2024/03/15. DOI: 10.1038/s41467-024-46194-y.
254. Samulski RJ, Chang LS and Shenk T. A recombinant plasmid from which an infectious adeno-associated virus genome can be excised in vitro and its use to study viral replication. *J Virol* 1987; 61: 3096-3101. 1987/10/01. DOI: 10.1128/JVI.61.10.3096-3101.1987.
255. McLaughlin SK, Collis P, Hermonat PL, et al. Adeno-associated virus general transduction vectors: analysis of proviral structures. *J Virol* 1988; 62: 1963-1973. 1988/06/01. DOI: 10.1128/JVI.62.6.1963-1973.1988.
256. Cunningham SC, Spinoulas A, Carpenter KH, et al. AAV2/8-mediated correction of OTC deficiency is robust in adult but not neonatal Spf(ash) mice. *Mol Ther* 2009; 17: 1340-1346. 2009/04/23. DOI: 10.1038/mt.2009.88.
257. Cunningham SC, Dane AP, Spinoulas A, et al. Gene delivery to the juvenile mouse liver using AAV2/8 vectors. *Mol Ther* 2008; 16: 1081-1088. 2008/04/17. DOI: 10.1038/mt.2008.72.
258. Cox DBT, Platt RJ and Zhang F. Therapeutic genome editing: prospects and challenges. *Nat Med* 2015; 21: 121-131. DOI: 10.1038/nm.3793.
259. Gaj T, Sirk SJ, Shui SL, et al. Genome-Editing Technologies: Principles and Applications. *Cold Spring Harb Perspect Biol* 2016; 8: a023754. 2016/12/03. DOI: 10.1101/cshperspect.a023754.
260. Jinek M, Chylinski K, Fonfara I, et al. A programmable dual-RNA-guided DNA endonuclease in adaptive bacterial immunity. *Science* 2012; 337: 816-821. 2012/06/30. DOI: 10.1126/science.1225829.
261. Jinek M, Chylinski K, Fonfara I, et al. A Programmable Dual-RNA-Guided DNA Endonuclease in Adaptive Bacterial Immunity. *Science* 2012; 337: 816-821. DOI: 10.1126/science.1225829.
262. Cohen J. A cut above: pair that developed CRISPR earns historic award. *Science* 2020; 370: 271-272. 2020/10/17. DOI: 10.1126/science.370.6514.271.
263. Wiedenheft B, Sternberg SH and Doudna JA. RNA-guided genetic silencing systems in bacteria and archaea. *Nature* 2012; 482: 331-338. 2012/02/18. DOI: 10.1038/nature10886.
264. Sorek R, Lawrence CM and Wiedenheft B. CRISPR-mediated adaptive immune systems in bacteria and archaea. *Annu Rev Biochem* 2013; 82: 237-266. 2013/03/19. DOI: 10.1146/annurev-biochem-072911-172315.
265. Ran FA, Hsu PD, Wright J, et al. Genome engineering using the CRISPR-Cas9 system. *Nat Protoc* 2013; 8: 2281-2308. 2013/10/26. DOI: 10.1038/nprot.2013.143.
266. Suzuki K, Yamamoto M, Hernandez-Benitez R, et al. Precise in vivo genome editing via single homology arm donor mediated intron-targeting gene integration for genetic disease correction. *Cell Res* 2019; 29: 804-819. 2019/08/25. DOI: 10.1038/s41422-019-0213-0.
267. Rouet P, Smih F and Jasin M. Introduction of double-strand breaks into the genome of mouse cells by expression of a rare-cutting endonuclease. *Mol Cell Biol* 1994; 14: 8096-8106. 1994/12/01. DOI: 10.1128/mcb.14.12.8096-8106.1994.
268. Bibikova M, Carroll D, Segal DJ, et al. Stimulation of homologous recombination through targeted cleavage by chimeric nucleases. *Mol Cell Biol* 2001; 21: 289-297. 2000/12/13. DOI: 10.1128/MCB.21.1.289-297.2001.
269. Bibikova M, Golic M, Golic KG, et al. Targeted chromosomal cleavage and mutagenesis in Drosophila using zinc-finger nucleases. *Genetics* 2002; 161: 1169-1175. 2002/07/24. DOI: 10.1093/genetics/161.3.1169.
270. Prakash V, Moore M and Yanez-Munoz RJ. Current Progress in Therapeutic Gene Editing for Monogenic Diseases. *Mol Ther* 2016; 24: 465-474. 2016/01/15. DOI: 10.1038/mt.2016.5.
271. Sadelain M, Papapetrou EP and Bushman FD. Safe harbours for the integration of new DNA in the human genome. *Nat Rev Cancer* 2011; 12: 51-58. 2011/12/02. DOI: 10.1038/nrc3179.
272. Orthwein A, Noordermeer SM, Wilson MD, et al. A mechanism for the suppression of homologous recombination in G1 cells. *Nature* 2015; 528: 422-426. 2015/12/10. DOI: 10.1038/nature16142.
273. Suzuki K, Tsunekawa Y, Hernandez-Benitez R, et al. In vivo genome editing via CRISPR/Cas9 mediated homology-independent targeted integration. *Nature* 2016; 540: 144-149. 2016/11/17. DOI: 10.1038/nature20565.
274. Ginn SL, Christina S and Alexander IE. Genome editing in the human liver: Progress and translational considerations. *Prog Mol Biol Transl Sci* 2021; 182: 257-288. 2021/06/28. DOI: 10.1016/bs.pmbts.2021.01.030.
275. Graves LE, Horton A, Alexander IE, et al. Gene Therapy for Paediatric Homozygous Familial Hypercholesterolaemia. *Heart Lung Circ* 2023; 32: 769-779. 2023/04/04. DOI: 10.1016/j.hlc.2023.01.017.

276. Suzuki K, Yamamoto M, Hernandez-Benitez R, et al. Precise in vivo genome editing via single homology arm donor mediated intron-targeting gene integration for genetic disease correction. *Cell Res* 2019; 29: 804-819. DOI: 10.1038/s41422-019-0213-0.
277. Nakade S, Tsubota T, Sakane Y, et al. Microhomology-mediated end-joining-dependent integration of donor DNA in cells and animals using TALENs and CRISPR/Cas9. *Nat Commun* 2014; 5: 5560. DOI: 10.1038/ncomms6560.
278. Taleei R and Nikjoo H. Biochemical DSB-repair model for mammalian cells in G1 and early S phases of the cell cycle. *Mutat Res* 2013; 756: 206-212. 2013/06/25. DOI: 10.1016/j.mrgentox.2013.06.004.
279. Anzalone AV, Koblan LW and Liu DR. Genome editing with CRISPR–Cas nucleases, base editors, transposases and prime editors. *Nat Biotechnol* 2020; 38: 824-844. DOI: 10.1038/s41587-020-0561-9.
280. Anzalone AV, Randolph PB, Davis JR, et al. Search-and-replace genome editing without double-strand breaks or donor DNA. *Nature* 2019; 576: 149-157. 2019/10/22. DOI: 10.1038/s41586-019-1711-4.
281. Tajima T, Okada T, Ma XM, et al. Restoration of adrenal steroidogenesis by adenovirus-mediated transfer of human cytochromeP450 21-hydroxylase into the adrenal gland of21-hydroxylase-deficient mice. *Gene Ther* 1999; 6: 1898-1903. 1999/12/22. DOI: 10.1038/sj.gt.3301018.
282. Naiki Y, Miyado M, Horikawa R, et al. Extra-adrenal induction of Cyp21a1 ameliorates systemic steroid metabolism in a mouse model of congenital adrenal hyperplasia. *Endocr J* 2016; 63: 897-904. 2016/11/01. DOI: 10.1507/endocrj.EJ16-0112.
283. Perdomini M, Dos Santos C, Goumeaux C, et al. An AAVrh10-CAG-CYP21-HA vector allows persistent correction of 21-hydroxylase deficiency in a Cyp21(-/-) mouse model. *Gene Ther* 2017; 24: 275-281. 2017/02/07. DOI: 10.1038/gt.2017.10.
284. Markmann S, De BP, Reid J, et al. Biology of the Adrenal Gland Cortex Obviates Effective Use of Adeno-Associated Virus Vectors to Treat Hereditary Adrenal Disorders. *Hum Gene Ther* 2018; 29: 403-412. 2018/01/11. DOI: 10.1089/hum.2017.203.
285. Naiki Y, Miyado M, Shindo M, et al. Adeno-Associated Virus-Mediated Gene Therapy for Patients' Fibroblasts, Induced Pluripotent Stem Cells, and a Mouse Model of Congenital Adrenal Hyperplasia. *Hum Gene Ther* 2022; 33: 801-809. 2022/07/16. DOI: 10.1089/hum.2022.005.
286. Gotoh H, Sagai T, Hata J, et al. Steroid 21-hydroxylase deficiency in mice. *Endocrinology* 1988; 123: 1923-1927. 1988/10/01. DOI: 10.1210/endo-123-4-1923.
287. Vinson GP. Functional Zonation of the Adult Mammalian Adrenal Cortex. *Front Neurosci* 2016; 10: 238. 2016/07/06. DOI: 10.3389/fnins.2016.00238.
288. Alesci S, Ramsey WJ, Bornstein SR, et al. Adenoviral vectors can impair adrenocortical steroidogenesis: clinical implications for natural infections and gene therapy. *Proc Natl Acad Sci U S A* 2002; 99: 7484-7489. 2002/05/29. DOI: 10.1073/pnas.062170099.
289. Macapagal MC, Slowinska BS, Nimkarn S, et al. Gene therapy of 21-hydroxylase deficient mice utilizing an adeno-associated virus vector. *ENDO 2002: The Endocrine Society's 84th Annual Meeting*. San Francisco2002, p. 1-503.
290. Naiki Y and Fukami M. Letter to the Editor: "Congenital Adrenal Hyperplasia Due to Steroid 21-Hydroxylase Deficiency: An Endocrine Society Clinical Practice Guideline". *J Clin Endocrinol Metab* 2019; 104: 1926-1927. 2018/12/19. DOI: 10.1210/jc.2018-02529.
291. Chuman Y, Zhan Z and Fojo T. Construction of gene therapy vectors targeting adrenocortical cells: enhancement of activity and specificity with agents modulating the cyclic adenosine 3',5'-monophosphate pathway. *J Clin Endocrinol Metab* 2000; 85: 253-262. 2000/01/14. DOI: 10.1210/jcem.85.1.6244.
292. Hong SA, Seo JH, Wi S, et al. In vivo gene editing via homology-independent targeted integration for adrenoleukodystrophy treatment. *Mol Ther* 2022; 30: 119-129. 2021/06/01. DOI: 10.1016/j.ymthe.2021.05.022.
293. Bougnères P and Gao G. *Adeno-associated virus gene therapy for 21-hydroxylase deficiency*. 2019.
294. Cabanes-Creus M, Navarro RG, Zhu E, et al. Novel human liver-tropic AAV variants define transferable domains that markedly enhance the human tropism of AAV7 and AAV8. *Mol Ther Methods Clin Dev* 2022; 24: 88-101. 2022/01/04. DOI: 10.1016/j.omtm.2021.11.011.
295. Westhaus A, Cabanes-Creus M, Jonker T, et al. AAV-p40 Bioengineering Platform for Variant Selection Based on Transgene Expression. *Hum Gene Ther* 2022; 33: 664-682. 2022/03/18. DOI: 10.1089/hum.2021.278.
296. Westhaus A, Cabanes-Creus M, Rybicki A, et al. High-Throughput In Vitro, Ex Vivo, and In Vivo Screen of Adeno-Associated Virus Vectors Based on Physical and Functional Transduction. *Hum Gene Ther* 2020; 31: 575-589. 2020/02/01. DOI: 10.1089/hum.2019.264.

297. Eclov RJ, Lewis TEW, Kapandia M, et al. Durable CYP21A2 gene therapy in non-human primates for treatment of congenital adrenal hyperplasia. *ESGCT 27th Annual Congress In collaboration with SETGyc*. Barcelona, Spain: Hum Gene Ther, 2019, p. A1-A221.
298. Nakai H, Yant SR, Storm TA, et al. Extrachromosomal recombinant adeno-associated virus vector genomes are primarily responsible for stable liver transduction in vivo. *J Virol* 2001; 75: 6969-6976. 2001/07/04. DOI: 10.1128/JVI.75.15.6969-6976.2001.
299. Miao CH, Snyder RO, Schowalter DB, et al. The kinetics of rAAV integration in the liver. *Nat Genet* 1998; 19: 13-15. 1998/05/20. DOI: 10.1038/ng0598-13.
300. Adrenas. Trial Update from Adrenas Therapeutics, https://cahgenetherapy.com/news/jan24 (2024, accessed 31st March 2024).
301. Nakade S, Tsubota T, Sakane Y, et al. Microhomology-mediated end-joining-dependent integration of donor DNA in cells and animals using TALENs and CRISPR/Cas9. *Nat Commun* 2014; 5: 5560. 2014/11/21. DOI: 10.1038/ncomms6560.
302. Anzalone AV, Koblan LW and Liu DR. Genome editing with CRISPR-Cas nucleases, base editors, transposases and prime editors. *Nat Biotechnol* 2020; 38: 824-844. 2020/06/24. DOI: 10.1038/s41587-020-0561-9.
303. Greenway CV and Stark RD. Hepatic vascular bed. *Physiol Rev* 1971; 51: 23-65. 1971/01/01. DOI: 10.1152/physrev.1971.51.1.23.
304. Haudebourg T, Dos Santos C, Colle M, et al. Gene therapy for the severe virilizing forms of congenital adrenal hyperplasia using direct intra-adrenal injection of recombinant AAV vector encoding human CYP21. *10th Annual Congress of the French Society of Cell and Gene Therapy* Nantes, France: Hum Gene Ther, 2011, p. A1-A29.
305. Butler A, Hoffman P, Smibert P, et al. Integrating single-cell transcriptomic data across different conditions, technologies, and species. *Nat Biotechnol* 2018; 36: 411-420. DOI: 10.1038/nbt.4096.
306. Lopez JP, Brivio E, Santambrogio A, et al. Single-cell molecular profiling of all three components of the HPA axis reveals adrenal ABCB1 as a regulator of stress adaptation. *Sci Adv* 2021; 7: eabe4497. 2021/02/12. DOI: 10.1126/sciadv.abe4497.
307. Huang L, Liao J, Chen Y, et al. Single-cell transcriptomes reveal characteristic features of cell types within the human adrenal microenvironment. *J Cell Physiol* 2021; 236: 7308-7321. 2021/05/03. DOI: 10.1002/jcp.30398.
308. Hanemaaijer ES, Margaritis T, Sanders K, et al. Single-cell atlas of developing murine adrenal gland reveals relation of Schwann cell precursor signature to neuroblastoma phenotype. *Proc Natl Acad Sci U S A* 2021; 118: e2022350118. 2021/01/28. DOI: 10.1073/pnas.2022350118.
309. Altieri B, Secener AK, Sai S, et al. Cell Atlas at Single-Nuclei Resolution of the Adult Human Adrenal Gland and Adrenocortical Adenomas. Cold Spring Harbor Laboratory, 2022.
310. Neirijnck Y, Sararols P, Kuhne F, et al. Single-cell transcriptomic profiling redefines the origin and specification of early adrenogonadal progenitors. *Cell Rep* 2023; 42: 112191. 2023/03/03. DOI: 10.1016/j.celrep.2023.112191.
311. Suzuki T, Takahashi K, Darnel AD, et al. Chicken ovalbumin upstream promoter transcription factor II in the human adrenal cortex and its disorders. *J Clin Endocrinol Metab* 2000; 85: 2752-2757. 2000/08/18. DOI: 10.1210/jcem.85.8.6730.
312. Lasorella A, Benezra R and Iavarone A. The ID proteins: master regulators of cancer stem cells and tumour aggressiveness. *Nat Rev Cancer* 2014; 14: 77-91. 2014/01/21. DOI: 10.1038/nrc3638.
313. Brown D, Altermatt M, Dobreva T, et al. Deep Parallel Characterization of AAV Tropism and AAV-Mediated Transcriptional Changes via Single-Cell RNA Sequencing. *Front Immunol* 2021; 12: 730825. 2021/11/12. DOI: 10.3389/fimmu.2021.730825.

Chapter 2

Materials and Methods

2.1 Materials

2.1.1 Chemicals and reagents

Chemicals and reagents used in this project are listed (Table 2-1). All were of analytical grade or higher.

Table 2-1 Chemicals and reagents.

	Source
General	
Agar	Scharlau
Agarose	Meridian Bioscience
Ammonium acetate	Sigma-Aldrich
15N Ammonium chloride	Sigma-Aldrich
Ampicillin sodium salt	Astral Scientific
Benzonase	Sigma-Aldrich
Caesium chloride	Invitrogen
Calcium Chloride	Sigma-Aldrich
Chloroform	VWR
Chloroform:Isoamyl alcohol 24:1 (v/v)	Sigma-Aldrich
CutSmart Restriction Enzyme Buffer	New England Biolabs
Dimethylsulphoxide (DMSO)	Sigma-Aldrich
Disodium phosphate	Sigma-Aldrich
DNA Loading Buffer 6×	New England Biolabs
DNase I	Sigma-Aldrich
dNTPs 10 mM	Bioline
Dithiothreitol (DTT)	Sigma-Aldrich

Ethylenediaminetetraacetic acid (EDTA)	Chem Supply
Ethanol 100% (v/v)	EMSURE
Ethanol 70% (v/v)	POCD
Foetal bovine serum (FBS)	Bovogen Biologicals
Glycerol	Chem Supply
4-(2-hydroxyethyl)-1-piperazineethanesulfonic acid (HEPES)	Astral Scientific
Hydrochloric acid	Merck
Hyperladder 1 kb	Bioline
Hyperladder 50 bp	Bioline
Isopropanol	Univar
Kanamycin Sulphate	A. G. Scientific
Magnesium acetate	Sigma-Aldrich
Magnesium Chloride	Sigma-Aldrich
Methanol	POCD Healthcare
MyTaq Red Mix 2×	Bioline
N-acetyl-L-glutamate	Sigma-Aldrich
NEBuffer r2.1	New England Biolabs
Neutral buffered formalin 10% (v/v)	Sigma-Aldrich
Paraformaldehyde	Sigma-Aldrich
Phosphate buffered saline tablets	MP
Phenol:Chloroform:Isoamyl alcohol 25:24:1 (v/v/v)	Sigma-Aldrich
Polyethylene glycol (PEG) 800	Sigma-Aldrich
Protease Inhibitor Cocktail	Roche
Proteinase K	Roche
PureLink DNase	Invitrogen
PureLink RNase A	Invitrogen
Q5 High-Fidelity DNA Polymerase + Buffer	New England Biolabs
RedSafe Nucleic Acid Staining Solution	INtRON Biotechnology
Restriction Enzyme Buffer 3.1	New England Biolabs
Restriction enzymes	New England Biolabs
Sodium Chloride	Sigma-Aldrich
Sucrose	Chem Supply
T4 DNA ligase + Buffer	New England Biolabs
Taq DNA polymerase	New England Biolabs
ThermoPol Buffer	New England Biolabs
Trisaminomethane (Tris)	Chem Supply
Triton X-100	Sigma-Aldrich
Trizol Reagent	Ambion
Tryptone	Sigma-Aldrich
UltraPure H_2O	Sigma-Aldrich
Yeast Extract	Scharlau
β-mercaptoethanol	

Cell culture	
Dulbecco's Modified Eagle's Medium (DMEM)	Sigma-Aldrich
Iscove's Modified Dulbecco's Medium (IMDM)	Sigma-Aldrich
Phosphate Buffered Saline (PBS) without calcium and magnesium	Sigma-Aldrich
Trypan blue solution (0.4% w/v)	
Trypsin/EDTA 0.05% (v/v)	Sigma-Aldrich
Immunohistochemistry	
4'-6-Diamidino-2-phenylindole dihydrochloride (DAPI)	Sigma-Aldrich
Donkey serum	Sigma-Aldrich
Goat serum	Sigma-Aldrich
Immu-Mount	ThermoFisher
Tissue-Tek Optimal Cutting Temperature (O.C.T) Compound	Sakura
Tween 20	Sigma-Aldrich
qPCR, ddPCR and dPCR	
2 × TB Green Premix Ex Taq	TAKARA
QX200 EvaGreen Supermix	BioRad
3 × QIAcuity EvaGreen Mastermix	Qiagen
Pharmacological agents for mice	
Corticosterone	Sigma
Dexamethasone	Ilium Veterinary Products
Fludrocortisone	Sigma
Isoflurane	Abbott Australia
Water for injection	Baxter

2.1.2 Buffers and solutions

Prepared buffers and solutions are listed (Table 2-2). Solutions were made up in Milli-Q water unless otherwise stated. Solutions were stored at room temperature unless otherwise stated.

Table 2-2 Buffers and solutions.

	Composition
General	
Agarose gel	1% - 3% (w/v) Agarose in 1 × TBE
Ammonium acetate 10M	77 g ammonium acetate in 100 mL H2O. Filter through 0.22 µm membrane.

DNA lysis buffer	10 mM Tris-Cl (pH 8), 0.1 M EDTA (pH 8), 0.5% SDS
Genotyping digestion buffer	5 mM EDTA, pH 8, 200 mM NaCl, 100 mM Tris, pH 8, 0.2% sodium dodecyl sulfate (SDS)
LB Agar	LB media containing 1.5% (w/v) Bacto-agar. Autoclaved. Antibiotic added before use.
Lysis buffer	0.5% (v/v) Triton-X100, 10 mM HEPES, Protease Inhibitor Cocktail. Filter through 0.22 µm membrane.
Lysogeny broth (LB) media	1% (w/v) Bacto-tryptone, 0.5% (w/v) Bacto-yeast extract, 1% (w/v) NaCl. Autoclaved.
Paraformaldehyde (PFA) 4% (w/v)	4% (w/v) Paraformaldehyde powder in 1 × PBS. 40 g Paraformaldehyde powder per 1 L. Raise pH by dropwise addition of NaOH until clear solution is formed. Store at -20°C.
Phosphate Buffered Saline (PBS)	1 PBS (no Ca^{2+}, no Mg^{2+}) tablet per 100 mL milliQ H_2O
TBE 5×	54 g Tris base, 27.5 g Boric acid, 10 mM EDTA pH 8.0 in 1 L dH_2O. Dilute 1 in 10 for working solution containing 45 mM Trisborate, 1 mM EDTA.
TBE 1×	1 in 5 dilution of 5 × TBE in H_2O.
TE (10%)	Tris 0.061 g (final conc 1 mM,) EDTA 0.019 g (final conc 0.1 mM). Make to 500 mL with milliQ water after adjusting to pH 8. Autoclav.
Cell culture	
Growth Media	DMEM + 10% (v/v) heat-inactivated FBS. Filter through 0.22 µm membrane and keep sterile. Store at 4°C
Maintenance Media	DMEM + 2% (v/v) heat-inactivated FBS. Filter through 0.22 µm membrane and keep sterile. Store at 4°C
Transfection Media	IMDM + 10% (v/v) heat-inactivated FBS. Filter through 0.22 µm membrane and keep sterile. Store at 4°C
Viral production	
Benzonase Buffer	50 mM Tris and 2 mM $MgCl_2$ in H2O, pH pH 8.5. 0.22 µm filter.
Calcium chloride 1 M	1 M $CaCl_2$ in H_2O. Autoclave.
Calcium chloride 2 M	2 M $CaCl_2$ in H_2O. Autoclave.
Caesium Chloride solutions	1.5 g/mL or 1.37 g/mL or 1.3 g/mL CsCl in PBS. 0.22 µm filter.
Dialysis buffer	PBS supplemented with 0.1 g/L $CaCl_2$ and 0.1 g/L $MgCl_2$. Prepare fresh.

Dialysis buffer with Glycerol	PBS supplemented with 0.1 g/L $CaCl_2$, 0.1 g/L $MgCl_2$, and 5% (v/v) glycerol. Prepare fresh.
HEPES/EDTA resuspension buffer	50mM HEPES, 0.15M NaCl, and 25 mM EDTA in H_2O, pH 7.40. 0.22 µm filter.
HEPES-Buffered Saline (HBS) 2×	280 mM NaCl and 50 mM HEPES in H_2O, pH 7.10. Autoclave.
Na_2HPO_4 0.15 M	0.15 M Na_2HPO_4 in H_2O, pH 7.10. Autoclave.
PEG 40% (w/v) in 2.5 M NaCl	40% (w/v) Polyethylene glycol 800, 2.5 M NaCl in H_2O. 0.22 µm filter.
Transfection solution A (per 10 cm tissue culture dish)	15 µg Plasmid DNA, 62.5 µL 2 M $CaCl_2$ made up to 500 µL 10% TE
Transfection solution B (per 10 cm tissue culture dish)	54.5 mL 2× HBS, 550 µL 0.15 M Na_2HPO_4
Immunohistochemistry	
10% sucrose (w/v)	10% (w/v) sucrose in PBS. 0.22 µm filter. Store at 4°C.
20% sucrose (w/v)	20% (w/v) sucrose in PBS. 0.22 µm filter. Store at 4°C.
30% sucrose (w/v)	30% (w/v) sucrose in PBS. 0.22 µm filter. Store at 4°C.
ddPCR	
Alkaline digestion buffer	1.25 mL of 1 M NaOH, 20 µL of 0.5 M EDTA, 48.73 mL H_2O.
Neutralisation buffer	2 mL of 1 M Tris, 25 µL of Tween 20, make up to 50 mL with H2O. pH 5, store at 4°C.

2.1.3 Kits

Commercial kits used are listed (Table 2-3).

Table 2-3 Kits.

Item	**Source**
AllPrep DNA/RNA Micro kit	Qiagen
Isolate II Plasmid Mini Kit	Bioline
Mouse/Rat ACTH SimpleStep ELISA Kit	Abcam
NucleoBond Xtra Maxi Kit	Macherey-Nagel
NucleoBond Xtra Midi Kit	Macherey-Nagel
On-column PureLink DNase treatment	Invitrogen
pGEM-T Easy Vector System I	Promega
PureLink RNA Mini Kit	Invitrogen

QIAcuity EG PCR Kit	Qiagen
QIA Shredder Kit	Qiagen
Qubit BR dsDNA Assay Kit	Invitrogen
Superscript IV First Strand Synthesis System	Invitrogen
TURBO DNA-free Kit	Invitrogen
Wizard SV Gel and PCR Clean-Up System	Promega

2.1.4 Antibodies

Antibodies used for immunohistochemistry are listed (Table 2-4).

Table 2-4 Antibodies.

Primary	**Species**	**Source**	**Catalogue Number**	**Conjugate**	**Dilution**
Anti-CYP21A2	Rabbit	Abcam	ab230327	N/A	1:50
Anti-CYP11B1	Rabbit	Abcam	ab197908	N/A	1:50
Anti-GFP	Chicken	Aves Labs	GFP-1020	N/A	1:150
Secondary					
Anti-rabbit	Donkey	Invitrogen	A32754	AlexaFluor 594	1:500
Anti-rabbit	Donkey	Invitrogen	A32790	AlexaFluor 488	1:500
Anti-chicken	Goat	Abcam	ab150173	AlexaFluor 488	1:500

2.1.5 Bacterial strains

Bacterial strains used for propagation of plasmids are listed (Table 2-5).

Table 2-5 Bacterial strains.

Strain	**Genotype**	**Source**
DH5 α	F– φ80lacZΔM15 Δ(lacZYA-argF)U169 recA1 endA1 hsdR17(rK–, mK+) phoA supE44 λ–thi-1 gyrA96 relA1	Thermo Scientific
JM109	endA1, recA1, gyrA96, thi, hsdR17 (rk – , mk +), relA1, supE44, Δ(lac-proAB), [F′ traD36, proAB, laqI qZΔM15]	Promega

2.1.6 Plasmids

The plasmids used for cloning and transfection are listed (Table 2-6).

Table 2-6 Plasmids.

Plasmid	Description	Source
pGEM®-T Easy	TA cloning plasmid	Promega
pAd5	Adenovirus helper plasmid	AddGene[1]
pAAV8	Packaging plasmid for rAAV2/8	Dr James Wilson, University of Pennsylvania[2]
pAAVRh10	Packaging plasmid for rAAV2/Rh10	Dr James Wilson, University of Pennsylvania[3]
pAAV2-BB2.ApoEhAAT.hOTCco	Backbone plasmid	Dr Sharon Cunningham, CMRI
pAAV2-GS.CMV.hCYP21A2	Cloning plasmid containing CYP21A2 cDNA (GenBank accession no: NM_000500.9)	GenScript
pUC-GW.hCYP11B1	Cloning plasmid containing CYP11B1 cDNA (GenBank accession no: NM_000497.4)	GeneWiz
pUC-GW.mCyp21a1co_donor1	Cloning plasmid containing *Cyp21a1* cDNA (exons 2-10) that had been codon-optimized for mouse.	GeneWiz
pAAV2-BB2.ApoEhAAT.hCYP21A2	AAV2 plasmid encoding human *CYP21A2* under a liver-specific promoter	Constructed by candidate
pAAV2-BB2.ApoEhAAT.hCYP11B1	AAV2 plasmid encoding human *CYP11B1* under a liver-specific promoter	Constructed by candidate
pX601-AAV-CMV::NLS-SaCas9-NLS-3xHA-bGHpA;U6::BsaI-sgRNA	pX601 plasmid encoding SaCas9 and the sgRNA scaffold	AddGene[4]

pX601-AAV.CMV.SaCas9.U6.guide15.sgRNA	pX601 plasmid encoding SaCas9 and the sgRNA for guide 1	Constructed by candidate
pX601-AAV.CMV.SaCas9.U6.guide02.sgRNA	pX601 plasmid encoding SaCas9 and the sgRNA for guide 2	Constructed by candidate
pX601-AAV.CMV.SaCas9.U6.guide03.sgRNA	pX601 plasmid encoding SaCas9 and the sgRNA for guide 3	Constructed by candidate
pscAAV-HITIvectorBB	Self-complimentary HITI vector plasmid backbone	Dr Samantha Ginn, CMRI
pAAV2-HITI.mCyp21a1co_donor1	AAV2 plasmid encoding the codon-optimised *Cyp21a1* (exons 2-10) donor cassette for use with sgRNA guide 1	Constructed by candidate

2.1.7 Vectors

Vectors used or produced during this thesis are listed (Table 2-7).

Table 2-7 Recombinant AAV vectors.

Vector	Description	Chapter	Source
AAV8-CYP21A2	Caesium-purified CYP21A2 expression cassette with liver-specific promoter, packaged in AAV8	4.1 & 4.2	Produced by candidate
AAV8-CYP11B1	Caesium-purified CYP11B1 expression cassette with liver-specific promoter, packaged in AAV8	4.2	Produced by candidate
AAV Vector Testing Kit, n=67.	Iodixanol-purified barcoded GFP expression cassettes packaged in a variety of AAV variants	5	Translational Vectorology Research Unit, Children's Medical Research Institute (TVRU, CMRI). Extended kit

			based on previously described.[5]
AAV10-CMV.GFP	Iodixanol-purified GFP expression cassettes packaged in AAV10	5	Vector Genome Engineering Facility (VGEF), CMRI
AAV8-CMV.GFP	Iodixanol-purified GFP expression cassettes packaged in AAV8	5	VGEF, CMRI
AAVAnc80-CMV.GFP	Iodixanol-purified GFP expression cassettes packaged in AAVAnc80	5	VGEF, CMRI
AAVKP1-CMV.GFP	Iodixanol-purified GFP expression cassettes packaged in AAVKP1	5	VGEF, CMRI
AAVKP3-CMV.GFP	Iodixanol-purified GFP expression cassettes packaged in AAVKP3	5	VGEF, CMRI
AAVNP22-CMV.GFP	Iodixanol-purified GFP expression cassettes packaged in AAVNP22	5	VGEF, CMRI
AAVRh10-CMV.GFP	Iodixanol-purified GFP expression cassettes packaged in AAVRh10	5	VGEF, CMRI
AAVRh10-SaCas9-guide1	Caesium-purified SaCas9 and sgRNA 1 expression cassette, packaged in Rh10	6	Plasmid cloned by candidate, vector packaged by VGEF, CMRI
AAVRh10-SaCas9-guide2	Caesium-purified SaCas9 and sgRNA 2 expression cassette, packaged in Rh10	6	Plasmid cloned by candidate, vector packaged by VGEF, CMRI
AAVRh10-SaCas9-guide3	Caesium-purified SaCas9 and sgRNA 3 expression cassette, packaged in Rh10	6	Plasmid cloned by candidate, vector packaged by VGEF, CMRI
AAVRh10-Cyp21a1.donor1	Caesium-purified codon optimized splice acceptor and Cyp21a1 exons 2-10, packaged in Rh10	6	Plasmid cloned by candidate, vector packaged by VGEF, CMRI

Abbreviations: VGEF, Vector Genome Engineering Facility; CMRI, Children's Medical Research Institute.

2.1.8 Primers

Primers used for PCR and sequencing are listed (Table 2-8).

Table 2-8 PCR and sequencing primers.

Primer Name	Direction	Sequence 5' to 3'	Description/target
Plasmid cloning			
LGcons1_004	Reverse	TATGATATCTCACTGGCTCTGGCCCGGGCTG	Amplify *CYP21A2* cDNA fragment from GeneScript plasmid. Add stop codon and EcoRV site 3' to *CYP21A2*
LGcons1_007	Forward	TATGATATCGCGGCCGCGCCACCATGCTGCTCCTGGG	Amplify *CYP21A2* cDNA fragment from GeneScript plasmid Add EcoRV and NotI sites 5' to *CYP21A2*
Titre allocation			
VG0057_bGH pA F	Forward	GCCTTCCTTGACCCTGGA	Bovine growth hormone polyA (ddPCR)
VG0058_bGH pA R	Reverse	ACTCAGACAATGCGATGCAA	
Genotyping			
LG_22	Forward	ACCACCCTGAGGTGCACT	Genotyping wild-type allele
LG_23	Reverse	GGGAGATTGATGCCAGCATAAG	
LG_34	Reverse	TCCTTGGGGATGTCATAGCCA	Genotyping mutant allele
LG_35	Forward	TCACCATCCTGAAGTGCACC	
Vector detection and quantification			
ddP_02F	Forward	TACCTCACCTTCGGAGACAA	*CYP21A2* target for vector copy number

ddP_04R	Reverse	CCACGATGTGATCCCTCTTC	(ddPCR) and *CYP21A2* expression (qPCR)
ddP_08F	Forward	TGTGGAAGGAGCACTTTGAG	*CYP11B1* target for vector copy number (ddPCR) and *CYP11B1* expression (qPCR)
ddP_08R	Reverse	CCCTGCAGTGAGTTCCATAG	
LB0042mouse ALB_F	Forward	AACTGCTACTCCCCTCCTAC	Murine albumin target for vector copy number normalisation (ddPCR and dPCR)
LB0042mouse ALB_R	Reverse	TTTACCCCAGTGCAGGAAAG	
SG330F	Forward	GATTCGACGTGTACCTGGAC	SaCas9 target for vector copy number (dPCR)
SG331R	Reverse	CGTTGTTGTAGAAGGAGGCG	
ddP_107	Reverse	TTCACGATGTGGTCCCTAGA	Codon-optimised murine *Cyp21a1* exons 5 and 6 target for vector copy number (dPCR)
ddP_108	Forward	GGAGCATTCAGATCCTGACC	
ddP_103	Reverse	CCTCGATGGTCCTATTGCTG	Target codon-optimised *Cyp21a1* exon 2 in donor template (dPCR)
ddP_104	Forward	CATCTACAGGATCCGCTTGG	Target native *Cyp21a1* exon 1 (dPCR)
ddP_112	Forward	GGGAAGACAATAGCAGGCAT	Target bovine growth hormone polyA in donor vector (dPCR)
ddP_115	Reverse	ATTTAGCATATGGGGTCGGC	Target native *Cyp21a1* exon 2 (dPCR)
Gene expression			
SG 381F	Forward	TACAGCGGAGCAACTGAAGA	Murine albumin expression for normalization (qPCR)
SG 382R	Reverse	TTGCAGCACAGAGACAAGAA	
LG_102F_tbp	Forward	CCCTTGTACCCTTCACCAATGAC	*Tbp* expression for normalization (qPCR and dPCR)
LG_103R_tbp	Reverse	TCACGGTAGATACAATATTTTGAAGCTG	
LG_104F_ren	Forward	CTCTGGGCACTCTTGTTGCT	*Ren1* expression (qPCR)

LG_105R_ren	Reverse	AGAAGGCATTTTCTTGAGCG	
LG_100F_mc2r	Forward	TTTCTCAGTCATCTTGCCGA	*Mc2r* expression (qPCR)
LG_101R_mc2r	Reverse	ATGCTCCTCTCCTTGGCTTT	
LG_029	Forward	ACAGGAACCGAATGCAGCTG	Wild-type murine *Cyp21a1* expression (qPCR)
LG_039	Reverse	CTTAGGGATGTCATAGCCGG	
LG_120F_11b2	Forward	GAGACGTGGTGTGTTCTTGC	*Cyp11b2* expression (qPCR)
LG_121R_11b2	Reverse	TCCCTTGCTACCATGTCCAC	
Barcode recovery and sequencing			
WPRE R	Reverse	GGATTTATACAAGGAGGAGAAAATGAAAG	WPRE gene-specific reverse primer. For cDNA synthesis from mRNA extracted from tissue treated with AAV barcode kit
NGS-R	Reverse	CAACATAGTTAAGAATACCAGTCAATCTTTCACAAATTTTGTAATCCAGAGG	Universal reverse primer for barcode amplification.
BC_00xx_GFP-BC_0x	Forward	NNNNNGCTGGAGTTCGTGACCGCCG	Barcoded forward primer for barcode amplification. Primer itself is also barcoded to allow cohorting multiple samples in one tube for NGS. Primer barcode sequences and primers numbers are detailed in Table 5-2.
Sequencing			
LG_008	Reverse	TGACCACAAGCTACCAAGGA	Murine *Cyp21a1* intron 2
LG_009	Reverse	AAGAGGAAGAGGAGCCATCG	Murine *Cyp21a1* intron 2
LG_011	Forward	GGGACTGTGCCAATGTGAAA	Murine *Cyp21a1* 5’ UTR

2.1.9 Mouse strains

The C57BL/10SnSlc-H-2^{aw18} mouse model was kindly provided by Toshihiko Shiroishi (National Institute of Genetics) and the RIKEN BRC through the National BioResource Project of the Ministry of Education, Culture, Sports, Science and Technology, Japan. The H-2^{aw18} mouse model has 21-hydroxylase deficiency, which is neonatally lethal.[6] Heterozygous (H-2$^{b/aw18}$; *Cyp21a1*$^{+/-}$) mice were bred to produce homozygous (H-2^{aw18}, *Cyp21a1*$^{-/-}$) offspring. Heterozygous (*Cyp21a1*+/-) and wild-type (*Cyp21a1*+/+) littermates were also used in some experiments, where specified.

2.2 Methods

2.2.1 Molecular biology

2.2.1.1 Plasmid DNA purification

2.2.1.1.1 Small-scale plasmid purification

A commercially available miniprep kit (Isolate II Plasmid Mini Kit) was used for small scale plasmid DNA purification (up to 20 µg) from bacterial clones. Briefly, single bacterial colonies were selected from LB/antibiotic agar plates and inoculated into 2 mL LB media with the relevant antibiotic (100 µg/mL ampicillin or 50 µg/mL kanamycin). Cultures were incubated at 37°C overnight in a shaking incubator (225 rpm, shaking orbit 19 mm). One millilitre of culture was pelleted in a 1.5 mL Eppendorf by centrifugation at 14 000 × *g* for 1 minute. Plasmid DNA was isolated from the bacterial pellet according to manufacturer's instructions. The remaining 1 mL culture was used to inoculate large cultures.

2.2.1.1.2 Large-scale plasmid purification

Large scale isolation of transfection-grade plasmid DNA was performed using Nucleobond Xtra Midi or Maxi kits (Macherey-Nagel, Germany) for up to 500 µg or 2000 µg DNA per column, respectively, according to the manufacturer's instructions. Single colonies were inoculated into 2 mL LB/antibiotic medium and grown at 37ºC in a rotary shaking incubator (225 rpm, shaking orbit 19 mm) over 6 hours or overnight. If required, 1 mL of this starting culture was used for small-scale plasmid purification (Section 2.2.1.1.1) to confirm the identity of the plasmid being propagated. The remaining 1 mL of culture broth was then used to inoculate a large culture flask containing LB broth (200 mL for midiprep, 400-500 mL for maxiprep) and the relevant antibiotic. Cultures were incubated overnight at 37ºC in a rotary shaking incubator (225

rpm, shaking orbit 19 mm). The bacteria were pelleted by centrifugation at 5660 ×g for 15 min. The DNA was then extracted immediately, or the pellet stored at -20ºC. DNA was purified as per the manufacturer's instructions.

2.2.1.2 Restriction enzyme digestion

Restriction enzymes reactions were preformed using the manufacturers recommended enzyme buffer for highest enzyme activity.

2.2.1.3 Agarose gel electrophoresis

Gel electrophoresis was performed to separate DNA bands according to size. Agarose gel was prepared (Table 2-2) and 5 µL/100 mL RedSafe Nucleic Acid Staining Solution (INtRON Biotechnology) was added before the gel was set. Each sample had 6 × DNA loading buffer (New England Biolabs) added before loading into gel wells. Gels were run at 80-100 volts.

2.2.1.4 Purification of PCR fragments from agarose gels

PCR fragments were purified from agarose gel using the Wizard Gel DNA Purification kit as per manufacturer's instructions. The excised DNA bands were dissolved in membrane binding solution (10 µL solution per 10 mg gel) at 50-65°C. The dissolved mixture was transferred to the SV minicolumn and incubated at room temperature for 1 min before centrifugation at 16 000 × *g* for 1 min. 700 µL membrane wash solution was added to the column which was then centrifuged at 16 000 × *g* for 1 min. This was repeated with 500 µL membrane wash solution for 5 min. The empty column was then centrifuged at 16 000 × *g* for 2 min with the lid open to allow any residual ethanol to evaporate. The minicolumn was transferred to a 1.5 ml Eppendorf tube and 35-50 µL (depending on expected yield) DNAse-free water was added to the tube before

incubation at room temperature for 1 min and then centrifugation at 16 000 × *g* for 2 min. The purified DNA was then stored at -20°C.

2.2.1.5 A-Tailing DNA fragments

The addition of an adenosine base to the 3' end of a DNA fragment is known as A-tailing. This was performed using 1 µL Taq DNA polymerase, 1 µL ThermoPol buffer 10×, 1 µL dATP (10 mM) and purified PCR product, made up to 10 µL reaction. The reaction was incubated at 72°C for 1 hour before proceeding to ligation.

2.2.1.6 DNA ligation

Ligation reactions were calculated at a ratio of 3:1, using the following formula:

$$\frac{x \text{ (ng of backbone)} \times y \text{ (kb insert)}}{w \text{ (kb backbone)}} \times 3 = z \text{ (ng insert)}$$

The relevant quantities of insert and backbone DNA fragments were added to 1 µL T4 DNA ligase buffer (10×) and 1 µL T4 DNA ligase and made up to 10 µL. The reaction was incubated at 4°C overnight and heat inactivated at 65°C for 20 min the following day. The ligation product was then used to transform bacteria (see Section 2.2.1.7)

2.2.1.7 Bacterial transformation

Plasmid DNA (3 µL) was added to 40 µL thawed DH5α cells and incubated on ice for 10-15 min. The bacteria were then heat-shocked at 42°C for 45-50 seconds to permit entry of the plasmid into the cells. The cells were incubated on ice for 2 min before 1 mL LB broth was added and then incubated at 37°C on the shaking incubator (225 rpm, shaking orbit 19 mm) for approximately 1 hour to facilitate bacterial growth. The transformation liquid was then plated onto agar plates embedded with the appropriate antibiotic, dried and incubated at 37°C overnight.

2.2.1.8 Glycerol stock

Culture broth was mixed with autoclaved glycerol to make up 25% of the volume, and stored at -80°C.

2.2.2 Cell culture

Culture of human embryonic kidney (HEK-293) cells was performed using aseptic technique within a Class II biohazard safety cabinet. Cells were cultured in disposable plastic flasks and dishes (Corning) and maintained at 37°C in a 5% CO_2 humidified incubator. Cell growth media, transfection media, and maintenance media (Table 2-2), washing buffers (1 × PBS), and dissociation agents (Trypsin) were warmed to 37°C in a water bath prior to contact with cells.

Adherent cells were passaged by aspirating to remove old media, washed with 10 mL PBS without magnesium and calcium, then incubated for 10 min at 37°C with 0.05% (v/v) Trypsin/EDTA (Sigma-Aldrich) to dissociate cells. After incubation, cells were manually agitated to facilitate lifting from flask surface and complete dissociation. Brightfield microscopy was used to confirm no cells remained adhered. Ten millilitres of growth media (or other appropriate media) was added to cells which were mixed by pipetting. The desired amount of cell suspension was seeded into a new tissue culture flask, usually split with a 1:10 dilution, with appropriate growth media. Cells were passaged again at 80% confluency. If required, cells were counted with a haemocytometer using Trypan Blue uptake to identify non-viable cells.

2.2.3 Viral vector production

2.2.3.1 Triple transfection

Vectors were packaged by triple transfection and purified by caesium chloride gradient as previously described.[7, 8] HEK293 cells were passaged and seeded at approximately 4.7 $\times 10^6$ cells per 10 cm diameter tissue culture dish on day 1 in Growth media (see Table 2-2). The following day, the media was changed to Transfection media, 1.5 to 2 hours before transfection. Triple plasmid transfection (3 µg vector plasmid, 3 µg capsid plasmid and 9 µg pAd5 [helper plasmid] per dish) was performed with the calcium phosphate method. Aliquots of 2 mL of Solution A was added slowly to 2 mL aliquots of solution B to precipitate DNA (Table 2-2). The mixtures were incubated for 15-20 min at room temperature and then added to cells at 1 mL per dish. The cells were incubated with the DNA mixture at 37°C overnight. On day 3 the media was changed to Maintenance media before harvest on day 4. Cells were scraped and pelleted at 530 ×*g* at 20°C for 10 min. The cell pellet was resuspended in benzonase buffer and stored at -80°C (freeze 1).

2.2.3.2 Caesium chloride gradient purification

The cells in benzonase buffer underwent three freeze/thaw cycles to lyse the cells. After the third thaw, Benzonase enzyme was incubated with the mixture at 37°C for 1 hour before centrifugation at 3500 × *g* for 10 min at 4°C to pellet cell debris. The supernatant was transferred to a new 50 mL Falcon tube. 1/39th of the volume of the supernatant of 1 M $CaCl_2$ (for 25 mM $CaCl_2$ final concentration) was added, and the mixture was incubated on ice for 1 hour. The mixture was then centrifuged at 3000 ×*g* for 30 min at 4°C. The supernatant was collected and ¼ this volume was added as 40% PEG 8000/NaCl. The mixture was incubated on ice at 4°C overnight. The following morning it was centrifuged at 3000 ×*g* for 30 min at 4°C. The supernatant was removed and the

pellet resuspended in 20 mL NaHepes/EDTA resuspension buffer by rotating the tube at 4°C overnight.

The following day, 12 mL of 1.3 g/mL CsCl in PBS was added to an Ultra-Clear Centrifuge Tube (BeckmanCoulter, Cat# 344058). 5 mL of 1.5 g/mL CsCl in PBS was then added to the bottom of the tube creating an interface between the two densities. 20-22 mL vector suspension was added to the top. The tubes were centrifuged at 106 800 ×*g* at 20°C for at least 24 hours. The vector band was collected by puncturing the tube below the visible virus band with an 18 G needle and the vector was collected with a 10 mL syringe. The clear contents of the tube was removed but the protein layer was left. The removed contents contained both empty and full vector particles. The collected vector was loaded into a 12 mL Ultra-Clear Centrifuge Tube (BeckmanCoulter, Cat# 344059) and topped up with 1.37 g/mL CsCl in PBS. It was then centrifuge at 247 600 ×*g* at 20°C for at least 24 hours. The vector was collected in 1 mL fractions using an 18 G needle to puncture the tube then slowly drip out the vector. qPCR was then utilized to determine which fraction/s contained vector: 2 µL from each fraction was diluted in 1 mL water for use in the qPCR. Primers to bovine growth hormone were used (Table 2-8). 10 µL Takara SYBR green 2×, 1 µL of each 10 µM primer and 5 µL diluted template was made up to 20 µL per reaction with water. The qPCR conditions were 95°C for 30 seconds; 35 cycles of 95°C for 5 seconds, 58°C for 15 seconds, 72°C for 20 seconds; and then ramp from 60-99°C to melt holding for 5 seconds for each step. The three to four fractions with the highest titre determined by qPCR were then pooled for the remaining steps. An appropriately sized dialysis cassette (Slide-A-Lyzer Gamma Irradiated Dialysis Cassette Extra-Strength, Thermo Scientific) was pre-wet with dialysis fluid and loaded with the pooled fractions. The vector was dialysed in 4 L

dialysis fluid overnight at 4°C, over the day in a fresh batch of the same dialysis fluid and then overnight in dialysis fluid that contained glycerol. The vector was then collected and concentrated by centrifugation in a Vivaspin 20 100,000 molecular weight cut-off (Satorius) at 3700 × *g* to achieve a final volume of 300µL-800µL. The final purified vector was stored at 4°C or -80°C.

2.2.3.3 Determining titre

Titre was determined using digital droplet PCR (C1000 Touch™ Thermal Cycler #1851196 and QX200 Droplet Reader #1864003, BioRad) using primers specific for the bovine growth hormone polyadenylation tail signal (Table 2-9) with QX200™ ddPCR™ EvaGreen Supermix (BioRad 1864034). The conditions were 95°C for 5 min, forty cycles of 95°C for 30 seconds and 60°C for 1 min, followed by 4°C for 5 min, 90°C for 5 min.

2.2.4 Animal procedures

All animal care and experimental procedures were evaluated and approved by the joint Children's Medical Research Institute and The Children's Hospital at Westmead Animal Care and Ethics Committee (Project C381). The C57BL/10SnSlc-H-2^{aw18} mouse model was kindly provided by Toshihiko Shiroishi (National Institute of Genetics) and the RIKEN BRC through the National BioResource Project of the Ministry of Education, Culture, Sports, Science and Technology, Japan.[6] Mice were housed in the Bioresources Facility of the Children's Medical Research Institute. Animals were maintained with 12-hour light/dark cycles with free access to standard mouse chow and water.

2.2.4.1 Treatment for homozygous mutant survival

The H-2^{aw18} mouse model has 21-hydroxylase deficiency, which is neonatally lethal.[6] Heterozygous (H-2$^{b/aw18}$; *Cyp21a1*$^{+/-}$) mice were bred to produce homozygous (H-2^{aw18}, *Cyp21a1*$^{-/-}$) offspring. Exogenous steroid rescue was required for survival of the homozygous offspring. Dams were examined daily to determine the presence of a vaginal plug, indicating day E0.5. All dams received 5 µg of dexamethasone (Ilium Dexason, Troy Animal Healthcare) subcutaneously daily from day E18 until the birth. Day E19 was the most common day of delivery in this colony. All pups received 10 µg corticosterone and 0.05 µg fludrocortisone subcutaneously from birth second daily until 3 weeks of age. Once genotype was available, steroid treatment was ceased prior to 3 weeks of age in non-homozygous pups. Adrenalectomized adult rats can survive with salt supplementation alone,[9] so dams with unweaned offspring and weaned *Cyp21a1*$^{-/-}$ mice were provided with rock salt three times per week. *Cyp21a1*$^{-/-}$ pups were weaned to small groups with other *Cyp21a1*$^{-/-}$ animals from the same litter or a single non-homozygous littermate to avoid resource competition.

2.2.4.2 Genotyping

2.2.4.2.1 Genomic DNA extraction from murine tissue for genotyping

Genotype was determined using a PCR-based assay with genomic DNA from toe removal during identification at 9 days of age. Toes were stored at -20°C until use. A rapid DNA extraction technique was used.[10] Essentially, 300 µL of genotyping digestion buffer and 6 µL proteinase K was added to each tube (aiming for final concentration of proteinase K 0.4 mg/mL buffer). The tubes were then vortexed and incubated overnight at 55°C. One millilitre of 100% ethanol was added to each tube and mixed gently. The tubes were centrifuged at 16 000 × *g* for 30 min at room temperature. The fluid was poured out of the tube and 1 mL of 70% ethanol was added, followed by

centrifugation at 16 000 × *g* for 20 min. Again, the fluid was poured out of the tube. 200 µL of 10% TE was then added to tube. The Eppendorf lids were left open to allowed excess ethanol evaporation for 2 hours at 55°C and then samples were stored at 4°C for immediate use or -20°C for later use.

2.2.4.2.2 Genotyping PCR

The genotyping PCR reaction components and conditions are shown (Table 2-9).

Table 2-9 Reaction components and conditions for genotyping PCR

	Wild-type allele (µL)	**Mutant allele (µL)**
MyTaq Red 2×	10	10
Primer LG_022 10 µM	1	-
Primer LG_023 10 µM	1	-
Primer LG_034 10 µM	-	1
Primer LG_035 10 µM	-	1
Water	6	6
DNA template	2	2
Total	**20**	**20**

The wild-type band is expected to be 832 bp, and the mutant band is expected to be 474 bp. The reaction conditions were 95°C 120sec; 35 cycles of 95°C 20 sec, 60°C 30 sec, 72°C 120 sec; 72°C 80 sec.

2.2.4.3 Minimally invasive conscious procedures

2.2.4.3.1 Dried blood spot collection from mandibular vein

Whole blood was collected on filter paper from the submandibular vein between 2 – 4 pm. Mice were restrained by hand and a 25-guage needle was used to puncture the mandibular vein. Blood was collected onto filter paper and haemostasis was ensured before mice returned to cage. Filter paper was dried overnight and then stored at 4°C[11] in a light protected, airtight bag with moisture absorbing crystals.

2.2.4.3.2 Intravenous injection via tail vein.

rAAV vector was diluted in sterile saline for injection to a total volume of 150 µl per mouse. Adult *Cyp21a1*$^{-/-}$ mice were warmed under a lamp to vasodilate the tail vein and then placed in a restrainer. The injection site was cleaned with alcohol and received the relevant vector intravenously via the lateral tail vein using a 29-gauge 1 mL syringe (BD Ultra-Fine Insulin Syringe, Becton Dickinson, USA). Haemostasis was ensured with gentle pressure to the site. Tail vein injections were performed by Cindy Zhu, Gene Therapy Research Unit, Children's Medical Research Institute.

2.2.4.4 Terminal sample collection and storage

After the specified treatment interval, treated and control animals were harvested between 2-4 pm if steroid profiles were to be part of the analysis, or at any time during the day if no steroid analysis was required. The same method was used to harvest untreated *Cyp21a1*$^{-/-}$ and wild-type (H-2^{b}, *Cyp21a1*$^{+/+}$) controls. The mice were deeply anaesthetised using isofluorane (5% v/v for induction in box, 3-5% v/v for maintenance via nose cone) to facilitate open cardiac puncture for blood collection. Blood was collected on filter paper and the remaining spun down to collect serum which was aliquoted and stored at -80°C until analysis. Dried whole blood on filter paper was dried overnight at room temperature, then stored in an airtight bag at 4°C. Following exsanguination, the animal was terminated with cervical dislocation and tissues harvested.

The adrenal glands were harvested first, and fat dissected away using 25-guage needles and a dissection microscope. Adrenal glands were either snap frozen or fixed in 4% PFA or 10% NBF. Liver was excised and small pieces were fixed in 4% PFA or 10%

NBF or snap frozen in liquid nitrogen. Other tissues that were collected were snap frozen in liquid nitrogen.

2.2.5 Analysis of animal samples

2.2.5.1 Microscopy

2.2.5.1.1 Immunohistochemistry

Adrenal glands and liver were fixed in overnight in 4% PFA. Following PFA fixation, tissue was dehydrated using a sucrose gradient. Tissue was then dried and placed in Tissue-Tek Cryomold Intermediate (Sakura) plastic cassette in Tissue-Tek Optimal Cutting Temperature (O.C.T) Compound (Sakura). Cassettes were snap-frozen in isopentane on the vapour-phase of liquid nitrogen then stored at -80°C.

2.2.5.1.1.1 Cryosectioning

Tissue blocks were incubated at -20°C for 20 min prior to sectioning and transported on dry-ice when removed from -20°C. Five µm and eight µm sections of PFA-fixed cryo-preserved liver and adrenal gland, respectively, were cut using a Leica Cryostat onto Menzel-Gläser Superfrost Plus Microscope Slides (Thermo Scientific). Slides with cut sections were stored at 4°C prior to staining.

2.2.5.1.1.2 Immunohistochemistry staining

Slides were washed in PBS for 5 min. Samples were permeablise in ice cold methanol for 20 min at -20°C, followed by 0.1% triton X-100 in PBS for 20 min. They were then washed in PBS for 5 min, then twice in 2% FBS in PBS for 5 min each. Slides were blocked with relevant blocking buffer (eg 10% donkey serum and 10% FBS in PBS) for 60 min at room temperature. They were then washed with 0.1% Tween-20 in PBS for 10 min. The primary antibody was incubated with the sections at 4°C overnight. The following day, slides were washed with 0.1% Tween-20 in PBS for 1 min, 5 min, 10

min and 15 min. Slides were then incubated with secondary antibody for 60 min at room temperature (light protected). The slides were washed with 0.1% Tween-20 in PBS three times for 5 min each then rinse in PBS. Next, 15 µL of 2 µg/mL DAPI was diluted in 50 mL PBS and incubated for 5 min. Slides were rinsed and dried and topped with coverslip. Stored at 4°C light protected. Slides were imaged with Zeiss Axio Imager M1 and A1 microscopes. Zeiss ZEN 3.8 software was used for microscope setup, capture, and image processing.

2.2.5.1.2 Histopathology

Adrenal glands were fixed in 10% NBF for 24 hours. Liver was fixed for 48 hours in 10% NBF. Haematoxylin and eosin slides were prepared by Li Ma, Histology Facility, The Westmead Institute for Medical Research (WIMR).

2.2.5.2 Blood profiles

2.2.5.2.1 Serum steroids

Serum steroids were analysed at the Endocrinology Laboratory, The Children's Hospital at Westmead by Dr Sundar Koyyalamudi. The steroid calibrators, controls and isotopically labelled Internal standard mix were obtained from Chromsystems Instruments & Chemicals Gmbh, Germany. The Optima LC-MS grade solvents including water, methanol, methyl t-butyl ether, acetonitrile and formic acid were obtained from Fisher Chemicals, UK. Internal standard solution was added to calibrators, controls and test samples and organic solvents were used for extraction. The extract supernatants were evaporated to dryness under nitrogen in a 37°C water bath. After evaporation, the extracted steroids were reconstituted in 50% methanol. Steroids were analysed by Ultra Performance Liquid Chromatography-Tandem Spectrometry (UPLC-MSMS) using validated in-house developed methods (Waters Acquity UPLC and Xevo TQ-S mass spectrometer).

2.2.5.2.2 Dried whole blood corticosterone

Dried whole blood corticosterone was analysed at the Newborn Screening Laboratory, The Children's Hospital at Westmead by Tiffany Wotton and Dinah Sung. The dried blood spot samples were collected on to filter paper and were extracted using an organic solvent (95% methanol) containing deuterated internal standards for each steroid. Whole blood corticosterone was measured using Liquid Chromatography Tandem Mass spectrometry (Waters Xevo TQ-S with Acquity UPLC system).

2.2.5.2.3 Serum ACTH

ACTH was measured after thawing snap frozen serum using the Mouse/Rat ACTH SimpleStep ELISA Kit as per manufacturer instructions (Ab263880, Abcam).

2.2.5.3 Genomic DNA extraction from tissue

A standard phenol-chloroform DNA extraction method was used. 400 µL DNA lysis buffer (Table 2-2) was added to a 1.5 mL Eppendorf containing the tissue sample and the tissue was homogenised. The appropriate amount of proteinase K (e.g. 2 µL for adrenal gland, 5 µL for liver sample) (stock 20 mg/mL) was added and the samples were incubated overnight at 57°C. 5 µL RNAse A (stock 20 mg/mL) was added and incubated for 1 hour at 37°C. Following this, 400 µL phenol:chloroform/isoamyl alcohol was added to the tube which was inverted for 10 minutes. The tubes were then centrifuged at 16 000 × *g* for 10 minutes. The aqueous phase was collected and again 400 µL phenol:chloroform/isoamyl alcohol was added, repeating the previous steps. Once the aqueous phase was collected for the second time, 0.25 times the sample volume of 10 M ammonium acetate (aiming for final concentration of 2 M) was added. And then 2 to 2.5 times the sample volume of 100% ethanol was added. The tube was then shaken vigorously by hand. The tubes were incubated at -20°C for at least 30 min (the protocol could be paused here if required and the tubes stored at this point). Next,

then tubes were centrifuged at 4°C for 30 min at maximum speed. The liquid was poured out and 1 mL 70% ethanol was added. The tubes were centrifuged at maximum speed for 10 min at room temperature. The liquid was removed and the tubes allowed to air dry for 2 min. The DNA pellets were then resuspended in appropriate amount of 10% TE and stored at 4°C overnight and then -20°C.

2.2.5.4 RNA extraction

Samples were homogenised in 300uL Trizol and then transferred to QIAshredder spin column and used as per manufacturer's instructions. The flow through was transferred to a new tube. 700uL Trizol was added and the samples were incubated for 5 min at room temperature. Choroform (200uL) was added and the tubes were shaken vigorously by hand for 15 seconds, followed by incubation at room temperature for 3 min. The samples were centrifuged at 12 000 × *g* for 15min at 4°C. The upper phase (contained RNA) was transferred to a fresh tube. At this point the Invitrogen Purelink RNA mini kit protocol was commenced as per manufacturer's instructions. DNase treatment was performed on-column as per manufacturer's instructions. The RNA was aliquoted and stored at -80°C.

2.2.5.4.1 cDNA synthesis

SuperScript IV First-Strand Synthesis System was used to synthesize cDNA as per manufacturer's instructions with Oligo $d(T)_{20}$ primer, unless otherwise specified in chapter-specific methods. Two µL of 50 µM Oligo $d(T)_{20}$ primer and 2 µL 40 mM dNTP mix was added to 500 ng RNA and made up to 20 µL per reaction to anneal the primer to the RNA template. This RNA mix was incubated at 65°C for 5 minutes then cooled on ice for at least 60 seconds. For reverse transcription, 4 µL of SuperScript IV buffer (5×), 1 µL 100 mM DTT, 1 µL ribonuclease inhibitor, and 1 µL SuperScript IV Reverse Transcriptase (RT+) and 10 µL of the annealed RNA was made up to 20 µL.

For the RT- reaction, the same volume of SuperScript IV buffer (5×), 100 mM DTT, ribonuclease inhibitor, and annealed RNA were made up to 20 µL without Reverse Transcriptase. Both reactions were incubated at 55°C for 10 min and 80°C for 10 min and stored at -20°C.

2.2.5.5 Genomic DNA and RNA quantification

DNA and RNA concentrations were determined by spectrophotometry using a Nanodrop 1000 (Thermo Scientific). Sample purity was estimated by A260/A280 and A260/A230 absorbance ratios. When increased accuracy was required, for example when preparing samples for ddPCR or dPCR, the Qubit dsDNA BR Assay Kit (Invitrogen) with the Qubit 4 Fluorometer (Invitrogen) was used. Samples and standards were prepared according to manufacturer directions.

2.2.5.6 Digital droplet PCR (ddPCR)

Genomic DNA was extracted from frozen tissue using a standard phenol-chloroform extraction method. It was digested with restriction enzyme HindIII-HF (New England BioLabs R3104L). Vector copy number (vcn) was determined using digital droplet PCR (C1000 Touch™ Thermal Cycler #1851196 and QX200 Droplet Reader #1864003, BioRad) using relevant primers (Table 2-8) with QX200™ ddPCR™ EvaGreen Supermix (BioRad 1864034). The conditions were 95°C for 5 min, forty cycles of 95°C for 30 seconds and 60°C for 1 min, followed by 4°C for 5 min, 90°C for 5 min. The vector count was normalised to two copies of murine albumin to determine vcn/diploid nucleus.

2.2.5.7 Digital PCR (dPCR)

Genomic DNA or cDNA synthesised from RNA was used. DNA was digested with restriction enzyme EcoRV at 37°C for two hours, and then inactivated at 72°C for 10

minutes. The digital PCR Qiagen Quick-Start protocol was run on the digital PCR machine QIAcuity One, 5plex Device (#911021, Qiagen) as per the manufacturer's instructions (QIAcuity® EG PCR Kit, Qiagen). The conditions were 95°C for 2 min, forty cycles of 95°C for 15 seconds, 60°C for 15 seconds, and 72°C for 15 seconds, followed by 40°C for 5 min. Imaging conditions were 500 ms exposure and gain of 6. Vector copy was normalised to two copies of murine albumin to determine vcn/diploid nucleus. Editing events were normalised to one copy of murine albumin to determine percentage events per total alleles.

2.2.5.8 Real-time quantitative PCR (qPCR)

qPCR was used to quantify expression of both vector and relevant genes. cDNA synthesized from liver RNA was diluted 1:10 with 10% TE and cDNA synthesized from adrenal RNA was diluted 1:20. The primers used are listed in Table 2-8. Reactions were prepared with 10 µL Takara TB green (2×), 1 µL of each relevant primer (10µM), 5 µL diluted template cDNA and made up to 20 uL. The conditions were 95°C for 30 seconds; 40 cycles of 95°C for 5 seconds, 57°C for 20 seconds, 80°C for 10 seconds; and then ramp from 60°C to 95°C to melt with 90 seconds held at first step then held for 5 seconds for each step thereafter.

2.2.6 Statistical analysis

GraphPad Prism software was used for statistical analysis and graph production. Data was not assumed to have a normal distribution so non-parametric statistics were utilised. Values graphed as individual data points with median and interquartile range displayed unless otherwise stated. Statistical significance was determined between two groups using the Mann-Whitney *U* test, between baseline and final corticosterone with

ANOVA and linear regression modelling for association between two variables. Statistical significance was defined as $p \leq 0.05$.

2.2.7 Figures

Figures were created with Biorender.com.

2.3 References

1. Miciak JJ, Hirshberg J and Bunz F. Seamless assembly of recombinant adenoviral genomes from high-copy plasmids. *PLoS One* 2018; 13: e0199563. 2018/06/28. DOI: 10.1371/journal.pone.0199563.
2. Gao GP, Alvira MR, Wang L, et al. Novel adeno-associated viruses from rhesus monkeys as vectors for human gene therapy. *Proc Natl Acad Sci U S A* 2002; 99: 11854-11859. 2002/08/23. DOI: 10.1073/pnas.182412299.
3. Mori S, Wang L, Takeuchi T, et al. Two novel adeno-associated viruses from cynomolgus monkey: pseudotyping characterization of capsid protein. *Virology* 2004; 330: 375-383. 2004/11/30. DOI: 10.1016/j.virol.2004.10.012.
4. Ran FA, Cong L, Yan WX, et al. In vivo genome editing using Staphylococcus aureus Cas9. *Nature* 2015; 520: 186-191. 2015/04/02. DOI: 10.1038/nature14299.
5. Westhaus A, Cabanes-Creus M, Rybicki A, et al. High-Throughput In Vitro, Ex Vivo, and In Vivo Screen of Adeno-Associated Virus Vectors Based on Physical and Functional Transduction. *Hum Gene Ther* 2020; 31: 575-589. 2020/02/01. DOI: 10.1089/hum.2019.264.
6. Shiroishi T, Sagai T, Natsuume-Sakai S, et al. Lethal deletion of the complement component C4 and steroid 21-hydroxylase genes in the mouse H-2 class III region, caused by meiotic recombination. *Proc Natl Acad Sci U S A* 1987; 84: 2819-2823. 1987/05/01. DOI: 10.1073/pnas.84.9.2819.
7. Snyder RO, Xiao X and Samulski RJ. Production of recombinant adenoassociated viral vectors. In: Dracopoli N, Haines J, Krof B, et al. (eds) *Current Protocols in Human Genetics*. Chichester, UK: John Wiley & Sons, Inc, 1996, pp.12.10.11–12.11.24.
8. Cunningham SC, Dane AP, Spinoulas A, et al. Gene delivery to the juvenile mouse liver using AAV2/8 vectors. *Mol Ther* 2008; 16: 1081-1088. 2008/04/17. DOI: 10.1038/mt.2008.72.
9. Richter CP. Increased Salt Appetite in Adrenalectomized Rats. *American Journal of Physiology-Legacy Content* 1936; 115: 155-161. DOI: 10.1152/ajplegacy.1936.115.1.155.
10. Wang Z and Storm DR. Extraction of DNA from mouse tails. *Biotechniques* 2006; 41: 410, 412. 2006/10/31. DOI: 10.2144/000112255.
11. Grecso N, Zadori A, Szecsi I, et al. Storage stability of five steroids and in dried blood spots for newborn screening and retrospective diagnosis of congenital adrenal hyperplasia. *PLoS One* 2020; 15: e0233724. 2020/05/30. DOI: 10.1371/journal.pone.0233724.

Chapter 3

Validating and extending the 21-hydroxylase deficient mouse model

3.1 Introduction

This chapter describes the establishment of the colony and validating and extending the characterisation of the model that was used for all later experiments. The C57BL/10SnSlc-H-2^{aw18} mouse model[1] was kindly provided by Toshihiko Shiroishi (National Institute of Genetics) and the RIKEN BRC through the National BioResource Project of the Ministry of Education, Culture, Sports, Science and Technology, Japan. While this model has been used in previous gene therapy studies, not all of the phenotypic parameters used in this thesis had been explored by previous groups, and thus clarification of the phenotype was warranted.

3.1.1 Comparison between human and murine adrenal cortex

Animal models are an important tool in the pre-clinical development of new treatments.[2] Mice have many similar biological functions as humans, however there are some important differences between the mouse and the human adrenal gland, both structurally and functionally. The human adrenal cortex is divided into three zones from superficial to deep: zona glomerulosa, zona fasciculata and zona reticularis. Deep to the zona

reticularis is the adrenal medulla.[3] The zona glomerulosa is regulated by the renin-angiotensin system, and the zona fasciculata and zona reticularis are dependent on ACTH secretion of the pituitary.[4] Aldosterone is produced in the zona glomerulosa and the major glucocorticoid produced by the zona fasciculata in humans is cortisol. The zona reticularis is unique to humans (and some non-human primates) and begins to appear from approximately age 3 to 5 years in children.[5] The zona reticularis produces adrenal androgens, and the onset of detectable androgen production, known as adrenarche, manifests as the development of pubic and axillary hair from age 6 to 8 years and onwards.[6]

However, rodents do not have a zona reticularis due to the lack expression of 17-hydroxylase (*Cyp17a1*) in the adrenal cortex, although it is expressed in the gonads for sex steroid production: Leydig cells (testis) in the male and thecal cells (ovary) in the female mouse.[7, 8] Thus the major glucocorticoid in rodents is corticosterone (Chapter 1, Section 1.3.5.1, Figure 1-3).[3, 9] The adult mouse adrenal does not produce androgens.[10] The foetal mouse adrenal transiently expresses 17-hydroxylase and therefore the adrenal may have a transient role in androgen production in the foetal mouse, but its expression is not present in post-natal life.[11] Between the zona fasciculata and the adrenal medulla the mouse has what is known as the X-zone, which is not responsive to ACTH.[12] This is similar to the human foetal zone, however it persists after birth until puberty in the male mouse and until the first pregnancy in the female mouse, where in both sexes involution appears to be related to exposure to androgens.[13-15] The role of the mouse X-zone is unclear,[3, 15] although it may be involved with progesterone catabolism.[16]

3.1.2 Murine model of 21-hydroxylase deficiency

3.1.2.1 Genetics of murine 21-hydroxylase deficiency

The human *CYP21A2* gene is located on the short arm of chromosome 6 within the major histocompatibility complex at 6p21.3 which is among one of the most complex regions in the human genome.[17, 18] Similar to humans, mice have a duplicated *C4* and *Cyp21* gene cluster with an associated 21-hydroxylase pseudogene.[19-21] In humans the *CYP21A2* gene is functional with 15 mutations rendering the human *CYP21A1-P* non-functional,[22] whereas in mice it is the *Cyp21a1* gene that is functional and the *Cyp21a2-ps* gene is the non-functional pseudogene primarily due to a large deletion which spans exon 2.[23, 24] There is high homology between the active and pseudo- genes with 98% exonic and 96% intronic homology in the human.[25, 26] This high homology results in risk of misalignment of chromosomes resulting in genetic recombination between the active and pseudogene, and accounts for more than 90% of the CAH-causing mutations.[27, 28] This can cause gene deletion from unequal cross-over or transfer of deleterious mutations from the pseudogene to the active gene.[28] When misalignment occurs during meiosis, one daughter chromosome may have three copies of *CYP21* and the other daughter chromosome may have one copy, and this single copy is a fusion of the 5' end of non-functional *CYP21A1P* and 3' end of *CYP21A2*.[27-30] This accounts for 20% of the recombination events that cause CAH.[28] Gene conversions, where there is transfer of genetic material from the pseudogene to the active gene through homologous recombination, take place in both somatic cells and gametes, and mostly occur during mitosis.[28] These recombination events are responsible for more than 90% of the pathogenic variants causing 21-hydroxylase deficiency.[28, 31] There are over 350 known variants in *CYP21A2* listed in the Human Gene Mutation Database (HGMD, http://www.hgmd.cf.ac.uk accessed 02/03/2024) spanning all 10 exons (Figure 3-1).

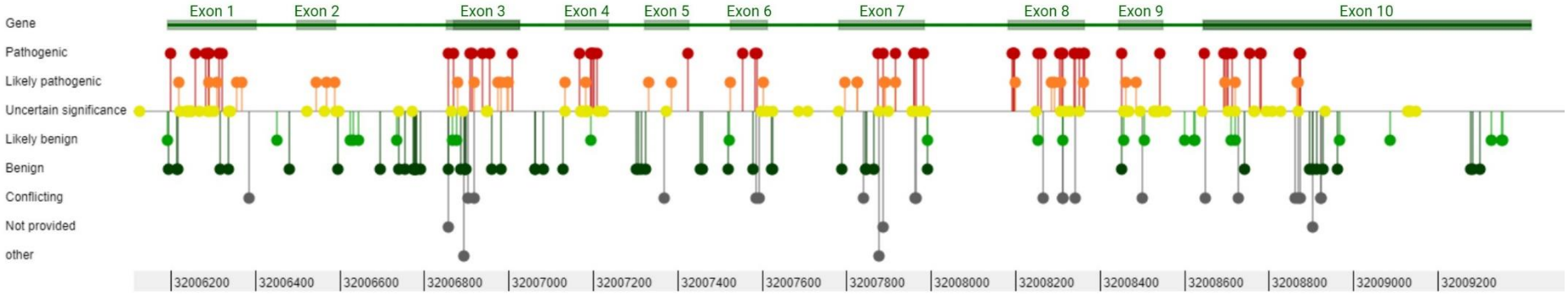

Figure 3-1 Graphical representation of known variants in *CYP21A2*

This figure is taken from ClinVar and demonstrates pathological variants span all 10 exons in the CYP21A2 gene. Source: https://www.ncbi.nlm.nih.gov/clinvar (accessed 17/3/24).

The mouse model for 21-hydroxylase deficient congenital adrenal hyperplasia (CAH) was developed in the 1980s when the C57BL/10-H-2^{aw18} recombinant mouse was produced by crossing C57BL/10-H-2^{a} and C57BL/10.MOL-SGR-H-2^{wm7} mice which had an H-2 complex from the Japanese wild mouse.[1] Homozygosity for the aw18 allele was lethal, and later determined to be due to 21-hydroxylase deficiency.[32] As there is no 17-hydroxylase in the murine adrenal, 21-hydroxylase deficiency causes an elevation of progesterone.[32] In the 1990s, it was shown that these mice could to be rescued by transgenesis, and this was the first indication that they could be used in a model for gene therapy in CAH.[33] The mutation was described in the early 2000s and found to be due to a complex gene rearrangement because of unequal crossing-over of the active *Cyp21a1* gene and the inactive *Cyp21a2* pseudogene,[34] This is similar to 20% of mutations that cause 21-hydroxylase deficient CAH in humans by unequal crossing-over between chromosomes in meosis.[28] The mutated *Cyp21a1* gene is a fusion of the wild-type exons 1-7 and non-functional pseudogene exons 8-10, which results in non-functional transcribed mRNA (Figure 3-2).[34] This resulted in an 80 kb deletion from the 3' end of *Cyp21a1*, to the 5' end of *Cyp21a2-ps* that includes *C4*.[34] The resulting mutant gene has 3 point mutations in exon 8 and 6 point mutations in exon 10 from the pseudogene that render it non-functional.[34] Additionally, there is a point mutation upstream of the fusion event in exon 6.[34]

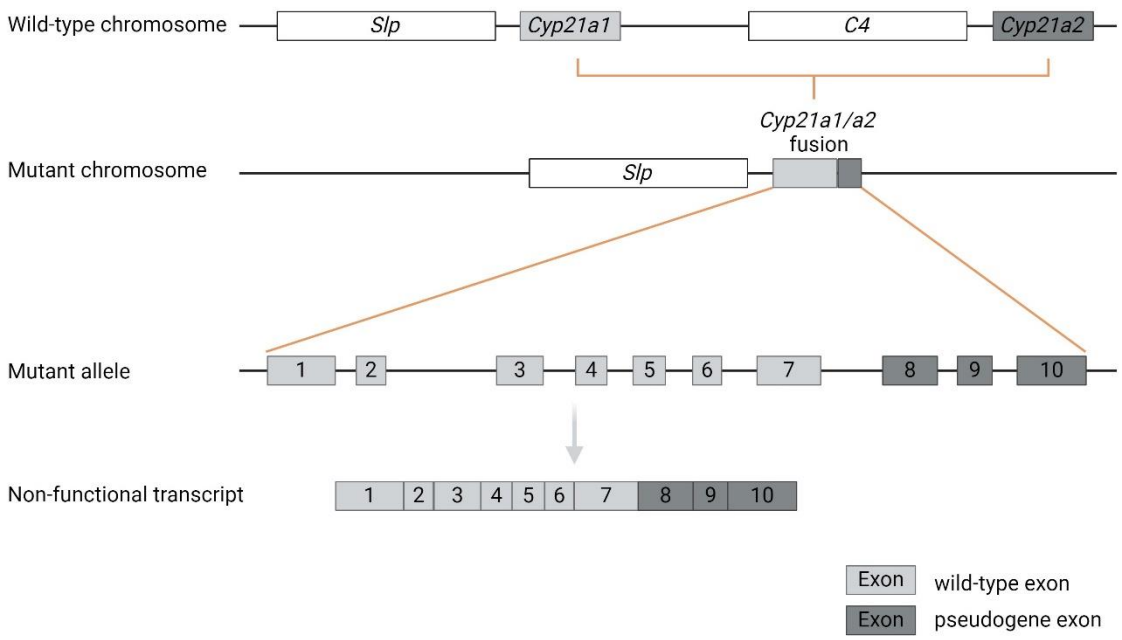

Figure 3-2 Mutant murine *Cyp21a1*

Unequal crossing over of chromosomes results in fusion of the *Cyp21a1* and *Cyp21a2-ps* genes and deletion of *C4*. Wild-type exons 1-7 form the 5' end of the new mutant gene and exons 8-10 from the pseudogene form the 3' end of the mutant gene, which results in a non-functional transcript. Abbreviations: *Slp*, sex-limited protein; *Cyp21a1*, 21-hydroxylase; *Cyp21a2-ps*, 21-hydroxylase pseudogene; *C4*, complement 4. Adapted from Riepe, *et al*, 2005.[34]

3.1.2.2 Rescue of the neonatally lethal murine 21-hydroxylase deficient model

Homozygosity for the mutated *Cyp21a1* gene is neonatally lethal, with death commonly occurring during birth or within the first few days of life, with none surviving beyond 15 days.[1] By treating with glucocorticoid or wild-type mouse adrenal homogenate, homozygous mice may survive,[33] however even with steroid rescue the expected survival rate is poor and estimated to be 12%.[35]

Various glucocorticoid regimens have been used in previous studies to improve neonatal survival:

- 20 µg hydrocortisone, 20 ng dexamethasone and 0.025 µg fludrocortisone dissolved in saline or olive oil and administered daily for the first 3 weeks of neonatal life.[33]
- 5ug dexamethasone dissolved in peanut oil and given to the pregnant dam from day 20 until delivery, followed by 5 µg corticosterone and 0.025 µg fludrocortisone daily for the first two weeks of life, followed by corticosterone in the drinking water for days 14-21.[36-38]
- 5ug dexamethasone daily from late pregnancy until day of delivery, followed by 5ug corticosterone and 0.025 µg fludrocortisone daily for the first 3 weeks of neonatal life.[39]
- 5 µg dexamethasone daily to the dam from gestational day 20 until day 7 post-natal , and the neonates received 10 µg corticosterone and 0.05 µg fludrocortisone every second day for two weeks of life.[35]
- 5 µg dexamethasone to the pregnant dams second daily[40] from late pregnancy The pups were administered wild-type adrenal homogenate daily from birth to day 3 (total 4 doses) into cryogenically sedated neonates (Jonathan B. Rosenberg, Senior Research Associate, Crystal Laboratory, personal communication, 12th June 2020).

Additionally, some studies utilised peanut oil as the diluent, however it has been found that this can increase maternal cannibalism, and ethanol may be used instead (Pierre Bougnères, personal communication, Emeritus Professor, Inserm, 18th June 2020).

3.1.2.3 Phenotype of murine 21-hydroxylase deficiency

The phenotype seen in 21-hydroxylase deficient mice is comparable to that seen in humans with severe salt-wasting disease; that is, there is elevation of a precursor

hormone, enlargement of the adrenal glands, loss of organised adrenocortical zonation and severe, potentially lethal disease in neonates.[32] The 21-hydroxylase deficient mouse has elevation of progesterone, when compared to heterozygotes and wild-type littermates.[32] Mild elevation of progesterone exists in heterozygotes when compared with wild-type littermates,[32] which may indicate that heterozygotes are partially affected, unlike most heterozygous humans. There is elevation in renin expression in adult homozygous mice,[35] indicative of chronic salt loss. Newborn mice homozygous for 21-hydroxylase deficiency have larger adrenal glands than heterozygous or wild-type, with cell hypertrophy and loss of organised zonation,[32, 35] which is also seen in affected humans.[41] When homozygous mice survive to adulthood, they have poor weight gain compared with their heterozygous and wild-type siblings.[35] In behavioural analyses, these mice show signs of anxiety and depressive-like behaviour.[35]

The majority of previous studies have utilised elevated serum or urine progesterone as the biomarker for disease and disease improvement.[35, 39, 40] Corticosterone is known to be deficient in this mouse model[36]; however, there is no previous characterisation of aldosterone production. While it has been shown that they have increased renin expression, which implies deficient mineralocorticoid production,[35] serum aldosterone has not been measured directly. We sought to use multiple biomarkers of disease therefore determined the wild-type reference ranges for serum progesterone, corticosterone and aldosterone and the expected levels in 21-hydroxylase deficiency in this model.

As mice do not express *Cyp17a1* in the adrenal gland, there is no hyperandrogenic phenotype in 21-hydroxylase deficiency, and the major glucocorticoid is corticosterone

rather than cortisol. While these minor differences mean that the model does not perfectly replicate human disease, there is sufficient similarity to make it a suitable candidate for early work in developing gene therapy for CAH, and it has been used previously for this purpose.[35, 36, 39, 40, 42] We sought to confirm the genotype and phenotype of this model, and to extend the biochemical phenotype to include aldosterone, prior to use in gene therapy experiments.

3.2 Chapter-specific methods

3.2.1 Genotyping

The PCR protocol provided by the Riken Laboratories was expected to yield a wild-type band of 1.7 kb and a mutant band of 2.3 kb but it was not reliably reproducible (universal forward primer ["Primer 1"]; wild-type specific reverse primer ["Primer 2"]; mutant specific reverse primer ["Primer 3"]) (Table 3-1). Optimisation of this protocol was attempted. DNA extraction methods that were tested included traditional phenol-chloroform, HotSHOT[43] and the Wang and Storm method.[44] PCR enzymes Q5 and Taq and PCR enzyme pre-mixes BioMix Red and MyTaq Red were tested and annealing temperature gradients were applied. Primer concentrations were tested from 1µL of 1µM stock in 20µL reaction (50nM final concentration) to 1.5 µL of 10µM stock (700nM final concentration). Despite this, the genotyping PCR remained unreliable therefore new primer sequences were designed for the wild-type (NC_000083.7) and mutant (GenBank AY613781) alleles (Table 3-1). Primers 1-14 were tested for genotyping, but the reaction remained unreliable. After sequencing, additional primers were designed to produce smaller PCR products (Primers 20-38).

Table 3-1 Primers for genotyping and sequencing.

Primer name	Primer number	Direction	Sequence 5’ to 3’	Target
LG_exon 2	1	forward	CATATGCTAAATGGTAAGGGTTAGG	Wild-type and mutant exon 2/intron 2
LG_intron 8_b	2	reverse	TACCCCCAGGGAATCACCTGCTCG	Wild-type exon 8/intron 8
LG_exon 41	3	reverse	AACTGAGGCACTAGGCTCATCC	Mutant 3’ UTR
LG_004	4	reverse	TGACTGCCGAGCACTGAGGG	Mutant 3’ UTR
LG_005	5	reverse	GCCGAGCACTGAGGGGTTGT	Mutant 3’ UTR
LG_006	6	reverse	CTCATCCTATCCTGTCAAGGATTT	Mutant 3’ UTR
LG_007	7	reverse	GTCTGTACCAACGTGCTGTC	Wild-type exon 5, Mutant intron 7
LG_008	8	reverse	TGACCACAAGCTACCAAGGA	Wild-type intron 2, Mutant intron 2
LG_009	9	reverse	AAGAGGAAGAGGAGCCATCG	Wild-type intron 2, Mutant intron 2
LG_010	10	forward	GAAGCAAAGGTCAGAGCCAC	Mutant 5’ UTR
LG_011	11	forward	GGGACTGTGCCAATGTGAAA	Mutant 5’ UTR
LG_012	12	forward	CCCATCGTGCAACTAAGGTT	Mutant exon 8
LG_013	13	forward	GGTCAGCTAGATGGCAGGAG	Wild-type intron 7, Mutant intron 7
LG_014	14	forward	CCTTTCCCTCAGCATCTCTG	Mutant intron 8/exon 9
LG_015	15	reverse	CATGTAGTCAATCATGTCTTTCCATTG	Wild-type exon 7, Mutant exon 7
LG_016	16	reverse	TCTTCCTCCCTCAACCCTTACCC	Wild-type intron 8, Wild intron 8
LG_020	20	reverse	GAAGCGATCTGTGGGTAGTAGAT	Wild-type intron 9/exon 10
LG_021	21	forward	GTCAAGCAGCAGCTGAAGCG	Wild-type exon 6
LG_022	22	forward	ACCACCCTGAGGTGCACT	Wild-type exon 7/intron 7
LG_023	23	reverse	GGGAGATTGATGCCAGCATAAG	Wild-type exon 10
LG_024	24	forward	CCTCTTGCCCACCCCTAAC	Wild-type intron 4
LG_025	25	forward	CCCTGGGGGATTACTCTCTC	Wild-type exon 3
LG_026	26	forward	CACCACTGCTGGACACACAA	Wild-type intron 6

LG_027	27	reverse	CCACAGTGCACCTCAGGG	Wild-type exon 7/intron 7
LG_028	28	forward	GCTCATGGCCACCATTGCC	Wild-type exon 8, Mutant exon 8
LG_029	29	forward	ACAGGAACCGAATGCAGCTG	Wild-type intron 7/exon 8
LG_030	30	reverse	GCCGCACCTAGAAAGGAGGA	Mutant exon 10
LG_031	31	reverse	GCCAGGTTCCAGGAAGCAAT	Mutant exon 10
LG_032	32	forward	CCCTCTTGCATACCCCTCAG	Mutant intron 4
LG_033	33	reverse	GGAAGGGCAAGGCTGGGT	Mutant intron 7
LG_034	34	reverse	TCCTTGGGGATGTCATAGCCA	Mutant exon 9
LG_035	35	forward	TCACCATCCTGAAGTGCACC	Mutant exon 7/intron 7
LG_036	36	reverse	CCACGGTGCACTTCAGGA	Mutant exon 7/intron 7
LG_037	37	forward	GTCCCTGGGGGATTACTCTCTA	Mutant exon 3
LG_038	38	forward	GTCAAGCAGCAGCTGAAGCA	Mutant exon 6
LG_039	39	reverse	CTTAGGGATGTCATAGCCGG	Wild-type exon 9, Mutant exon 9
LG_040	40	reverse	AGTCCACCCACTTTTGGATC	Wild-type exon 2, Mutant exon 2
LG_041	41	forward	TTCCTACAGCCTAACCTTCCCA	Wild-type exon 1, Mutant exon 1
LG_042	42	forward	CAATGGAAGCTCCGGAAGC	Wild-type exon 1, Mutant exon 1
LG_043	43	reverse	CATTTAGCATATGGGGTCGGC	Wild-type exon 2, Mutant exon 2

3.2.2 Sequencing

The published sequence for the mutant *Cyp21a1* gene in the C57BL/10SnSlc-H-2^{aw18} mouse model[34] was sourced from GenBank (accession no. AY613781). Primers were designed to be unique to the wild and mutant *Cyp21a1* gene and not bind in the *Cyp21a2-ps* (Table 3.1). DNA from a *Cyp21a1*+/+ and a *Cyp21a1*-/- mouse were used for template. Primers 1, 2, 7, 8, 9, 10, 11, 15, 22, 23, 24, 26, and 27 were used to amplify segments of the wild allele. Primers 1, 6, 7, 8, 9, 10, 11, 13 and 15 were used to amplify segments of the mutant allele. PCR products were purified from electrophoresis gel and sent to the Australian Genome Research Facility (AGRF, Westmead) for Sanger sequencing.

3.3 Results

3.3.1 Genotyping

The reliability of the genotyping PCR increased when smaller PCR products were targeted. The final genotyping methodology utilised the Wang and Storm DNA extraction method,[44] MyTaq Red PCR enzyme pre-mix and Primers 22 and 23 (10µM) for the wild-type allele (832bp) and 34 and 35 for the mutant allele (474bp). The final cycling conditions were 95°C 120sec; 35 cycles of 95°C 20sec, 60°C 30sec, 72°C 120sec; 72°C 80sec.

3.3.2 Sequencing the wild-type and mutant gene

Unlike the published mutant *Cyp21a1* gene sequence (GenBank accession no. AY613781), intron 1 of the mutant gene was found to have the same sequence as the published reference sequence for the wild-type *Cyp21a1* gene (NC_000083.7). Therefore,

there was an additional cytosine in the middle of intron 1 not present in the published mutant *Cyp21a1* gene (c.204-33_204-34insC) (Figure 3-3). This was of particular importance for Chapter 6, as it fell within a PAM site target sequence for Cas9 which was used for gene editing. Additionally, there was a second location where the sequenced mutant gene matched the wild-type sequence rather than the published mutant sequence, however this did not have downstream implications. There was a guanine inserted 6 base pairs upstream of exon 1 (c.-15_c-16insG) (Figure 3-4). The mutant gene was otherwise accurate to the published mutant sequence.

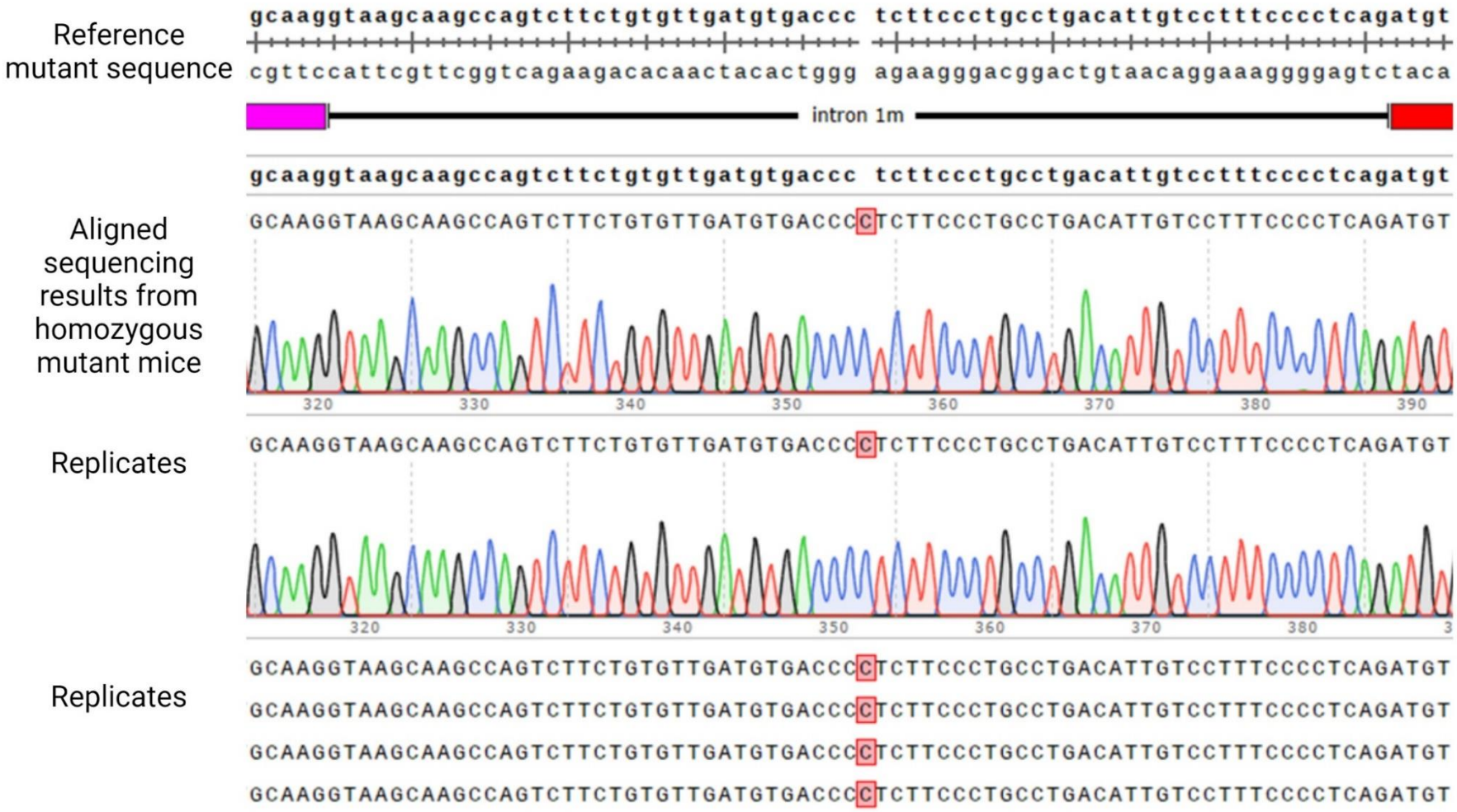

Figure 3-3 Sequencing intron 1 from mutant allele.

Sequencing revealed c.204-33_204-34insC. The sequence in the mutant intron 1 was consistent with the published wild-type sequence, and not the published mutant sequence.

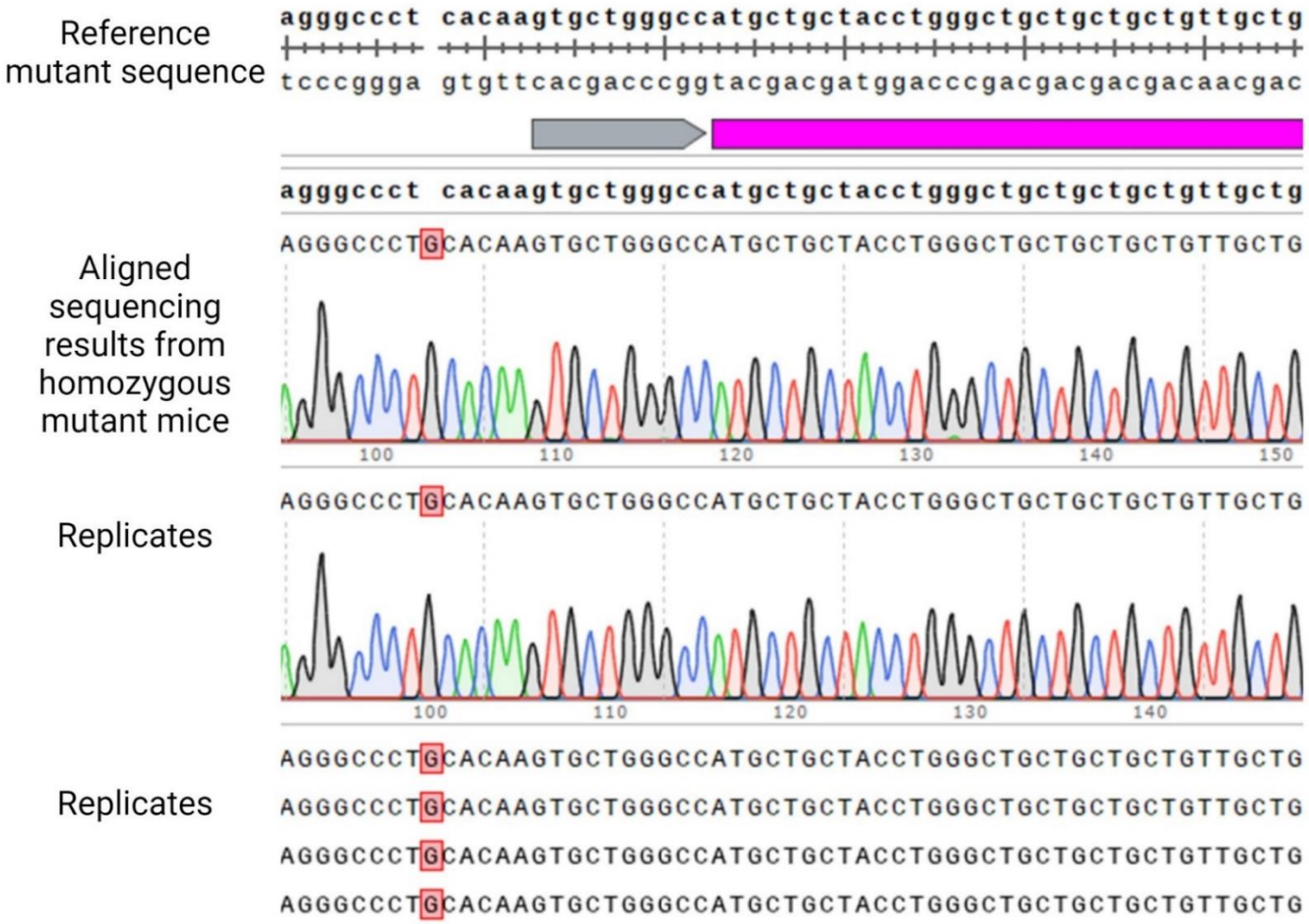

Figure 3-4 Sequencing 5’ UTR of mutant allele.

Sequencing revealed c.-15_c-16insG. The variant in the published mutant sequence 5’UTR was not present in the sequencing and was consistent with the published wild-type 5’UTR.

3.3.3 Increased homozygous neonatal survival

Prior to steroid rescue, no homozygous pups were detected, including recovered stillborn carcasses. Steroid rescue was commenced in February 2021 and survival rates were closely monitored until August 2021. In that time 25 dams had 48 litters that were treated with steroids. Twenty-three litters were delivered to experienced dams (one or more previous pregnancies) with 9/25 primiparous litters and 15/23 multiparous litters containing surviving homozygotes. From these litters 296 mouse pups reached 3 weeks of age following steroid treatment. Of these pups, 81 were determined to be wild-type, 147 were heterozygous and 41 were homozygous. Assuming 100% survival of wild-type and heterozygous pups which should make up 75% of the total births, the survival rate was estimated to be 48% in homozygous mice (41/85) (Table 3-2), although the survival rate for this colony has fluctuated over time from 35-50%. The survival rate was lower in litters from inexperienced dams (35%) and higher with experienced dams (50%). Male homozygous offspring had a 2-fold higher survival rate than female homozygous offspring.

Table 3-2 Survival of pups born to 48 litters.

	+/+	+/-	-/-	**Total**
Surviving pups	81	147	41	296
Expected birth rate	25%	50%	25%	
Expected number if 100% survival of homozygous	81	147	85	313
Survival rate			41/85 (48%)	

Abbreviations: +/+, wild-type; +/-, heterozygous; -/-, homozygous.

3.3.4 Body weight and adrenal cortex hyperplasia

Adrenal glands were harvested from adult wild-type and homozygous mice. At the time of harvesting, the median body weight for the wild-type controls was 22.5g for females and 30.9g for males. The median body weight for untreated 21-hydroxylase deficient mice was 22.4g for females and 28.9g for males. The median bilateral adrenal mass was 2.6 times greater in 21-hydroxylase deficient females and 3.4 times greater in males compared with wild-type adrenal glands (Figure 3-5A and B). There was a relationship between body weight and absolute adrenal mass in the homozygous mice (Figure 3-5C), therefore the adrenal mass is presented as both absolute mass and mass relative to body weight (Figure 3-5B to D). No strong correlation was demonstrated between adrenal mass and age (Figure 3-5E to F).

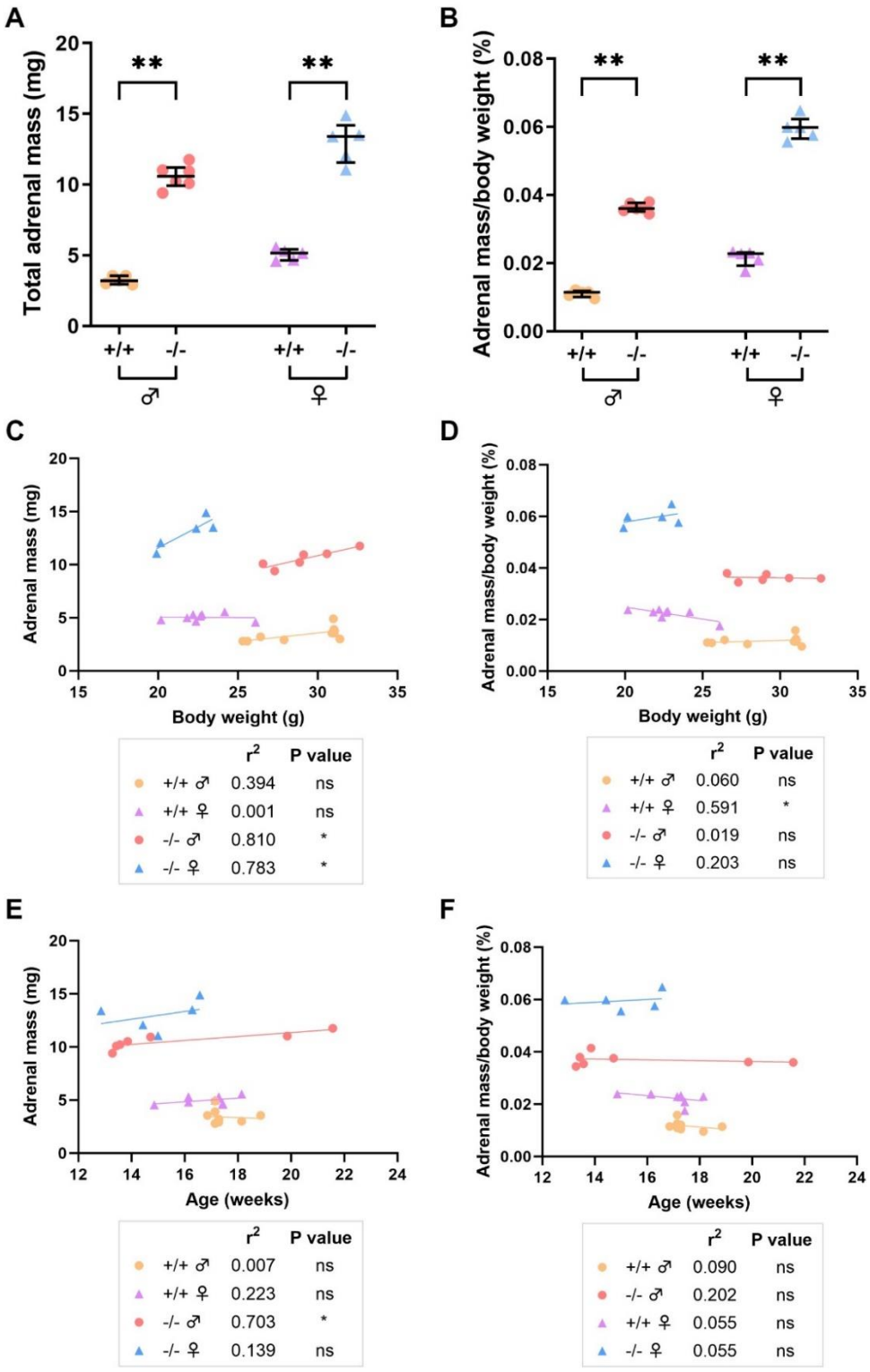

Figure 3-5 Adrenal size in adult mice.

A. Total bilateral adrenal mass. **B.** Adrenal mass represented as a percentage of total body weight. **C.** Relationship between body weight and bilateral adrenal mass. **D.** Relationship between body weight and relative adrenal mass. **E.** Relationship between age and bilateral adrenal mass. **F.** Relationship between age and relative adrenal mass. Abbreviations: +/+, wild-type; +/-, heterozygous; -/-, homozygous; ♂, male; ♀, female; ns, not significant. Individual data points are shown. Error bars in A and B represent median and interquartile range. * $p<0.05$, ** $p<0.01$ on Mann-Whitney *U* test or linear regression modelling.

Haematoxylin and eosin-stained adrenal sections revealed that cells of the zona fasciculata were enlarged with increased cytoplasm and the zone was expanded in homozygous mice compared with wild-type mice (Figure 3-6). Due to the irregular shape of the 21-hydroxylase deficient adrenal glands it was challenging to ensure sections included medulla.

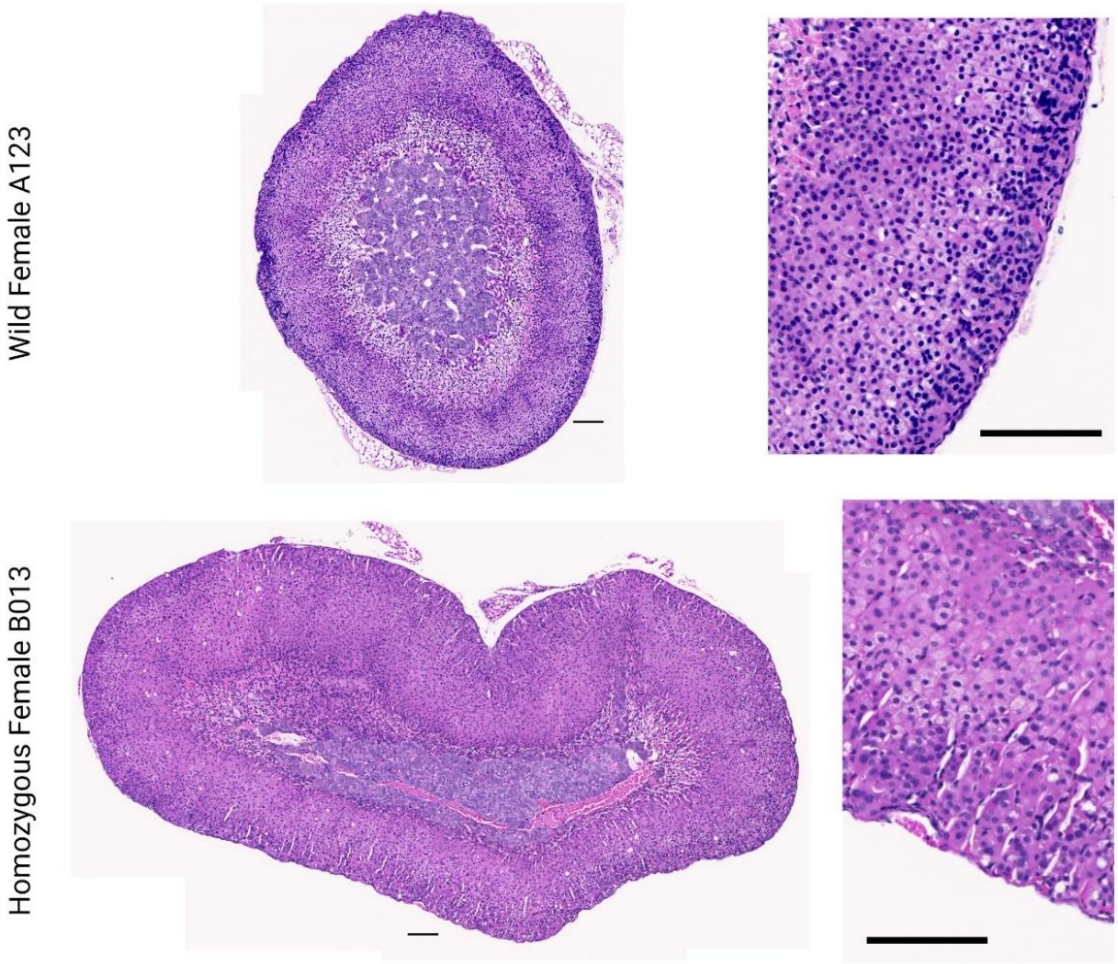

Figure 3-6 Wild-type and mutant adrenal histology.
Haematoxylin and eosin-stained sections of representative murine adrenal glands demonstrating irregular shape and enlarged, pale cytoplasm in the homozygotes, particularly in the zona fasciculata cells. The scale bar represents 100 µm. Slide scanning and image exportation by Eva van Dijk, GTRU, CMRI and Clare Loudon, ProCan Cancer Pathology, CMRI.

3.3.5 Steroid profiles

There was significantly elevated progesterone and reduced corticosterone and aldosterone in homozygotes compared with wild-type and heterozygotes. Aldosterone was 3.3-fold lower in homozygous females compared with wild-type and 2.5-fold lower in males (Figure 3-7A). In the homozygotes, corticosterone was 23-fold lower in females and 12-fold lower in males compared with wild-type (Figure 3-7B). The homozygotes had progesterone 28-fold higher and 42-fold higher than wild-type in females and males, respectively. Heterozygotes males had 1.9-fold elevated progesterone compared with their wild-type counterparts and their progesterone levels were similar to wild-type females (Figure 3-7C). The homozygotes also had elevated progesterone-to-corticosterone ratios (Figure 3-7D). No female mice had elevated androgens, regardless of genotype (Figure 3-8). Median serum testosterone was 3-fold higher in wild-type males compared to homozygous males.

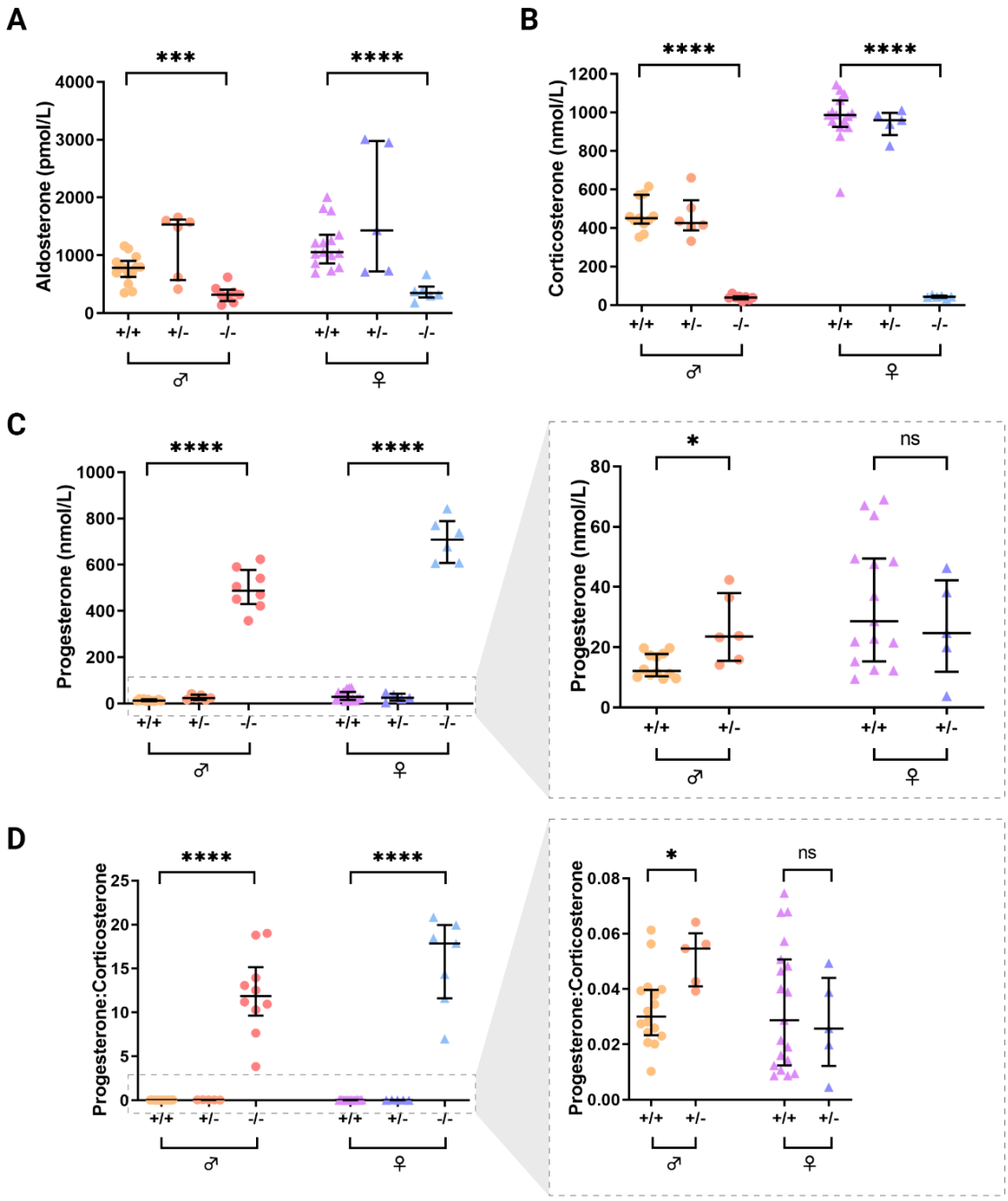

Figure 3-7 Steroid profiles in adult mice.

A. Serum aldosterone. **B.** Serum corticosterone. **C.** Serum progesterone. Call-out box has homozygous samples removed to demonstrate the mild elevation in heterozygous male serum progesterone. **D.** Progesterone-to-corticosterone ration. Call-out box has homozygous samples removed to demonstrate the mild elevation in heterozygous male serum progesterone-to-corticosterone ratio. Individual data points are shown. Abbreviations: +/+, wild-type; +/-, heterozygous; -/-, homozygous; ♂, male; ♀, female; ns, not significant. Error bars represent median and interquartile range. * $p<0.05$, *** $p<0.001$, **** $p<0.0001$ on Mann-Whitney *U* test.

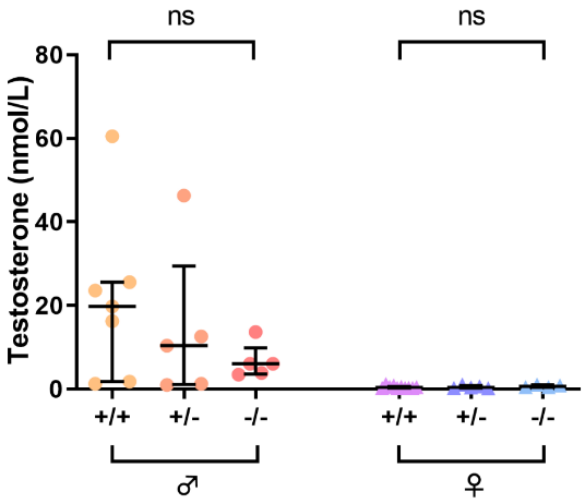

Figure 3-8 Serum testosterone in adult mice.
No female mouse had elevated serum testosterone regardless of genotype. Individual data points are shown. Abbreviations: +/+, wild-type; +/-, heterozygous; -/-, homozygous; ♂, male; ♀, female; ns, not significant. Error bars represent median and interquartile range.

3.3.6 Hydrocephalus

Hydrocephalus was noted in the mouse colony, with generational anticipation. The first mice noted to have hydrocephalus that was impacting their quality of life were 10-11 months of age. In later generations, hydrocephalus was the reason for termination at younger ages from 4-5 months, then 10-12 weeks then 6-8 weeks. The pedigree was followed to determine likely founder mice and these were removed from the breeding colony (Figure 3-9). The colony was refreshed by crossing heterozygous mice with wild-type black 6 mice (source: Jackson Laboratories) and the subsequent heterozygous off-spring were used to replace the breeding stock. This combination of approaches was able to eliminate hydrocephalus from the colony.

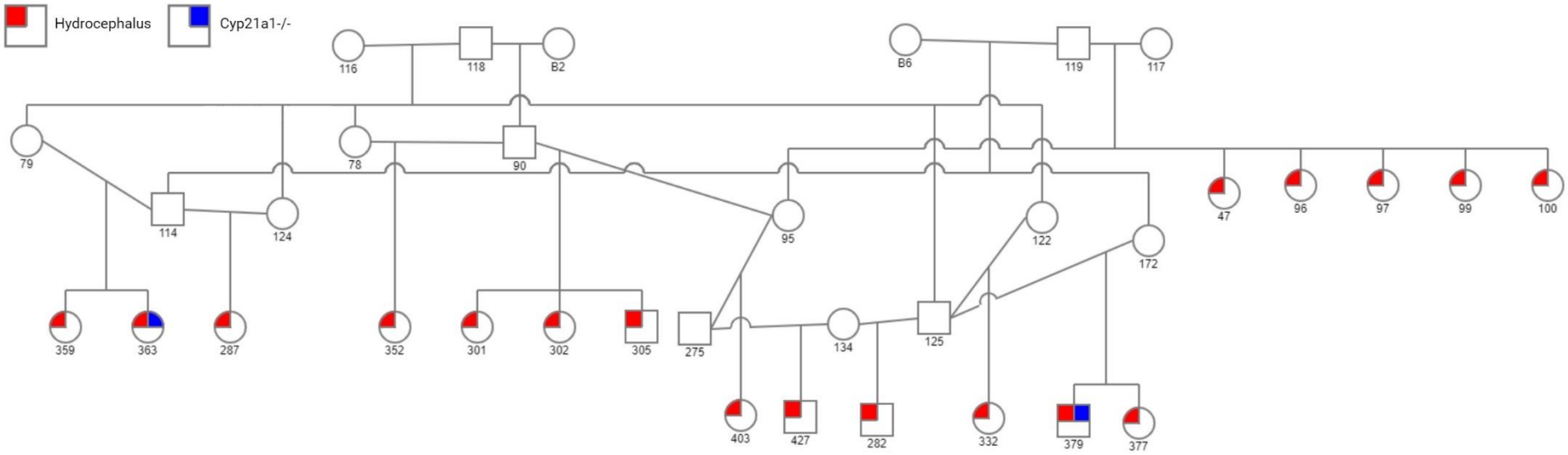

Figure 3-9 Hydrocephalus pedigree.
Representative pedigree of mice affected with hydrocephalus (red). Homozygous 21-hydroxylase deficient mice in this pedigree also shown (blue).

3.4 Discussion

These data show that the H-2aw18 mouse was a suitable model for CAH gene therapy through demonstration of a comparative genotype and phenotype to the human disease. The genetic basis for disease is similar to humans with cross over from the pseudogene.[34] The mutant gene was sequenced and two variations from the published reference mutant sequence were found, one of which had implications for guide selection in Chapter 6. Once the colony was able to be genotyped reliably, exogenous steroid rescue was introduced. With the subcutaneous steroid regimen, 35-50% of homozygous offspring survived the neonatal period with the higher survival rate seen with experienced dams. The surviving homozygous mice had higher adult body weight than previously described. The phenotype of the CAH mouse model was confirmed, including elevated progesterone, low corticosterone, and increased adrenal mass and protocols optimised for use in subsequent experiments. Additionally, the model was shown to have low serum aldosterone, which had not been previously demonstrated.

The genetic sequence of the mutant *Cyp21a1* gene was confirmed by Sanger sequencing. There were two nucleotides present in the mutant *Cyp21a1* sequence, also present in the published wild-type *Cyp21a1* sequence that were not present in the published mutant *Cyp21a1* sequence. This was particularly important for the selection of PAM and guide target sequences in Chapter 6. Had the published mutant sequence been used without confirmation, the designed guide may not have been effective. This had the potential to lead to conclusions that the strategy did not work, rather than the guide sequence being incorrect. Furthermore, the other variation in the mutant sequence that was not present in the published mutant sequence was upstream of exon 1, potentially in the

promoter/enhancer region. However, this was unlikely to affect the promoter/enhancer at this locus, as the same sequence is present in the functional wild-type gene.

The survival rate was higher than the previously published 12% survival rate.[35] Homozygous males outnumbered homozygous females in the surviving offspring approximately 2:1, implying a survival advantage in males or disadvantage in females. Female mice are known to have higher serum corticosterone levels than males,[45] so the corticosterone deficiency may have had a more profound effect on female mice due to an increased absolute requirement. Furthermore, it has been reported that homozygous mice have reduced body weight, with homozygous mice weighing ~16g and wild-type controls 26-28g at the same age.[35] In our study, this large discrepancy between the body weight of homozygous and wild-type mice was not seen. The management of 21-hydroxylase colonies has differed across research centres that have utilised this model. The majority administered 5 µg dexamethasone to pregnant dams from day 20 or "late pregnancy" until delivery.[36, 38, 39, 46] One group continued to administer subcutaneous dexamethasone to dams for 7 days post-partum,[35] however more recently they changed their protocol from giving subcutaneous dexamethasone to providing corticosterone in drinking water to pregnant dams (Pierre Bougnères, personal communication, Emeritus Professor, Inserm, 18th June 2020). Offspring have been variously given 5 µg corticosterone and 0.025 µg fludrocortisone subcutaneously daily for two[36, 38] or three[39] weeks or given 10ug corticosterone and 0.05 µg fludrocortisone second daily for two weeks.[35] One group injected wild-type adrenal homogenate in to pups as survival rate was poor with injected steroids (Jonathan B. Rosenberg, Senior Research Associate, Crystal Laboratory, personal communication, 12th June 2020). The adrenal glands were comparatively larger in our homozygous mice than previously published[35] and we hypothesise that this is due

to better overall body weight in our homozygous animals, as we found a relationship between adrenal size and body weight in the homozygous mice. The reason for the improvement in survival and body weight in our colony is unclear, however perhaps it is due to our different husbandry practices: pregnant dams commenced dexamethasone treatment earlier (day 18), neonatal mice were treated with subcutaneous steroids second daily for longer (until age 21 days), pregnant dams and all homozygous mice were provided with *ad lib* salt supplementation, diet gel was offered to lactating dams for the first 9-10 days following pregnancy and weaned homozygous mice were housed in small groups, preferentially with other homozygous mice if possible (2-4 mice per cage) to minimise resource competition. Reduced resource competition and increased high calorie diet supplementation in conjunction with salt-supplementation may have contributed to retention of body mass in this model.

We demonstrated that aldosterone is lower in homozygous mice than wild-type, which has not previously been shown, confirming the suspected mineralocorticoid deficiency suggested by elevated renin expression.[35] As the mutant mRNA is prematurely truncated, it was expected that this was associated with a severe phenotype and salt-wasting.

The heterozygous mice had a mild biochemical phenotype with mildly elevated progesterone which did not appear to impact fertility or survival. Human heterozygous carriers of pathogenic CAH variants have an increased 17OHP response to ACTH stimulation,[47] but do not reliably have elevated basal 17OHP to distinguish them from unaffected individuals.[48] The murine serum samples were collected during terminal exsanguination, which is a physiologically stressful event and expected to result in elevated ACTH levels, therefore the serum progesterone levels could be considered to be

ACTH stimulated levels. Heterozygous mice were not used in experiments, only in breeding and colony maintenance.

The main limitation of this model for human disease is the lack of adrenal androgen synthesis in rodents. We confirmed that in 21-hydroxylase deficiency mice do not develop hyperandrogenism. One of the hallmarks of CAH is hyperandrogenism, a characteristic that is present across the phenotypic severity spectrum. Thus, presence of androgen excess including the canonical androgen pathway, backdoor androgen pathway and C-11 androgen pathways could not be characterised, nor compared following gene therapy treatment. With the absence of adrenal androgen production, we are unable to determine if one androgen pathway would be better suppressed following gene therapy than another, or if there is an effect on the androgen pathway at all. In lieu of hyperandrogenism, elevated progesterone was used as a marker for increased upstream products which would be shunted into androgen pathways in the human.

The anatomical phenotype seen in the 21-hydroxylase deficient mice was comparable to that seen with humans with CAH: large adrenal glands with disordered histological structure, elevated precursor steroids and reduced glucocorticoid and mineralocorticoid levels. This model is therefore an appropriate recapitulation of the human CAH disease, other than the lack of hyperandrogenisation. Thus, this model was well validated in anticipation of use in downstream experimental work, described in later chapters.

3.5 References

1. Shiroishi T, Sagai T, Natsuume-Sakai S, et al. Lethal deletion of the complement component C4 and steroid 21-hydroxylase genes in the mouse H-2 class III region, caused by meiotic recombination. *Proc Natl Acad Sci U S A* 1987; 84: 2819-2823. 1987/05/01. DOI: 10.1073/pnas.84.9.2819.
2. Barre-Sinoussi F and Montagutelli X. Animal models are essential to biological research: issues and perspectives. *Future Sci OA* 2015; 1: FSO63. 2016/12/30. DOI: 10.4155/fso.15.63.
3. Vinson GP. Functional Zonation of the Adult Mammalian Adrenal Cortex. *Front Neurosci* 2016; 10: 238. 2016/07/06. DOI: 10.3389/fnins.2016.00238.
4. Vinson GP. Adrenocortical zonation and ACTH. *Microsc Res Tech* 2003; 61: 227-239. 2003/05/28. DOI: 10.1002/jemt.10331.
5. Rosenfield RL. Normal and Premature Adrenarche. *Endocr Rev* 2021; 42: 783-814. 2021/04/01. DOI: 10.1210/endrev/bnab009.
6. Dumontet T and Martinez A. Adrenal androgens, adrenarche, and zona reticularis: A human affair? *Mol Cell Endocrinol* 2021; 528: 111239. 2021/03/08. DOI: 10.1016/j.mce.2021.111239.
7. Perkins LM and Payne AH. Quantification of P450scc, P450(17) alpha, and iron sulfur protein reductase in Leydig cells and adrenals of inbred strains of mice. *Endocrinology* 1988; 123: 2675-2682. 1988/12/01. DOI: 10.1210/endo-123-6-2675.
8. Payne AH and Hales DB. Overview of steroidogenic enzymes in the pathway from cholesterol to active steroid hormones. *Endocr Rev* 2004; 25: 947-970. 2004/12/08. DOI: 10.1210/er.2003-0030.
9. Nandi J, Bern HA, Biglieri EG, et al. In vitro steroidogenesis by the adrenal glands of mice. *Endocrinology* 1967; 80: 576-582. 1967/04/01. DOI: 10.1210/endo-80-4-576.
10. Pihlajoki M, Dorner J, Cochran RS, et al. Adrenocortical zonation, renewal, and remodeling. *Front Endocrinol (Lausanne)* 2015; 6: 27. 2015/03/24. DOI: 10.3389/fendo.2015.00027.
11. Keeney DS, Jenkins CM and Waterman MR. Developmentally regulated expression of adrenal 17 alpha-hydroxylase cytochrome P450 in the mouse embryo. *Endocrinology* 1995; 136: 4872-4879. 1995/11/01. DOI: 10.1210/endo.136.11.7588219.
12. Jones IC. Role of the adrenal cortex in reproduction. *Br Med Bull* 1955; 11: 156-160. 1955/05/01. DOI: 10.1093/oxfordjournals.bmb.a069470.
13. Jones IC. The action of testosterone on the adrenal cortex of the hypophysectomized, prepuberally castrated male mouse. *Endocrinology* 1949; 44: 427-438. 1949/05/01. DOI: 10.1210/endo-44-5-427.
14. Jones IC. The disappearance of the X zone of the mouse adrenal cortex during first pregnancy. *Proc R Soc Lond B Biol Sci* 1952; 139: 398-410. 1952/04/24. DOI: 10.1098/rspb.1952.0020.
15. Huang CC and Kang Y. The transient cortical zone in the adrenal gland: the mystery of the adrenal X-zone. *J Endocrinol* 2019; 241: R51-R63. 2019/03/01. DOI: 10.1530/JOE-18-0632.
16. Hershkovitz L, Beuschlein F, Klammer S, et al. Adrenal 20alpha-hydroxysteroid dehydrogenase in the mouse catabolizes progesterone and 11-deoxycorticosterone and is restricted to the X-zone. *Endocrinology* 2007; 148: 976-988. 2006/11/24. DOI: 10.1210/en.2006-1100.
17. Cunliffe V and Trowsdale J. The molecular genetics of human chromosome 6. *J Med Genet* 1987; 24: 649-658. 1987/11/01. DOI: 10.1136/jmg.24.11.649.
18. Miller WL and Auchus RJ. The molecular biology, biochemistry, and physiology of human steroidogenesis and its disorders. *Endocr Rev* 2011; 32: 81-151. 2010/11/06. DOI: 10.1210/er.2010-0013.
19. Amor M, Tosi M, Duponchel C, et al. Liver mRNA probes disclose two cytochrome P-450 genes duplicated in tandem with the complement C4 loci of the mouse H-2S region. *Proc Natl Acad Sci U S A* 1985; 82: 4453-4457. 1985/07/01. DOI: 10.1073/pnas.82.13.4453.
20. Carroll MC, Campbell RD and Porter RR. Mapping of steroid 21-hydroxylase genes adjacent to complement component C4 genes in HLA, the major histocompatibility complex in man. *Proc Natl Acad Sci U S A* 1985; 82: 521-525. 1985/01/01. DOI: 10.1073/pnas.82.2.521.
21. White PC, Grossberger D, Onufer BJ, et al. Two genes encoding steroid 21-hydroxylase are located near the genes encoding the fourth component of complement in man. *Proc Natl Acad Sci U S A* 1985; 82: 1089-1093. 1985/02/01. DOI: 10.1073/pnas.82.4.1089.
22. Narasimhan ML and Khattab A. Genetics of congenital adrenal hyperplasia and genotype-phenotype correlation. *Fertil Steril* 2019; 111: 24-29. 2019/01/07. DOI: 10.1016/j.fertnstert.2018.11.007.
23. Chaplin DD, Galbraith LJ, Seidman JG, et al. Nucleotide sequence analysis of murine 21-hydroxylase genes: mutations affecting gene expression. *Proc Natl Acad Sci U S A* 1986; 83: 9601-9605. 1986/12/01. DOI: 10.1073/pnas.83.24.9601.
24. Parker KL, Chaplin DD, Wong M, et al. Expression of murine 21-hydroxylase in mouse adrenal glands and in transfected Y1 adrenocortical tumor cells. *Proc Natl Acad Sci U S A* 1985; 82: 7860-7864. 1985/12/01. DOI: 10.1073/pnas.82.23.7860.

25. White PC, New MI and Dupont B. Structure of human steroid 21-hydroxylase genes. *Proc Natl Acad Sci U S A* 1986; 83: 5111-5115. 1986/07/01. DOI: 10.1073/pnas.83.14.5111.
26. Rodrigues NR, Dunham I, Yu CY, et al. Molecular characterization of the HLA-linked steroid 21-hydroxylase B gene from an individual with congenital adrenal hyperplasia. *EMBO J* 1987; 6: 1653-1661. 1987/06/01. DOI: 10.1002/j.1460-2075.1987.tb02414.x.
27. White PC, Vitek A, Dupont B, et al. Characterization of frequent deletions causing steroid 21-hydroxylase deficiency. *Proc Natl Acad Sci U S A* 1988; 85: 4436-4440. 1988/06/01. DOI: 10.1073/pnas.85.12.4436.
28. White PC and Speiser PW. Congenital adrenal hyperplasia due to 21-hydroxylase deficiency. *Endocr Rev* 2000; 21: 245-291. 2000/06/17. DOI: 10.1210/edrv.21.3.0398.
29. Donohoue PA, Jospe N, Migeon CJ, et al. Two distinct areas of unequal crossingover within the steroid 21-hydroxylase genes produce absence of CYP21B. *Genomics* 1989; 5: 397-406. 1989/10/01. DOI: 10.1016/0888-7543(89)90002-5.
30. Gitelman SE, Bristow J and Miller WL. Mechanism and consequences of the duplication of the human C4/P450c21/gene X locus. *Mol Cell Biol* 1992; 12: 2124-2134. DOI: 10.1128/mcb.12.5.2124.
31. Tajima T, Fujieda K, Nakayama K, et al. Molecular analysis of patient and carrier genes with congenital steroid 21-hydroxylase deficiency by using polymerase chain reaction and single strand conformation polymorphism. *J Clin Invest* 1993; 92: 2182-2190. 1993/11/01. DOI: 10.1172/JCI116820.
32. Gotoh H, Sagai T, Hata J, et al. Steroid 21-hydroxylase deficiency in mice. *Endocrinology* 1988; 123: 1923-1927. 1988/10/01. DOI: 10.1210/endo-123-4-1923.
33. Gotoh H, Kusakabe M, Shiroishi T, et al. Survival of steroid 21-hydroxylase-deficient mice without endogenous corticosteroids after neonatal treatment and genetic rescue by transgenesis as a model system for treatment of congenital adrenal hyperplasia in humans. *Endocrinology* 1994; 135: 1470-1476. 1994/10/01. DOI: 10.1210/endo.135.4.7925109.
34. Riepe FG, Tatzel S, Sippell WG, et al. Congenital adrenal hyperplasia: the molecular basis of 21-hydroxylase deficiency in H-2(aw18) mice. *Endocrinology* 2005; 146: 2563-2574. 2005/02/26. DOI: 10.1210/en.2004-1563.
35. Perdomini M, Dos Santos C, Goumeaux C, et al. An AAVrh10-CAG-CYP21-HA vector allows persistent correction of 21-hydroxylase deficiency in a Cyp21(-/-) mouse model. *Gene Ther* 2017; 24: 275-281. 2017/02/07. DOI: 10.1038/gt.2017.10.
36. Tajima T, Okada T, Ma XM, et al. Restoration of adrenal steroidogenesis by adenovirus-mediated transfer of human cytochromeP450 21-hydroxylase into the adrenal gland of21-hydroxylase-deficient mice. *Gene Ther* 1999; 6: 1898-1903. 1999/12/22. DOI: 10.1038/sj.gt.3301018.
37. Tajima T, Ma XM, Bornstein SR, et al. Prenatal dexamethasone treatment does not prevent alterations of the hypothalamic pituitary adrenal axis in steroid 21-hydroxylase deficient mice. *Endocrinology* 1999; 140: 3354-3362. 1999/06/29. DOI: 10.1210/endo.140.7.6755.
38. Bornstein SR, Tajima T, Eisenhofer G, et al. Adrenomedullary function is severely impaired in 21-hydroxylase-deficient mice. *FASEB J* 1999; 13: 1185-1194. 1999/07/01. DOI: 10.1096/fasebj.13.10.1185.
39. Naiki Y, Miyado M, Horikawa R, et al. Extra-adrenal induction of Cyp21a1 ameliorates systemic steroid metabolism in a mouse model of congenital adrenal hyperplasia. *Endocr J* 2016; 63: 897-904. 2016/11/01. DOI: 10.1507/endocrj.EJ16-0112.
40. Markmann S, De BP, Reid J, et al. Biology of the Adrenal Gland Cortex Obviates Effective Use of Adeno-Associated Virus Vectors to Treat Hereditary Adrenal Disorders. *Hum Gene Ther* 2018; 29: 403-412. 2018/01/11. DOI: 10.1089/hum.2017.203.
41. Bongiovanni AM and Root AW. The adrenogenital syndrome. *N Engl J Med* 1963; 268: 1283-1289 contd. 1963/06/06. DOI: 10.1056/NEJM196306062682308.
42. Macapagal MC, Slowinska BS, Nimkarn S, et al. Gene therapy of 21-hydroxylase deficient mice utilizing an adeno-associated virus vector. *ENDO 2002: The Endocrine Society's 84th Annual Meeting*. San Francisco2002, p. 1-503.
43. Truett GE, Heeger P, Mynatt RL, et al. Preparation of PCR-quality mouse genomic DNA with hot sodium hydroxide and tris (HotSHOT). *Biotechniques* 2000; 29: 52, 54. 2000/07/25. DOI: 10.2144/00291bm09.
44. Wang Z and Storm DR. Extraction of DNA from mouse tails. *Biotechniques* 2006; 41: 410, 412. 2006/10/31. DOI: 10.2144/000112255.
45. Bielohuby M, Herbach N, Wanke R, et al. Growth analysis of the mouse adrenal gland from weaning to adulthood: time- and gender-dependent alterations of cell size and number in the cortical compartment. *Am J Physiol Endocrinol Metab* 2007; 293: E139-146. 2007/03/22. DOI: 10.1152/ajpendo.00705.2006.

46. Riepe FG, Tatzel S, Sippell WG, et al. Congenital Adrenal Hyperplasia: The Molecular Basis of 21-Hydroxylase Deficiency in H-2aw18Mice. *Endocrinology* 2005; 146: 2563-2574. DOI: 10.1210/en.2004-1563.
47. Azziz R, Wells G, Zacur HA, et al. Abnormalities of 21-hydroxylase gene ratio and adrenal steroidogenesis in hyperandrogenic women with an exaggerated 17-hydroxyprogesterone response to acute adrenal stimulation. *J Clin Endocrinol Metab* 1991; 73: 1327-1331. 1991/12/01. DOI: 10.1210/jcem-73-6-1327.
48. Napolitano E, Manieri C, Restivo F, et al. Correlation between genotype and hormonal levels in heterozygous mutation carriers and non-carriers of 21-hydroxylase deficiency. *J Endocrinol Invest* 2011; 34: 498-501. 2010/07/31. DOI: 10.3275/7225.

Chapter 4.1

AAV-delivered hepato-adrenal cooperativity in steroidogenesis: implications for gene therapy for congenital adrenal hyperplasia

4.1.1 Preface

This chapter has been published[1] and is reproduced here verbatim. The journal-formatted publication is included in the appendix.

Additional detail that was not included in the publication has been added to the chapter-specific methodology (Section 4.1.4.2.1), and the results have been moved to after the methodology for thesis structure. A figure legend has been added for the graphical abstract. Figures 4.1-3 and 4.1-8 are additional and were not included in the published manuscript.

4.1.2 Abstract

Despite the availability of life-saving corticosteroids for 70 years, treatment for adrenal insufficiency is not able to recapitulate physiological diurnal cortisol secretion and results in numerous complications. Gene therapy is an attractive possibility for monogenic adrenocortical disorders such as congenital adrenal hyperplasia; however, requires further development of gene transfer/editing technologies and knowledge of the target progenitor cell populations. Vectors based on adeno-associated virus are the leading system for direct in vivo gene delivery but have limitations in targeting replicating cell populations such as in the adrenal cortex. One strategy to overcome this technological limitation is to deliver the relevant adrenocortical gene to a currently targetable organ outside of the adrenal cortex. To explore this possibility, we developed a vector encoding human 21-hydroxylase and directed expression to the liver in a mouse model of congenital adrenal hyperplasia. This extra-adrenal expression resulted in reconstitution of the steroidogenic pathway. Aldosterone and renin levels normalized, and corticosterone levels improved sufficiently to reduce adrenal hyperplasia (Figure 4.1-1). This strategy could provide an alternative treatment option for monogenic adrenal disorders, particularly for mineralocorticoid defects. These findings also demonstrate, when targeting the adrenal gland, that inadvertent liver transduction should be precluded as it may confound data interpretation.

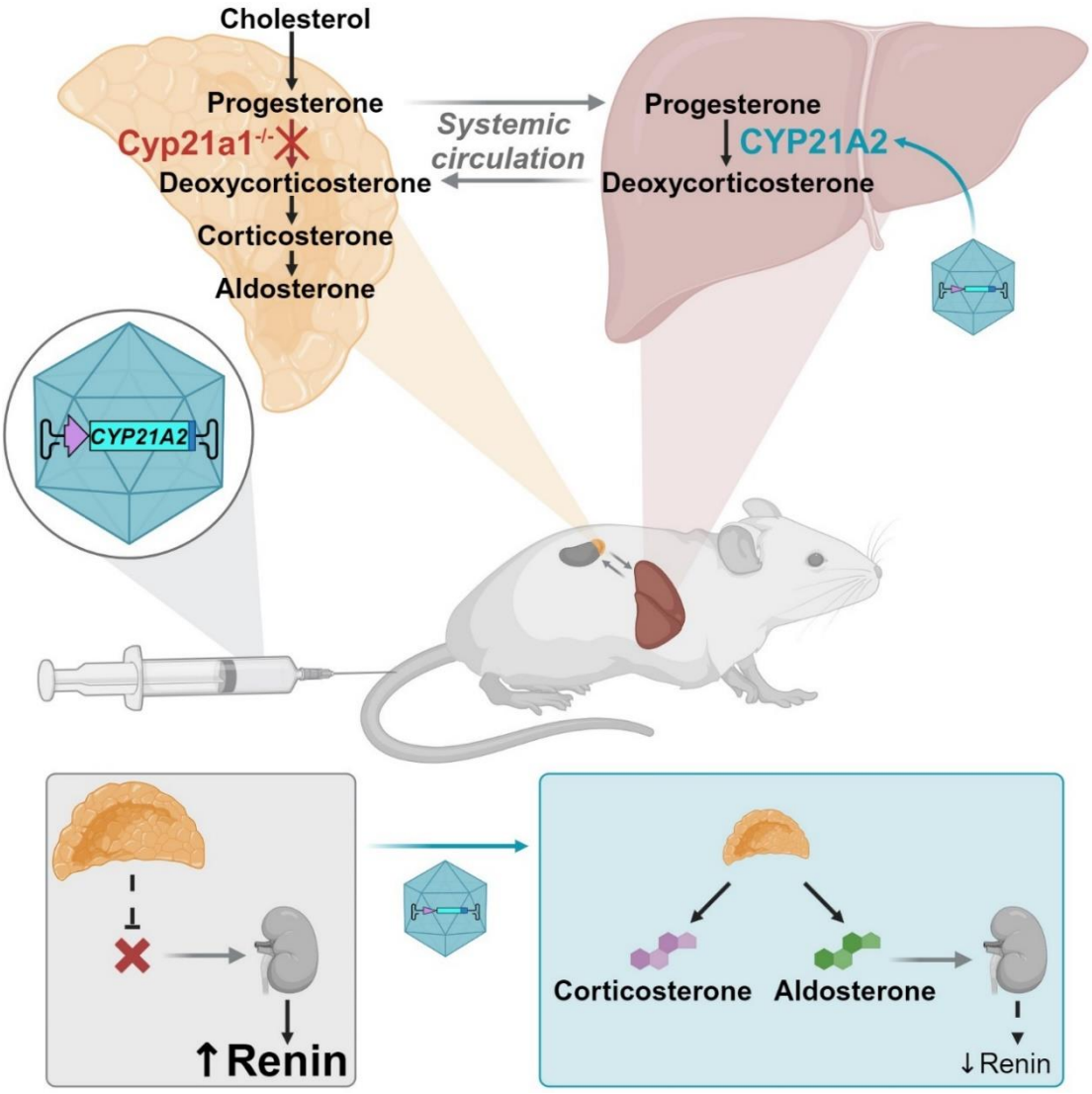

Figure 4.1-1 Graphical abstract.

In the absence of sufficient 21-hydroxylase function, excess progesterone accumulates, enters the systemic circulation and travels to the liver. Using rAAV to deliver specific hepatically expressed *CYP21A2*, this could convert the progesterone that reaches the liver to deoxycorticosterone, which could then re-enter the systemic circulation, and travel back to the adrenal gland to complete steroidogenesis. This resulted in improved corticosterone and aldosterone production with reduction in adrenal size and renin expression.

4.1.3 Introduction

Little has changed in the treatment for congenital adrenal hyperplasia (CAH) since exogenous steroids were first introduced 70 years ago.[2-4] CAH encompasses seven monogenic disorders of the adrenal that disrupt enzymatic function and result in a deficiency of one or more adrenal steroids with compensatory adrenal hyperplasia secondary to adrenocorticotropic hormone (ACTH) stimulation.[5] Deficiency of 21-hydroxylase is the most common cause of CAH with a global incidence of classical salt-wasting CAH estimated to be between 1 in 10,000 to 1 in 22,000.[6-8] There is resultant deficiency of cortisol and aldosterone, and upstream precursor steroids are shunted along the 17-hydroxylase-facilitated pathway to form adrenal androgens in excess causing pre- and postnatal virilization.[5] While exogenous corticosteroids are life-saving, treatment is far from perfect and cannot mimic the diurnal rhythm and physiological control of cortisol secretion, resulting in intervals of over- and undertreatment within a 24-h period. Adrenal crisis remains the most common cause of death and there is shorter life expectancy in those with CAH than the general population.[9]

Superior treatment options are needed to overcome the burden of disease in CAH.[10] As current standard management is imperfect, alternative and adjunctive treatment options have been explored, including subcutaneous hydrocortisone pumps[11, 12] and modified-release once-daily hydrocortisone.[13, 14] Neither of these alternatives is ideal, as pump management is complex and the modified-release hydrocortisone has not been shown to be superior to standard management.[15] Recent success with gene therapy for conditions such as spinal muscular atrophy has paved the way for other genetic treatments.[16] There is a paucity of gene therapy studies targeting the adrenal cortex, despite publication of the first pre-clinical gene therapy study for CAH over 20 years ago.[10] The murine adrenal

cortex lacks 17-hydroxylase expression so does not produce adrenal androgens, and the major glucocorticoid in the mouse is corticosterone[17]: thus in the 21-hydroxylase-deficient mouse model, serum progesterone levels are elevated rather than 17-hydroxyprogesterone (17OHP).[18] While there is no hyperandrogenism, the model otherwise appropriately recapitulates the human classical salt-wasting CAH phenotype with inadequate glucocorticoid and mineralocorticoid production to sustain neonatal life. Murine studies using intra-adrenal or intravenous delivery of a viral vector with 21-hydroxylase cDNA has demonstrated short-term improvement in progesterone.[19-21] Based on these pre-clinical studies a human clinical trial is now under way using a gene addition strategy with rAAV5-CYP21A2 (ClinicalTrials.gov: NCT04783181).

However, these studies do not address the rapid cellular turnover in the adrenal cortex. The recombinant adeno-associated virus (rAAV) genome is maintained predominantly as extra-chromosomal episomes that are lost during cellular replication. Therefore, a gene addition strategy using rAAV will not provide a lasting effect.[21, 22] Furthermore, the development of neutralizing antibodies currently limits the use of rAAV therapy to a single treatment.[23, 24] For durable adrenal-directed gene therapy, the new genetic material must be integrated into the genome of adrenocortical progenitor cells, a feat that is beyond current technology due to difficulties in targeting this cell population.[10] One strategy that could overcome this technological limitation is to deliver ectopic expression of 21-hydroxylase in a readily targetable organ outside of the adrenal cortex. We explored this theoretical possibility by developing an rAAV encoding human 21-hydroxylase (*CYP21A2*) and directing expression specifically to the liver in a mouse model of CAH. We hypothesized that hepatically expressed human *CYP21A2* could participate in steroidogenesis and facilitate downstream adrenal production of corticosterone and

aldosterone (Figure 4.1-2A). We found that extra-adrenal expression of a deficient adrenocortical enzyme could indeed co-operatively reconstitute adrenal steroidogenesis.

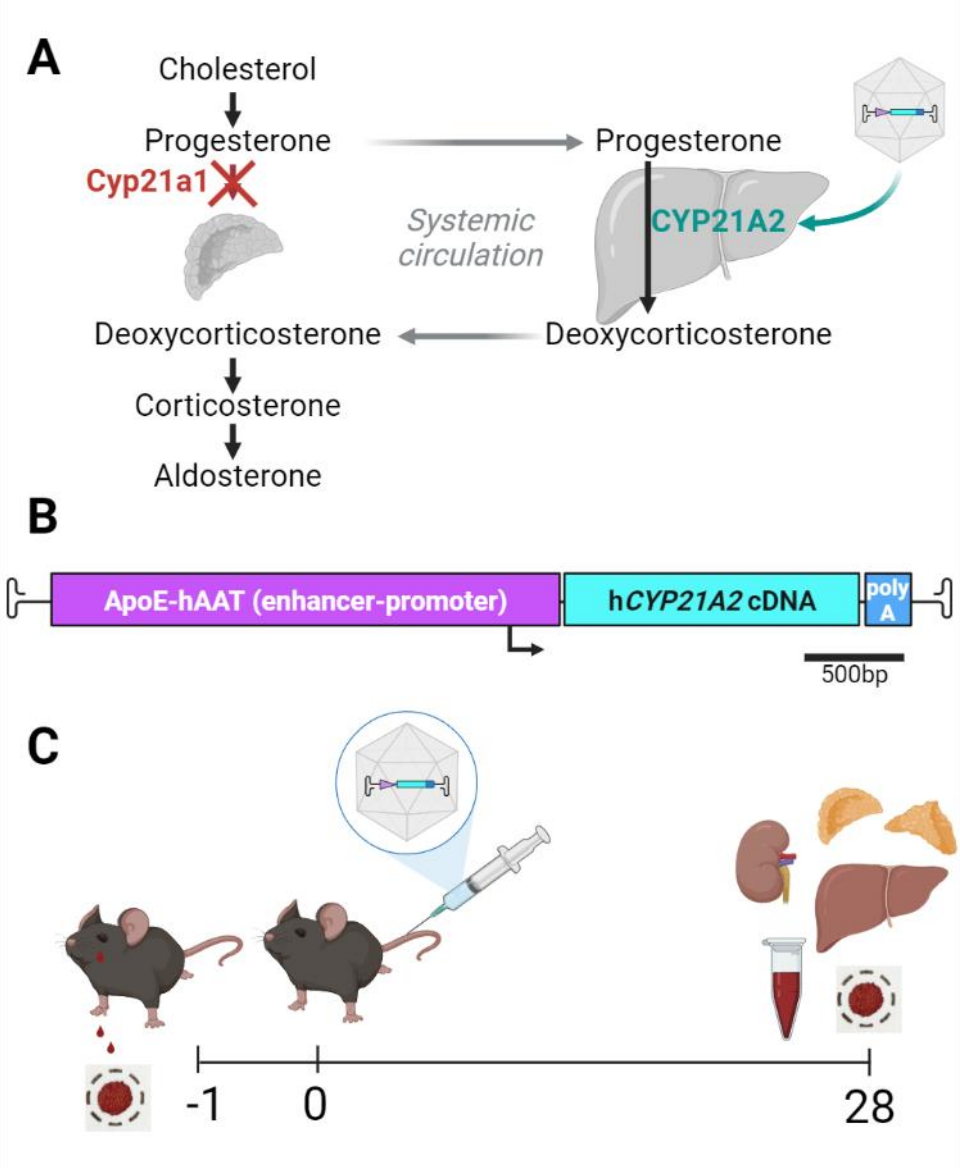

Figure 4.1-2 Study set up to assess hepato-adrenal cooperativity in steroidogenesis. **A.** Hypothesis: in 21-hydroxylase deficiency, the precursor steroid (progesterone in the mouse, 17-hydroxyprogesterone in the human) accumulates and enters the systemic circulation where it will circulate to the liver. Recombinant AAV-derived human 21-hydroxylase expressed in the liver will convert progesterone to deoxycorticosterone, which will then enter the systemic circulation, reaching the adrenal gland. Enzymes downstream of 21-hydroxylase will be unaffected and will be able to complete steroidogenesis. **B.** Recombinant AAV vector genome; liver-specific enhancer-promoter (ApoE-hAAT), human 21-hydroxylase cDNA (h*CYP21A2*), and bovine growth hormone poly-adenylated tail (polyA). The scale bar represents 500 base pairs. **C.** Prior to treatment, dried whole blood was collected on to filter paper. Mice (n = 5 male, n = 5 female) were administered the purified vector intravenously via the tail vein and harvested 4 weeks later. AAV, adeno-associated virus.

4.1.4 Methods

4.1.4.1 Animal procedures

All animal care and experimental procedures were evaluated and approved by the joint Children's Medical Research Institute and The Children's Hospital at Westmead Animal Care and Ethics Committee (Project C381). The C57BL/10SnSlc-H-2^{aw18} mouse model was kindly provided by Toshihiko Shiroishi (National Institute of Genetics) and the RIKEN BRC through the National BioResource Project of the Ministry of Education, Culture, Sports, Science and Technology, Japan. The H-2^{aw18} mouse model has 21-hydroxylase deficiency, which is neonatally lethal.[25] Heterozygous (H-2$^{b/aw18}$; *Cyp21a1*$^{+/-}$) mice were bred to produce homozygous (H-2^{aw18}, *Cyp21a1*$^{-/-}$) offspring. Exogenous steroid rescue was required for survival of the homozygous offspring. Exogenous steroid rescue was required for survival of the homozygous offspring. Dams were examined daily to determine the presence of a vaginal plug, indicating E0.5. All dams received 5 µg of dexamethasone (Ilium Dexason, Troy Animal Healthcare) subcutaneously daily from gestational day 18 until the birth. Day 19 was the most common day of delivery in this colony. All pups received 10 µg corticosterone and 0.05 µg fludrocortisone subcutaneously from birth second daily until 3 weeks of age. Once genotype was available, steroid treatment was ceased prior to 3 weeks of age in non-homozygous pups. Genotype was determined using a PCR-based assay with genomic DNA from toe removal during identification at 9 days of age. Dams, pups, and weaned *Cyp21a1*$^{-/-}$ mice were provided with table rock salt thrice weekly. *Cyp21a1*$^{-/-}$ pups were weaned to small groups with other *Cyp21a1*$^{-/-}$ animals from the same litter or a single non-homozygous littermate to avoid resource competition. Animals were maintained with 12-h light/dark cycles with free access to standard mouse chow and water.

With exogenous steroid rescue, 35%–50% of *Cyp21a1*$^{-/-}$ offspring survived the neonatal period with the higher survival rate seen with experienced dams. This is higher than the previously published 12% survival rate.[20] *Cyp21a1*$^{-/-}$ males outnumbered *Cyp21a1*$^{-/-}$ females in the surviving offspring approximately 2:1, implying a survival advantage in males or disadvantage in females. Female mice are known to have higher serum corticosterone levels than males[26] so the corticosterone deficiency may have had a more profound effect on female mice due to an increased absolute requirement. The median bilateral adrenal mass was 2.6 times greater in *Cyp21a1*$^{-/-}$ females and 3.4 times greater in *Cyp21a1*$^{-/-}$ males compared with wild-type adrenals.

Prior to injection, a whole blood spot was collected on filter paper between 2 and 4 p.m. from a conscious submandibular bleed. Adult *Cyp21a1*$^{-/-}$ mice received the rAAV8-CYP21A2 vector at a dose of 5×10^{11} vgc/mouse intravenously via the tail vein. Four weeks later the treated *Cyp21a1*$^{-/-}$ animals were harvested between 2 and 4 p.m (Figure 4.1-2C). The same method was used to harvest untreated *Cyp21a1*$^{-/-}$ and wild-type (H-2^{b}, *Cyp21a1*$^{+/+}$) controls. The mice were anesthetized using isoflurane (3%–5%) to facilitate open cardiac puncture for blood collection. Blood was collected on filter paper and the remaining spun down to collect serum that was stored at −80°C until analysis. Following exsanguination, the animal was terminated with cervical dislocation and tissues harvested. Tissues for biochemical and molecular analysis were snap frozen in liquid nitrogen and stored at −80°C. Samples for immunohistochemistry were fixed in 4% (w/v) PFA overnight at 4°C and then underwent a sucrose gradient until embedding in optimal cutting temperature compound and snap frozen in isopentane chilled in liquid nitrogen.

4.1.4.2 Vector construction and production

4.1.4.2.1 Generating rAAV vector encoding hCYP21A2

The plasmids used for the construction of the CYP21A2 expression vector are listed in Table 2-6. The human *CYP21A2* cDNA (GenBank: NM_000500.9) was cloned into an AAV2 backbone that had an ApoE-hAAT enhancer-promoter (liver-specific) that was provided by S. Cunningham[22] (Figures 4.1-2B and 4.1-3).

To achieve this, the h*CYP21A2* cDNA (GenBank NM_000500.9) was amplified from a GenScript ORF clone plasmid using Q5 DNA polymerase. The forward primer (LGcons1_007, 5'-TATGATATCGCGGCCGCGCCACCATGCTGCTCCTGGG-3') included *Eco*RV and *NotI* sites, followed by a Kozak sequence and the 5' end of the coding sequence for the h*CYP21A2* cDNA and the reverse primer (LGcons1_004, 5'-TATGATATCTCACTGGCTCTGGCCCGGGCTG- 3') contained an *Eco*RV site and stop codon followed by a reverse complement sequence to 3' end of the h*CYP21A2* cDNA.. The PCR product was A-tailed and then ligated into a pGEM®-T Easy cloning vector with T4 DNA ligase, and bacterially propagated in transformed DH5α cells. The insert was confirmed to be correct through restriction digestion and Sanger sequencing. Purified plasmid was digested with *Not*I and *Eco*RV and the h*CYP21A2* fragment that now also included cloning sites and a stop codon was purified from electrophoresis gel. The recipient AAV2 vector backbone was prepared by digesting out the existing h*OTC* transgene with *Not*I and *Eco*RV and purifying the backbone from an electrophoresis gel. The h*CYP21A2* fragment was then ligated into the prepared recipient backbone using T4 DNA ligase. The resulting plasmid, designated pAAV2.ApoEhAAT.hCYP21A2 was amplified by transforming chemically competent *E. coli* (DH5α) using heat shock and bacterial culture. Plasmid DNA was purified using a commercial kit (Nucleobond Xtra

Maxi Kit, Macherey-Nagel). pAAV2.ApoEhAAT.CYP21A2 contained an AAV expression cassette of 4729 bp in length which included flanking AAV2 ITRs. Presence of the correct insert and ITRs was confirmed with restriction digestion with *Eco*RV, *Not*I, *Ava*I, and *Msc*I.

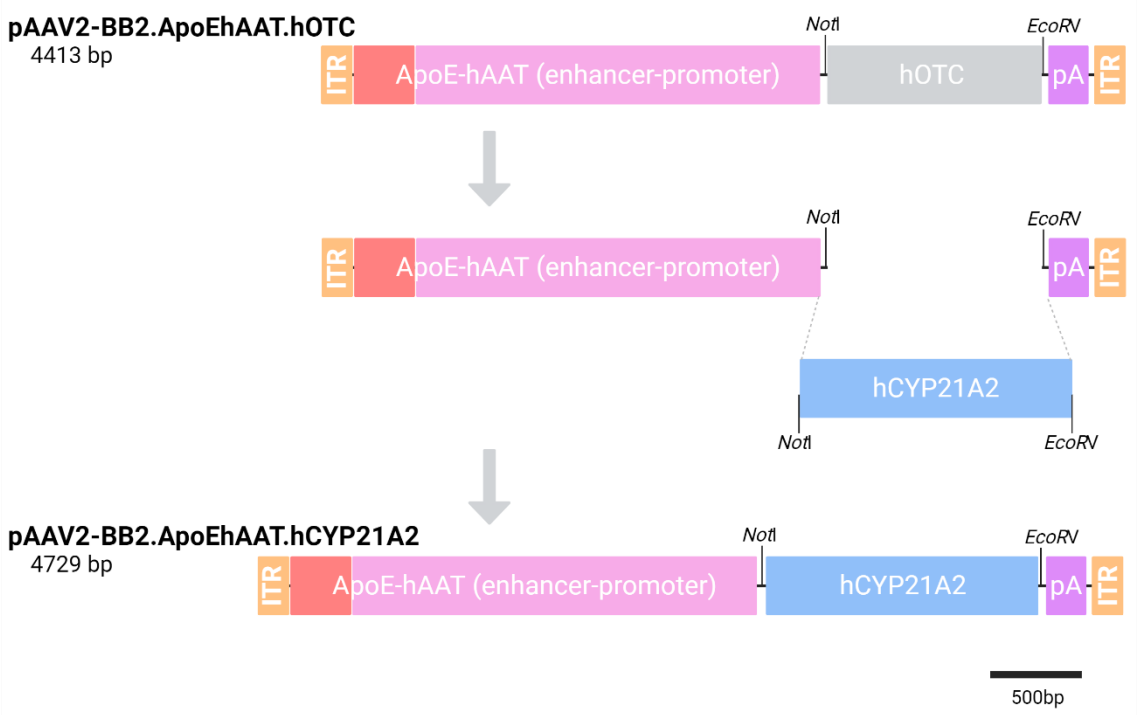

Figure 4.1-3 Molecular subcloning to generate the CYP21A2 vector plasmid.
Flow diagram of molecular subcloning steps taken to generate pAAV2-BB2.ApoEhAAT.hCYP21A2. pAAV2-BB2.ApoEhAAT.hOTC was digested with NotI and EcoRV to remove the human OTC transgene. Human *CYP21A2* was prepared using pGEM T Easy (not shown). The prepared human *CYP21A2* transgene was ligated to the backbone. AAV2 ITRs (orange) flank the transgene expression cassette. The expression cassette contains the liver-specific enhancer/promoter, ApoE hAAT (red and pink), human CYP21A2 transgene (blue), bovine growth hormone polyadenylation tail (pA, purple). Scale bar = 500 bp.

4.1.4.2.2 Vector production

The vector was packaged by triple transfection of human embryonic kidney 293 cells, as previously described,[22] and was pseudo-serotyped with the AAV8 capsid (rAAV2/8). Vector particles were purified from cell lysate using standard cesium chloride gradient centrifugation. Titer was assigned using digital droplet PCR (C1000 Touch Thermal Cycler #1851196 and QX200 Droplet Reader #1864003, BioRad) using primers specific for the bovine growth hormone polyadenylation tail signal (Table S4.1-1) with QX200 ddPCR EvaGreen Supermix (BioRad 1864034). The conditions were 95°C for 5 min, 40 cycles of 95°C for 30 s and 60°C for 1 min, followed by 4°C for 5 min, 90°C for 5 min.

4.1.4.3 Immunohistochemistry

Frozen liver sections (5 μm) were permeabilized in methanol and then 0.1% (v/v) Triton X-100. They were then blocked with 10% (v/v) donkey serum and 10% (v/v) fetal bovine serum in phosphate buffered saline without magnesium or calcium (PBS). After washing with 0.1% (v/v) Tween 20, the sections were incubated overnight with the rabbit primary CYP21A2 antibody (Abcam ab230327) diluted 1:50. After washing with 0.1% (v/v) Tween 20, the sections were incubated with the secondary antibody (AlexaFluor Donkey anti-rabbit 594, Invitrogen A32754) diluted 1:500, and then counterstained with DAPI, diluted to 0.03 μg/mL.

4.1.4.4 Vector copy number determination

Genomic DNA was extracted from frozen liver using a standard phenol-chloroform extraction method. It was digested with restriction enzyme HindIII-HF (New England BioLabs R3104L).

Vector copy number (vcn) was determined using digital droplet PCR (C1000 Touch Thermal Cycler #1851196 and QX200 Droplet Reader #1864003, BioRad) using primers specific for human CYP21A2 and murine albumin (Table S4.1-1) with QX200 ddPCR EvaGreen Supermix (BioRad 1864034). The conditions were 95°C for 5 min, 40 cycles of 95°C for 30 s and 60°C for 1 min, followed by 4°C for 5 min, 90°C for 5 min. The CYP21A2 count was normalized to two copies of murine albumin to determine vcn/diploid nucleus.

4.1.4.5 Quantitative real-time PCR

RNA was extracted using the Purelink RNA Mini Kit (Invitrogen 12183018A) and stored at −80°C. cDNA was generated from extracted RNA using the SuperScript IV First-Strand Synthesis System (Invitrogen 18091050) using the Oligo $d(T)_{20}$ primer and stored at −20°C. Primers were used to detect gene expression for *CYP21A2* (normalized to murine albumin as the reference transcript) in liver, *Ren1* (normalized to *Tbp* as the reference transcript) in kidney and *Mc2r*, the ACTH receptor (normalized to *Tbp*) in adrenal cDNA, (Table S4.1-1). TB Green Premix Ex Taq II (Takara RR82WR) was used in the reaction with conditions as follows: 95°C for 30 s, 40 cycles of 95°C for 5 s, 60°C for 20 s, and 76°C for 10 s followed by melt 60°C–95°C (Qiagen Rotor-Gene Q).

4.1.4.6 Steroid profiles

4.1.4.6.1 Serum aldosterone, corticosterone and progesterone

The steroid calibrators, controls, and isotopically labeled internal standard mix were obtained from Chromsystems Instruments & Chemicals Gmbh, Germany. The Optima

LC-MS grade solvents including water, methanol, methyl t-butyl ether, acetonitrile, and formic acid were obtained from Fisher Chemicals, UK. Internal standard solution was added to calibrators, controls, and test samples and organic solvents were used for extraction. The extract supernatants were evaporated to dryness under nitrogen in a 37°C water bath. After evaporation, the extracted steroids were reconstituted in 50% methanol. Steroids were analyzed by ultra performance liquid chromatography-tandem mass spectrometry (UPLC-MSMS) using validated in-house developed methods (Waters Acquity UPLC and Xevo TQ-S mass spectrometer).

4.1.4.6.2 Whole blood corticosterone

The dried blood spot samples were collected onto filter paper and were extracted using an organic solvent (95% methanol) containing deuterated internal standards for each steroid. Whole blood corticosterone was measured using liquid chromatography-tandem mass spectrometry (Waters Xevo TQ-S with Acquity UPLC system).

4.1.4.7 ACTH ELISA

ACTH was measured after thawing snap frozen serum using the Mouse/Rat ACTH SimpleStep ELISA Kit as per manufacturer instructions (Ab263880, Abcam).

4.1.4.8 Statistical analysis

GraphPad Prism 9 was used for statistical analysis and graph production. Non-parametric statistical methods including the Mann-Whitney *U* test were used.

4.1.5 Results

4.1.5.1 Expression of human *CYP21A2* in murine liver following rAAV-mediated delivery

An rAAV2/8 vector utilizing a liver-specific promoter with the human *CYP21A2* cDNA (Figure 4.1-2B) was intravenously delivered to 21-hydroxylase-deficient (C57BL/10SnSlc-H-2^{aw18}; *Cyp21a1*$^{-/-}$) adult mice, homozygous for a pathogenic variant in *Cyp21a1*, at a dose of 5×10^{11} vector genomes per mouse (Figure 4.1-2C). Four weeks after administration, liver transduction was confirmed by vector copy number (vcn) per diploid nucleus and vector encoded mRNA detected in the livers of treated *Cyp21a1*$^{-/-}$ mice (Figure 4.1-4A, and B, respectively, and Table S4.1-2). The median vcn/diploid nucleus was similar in males and females; however, there was 3-fold higher vector transcription into mRNA in males than females, as expected.[27] In both sexes, the mouse with the lowest vcn/diploid nucleus had the lowest mRNA transcription (Figure 4.1-4C). Protein translation was demonstrated by immunohistochemical staining for CYP21A2 (Figure 4.1-4D). While human *CYP21A2* mRNA was detectable in the treated *Cyp21a1*$^{-/-}$ mouse adrenals, levels were 300- to 800-fold lower than native *Cyp21a1* mRNA in wild-type (*Cyp21a1*$^{+/+}$) adrenals (Figure S4.1-7A).

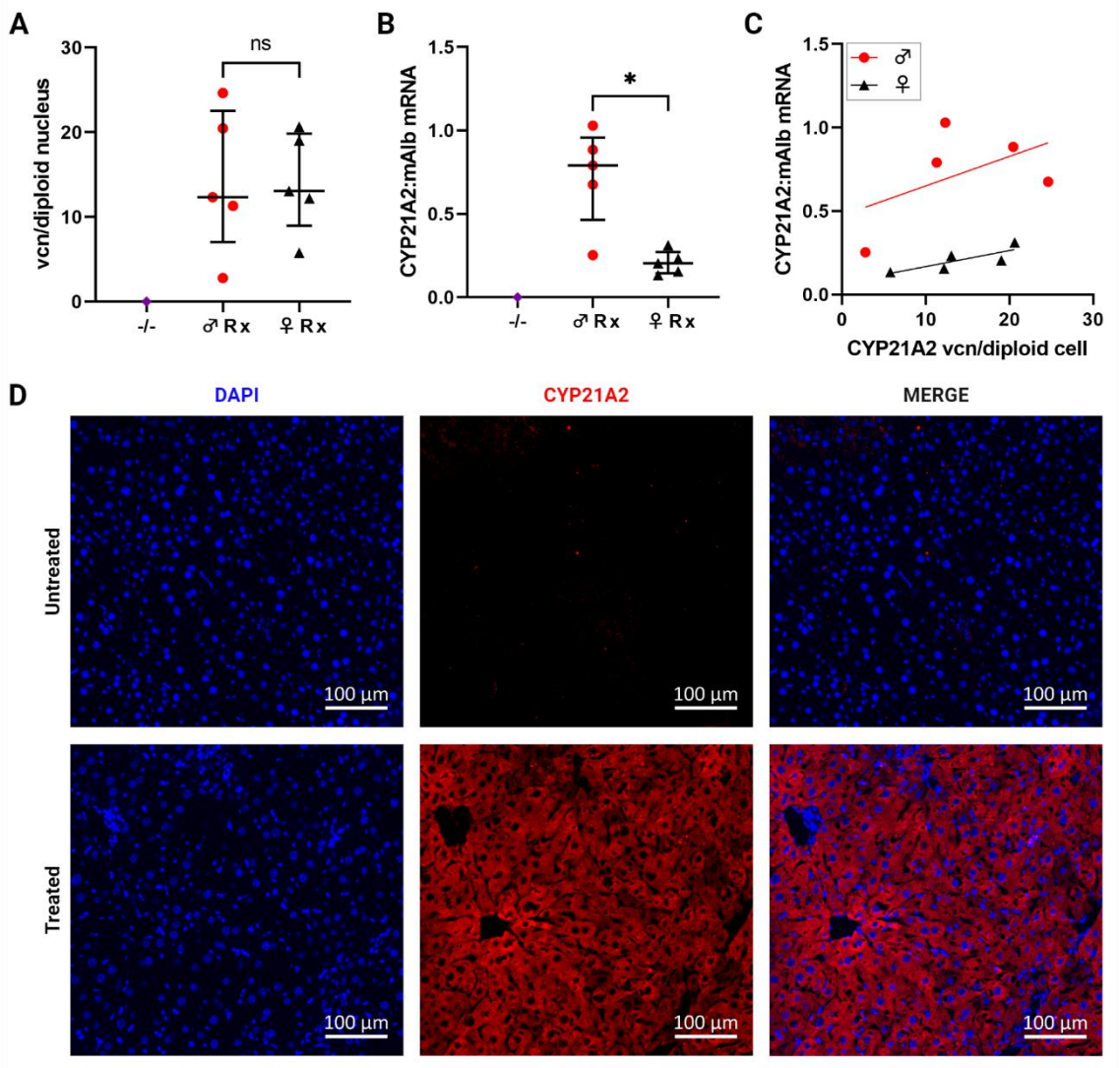

Figure 4.1-4 Robust delivery to and expression of human *CYP21A2* in the murine liver.

A. Vector DNA detected in the livers of treated mice. **B.** The ratio of vector-derived mRNA transcripts to murine albumin transcripts. **C.** Vector copy number vs. vector expression in males (red) and females (black). **D.** IHC staining demonstrated CYP21A2 protein (red) in the liver from a representative treated male −/− mouse with 20.5 vcn/diploid nucleus and transcript mRNA ratio 0.88. Scale bar represents 100 µm. DAPI nuclear staining in blue. vcn, vector copy number; IHC, immunohistochemistry; −/−, homozygous 21-hydroxylase deficiency; ♂, male; ♀, female; Rx, homozygous 21-hydroxylase deficient mice that were treated with vector; *CYP21A2*, human 21-hydroxylase; mAlb, murine albumin; ns, not significant. Individual data points are shown, and error bars represent median and interquartile range. $*p < 0.05$ on Mann-Whitney *U* test.

4.1.5.2 Human *CYP21A2* expression in the liver co-operatively improved adrenal steroidogenesis

Serum aldosterone in the vector-treated *Cyp21a1*$^{-/-}$ mice was restored to *Cyp21a1*$^{+/+}$ levels (Figure 4.1-5A; Table S4.1-2). Serum corticosterone in the treated *Cyp21a1*$^{-/-}$ mice was increased 4- to 5-fold compared with untreated *Cyp21a1*$^{-/-}$ controls; however *Cyp21a1*$^{+/+}$ serum corticosterone levels were not achieved following vector administration (Figure 4.1-5B; Table S4.1-2). *Cyp21a1*$^{+/+}$ females had 2-fold higher serum corticosterone than their *Cyp21a1*$^{+/+}$ male counterparts, as has been previously demonstrated by other researchers.[26] The change in individual dried whole blood corticosterone improved in all but one *Cyp21a1*$^{-/-}$ mouse (Figure 4.1-5C). Although this mouse had the lowest vcn/diploid nucleus, lowest vector expression among the males, and lowest serum corticosterone (69.8 nmol/L), vcn/diploid nucleus did not always correlate with steroidogenic effect in other treated mice. Progesterone improved in the treated *Cyp21a1*$^{-/-}$ female mice but there was no change in the *Cyp21a1*$^{-/-}$ male progesterone levels (Figure 4.1-5D; Table S4.1-2). The progesterone remained 17- and 35-fold higher in *Cyp21a1*$^{-/-}$ females and males than *Cyp21a1*$^{+/+}$ levels, respectively.

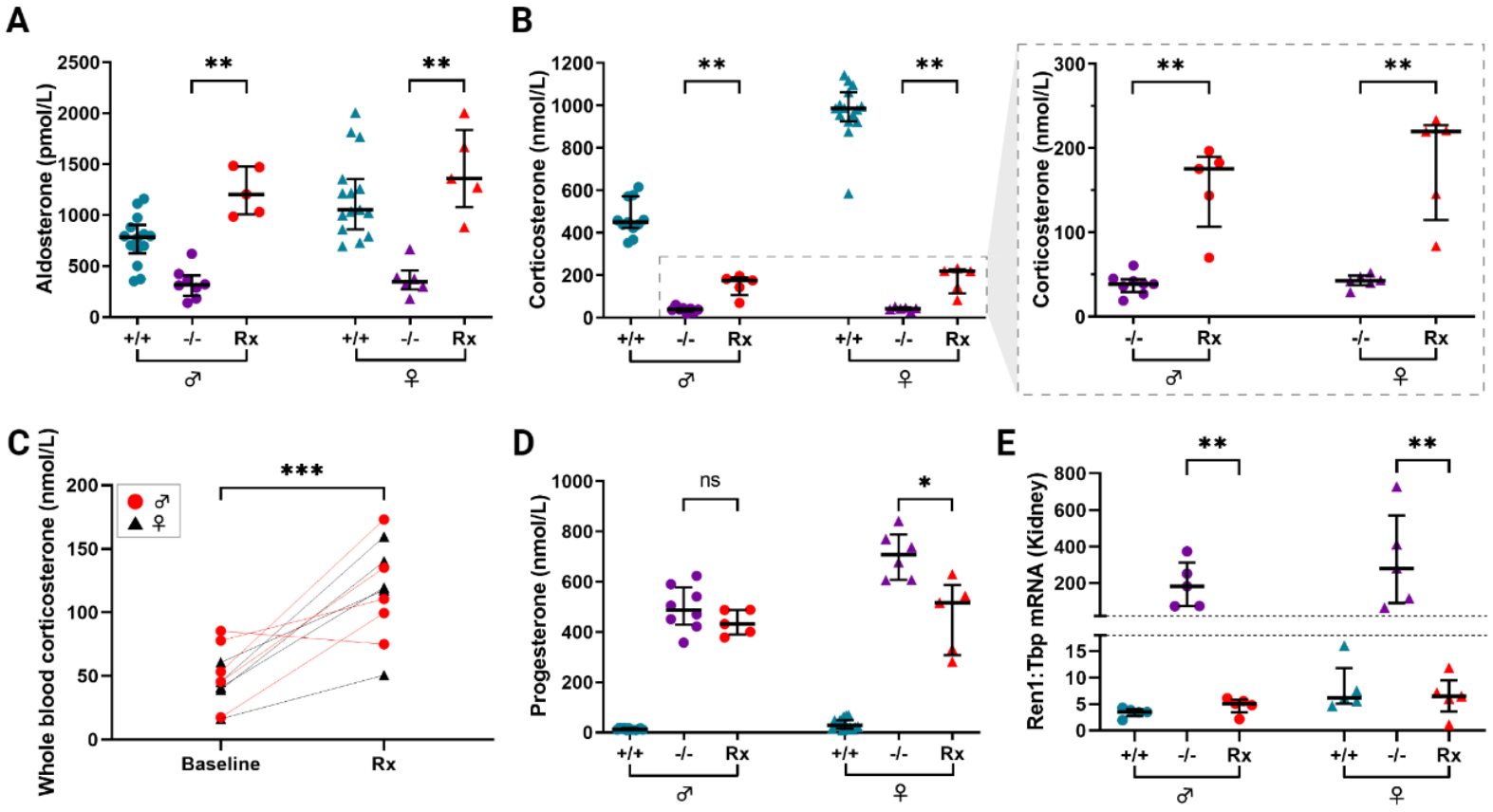

Figure 4.1-5 Improvement in steroidogenesis following hepatic *CYP21A2* expression.

A. Serum aldosterone. **B.** Serum corticosterone. In the call-out box, +/+ controls were removed to demonstrate more clearly the change in serum corticosterone levels in −/− treated vs. −/− untreated. **C.** Dried whole blood corticosterone before treatment and at harvest in males (red) and females (black). **D.** Serum progesterone. **E.** Renin expression demonstrated as the ratio of renal renin (*Ren1*) mRNA transcripts to *Tbp* transcripts. +/+, wild-type 21-hydroxylase sufficiency; −/−, homozygous 21-hydroxylase deficiency; ♂, male; ♀, female; Rx, homozygous 21-hydroxylase deficient mice that were treated with vector; *Ren1*, renin; *Tbp*, TATA-box binding protein; ns, not significant. Individual data points are shown, and error bars represent median and interquartile range. ∗p < 0.05; ∗∗p < 0.01 on Mann-Whitney *U* test. ∗∗∗p < 0.001 on two-way ANOVA.

4.1.5.3 Renin expression normalised and adrenal hyperplasia reduced following human *CYP21A2* expression in the liver

Given that renin increases in response to reduced renal perfusion and reduced tubular sodium content to activate the renin-angiotensin-aldosterone system,[28, 29] renin (*Ren1*) expression was measured as a marker of mineralocorticoid function. *Ren1* mRNA expression in the kidneys was normalized to TATA-box binding protein (*Tbp*) mRNA as the chosen reference housekeeping transcript.[20, 30-32] Renin expression was 25- to 30-fold higher in untreated *Cyp21a1*$^{-/-}$ mice compared with *Cyp21a1*$^{+/+}$. Renin expression in *Cyp21a1*$^{-/-}$ mice was restored to *Cyp21a1*$^{+/+}$ levels following treatment with the vector (Figure 4.1-5E, Table S4.1-2).

Female mice are known to have larger adrenal glands than males.[26] This pattern remained consistent in the *Cyp21a1*$^{-/-}$ mice with the bilateral adrenal mass 20% higher in *Cyp21a1*$^{-/-}$ females than *Cyp21a1*$^{-/-}$ males. *Cyp21a1*$^{-/-}$ females had adrenal mass 2.6-fold larger than *Cyp21a*$^{+/+}$ females and *Cyp21a1*$^{-/-}$ male adrenal mass was 3.2-fold larger than *Cyp21a1*$^{+/+}$ male adrenal mass. While the effect on corticosterone was partial, there was a reduction in size of the bilateral adrenal mass by one-third following treatment in both *Cyp21a1*$^{-/-}$ males and females (Figure 4.1-6A, Table S4.1-2). The bilateral adrenal mass was also measured as a percentage of the total body mass to account for any variation in body size and the reduction in adrenal size persisted (Figure S4.1-7B). Upon direct macroscopic examination, the adrenal glands from the treated *Cyp21a1*$^{-/-}$ animals were collapsed and flat, consistent with a reduction in volume, compared with the round untreated *Cyp21a1*$^{-/-}$ glands. The difference was visible macroscopically (Figure 4.1-6B). There was no change in the histological architecture of the adrenal cortex following

treatment (Figure S4.1-8).

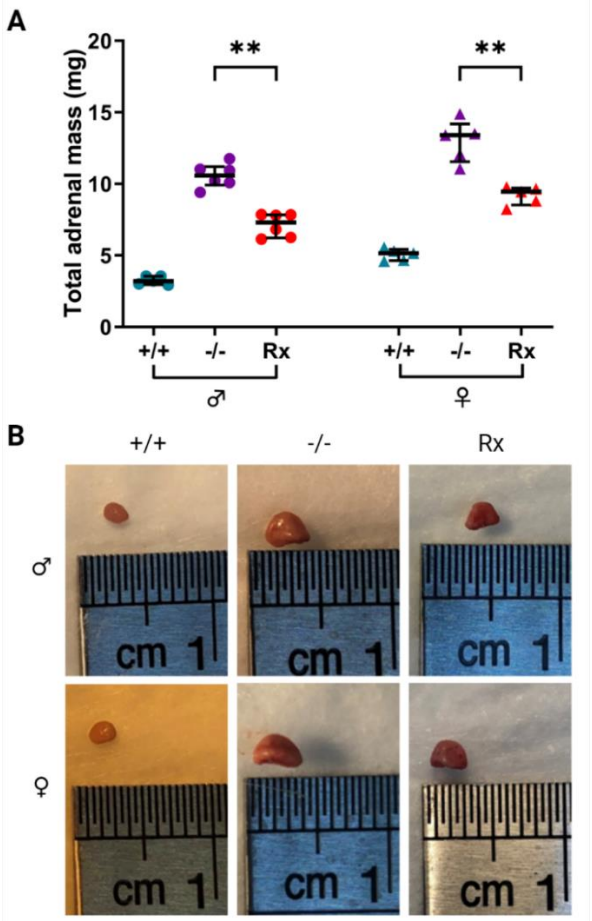

Figure 4.1-6 Reduction in adrenal hyperplasia after hepatic *CYP21A2* expression. **A.** Absolute bilateral adrenal mass. **B.** Macroscopic photographs of representative adrenal glands after fat dissection. +/+, wild-type 2-hydroxylase sufficiency; −/−, homozygous 21-hydroxylase deficiency; ♂, male; ♀, female; Rx, homozygous 21-hydroxylase-deficient mice that were treated with vector. Individual data points are shown, and error bars represent as median and interquartile range. ∗∗p < 0.01 on Mann-Whitney *U* test.

Blood was collected during exsanguination causing physiological stress. The difference in maximal ACTH secretion in the treated *Cyp21a1*$^{-/-}$ mice was not statistically significant compared with the untreated *Cyp21a1*$^{-/-}$ mice (Figure S4.1-7C). Due to the short half-life of ACTH, expression of the ACTH receptor (*Mc2r*) was also examined. Although the expression of *Mc2r* did not change in the female mice following treatment, expression was reduced by 28% in treated *Cyp21a1*$^{-/-}$ male mice compared with untreated *Cyp21a1*$^{-/-}$ (Figure S4.1-7C).

4.1.6 Discussion

The adrenal cortex is an attractive gene therapy target, but its challenging biological properties have yet to be surmounted by contemporary gene delivery technology. Adeno-associated virus has natural tropism for the liver and is a logical target for gene therapies. Our approach exploits this characteristic with good clinical effect. This study demonstrated that extra-adrenal expression of human *CYP21A2* facilitated by rAAV gene delivery to the liver successfully conferred hepato-adrenal co-operativity in steroidogenesis resulting in significant phenotypic correction in a 21-hydroxylase-deficient mouse. In adults with completed liver growth, this strategy overcomes the limitations imposed by adrenocortical cellular turnover, rAAV gene delivery, and targeting stem/progenitor cell populations that are not fully characterized.[10, 21] Mineralocorticoid function was restored and glucocorticoid production improved. This is the first study that has looked at the effect of rAAV-mediated adrenocortical gene delivery to the liver. Based on these data, this strategy could provide a treatment option for mineralocorticoid disorders such as aldosterone synthase deficiency; however, requires further development for use in disorders that impact glucocorticoid production. This study also highlights a need for caution in the interpretation of the effects of systemically administered therapies that may result from inadvertent liver transduction.

The clinically relevant outcomes of our strategy include improved steroidogenesis with subsequent phenotypic benefit. Restoration of aldosterone production would likely result in resolution of the salt-wasting component of the phenotype and therefore could improve the clinical phenotype from severe salt-wasting to simple virilizing CAH. This is important as the most severe form, salt-wasting CAH, has a higher mortality rate than milder phenotypes.[33] While blood pressure and urine sodium were unable to be measured,

renin expression was considered an appropriate surrogate marker for mineralocorticoid function. Following normalization of aldosterone production, renin expression in the kidney also normalized. The aldosterone likely allowed appropriate salt retention, which removed stimulation on the renin-angiotensin-aldosterone system and thus increased renin expression was no longer required.

Aldosterone is produced in picomolar serum concentrations, whereas corticosterone is produced in nanomolar concentrations. This means the amount of aldosterone required for physiological normalization is 1,000-fold less than corticosterone and is therefore more achievable. Corticosterone production improved 4- to 5-fold in the treated *Cyp21a1*$^{-/-}$ mice compared with untreated *Cyp21a1*$^{-/-}$ mice. However, it was still only 40% of wild-type level in males and 22% of wild-type level in females. Despite the corticosterone production not reaching wild-type levels, the increased corticosterone production was sufficient to reduce the hypothalamic-pituitary-adrenal axis stimulation, demonstrated by a reduction in adrenal size. As the serum was collected during a terminal procedure, the ACTH level detected was the maximum secretory capacity. When the pituitary is subject to chronic corticotropic releasing hormone stimulation from the hypothalamus, the pituitary ACTH-producing corticotrophic cells undergo hyperplasia.[34] ACTH secretion is biphasic with the immediate release of stored ACTH followed by sustained release of newly synthesized ACTH.[35] Untreated *Cyp21a1*$^{-/-}$ mice had a greater maximal ACTH secretory capacity than the treated *Cyp21a1*$^{-/-}$ mice. This indicates that either the storage or secretory capacity of ACTH by pituitary corticotrophs reduced following the vector treatment, likely due to reduced hypothalamic stimulation upon the pituitary as a direct result of increased corticosterone production by the adrenal cortex. Improvement in expression of the ACTH receptor in our *Cyp21a1*$^{-/-}$ male treatment

group was similar to that of a previous study in which males and females were combined into a single treatment group, although the proportion of males and females in that study was not described.[20] The finding was not detected in our treated *Cyp21a1*$^{-/-}$ female group demonstrating the importance of documenting both sexes separately as results are not generalizable between the sexes.

Despite these improvements, and some reduction in progesterone in the treated *Cyp21a1*$^{-/-}$ females, progesterone remained elevated and if recapitulated in humans would be associated with persistent androgen elevation. This could contribute to morbidity, particularly in women with CAH, and anti-androgen treatment may be required. Elevated progesterone may be required for the continual corticosterone production as increased progesterone production by the adrenal cortex allows spill-over into the systemic circulation, allowing the precursor to reach the newly expressed 21-hydroxylase in the liver, and therefore conversion to corticosterone. Should progesterone normalize, it is unclear whether that would still provide enough circulating substrate for hepatic 21-hydroxylation.

To our knowledge, this is the first study that has examined the effect of rAAV-mediated adrenocortical gene delivery to the liver. This could provide an alternative treatment option for CAH. The adrenal cortex can regenerate itself when only the capsule remains,[36] from populations of cells located in the capsule and subcapsular region.[37] Cells from the peripheral layers differentiate into zona glomerulosa cells and then undergo lineage conversion as they migrate centripetally to populate the deeper zones until they reach the cortico-medullary junction where they apoptose.[38-40] While rAAV is the most popular vector-based gene delivery system *in vivo*,[41, 42] and has shown long-term durability of

expression in the liver of adults,[43] one caveat is that it is predominantly episomal. Thus, during pediatric organ growth or in organs with life-long cellular turnover such as the adrenal cortex, the effect of gene therapy will be transient as the episomal vector genomes will be lost during cellular division.[21, 22, 44] Moreover, repeated doses of rAAV therapy are not currently feasible due to the development of neutralizing antibodies and immunomodulatory technology has not yet been clinically validated.[23, 24] Thus, effective treatment must be durable after a single dose. We have demonstrated that hepatically expressed adrenal enzymes are able to contribute to adrenal steroidogenesis, and this gene addition approach is directly applicable to adults with monogenic adrenocortical disorders. Conventional gene addition strategies using rAAV do not address hepatocellular proliferation, which is a particular challenge in the pediatric liver.[22, 45] However, this could be surmounted in the pediatric CAH population, by use of a gene editing approach whereby the newly introduced genetic material is stably integrated into the host genome, which has been shown to be an effective method to provide durable hepatic transgene expression in the growing liver.[46]

Our study also provides evidence supporting the possibility that enzyme activity from inadvertent extra-adrenal organ transduction could contribute to the biochemical effects seen when rAAV is used to deliver adrenocortical genes systemically, particularly when ubiquitously expressing enhancer-promoters are used. This unrecognized effect may lead to misinterpretation of results, attributing delivery of vector to the adrenal cortex as the cause of the phenotypic effect rather than vector expressed outside the adrenal gland. A persistent effect may be seen despite anticipated adrenal turnover. Despite this, a phase I/II clinical trial is under way whereby rAAV5 is used to deliver *CYP21A2* with a ubiquitous promoter to adults with 21-hydroxylase deficiency (ClinicalTrials.org:

NCT04783181), and at least four adults with CAH have been treated thus far.[47] Use of the rAAV5 capsid serotype and a ubiquitous promoter means that the *CYP21A2* will be expressed extensively throughout the body, including the liver, and not just in the adrenal cortex. Indeed the rAAV5 capsid is used for liver-targeted delivery of factor IX in the approved product Hemgenix.[48] There is some caution regarding the potential prematurity of this clinical trial in CAH, given concerns about safety and durability, particularly when traditional inexpensive steroid treatment (although not perfect) can suffice.[49]

rAAV-delivered extra-adrenal 21-hydroxylase has been previously attempted; however, did not achieve statistically significant results.[50] To date, most of the pre-clinical gene therapy studies for CAH have focused on gene delivery to the adrenal cortex and none has proven durability beyond the adrenocortical cellular turnover period.[19-21, 51] While one group demonstrated a positive effect on the *Cyp21a1*$^{-/-}$ phenotype for at least 15 weeks despite very low levels of residual vector DNA in the adrenal glands,[20] another demonstrated the effect was transient, lasting only 8 weeks in female *Cyp21a1*$^{-/-}$ mice.[21] Use of a ubiquitous promoter can allow persistent expression of vector-derived DNA delivered to stable organs such as liver and muscle, implicating expression of vector from sites external to the target organ.[52] In non-human primates that were treated with rAAV5-CYP21A2, the vector DNA in adrenal glands waned with time and there was more vector DNA and transgene expression in the liver than adrenal glands.[53] While our *CYP21A2* vector had a liver-specific promoter, a very small amount of *CYP21A2* mRNA was expressed in the adrenal gland at detectable levels. However, it was up to 800-fold lower than native *Cyp21a1* expression in wild-type adrenal glands and therefore unlikely to have exerted a clinical effect. Our study demonstrated that *CYP21A2* specifically expressed in the liver can exert a steroidogenic effect, implying that some of the effect

seen in other studies may have been due to 21-hydroxylase expressed extra-adrenally. Female mice have a more rapid adrenocortical cellular turnover rate than males (3 months vs. 9 months).[54] Use of predominantly male mice may also prolong the duration of effect of rAAV gene delivery to the adrenal cortex. Ours is the first pre-clinical adrenocortical gene therapy study to report male and female data separately. It is known that female mice have larger adrenal cortices due to a larger zona fasciculata and as such, have higher corticosterone levels at baseline.[26] Therefore, we considered it important to demonstrate the changes following gene therapy in both sexes.

While human clinical translation is plausible, the approach described would require refinement. From a gene delivery perspective, this would include pseudo-serotyping the rAAV vector with a highly human liver tropic capsid such as the AAV-SYDs[55] or AAV-LK03,[56] ather than the murine liver tropic AAV8 capsid serotype. This in turn would facilitate the use of lower vector doses with an associated reduction in unwanted immune-mediated adverse events currently being observed in high-dose rAAV trials, such as thrombotic microangiopathy. These are being increasingly well managed with short courses of glucocorticoids and other immune-modulating drugs.[57, 58] No other changes to the vector construct are likely to be required, such as inclusion of an inducible promoter-enhancer, given that upstream and downstream glucocorticoid production remains under physiological control. In women with CAH, as already discussed, the only other refinement would be inclusion of strategies to manage ongoing elevation of androgens and related sequelae with or without stress precautions in both sexes.

With current technology, simple gene delivery to the adrenal cortex using rAAV will not have a durable effect. We have demonstrated an alternative whereby adrenocortical genes

can be delivered to a stable organ outside of the adrenal cortex using contemporary technology. The future of adrenal-directed gene therapy is to stably integrate new genetic material into the genome of adrenocortical progenitor cells such that the daughter cells maintain the correction.[10] This method is impeded by the difficulty in identifying adrenocortical progenitor cells, which is required for the development or discovery of rAAV capsids that can transduce this cell population. Alternatively, a method that allows rAAV to evade the immune system would allow repeated administration of rAAV without the need to target the elusive progenitor population.

We have demonstrated that specifically expressing human *CYP21A2* in the livers of 21-hydroxylase-deficient mice can correct the CAH phenotype through hepato-adrenal cooperativity in steroidogenesis with resultant normalization of aldosterone production and renin expression, and sufficient improvement in corticosterone production to allow reduction in adrenal gland hyperplasia. This strategy has the potential to overcome the current technological limitations of direct adrenal cortex targeting with rAAV. While this could be directly applied to an adult population with completed liver growth, it would need to be adapted to a gene editing approach for a durable effect in the pediatric CAH population. This work also demonstrates that extra-adrenal 21-hydroxylation has a meaningful clinical effect and any biochemical effect seen when utilizing systemically delivered rAAV with a ubiquitous promoter-enhancer cannot be definitively attributed to adrenal 21-hydroxylase expression.

4.1.7 Supplementary figures and tables

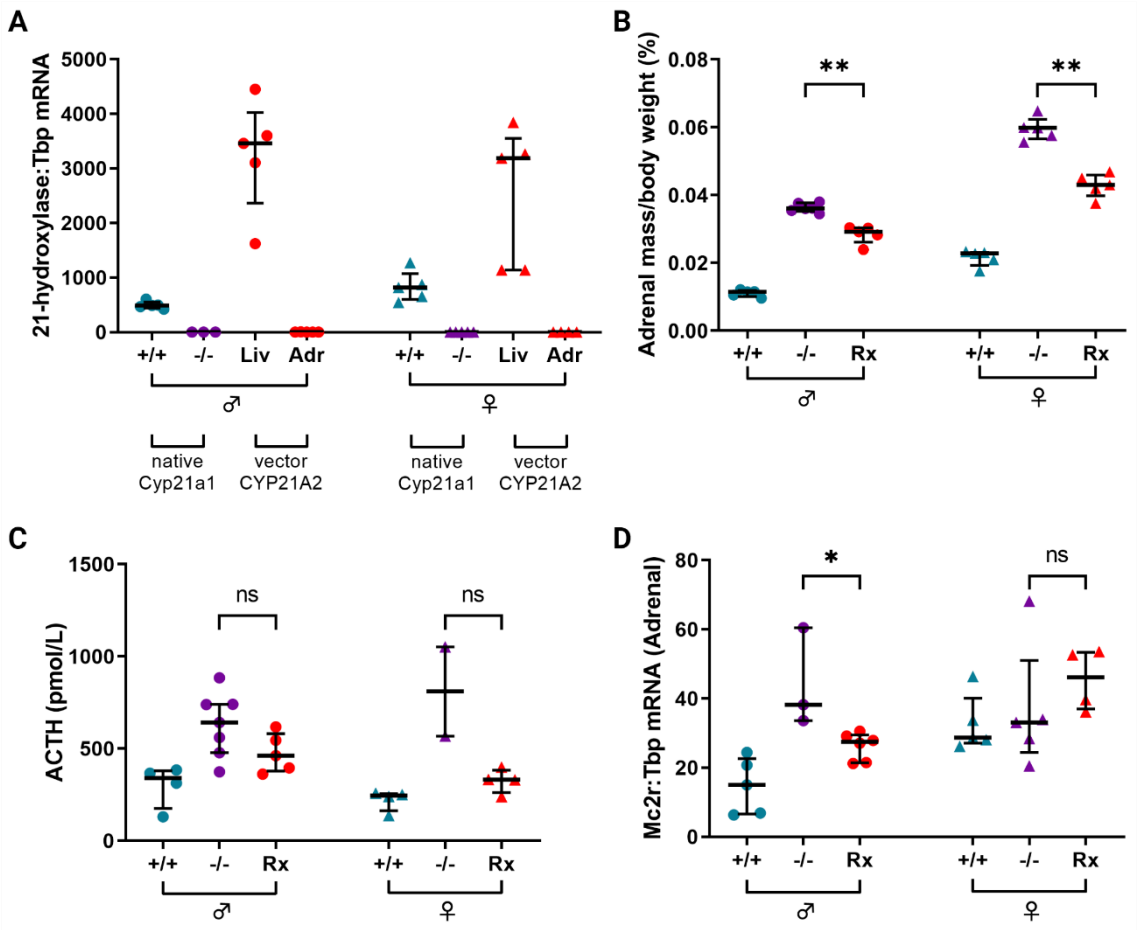

Figure S4.1-7 Supplementary figures.

A. 21-hydroxylase mRNA transcripts. Native murine Cyp21a1 transcripts in the adrenal gland or vector-derived human CYP21A2 transcripts in the liver or adrenal gland of vector-treated mice are shown as a ratio to Tbp transcripts. **B.** Relative bilateral adrenal mass as a ratio to body weight as a percentage to account for any variation in body size. **C.** Serum ACTH. **D.** ACTH receptor (Mc2r) transcripts normalised to Tbp. Abbreviations: +/+, wild-type 21-hydroxylase sufficient controls; -/-, homozygous 21-hydroxylase deficient controls; ♂, male; ♀, female; Rx, homozygous 21-hydroxylase deficient mice that were treated with vector; Liv, liver; Adr, adrenal; ACTH, adrenocorticotropic hormone; Tbp, TATA-box binding protein; Cyp21a1, murine 21-hydroxylase; CYP21A2, vector-derived human 21-hydroxylase. Individual data points are shown, and error bars represent as median and interquartile range. * $p<0.05$ and ** $p<0.01$ on Mann-Whitney U test.

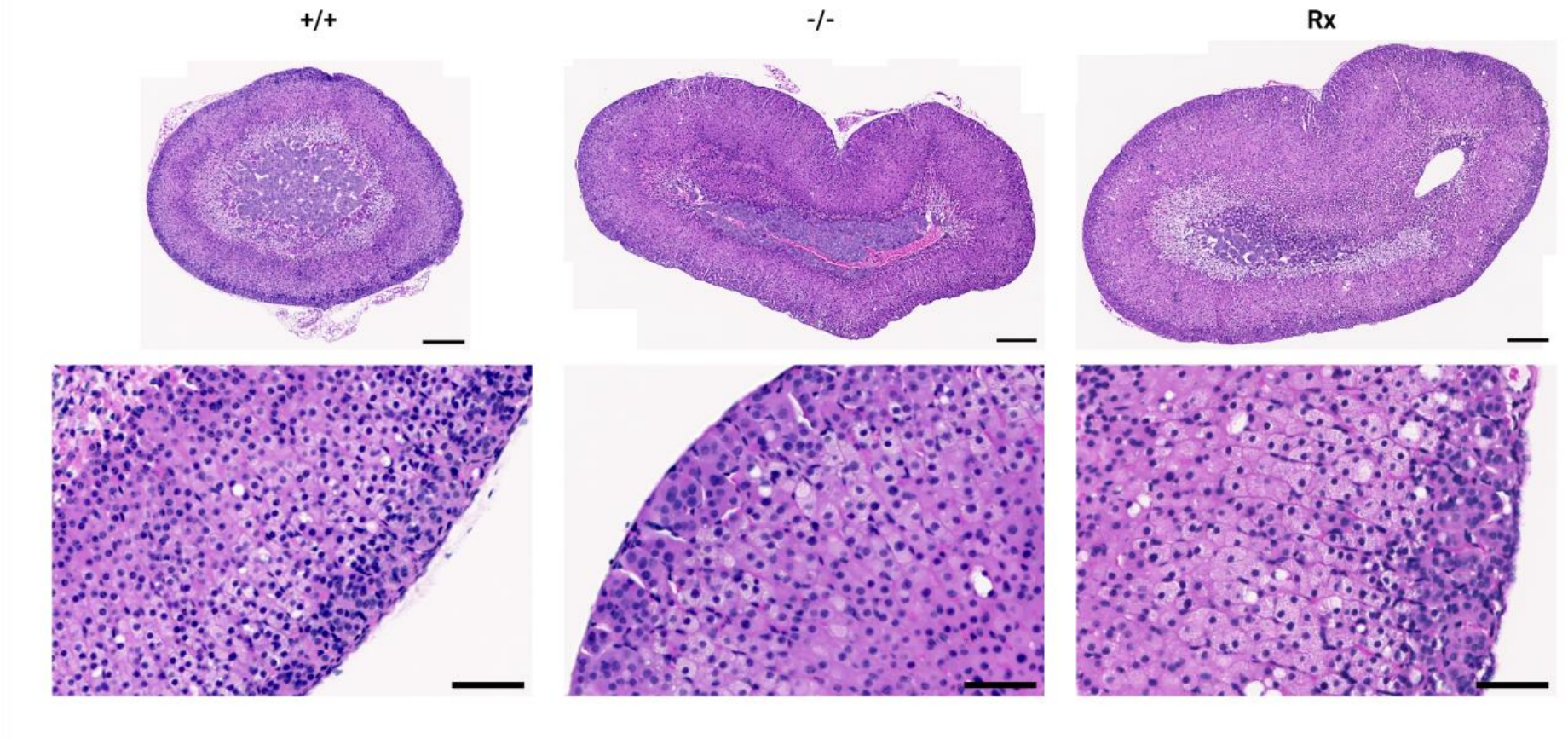

Figure S4.1-8 Additional figure: adrenal histopathology.

Haematoxylin and eosin stained histopathological sections from representative adrenal glands. Homozygous 21-hydroxylase deficient adrenal glands were larger and had increased thickness of the cortex compared with wild-type. The glands had inconsistent shapes. Adrenocortical cells had dilated cytoplasm. Abbreviations: +/+, wild-type 21-hydroxylase sufficient controls; -/-, homozygous 21-hydroxylase deficient controls; Rx, homozygous 21-hydroxylase deficient mice that were treated with vector. Scale bar represents 200uM in top row, 50uM in bottom row.

Table S4.1-1 Primers.

Purpose	Target	Sequence (5'-3')
Genotyping (PCR)	Wild-type *Cyp21a1* allele	ACCACCCTGAGGTGCACT
		GGGAGATTGATGCCAGCATAAG
	Mutant *Cyp21a1* allele	TCCTTGGGGATGTCATAGCCA
		TCACCATCCTGAAGTGCACC
Vector genome titre (ddPCR)	Bovine growth hormone polyA	GCCTTCCTTGACCCTGGA
		ACTCAGACAATGCGATGCAA
Vector genome copies (ddPCR) and *CYP21A2* expression (qPCR)	Human *CYP21A2*	TACCTCACCTTCGGAGACAA
		CCACGATGTGATCCCTCTTC
Vector copy number normalisation (ddPCR)	Albumin	AACTGCTACTCCCCTCCTAC
		TTTACCCCAGTGCAGGAAAG
Albumin expression (qPCR)	Albumin	TACAGCGGAGCAACTGAAGA
		TTGCAGCACAGAGACAAGAA
Renin expression (qPCR)	*Ren1*	CTCTGGGCACTCTTGTTGCT
		AGAAGGCATTTTCTTGAGCG
ACTH receptor expression (qPCR)	*Mc2r*	TTTCTCAGTCATCTTGCCGA
		ATGCTCCTCTCCTTGGCTTT
Cyp21a1 expression (qPCR)	Murine wild-type *Cyp21a1*	ACAGGAACCGAATGCAGCTG
		CTTAGGGATGTCATAGCCGG
TATA-box binding protein expression for normalisation (qPCR)	*Tbp*	CCCTTGTACCCTTCACCAATGAC
		TCACGGTAGATACAATATTTTGAAGCTG

Table S4.1-2 Median values for results presented in figures.

Measurement	Genotype	Treated	Male	Female
Vector DNA (vcn/diploid nucleus)	-/-	Yes	13.1	12.3
Vector RNA (ratio of *CYP21A2* mRNA transcripts to albumin transcripts)	-/-	Yes	0.79	0.20
Serum aldosterone (pmol/L)	+/+	No	784	1056
	-/-	No	341	390
	-/-	Yes	1206	1360
Serum corticosterone (nmol/L)	+/+	No	436	987
	-/-	No	39	43
	-/-	Yes	175	220
Serum progesterone (nmol/L)	+/+	No	12.1	28.6
	-/-	No	506	723
	-/-	Yes	443	517
Renal renin expression (ratio of *Ren1* mRNA	+/+	No	3.5	6.2

transcripts to *Tbp* transcripts)	-/-	No	129	197
	-/-	Yes	5.1	6.5
Bilateral adrenal mass (mg)	+/+	No	3.2	5.1
	-/-	No	10.9	13.4
	-/-	Yes	7.3	9.5

Abbreviations: vcn, vector copy number; *Tbp*, TATA-box binding protein; +/+, wild-type 21-hydroxylase sufficiency; -/-, homozygous 21-hydroxylase deficiency

4.1.8 Author contributions

The candidate performed the bulk of the work for this chapter and wrote the manuscript. Cindy Zhu, GTRU, CMRI performed the intravenous injections. The serum steroid profiles were analysed by Sundar Koyyalamudi, Endocrinology Lab, The Children's Hospital at Westmead. The dried whole blood corticosterone measurements were analysed by Tiffany Wotton and Dinah Sung, Newborn Screening, The Children's Hospital at Westmead. Fixed adrenal glands were mounted, sectioned, and stained with haematoxylin and eosin by Li Ma, Histology Facility, Westmead Institute for Medical Research (WIMR).

4.1.9 References

1. Graves LE, van Dijk EB, Zhu E, et al. AAV-delivered hepato-adrenal cooperativity in steroidogenesis: Implications for gene therapy for congenital adrenal hyperplasia. *Mol Ther Methods Clin Dev* 2024; 32: 101232. 2024/04/01. DOI: 10.1016/j.omtm.2024.101232.
2. Wilkins L, Lewis RA, Klein R, et al. The suppression of androgen secretion by cortisone in a case of congenital adrenal hyperplasia. *Bull Johns Hopkins Hosp* 1950; 86: 249-252. 1950/04/01.
3. Wilkins L, Lewis RA, Klein R, et al. Treatment of congenital adrenal hyperplasia with cortisone. *J Clin Endocrinol Metab* 1951; 11: 1-25. 1951/01/01. DOI: 10.1210/jcem-11-1-1.
4. Bartter FC, Albright F, Forbes AP, et al. The effects of adrenocorticotropic hormone and cortisone in the adrenogenital syndrome associated with congenital adrenal hyperplasia: an attempt to explain and correct its disordered hormonal pattern. *J Clin Invest* 1951; 30: 237-251. 1951/03/01. DOI: 10.1172/JCI102438.
5. El-Maouche D, Arlt W and Merke DP. Congenital adrenal hyperplasia. *Lancet* 2017; 390: 2194-2210. 2017/06/04. DOI: 10.1016/S0140-6736(17)31431-9.
6. Lai F, Srinivasan S and Wiley V. Evaluation of a Two-Tier Screening Pathway for Congenital Adrenal Hyperplasia in the New South Wales Newborn Screening Programme. *Int J Neonatal Screen* 2020; 6: 63. 2020/10/30. DOI: 10.3390/ijns6030063.

7. Navarro-Zambrana AN and Sheets LR. Ethnic and National Differences in Congenital Adrenal Hyperplasia Incidence: A Systematic Review and Meta-Analysis. *Horm Res Paediatr* 2023; 96: 249-258. 2022/08/17. DOI: 10.1159/000526401.
8. Berglund A, Ornstrup MJ, Lind-Holst M, et al. Epidemiology and diagnostic trends of congenital adrenal hyperplasia in Denmark: a retrospective, population-based study. *Lancet Reg Health Eur* 2023; 28: 100598. 2023/03/10. DOI: 10.1016/j.lanepe.2023.100598.
9. Claahsen-van der Grinten HL, Speiser PW, Ahmed SF, et al. Congenital Adrenal Hyperplasia-Current Insights in Pathophysiology, Diagnostics, and Management. *Endocr Rev* 2022; 43: 91-159. 2021/05/08. DOI: 10.1210/endrev/bnab016.
10. Graves LE, Torpy DJ, Coates PT, et al. Future Directions for Adrenal Insufficiency: Cellular Transplantation and Genetic Therapies. *J Clin Endocrinol Metab* 2023; 108: 1273-1289. 2023/01/08. DOI: 10.1210/clinem/dgac751.
11. Nella AA, Mallappa A, Perritt AF, et al. A Phase 2 Study of Continuous Subcutaneous Hydrocortisone Infusion in Adults With Congenital Adrenal Hyperplasia. *J Clin Endocrinol Metab* 2016; 101: 4690-4698. 2016/09/30. DOI: 10.1210/jc.2016-1916.
12. Mallappa A, Nella AA, Sinaii N, et al. Long-term use of continuous subcutaneous hydrocortisone infusion therapy in patients with congenital adrenal hyperplasia. *Clin Endocrinol (Oxf)* 2018; 89: 399-407. 2018/07/14. DOI: 10.1111/cen.13813.
13. Mallappa A, Sinaii N, Kumar P, et al. A phase 2 study of Chronocort, a modified-release formulation of hydrocortisone, in the treatment of adults with classic congenital adrenal hyperplasia. *J Clin Endocrinol Metab* 2015; 100: 1137-1145. 2014/12/17. DOI: 10.1210/jc.2014-3809.
14. Jones CM, Mallappa A, Reisch N, et al. Modified-Release and Conventional Glucocorticoids and Diurnal Androgen Excretion in Congenital Adrenal Hyperplasia. *J Clin Endocrinol Metab* 2017; 102: 1797-1806. 2016/11/16. DOI: 10.1210/jc.2016-2855.
15. Speiser PW. Emerging medical therapies for congenital adrenal hyperplasia. *F1000Res* 2019; 8: 363. 2019/04/16. DOI: 10.12688/f1000research.17778.1.
16. Pascual-Morena C, Cavero-Redondo I, Luceron-Lucas-Torres M, et al. Onasemnogene Abeparvovec in Type 1 Spinal Muscular Atrophy: A Systematic Review and Meta-Analysis. *Hum Gene Ther* 2023; 34: 129-138. 2022/09/23. DOI: 10.1089/hum.2022.161.
17. Vinson GP. Functional Zonation of the Adult Mammalian Adrenal Cortex. *Front Neurosci* 2016; 10: 238. 2016/07/06. DOI: 10.3389/fnins.2016.00238.
18. Gotoh H, Sagai T, Hata J, et al. Steroid 21-hydroxylase deficiency in mice. *Endocrinology* 1988; 123: 1923-1927. 1988/10/01. DOI: 10.1210/endo-123-4-1923.
19. Tajima T, Okada T, Ma XM, et al. Restoration of adrenal steroidogenesis by adenovirus-mediated transfer of human cytochromeP450 21-hydroxylase into the adrenal gland of21-hydroxylase-deficient mice. *Gene Ther* 1999; 6: 1898-1903. 1999/12/22. DOI: 10.1038/sj.gt.3301018.
20. Perdomini M, Dos Santos C, Goumeaux C, et al. An AAVrh10-CAG-CYP21-HA vector allows persistent correction of 21-hydroxylase deficiency in a Cyp21(-/-) mouse model. *Gene Ther* 2017; 24: 275-281. 2017/02/07. DOI: 10.1038/gt.2017.10.
21. Markmann S, De BP, Reid J, et al. Biology of the Adrenal Gland Cortex Obviates Effective Use of Adeno-Associated Virus Vectors to Treat Hereditary Adrenal Disorders. *Hum Gene Ther* 2018; 29: 403-412. 2018/01/11. DOI: 10.1089/hum.2017.203.
22. Cunningham SC, Dane AP, Spinoulas A, et al. Gene delivery to the juvenile mouse liver using AAV2/8 vectors. *Mol Ther* 2008; 16: 1081-1088. 2008/04/17. DOI: 10.1038/mt.2008.72.
23. Boutin S, Monteilhet V, Veron P, et al. Prevalence of serum IgG and neutralizing factors against adeno-associated virus (AAV) types 1, 2, 5, 6, 8, and 9 in the healthy population: implications for gene therapy using AAV vectors. *Hum Gene Ther* 2010; 21: 704-712. 2010/01/26. DOI: 10.1089/hum.2009.182.
24. Li A, Tanner MR, Lee CM, et al. AAV-CRISPR Gene Editing Is Negated by Pre-existing Immunity to Cas9. *Mol Ther* 2020; 28: 1432-1441. 2020/04/30. DOI: 10.1016/j.ymthe.2020.04.017.
25. Shiroishi T, Sagai T, Natsuume-Sakai S, et al. Lethal deletion of the complement component C4 and steroid 21-hydroxylase genes in the mouse H-2 class III region, caused by meiotic recombination. *Proc Natl Acad Sci U S A* 1987; 84: 2819-2823. 1987/05/01. DOI: 10.1073/pnas.84.9.2819.
26. Bielohuby M, Herbach N, Wanke R, et al. Growth analysis of the mouse adrenal gland from weaning to adulthood: time- and gender-dependent alterations of cell size and number in the cortical compartment. *Am J Physiol Endocrinol Metab* 2007; 293: E139-146. 2007/03/22. DOI: 10.1152/ajpendo.00705.2006.
27. Dane AP, Cunningham SC, Graf NS, et al. Sexually dimorphic patterns of episomal rAAV genome persistence in the adult mouse liver and correlation with hepatocellular proliferation. *Mol Ther* 2009; 17: 1548-1554. 2009/07/02. DOI: 10.1038/mt.2009.139.

28. Page IH and Helmer OM. A Crystalline Pressor Substance (Angiotonin) Resulting from the Reaction between Renin and Renin-Activator. *J Exp Med* 1940; 71: 29-42. 1940/01/01. DOI: 10.1084/jem.71.1.29.
29. Braun-Menendez E, Fasciolo JC, Leloir LF, et al. The substance causing renal hypertension. *J Physiol* 1940; 98: 283-298. 1940/07/24. DOI: 10.1113/jphysiol.1940.sp003850.
30. Radonic A, Thulke S, Mackay IM, et al. Guideline to reference gene selection for quantitative real-time PCR. *Biochem Biophys Res Commun* 2004; 313: 856-862. 2004/01/07. DOI: 10.1016/j.bbrc.2003.11.177.
31. Costello HM, Krilis G, Grenier C, et al. High salt intake activates the hypothalamic-pituitary-adrenal axis, amplifies the stress response, and alters tissue glucocorticoid exposure in mice. *Cardiovasc Res* 2023; 119: 1740-1750. 2022/11/12. DOI: 10.1093/cvr/cvac160.
32. Witt A, Mateska I, Palladini A, et al. Fatty acid desaturase 2 determines the lipidomic landscape and steroidogenic function of the adrenal gland. *Sci Adv* 2023; 9: eadf6710. 2023/07/21. DOI: 10.1126/sciadv.adf6710.
33. Falhammar H, Frisen L, Norrby C, et al. Increased mortality in patients with congenital adrenal hyperplasia due to 21-hydroxylase deficiency. *J Clin Endocrinol Metab* 2014; 99: E2715-2721. 2014/10/04. DOI: 10.1210/jc.2014-2957.
34. Scheithauer BW, Kovacs K and Randall RV. The pituitary gland in untreated Addison's disease. A histologic and immunocytologic study of 18 adenohypophyses. *Arch Pathol Lab Med* 1983; 107: 484-487. 1983/09/01.
35. DeBold CR, DeCherney GS, Jackson RV, et al. Effect of synthetic ovine corticotropin-releasing factor: prolonged duration of action and biphasic response of plasma adrenocorticotropin and cortisol. *J Clin Endocrinol Metab* 1983; 57: 294-298. 1983/08/01. DOI: 10.1210/jcem-57-2-294.
36. Ingle DJ and Higgins GM. Autotransplantation and Regeneration of the Adrenal Gland. *Endocrinology* 1938; 22: 458-464. DOI: 10.1210/endo-22-4-458.
37. Zwemer RL, Wotton RM and Norkus MG. A study of corticoadrenal cells. *The Anatomical Record* 1938; 72: 249-263. DOI: 10.1002/ar.1090720210.
38. Chang SP, Morrison HD, Nilsson F, et al. Cell proliferation, movement and differentiation during maintenance of the adult mouse adrenal cortex. *PLoS One* 2013; 8: e81865. 2013/12/11. DOI: 10.1371/journal.pone.0081865.
39. Freedman BD, Kempna PB, Carlone DL, et al. Adrenocortical zonation results from lineage conversion of differentiated zona glomerulosa cells. *Dev Cell* 2013; 26: 666-673. 2013/09/17. DOI: 10.1016/j.devcel.2013.07.016.
40. Zwemer RL. A Study of Adrenal Cortex Morphology. *Am J Pathol* 1936; 12: 107-114 101. 1936/01/01. DOI: 10.1097/00005053-193607000-00010.
41. Wang D, Tai PWL and Gao G. Adeno-associated virus vector as a platform for gene therapy delivery. *Nat Rev Drug Discov* 2019; 18: 358-378. 2019/02/03. DOI: 10.1038/s41573-019-0012-9.
42. Barrett D, Nguyen-Jatkoe L, Foss-Campbell B, et al. *Gene, Cell, & RNA Therapy Landscape, Q2 2021 Quarterly Data Report*. 2021.
43. Nathwani AC, Reiss UM, Tuddenham EG, et al. Long-term safety and efficacy of factor IX gene therapy in hemophilia B. *N Engl J Med* 2014; 371: 1994-2004. 2014/11/20. DOI: 10.1056/NEJMoa1407309.
44. Alexander IE, Cunningham SC, Logan GJ, et al. Potential of AAV vectors in the treatment of metabolic disease. *Gene Ther* 2008; 15: 831-839. 2008/04/11. DOI: 10.1038/gt.2008.64.
45. Cunningham SC, Spinoulas A, Carpenter KH, et al. AAV2/8-mediated correction of OTC deficiency is robust in adult but not neonatal Spf(ash) mice. *Mol Ther* 2009; 17: 1340-1346. 2009/04/23. DOI: 10.1038/mt.2009.88.
46. Ginn SL, Amaya AK, Liao SHY, et al. Efficient in vivo editing of OTC-deficient patient-derived primary human hepatocytes. *JHEP Rep* 2020; 2: 100065. 2020/02/11. DOI: 10.1016/j.jhepr.2019.100065.
47. Adrenas. Trial Update from Adrenas Therapeutics, https://adrenastx.com/wp-content/uploads/CAH-Letter-to-Community-Q1-2023-Update-FINAL.pdf (2023, accessed 28th July 2023).
48. Heo YA. Etranacogene Dezaparvovec: First Approval. *Drugs* 2023; 83: 347-352. 2023/02/22. DOI: 10.1007/s40265-023-01845-0.
49. White PC. Emerging treatment for congenital adrenal hyperplasia. *Curr Opin Endocrinol Diabetes Obes* 2022; 29: 271-276. 2022/03/15. DOI: 10.1097/MED.0000000000000723.
50. Naiki Y, Miyado M, Horikawa R, et al. Extra-adrenal induction of Cyp21a1 ameliorates systemic steroid metabolism in a mouse model of congenital adrenal hyperplasia. *Endocr J* 2016; 63: 897-904. 2016/11/01. DOI: 10.1507/endocrj.EJ16-0112.

51. Naiki Y, Miyado M, Shindo M, et al. Adeno-Associated Virus-Mediated Gene Therapy for Patients' Fibroblasts, Induced Pluripotent Stem Cells, and a Mouse Model of Congenital Adrenal Hyperplasia. *Hum Gene Ther* 2022; 33: 801-809. 2022/07/16. DOI: 10.1089/hum.2022.005.
52. Pontoizeau C, Simon-Sola M, Gaborit C, et al. Neonatal gene therapy achieves sustained disease rescue of maple syrup urine disease in mice. *Nat Commun* 2022; 13: 3278. 2022/06/08. DOI: 10.1038/s41467-022-30880-w.
53. Eclov RJ, Lewis TEW, Kapandia M, et al. Durable CYP21A2 gene therapy in non-human primates for treatment of congenital adrenal hyperplasia. *ESGCT 27th Annual Congress In collaboration with SETGyc*. Barcelona, Spain: Hum Gene Ther, 2019, p. A1-A221.
54. Grabek A, Dolfi B, Klein B, et al. The Adult Adrenal Cortex Undergoes Rapid Tissue Renewal in a Sex-Specific Manner. *Cell Stem Cell* 2019; 25: 290-296 e292. 2019/05/21. DOI: 10.1016/j.stem.2019.04.012.
55. Cabanes-Creus M, Navarro RG, Zhu E, et al. Novel human liver-tropic AAV variants define transferable domains that markedly enhance the human tropism of AAV7 and AAV8. *Mol Ther Methods Clin Dev* 2022; 24: 88-101. 2022/01/04. DOI: 10.1016/j.omtm.2021.11.011.
56. Lisowski L, Dane AP, Chu K, et al. Selection and evaluation of clinically relevant AAV variants in a xenograft liver model. *Nature* 2014; 506: 382-386. 2014/01/07. DOI: 10.1038/nature12875.
57. Au HKE, Isalan M and Mielcarek M. Gene Therapy Advances: A Meta-Analysis of AAV Usage in Clinical Settings. *Front Med (Lausanne)* 2021; 8: 809118. 2022/03/01. DOI: 10.3389/fmed.2021.809118.
58. Merke DP, Auchus RJ, Sarafoglou K, et al. Design of a Phase 1/2 Open-Label, Dose-Escalation Study of the Safety and Efficacy of Gene Therapy in Adults with Classic Congenital Adrenal Hyperplasia (CAH) Due to 21-Hydroxylase Deficiency through Administration of an Adeno-Associated Virus (AAV) Serotype 5-Based Recombinant Vector Encoding the Human CYP21A2 Gene. *Endo*. Virtual event 2021.

Chapter 4.2

Recombinant AAV-mediated dual adrenal enzyme gene delivery to the liver

4.2.1 Introduction

Chapter 4.1 demonstrated that a hepatically-expressed adrenal enzyme, delivered by rAAV, can contribute to adrenocortical steroidogenesis. Additionally, when targeting the adrenal gland with systemically administered rAAV vectors, inadvertent liver transduction may confound data interpretation. In a mouse model of CAH, delivery of rAAV8-CYP21A2 with a liver-specific promoter restored aldosterone production, improved corticosterone production, reduced adrenal hyperplasia, and normalised renal renin (*Ren1*) expression. However, progesterone only reduced marginally in females and did not change in males. Although corticosterone improved, it did not reach wild-type levels. Most of the enzymatic steps for steroidogenesis occur in adrenocortical cell mitochondria[1, 2]. Steroidogenesis is facilitated by close communication between the mitochondria and the endoplasmic reticulum facilitated through mitochondria-associated endoplasmic reticulum membranes[2, 3]. 11ß-hydroxylase (encoded by *Cyp11b1*) is a mitochondrial enzyme, whereas 21-hydroxylase (encoded by *Cyp21a1*) resides in the endoplasmic reticulum. Normally, corticosterone is produced from cholesterol by cells

located in the murine zona glomerulosa in a cascade of enzymatic reactions. The final step converts microsomal 21-hydroxylase derived 11-deoxycorticosterone to corticosterone, and this final step is catalysed by mitochondrial 11ß hydroxylase[4].

In the mice treated in Chapter 4.1, progesterone is produced in the adrenal gland, and must travel to the liver for conversion to 11-deoxycorticosterone by hepatically expressed *CYP21A2*. For subsequent conversion to corticosterone, the 11-deoxycorticosterone must travel back to the adrenal gland to become a substrate for 11ß-hydroxylase. This requires the steroid substrates to leave the cell's closely associated mitochondria and endoplasmic reticulum. We hypothesised that co-locating *CYP21A2* and *CYP11B1* in the same cells may facilitate more efficient steroidogenesis, allowing efficient passage of 11-deoxycorticosterone to *CYP11B1* to improve corticosterone production further. Thus although the mice were only deficient in 21-hydroxylase, both *CYP21A2* and *CYP11B1* were delivered for specific hepatic expression, to determine if this combination could further improve corticosterone production and reduce serum progesterone, compared with delivery of *CYP21A2* alone.

4.2.2 Chapter-specific methods

Vector copy number determination, quantitative real-time PCR, steroid profiles, ACTH ELISA, and statistical analysis were performed as described in Section 4.1.4.

4.2.2.1 Animal procedures: vector dosing

All mice in the experimental group were treated with 5×10^{11} vg/mouse rAAV8-CYP21A2 and 5×10^{11} vg/mouse rAAV8-CYP11B1, for a total rAAV dose of 1×10^{12} vg/mouse.

Mice were injected intravenously with a stoichiometric mix of both vectors and harvested four weeks later.

4.2.2.2 Vector construction and production

The rAAV8-CYP21A2 vector from Chapter 4.1 was utilised (Section 4.1.4.2).

4.2.2.2.1 Generating rAAV vector encoding hCYP11B1

For the rAAV8-CYP11B2 vector, human *CYP11B1* (h*CYP11B1*) cDNA (Genbank accession no. NM_000497.4) with added *Not*I and *EcoR*V restriction sites and a Kozak sequence upstream of the h*CYP11B1* cDNA, was purchased from GeneWiz (Azenta Life Sciences). The h*CYP11B1* cDNA was cloned into the same AAV2 backbone plasmid (pAAV2-BB2.ApoEhAAT.hOTC) as the previously constructed CYP21A2 plasmid, which had a liver-specific ApoE-hAAT enhancer-promoter, to produce the rAAV8-CYP11B1 vector (Figure 4.2-1). The GeneWiz h*CYP11B1* plasmid was digested with *Not*I and *Eco*RV and the h*CYP11B1* fragment was purified from an electrophoresis gel. The recipient AAV2 vector backbone was prepared as per Section 4.1.4.2.1. The h*CYP11B1* fragment was ligated into the prepared recipient AAV2 backbone with T4 DNA ligase. The resulting plasmid, designated pAAV2-BB2.ApoEhAAT.hCYP11B1 was amplified by transforming chemically competent E. coli (DH5α) using heat shock and bacterial culture. Plasmid DNA was purified using a commercial kit (Nucleobond Xtra Maxi Kit, Macherey-Nagel). pAAV2.ApoEhAAT.hCYP11B1 contained an AAV expression cassette of 4753 bp in length which included flanking AAV2 ITRs. Presence of the correct insert and ITRs was confirmed with restriction digestion with *Eco*RV, *Not*I, *Ava*I, and *Msc*I.

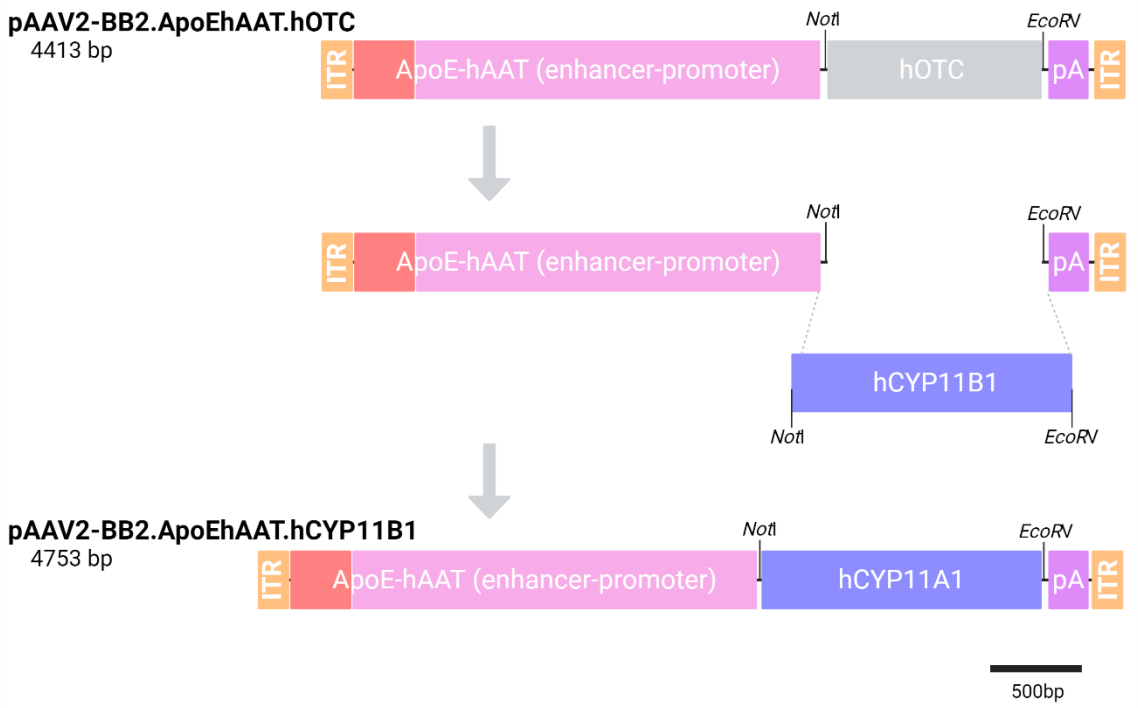

Figure 4.2-1 Molecular subcloning to generate the *CYP11B1* vector plasmid.
Flow diagram of the molecular subcloning steps taken to generate pAAV2-BB2.ApoEhAAT.hCYP11B1. pAAV2-BB2.ApoehAAT.hOTC was digested with *Not*I and *Eco*RV to remove the human OTC transgene. h*CYP11B1* cDNA was prepared by digesting it from the GeneWiz plasmid with *Not*I and *Eco*RV (not shown). The prepared h*CYP11B1* transgene was ligated to the backbone. AAV2 ITRs (orange) flank the transgene expression cassette. The expression cassette contained the liver-specific enhancer/promoter, ApoE hAAT (red and pink), human *CYP11B1* (dark blue) and bovine growth hormone polyadenylation tail (pA, purple). Scale bar = 500 bp.

4.2.2.2.2 Vector production

The vector was produced using standard triple transfection, purified with a caesium chloride gradient and titre was assigned with digital droplet PCR as described in Section 4.1.4.2.2.[5]

4.2.2.3 Immunohistochemistry

Immunohistochemistry slides stained for CYP21A2 protein were prepared as described in Section 4.1.4.3. This same method was used to produce the slides stained for CYP11B1

protein using the primary rabbit CYP11B1 antibody (Abcam ab197908) diluted 1:50. Cryo-sectioning, staining and imaging was performed by Lakshmy Viswanath, research assistant.

4.2.3 Results

4.2.3.1 Human *CYP21A2* and *CYP11B1* were detected in the murine liver

Vector copy number (vcn) per diploid nucleus in the liver was assigned by digital droplet PCR. Liver transduction was confirmed by vcn/diploid nucleus and detection of vector encoded mRNA in the livers of treated mice (Figures 4.2-2 A and B). *CYP21A2* vector copies were detected at lower rates in the dual vector (AAV8-CYP21A2 and AAV8-CYP11B1) treated mice than the single vector (AAV8-CYP21A2) treated mice. There were similar copies of *CYP21A2* and *CYP11B1* in dual vector treated mice. There was a linear association between *CYP21A2* and *CYP11B1* vector copies in dual vector treated mice, suggesting possible dose effect (Figure 4.2-2C).

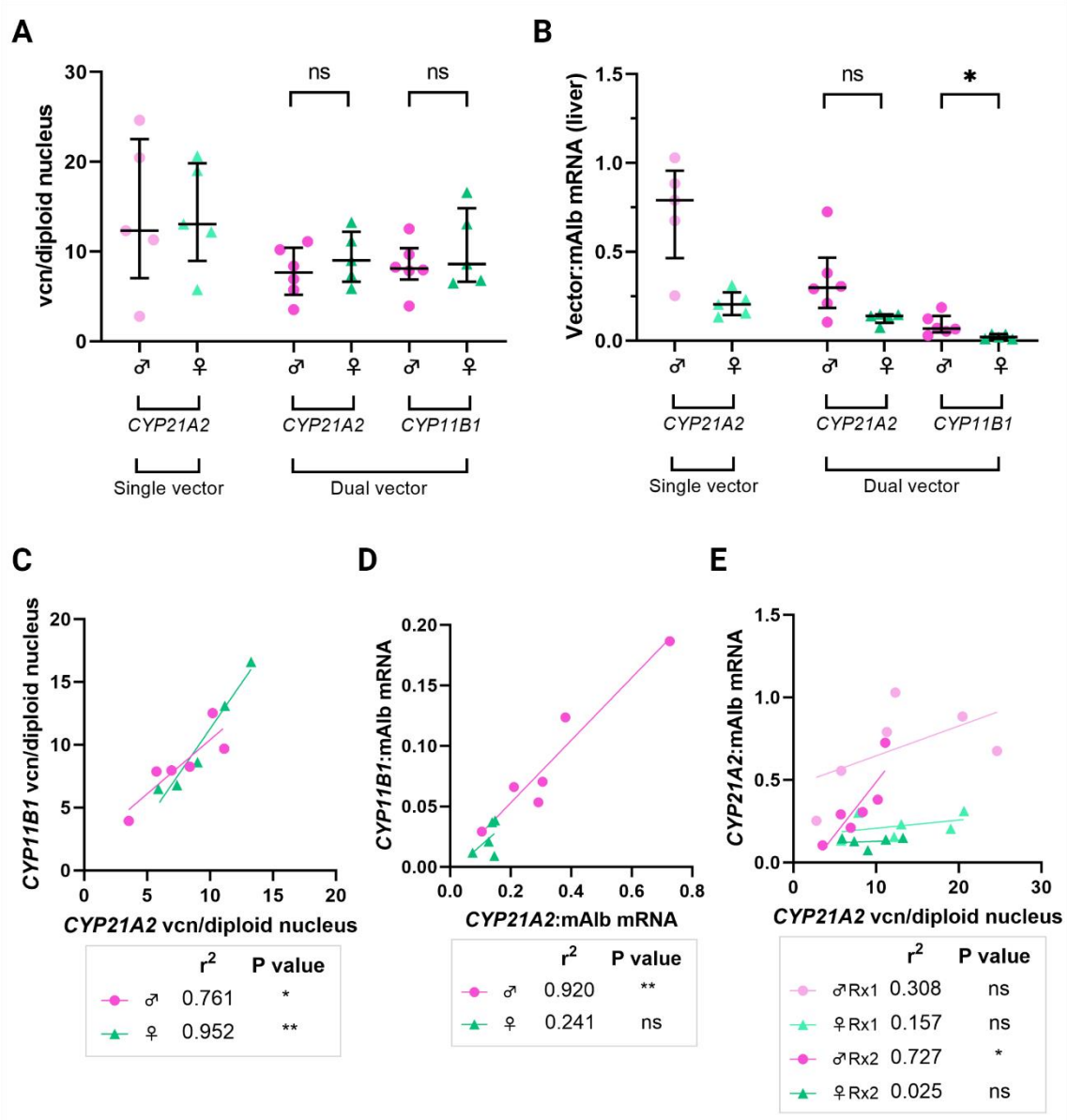

Figure 4.2-2 Delivery and expression of vectors.

A. Vector DNA detected in the livers of dual vector-treated mice, compared with single vector treated mice. **B.** The ratio of vector-derived mRNA transcripts to murine albumin transcripts. **C.** *CYP21A2* vcn vs *CYP11B1* vcn. **D.** *CYP21A2* mRNA transcripts vs *CYP11B1* transcripts. **E.** *CYP21A2* transcripts vs *CYP21A2* vector DNA. Abbreviations: vcn, vector copy number; Rx1, single vector; Rx2, dual vector; mAlb, murine albumin; ♂, male; ♀, female; ns not significant, * $p<0.05$; ** $p<0.01$. Mann Whitney *U* test for significance in A-B, linear regression modelling for C-E.

Vector expression was determined by quantitative PCR following reverse transcription and was normalised to murine albumin expression (Figure 4.2-2B). Expression of *CYP21A2* was 1.6-fold lower in females and 2.5-fold lower in males in the dual vector treated mice than in single vector treated. In the dual vector treated mice *CYP11B1* expression was 6.7-fold lower in the females and 4.4-fold lower in the males than *CYP21A2* expression. *CYP21A2* expression was 2.1-fold higher in dual treated males than dual treated females. There was a linear association between *CYP11B1* expression and *CYP21A2* expression in males (Figure 4.2-2D). There was a linear association between *CYP21A2* vcn and vector expression in the dual treated males, but this association was not present in single vector treated males or either female group (Figure 4.2-2E). There was a linear association between *CYP11B1* expression and *CYP21A2* expression, particularly in males (Figure 4.2-2E). There was no association between vcn/diploid cell or vector expression and corticosterone (Figures 4.2-3A and B, respectively).

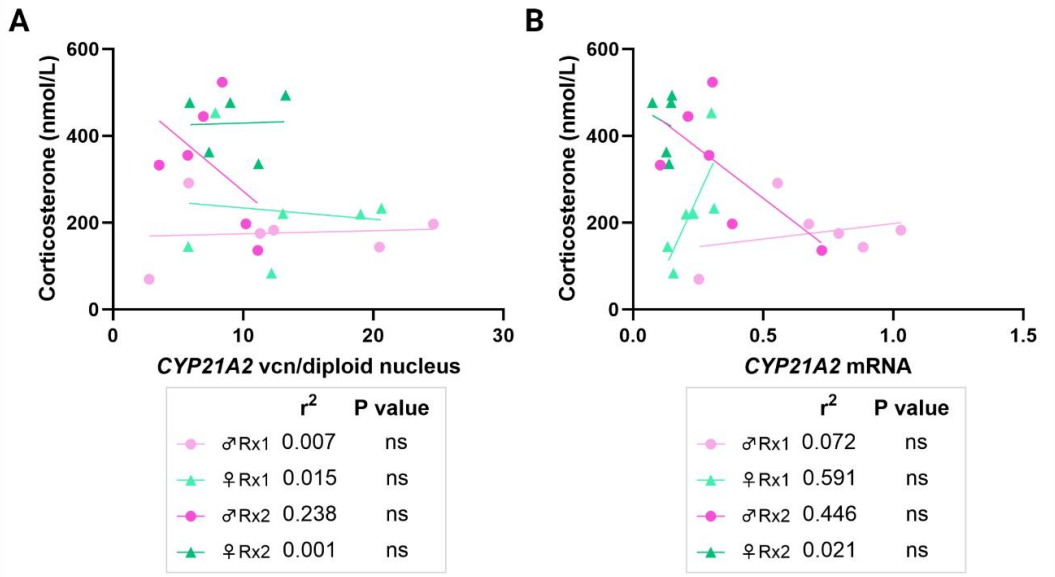

Figure 4.2-3 No relationship between serum corticosterone and vector copy number or expression.

A. Serum corticosterone versus *CYP21A2* vector copies. **B.** Serum corticosterone versus *CYP21A2* vector transcripts. Abbreviations: vcn, vector copy number; Rx1, single vector; Rx2, dual vector; mAlb, murine albumin; ♂, male; ♀, female; ns; not significant on linear regression modelling.

Vector expression was also normalised to *Tbp* to compare to native *Cyp21a1* expression in wild-type and untreated 21-hydroxylase deficient mice (Figure 4.2-4). Vector derived *CYP21A2* expression was 2000-fold higher in the liver than in the adrenal gland of the treated mice. Native *Cyp21a1* expression was 300-fold higher in the wild-type adrenal glands than vector-derived *CYP21A2* in treated adrenal glands. Immunohistochemical staining demonstrated protein translation of both *CYP11B1* and *CYP21A2* in the livers of the treated mice (Figure 4.2-5 to 4.2-8) and was not present in the untreated control (Figure 4.2-9).

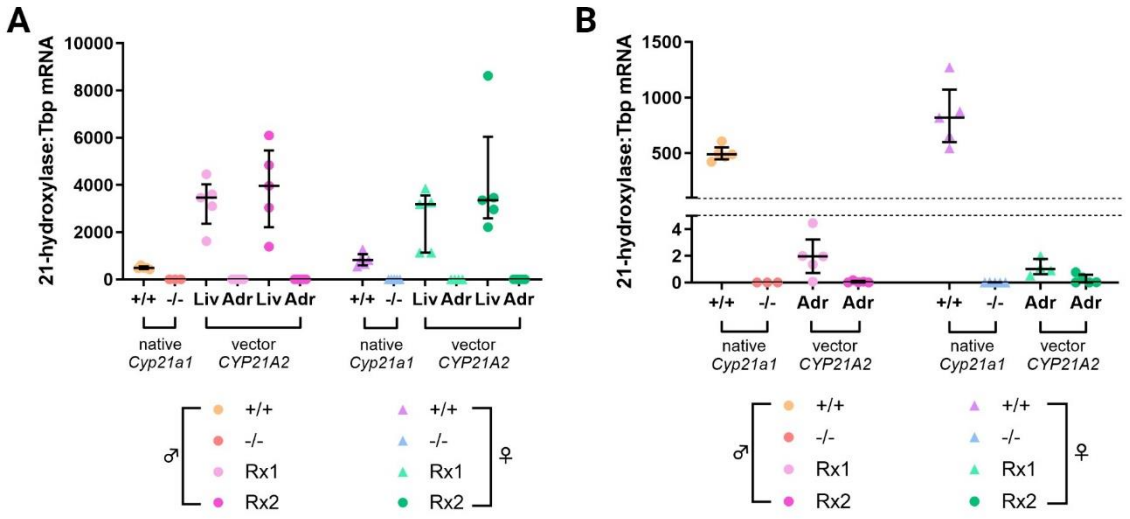

Figure 4.2-4 Comparing vector-derived and native 21-hydroxylase expression.
All are normalised to *Tbp*. **A.** Liver *CYP21A2* expression included. **B.** Liver expression excluded, note that the y axis is split. Abbreviations: +/+, wild-type 21-hydroxylase sufficiency; -/-, homozygous 21-hydroxylase deficiency; Rx1, homozygous 21-hydroxylase deficient mice that were treated with the *CYP21A2* vector alone; Rx2, homozygous 21-hydroxylase deficient mice that were treated with both the *CYP21A2* and *CYP11B1* vectors; ♀, female; ♂, male; *Tbp*, TATA-box binding protein. Individual data points are shown, and error bars represent median and interquartile range.

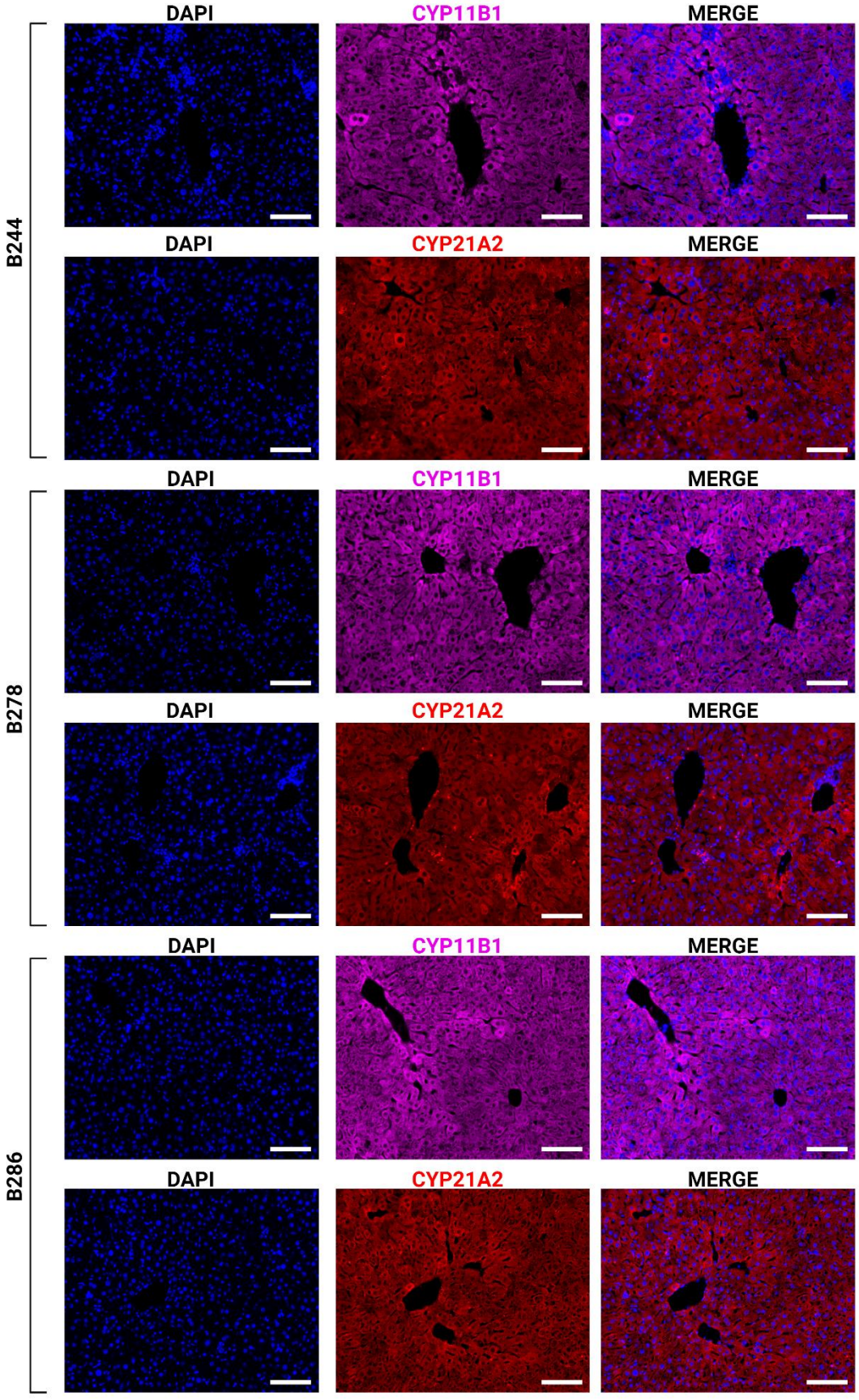

Figure 4.2-5 Immunohistochemistry slides from females B244, B278 and B286.
IHC staining demonstrated CYP11B1 (purple) and CYP21A2 protein (red) in the liver of treated mice. DAPI nuclear staining in blue. Scale bar represents 100µm.

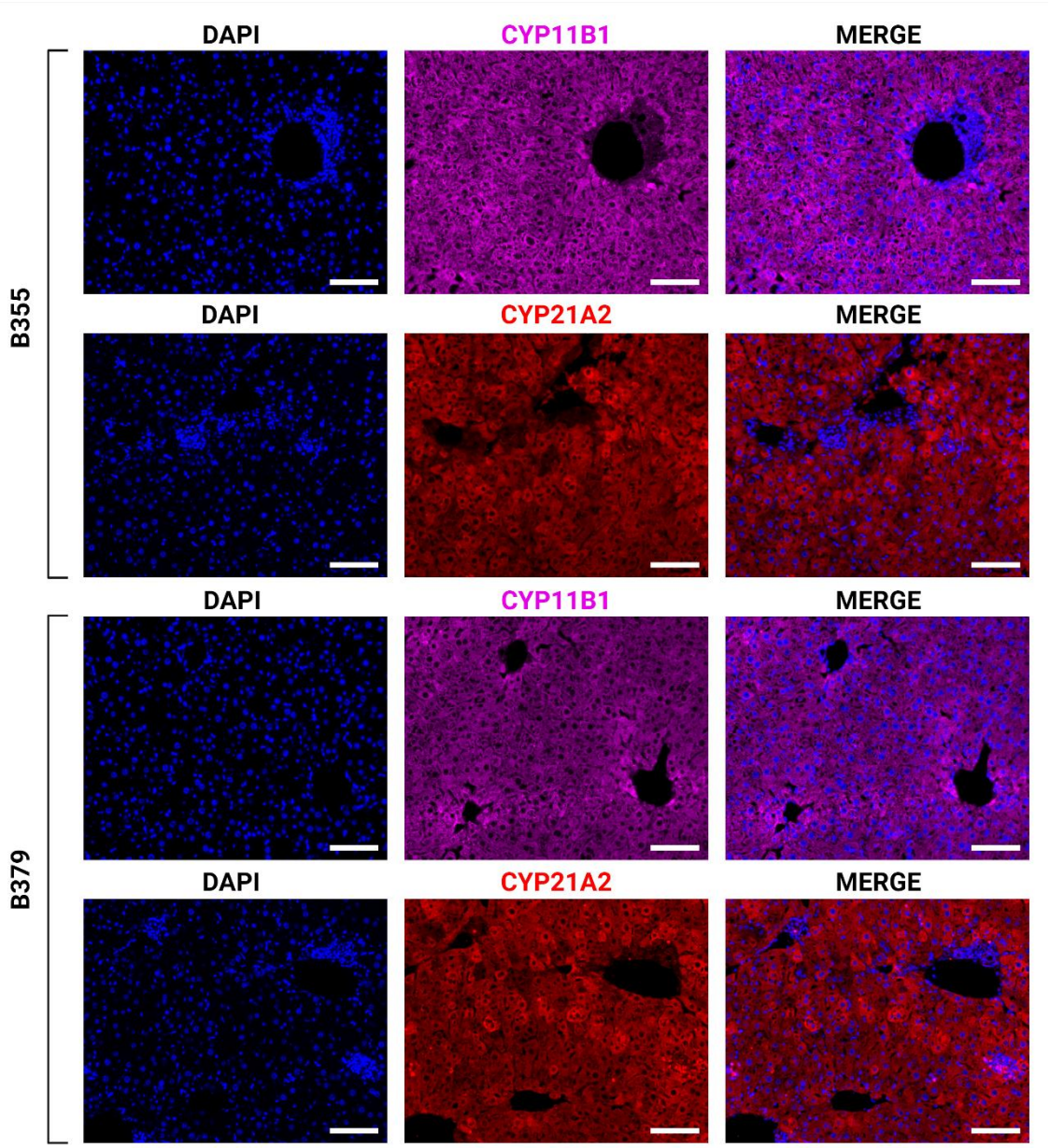

Figure 4.2-6 Immunohistochemistry slides of females B355 and B379.
IHC staining demonstrated CYP11B1 (purple) and CYP21A2 protein (red) in the liver of treated mice. DAPI nuclear staining in blue. Scale bar represents 100µm.

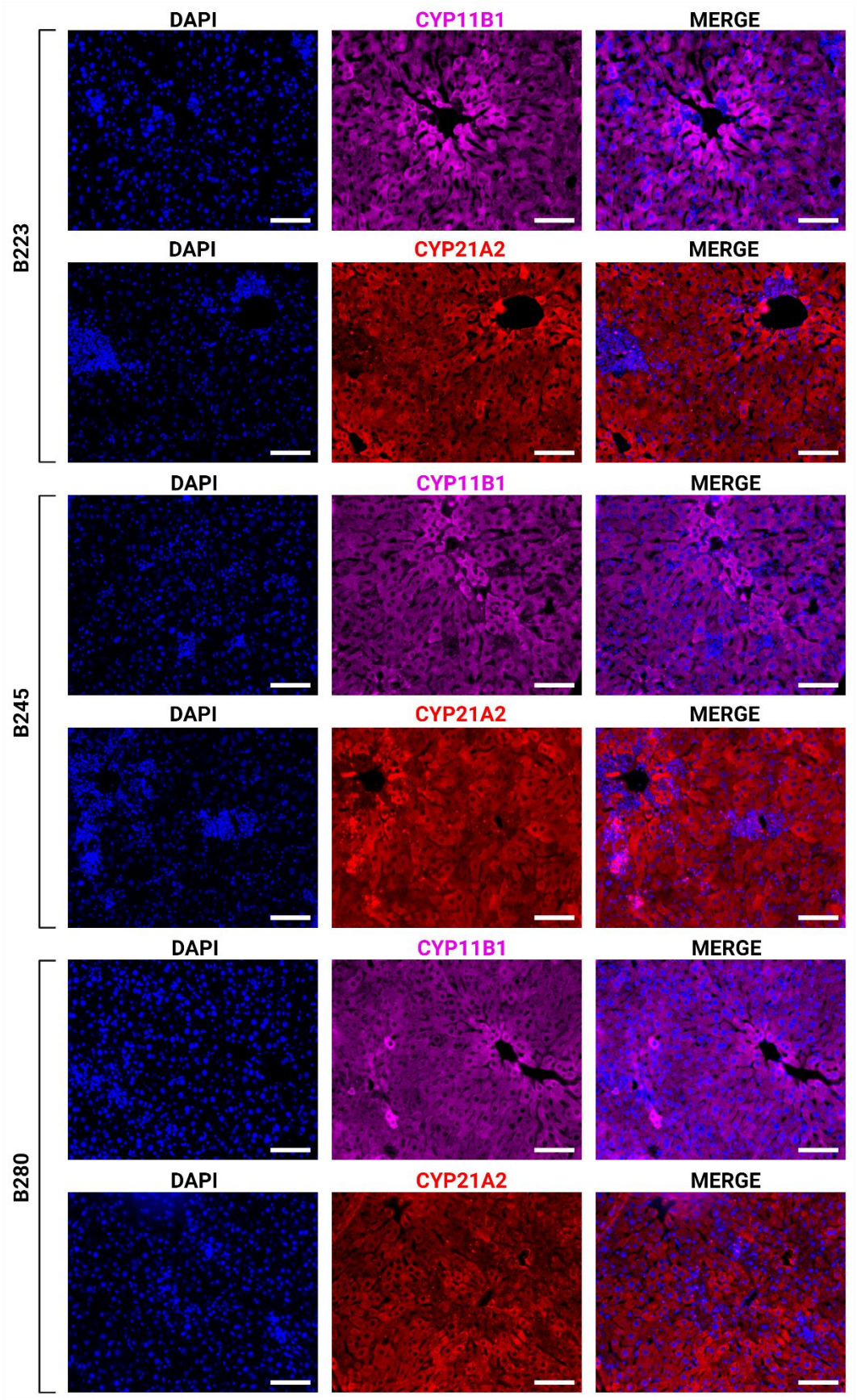

Figure 4.2-7 Immunohistochemistry slides from males B223, B245 and B280.
IHC staining demonstrated CYP11B1 (purple) and CYP21A2 protein (red) in the liver of treated mice. DAPI nuclear staining in blue. Scale bar represents 100µm.

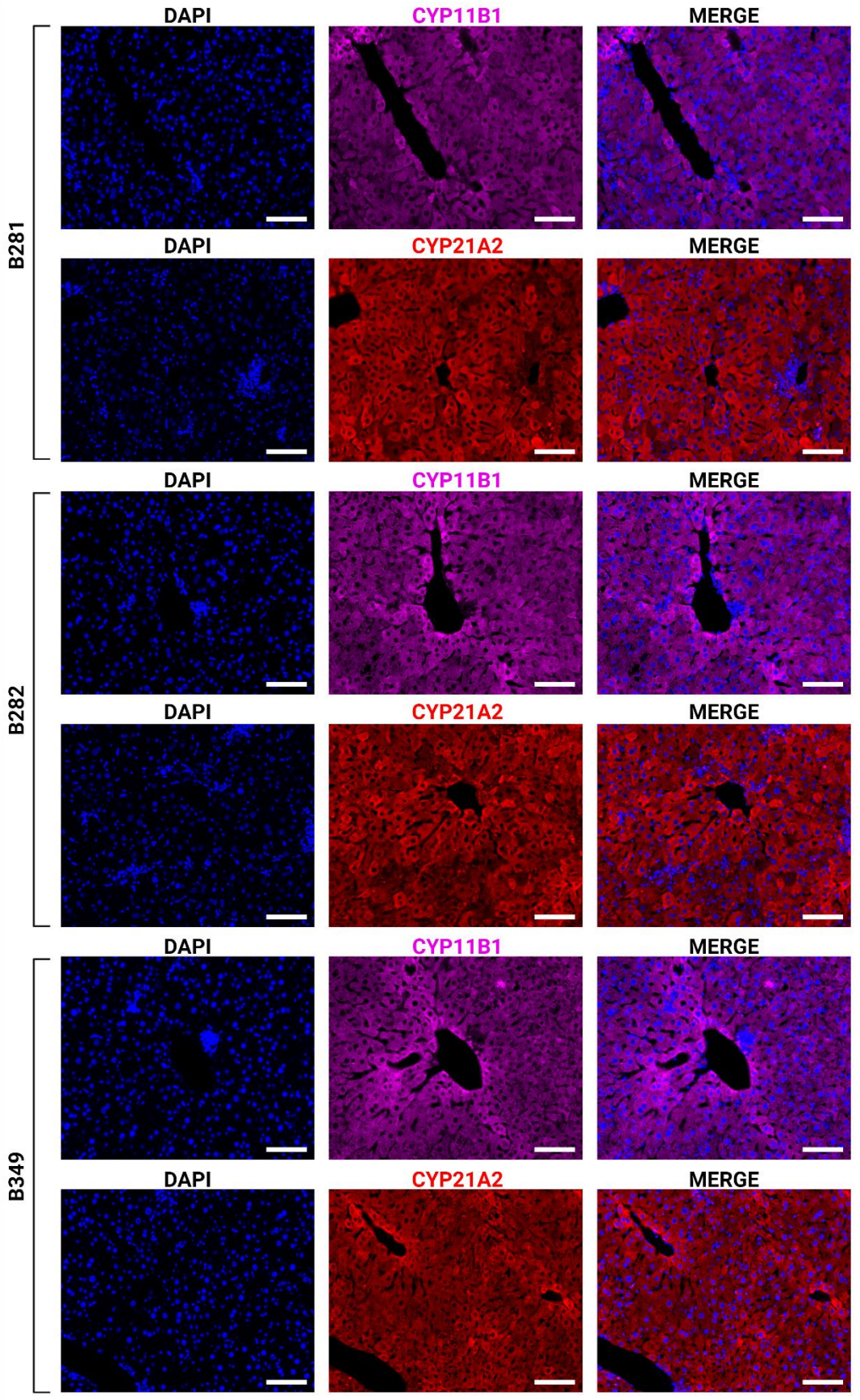

Figure 4.2-8 Immunohistochemistry slides from males B281, B282 and B349.
IHC staining demonstrated CYP11B1 (purple) and CYP21A2 protein (red) in the liver of treated mice. DAPI nuclear staining in blue. Scale bar represents 100µm.

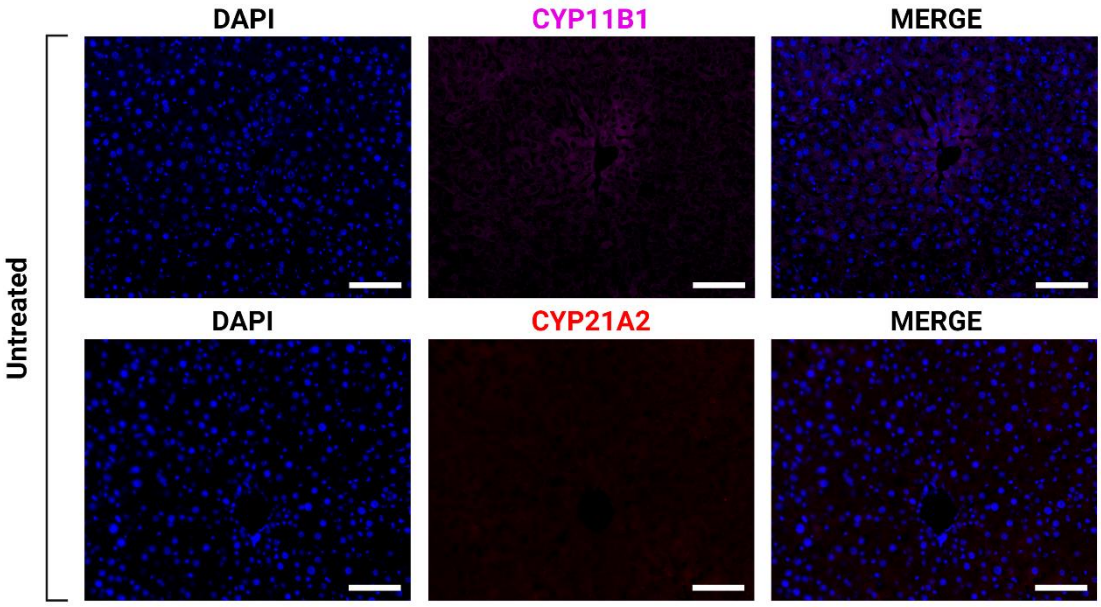

Figure 4.2-9 Immunohistochemistry slides of liver from untreated control.
IHC staining demonstrated absence of CYP11B1 (purple) and CYP21A2 protein (red) in the liver of an untreated control. DAPI nuclear staining in blue. Scale bar represents 100µm

4.2.3.2 Improved steroidogenesis following combined expression of *CYP11B1* and *CYP21A2* over *CYP21A2* alone

Following the addition of *CYP11B1* expression in the liver, the corticosterone production increased 2.2-fold in females and 1.9-fold in males over the single vector treated mice (Figure 4.2-10A). While the corticosterone production in female dual vector treated mice was higher than single vector treated and reached that of male wild-type mice, it was only 48% of female wild-type levels. There was also increased dried whole blood corticosterone in the dual vector treated mice compared with the single vector treated (Figure 4.2-10B). The aldosterone production significantly increased above that of wild-type levels in the dual vector treated mice (Figure 4.2-11A). For comparison, two extra single vector treated mice were added to the cohort and were found to also have significantly increased aldosterone levels compared with the previous cohort of single-

vector treated mice. Despite this documented increased aldosterone level, renin expression was normal in all vector treated mice, indicating this hyperaldosteronism was not renin-driven (Figure 4.2-11B). Aldosterone synthase (*Cyp11b2*) expression was 50-fold higher in *Cyp21a1*$^{-/-}$ than wild-type, and this upregulation of *Cyp11b2* remained markedly elevated post-treatment, despite improved aldosterone production (Figure 4.2-11C). There was no relationship between serum aldosterone and *Cyp11b2* expression in the treated mice (Figure 4.2-11D). While the corticosterone production improved, progesterone did not (Figure 4.2-11E), although the dual vector treatment did improve the ratio of progesterone to corticosterone in the males (Figure 4.2-11F).

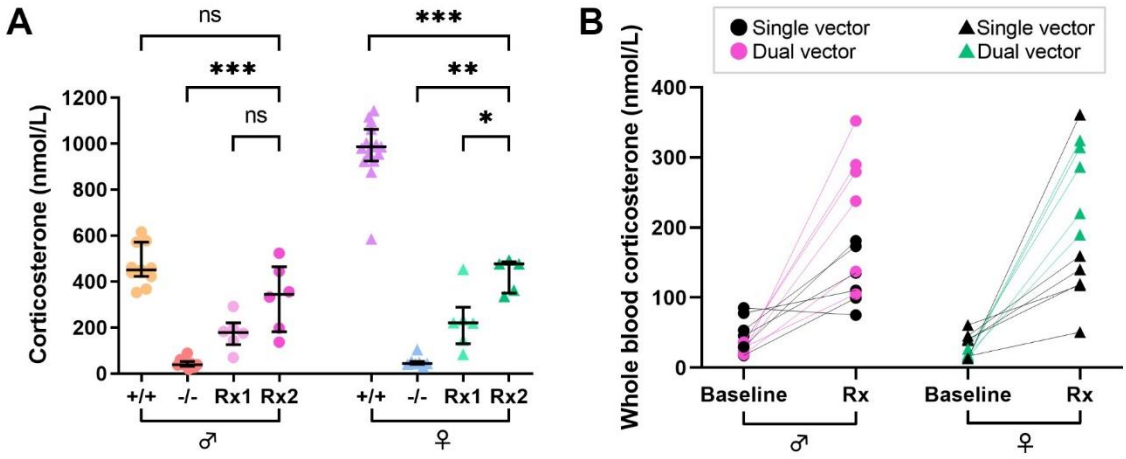

Figure 4.2-10 Corticosterone production following dual vector delivery.
A. Serum corticosterone. **B.** Dried whole blood corticosterone before treatment and at harvest. Single vector (black), dual vector males (pink), dual vector females (green). Abbreviations: +/+, wild-type 21-hydroxylase sufficiency; -/-, homozygous 21-hydroxylase deficiency; Rx1, homozygous 21-hydroxylase deficient mice that were treated with the CYP21A2 vector alone; Rx2, homozygous 21-hydroxylase deficient mice that were treated with both the CYP21A2 and CYP11B1 vectors; ♀, female; ♂, male; ns not significant. Individual data points are shown, and error bars represent median and interquartile range. * p<0.05, ** p<0.01, *** p<0.001 on Mann Whitney U test.

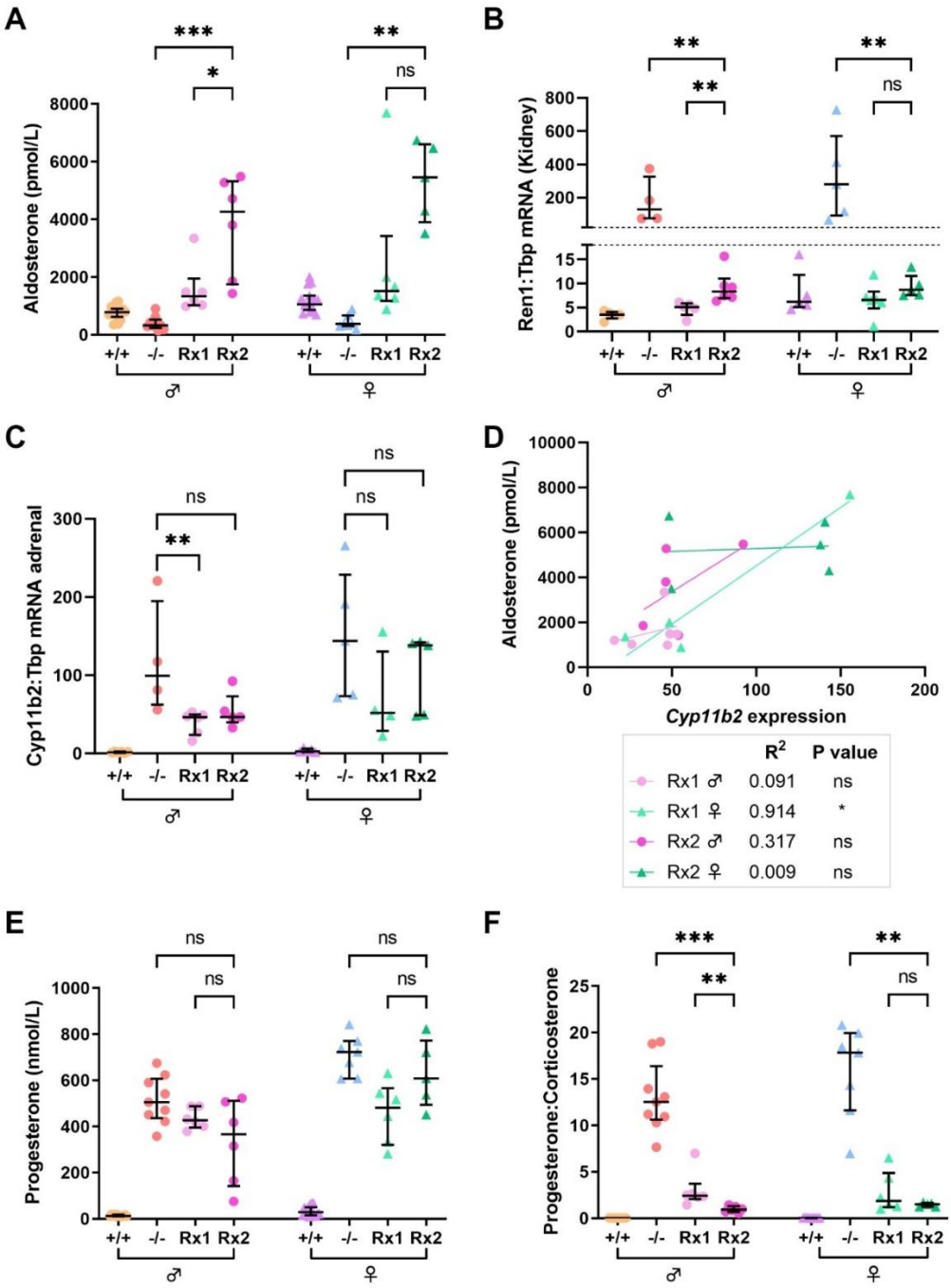

Figure 4.2-11 Aldosterone and progesterone following dual vector delivery.

A. Serum aldosterone. **B.** Renin expression demonstrated as the ratio of renal renin (*Ren1*) mRNA transcripts to *Tbp* transcripts. **C.** Aldosterone synthase expression demonstrated as the ratio of adrenal *Cyp11b2* mRNA transcripts to *Tbp* transcripts. **D.** No relationship between *Cyp11b2* expression and serum aldosterone in treated mice. **E.** Serum progesterone. **F.** Ratio of serum progesterone to serum corticosterone. Abbreviations: +/+, wild-type 21-hydroxylase sufficiency; -/-, homozygous 21-hydroxylase deficiency; Rx1, homozygous 21-hydroxylase deficient mice that were treated with the *CYP21A2* vector alone; Rx2, homozygous 21-hydroxylase deficient mice that were treated with both the CYP21A2 and CYP11B1 vectors; ♀, female; ♂, male; *Ren1*, renin; *Tbp*, TATA-box binding protein; *Cyp11b2*, aldosterone synthase; ns not significant. Individual data points are shown, and error bars represent median and interquartile range. * $p<0.05$, ** $p<0.01$, *** $p<0.001$ on Mann Whitney *U* test or linear regression modelling.

4.2.3.3 Reduction of adrenal hyperplasia

The improvement in adrenal hyperplasia compared with untreated mice was visible grossly (Figure 4.2-12), however the addition of *CYP11B1* expression did not further reduce the adrenal hyperplasia seen with *CYP21A2* vector treatment alone (Figure 4.2-13A and B). Similarly, the addition of *CYP11B1* did not reduce serum ACTH levels (ACTH levels would be expected to be stimulated by lethal exsanguination) or ACTH receptor expression (*Mc2r*) (Figures 4.2-13C and D).

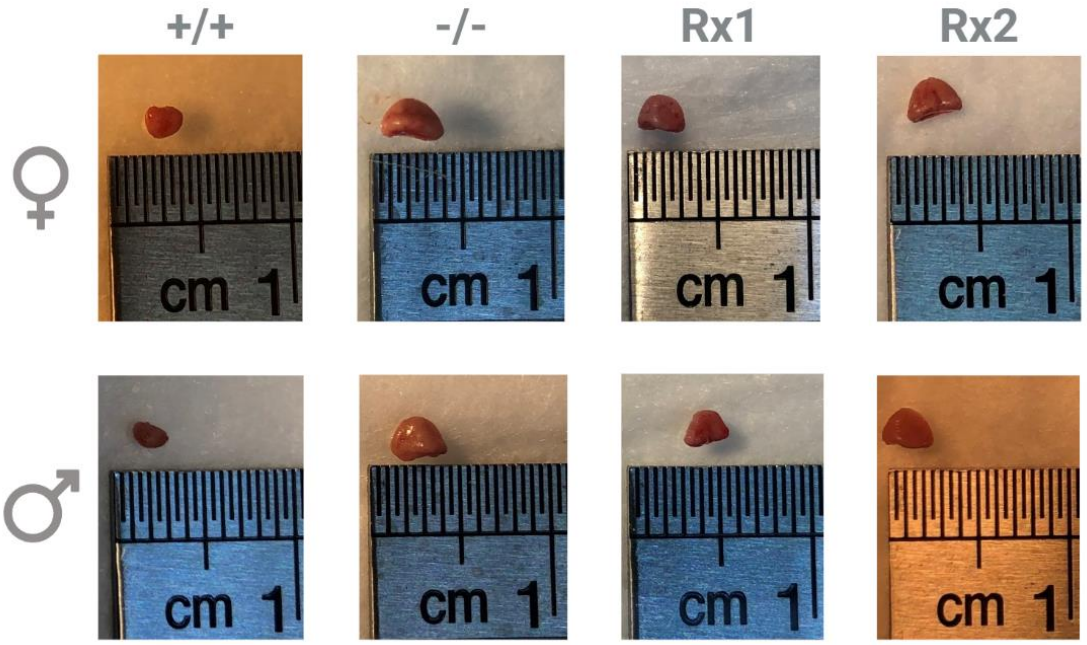

Figure 4.2-12 Adrenal gland photographs.
Macroscopic photographs of representative adrenal glands after fat dissection. Top row females: wild-type (mouse A386), 21-hydroxylase deficient (B097), single vector treated 21-hydroxylase deficient (A652), dual vector treated 21-hydroxylase deficient (B355). Bottom row males: wild-type (A503), 21-hydroxylase deficient (A560), single vector treated 21-hydroxylase deficient (A425), dual vector treated 21-hydroxylase deficient (B280). Abbreviations: +/+, wild-type; -/-, 21-hydroxylase deficient; Rx1, single vector treated; Rx2, dual vector treated; ♀, female; ♂, male.

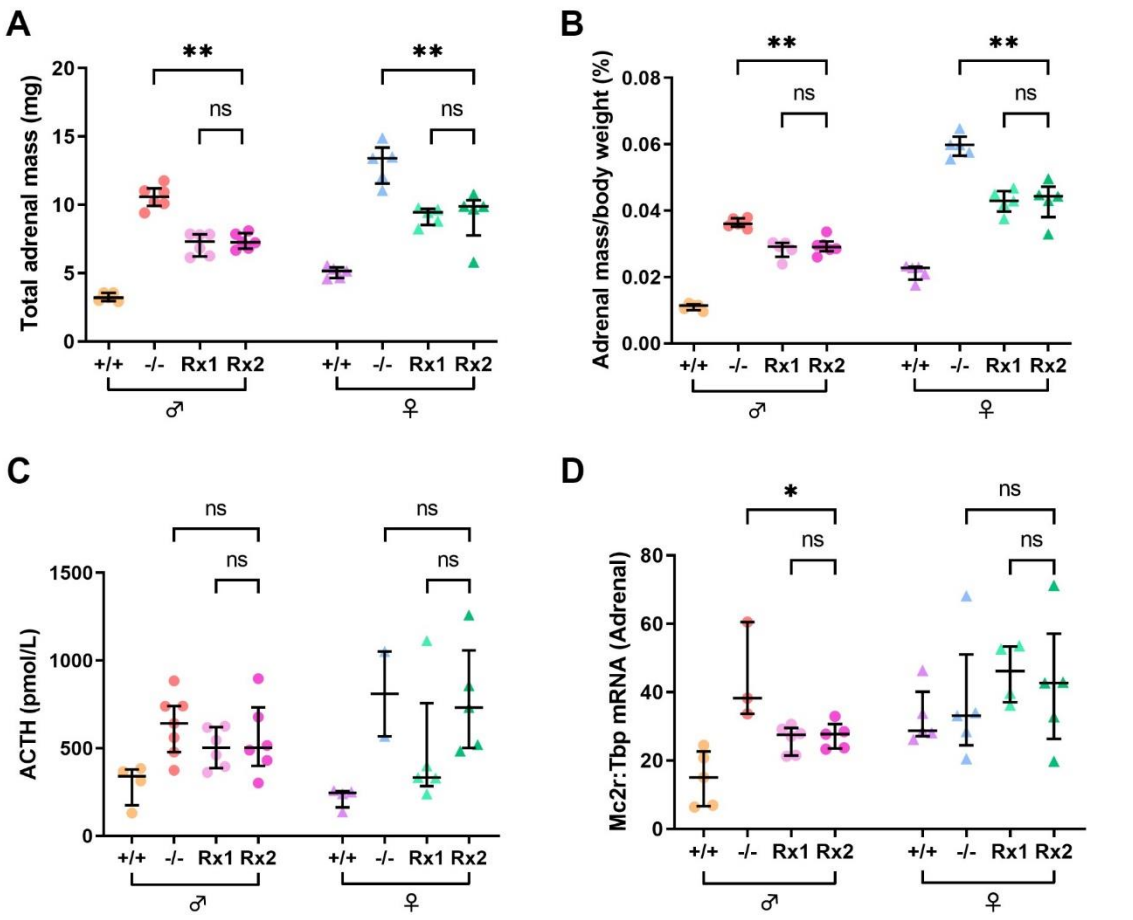

Figure 4.2-13 Adrenal hyperplasia and ACTH.

A. Absolute bilateral adrenal mass. **B.** Bilateral adrenal mass expressed as a percentage of total body mass. **C.** Serum ACTH. **D.** *Mc2r* expression demonstrated as the ratio of adrenal ACTH receptor (*Mc2r*) mRNA transcripts to *Tbp* transcripts. Abbreviations: +/+, wild-type; -/-, 21-hydroxylase deficient; Rx1, single vector treated; Rx2, dual vector treated; ♀, female; ♂, male; ACTH, adrenocorticotropic hormone; *Mc2r*, melanocortin 2 receptor; *Tbp*, TATA-box binding protein; ns not significant. Individual data points are shown, and error bars represent median and interquartile range. * $p<0.05$, ** $p<0.01$ on Mann Whitney *U* test.

4.2.4 Discussion

Co-expression of human enzymes *CYP21A2* and *CYP11B1* in hepatocytes of 21-hydroxylase deficient mice increased production of corticosterone further than ectopic *CYP21A2* expression alone, as described in Chapter 4.1. Ectopic 21-hydroxylase expression could be an alternative genetic therapeutic option that overcomes the limitations of standard rAAV gene therapy in adrenal cortex due to rapid cellular turnover.

Vector expression in the liver was higher in males than in females. This is a known phenomenon in mice,[6] which appears to be related to androgens as castration of male mice reduced transgene expression while administration of dihydrotestosterone (DHT) to female mice increased transgene expression.[6] Although mice with 21-hydroxylase deficiency do not produce androgens in excess, humans with CAH experience hyper-androgenisation and we postulate that if there is an effect on androgens in AAV transduction in humans, this could help facilitate improved transgene expression for liver-directed gene therapy in women. There is no known sex-difference in the expression of AAV-delivered transgenes in lung, spleen or kidney.[6] It is unclear if there is variation in vector expression in the adrenal glands, but as this study used a liver-specific promoter, adrenal vector expression was negligible. Chapter 5 demonstrates that vector expression in the adrenal is both sex and serotype-dependant, but AAV vectors pseudo-typed with the Rh10 capsid had similar expression in both male and female adrenal glands.

Corticosterone production in the mice that received both vectors was approximately double that of those that received *CYP21A2* alone. Indeed, there was no significant difference between the wild-type male corticosterone levels and the dual vector treated

males. However, the treated females produced corticosterone at about half that of wild-type females. Female rodents are known to produce higher levels of corticosterone than males.[7, 8] Co-expression of two enzymes required for steroidogenesis more closely mimics the native condition where 11ß-hydroxylase, expressed in the mitochondria receives 11-deoxycorticosterone that has been produced by 21-hydroxylase in the endoplasmic reticulum via mitochondria-associated endoplasmic reticulum membranes.[2, 3] The ectopic production of corticosterone is, therefore, probably more efficient when the final enzymatic steps are in the same cells.

Restoration of corticosterone would be expected to normalise progesterone production; however, this was not the case. Serum progesterone improved in 21-hydroxylase deficient mice two weeks after systemic treatment with AAVRh10-CYP21A2 that utilised a ubiquitous promoter.[9] In a similar study, urine progesterone was significantly improved although had not normalised at 5 weeks after AAVRh10-CYP21A2 with a ubiquitous promoter.[10] Urinary progesterone may not be directly comparable to serum progesterone as the major route of excretion of progesterone in mice is via the enteric route.[11, 12] However, it is unclear if the high serum progesterone concentration is required to drive flux through the ectopic 21-hydroxylation pathway and if normalisation of progesterone would prevent the ectopic production of corticosterone. While corticosterone was restored, which could greatly improve the CAH phenotype in humans, persistently elevated progesterone suggests that if applied to humans, there would be persistence of hyperandrogenism. In humans with CAH, progesterone is 17-hydroxylated to 17OHP which will then enter the canonical androgen pathway to produce androstenedione, testosterone and DHT (Chapter 1, Figure 1-7). Additionally, the excess progesterone and 17OHP may provide substrate for the backdoor androgen pathway, with eventual

production of further DHT.[13] Furthermore, the excess production of androstenedione and the 11ß-hydroxylation of 21-deoxycorticosterone and 21-deoxycortisol in the adrenal cortex may be used to produce 11-ketoandrostenedione and eventually 11-ketotestosterone and 11-ketoDHT which are known to have equal potency to testosterone and DHT, respectively.[14, 15] Thus despite the glucocorticoid and mineralocorticoid "cure", there would remain a hyperandrogenic state, similar to non-classical CAH, which is particularly an issue for women. Androgen-receptor agonists could be considered in women with CAH.[16] Anti-androgen/oestrogen therapy, such as *CYP17A1* inhibitors, are not appropriate in peripubertal children, pubertal adolescents or adults (unless adults with completed puberty take concomitant hormone replacement therapy), as it blocks the production of all gonadal sex hormones.[16]

Despite improved corticosterone production with the addition of *CYP11B1* expression in the liver, progesterone remained elevated and the corticosterone level in females was only half that of wild-type. Higher vector doses were not considered, as there was no relationship between vector expression and corticosterone levels in individual mice. Furthermore, despite a large difference in vector expression between males and females, the absolute corticosterone production was similar. Therefore, this implies that increasing the vector dose would be unlikely to have an effect, and we likely reached the pinnacle of ectopic adrenal enzyme efficiency with the doses used. This is a limitation of delivering new functions to the transduced hepatocytes, rather than a limitation imposed by AAV gene transfer.

The serum aldosterone levels were higher in this experiment than Chapter 4.1, so variables were examined. The possibility that there were changes in the husbandry of the

colony was considered between 2021 and 2022 but none were found. Most of the single vector treated mice were treated May – October 2021 whereas the dual vector treated mice were treated in March – May 2022 and two additional single vector treated mice were treated in June – July 2022. The mice treated in 2022 had much higher aldosterone levels than those treated in 2021. There were no changes that we could identify including diet, salt supplementation, timing of blood collection or any other known variable. *CYP11B1* cannot produce aldosterone,[17] rather its production is catalysed by aldosterone synthase (*CYP11B2*), and this possibility was negated by the elevated aldosterone in the *CYP21A2*-only treated mice. *Cyp11b2* has 40-fold increased expression in 21-hydroxylase deficient mice compared with wild-type.[10] When AAVRh10 was used to deliver human *CYP21A2* to 21-hydroxylase deficient mice systemically, there was persistent elevation in *Cyp11b2* up to 18 weeks after treatment. While it was reported in this study that *Cyp11b2* expression near normalised, inspection of the results revealed *Cyp11b2* expression was markedly elevated over wild-type, even 18 weeks after treatment.[10] Aldosterone was not measured in that study, therefore it is unclear if there was similar over production of aldosterone. We found similar upregulation of aldosterone synthase pre- and post-treatment, which is likely the cause of increased aldosterone production above physiological levels. We expect that this would be transient if the mice were followed for long enough to allow equilibration. This strategy could be applied to mineralocorticoid defects. If *CYP11B2* was delivered to the liver in aldosterone synthase deficiency, then the aldosterone would only be produced by the transgene as the native *CYP11B2* would be defective. This would prevent rebound hyperaldosteronism in this situation.

Renin expression in the 21-hydroxylase deficient mice was increased 20 to 30-fold over wild-type, however others found a 120-fold increase.[10] We postulate that salt supplementation contributed to slightly reduced renin stimulation, and may also be related to our improved body mass pre-treatment (see Chapter 3).

General anaesthesia is a physiologically stressful event and in humans with adrenal insufficiency, a large dose of hydrocortisone is required on induction.[16] Steroids were not provided on induction in this experiment to avoid any effect on the measured serum steroids. The treated *Cyp21a1*$^{-/-}$ mice were subjectively more robust than the untreated *Cyp21a1*$^{-/-}$ mice were under anaesthetic, allowing for larger blood volume collection prior to cardiac arrest. One untreated *Cyp21a1*$^{-/-}$ female mouse died on anaesthetic induction, prior to cardiac puncture. We postulate that the improved corticosterone production may have allowed improved tolerance of the physiological stress associated with general anaesthesia.

This approach would need refinement for human clinical translation. While AAV8 can transduce the human liver, there are serotypes with much higher human liver tropism such as AAV-SYDs, AAV-KPs and AAV-LK03,[18-20] and pseudo-serotyping for a highly human liver tropic capsid would make this strategy more efficient for human clinical translation. This could allow the use of lower total vector doses . Furthermore, for human clinical translation, determining the stability of the ITRs is imperative. ITRs are prone to large truncations during bacterial propagation, which can affect the amount of therapeutic vector in a preparation.[21] By treating with vector that is not packaged correctly, the dose would need to be increased, exposing the patient to unnecessarily large amounts of immunogenic, ineffective vector. Therefore, it is imperative that strategies are developed

to minimise acquired mutations in plasmids during bacterial propagation for commercial use. Furthermore, this approach has not yet been shown to reduce progesterone levels. It would be important to determine if progesterone levels improve after a longer period of time post-treatment, and if not, women with CAH would require additional anti-androgen treatment in conjunction with the gene therapy.

Specifically expressing human *CYP21A2* and *CYP11B1* in the livers of 21-hydroxylase deficient mice can further correct the CAH phenotype above *CYP21A2* alone, through hepato-adrenal cooperativity in steroidogenesis, with resultant normalisation of corticosterone production in males, 50% of normal corticosterone in females, and normalisation of renal renin expression. This strategy has the potential to overcome the current technological limitations of direct adrenal cortex targeting with rAAV, and has particular relevance to men with classical CAH, where excess androgen is tolerated.

4.2.5 References

1. Payne AH and Hales DB. Overview of steroidogenic enzymes in the pathway from cholesterol to active steroid hormones. *Endocr Rev* 2004; 25: 947-970. 2004/12/08. DOI: 10.1210/er.2003-0030.
2. Doghman-Bouguerra M and Lalli E. The ER-mitochondria couple: In life and death from steroidogenesis to tumorigenesis. *Mol Cell Endocrinol* 2017; 441: 176-184. 2016/09/07. DOI: 10.1016/j.mce.2016.08.050.
3. Vance JE. Phospholipid synthesis in a membrane fraction associated with mitochondria. *J Biol Chem* 1990; 265: 7248-7256. 1990/05/05.
4. Domalik LJ, Chaplin DD, Kirkman MS, et al. Different isozymes of mouse 11 beta-hydroxylase produce mineralocorticoids and glucocorticoids. *Mol Endocrinol* 1991; 5: 1853-1861. 1991/12/01. DOI: 10.1210/mend-5-12-1853.
5. Cunningham SC, Dane AP, Spinoulas A, et al. Gene delivery to the juvenile mouse liver using AAV2/8 vectors. *Mol Ther* 2008; 16: 1081-1088. 2008/04/17. DOI: 10.1038/mt.2008.72.
6. Davidoff AM, Ng CY, Zhou J, et al. Sex significantly influences transduction of murine liver by recombinant adeno-associated viral vectors through an androgen-dependent pathway. *Blood* 2003; 102: 480-488. 2003/03/15. DOI: 10.1182/blood-2002-09-2889.
7. Kitay JI. Sex differences in adrenal cortical secretion in the rat. *Endocrinology* 1961; 68: 818-824. 1961/05/01. DOI: 10.1210/endo-68-5-818.
8. Bielohuby M, Herbach N, Wanke R, et al. Growth analysis of the mouse adrenal gland from weaning to adulthood: time- and gender-dependent alterations of cell size and number in the cortical

compartment. *Am J Physiol Endocrinol Metab* 2007; 293: E139-146. 2007/03/22. DOI: 10.1152/ajpendo.00705.2006.
9. Markmann S, De BP, Reid J, et al. Biology of the Adrenal Gland Cortex Obviates Effective Use of Adeno-Associated Virus Vectors to Treat Hereditary Adrenal Disorders. *Hum Gene Ther* 2018; 29: 403-412. 2018/01/11. DOI: 10.1089/hum.2017.203.
10. Perdomini M, Dos Santos C, Goumeaux C, et al. An AAVrh10-CAG-CYP21-HA vector allows persistent correction of 21-hydroxylase deficiency in a Cyp21(-/-) mouse model. *Gene Ther* 2017; 24: 275-281. 2017/02/07. DOI: 10.1038/gt.2017.10.
11. Bamberg E, Palme R and Meingassner JG. Excretion of corticosteroid metabolites in urine and faeces of rats. *Lab Anim* 2001; 35: 307-314. 2001/10/24. DOI: 10.1258/0023677011911886.
12. Busso JM and Ruiz RnD. Excretion of Steroid Hormones in Rodents: An Overview on Species Differences for New Biomedical Animal Research Models. In: Evanthia D-K (ed) *Contemporary Aspects of Endocrinology*. Rijeka: IntechOpen, 2011, pp.Ch. 16.
13. Kamrath C, Hochberg Z, Hartmann MF, et al. Increased activation of the alternative "backdoor" pathway in patients with 21-hydroxylase deficiency: evidence from urinary steroid hormone analysis. *J Clin Endocrinol Metab* 2012; 97: E367-375. 2011/12/16. DOI: 10.1210/jc.2011-1997.
14. Storbeck KH, Bloem LM, Africander D, et al. 11beta-Hydroxydihydrotestosterone and 11-ketodihydrotestosterone, novel C19 steroids with androgenic activity: a putative role in castration resistant prostate cancer? *Mol Cell Endocrinol* 2013; 377: 135-146. 2013/07/17. DOI: 10.1016/j.mce.2013.07.006.
15. Turcu AF, Nanba AT, Chomic R, et al. Adrenal-derived 11-oxygenated 19-carbon steroids are the dominant androgens in classic 21-hydroxylase deficiency. *Eur J Endocrinol* 2016; 174: 601-609. 2016/02/13. DOI: 10.1530/EJE-15-1181.
16. Speiser PW, Arlt W, Auchus RJ, et al. Congenital Adrenal Hyperplasia Due to Steroid 21-Hydroxylase Deficiency: An Endocrine Society Clinical Practice Guideline. *J Clin Endocrinol Metab* 2018; 103: 4043-4088. 2018/10/03. DOI: 10.1210/jc.2018-01865.
17. Mulatero P, Curnow KM, Aupetit-Faisant B, et al. Recombinant CYP11B genes encode enzymes that can catalyze conversion of 11-deoxycortisol to cortisol, 18-hydroxycortisol, and 18-oxocortisol. *J Clin Endocrinol Metab* 1998; 83: 3996-4001. 1998/11/14. DOI: 10.1210/jcem.83.11.5237.
18. Cabanes-Creus M, Navarro RG, Zhu E, et al. Novel human liver-tropic AAV variants define transferable domains that markedly enhance the human tropism of AAV7 and AAV8. *Mol Ther Methods Clin Dev* 2022; 24: 88-101. 2022/01/04. DOI: 10.1016/j.omtm.2021.11.011.
19. Lisowski L, Dane AP, Chu K, et al. Selection and evaluation of clinically relevant AAV variants in a xenograft liver model. *Nature* 2014; 506: 382-386. 2014/01/07. DOI: 10.1038/nature12875.
20. Pekrun K, De Alencastro G, Luo QJ, et al. Using a barcoded AAV capsid library to select for clinically relevant gene therapy vectors. *JCI Insight* 2019; 4 2019/11/15. DOI: 10.1172/jci.insight.131610.
21. Wilmott PG. *Endogenous UMIs as quantifiable reporter elements–validation studies & applications in rAAV vectorology*. University of Sydney, 2023.

Chapter 5

Towards determining rAAV capsid tropism for the adrenocortical progenitor cells

5.1 Introduction

Gene therapy has the potential to replace standard glucocorticoid treatment in the management of CAH whereby the gene coding the defective enzyme is replaced or repaired, thus allowing the enzyme expression to increase and overcome the deficiency. However, a major obstacle to genome editing is the delivery of editing reagents to the appropriate cell population.

Despite gene therapy for monogenic adrenocortical disorders being conceptually promising treatment options, there is a paucity of gene therapy studies in the adrenal cortex. Thus far, no adrenocortical targeting gene therapy has shown durability of effect beyond the cellular turnover period.[1-3] The adrenal cortex can regenerate itself[4] from populations of cells located in the capsular/subcapsular region.[5] Cells from the peripheral layers differentiate into steroidogenic cells, migrate centripetally while undergoing lineage conversion, and finally reach the cortico-medullary junction where they apoptose.[6, 7] The differentiated cells do not undergo significant cellular replication before they apoptose and the cortex is populated from the stem and progenitor cells. There are

multiple populations of long-lived stem cells in the adult adrenal capsule and outer cortex. Within the capsule are stem cells that variously express Wilms tumour protein homolog 1 (WT1), and GLI family zinc finger 1 (GLI1), among others.[8] Cells expressing GLI1+ are the largest population of capsular cells and they give rise to cortical SF1+ progenitor and SF1+ differentiated steroidogenic cells of the zona glomerulosa.[9, 10] With this constant cell renewal, the mouse adrenal cortex is almost entirely replaced in 200 days, a process thought to be faster in female mice.[11, 12] In an attempt to overcome the limitations imposed by the adrenocortical biology and standard rAAV therapy, in Chapter 4, delivery of adrenal enzyme transgenes for specific hepatic expression outside the adrenal cortex was achieved.[13] While this improved the downstream corticosteroid production such that there was phenotypic improvement in adrenal size and renin expression, the progesterone precursor levels did not reduce, thus adrenal-targeting gene therapy is still sought.

A critical advantage of rAAV is that the AAV2 genome can be cross-packaged into an alternate capsid serotype, known as pseudo-serotyping. The rAAV capsid proteins determine vector-host interactions, including tissue tropism. There have been no systematic studies examining rAAV delivery to the adrenal gland. In the murine adrenal gland, Rh10 and AAV9 were compared following intravenous administration, with Rh10 shown superior[2]. In another study, AAV2 and AAV9 were compared following intra-adrenal administration, with AAV9 shown to be superior[14]. In a non-human primate (NHP) AAV1, AAV5 and AAV6 were compared following both intra-adrenal and intravenous administration and AAV5 was shown to result in the highest vector levels detected in the adrenal gland.[15] These limited comparisons are not systematic capsid tropism studies and capsid technology has evolved such that unique capsid serotypes have been developed which can target relatively specific cell populations with high tropism. ,

Furthermore, there are now over one hundred capsids available due to the rapid expansion of the capsid engineering field.[16-18] Determining the optimal rAAV serotype for transgene delivery to the adrenal cortex is the first step in improving gene therapy delivery, however the crucial caveat is that the terminally differentiated adrenocortical cells undergo minimal cellular replication and thus targeting the progenitor population is required. However, these techniques are yet to be adequately described.

There are multiple populations of long-lived stem and progenitor cells in the adult adrenal capsule and cortex. The largest somatic stem population resides in the capsule, expresses *Gli1* and gives rise to Gli1- cortical progenitor cells.[9, 10] Peripheral progenitor cells of the subcapsular zona glomerulosa in mice are characterised by nuclear beta-catenin, SF1 (*Nr5a1*) and *Shh* expression and lack *Gli1* and *Cyp11b2* expression.[7, 9] SF1+/Shh+ progenitor cells of the zona glomerulosa differentiate into Cyp11b2+ steroidogenic cells that produce aldosterone, and then migrate and undergo lineage conversion to become Cyp11b1+ steroidogenic cells of the zona fasciculata that produce corticosterone in the mouse or cortisol in the human.[7, 8] Female mice have 6.3-fold higher rate of proliferation in the adrenal cortex than males.[12] In juvenile mice, Gli1+ capsular stem cells contribute to the differentiated adrenocortical population in both sexes, however by sexual maturity, the main source of cells that populate the male murine adrenal cortex are Gli1-, Shh+ progenitor cells located in the zona glomerulosa., In females both the capsular stem cells and the subcapsular progenitor cells populate the differentiated cortex.[12] Therefore, the adrenocortical progenitor cells were considered an appropriate target for gene therapy as they populate the adrenal cortex in both males and females. In a published study of the single cell transcriptome of the hypothalamic-pituitary-adrenal axis in the mouse, a population of cycling/dividing adrenocortical cells was found, however progenitor cells

were not specifically described.[19] This may have been as the progenitor cells did not form a distinct cluster and were not specifically examined for; however, it is possible to interrogate for cell populations that are present in numbers that are too small to form a distinct cluster.

AAV genomes are predominantly episomal and standard gene therapy using rAAV vectors, applied to the adrenal cortex, will be lost due to cellular turnover. Furthermore, differentiated adrenal cortical cells apoptose without significant cellular replication and therefore genome modification of differentiated cells will only provide a transient effect. To overcome this, the genomic repair must be integrated into the genome of the adrenal progenitor cells, to ensure daughter cells maintain the correction. Genomic editing has the potential to provide a robust curative treatment for adrenocortical disorders, although current limits in knowledge of the adrenal stem/progenitor cell system precludes its use. A gap in the knowledge regarding the characterisation of adrenal stem/progenitor cells exists and further information is required to design adrenal-targeting gene therapy vector targets.

Despite knowledge of their existence, little is known about the adrenocortical progenitor populations and they have not previously been identified in single cell RNA sequencing (scRNA-Seq) transcriptomic analysis.[19] We postulated that additional ACTH stimulation in the context of 21-hydroxylase deficiency may affect the progenitor population. The aims of this study were to set the foundation for further investigation into determining appropriate capsid choice for adrenal-targeting gene therapy. Firstly, we sought to identify the top rAAV serotypes from a known pool of candidates for adrenal cortex transduction. Secondly, using 21-hydroxylase deficiency as a model for excessive ACTH

stimulation, we aimed to compare the adrenal single nuclei transcriptome in wild-type and 21-hydroxylase deficient mice and to identify potential adrenocortical progenitor cells. This study provides foundations for future downstream study of capsid tropism for the adrenocortical progenitor population.

5.2 Chapter-specific methods

5.2.1 Vectors

5.2.1.1 AAV testing kit

A stoichiometric mix of multiple vectors, each with a unique capsid and encoding a unique barcode was developed by the Translational Vectorology Research Unit (TVRU), CMRI,[18] and known as an AAV Testing Kit. This barcode can be detected using next generation sequencing and allows for rapid screening of a large number of capsid serotypes in individual animals. This kit was expanded to include a total of 67 unique capsids (TVRU, CMRI) (Table 5-1). Each vector encodes the same genome except for a unique 6 nucleotide sequence, known as a barcode (Figure 5-1). The barcode is within the expression cassette and in addition to being detectable in gDNA it is also present in mRNA transcripts. This allows the detection of vector "entry" (presence of barcode in cellular gDNA) and "expression" (presence of barcode in mRNA). All vectors include an eGFP reporter sequence allowing detection of vector expression by immunohistochemistry or fluorescence microscopy.

5.2.1.2 Individual vectors

In the second part of this study, the top capsid serotypes from the capsid kit were chosen and delivered as individual vectors to the mice. The vectors were purchased from Vector

Genome Engineering Facility (VGEF), CMRI and contained the same genome as those in the AAV Testing Kit (Figure 5-1).

Table 5-1 Capsid variants included in the AAV Testing Kit.

Variant	Source	Reference
AAV1	Natural serotype	Atchison, et al. 1965[20]
AAV2	Natural serotype	Hoggan, et al. 1966[21]
AAV3b	Natural serotype	Hoggan, et al. 1966[21] and Rutledge, et al. 1998[22]
AAV4	Natural serotype	Parks, et al, 1967[23]
AAV5	Natural serotype	Bantel-Schaal and zur Hausen, 1984[24]
AAV6	Natural serotype	Rutledge, et al. 1998[22]
AAV7	Natural serotype	Gao, et al. 2002[25]
AAV8	Natural serotype	Gao, et al. 2002[25]
AAV9	Natural serotype	Gao, et al. 2004[26]
AAV10	Natural serotype	Mori, et al. 2004[27]
AAV11	Natural serotype	Mori, et al. 2004[27]
AAV12	Natural serotype	Schmidt, et al. 2008a[28]
AAV13	Natural serotype	Schmidt, et al. 2008b[29]
Rh10	Natural isolate	Gao, et al. 2003[30]
2i8	Rational design	Asokan, et al. 2010[31]
AAV2.hSC1	Peptide display	*
AAV2.hSC10	Peptide display	*
AAV2.hSC2	Peptide display	*
AAV2-FT01	Peptide display	Westhaus, et al. 2022[17]
AAV2-FT11	Peptide display	Westhaus, et al. 2022[17]
AAV2-L1	Peptide display	Westhaus, et al. 2023[32]
AAV2-L2	Peptide display	Westhaus, et al. 2023[32]
AAV2-M1	Peptide display	Westhaus, et al. 2023[32]
AAV2-M4	Peptide display	Westhaus, et al. 2023[32]
AAV2-RC01	Peptide display	Westhaus, et al. 2022[17]
AAV2-RC02	Peptide display	Westhaus, et al. 2022[17]
AAV2-RC06	Peptide display	Westhaus, et al. 2022[17]
AAV2-Retro	Peptide display	Tervo, et al. 2016[33]
AAV6.2	Rational design	Wu, et al. 2006[34]
AAV6.TM	Rational design	Ling, et al. 2016[35]
AAV-7m8	Peptide display	Dalkara, et al. 2013[36]
AAV9 Full Mutant	Rational design	*
AAV-DJ	DNA family shuffling	Grimm, et al. 2008[37]

AAV-DJ8	DNA family shuffling	Grimm, et al. 2008[37]
AAV-PHP.eB	Peptide display	Chan, et al. 2017[38]
Anc80	Reconstructed capsid	Zinn, et al. 2015[39]
CAP-B10	Peptide display	Goertsen, et al. 2022[40]
CD15	DNA family shuffling	Cabanes-Creus 2019[41]
CD34-SYD01	DNA family shuffling	Cabanes-Creus 2019[41]
CD34-SYD03	DNA family shuffling	Cabanes-Creus 2019[41]
CD34-SYD09	DNA family shuffling	Cabanes-Creus 2019[41]
h.Lvr6	Natural isolate	Cabanes-Creus, et al. 2020[42]
HRP5	DNA family shuffling	Cabanes-Creus 2019[41]
HRS1	DNA family shuffling	Cabanes-Creus 2019[41]
HRS19	DNA family shuffling	Cabanes-Creus 2019[41]
KP1	DNA family shuffling	Pekrun, et al. 2019[43]
KP2	DNA family shuffling	Pekrun, et al. 2019[43]
KP3	DNA family shuffling	Pekrun, et al. 2019[43]
LK01	DNA family shuffling	Lisowski, et al. 2014[44]
LK02	DNA family shuffling	Lisowski, et al. 2014[44]
LK03	DNA family shuffling	Lisowski, et al. 2014[44]
LK03 HSPG	Rational design	Cabanes-Creus, et al. 2023[45]
LK19	DNA family shuffling	Lisowski, et al. 2014[44]
N496D	DNA family shuffling	Cabanes-Creus, et al. 2020[46]
NP22	DNA family shuffling	Paulk, et al, 2018b[47]
NP40	DNA family shuffling	Paulk, et al. 2018a[48]
NP59	DNA family shuffling	Paulk, et al. 2018a[48]
NP6	DNA family shuffling	Paulk, et al. 2018b[47]
NP66	DNA family shuffling	Paulk, et al. 2018b[47]
NP84	DNA family shuffling	Paulk, et al. 2018a[48]
NP94	DNA family shuffling	Paulk, et al. 2018b[47]
R588I	DNA family shuffling	Cabanes-Creus , et al. 2020[42]
shH10	DNA family shuffling	Klimczak, et al. 2009[49]
SYD04	DNA family shuffling	Cabanes-Creus, et al. 2022[16]
SYD11	DNA family shuffling	Cabanes-Creus, et al. 2022[16]
SYD12	DNA family shuffling	Cabanes-Creus, et al. 2022[16]
T33	DNA family shuffling	Cabanes-Creus 2019[41]

AAV Testing kit with 67 capsid serotypes developed by the Translational Vectorology Research Unit (TVRU, CMRI).

*Unpublished TVRU research capsid

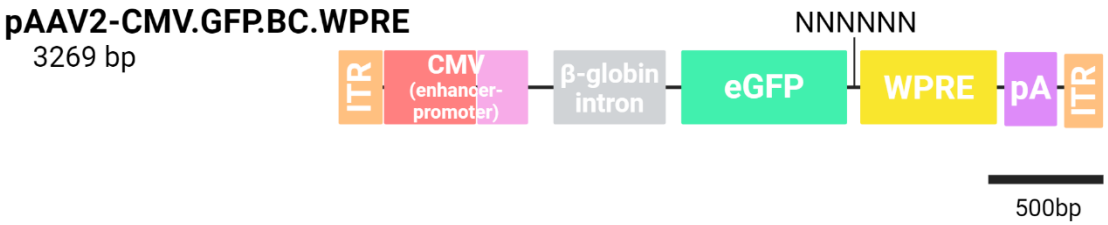

Figure 5-1 Schematic of genome for vectors in the capsid kit.
Between the ITRs, the sequence included a CMV enhancer (red) promoter (pink), beta globin intron (grey), green fluorescent protein sequence (eGFP, green), Woodchuck Hepatitis Virus Posttranscriptional Regulatory Element (WPRE, yellow), unique 6 nucleotide barcode (NNNNNN), bovine growth hormone polyadenylated tail (pA, purple).

5.2.2 Mouse procedures

Wild-type C57BL/10SnSlc-H-2^{aw18} mice[50] were used for the capsid study, as they have the same background genetics as the 21-hydroxylase deficient mice used in other studies in this thesis. The AAV testing kit was administered intravenously to two adult wild-type mice: one female, and one male at a dose of 3.25 $\times 10^{11}$ vector genomes (vg) per mouse, which is equivalent to a dose of 4.85 $\times 10^{9}$ vg per unique capsid per mouse (Figure 5-2A). The mice were harvested two weeks later: one adrenal gland was fixed in 4% (w/v) PFA, followed by treatment with a sucrose gradient for immunohistochemistry and the other adrenal gland was snap frozen in liquid nitrogen for molecular studies. The 7 chosen top individual capsid serotypes were administered intravenously to one adult male and one adult female wild-type mouse each, at a dose of 5 $\times 10^{10}$ vg per mouse (n=14 total) (Figure 5-2B). The mice were harvested one week later: the adrenal glands were fixed in 4% (w/v) PFA for immunohistochemistry.

For the transcriptomic study, both adrenal glands from one male wild-type, one female wild-type, one male 21-hydroxylase deficient and one female 21-hydroxylase deficient

adult mice were harvested after anaesthetisation (Figure 5-2C). The fat was dissected from the glands before they were snap frozen and subsequently dissociated into single nuclei.

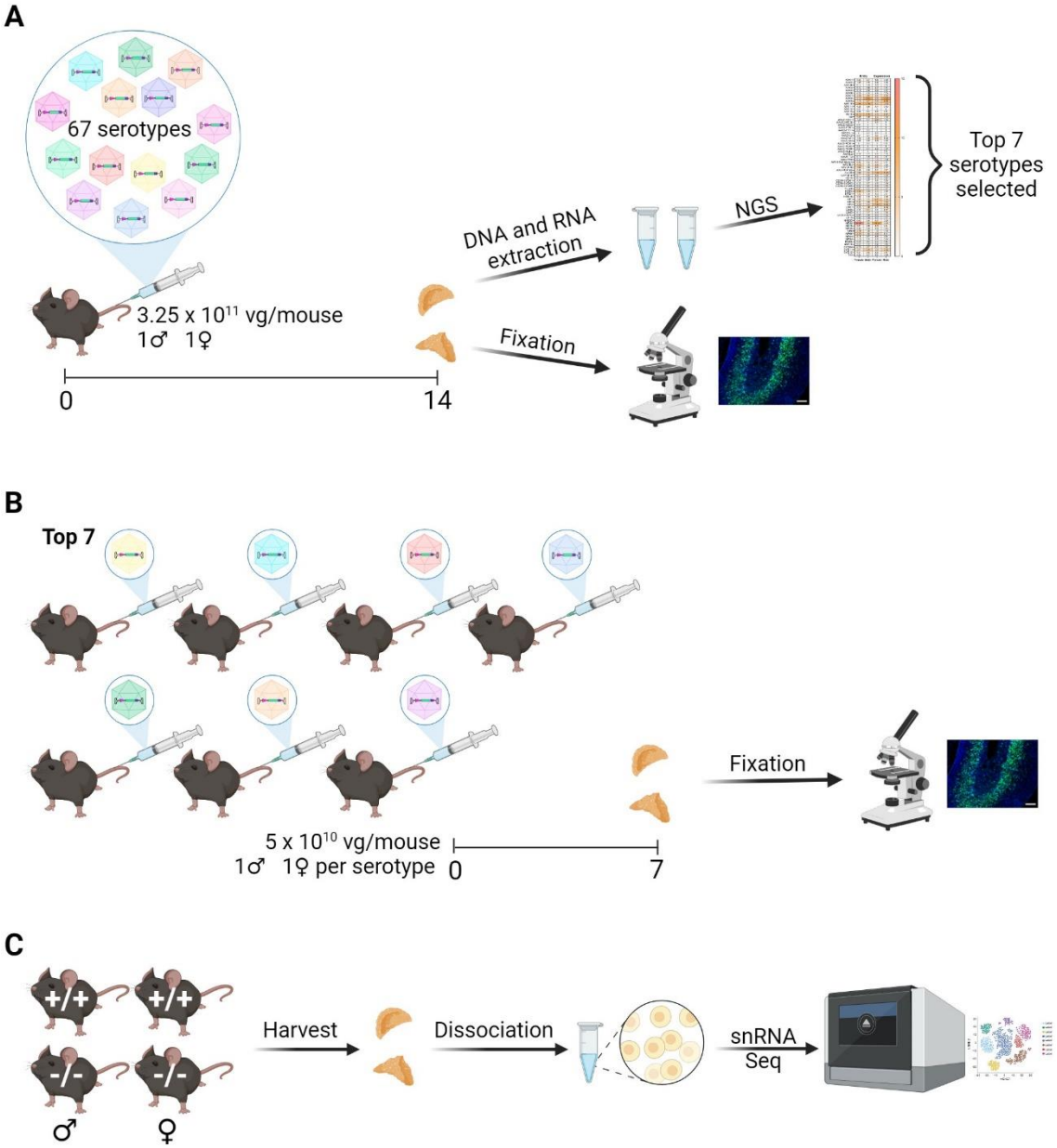

Figure 5-2 Schematic of mouse procedures

A. Two mice were intravenously injected with the AAV testing kit (67 capsid serotypes) and harvested 2 weeks later. One adrenal gland was used for molecular studies and one for immunohistochemistry. **B.** The 7 serotypes with the highest functional transduction were each injected into individual mice. Adrenal glands were harvested 1 week later for immunohistochemistry. **C.** Adrenal glands from two wild-type and two 21-hydroxylase deficient mice were dissociated into single nuclei preparations and underwent single nuclei RNA sequencing. Abbreviations: vg, vector genomes; ♂ male; ♀ female; NGS, next generation sequencing; +/+, wild-type; -/-, 21-hydroxylase deficient; snRNA Seq, single nuclei RNA sequencing.

5.2.3 Molecular studies

5.2.3.1 DNA and RNA preparation for AAV testing kit samples

5.2.3.1.1 DNA and RNA extraction

Snap frozen samples were manually homogenised in Buffer RLT Plus (AllPrep DNA/RNA Micro Kit, Qiagen, Germany) and then transferred to the QIA shredder spin column for centrifugation at 16 000 ×*g* for 2 min. The spin column was then removed, a lid was applied to the tube and centrifuged for a further 3 min at the same speed. The supernatant was transferred to an AllPrep DNA spin column and centrifuged at 8000 ×*g* for 30 seconds. The spin column contained DNA and the flow through contained RNA. The spin column was moved to a new tube and stored at 4°C until DNA purification was continued. The flow through was used for RNA purification. The purification proceeded as per the manufacturer's instructions for the AllPrep DNA/RNA Micro Kit (Qiagen).

Seven hundred and fifty nanograms of total RNA was incubated at 37°C with 2 units of TURBO DNase (Cat# AM2238; Invitrogen) for 60 min followed by incubation with the DNAse inactivation reagent for 5 min at room temperature. The mixture was centrifuged at 10,000 × *g* for 2 min and the supernatant was used as the purified RNA for cDNA synthesis.

5.2.3.1.2 cDNA synthesis

cDNA was synthesised using the SuperScript™ IV First-Strand Synthesis System (Cat# 18091050, Invitrogen) as per manufacturer instructions using a gene-specific reverse primer (WPRE-R, Table 5-2) to synthesis the AAV encoded transgene cDNA. The reactions were made up in a larger volume to allow for increased accuracy. 3 µL of the 2 µM gene-specific reverse primer WPRE-R, 3 µL of 10 mM dNTP mix and 4 µL nuclease-free water was added to 20 µL DNAse treated RNA. The RNA-primer mix was incubated

at 80°C for 1 min, 65°C for 5 min and then on ice for 1 min. From this, 10 µL was removed and added to a mixture of 3 µL water, 4 µL SuperScript IV buffer, 1 µL 100 mM DTT, 1 µL RNAseOUT Recombinant RNAse Inhibitor and 1 µL SuperScript IV reverse transcriptase (RT+). A second aliquot was added to a mixture the same as previously described but without SuperScript IV reverse transcriptase and an additional 1 µL water (RT-). Both mixtures were incubated at 53°C for 30 min and then inactivated by incubating at 80°C for 10 min.

5.2.3.2 Nucleotide barcode PCR amplification

PCR was used for nucleotide barcode amplification with genomic DNA, RT+ cDNA and RT- cDNA samples. Forward primers were barcoded to allow multiple separate PCR products to be combined into a single tube for NGS. 50 ng gDNA or 5 µL of cDNA reaction was added to 2.5 µL 10 µM barcoded forward primers, 2.5 µL 10 µM universal reverse primer (NGS-R), 10 µL Q5 reaction buffer, 1 µL dNPT 0.5 µL Q5 enzyme and made up to 50 µL volume with water. The thermocycler reaction conditions were 98°C 30 sec; 35 cycles of 98°C 10 sec, 62°C 10 sec, 72°C 10 sec; 72°C 2 min. The PCR products were run on a 2% (w/v) agarose electrophoresis gel with an expected product size of 155 bp. The PCR bands were purified using Wizard SV Gel and PCR Clean-Up System (Promega) as per manufacturer instructions. The purified PCR products were mixed in a 1.5 mL DNA LoBind Eppendorf with a maximum total DNA 1 µg and sent for NGS.

Table 5-2 Primers used for cDNA synthesis.

Primer name	Short name	Sequence 5’ to 3’	Description
Universal Reverse (NGS)_R	WPRE-R	GGATTTATACAAGGAGGAGAAAATGAAAG	WPRE gene-specific reverse primer for cDNA construction.
BC2-NGS-R	NGS-R	CAACATAGTTAAGAATACCAGTCAATCTTTCACAAATTTTGTAATCCAGAGG	Reverse barcode recovery
BC_0039_GFP_BC_01	BC_01	GTTCAGCTGGAGTTCGTGACCGCCG	Forward barcode recovery (barcoded with GTTCA)
BC_0041_GFP_BC_03	BC_03	CTGTAGCTGGAGTTCGTGACCGCCG	Forward barcode recovery (barcoded with CTGTA)
BC_0042_GFP_BC_04	BC_04	GTATTGCTGGAGTTCGTGACCGCCG	Forward barcode recovery (barcoded with GTATT)
BC_0043_GFP_BC_05	BC_05	CTAGTGCTGGAGTTCGTGACCGCCG	Forward barcode recovery (barcoded with CTAGT)
BC_0044_GFP_BC_06	BC_08	ACTGAGCTGGAGTTCGTGACCGCCG	Forward barcode recovery (barcoded with ACTGA)
BC_0045_GFP_BC_07	BC_09	TCCAAGCTGGAGTTCGTGACCGCCG	Forward barcode recovery (barcoded with TCCAA)

Forward primers for barcode recovery are barcoded themselves, to allow multiplexing Next Generation Sequencing.

5.2.4 Analysis of next generation sequencing results

The raw NGS data was prepared by Marti Cabanes-Crues from TVRU, CMRI using previously published methods.[18] The NGS reads were normalised to the final concentrations of the kit mix to create normalised entry and normalized expression indices. As there were 67 unique capsid barcodes in this kit, each barcode should make up 1.47% of the NGS reads in the kit prior to injection. Although the kit was mixed stoichiometrically, a normalisation step was taken to account for any variation in concentration of the original kit by using these calculations to rank the entry and expression:

$$\text{Entry index} = \frac{\%\text{ of NGS reads for given capsid in mouse gDNA}}{\%\text{ of NGS reads for given capsid in kit pre-injection}}$$

$$\text{Normalised expression} = \frac{\%\text{ of NGS reads for given capsid in mouse cDNA}}{\%\text{ of NGS reads for given capsid in kit pre-injection}}$$

5.2.5 Single nuclei dissociation

Snap frozen adrenal glands were dissociated into single nuclei preparations and the 10X Single Nuclei Sequencing samples were processed by Hilary Knowles (Embryology Unit, CMRI). Glands were cut into smaller pieces on dry ice to allow buffer to contact tissue internal to the capsule. Nuclear lysis buffer (10mM Tris-HCl, 10mM NaCl, 3mM MgCl2, 0.1% (v/v) IGFEPAL® CA-630 [I8896, Sigma-Aldrich]) was added and the tissue further minced. The samples were then incubated on ice for 10 min with frequent mixing by pipette. The sample was passed through a 70 µM filter and spun at low speed (500 × g) for 10 min at 4°C. The supernatant was discarded, and pellets resuspended in fresh nuclear lysis buffer. The samples were spun at 500 × g for 5 min at 4 °C and the process of removing the supernatant and resuspending the pellet in lysis buffer was repeated for a

total of 3 runs. The final spun sample was then resuspended in 0.4% (v/v) bovine foetal serum and passed through a 35 µM flow cytometry filter. Sample concentrations were adjusted to obtain an output of 10,000 nuclei/sample. Single nuclei droplet capture was obtained using the 10X Chromium Controller. Sample and library preparation was performed as specified in the Chromium Next GEM Single Cell 3′ Reagent Kits v3.1 (Dual Index) protocol (CG000315 Rev D).

5.2.6 Bioinformatic analysis

The scRNA-Seq library was prepared using 10x Chromium technology and sequenced on the Illumina NovaSeq platform. The transcriptome was mapped to the mouse mm10 reference genome using the *CellRanger* pipeline, followed by scRNA-Seq analysis using the *Seurat v4.0* package. Cell types were annotated using a combination of the Clustifyr package and manual annotation using gene expression patterns. Manual annotation was performed by the candidate, the previous bioinformatic pathway steps were performed by Nader Aryamanesh (Bioinformatics Facility, CMRI). The genes used for manual annotation are listed (Table 5-3). Adrenocortical progenitor cells were defined as co-expression of *Nr5a1* (encodes SF1 protein), *Shh* and *Ctnnb1* without expression of *Cyp11b1* or *Cyp11b2* (markers of differentiated adrenocortical cells).[8-10]

Table 5-3 Genes interrogated for manual annotation of clusters.

Gene	Tissue associated
Abcb1b	zFasc
Adh1	zFasc
Agtr1a	zGlom
Agtr1b	zGlom
Agtr2	zGlom
Akr1b7	zFasc
Akr1cl	zFasc

Akr1c18	X-zone
Btg2	zFasc
Cd300a	Macrophages
Chga	Medulla
Chgb	Medulla
Chrm1	Medulla
Chrm3	Muscarinic receptor
Chrna3	Medulla
Chrnb4	Medulla
Col1a1	Connective tissue
Cyp11a1	Steroidogenic cells
Cyp11b1	zFasc and tZone
Cyp11b2	zGlom and tZone
Cyp21a1	zGlom, tZone and zFasc
Dab2	zGlom
Dach1	zGlom
Dbh	Medulla
Gadd45g	zFasc
Gli1	capsular stem cells
Hmgb3	zGlom
Igfbp7	zFasc
Ighm	B cells/immune
Kdr	Endothelial
Mc2r	zFasc (and zGlom to lesser extent)
Me1	zFasc
Mgarp	Adrenocortical
Npy	Medulla
Nr5a1	Steroidogenic cells and progenitor cells
Pecam1	Endothelial
Pik3c2g	X-zone
Pnmt	Medulla
Ptprc	Immune
Rspo3	Adrenal capsule
S100b	Glial
Sox10	Glial
Sparcl1	Capsule
Srd5a2	zFasc
Star	Steroidogenic cells
Tek	Endothelial
Th	Medulla
Tie1	Endothelial

5.3 Results

5.3.1 rAAV capsid tropism for the adrenal gland

5.3.1.1 The AAV testing kit delivered GFP expression to the adrenal cortex

Two weeks after intravenous administration of the AAV Testing Kit containing 67 capsid serotypes, adrenal glands were harvested. Immunofluorescence of the gland revealed expression of the GFP transgene throughout the adrenal cortex, predominantly in the zona fasciculata (Figure 5-3).

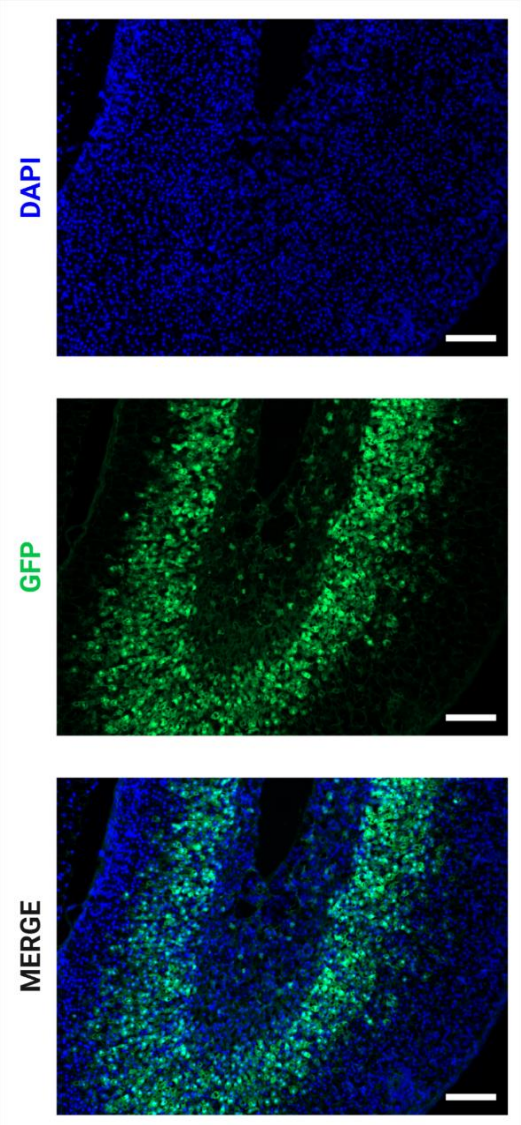

Figure 5-3 Demonstration of vector in adrenal gland.
Immunohistochemically stained adrenal gland from the female mouse treated with the AAV testing kit, demonstrating GFP expression (green). Scale bar represents 100 µm.

5.3.1.2 Identification of AAV capsids capable of physical transduction (cell entry) of the adrenal gland

The presence of vector genomes in DNA extracted from tissue 2 weeks after treatment is consistent with entry of the vector into the cell, but not necessarily whether it is then able to express its genetic cargo. Cellular entry (physical transduction) was determined by normalising the percentage of barcode reads on a genomic DNA sample to the expected percentage from the pre-injection kit concentration for that capsid serotype, as per the previously published methodology[18] (Figure 5-4). High entry efficiency in the female mouse did not necessarily mean high entry efficiency in the male mouse (e.g. NP22) and vice versa (e.g. AAV8). Some capsids had relatively similar entry in both the male and female mice (e.g. AAV10, Rh10).

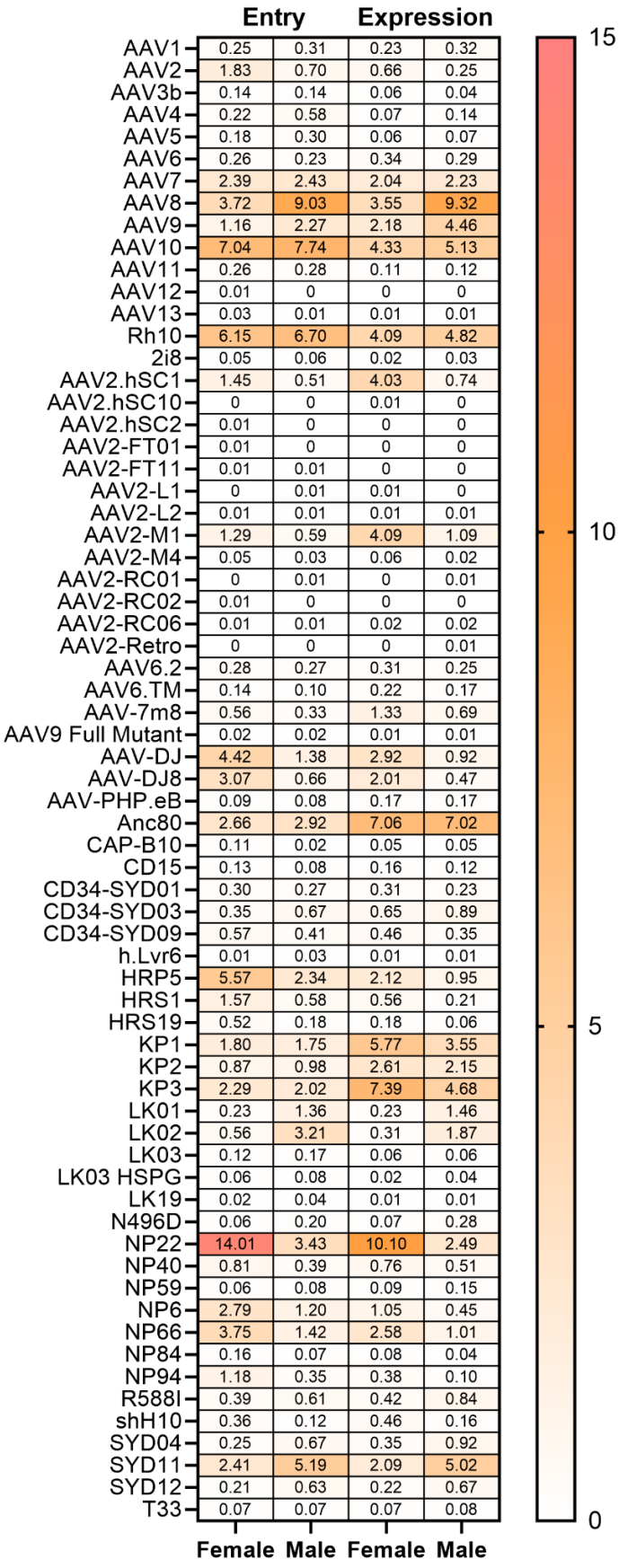

Figure 5-4 AAV Testing kit entry and expression.

Heat map showing entry index (physical transduction) and normalised expression (functional transduction) for 67 capsid serotypes in murine adrenal glands.

5.3.1.3 Identification of capsids capable of functional transduction (expression) of the adrenal gland

Through reverse transcription, cDNA was synthesised from adrenal gland RNA. Next generation sequencing of the resultant cDNA revealed the percentage of each capsid serotype present, and this was normalised against the percentage of each serotype in the injected kit to create the "normalised expression" value. The serotypes that conferred enriched expression of the transgene were those with a normalised expression value >1 (Figure 5-5). Serotype Rh10 has been used in most pre-clinical gene delivery studies in the mouse for adrenal targeting and is known to transduce the adrenal zona fasciculata[2] but there were multiple capsid serotypes detected with greater expression efficiency in the murine adrenal gland, including NP22, KP3, Anc80, and KP1 in the female and AAV8, Anc80 and AAV10 in the male. The 7 capsids with the highest expression overall were selected for individual analysis. AAV8, AAV10 and Rh10 are natural serotypes, KP1, KP3 and NP22 are engineered capsids and Anc80 is an *in silico* reconstructed ancestral capsid. AAV9 and SYD11 were not chosen for individual analysis as although they had high expression in the male, the expression in females was not as high. Similarly, for AAV2.hSC1 and AAV2-M1 expression was high in females but not in males so they were not chosen for downstream experiments.

Overall, the serotype with the highest median normalised expression was Anc80, although the replicates in the male were discrepant with one replicate 3.92 and one 10.12 (compared with the female replicates of 7.01 and 7.10). The serotype with the second highest overall median was NP22, but this capsid performed much better in the female samples than the male. KP3 performed similarly to NP22, however the performance in the female versus male was more closely matched in KP3 than in NP22. The replicates in the male for AAV8 skewed the results as one replicate had a normalised expression index

of 15.54 and one was 3.09, the latter of which more closely matched the performance in the female.

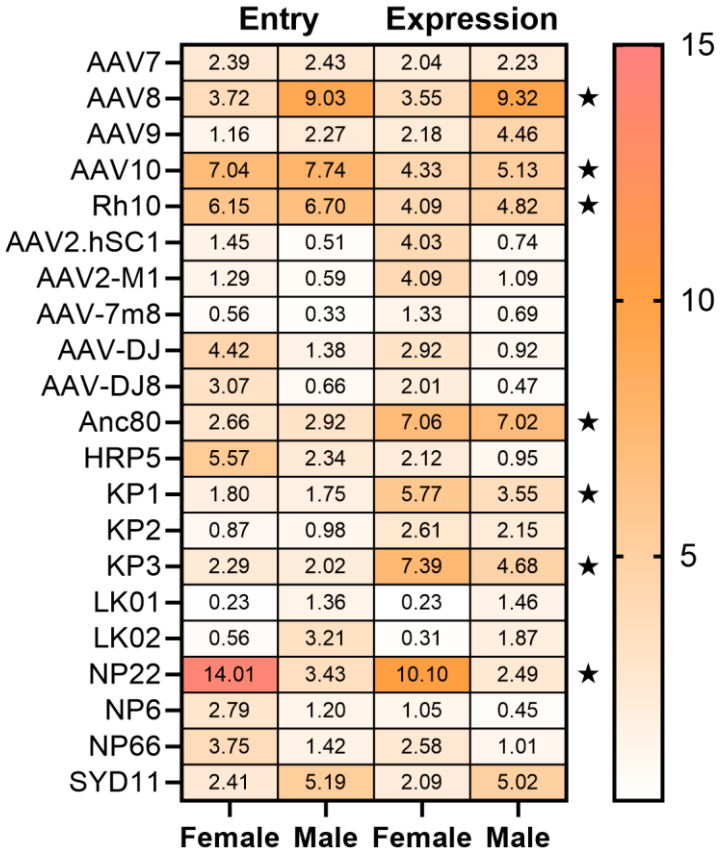

Figure 5-5 Entry index and normalised expression in the serotypes enriched for expression.
AAV capsid serotypes with a normalised expression index of >1 for male and/or female samples. The top 7 are highlighted (★).

5.3.1.4 Evaluation of the seven rAAV capsid serotypes with greatest transgene expression

The functional transduction performance by GFP expression was examined individually for the top 7 serotypes: AAV8, AAV10, Rh10, KP1, KP3, NP22 and Anc80 packaged a GFP expression cassette (Figure 5-1) and were each delivered to one male and one female mouse for a total of 14 mice. The mice were harvested 1 week later. The natural serotypes AAV8, AAV10 and Rh10 performed similarly with transduction of the zona fasciculata

but minimal transduction of the zona glomerulosa (Figure 5-6). The bioengineered serotypes showed some evidence of transduction of cells in the zona glomerulosa, with KP3 in the female mouse showing the most evidence of zona glomerulosa transduction (Figure 5-7). Anc80 had minimal transduction of the zona glomerulosa, but strong expression in the zona fasciculata (Figure 5-8). Generally, AAV appears to preferentially transduce the zona fasciculata over the capsule and zona glomerulosa. Many of the capsid serotypes appear to have performed better in females than males (particularly the bioengineered and reconstructed ancestral capsids), however females have a larger zona fasciculata than males, which may be skewing the transduction appearance, as there is more cell mass available in the females.

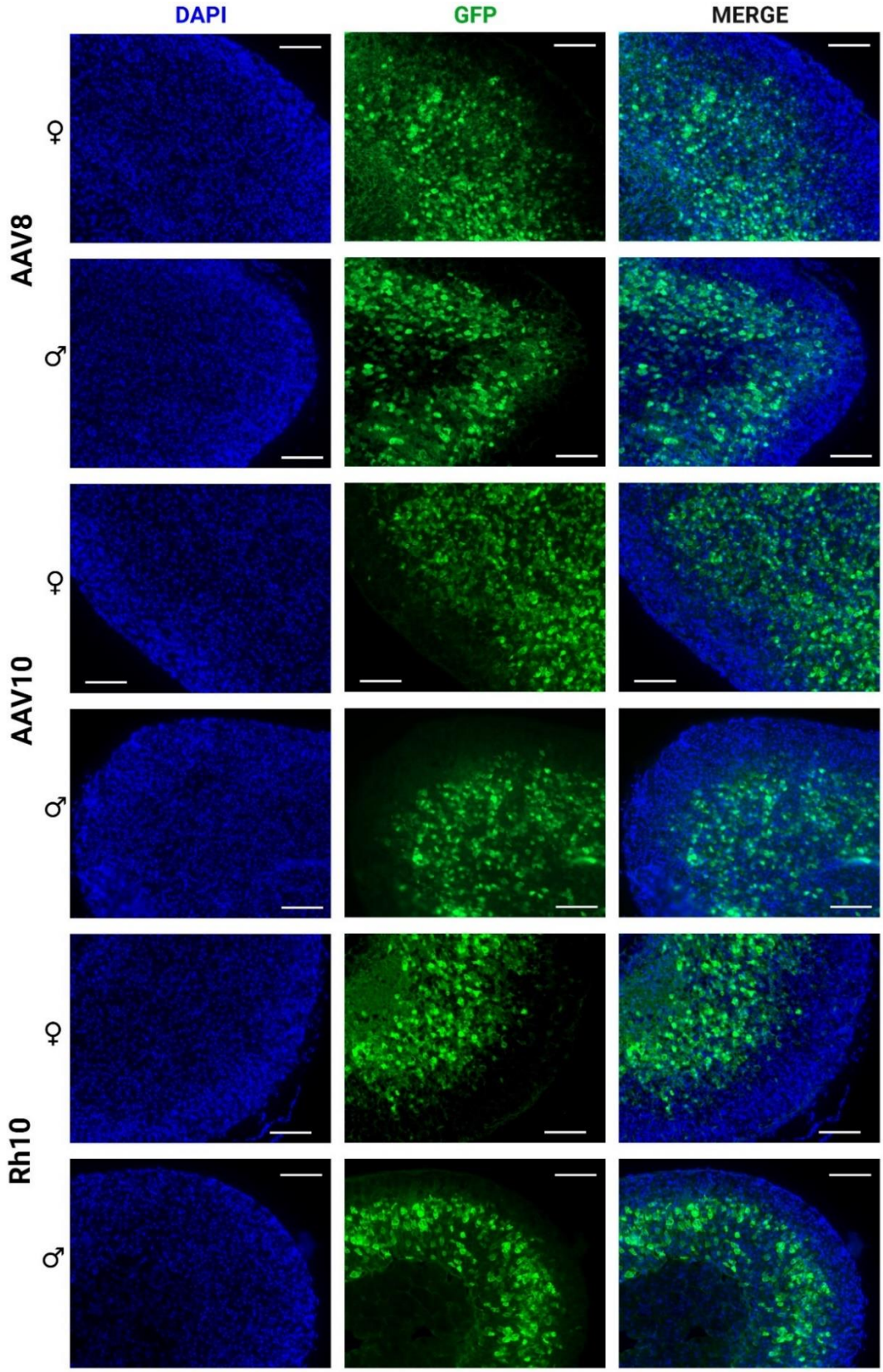

Figure 5-6 Natural serotypes with the highest functional transduction of the adrenal cortex.

Immunohistochemistry staining demonstrated GFP expression (green) in the adrenal cortex delivered by AAV8, AAV10 or Rh10. ♂, male; ♀, female. Scale bar represents 100 μm.

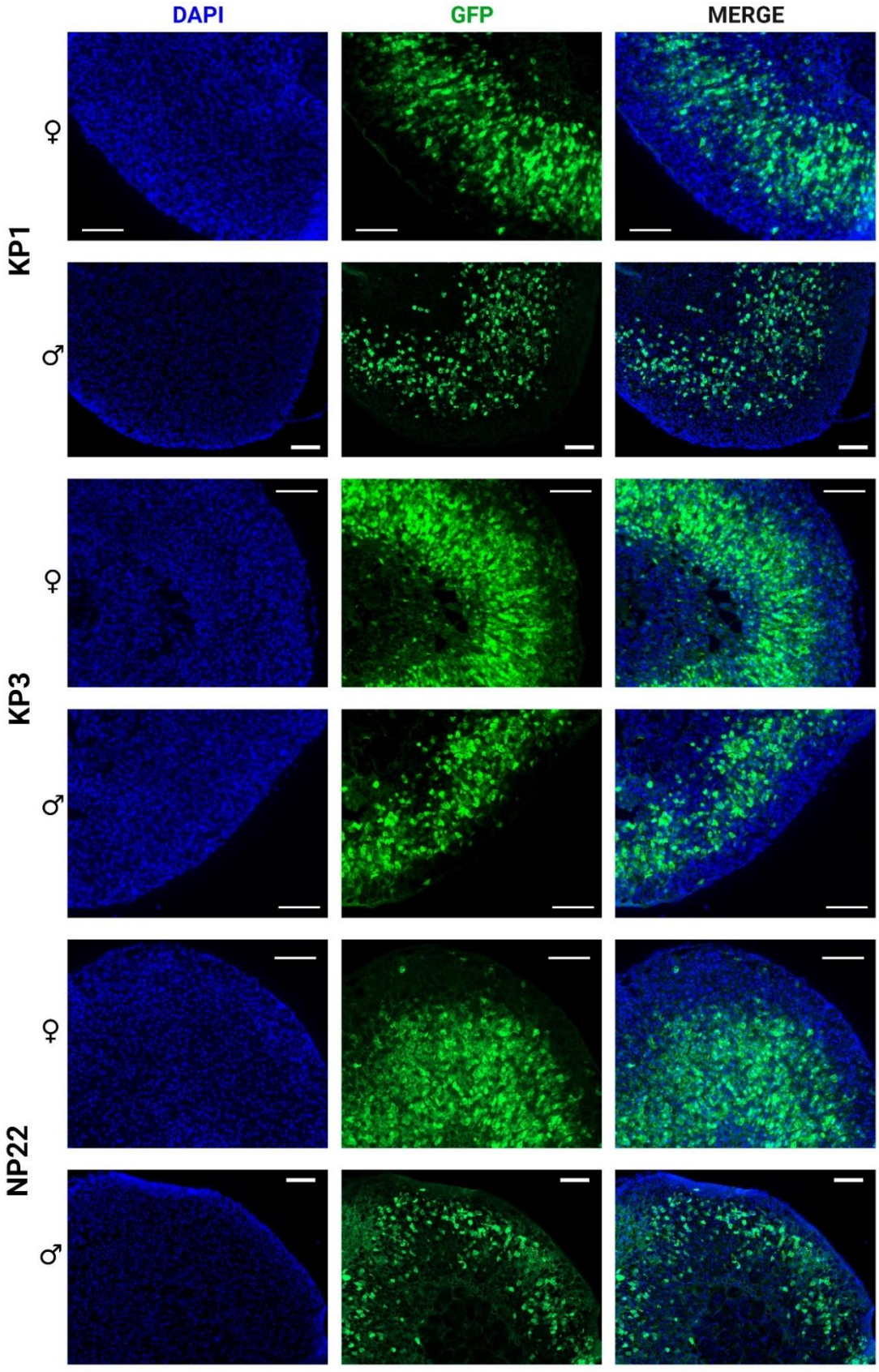

Figure 5-7 Engineered capsids with the highest functional transduction of the adrenal cortex.

Immunohistochemistry staining demonstrated GFP expression (green) in the adrenal cortex delivered by KP1, KP3 or NP22. ♂, male; ♀, female. Scale bar represents 100 μm.

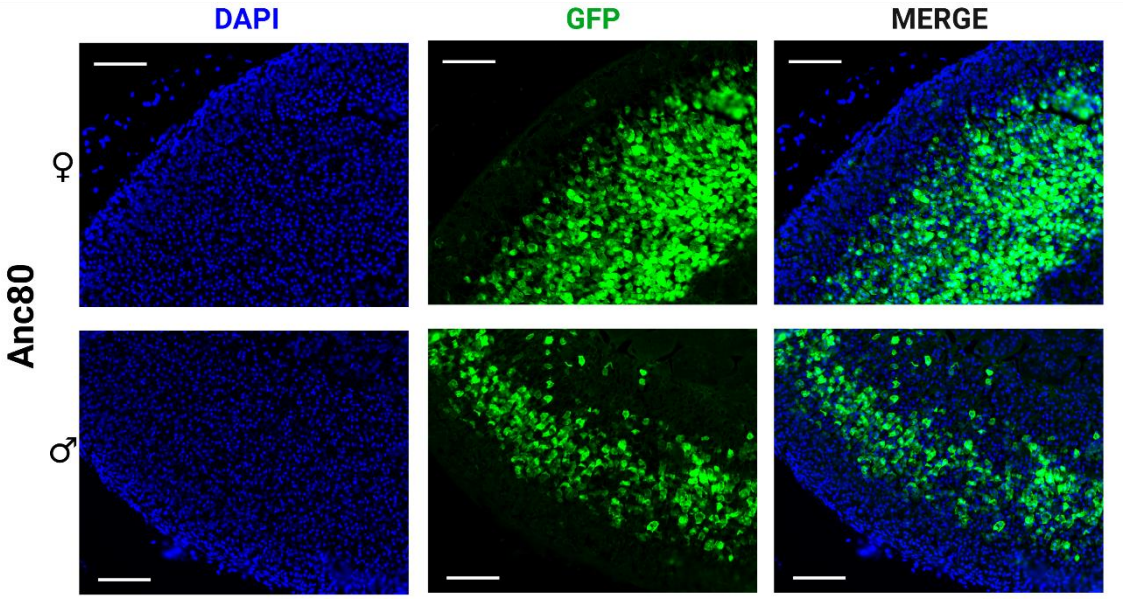

Figure 5-8 Reconstructed ancestral capsid with the efficient functional transduction of the adrenal cortex.
Immunohistochemistry staining demonstrated GFP expression (green) in the adrenal cortex delivered by Anc80. ♂, male; ♀, female. Scale bar represents 100 μm.

Using the pattern analysis tool Xover 3.0 [http://qpmf.rx.umaryland.edu/xover.html],[51] the bioengineered sequences were aligned against AAV1 to AAV12 and Rh10 (Figure 5-9). There were no apparent commonalities identified when the bioengineered sequences were aligned against the parent sequences. Nor were the bioengineered sequences similar to the same parent sequence: KP1 and KP3 were closest to parent sequences AAV3, NP22 was closest to AAV2 and Anc80 was closest to Rh10 (Figure 5-10).

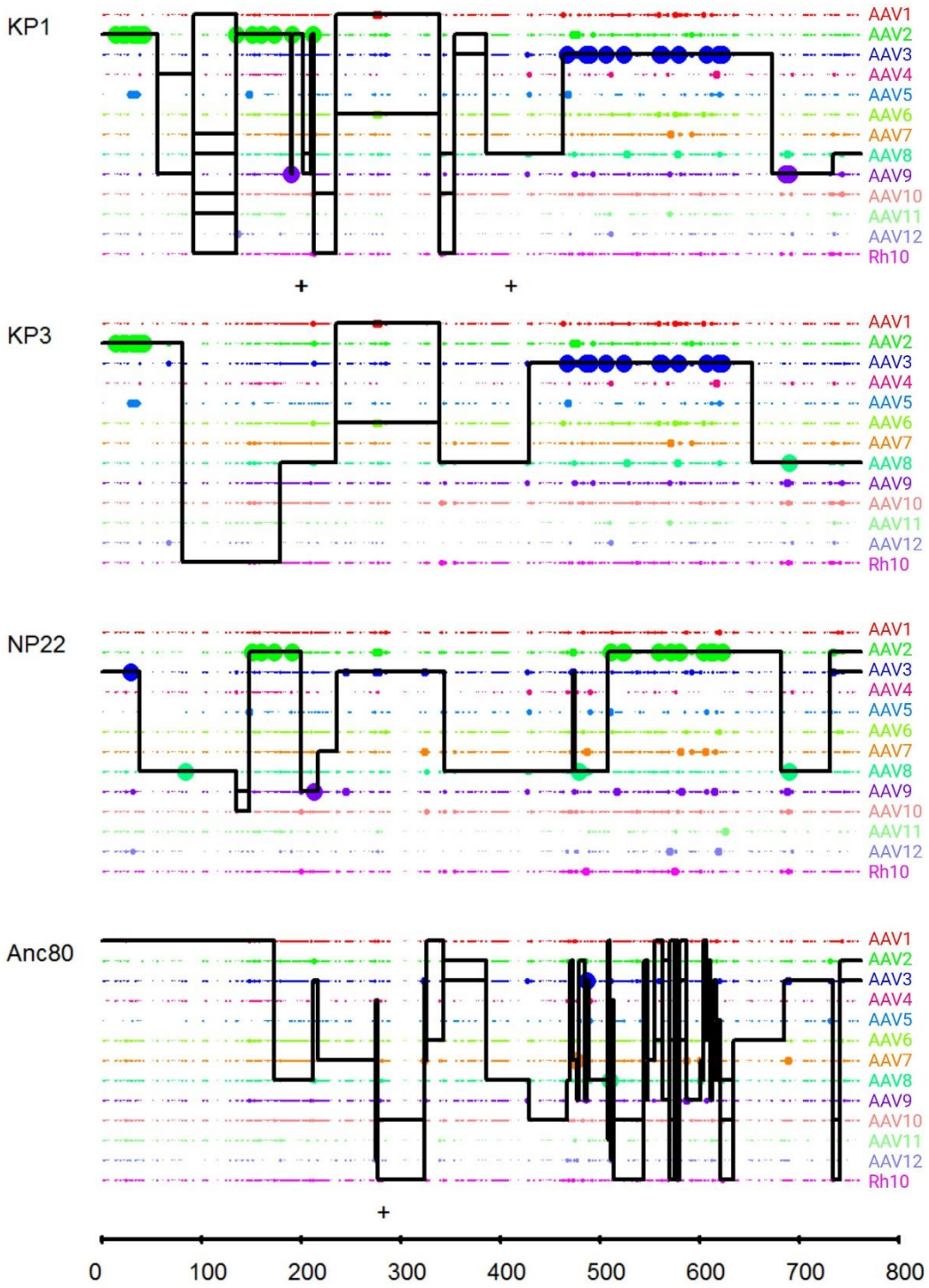

Figure 5-9 Bioengineered capsid amino acid aligned with parental sequences.
The amino acid sequences for the top bioengineered capsids (KP1, KP3, NP22 and Anc80) were compared against parental sequences AAV1-12 and Rh10. Large dots represent 100% parental match (i.e. the position in question matches only one parent) and small dots represent more than one parental match (i.e. the position matches more than one parent) at each position. The solid line for each chimera represents the library parents identified within the sequence between crossovers. A set of thin horizontal parallel lines between crossovers indicates multiple parents match at an equal probability. A mutation is recorded as a plus sign when a position of a chimera does not match the corresponding position in any parental sequence.

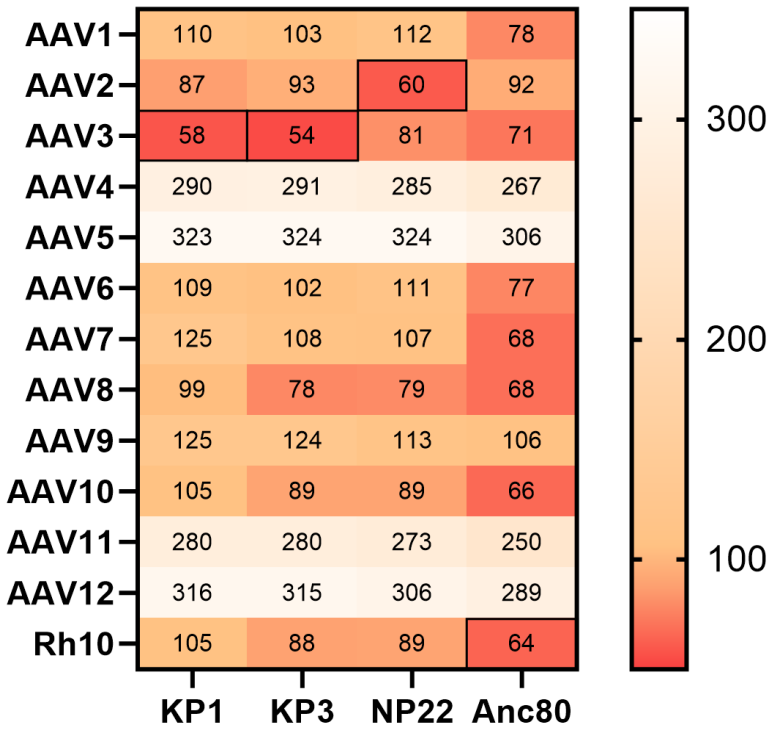

Figure 5-10 Measurement of Levenshtein Distance and Effective Mutation.
Levenshtein distance measures sequence difference between mutants and parents, i.e. minimum point mutations required to convert a parent into a mutant. It indicates the closeness between mutants and parents. Effective mutation (boxed value) is the minimum point mutations required to back-mutate a mutant to its closest parent, i.e. the shortest Levenshtein distance to parents. It indicates the closest parent and the actual diversity introduced.

Using Molecular Evolutionary Genetics Analysis version 11 (MEGA11) software [https://www.megasoftware.net/][52] a phylogeny tree was constructed using the maximum likelihood method, and included parental sequences AAV1-12, and the engineered capsid sequences KP1, KP3, NP22 and Anc80 (Figure 5-11).[53] There was a close evolutionary relationship between KP3, AAV8, AAV10 and Rh10. Anc80 was closer to KP1 than any other engineered capsid.

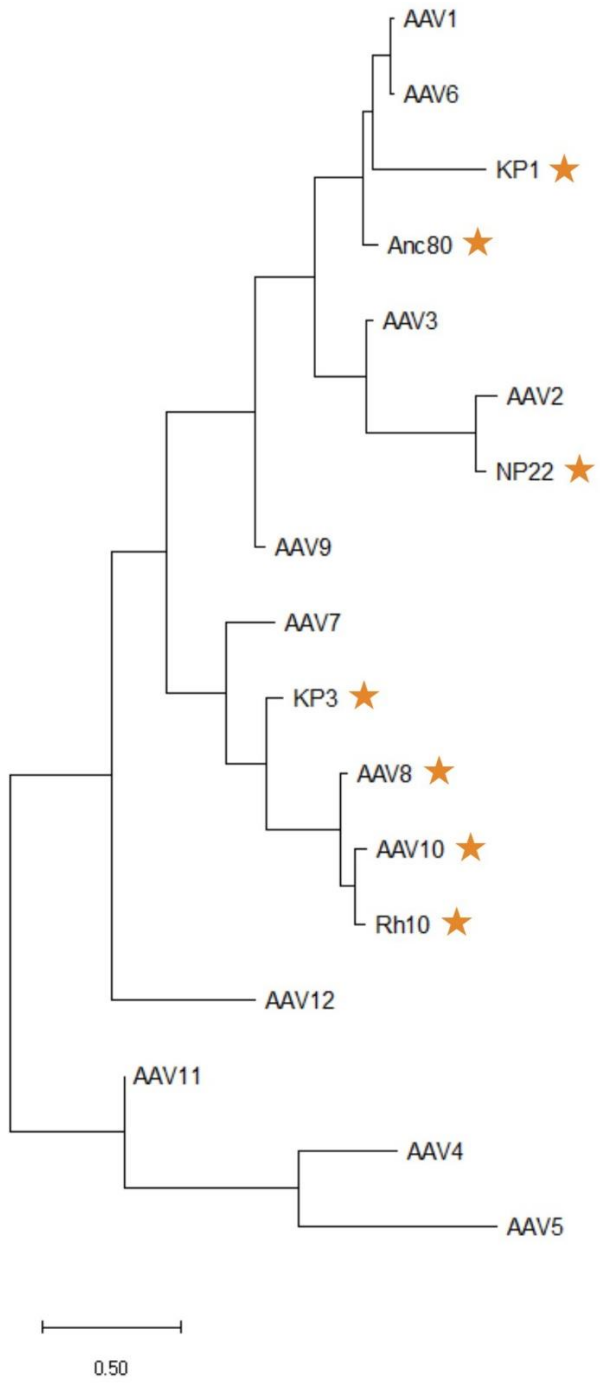

Figure 5-11 Evolutionary analysis of AAV1-12, Rh10, KP1, KP3, Anc80 and NP22 by Maximum Likelihood method.

The evolutionary history was inferred by using the Maximum Likelihood method and Tamura-Nei model.[53] The tree with the highest log likelihood (-33639.37) is shown. Initial tree(s) for the heuristic search were obtained automatically by applying Neighbor-Join and BioNJ algorithms to a matrix of pairwise distances estimated using the Tamura-Nei model, and then selecting the topology with superior log likelihood value. The tree is drawn to scale, with branch lengths measured in the number of substitutions per site. This analysis involved 17 nucleotide sequences. Codon positions included were 1^{st} + 2^{nd} + 3^{rd} + Noncoding. There were a total of 2229 positions in the final dataset. Evolutionary analyses were conducted in MEGA11.[52] The AAV serotypes with the most efficient functional transduction are highlighted (★).

5.3.2 Analysis of the murine adrenal transcriptome

5.3.2.1 Wild-type murine adrenal gland transcriptome

Determining capsid tropism to the murine adrenal gland *en bloc* is the first step to improve adrenal transduction with gene therapy, however, a method to identify the adrenocortical progenitors is required. Therefore, single nuclei RNA sequencing (snRNA Seq) was used to determine whether this cell population could be identified. The transcriptome was analysed for 4153 and 4141 individual cell nuclei in the wild-type female and male samples, respectively. The snRNA Seq clustering pattern revealed 16 unique clusters by the Clustifyr package, two of which were subsequently manually divided (clusters 8 and 13) (Table 5-4, Figure 5-12). Adrenocortical cells made up 56% (n=2313) and 58% (n=2399) of cells in the female and male samples, respectively. There were 3 zona glomerulosa and 4 zona fasciculata clusters, and one that had gene markers from both zones which was considered transitional. Cluster 8 was difficult to identify, as it expressed genes consistent with both endothelial cells and adrenocortical cells, which are not expected to originate from the same cell lineage.

Table 5-4 Wild-type transcriptome cluster annotation.

Cluster number	Annotation
0	zGlom2_0
1	zFasc2_1
2	zTran_2
3	zFasc3_3
4	Endothelial_4
5	zGlom1_5
6	Endothelial_6
7	Medulla_7
8	Endothelial_8 zFasc4_8 Unknown_8
9	Medulla_9
10	Medulla_10
11	Medulla_11
12	Macrophage_12
13	zFasc1_13a zGlom3_13b
14	Capsule_14
15	Glial_15

The Clustifyr package divided the cells into 16 clusters (clusters 0-15), two of which were manually split further (cluster 8 and 13).

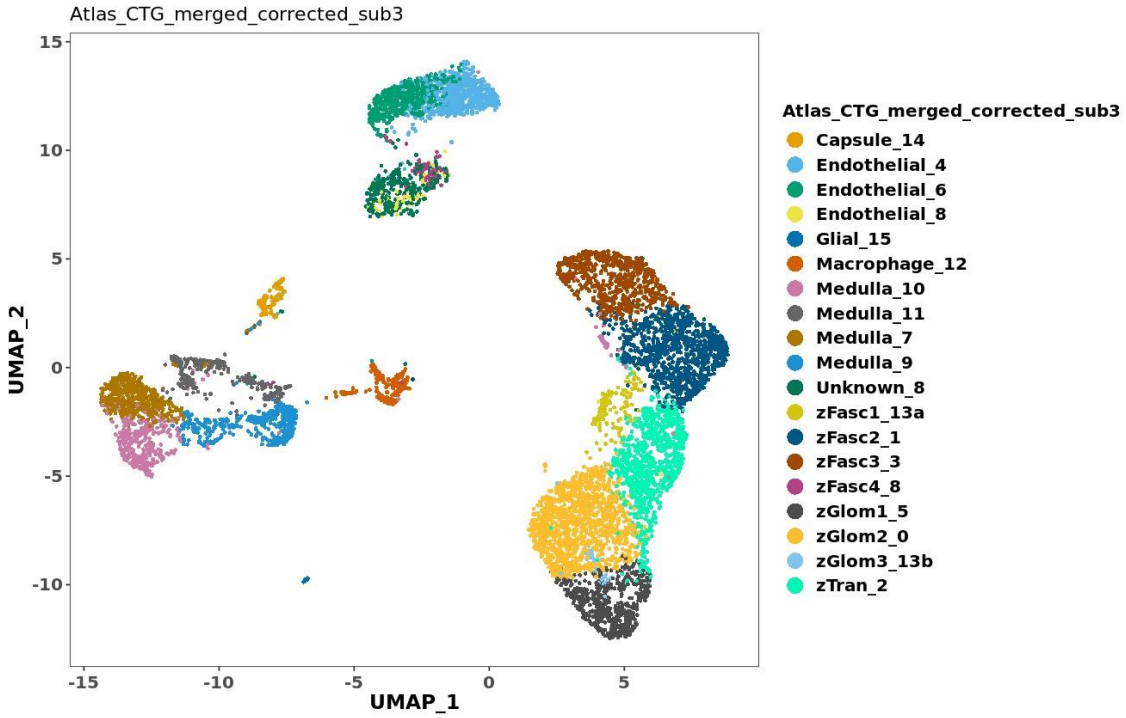

Figure 5-12 Wild-type adrenal gland nuclei transcriptome UMAP.
Using the Seurat package, 16 distinct cellular clusters were determined when the wild-type male and female single nuclei transcriptomic data was combined. The Uniform Manifold Approximation and Projection (UMAP) non-linear dimensional reduction technique with annotated clusters is shown. Clusters 0 and 5 were zona glomerulosa cells (zG), clusters 1, 3 and 13 were zona fasciculata (zF) cells and cluster 2 was a mixture of zG and zF cells, likely making up a transitional zone.

Heat maps were made for all genes listed (Table 5-3), and an example is provided for two genes expressed primarily in the zona glomerulosa, *Agtr1b* and *Cyp11b2* (Figure 5-13). Additional representative genes are provided for the zona fasciculata, steroidogenic cells, endothelial cells, immune cells and the adrenal medulla (Figures S5-22 to S5-25) but the complete gene list is not included. Due to the analytical need to start with one sample and compare it to the other, the heatmaps were made based on the female analysis, and the male heatmaps have 0 as slightly red. Therefore, genes with low expression in the male are shown in light red, rather than grey. Endothelial cells express *Chrm3* and *Pecam1* and were used to distinguish the sub-clusters of cluster 8 (Figure S5-24).

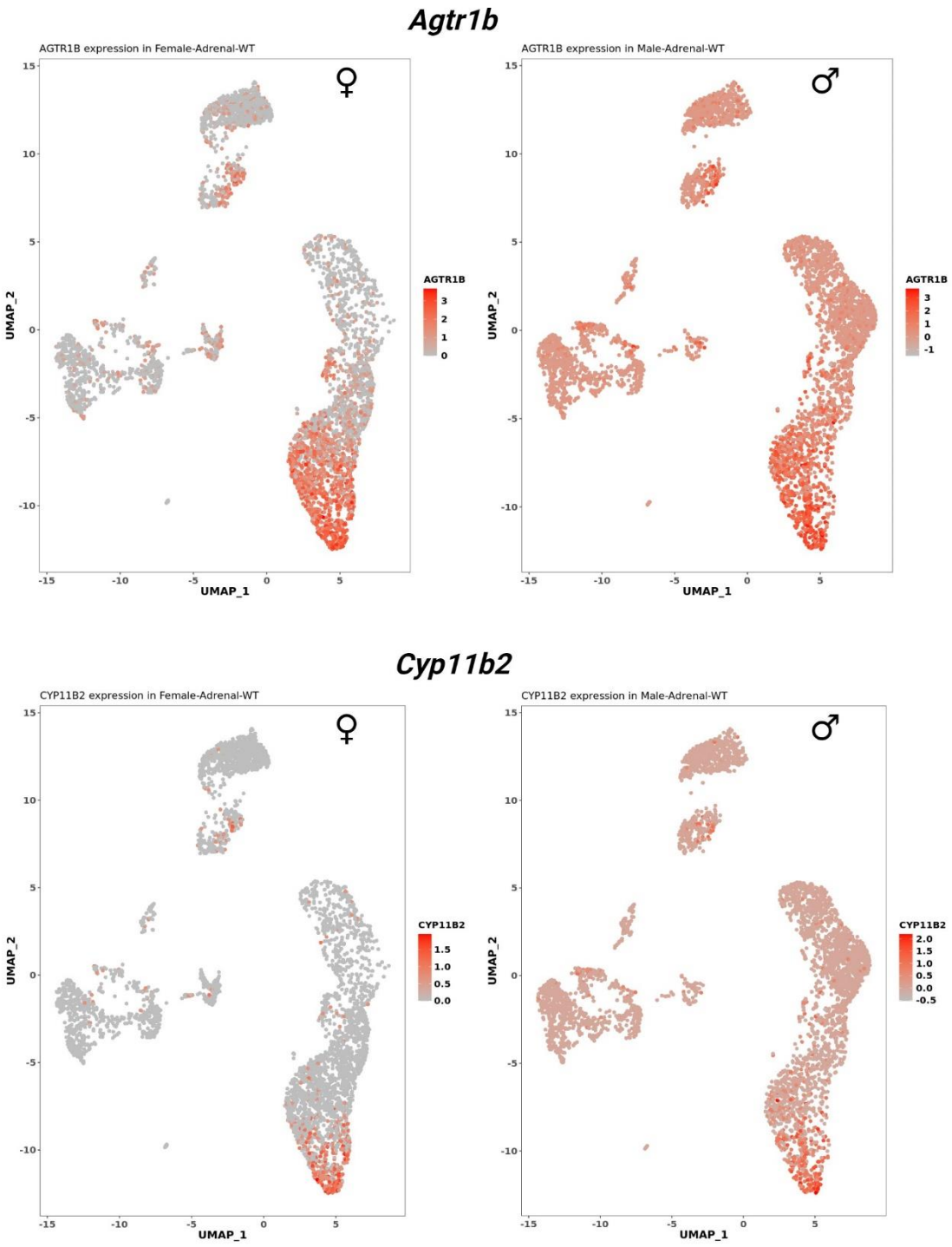

Figure 5-13 Selected genes highly expressed in by cells in the zona glomerulosa. Note 0 on the heat map for the male samples is not grey.

5.3.2.1.1 Identification of adrenocortical Shh+ progenitor cells

Adrenocortical progenitor cells were defined by their expression pattern. The progenitor population did not form a distinct cluster. However, cells co-expressing *Nr5a1* (encodes SF1 protein), *Shh* and *Ctnnb1* that did not express *Cyp11b2* or *Cyp11b1* (markers of differentiated adrenocortical cells from the zona glomerulosa and zona fasciculata, respectively) were detected with most located in cluster 0 (zona glomerulosa), consistent with SF1+/SHH+ progenitors (Figure 5-14). There were 14 cells with this transcriptomic pattern detected in the female adrenals (of 4153 total cells) and 9 cells in the male (of 4141 total cells). Other genes that were highly expressed by these possible adrenocortical progenitor cells included *Bcat1* (essential for cell growth), *Bicc1* (regulation of gene expression during cell differentiation), *Daam2* (nervous system development and regulation of Wnt signalling), *Dzip3* (developmental gene regulation), and *Ly6d* (B-cell progenitor differentiation) (Figure 5-15). Other genes that were expressed by the possible progenitor cells are shown (Table 5-5).

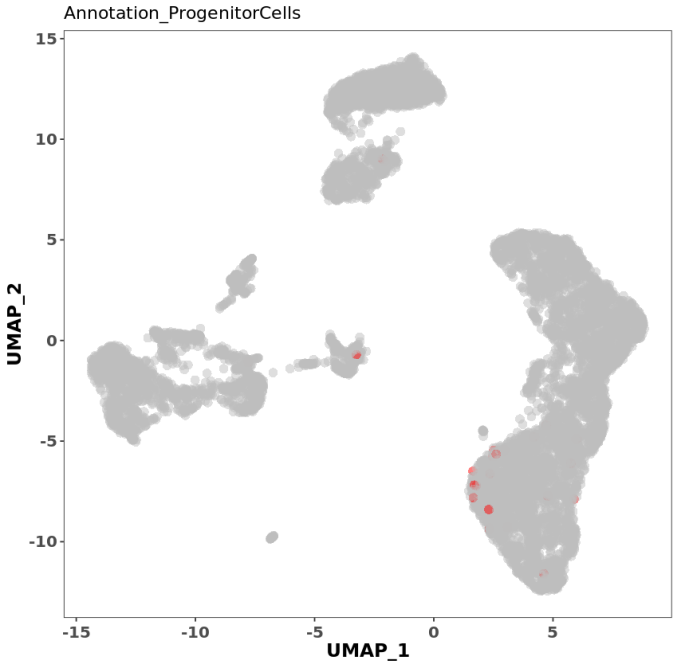

Figure 5-14 Potential progenitor cells (UMAP).

Cells that expressed *Nr5a1* (encodes SF1 protein), *Shh* and *Ctnnb1* that did not express *Cyp11b1* or *Cyp11b2* were detected. This transcriptomic pattern is consistent with adrenocortical progenitor cells. Each cell in the analysis is represented as a single dot and this dataset represents male and female cells combined. This figure is a true/false UMAP where cells that do not meet the expression pattern criteria are represented in grey (False) and cells that do meet the expression pattern criteria for progenitor cells are represented in red (True).

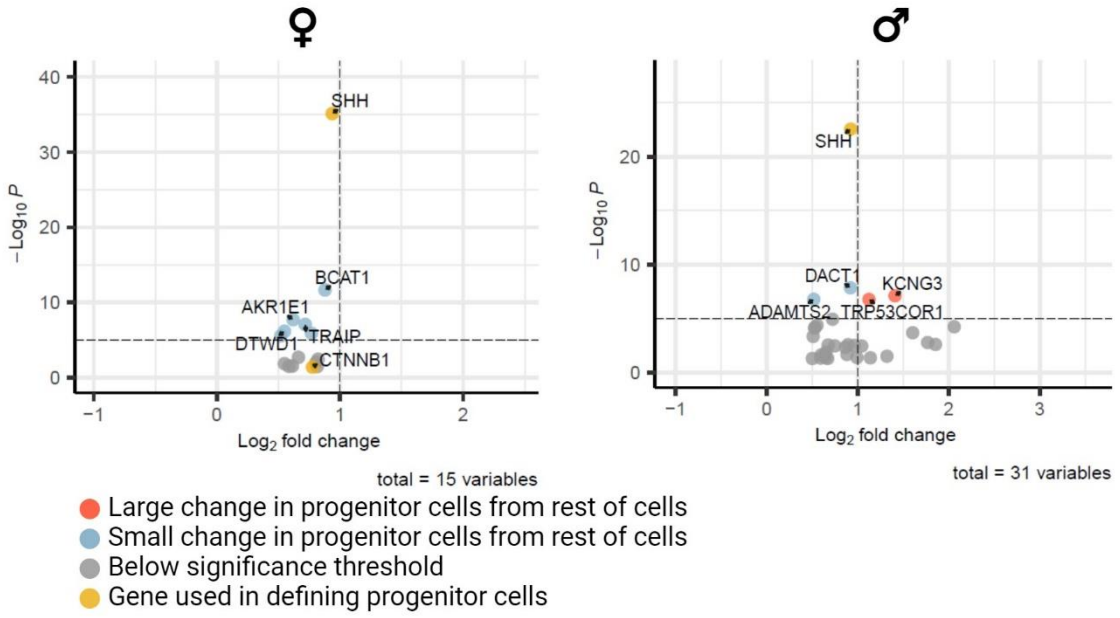

Figure 5-15 Volcano plots comparing gene expression in progenitor cells to other cells.

Genes that are more highly expressed in progenitor cells compared with the rest of the cells in the analysis are on the right of the 0 point on the *x* axis of the plots. Volcano plots were prepared by Eva van Dijk, GTRU, CMRI.

Table 5-5 Gene expression in progenitor cells.

Female	Male
Shh	*6330411d24rik*
Bcat1	*Daam2*
Utp11	*Fat3*
6030469f06rik	*Col23a1*
Dzip3	*Kcng3*
Ctnnb1	*Skap1*
Gars	*Bicc1*
Traip	*Trp53cor1*
Sptb	*Lancl3*
Akr1e1	*Ly6d*
Hsd3b6	*Elovl7*
Itga3	*Shh*
Fgd1	*Dact1*
Dtwd1	*6030469f06rik*
Mrpl13	*Mybpc1*
	C77080
	Dyrk1b
	Pygm
	Tcp11l2
	Sorcs2
	Slc25a43
	Sphk2
	Lrrc55
	Bnip3
	Sigmar1
	9330111n05rik
	Gm26559
	Camkv
	Adamts2
	Gm42567
	Msto1

Genes expressed more highly by cells that met definition for progenitor cells than the rest of the cell population of the wild-type samples.

5.3.2.2 Analysis of the wild-type and 21-hydroxylase deficient transcriptomes

The transcriptome was analysed for 10 451 and 10 017 individual cell nuclei in the *Cyp21a1*-/- female and male samples, respectively, and clustered with the wild-type cells in Section 5.3.2.1. This revealed 22 unique clusters using the Clustifyr package (Table 5-6 and Figures 5-16, 5-17). Cluster 8, that was difficult to annotate in the wild-type only analysis, contributed to endothelial (cluster 5), macrophage (9), zona fasciculata (11), capsule (14, 16) and adipocyte (20) clusters in the combined analysis. No progenitor cells were identified in the *Cyp21a1*-/- samples. Cells identified as belonging to the X-zone were identified in this analysis (zX_3_21) and were more prominent in the mutant samples (Figure 5-17).

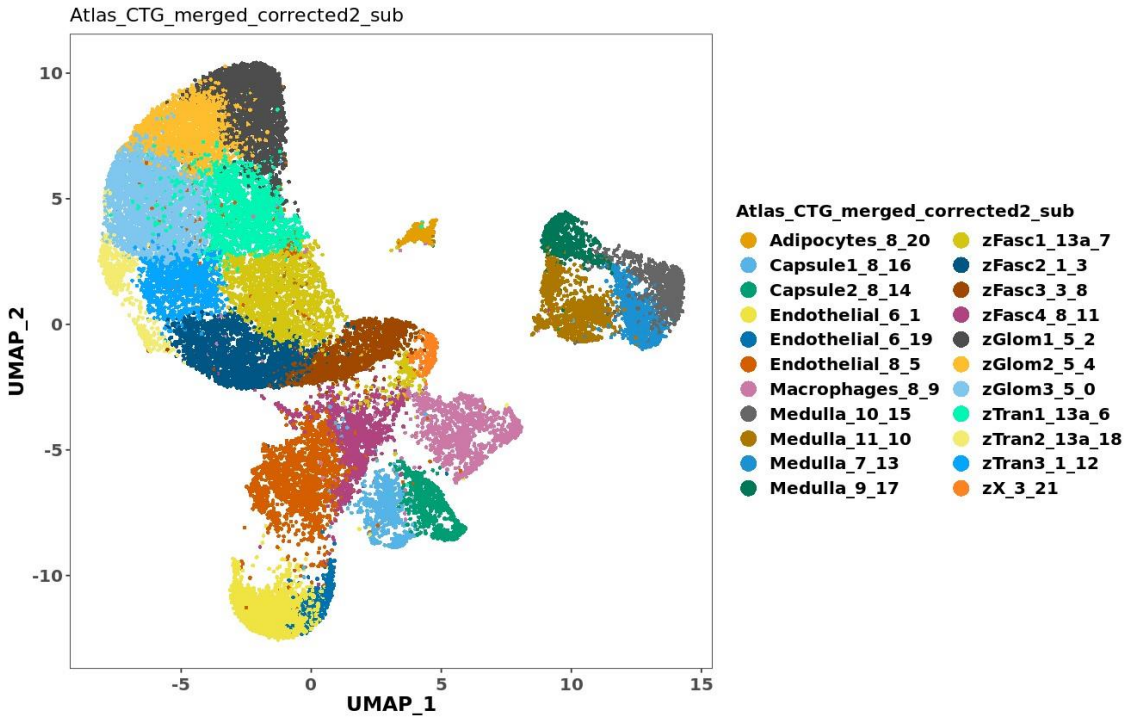

Figure 5-16 Wild-type and homozygous clusters (UMAP).
The Clustifyr package divided the combined wild-type and mutant transcriptome cells into 22 clusters (clusters 0-21).

Table 5-6 Cluster annotations in wild-type and mutant transcriptome.

Cluster number	Annotation
0	zGlom3_5_0
1	Endothelial_6_1
2	zGlom1_5_2
3	zFasc2_1_3
4	zGlom2_5_4
5	Endothelial_8_5
6	zTran1_13a_6
7	zFasc1_13a_7
8	zFasc3_3_8
9	Macrophages_8_9
10	Medulla_11_10
11	zFasc4_8_11
12	zTran3_1_12
13	Medulla_7_13
14	Capsule2_8_14
15	Medulla_10_15
16	Capsule1_8_16
17	Medulla_9_17
18	zTran2_13a_18
19	Endothelial_6_19
20	Adipocytes_8_20
21	zX_3_21

The Clustifyr package divided the combined wild-type and mutant transcriptome cells into 22 clusters (clusters 0-21). The last number refers to the cluster from this analysis, the second last number refers to the cluster the package allocated from the wild-type only analysis.

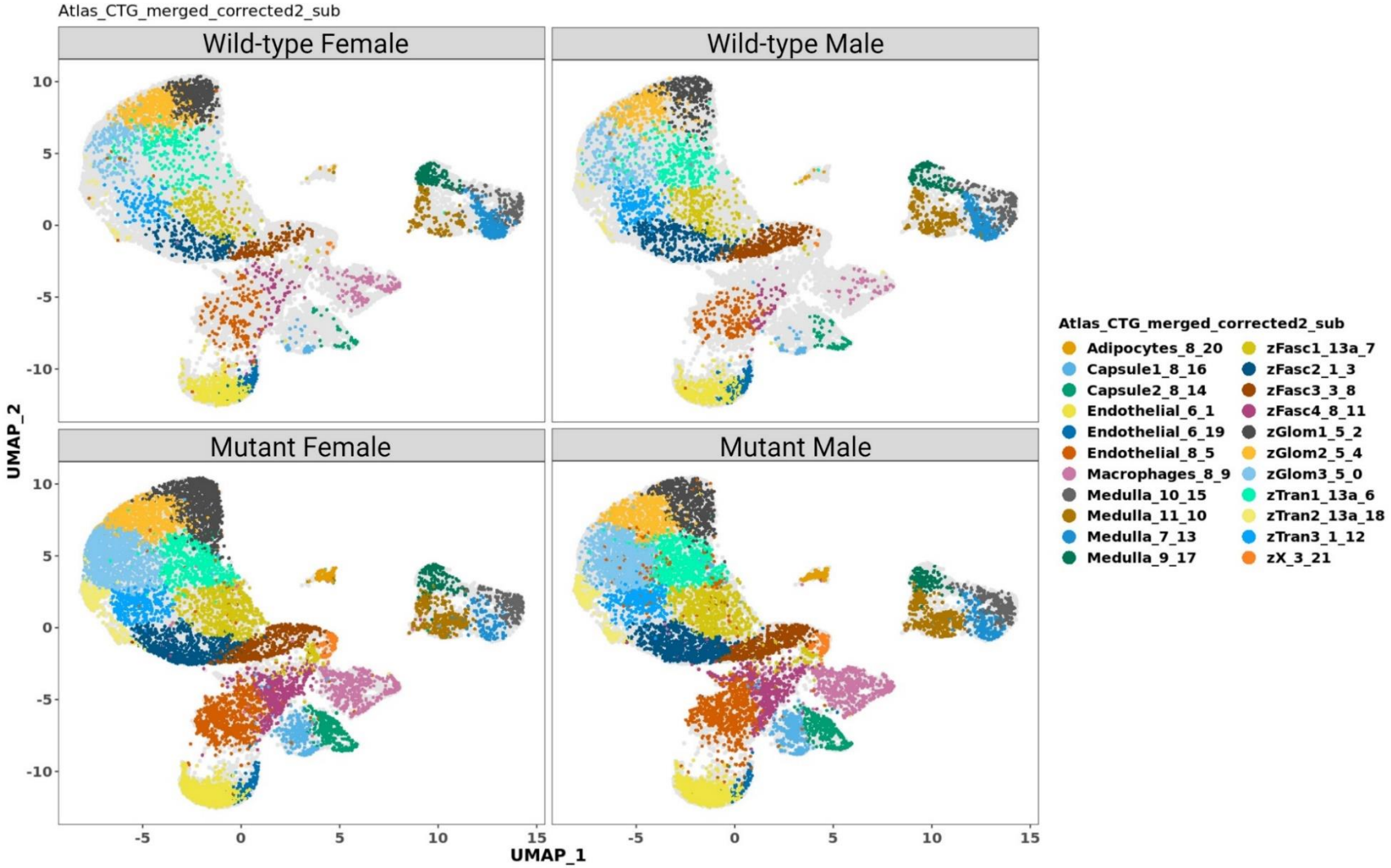

Figure 5-17 UMAP showing clusters from each mouse sample.

5.3.2.3 Pseudotime trajectory

The cells of the adrenal cortex undergo lineage conversion as they migrate centripetally. A pseudotime trajectory map can show the direction of this lineage conversion in a UMAP cluster. Three pathways were determined on pseudotime trajectory analysis (Figure 5-18). The shortest pathway stopped in the cluster that was annotated as transitional zone. This zone had a high level of mitochondrial genes and may have represented poor quality samples. The remaining two trajectories terminate near the X-zone and towards endothelial cells.

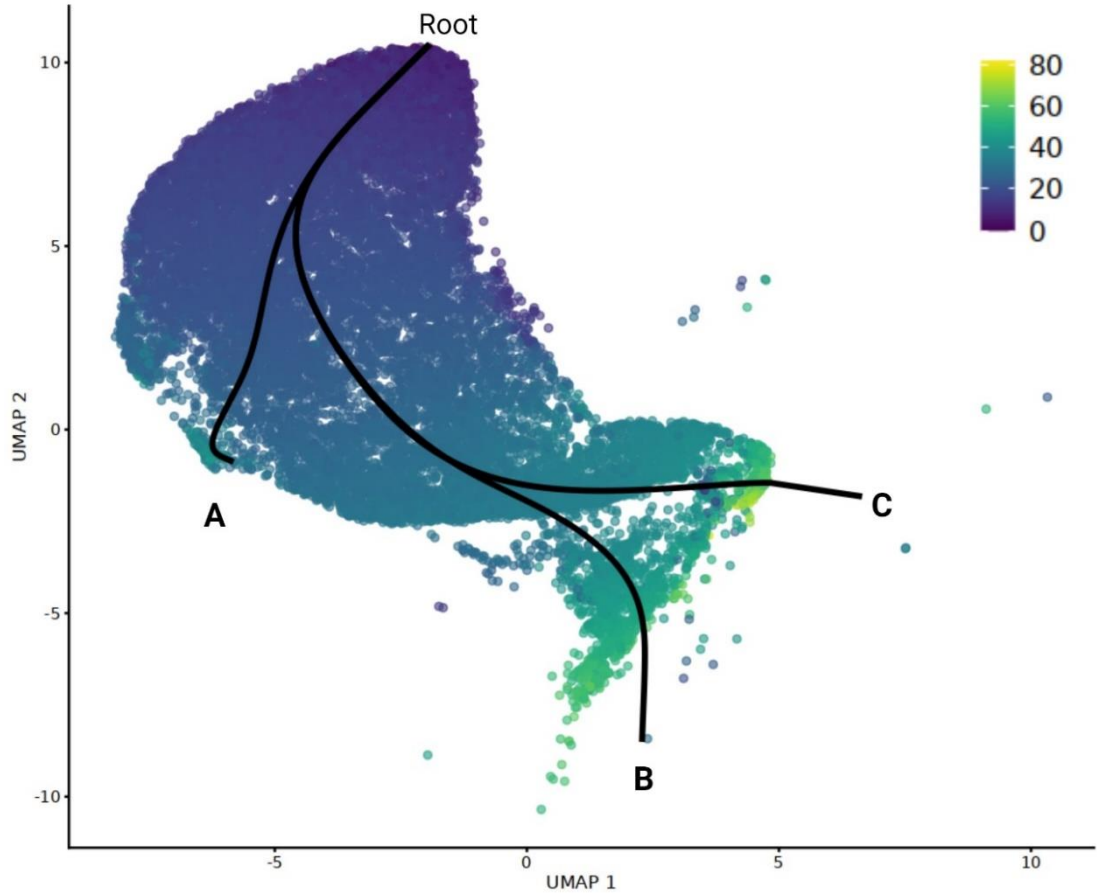

Figure 5-18 Pseudotime trajectory analysis.
The cells used in this analysis were restricted to the clusters identified as adrenocortical (clusters zGlom1, zGlom2, zGlom3, zTran1, zTran2, zTran3, zFasc1, zFasc2, zFasc3, zFasc4 and zX). Black lines on the UMAP plots represent the trajectory graph. Root of the pseudotime trajectory was selected as cluster zGlom1 (dark blue). Three trajectories were detected, terminating in the transitional zone (A), endothelial cells (B) and the X-zone (C).

5.3.2.4 Comparing the mutant and wild-type transcriptome

Selected genes that showed increased expression in the mutant zona glomerulosa compared with the wild-type included *Tafa2*, *Ntrk2*, *Fdx1* and *Akr1b7* (Figure 5-19). Selected genes that showed decreased expression included *Ptprd* and *Auts2*. In addition to increased expression of *Tafa2* and *Fdx1* in the zona fasciculata of mutant adrenals, there was increased expression of *Hsd3b1*, and decreased expression of *Me1* and *Pbx3* (Figure 5-20). The top 10 genes with increased expression in the mutant compared with the wild-type are shown (Table 5-7).

Table 5-7 Top 10 genes highly expressed in mutant compared with wild-type.

Cluster	zGlom1	zGlom2	zGlom3	zFasc1	zFasc2	zFasc3
Female	*Tafa2*	*Tafa2*	*Fdx1*	*Tafa2*	*Mt-Co3*	*Abcb1b*
	Fam155A	*Fdx1*	*Tafa2*	*Pde10a*	*Mt-Co2*	*Fdx1*
	Nebl	*Ctnnd2*	*Gm17276*	*Rnf220*	*Fdx1*	*Mt-Co3*
	Ctnnd2	*Gm17276*	*Akr1b7*	*Ctnnd2*	*Hsd3b1*	*Hsd3b1*
	Gm17276	*Akr1b7*	*Lrrc4*	*Nr4a2*	*Rnf220*	*Rnf220*
	Akr1b7	*Nebl*	*Ctnnd2*	*Ccdc57*	*Mt-Co1*	*Mt-Co2*
	Ntrk2	*Fam155a*	*Slc6a5*	*Clc6a5*	*Nr4a2*	*Mt-Atp6*
	Lrrc4	*Lrrc4*	*Pde10a*	*Fdx1*	*Mt-Atp6*	*Nr4a2*
	Notch3	*Slc6a5*	*Mt-Co3*	*Lrrc4*	*Abcb1b*	*Gm7247*
	Grk5	*Mt-Co3*	*Nebl*	*Mt-Co3*	*Tafa2*	*Mt-Co1*
Male	*Tafa2*	*Tafa2*	*Tafa2*	*Tafa2*	*Adh1*	*Chka*
	Ntrk2	*Ntrk2*	*Slc6a5*	*Slc6a5*	*Mt-Co3*	*Man1a*
	Pex5l	*Hspe1*	*Mt-Co3*	*Cyp11b2*	*Hspe1*	*Prlr*
	Procr	*Akr1b7*	*Hspe1*	*Ntrk2*	*Mt-Co2*	*Hspe1*
	Fam155a	*Procr*	*Mt-Co2*	*Ctnnd2*	*Tafa2*	*Mt-Co3*
	Akr1b7	*Mt-Co3*	*Ntrk2*	*Adh1*	*Chka*	*Nr4a2*
	Prkg1	*Pex5l*	*Pex5l*	*Ccdc57*	*Mt-Co1*	*Rgs2*
	Hspe1	*Pdx1*	*Cyp11b2*	*Prr16*	*Nr4a2*	*Appl2*
	Slc16a3	*Slc6a5*	*Adh1*	*Mt-Co3*	*Prr16*	*Mt-Co2*
	Ccdc57	*Mt-Co2*	*Ctnnd2*	*Mt-Co2*	*Mt-Atp6*	*Slc25a3*

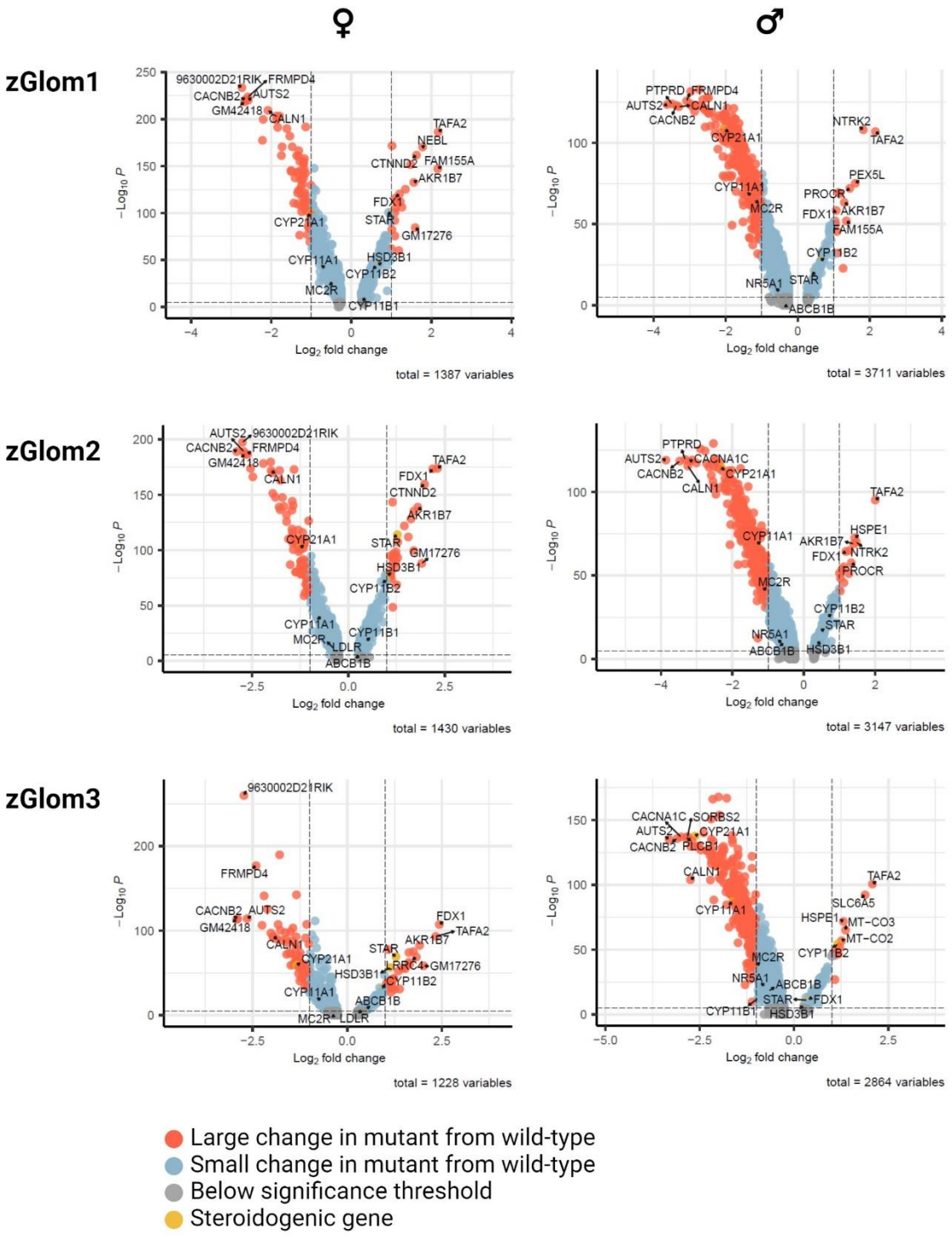

Figure 5-19 Volcano plots displaying gene expression in mutant compared with wild-type adrenal gland zona glomerulosa.

Three zona glomerulosa clusters are shown. Genes towards the right have increased expression in the mutant adrenal compared with the wild-type and genes towards the left have decreased expression. Volcano plots were prepared by Eva van Dijk, GTRU, CMRI.

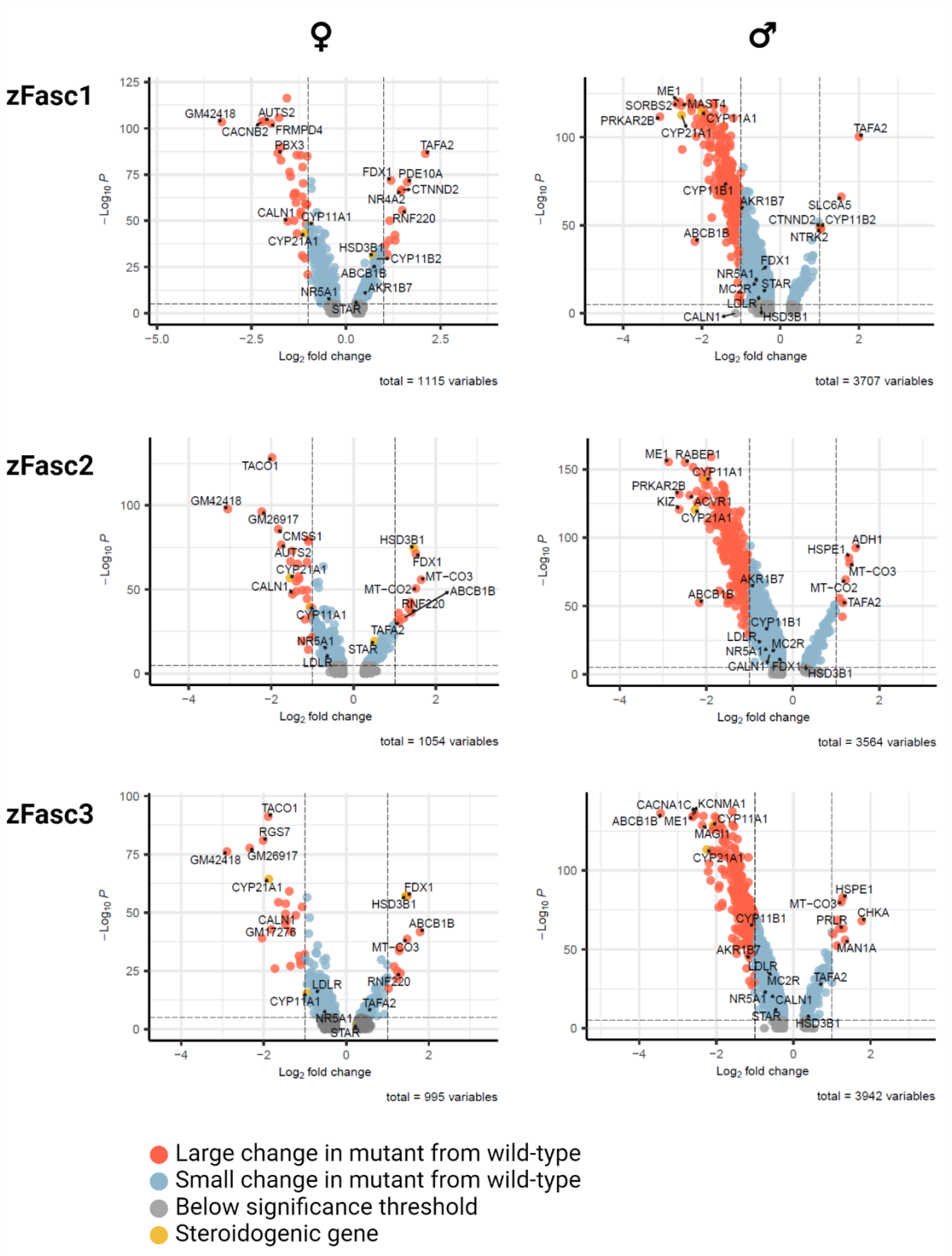

Figure 5-20 Volcano plots displaying gene expression in mutant compared with wild-type adrenal gland zona fasciculata.

Three zona fasciculata clusters are shown. Genes towards the right have increased expression in the mutant adrenal compared with the wild-type and genes towards the left have decreased expression. Volcano plots were prepared by Eva van Dijk, GTRU, CMRI.

5.3.2.5 Annotation of the Cyp21a1-/- transcriptome without clustering influence from Cyp21+/+ analysis

The *Cyp21a1*-/- samples were originally annotated with the *Cyp21a1*+/+ samples, as they had already been annotated. However, if a gene is not expressed by all samples during the clustering, it will be eliminated from the analysis. This was important to consider when the *Cyp21a1*-/- transcriptome is likely to be different to the *Cyp21a1*+/+ transcriptome, so the process was repeated with the *Cyp21a1*-/- samples alone (Table 5-8). The UMAP for the Cyp21a1-/- samples alone is shown (Figure 5-21). The cluster identities for each analysis only had small variations, except cluster 8 from the wild-type only analysis that was further divided into multiple cell types (Table S5-9).

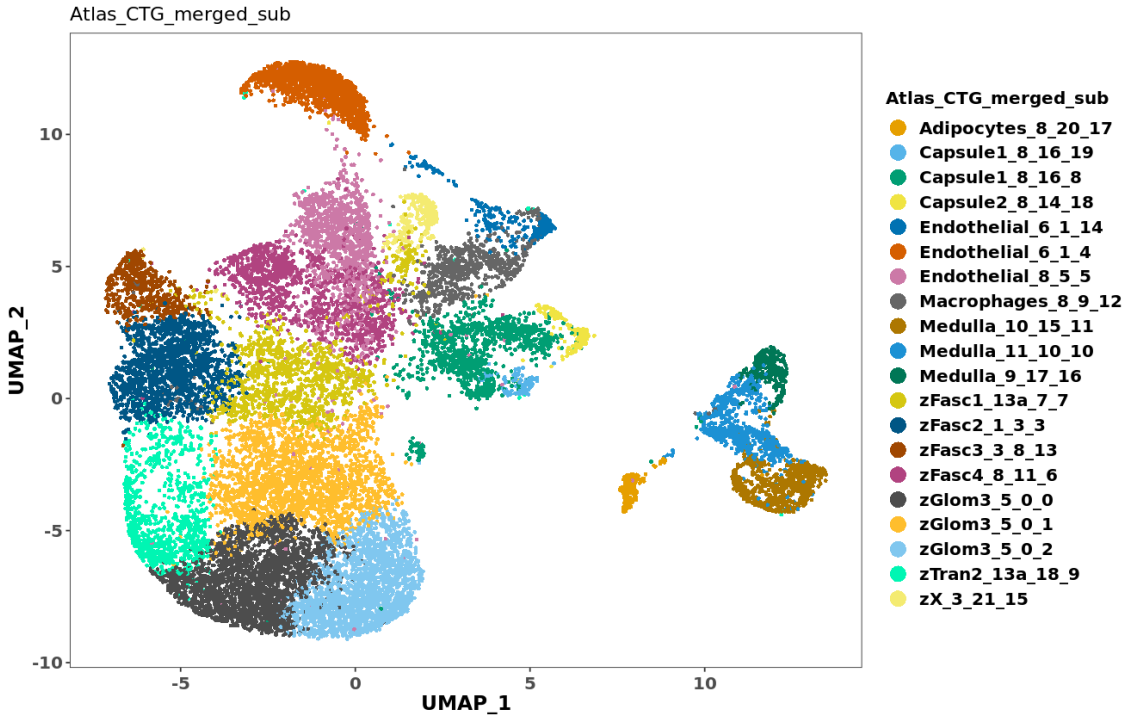

Figure 5-21 UMAP showing clusters from mutant-only adrenal glands.
This analysis was performed without including the wild-type samples.

Table 5-8 Annotation for the clusters of the mutant-only transcriptomic analysis.

Cluster number	Annotation
0	zGlom3_5_0_0
1	zGlom3_5_0_1
2	zGlom3_5_0_2
3	zFasc2_1_3_3
4	Endothelial_6_1_4
5	Endothelial_8_5_5
6	zFasc4_8_11_6
7	zFasc1_13a_7_7
8	Capsule1_8_16_8
9	zTran2_13a_18_9
10	Medulla_11_10_10
11	Medulla_10_15_11
12	Macrophages_8_9_12
13	zFasc3_3_8_13
14	Endothelial_6_1_14
15	zX_3_21_15
16	Medulla_9_17_16
17	Adipocytes_8_20_17
18	Capsule2_8_14_18
19	Capsule1_8_16_19

The Clustifyr package divided the mutant-only transcriptome cells into 20 clusters (clusters 0-19). The last number refers to the cluster from this analysis, the second last number refers to the cluster the package allocated from the combined analysis and the third last number refers to the cluster allocated during the wild-type only analysis.

There was a high level of mitochondrial gene expression in zTran2_13a_18_9. This can be a sign of a low-quality sample or possibly presence of apoptosis.[54] There was a small subset of cells consistent with the X-zone in both the male and female samples (expression of *Pik3c2g*[55] and/or *Akr1c18*[56]). This was unexpected as the male X-zone is expected to involute at puberty,[57] however perhaps there is abnormal puberty in 21-hydroxylase deficient mice. The cluster annotated as the X-zone had lower expression of *Pik3c2g* in the male than female homozygote.

5.4 Discussion

This study provides the foundation for further investigation of rAAV-mediated gene delivery to the adrenal cortex for durable effect. We demonstrated the most comprehensive analysis of rAAV serotype transduction of the adrenal gland to date and the first timepotential adrenocortical progenitor cells on single nuclei RNA sequencing have been identified. In combination, these results provide the basis for further analysis of transducing the adrenocortical cells through either single nuclei RNA sequencing-compatible rAAV testing kit development or through the use of these top serotypes with a reporter mouse and studies that go beyond the cellular turnover period.

There were 8 rAAV serotypes (AAV8, Anc80, AAV10, SYD11, NP22, KP3, KP1, AAV2-M1) that may deliver better gene expression to either the male or the female murine adrenal gland *en bloc* than Rh10, the most popular serotype used in murine adrenal studies.[2, 3] Of these, 5 were bioengineered capsids, one was an *in silico* predicted ancestral capsid and the remaining two were natural serotypes. There was a slight difference in hierarchy in males and females. Based on functional transduction efficiency, the top 7 serotypes were Anc80, NP22, KP3, KP1, AAV10, Rh10 and AAV8. Overall, the bioengineered capsids that delivered the best gene expression had sequence similarities to AAV2, AAV3, AAV8, AAV10 and Rh10. The gene expression delivered by AAV2 and AAV3 was poor but AAV8, AAV10 and Rh10 were in the top 7 capsid serotypes, suggesting there may be a commonality between these sequences that is conferring adrenal tropism. On our phylogenetic analysis, KP3 was determined to have a close evolutionary genetic relationship with AAV8, AAV10 and Rh10, all of which also had efficient functional transduction. NP22 had a close phylogenetic relationship with AAV2 and AAV3, neither of which had efficient functional transduction. Similarly, Anc80 and

KP1 were phylogenetically related to AAV1 and AAV6. None of the serotypes was able to efficiently functionally transduce the capsule and zona glomerulosa. These zones appear to be resistant to functional transduction but a limitation of this study was that we were not able to determine whether physical transduction had occurred in specific zones of the gland.

Anc80 is an *in silico* reconstructed ancestor of AAV1, AAV2, AAV8 and AAV9.[39] AAV1 and AAV2 had low transduction efficiency in the adrenal glands. Interestingly, the closest reported homolog to Anc80 is Rh10, the capsid that has been used in most murine adrenal gene therapy studies[2, 3]; however, Anc80 delivered better gene expression than Rh10 and in our phylogenetic analysis Anc80 was not mapped close to Rh10. Anc80 has been shown to provide efficient transduction of the murine and non-human primate liver, murine skeletal muscle, and murine retina,[39] but to our knowledge it has not been used in the adrenal gland or other endocrine glands previously.

NP22 was developed by selecting for efficient human skeletal muscle transduction.[47] NP22 performed better than AAV1 and AAV8 for the *in vitro* and *ex vivo* transduction of human skeletal muscle cells.[47] NP22 was highly shuffled, with unique regions contributed from AAV3b, AAV8, AAV6, AAV9_hu14 and AAV2, as well as some *de novo* mutations not present in the parent sequence from which the shuffled capsid was derived.[47] While NP22 delivered good gene expression , AAV2, AAV3b, AAV6 performed poorly in our murine adrenal glands. However, the results were enriched for AAV8 and AAV9. The AAV9 variant AAV9_hu14 was not included in the Testing Kit.

KP1 and KP3 were developed by selecting for high efficiency in transducing human pancreatic islet cells.[43] It is interesting that they also conferred good tropism to another endocrine organ, the adrenal cortex, particularly as they have different embryological origins. Pancreatic islet cells arise from the endoderm,[58] however steroid-secreting endocrine organs arise from the mesoderm. These variants had excellent transduction across a range of human cell types, as well as the murine liver,[43] and so perhaps are all-round good tissue transducers, regardless of tissue type. AAV3B was reported to be most similar to the KP sequences,[43] however this serotype performed poorly in the adrenal gland. KP3 was phylogenetically close to AAV9, AAV10 and Rh10 whereas KP1 was close to AAV1 and AAV6 on our analysis. The commonality that is conferring adrenal performance across these sequences is unclear.

A limitation of this study was that only known capsid serotypes were included in the analysis. For more thorough determining of capsid serotype transduction, shuffled DNA libraries can be used whereby the capsid sequence is not known at the time of the experiment. However, due to the difficulty in identifying progenitor cells, it is unclear if *en bloc* analysis of the adrenal gland for capsid enrichment would be an appropriate method for determining this, as it is plausible that a serotype that transduces the progenitor cells may not be the major serotype present in an adrenal gland. Additionally, due to the low level of general protein expression in stem and progenitor cells, there may be effective physical transduction, but the cells may express the transgene poorly, which would be indicative of poor functional transduction. This could be missed by standard techniques to analyse transduction efficiency. Therefore, an appropriate serotype could be artificially selected against.

The identification of the adrenocortical progenitor cells is elusive, and a method to identify them would be useful for future rAAV capsid tropism studies in the adrenal cortex. We explored whether this elusive cell population could be identified using single nuclei RNA sequencing in wild-type and 21-hydroxylase deficient murine adrenal glands. This is the first time that single nuclei RNA sequencing has detected potential progenitor cells in the adrenal gland. One of the limiting factors with this technology is the exclusion of small cell populations and cells with small numbers of genes expressed and the exclusion of genes with low levels of expression. As, by definition, a progenitor cell does not have much in the way of cellular functions, it would likely have limited gene expression. Furthermore, the population is very small and likely to be excluded from most standard analyses. Indeed, a specific cluster of "progenitor" cells was not found, however a subset of cells that had the expression criteria were detected. It was postulated that there may be an enlarged progenitor pool in the 21-hydroxylase deficient adrenal glands due to increased ACTH drive, however there were no progenitor cells found in these samples. Perhaps the ACTH stimulation is driving the rapid differentiation of progenitor cells, and they are spending less time in a progenitor state, therefore harder to detect. Dissociation of the adrenal tissue was challenging, particularly the tough capsule. Therefore, the capsular cells are not well represented in the analysis, and this is where the adrenocortical stem cells reside.

The development of a single nuclei atlas that includes the 21-hydroxylase deficient transcriptome is required for future use for rAAV capsid tropism studies for the development of gene therapy for CAH. Specific gene expression pattern differences between the wild-type and 21-hydroxylase deficient adrenal cortices were noted. *Tafa2* was upregulated in the 21-hydroxylase deficient adrenal cortex. This gene has a role in

neuronal tissue survival and may act as a chemokine.[59] Additionally, it induces skeletal stem cell migration.[60] While it is ubiquitously expressed, its specific role in the adrenal cortex is unclear, however it is plausible that it may have a similar role in the adrenal cortex where it mobilises the stem cells in the context of 21-hydroxylase deficiency. *Ntrk2* was also upregulated in the zona glomerulosa, and expression of this gene in neuroblastoma tissue is associated with higher risk and poor outcome.[61] *Ntrk2* expression in the adrenal gland is associated with highly fecund sheep,[62] and we postulate that it may be related to high progesterone levels found in 21-hydroxylase deficiency. Ferredoxin 1 (*Fdx1*), also known as adrenodoxin, is essential for steroidogenesis in adrenal glands,[63, 64] and was upregulated in the 21-hydroxylase deficient adrenocortical cells, likely due to upregulated steroidogenic pathways. *Fdx1* reduces mitochondrial cytochrome P450 enzymes to enable the catalyst of various reactions for steroidogenesis. The adrenal cortex generates a large amount of harmful byproducts of lipid peroxidation and steroidogenesis.[65] *Akr1b7*, which is orthologous to human *AKR1B10*, was upregulated in the 21-hydroxylase deficient zona glomerulosa and has a role in the detoxification of these lipid peroxidation by-products.[66] *Akr1b7* expression is decreased when ACTH is suppressed,[67] and thus in the context of elevated ACTH exposure in 21-hydroxylase deficiency it follows that it will be upregulated. Previously, it was shown that *Akr1b7* expression was limited to the zona fasciculata in wild-type adrenal glands and while it is expressed in the zona fasciculata,[67] it is also abnormally upregulated in the zona glomerulosa of the mutant adrenal glands. In terms of reduced expression in 21-hydroxylase deficient adrenal glands, *Ptprd* and *Auts2* was shown to have reduced expression in the zona glomerulosa. *Ptprd* has a role in neuronal differentiation, so its reduced expression in 21-hydroxylase deficiency is unclear. *Auts2* has a role in repressing transcription of gene expression, therefore reduced expression of *Auts2* in 21-hydroxylase

deficiency will allow the increased gene expression required of enzymes involved in steroidogenesis in the presence of 21-hydroxylase deficiency. In the zona fasciculata, *Me1* and *Pbx3* were both down regulated in the mutant adrenal glands. *Me1* is involved in generation NADPH for fatty acid biosynthesis and *Pbx3* has a role in the regulation of transcription. A limitation of this study was that only four mice were included in the transcriptomic study, one mouse for each sex and genotype. Therefore, the reproducibility of the findings was not able to be demonstrated. Furthermore, the presence of changes in gene expression was not validated with a second method.

The X-zone was identified as a distinct cluster, more prominent in the mutant transcriptome. The function of the X-zone is unclear, but postulated to be involved with metabolism of placentally-derived progesterone due to the expression of *Akr1c18*.[56] It persists in the male mouse until puberty and in the female mouse until their first pregnancy.[68-70] Without pregnancy, the X-zone degenerates between 3-7 months of age in female mice.[70] The presence of androgens drive this regression.[71] The mice were approximately 3 months old in this study. The prominence of the X-zone in the mutant clusters suggests perhaps either the hormones required for its involution are not produced in adequate amounts, or it is required for additional progesterone metabolism in the context of elevated serum progesterone due to 21-hydroxylase deficiency. Although the difference in testosterone production by wild-type and mutant male mice was not significant, there was a trend towards lower testosterone production in the mutants with 3-fold lower median serum testosterone (Chapter 3, Figure 3-8).

These top serotypes provide a shortlist for downstream analysis for determining tissue tropism for the adrenocortical progenitor cells. One strategy is to directly identify capsids

that can transduce the adrenocortical progenitor cells, by developing a 10X compatible mini AAV Testing kit, and determining if any capsid barcodes are expressed by the cells that also express *Nr5a1* and *Shh* but not *Cyp11b2* or *Cyp11b1*. The 10X compatible mini kit would need the barcode to be within 300 bp of the polyA signal to ensure that it is detected by the 10X technology, so the standard AAV Testing Kit cannot be used. A second strategy could be to indirectly identify serotypes that transduce progenitor cells through demonstration of durable effect, without proving transduction of the progenitor cells directly. A reporter mouse such as the Ai9 could be used whereby exposure to cre permanently turns on expression of the tdTomato expression cassette. By treating mice with various AAV serotypes that encode cre DNA and harvesting at various timepoints, one could determine in retrospect that if the tdTomato expression was permanent, then this serotype must have transduced the correct cell population as all daughter cells had the reporter expressed.

While small animal models are often a good approximation to humans, there are some differences. Gene therapy and AAV targeting that is robust in the mouse may fail in the human. This study has focussed on determining optimal capsid use for gene delivery to the murine adrenocortical progenitor cells, however AAV serotypes that perform well in one species do not necessarily confer efficient performance in another species. Therefore, this study provides a proof of concept, but determining AAV serotype specificity for human adrenocortical progenitor cells is still required. This is a challenging next step. It could be achieved through *in vitro* modelling with adrenocortical organoids, however the difficulty in identifying progenitor cells means it is unclear whether these organoids possess all the appropriate cell populations for these studies. Furthermore, it is easier to reconstitute foetal organoids and cell populations than adult populations,[72] but the adult

adrenal cortex is quite different to the foetal cortex. Alternatively, cadaveric organs or organs sourced following therapeutic adrenalectomy could provide an alternate source of human tissue for capsid studies, however the limited life span of these organs may impact on its usefulness.

In conclusion, rAAV serotypes that were highly adrenally-tropic were identified, and a transcriptomic atlas for wild-type and 21-hydroxylase deficient adrenals was developed. Furthermore, potential adrenocortical progenitors were identified. These results provide the foundation for further work in identifying capsids that can transduce specific populations in the adrenal cortex, providing the pathway to robust gene delivery such as the gene editing strategy that is described in Chapter 6.

5.5 Supplementary data

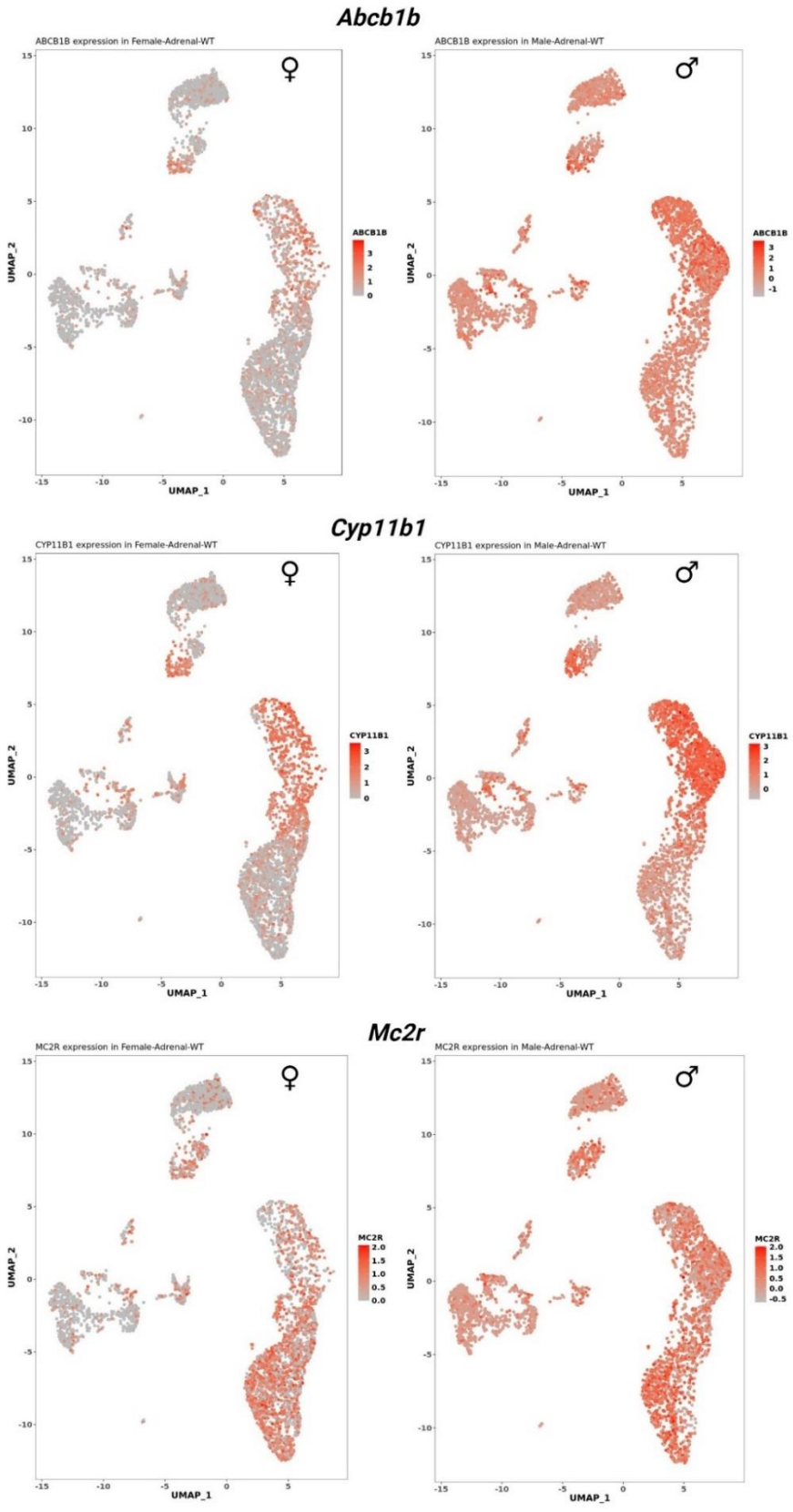

Figure S5-22 Heatmaps showing selected genes highly expressed in zona fasciculata.

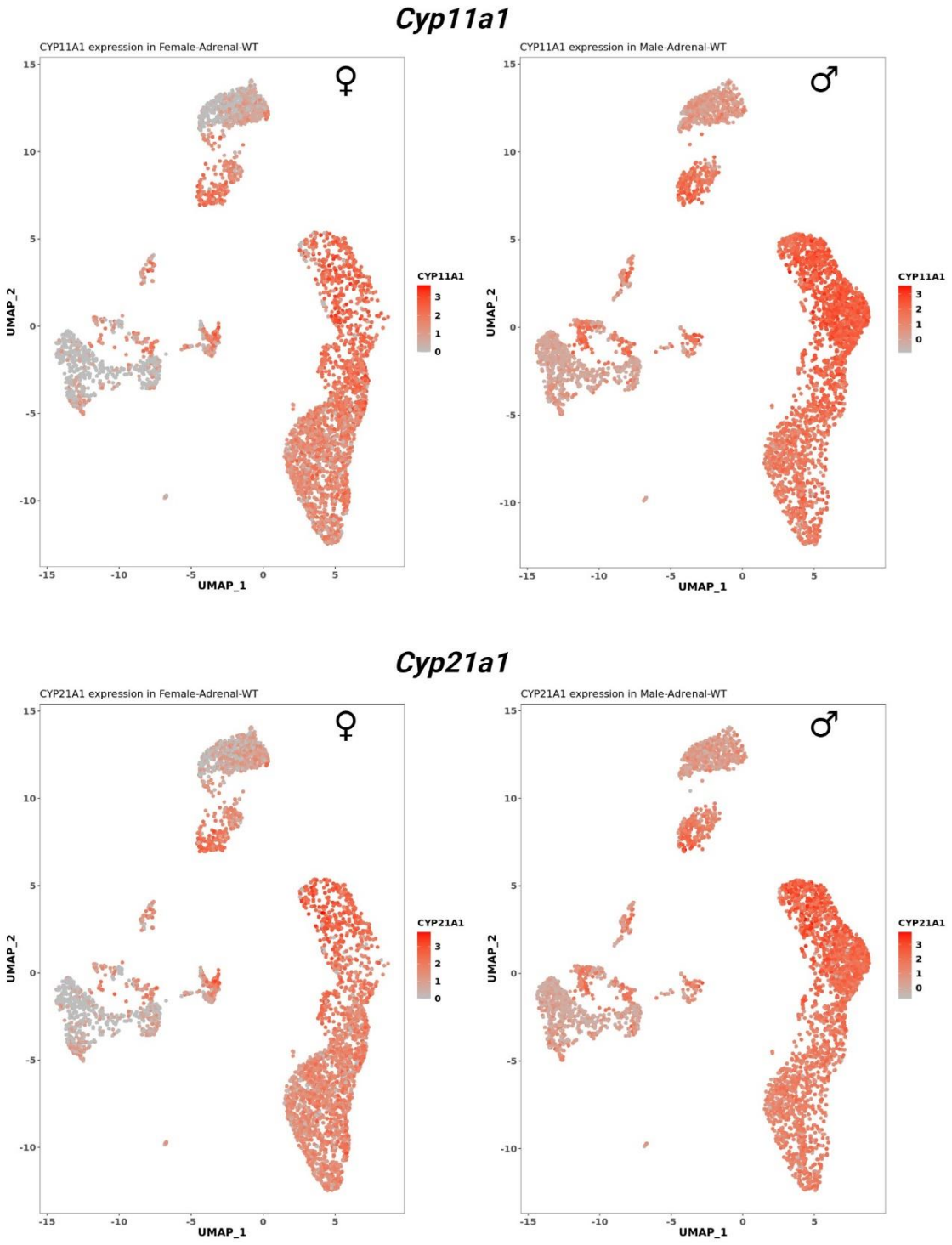

Figure S5-23 Heatmaps showing selected genes that are expressed by steroidogenic cells.

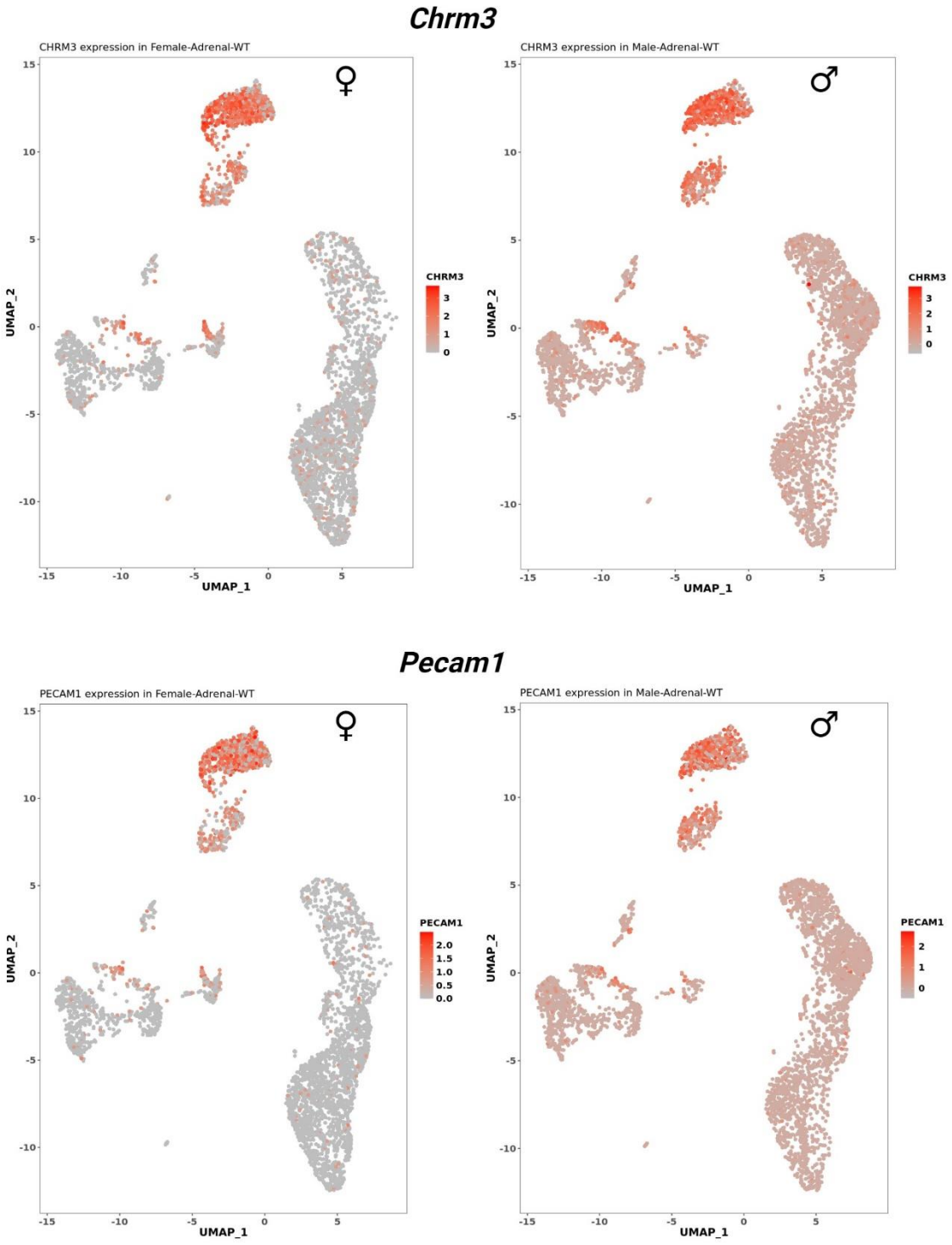

Figure S5-24 Heatmaps showing selected genes that are expressed by endothelial cells.

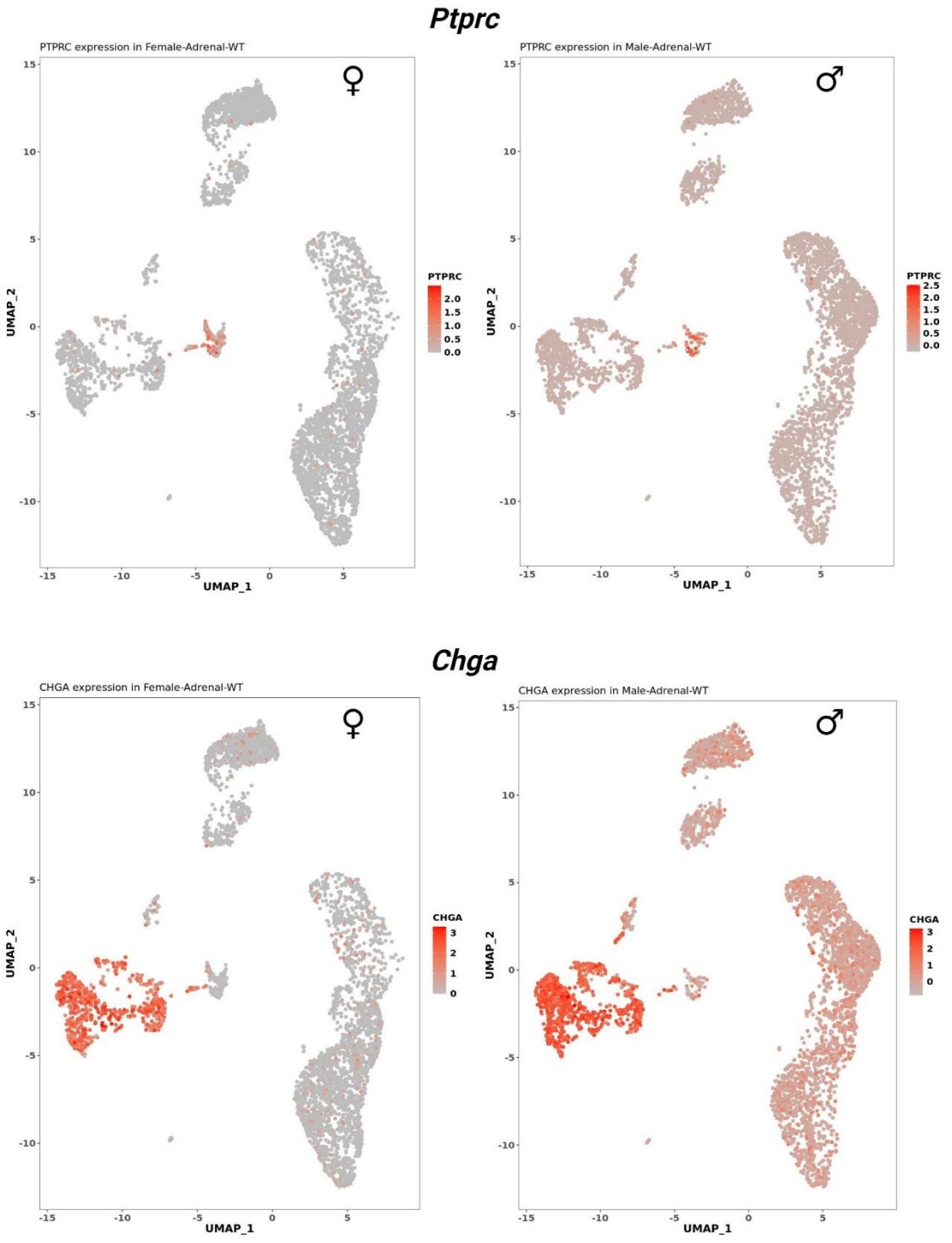

Figure S5-25 Heatmaps with selected genes expressed outside of the adrenal cortex. *Ptprc* is a marker of immune cells. *Chga* is a marker of the adrenal medulla.

Table S5-9 Comparing the annotations for each cluster analysis.

	Wild only		Combined		Mutant only	
	#	Annotation	#	Annotation	#	Annotation
Adrenal cortex	5	zGlom1_5	0	zGlom3_5_0	0	zGlom3_5_0_0
					1	zGlom3_5_0_1
					2	zGlom3_5_0_2
			2	zGlom1_5_2		
			4	zGlom2_5_4		
	0	zGlom2_0				
	2	zTran_2				
	13	zFasc1_13a zGlom3_13b	6	zTran1_13a_6		
			7	zFasc1_13a_7	7	zFasc1_13a_7_7
			18	zTran2_13a_18	9	zTran2_13a_18_9
	1	zFasc2_1	3	zFasc2_1_3	3	zFasc2_1_3_3
			12	zTran3_1_12		
	3	zFasc3_3	8	zFasc3_3_8	13	zFasc3_3_8_13
			21	zX_3_21	15	zX_3_21_15
Other (incl zFasc4)	4	Endothelial_4				
	6	Endothelial_6	1	Endothelial_6_1	4	Endothelial_6_1_4
					14	Endothelial_6_1_14
			19	Endothelial_6_19		
	8	Endothelial_8 zFasc4_8 Unknown_8	5	Endothelial_8_5	5	Endothelial_8_5_5
			9	Macrophages_8_9	12	Macrophages_8_9_12
			11	zFasc4_8_11	6	zFasc4_8_11_6
			14	Capsule2_8_14	18	Capsule2_8_14_18
			16	Capsule1_8_16	8	Capsule1_8_16_8
					19	Capsule1_8_16_19
			20	Adipocytes_8_20	17	Adipocytes_8_20_17
	14	Capsule_14				
	15	Glial_15				
	12	Macrophage_12				
Adrenal medulla	7	Medulla_7	13	Medulla_7_13		
	9	Medulla_9	17	Medulla_9_17	16	Medulla_9_17_16
	10	Medulla_10	15	Medulla_10_15	11	Medulla_10_15_11
	11	Medulla_11	10	Medulla_11_10	10	Medulla_11_10_10

Cluster 8 from the wild-only analysis was subdivided by the subsequent two analyses.

5.6 References

1. Eclov RJ, Lewis TEW, Kapandia M, et al. Durable CYP21A2 gene therapy in non-human primates for treatment of congenital adrenal hyperplasia. *ESGCT 27th Annual Congress In collaboration with SETGyc*. Barcelona, Spain: Hum Gene Ther, 2019, p. A1-A221.
2. Markmann S, De BP, Reid J, et al. Biology of the Adrenal Gland Cortex Obviates Effective Use of Adeno-Associated Virus Vectors to Treat Hereditary Adrenal Disorders. *Hum Gene Ther* 2018; 29: 403-412. 2018/01/11. DOI: 10.1089/hum.2017.203.
3. Perdomini M, Dos Santos C, Goumeaux C, et al. An AAVrh10-CAG-CYP21-HA vector allows persistent correction of 21-hydroxylase deficiency in a Cyp21(-/-) mouse model. *Gene Ther* 2017; 24: 275-281. 2017/02/07. DOI: 10.1038/gt.2017.10.
4. Ingle DJ and Higgins GM. Autotransplantation and Regeneration of the Adrenal Gland. *Endocrinology* 1938; 22: 458-464. DOI: 10.1210/endo-22-4-458.
5. Zwemer RL, Wotton RM and Norkus MG. A study of corticoadrenal cells. *The Anatomical Record* 1938; 72: 249-263. DOI: 10.1002/ar.1090720210.
6. Chang SP, Morrison HD, Nilsson F, et al. Cell proliferation, movement and differentiation during maintenance of the adult mouse adrenal cortex. *PLoS One* 2013; 8: e81865. 2013/12/11. DOI: 10.1371/journal.pone.0081865.
7. Freedman BD, Kempna PB, Carlone DL, et al. Adrenocortical zonation results from lineage conversion of differentiated zona glomerulosa cells. *Dev Cell* 2013; 26: 666-673. 2013/09/17. DOI: 10.1016/j.devcel.2013.07.016.
8. Finco I, Mohan DR, Hammer GD, et al. Regulation of stem and progenitor cells in the adrenal cortex. *Curr Opin Endocr Metab Res* 2019; 8: 66-71. 2020/04/08. DOI: 10.1016/j.coemr.2019.07.009.
9. King P, Paul A and Laufer E. Shh signaling regulates adrenocortical development and identifies progenitors of steroidogenic lineages. *Proc Natl Acad Sci U S A* 2009; 106: 21185-21190. 2009/12/04. DOI: 10.1073/pnas.0909471106.
10. Wood MA, Acharya A, Finco I, et al. Fetal adrenal capsular cells serve as progenitor cells for steroidogenic and stromal adrenocortical cell lineages in M. musculus. *Development* 2013; 140: 4522-4532. 2013/10/18. DOI: 10.1242/dev.092775.
11. Kataoka Y, Ikehara Y and Hattori T. Cell proliferation and renewal of mouse adrenal cortex. *J Anat* 1996; 188 (Pt 2): 375-381. 1996/04/01.
12. Grabek A, Dolfi B, Klein B, et al. The Adult Adrenal Cortex Undergoes Rapid Tissue Renewal in a Sex-Specific Manner. *Cell Stem Cell* 2019; 25: 290-296 e292. 2019/05/21. DOI: 10.1016/j.stem.2019.04.012.
13. Graves LE, van Dijk EB, Zhu E, et al. AAV-delivered hepato-adrenal cooperativity in steroidogenesis: Implications for gene therapy for congenital adrenal hyperplasia. *Mol Ther Methods Clin Dev* 2024; 32: 101232. 2024/04/01. DOI: 10.1016/j.omtm.2024.101232.
14. Naiki Y, Miyado M, Shindo M, et al. Adeno-Associated Virus-Mediated Gene Therapy for Patients' Fibroblasts, Induced Pluripotent Stem Cells, and a Mouse Model of Congenital Adrenal Hyperplasia. *Hum Gene Ther* 2022; 33: 801-809. 2022/07/16. DOI: 10.1089/hum.2022.005.
15. Bougnères P and Gao G. *Adeno-associated virus gene therapy for 21-hydroxylase deficiency*. 2019.
16. Cabanes-Creus M, Navarro RG, Zhu E, et al. Novel human liver-tropic AAV variants define transferable domains that markedly enhance the human tropism of AAV7 and AAV8. *Mol Ther Methods Clin Dev* 2022; 24: 88-101. 2022/01/04. DOI: 10.1016/j.omtm.2021.11.011.
17. Westhaus A, Cabanes-Creus M, Jonker T, et al. AAV-p40 Bioengineering Platform for Variant Selection Based on Transgene Expression. *Hum Gene Ther* 2022; 33: 664-682. 2022/03/18. DOI: 10.1089/hum.2021.278.
18. Westhaus A, Cabanes-Creus M, Rybicki A, et al. High-Throughput In Vitro, Ex Vivo, and In Vivo Screen of Adeno-Associated Virus Vectors Based on Physical and Functional Transduction. *Hum Gene Ther* 2020; 31: 575-589. 2020/02/01. DOI: 10.1089/hum.2019.264.
19. Lopez JP, Brivio E, Santambrogio A, et al. Single-cell molecular profiling of all three components of the HPA axis reveals adrenal ABCB1 as a regulator of stress adaptation. *Sci Adv* 2021; 7: eabe4497. 2021/02/12. DOI: 10.1126/sciadv.abe4497.
20. Atchison RW, Casto BC and Hammon WM. Adenovirus-Associated Defective Virus Particles. *Science* 1965; 149: 754-756. 1965/08/13. DOI: 10.1126/science.149.3685.754.
21. Hoggan MD, Blacklow NR and Rowe WP. Studies of small DNA viruses found in various adenovirus preparations: physical, biological, and immunological characteristics. *Proc Natl Acad Sci USA* 1966; 55: 1467-1474. 1966/06/01. DOI: 10.1073/pnas.55.6.1467.

22. Rutledge EA, Halbert CL and Russell DW. Infectious clones and vectors derived from adeno-associated virus (AAV) serotypes other than AAV type 2. *J Virol* 1998; 72: 309-319. 1998/01/07. DOI: 10.1128/JVI.72.1.309-319.1998.
23. Parks WP, Melnick JL, Rongey R, et al. Physical assay and growth cycle studies of a defective adeno-satellite virus. *J Virol* 1967; 1: 171-180. 1967/02/01. DOI: 10.1128/JVI.1.1.171-180.1967.
24. Bantel-Schaal U and zur Hausen H. Characterization of the DNA of a defective human parvovirus isolated from a genital site. *Virology* 1984; 134: 52-63. 1984/04/15. DOI: 10.1016/0042-6822(84)90271-x.
25. Gao GP, Alvira MR, Wang L, et al. Novel adeno-associated viruses from rhesus monkeys as vectors for human gene therapy. *Proc Natl Acad Sci U S A* 2002; 99: 11854-11859. 2002/08/23. DOI: 10.1073/pnas.182412299.
26. Gao G, Vandenberghe LH, Alvira MR, et al. Clades of Adeno-associated viruses are widely disseminated in human tissues. *J Virol* 2004; 78: 6381-6388. 2004/05/28. DOI: 10.1128/JVI.78.12.6381-6388.2004.
27. Mori S, Wang L, Takeuchi T, et al. Two novel adeno-associated viruses from cynomolgus monkey: pseudotyping characterization of capsid protein. *Virology* 2004; 330: 375-383. 2004/11/30. DOI: 10.1016/j.virol.2004.10.012.
28. Schmidt M, Voutetakis A, Afione S, et al. Adeno-associated virus type 12 (AAV12): a novel AAV serotype with sialic acid- and heparan sulfate proteoglycan-independent transduction activity. *J Virol* 2008; 82: 1399-1406. 2007/11/30. DOI: 10.1128/JVI.02012-07.
29. Schmidt M, Govindasamy L, Afione S, et al. Molecular characterization of the heparin-dependent transduction domain on the capsid of a novel adeno-associated virus isolate, AAV(VR-942). *J Virol* 2008; 82: 8911-8916. 2008/06/06. DOI: 10.1128/JVI.00672-08.
30. Gao G, Alvira MR, Somanathan S, et al. Adeno-associated viruses undergo substantial evolution in primates during natural infections. *Proc Natl Acad Sci U S A* 2003; 100: 6081-6086. 2003/04/30. DOI: 10.1073/pnas.0937739100.
31. Asokan A, Conway JC, Phillips JL, et al. Reengineering a receptor footprint of adeno-associated virus enables selective and systemic gene transfer to muscle. *Nat Biotechnol* 2010; 28: 79-82. 2009/12/29. DOI: 10.1038/nbt.1599.
32. Westhaus A, Eamegdool SS, Fernando M, et al. AAV capsid bioengineering in primary human retina models. *Sci Rep* 2023; 13: 21946. 2023/12/12. DOI: 10.1038/s41598-023-49112-2.
33. Tervo DG, Hwang BY, Viswanathan S, et al. A Designer AAV Variant Permits Efficient Retrograde Access to Projection Neurons. *Neuron* 2016; 92: 372-382. 2016/10/21. DOI: 10.1016/j.neuron.2016.09.021.
34. Wu Z, Asokan A, Grieger JC, et al. Single amino acid changes can influence titer, heparin binding, and tissue tropism in different adeno-associated virus serotypes. *J Virol* 2006; 80: 11393-11397. 2006/09/01. DOI: 10.1128/JVI.01288-06.
35. Ling C, Li B, Ma W, et al. Development of Optimized AAV Serotype Vectors for High-Efficiency Transduction at Further Reduced Doses. *Hum Gene Ther Methods* 2016; 27: 143-149. 2016/07/20. DOI: 10.1089/hgtb.2016.054.
36. Dalkara D, Byrne LC, Klimczak RR, et al. In vivo-directed evolution of a new adeno-associated virus for therapeutic outer retinal gene delivery from the vitreous. *Sci Transl Med* 2013; 5: 189ra176. 2013/06/14. DOI: 10.1126/scitranslmed.3005708.
37. Grimm D, Lee JS, Wang L, et al. In vitro and in vivo gene therapy vector evolution via multispecies interbreeding and retargeting of adeno-associated viruses. *J Virol* 2008; 82: 5887-5911. 2008/04/11. DOI: 10.1128/JVI.00254-08.
38. Chan KY, Jang MJ, Yoo BB, et al. Engineered AAVs for efficient noninvasive gene delivery to the central and peripheral nervous systems. *Nat Neurosci* 2017; 20: 1172-1179. 2017/07/04. DOI: 10.1038/nn.4593.
39. Zinn E, Pacouret S, Khaychuk V, et al. In Silico Reconstruction of the Viral Evolutionary Lineage Yields a Potent Gene Therapy Vector. *Cell Rep* 2015; 12: 1056-1068. 2015/08/04. DOI: 10.1016/j.celrep.2015.07.019.
40. Goertsen D, Flytzanis NC, Goeden N, et al. AAV capsid variants with brain-wide transgene expression and decreased liver targeting after intravenous delivery in mouse and marmoset. *Nat Neurosci* 2022; 25: 106-115. 2021/12/11. DOI: 10.1038/s41593-021-00969-4.
41. Cabanes-Creus M. *Novel AAV engineering technology: identification of improved AAV variants for gene addition and genome engineering in primary human cells*. Doctoral thesis, University College London, 2019.
42. Cabanes-Creus M, Hallwirth CV, Westhaus A, et al. Restoring the natural tropism of AAV2 vectors for human liver. *Sci Transl Med* 2020; 12: eaba3312. 2020/09/11. DOI: 10.1126/scitranslmed.aba3312.

43. Pekrun K, De Alencastro G, Luo QJ, et al. Using a barcoded AAV capsid library to select for clinically relevant gene therapy vectors. *JCI Insight* 2019; 4 2019/11/15. DOI: 10.1172/jci.insight.131610.
44. Lisowski L, Dane AP, Chu K, et al. Selection and evaluation of clinically relevant AAV variants in a xenograft liver model. *Nature* 2014; 506: 382-386. 2014/01/07. DOI: 10.1038/nature12875.
45. Cabanes-Creus M, Navarro RG, Liao SHY, et al. Characterization of the humanized FRG mouse model and development of an AAV-LK03 variant with improved liver lobular biodistribution. *Mol Ther Methods Clin Dev* 2023; 28: 220-237. 2023/01/27. DOI: 10.1016/j.omtm.2022.12.014.
46. Cabanes-Creus M, Westhaus A, Navarro RG, et al. Attenuation of Heparan Sulfate Proteoglycan Binding Enhances In Vivo Transduction of Human Primary Hepatocytes with AAV2. *Mol Ther Methods Clin Dev* 2020; 17: 1139-1154. 2020/06/04. DOI: 10.1016/j.omtm.2020.05.004.
47. Paulk NK, Pekrun K, Charville GW, et al. Bioengineered Viral Platform for Intramuscular Passive Vaccine Delivery to Human Skeletal Muscle. *Mol Ther Methods Clin Dev* 2018; 10: 144-155. 2018/08/14. DOI: 10.1016/j.omtm.2018.06.001.
48. Paulk NK, Pekrun K, Zhu E, et al. Bioengineered AAV Capsids with Combined High Human Liver Transduction In Vivo and Unique Humoral Seroreactivity. *Mol Ther* 2018; 26: 289-303. 2017/10/23. DOI: 10.1016/j.ymthe.2017.09.021.
49. Klimczak RR, Koerber JT, Dalkara D, et al. A novel adeno-associated viral variant for efficient and selective intravitreal transduction of rat Muller cells. *PLoS One* 2009; 4: e7467. 2009/10/15. DOI: 10.1371/journal.pone.0007467.
50. Shiroishi T, Sagai T, Natsuume-Sakai S, et al. Lethal deletion of the complement component C4 and steroid 21-hydroxylase genes in the mouse H-2 class III region, caused by meiotic recombination. *Proc Natl Acad Sci U S A* 1987; 84: 2819-2823. 1987/05/01. DOI: 10.1073/pnas.84.9.2819.
51. Huang W, Johnston WA, Boden M, et al. ReX: A suite of computational tools for the design, visualization, and analysis of chimeric protein libraries. *Biotechniques* 2016; 60: 91-94. 2016/02/05. DOI: 10.2144/000114381.
52. Tamura K, Stecher G and Kumar S. MEGA11: Molecular Evolutionary Genetics Analysis Version 11. *Mol Biol Evol* 2021; 38: 3022-3027. 2021/04/24. DOI: 10.1093/molbev/msab120.
53. Tamura K and Nei M. Estimation of the number of nucleotide substitutions in the control region of mitochondrial DNA in humans and chimpanzees. *Mol Biol Evol* 1993; 10: 512-526. 1993/05/01. DOI: 10.1093/oxfordjournals.molbev.a040023.
54. Ilicic T, Kim JK, Kolodziejczyk AA, et al. Classification of low quality cells from single-cell RNA-seq data. *Genome Biol* 2016; 17: 29. 2016/02/19. DOI: 10.1186/s13059-016-0888-1.
55. Pihlajoki M, Gretzinger E, Cochran R, et al. Conditional mutagenesis of Gata6 in SF1-positive cells causes gonadal-like differentiation in the adrenal cortex of mice. *Endocrinology* 2013; 154: 1754-1767. 2013/03/09. DOI: 10.1210/en.2012-1892.
56. Huang CC and Kang Y. The transient cortical zone in the adrenal gland: the mystery of the adrenal X-zone. *J Endocrinol* 2019; 241: R51-R63. 2019/03/01. DOI: 10.1530/JOE-18-0632.
57. Howard-Miller E. A transitory zone in the adrenal cortex which shows age and sex relationships. *Am J Anat* 1927; 40: 251-293. DOI: 10.1002/aja.1000400204.
58. Yamaoka T and Itakura M. Development of pancreatic islets (review). *Int J Mol Med* 1999; 3: 247-261. 1999/02/24. DOI: 10.3892/ijmm.3.3.247.
59. Wang X, Shen C, Chen X, et al. Tafa-2 plays an essential role in neuronal survival and neurobiological function in mice. *Acta Biochim Biophys Sin (Shanghai)* 2018; 50: 984-995. 2018/08/24. DOI: 10.1093/abbs/gmy097.
60. Jafari A, Isa A, Chen L, et al. TAFA2 Induces Skeletal (Stromal) Stem Cell Migration Through Activation of Rac1-p38 Signaling. *Stem Cells* 2019; 37: 407-416. 2018/11/30. DOI: 10.1002/stem.2955.
61. Brodeur GM and Bagatell R. Mechanisms of neuroblastoma regression. *Nat Rev Clin Oncol* 2014; 11: 704-713. 2014/10/22. DOI: 10.1038/nrclinonc.2014.168.
62. Xia Q, Li Q, Gan S, et al. Exploring the roles of fecundity-related long non-coding RNAs and mRNAs in the adrenal glands of small-tailed Han Sheep. *BMC Genet* 2020; 21: 39. 2020/04/08. DOI: 10.1186/s12863-020-00850-6.
63. Sheftel AD, Stehling O, Pierik AJ, et al. Humans possess two mitochondrial ferredoxins, Fdx1 and Fdx2, with distinct roles in steroidogenesis, heme, and Fe/S cluster biosynthesis. *Proc Natl Acad Sci U S A* 2010; 107: 11775-11780. 2010/06/16. DOI: 10.1073/pnas.1004250107.
64. Vickery LE. Molecular recognition and electron transfer in mitochondrial steroid hydroxylase systems. *Steroids* 1997; 62: 124-127. 1997/01/01. DOI: 10.1016/s0039-128x(96)00170-5.
65. Pastel E, Pointud JC, Martinez A, et al. Aldo-Keto Reductases 1B in Adrenal Cortex Physiology. *Front Endocrinol (Lausanne)* 2016; 7: 97. 2016/08/09. DOI: 10.3389/fendo.2016.00097.
66. Endo S, Matsunaga T and Nishinaka T. The Role of AKR1B10 in Physiology and Pathophysiology. *Metabolites* 2021; 11: 332. 2021/06/03. DOI: 10.3390/metabo11060332.

67. Aigueperse C, Martinez A, Lefrancois-Martinez AM, et al. Cyclic AMP regulates expression of the gene coding for a mouse vas deferens protein related to the aldo-keto reductase superfamily in human and murine adrenocortical cells. *J Endocrinol* 1999; 160: 147-154. 1998/12/17. DOI: 10.1677/joe.0.1600147.
68. Jones IC. The disappearance of the X zone of the mouse adrenal cortex during first pregnancy. *Proc R Soc Lond B Biol Sci* 1952; 139: 398-410. 1952/04/24. DOI: 10.1098/rspb.1952.0020.
69. Lanman JT. The fetal zone of the adrenal gland: its developmental course, comparative anatomy, and possible physiologic functions. *Medicine (Baltimore)* 1953; 32: 389-430. 1953/12/01. DOI: 10.1097/00005792-195312000-00001.
70. Howard-Miller E. A transitory zone in the adrenal cortex which shows age and sex relationships. *Am J Anat* 2005; 40: 251-293. DOI: 10.1002/aja.1000400204.
71. Gannon AL, O'Hara L, Mason JI, et al. Androgen receptor signalling in the male adrenal facilitates X-zone regression, cell turnover and protects against adrenal degeneration during ageing. *Sci Rep* 2019; 9: 10457. 2019/07/20. DOI: 10.1038/s41598-019-46049-3.
72. Sakata Y, Cheng K, Mayama M, et al. Reconstitution of human adrenocortical specification and steroidogenesis using induced pluripotent stem cells. *Dev Cell* 2022; 57: 2566-2583 e2568. 2022/11/23. DOI: 10.1016/j.devcel.2022.10.010.

Chapter 6

A genomic editing approach to congenital adrenal hyperplasia

6.1 Introduction

Despite the development of glucocorticoid replacement therapy for congenital adrenal hyperplasia (CAH) in the mid-20th century, such treatment cannot recapitulate physiological requirements, resulting in excess morbidity and mortality for affected patients. Alternative treatment options are sought. The gene therapy field is revolutionising the treatment of monogenic disorders, and rAAV is the leading viral vector for *in vivo* gene delivery. Physiological cortisol secretion regulated by pituitary adrenocorticotropin could be achieved through genomic editing to repair the defective 21-hydroxylase gene *in situ*, thereby offering the potential to restore normal adrenal function without the requirement for regular patient intervention. However, the adrenal cortex is continually replaced from progenitor cells and therefore correcting the 21-hydroxylase locus in the genome of adrenocortical progenitor cells is required for a durable effect.

AAV has an advantage over many other viral vector gene delivery systems as the capsid can be engineered to increase delivery to certain targeted cell populations. Chapter 5

provided the foundation for determining rAAV capsid serotypes that provide gene delivery to the adrenocortical progenitor cells. However, it remains unknown whether any of the capsid serotypes tested can transduce this elusive and difficult to identify cell population. Nevertheless, a genomic editing approach can be developed without specific knowledge of the rAAV capsid serotype that will transduce the progenitor cells. Editing the locus in differentiated adrenocortical progenitor cells proves that the locus is amenable to editing and reagents could be repacked into an effective capsid once that is determined.

Early genomic editing techniques such as zinc-finger nucleases have largely been superseded by strategies that employ CRISPR/Cas9 technology.[1] This system allows RNA-guided precise double-stranded DNA breaks, and in the presence of a repair template the host's DNA repair mechanisms can be exploited to facilitate a site-specific modification into the host's genome.[2] Homology-independent targeted integration (HITI) has the advantage over homology directed repair (HDR)-based editing as it exploits non-homologous end-joining (NHEJ) DNA repair which is efficient in both dividing and non-dividing cells.[3] Guide RNA (sgRNA) within the CRISPR/Cas9 complex ensures the host DNA is precisely cleaved in the guide sequence. Similarly, when the target sequence is provided in the donor genome, CRISPR/Cas9 creates double-stranded DNA cleavage in the donor genome. The donor sequence is then integrated into the host DNA, at the target site. Theoretically, this system is self-correcting: if the donor sequence is integrated in the reverse orientation, the guide sequence and PAM sites re-align, and CRISPR/Cas9 will cleave the donor sequence out again. If the donor sequence is integrated in the correct position, the guide sequence and PAM sites do not align, and no further DNA breaks occur.[4] In reality, donor segments may remain in the reverse orientation due to DNA

repair via NHEJ inducing indels that destroy the target sequence.[5] Furthermore, there is mounting evidence,[6, 7] including unpublished data from our lab, that multiple unintended events can occur following DNA cleavage including integration of subgenomic fragments from either the donor vector or the Cas9 vector genomes, all of which would be expected to be detrimental and compete with integration of the correctly oriented complete donor segment at the cut site. These caveats must be considered with utilising HITI-based gene editing.

6.1.1 Special considerations for the 21-hydroxylase locus

6.1.1.1 Locus complexity

The gene for 21-hydroxylase, *CYP21A2*, lies within the MHC class III sequence which is considered one of the most complex regions of the human genome.[8, 9] There are at least 14 distinct transcripts in the 140 kb region, and this includes genes that overlap and genes within genes.[10, 11] *CYP21A2* has a homologous pseudogene, *CYP21A1P*, 30 kb upstream, and this pair of genes lie in tandem repeat with two complement 4 genes (*C4A* and *C4B*) (Chapter 1, Figure 1-6). *CYP21A1P* shares 98% exonic and 96% intronic homology with *CYP21A2*,[12] however the pseudogene has multiple mutations along its length, rendering the transcribed mRNA non-functional.[12, 13] It is the presence of this pseudogene which is thought to be the reason why 21-hydroxylase deficiency is far more common than any of the other forms of CAH, as the high level of homology leads to an increased risk of erroneous recombination events during meiosis.[12, 14-22] There is a similar tandem genetic arrangement in the mouse, however the functional gene is upstream (*Cyp21a1*), and the pseudogene is 80 kb downstream (*Cyp21a1-ps*). There is high level of homology between the murine 21-hydroxylase genes, however the murine pseudogene lacks the equivalent of exon 2.

The high homology between the active and pseudogene for 21 hydroxylase has implications for the choice of target sequence when utilising a CRISPR/Cas9-based approach, as a double stranded break in both genes could result in dropping out 30 kb in the human, (and 80 kb in the mouse) genomic sequence between them, which would notably include the *C4B* gene. This issue is not as relevant to the H-2aw18 CAH mouse model due to a large 80 kb deletion which includes the 3' end of *Cyp21a1* (from exon 8), *C4*, and the 5' end of *Cyp21a2-ps* (Chapter 3, Figure 3-2).[23] Thus the 5' region of interest is only present in the *Cyp21a1* gene in the H-2aw18 homozygous mouse.

6.1.1.2 Spectrum of gene mutations

There are over 350 known variants in *CYP21A2* listed in the Human Gene Mutation Database (HGMD, http://www.hgmd.cf.ac.uk, accessed 26/04/2024)[24] spanning the promoter region and all 10 exons and associated intronic regions. The variants include over 55 complex rearrangements, over 15 large deletions/insertions or duplications, and many other mutation types. This has implications for the choice of editing technique, as a highly localised technique such as prime editing[25] would not be a practical choice. Furthermore, any repair mechanism for humans requiring homology arms (see Chapter 1.4.3) would be similarly impractical as a new set of reagents would be required for each individual's polymorphisms in the homology arm sites. Therefore, the most feasible editing technique is to utilise HITI to introduce the entire or most of the wild-type 21-hydroxylase cDNA deep within a non-coding sequence, such that most if not all potential mutations could be cured with a single set of reagents.

6.1.1.3 Non-coding regions

Ideally, the target sequence for a double-stranded break should be deep within a non-coding region, to avoid the risk of knocking out residual function in a hypomorphic (ie weakly functional or under expressed) allele. However, the introns in *Cyp21a1* are very small, limiting the choices for target sites within non-coding regions. Intron 1 is 64 bp and intron 2 is 352 bp (NCBI RefSeq: NC_000083.7); in comparison to other murine genes such as the *Otc* gene which has a much larger first intron of 14 517 bp (NC_000086.8) or 16 466 bp in intron 1 of the murine *Cps1* gene (NC_000067.7).

6.1.2 Special considerations for the adrenal cortex

The adrenal cortex continuously renews from progenitor cells situated beneath the capsule and differentiated adrenocortical cells undergo minimal replication as they pass down the cortex towards the medulla. Furthermore, rAAV treatment can currently only be administered once as neutralising antibodies induced by the initial exposure render further doses ineffective. Thus, for durable gene therapy, the genome of the adrenal progenitor cells must be repaired to ensure daughter cells maintain the correction. As progenitor cells may be quiescent, a HITI strategy is the more appropriate method than HDR to edit the genome of progenitor cells.[5] However, targeting the adrenal progenitor cells is challenging with the current state of contemporary technology reach and biological knowledge. This chapter seeks to demonstrate a proof-of-concept approach by introducing targeted editing events in the 21-hydroxylase locus in differentiated adrenocortical cells *in vivo* through rAAV-mediated CRISPR/Cas9 delivery, using a homology-independent targeted integration strategy (Figure 6-1). If successful, the editing reagents developed by this strategy could be re-packaged into an appropriate

capsid for future targeting of the adrenal cortex progenitor cells, once the rAAV serotype that can transduce this specific cell population is identified.

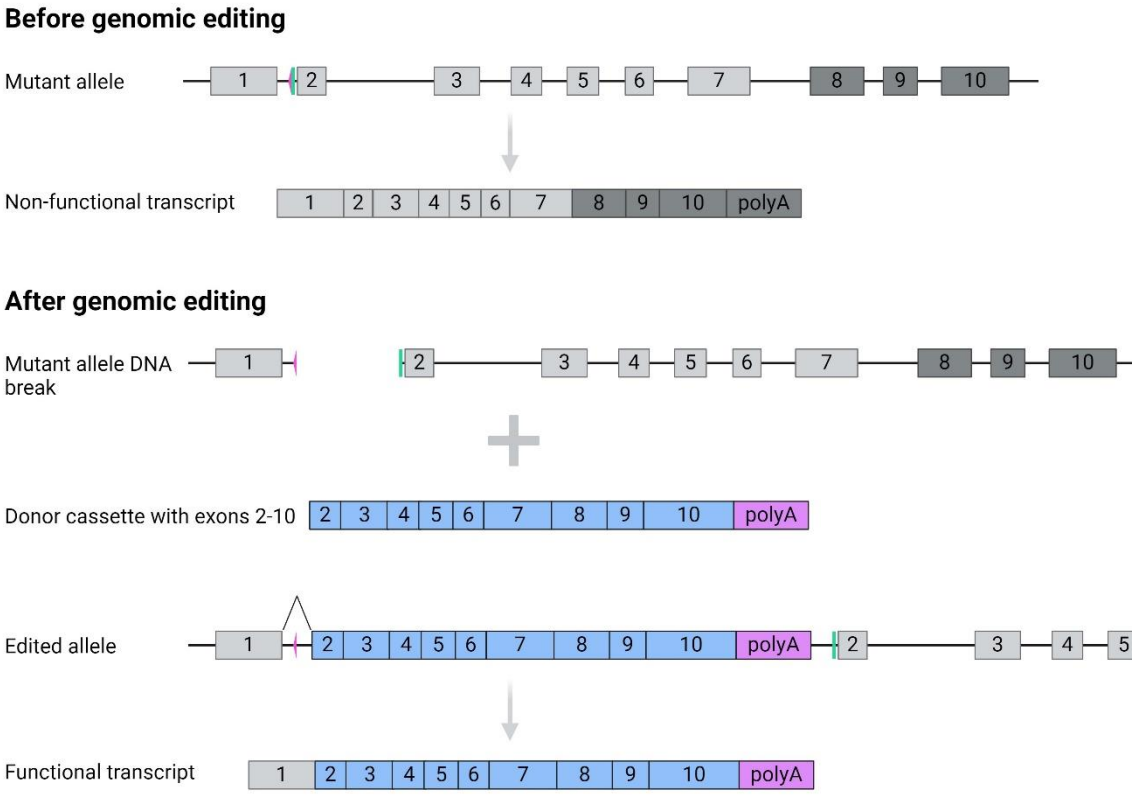

Figure 6-1 A HITI strategy was used to integrate the donor at the target locus.
In the mouse model for CAH, the mutant locus is a fusion of the wild-type exons 1-7 and pseudogene exons 8-10. While it is transcribed, the resultant mRNA is non-functional. In this HITI approach, a double stranded break is made in the first intron. The donor cassette with codon optimised exons 2-10 and a splice acceptor is integrated into the cut site. The native promoter is captured, and the mRNA transcribed, which is a fusion of the native exon 1 and the donor exons 2-10. This mRNA is functional. PAM sequence (pink), target sequence (green), mutant exons (dark grey), functional exons (light grey), codon optimised donor exons (blue), donor polyA (purple).

6.2 Chapter-specific methods

6.2.1 Vectors

6.2.1.1 Guide design, sub-cloning and vector production

Guide RNAs were designed *in silico* using CRISPOR (http://crispor.tefor.net/) to target protospacer adjacent motif (PAM) sequences in intronic sequences of the mutant murine *Cyp21a1* gene, that were not present in the pseudogene. As intron 1 was small (64 bp), guides were selected from both intron 1 and intron 2 (355 bp). There was one potentially viable target site identified in intron 1 and two identified in intron 2. The top 3 guide sequences were selected (Table 6-1, Figure 6-2). Each sequence was cloned into the Cas9 plasmid (Addgene plasmid # 61591)[26] backbone (Figure 6-3). Custom DNA oligos were ordered for each guide and complementary sequences with 5'-CACC and 5'AAAC overhangs, and G addition to guide 3 as a G at the 5' end of the guide sequence improves expression from the U6 promoter (Table 6-2). The vectors were pseudo-serotyped with AAVRh10 (rAAV2/Rh10) and packaged by the Vector Genome Engineering Facility, CMRI using standard triple transfection, caesium purification, and vector genome titre determination with digital droplet PCR.

Table 6-1 Guide sequences designed with CRISPOR.

Guide no.	Location	ID	Guide sequence 5' to 3'	PAM
1	Intron 1	31rev	GGACAATGTCAGGCAGGGAAG	AGGGGT
2	Intron 2	13rev	GGAAGGGAGGGGAAACTGAGC	AAGGGT
3	Intron 2	189rev	AAGACCTAATCTTAAAGAAGA	GGGAGT

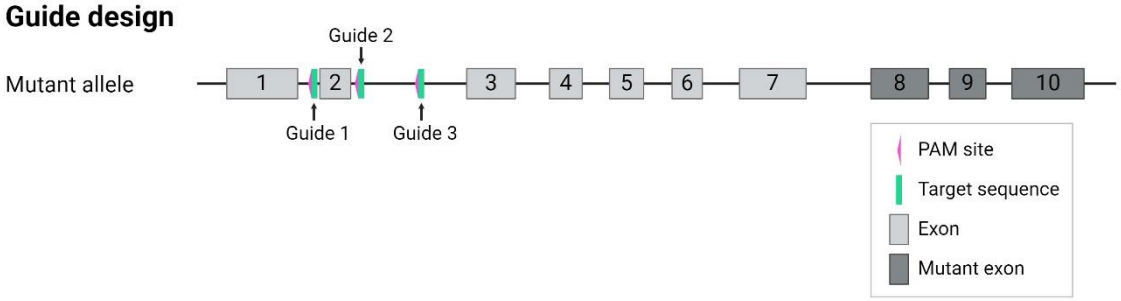

Figure 6-2 Target sequence locations.
Guides were chosen from introns 1 and 2. Target sequence (green), PAM site (pink).

Table 6-2 Custom oligo sequences ordered for each guide.

Guide no.	Oligo sequence 5' to 3'	Complimentary oligo sequence 5' to 3'
1	CACCGGACAATGTCAGGCAGGGAAG	AAACCTTCCCTGCCTGACATTGTCC
2	CACCGGAAGGGAGGGGAAACTGAGC	AAACGCTCAGTTTCCCCTCCCTTCC
3	CACCGAAGACCTAATCTTAAAGAAGA	AAACTCTTCTTTAAGATTAGGTCTTC

5'-CAAC and 5'AAAC overhands are shown in brown and G addition to guide 3 is shown in blue.

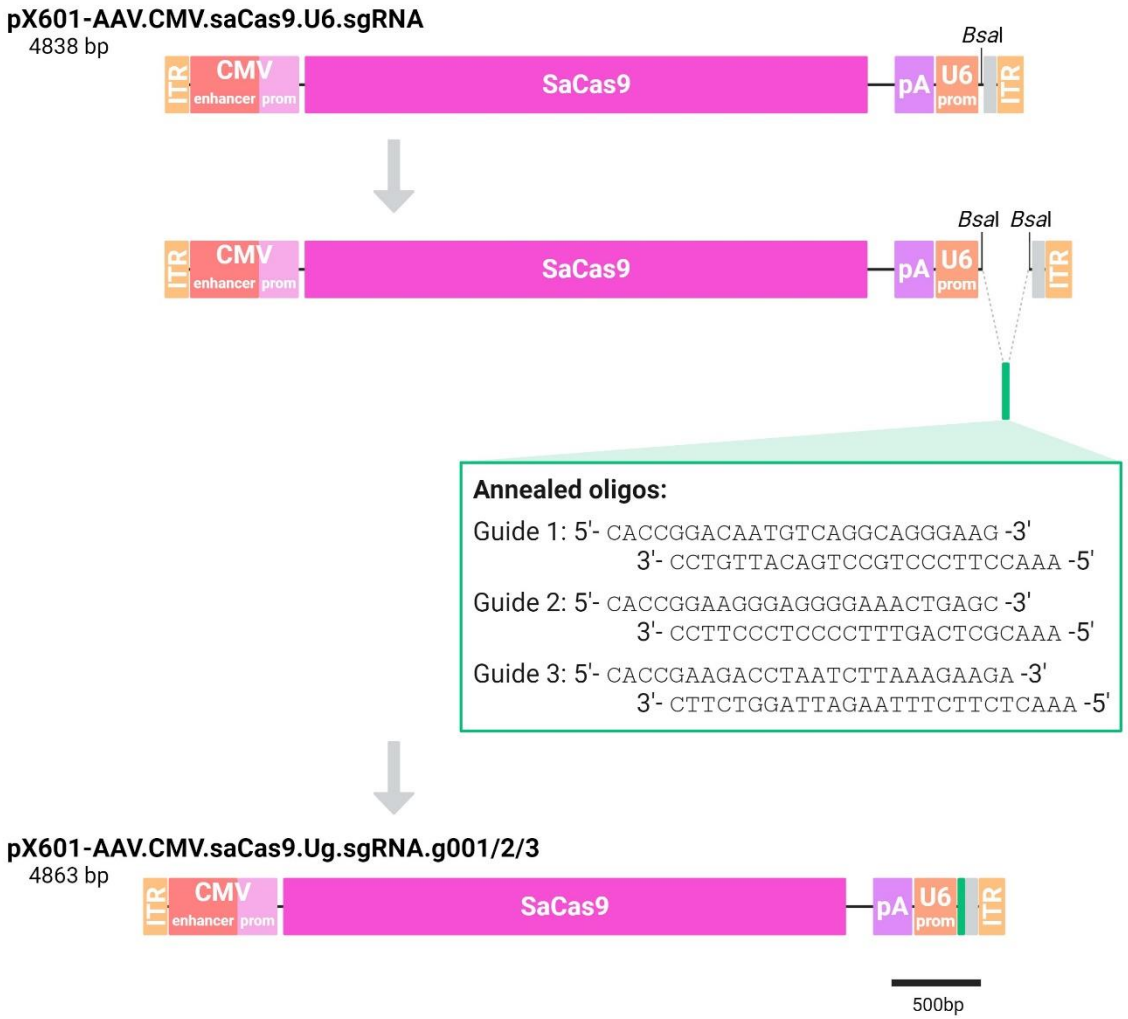

Figure 6-3 Cloning steps to construct SaCas9 and guide vector plasmids.

Flow diagram of the molecular subcloning steps taken to generate the guide vectors. The PX601-AAV.CMV.saCas9.U6.sgRNA backbone was prepared by digesting with BsaI. The oligos were annealed and ligated to the backbone. AAV2 ITRs (orange) flank the expression cassette. The expression cassette contains the ubiquitous CMV enhancer/promoter (red and pink), SaCas9 (magenta), bovine growth hormone polyadenylation tail (pA, purple), U6 promoter (dark orange), guide sequence (green), Sa gRNA scaffold (grey). Scale bar = 500 bp.

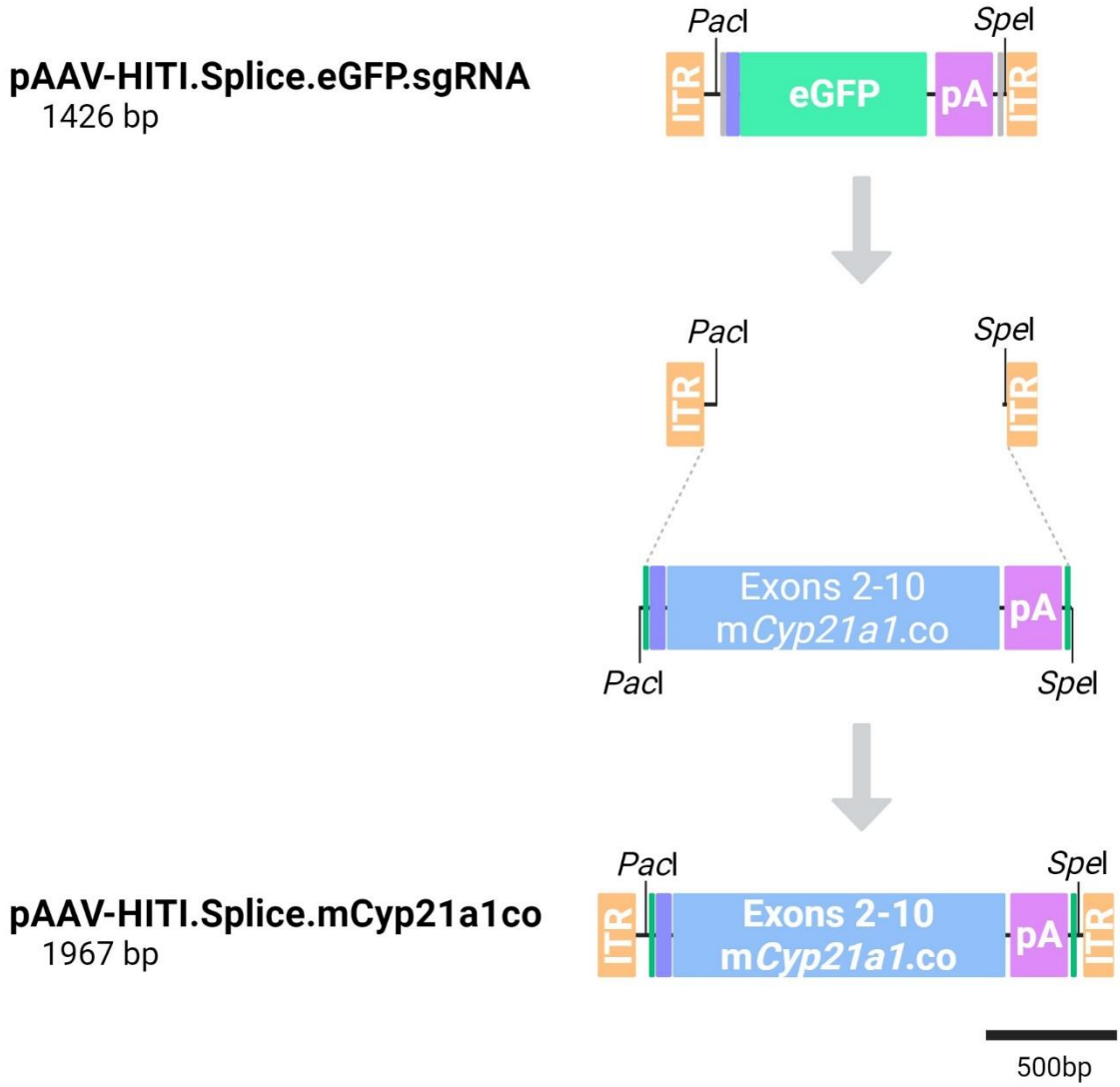

Figure 6-4 Cloning steps to construct the donor vector plasmid.

The pAAV-HITI.Splice.eGFP.sgRNA backbone was prepared by digesting with PacI and SpeI to remove the eGFP expression cassette. The donor construct was prepared by digesting the GeneWiz plasmid with PacI and SpeI. The donor cassette was ligated into the backbone. AAV2 ITRs (orange) flank the expression cassette. The expression cassette contains the guide target sequence and PAM site (dark green), splice acceptor site (dark blue), codon optimised exons 2-10 for *Cyp21a1* (blue), bovine growth hormone polyadenylation tail (pA, purple). Scale bar = 500 bp.

6.2.1.2 Donor cassette design, sub-cloning and production

Guide 1 was chosen, and a donor cassette was designed to complement this target site. As the target site and PAM sequences were located in intron 1 in the splice acceptor region, a donor cassette was designed which included a splice acceptor site and branch point, codon optimised exons 2-10 from the wild type *Cyp21a1* gene and a bovine growth hormone polyA signal. The splice acceptor site and branch point sequence were designed by S. Ginn, GTRU, CMRI. The cDNA was purchased from GeneWiz. The donor cassette was cloned into the eGFP HITI backbone (provided by S. Ginn) (Figure 6-4). The vector was pseudo-serotyped with AAVRh10 (rAAV2/Rh10) and packaged by the Vector Genome Engineering Facility, CMRI using standard methods.

6.2.2 Animal procedures

6.2.2.1 *In vivo* guide testing

As the guides targeted sites present in the mutant locus, *in vivo* testing was required. Older homozygous mutant males were used which had been bred but not yet used experimentally and were too old to compare serum steroids. Each guide vector was dosed at 5×10^{11} vc/mouse (n=3 per guide vector). Mice were harvested 3-4 weeks after treatment. A further 3 mice were treated with the most promising guide at a dose of 2.5×10^{12} vc/mouse.

6.2.2.2 *In vivo* editing

Male and female 21-hydroxylase deficient mice (average weight 19.2g) were injected intravenously via the tail vein with vector. The HITI treated mice received 2.5×10^{12} vc/mouse of the CRISPR/guide vector and 1×10^{12} vc/mouse of the donor vector (total

vector dose 3.5×10^{12} vc/mouse). Donor-only control mice received 1×10^{12} vc/mouse of the donor vector.

6.2.3 Analysis of animal samples

6.2.3.1 Indel determination

For the *in vivo* guide testing, the presence of insertions/deletions (indels) was used to determine guide efficiency. Following standard DNA extraction, a PCR using the primers LG_008 and LG_011 (Chapter 2, Table 2-8) was performed to extract the mutant locus between exon 1 and exon 3. This PCR product was isolated by gel electrophoresis, the band excised, purified and sent for Sanger sequencing at AGRF. The sequences were aligned with the control sequence using Synthego ICE (https://ice.synthego.com/)[27] to determine the rate of insertions/deletions (indels) as a marker of targeted double stranded DNA breaks.

6.2.3.2 Quantifying vector copy number and editing events

DNA from liver and adrenal glands were analysed by digital PCR (dPCR) to determine the vector genome copy number per cell (Primers 107 and 108, Table 6-3; and SG330R and SG331R, Chapter 2, Table 2-8), normalising to two copies of murine albumin (diploid nucleus) (Primers LB0042mouse ALB_F and LB0042mouse ALB_R, Chapter 2, Table 2-8). Editing events were normalised to one copy of murine albumin to determine percentage of alleles. The editing events examined are listed (Table 6-3).

Table 6-3 Chapter-specific primers used in dPCR analysis.

Purpose	Spanning	Primers	Sequences 5' to 3'
Vector copy number donor cassette	Donor exons 5 and 6 target	107	TTCACGATGTGGTCCCTAGA
		108	GGAGCATTCAGATCCTGACC
Unedited *Cyp21a1* alleles	native exon 1 to native exon 2	104	CATCTACAGGATCCGCTTGG
		115	ATTTAGCATATGGGGTCGGC
5' junction HITI editing event	native exon 1 to donor exon 2	103	CCTCGATGGTCCTATTGCTG
		104	CATCTACAGGATCCGCTTGG
3' junction HITI editing event	donor polyA to native exon 2	112	GGGAAGACAATAGCAGGCAT
		115	ATTTAGCATATGGGGTCGGC
5' junction reverse donor insertion	Native exon 1 to donor poly A	104	CATCTACAGGATCCGCTTGG
		112	GGGAAGACAATAGCAGGCAT
3' junction reverse donor insertion	Donor exon 2 to native exon 2	103	CCTCGATGGTCCTATTGCTG
		115	ATTTAGCATATGGGGTCGGC

6.2.3.3 Quantifying edited transcripts

Complementary DNA (cDNA) was synthesised from RNA as per methods listed in Chapter 2. Digital PCR was used to quantify edited transcripts and normalised to *Tbp* (LG_102F_tbp and LG_103R_tbp, Chapter 2, Table 2-8). Primer pairs 104 & 115, 103 & 104 and 104 & 112 were used to quantify the events in cDNA (Table 6-3). RNA extraction, cDNA synthesis and dPCR was performed by Lakshmy Viswanath, research assistant.

6.2.4 Immunohistochemistry

Immunohistochemistry slides made from PFA fixed adrenal glands and stained for 21-hydroxylase protein were prepared as described in Chapter 2, Section 2.2.5.1.1 using the primary rabbit CYP21A2 antibody (Abcam ab230327) diluted 1:50. Cryo-sectioning, staining and imaging was performed by Lakshmy Viswanath, research assistant.

6.3 Results

6.3.1 SaCas9/guide vector testing *in vivo*

6.3.1.1 Standard dose guide testing

Guides were tested *in vivo* by intravenous administration to homozygous mutants at a dose of 5×10^{11} vg/mouse. Mice were harvested 4 weeks after vector treatment. DNA was extracted from the liver and adrenal glands. Non homologous end-joining DNA repair following DNA cleavage is error prone and introduces insertions/deletions (indels) that can be detected by sequencing. Amplification by PCR across the predicted SaCas9 cleavage site was performed, the band excised and purified. The purified products were Sanger sequenced and quantification of indels was performed using Synthego ICE.

6.3.1.1.1 Guide 2 and 3

Intron 2 had 16 repeats of the nucleotide cytosine which interfered with the accuracy of PCR. This impeded the ability to accurately determine the indel rate when using guide 2. Guide 3 did not induce detectable indels in either liver or adrenal DNA.

6.3.1.1.2 Guide 1

Analysis of the sequencing results for Guide 1 in Synthego ICE demonstrated editing events (indels) at the desired genomic locus within the murine *Cyp21a1* gene in the liver of the treated mice (Table 6-4, Figure 6-5). However, no indels in the adrenal gland DNA were detected. If the plots and traces are examined, there appear to be sub-threshold events occurring in the adrenal glands (Figure 6-6) therefore the experiment was repeated at a higher dose.

Table 6-4 Indels following standard dose guide 1 treatment.

Mouse ID	Liver indel rate	Adrenal indel rate
A684	10%	0%
B059	0%	0%
B368	17%	0%

Percent of insertions/deletions (indels) detected in the liver and adrenal DNA of the mice treated with a standard dose of guide 1.

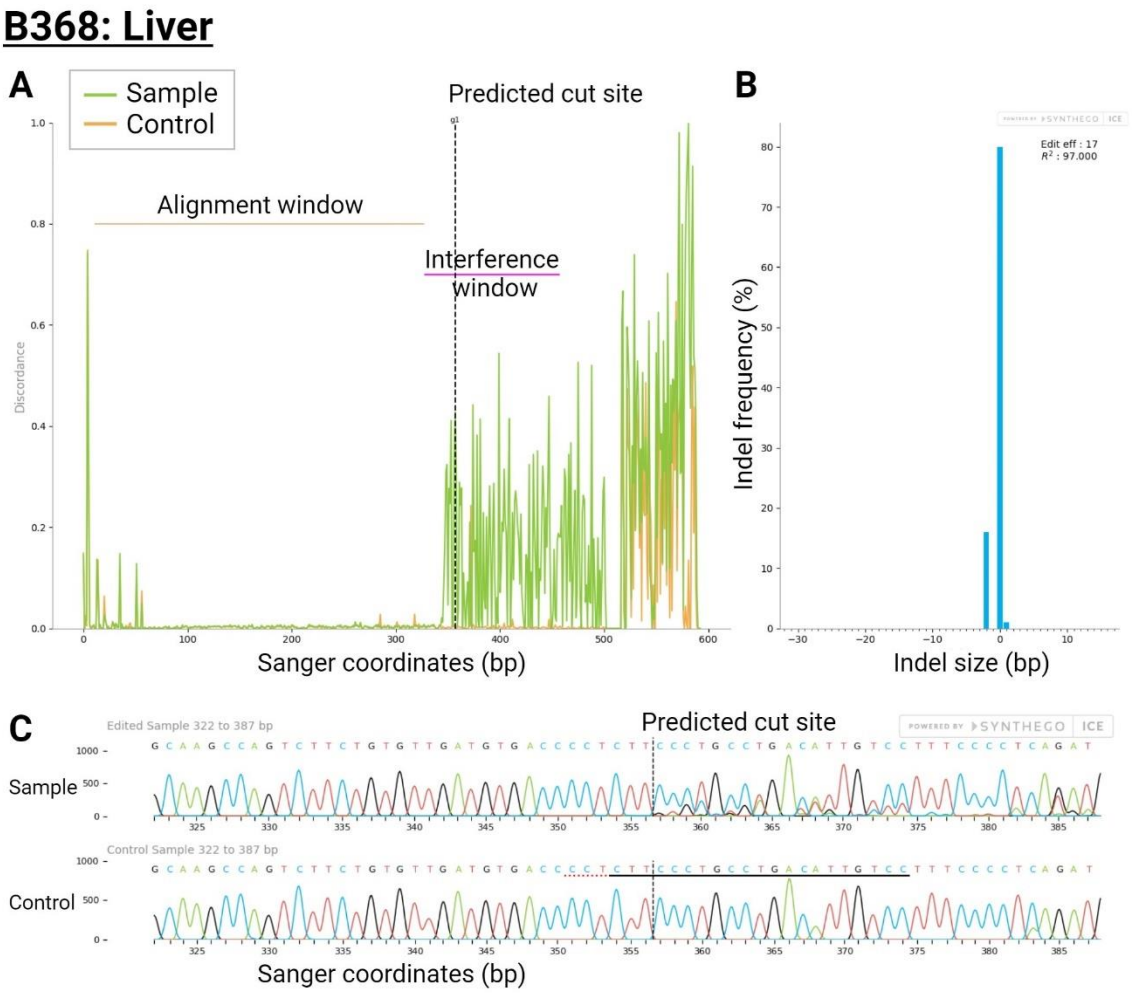

Figure 6-5 Liver DNA plots and traces from representative mouse (B368) treated with standard dose Guide 1.

The PCR was unable to cross the C repeats which is demonstrated in noise in the control (orange) as well as the green treated samples. **A.** Discordance for the sample (green) and control (orange) trace files. The vertical dotted line marks the expected cut site. **B.** Insertion or deletion (indel) sizes (blue), as calculated by ICE. **C.** Trace segments spanning the cut site from the control and the edited samples. The guide target sequence is underlined in black, and the protospacer adjacent motif sequence is marked by a dotted red underline in the control sample. Vertical dotted lines denote the expected cut site.

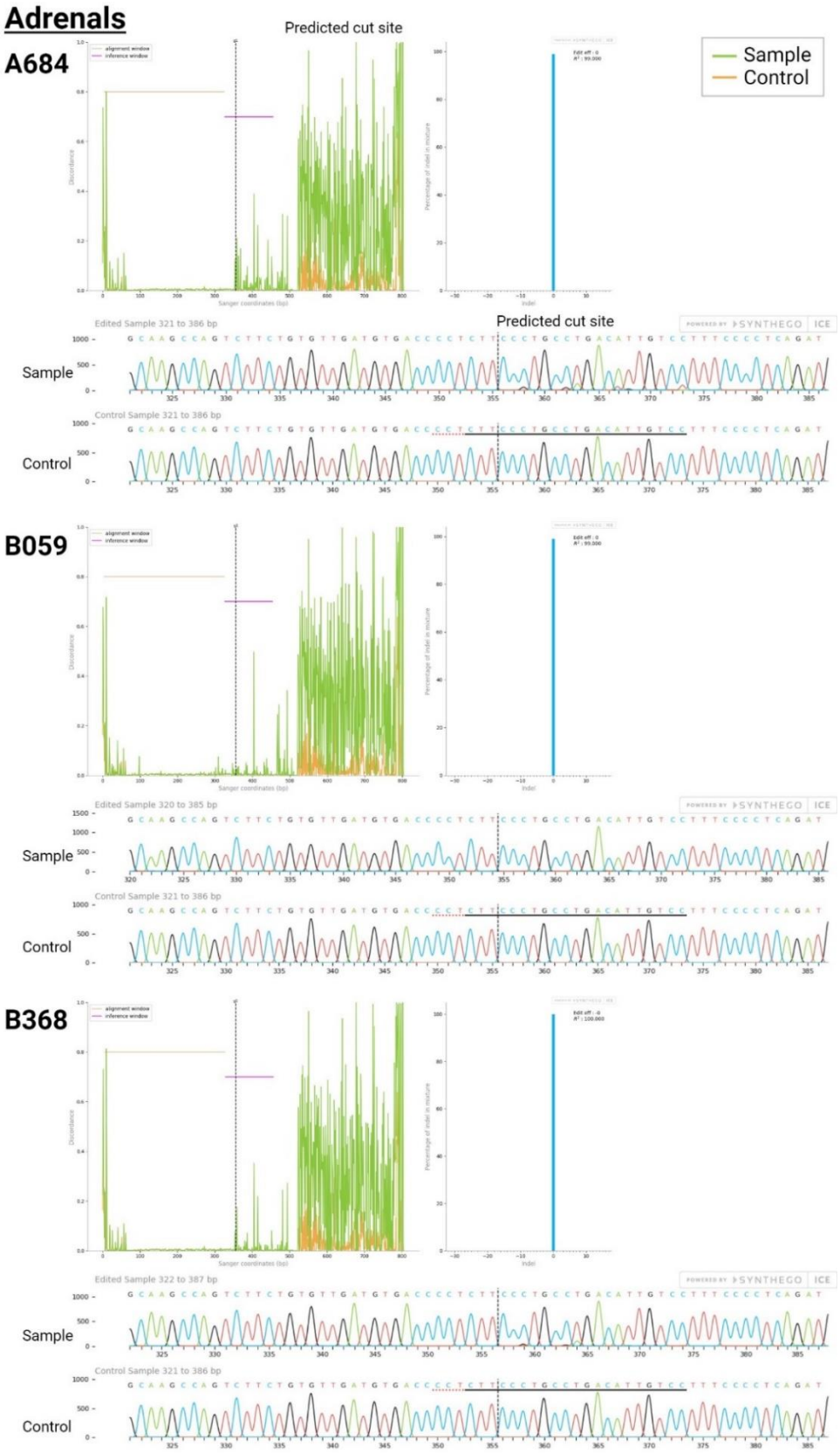

Figure 6-6 Adrenal gland DNA plots and traces for standard dose guide 1.

Discordance for sample (green) and control (orange) and trace segments spanning the expected cut site demonstrate possible subthreshold indels in the adrenal gland standard dose-treated mice that received Guide 1.

6.3.1.2 Delivery of a high dose of guide 1 vector *in vivo*

The experiment was repeated with guide 1 at a high dose (2.5×10^{12} vg/mouse) and editing events (indels) were detected in the adrenal DNA (Table 6-5, Figure 6-7). As there was evidence of site-specific modification in the adrenal after using guide 1, a complementary donor cassette was designed. Vector copy number per diploid cell and indel rates (percentage) for all guide treated mice are shown (Figure 6-8).

Table 6-5 Indels following high dose guide treatment.

Mouse ID	Liver indel rate	Adrenal indel rate
B330	13%	9%
B406	10%	9%
B434	2%	4%

Percent of insertions/deletions (indels) detected in the liver and adrenal DNA of the mice treated with a high dose of guide 1.

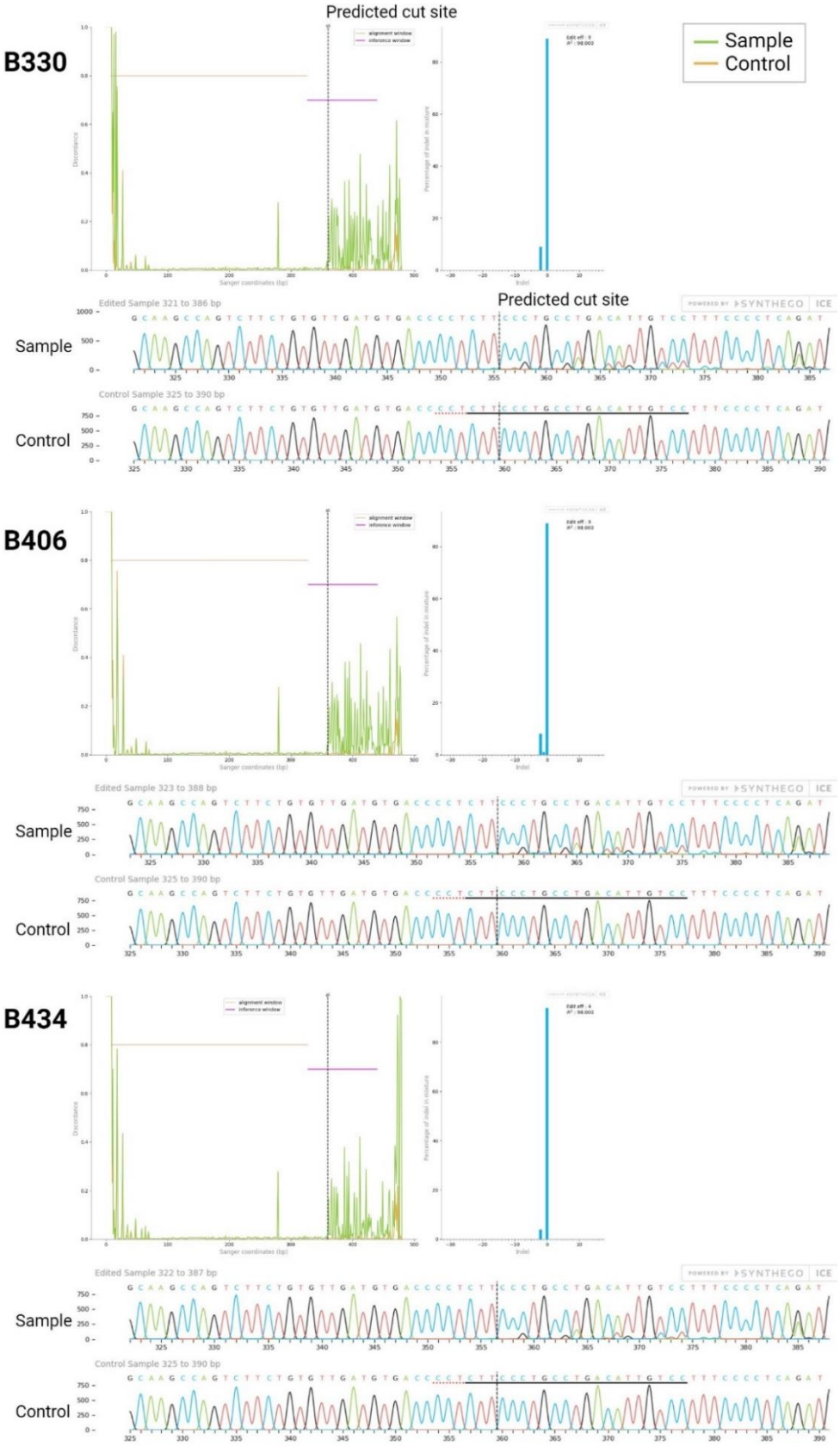

Figure 6-7 Adrenal gland DNA plots and traces for high dose guide 1.
Discordance, indel size and traces from SynthegoICE from the adrenal glands of the mice treated with high-dose guide 1 demonstrating presence of indels at the expected cut site.

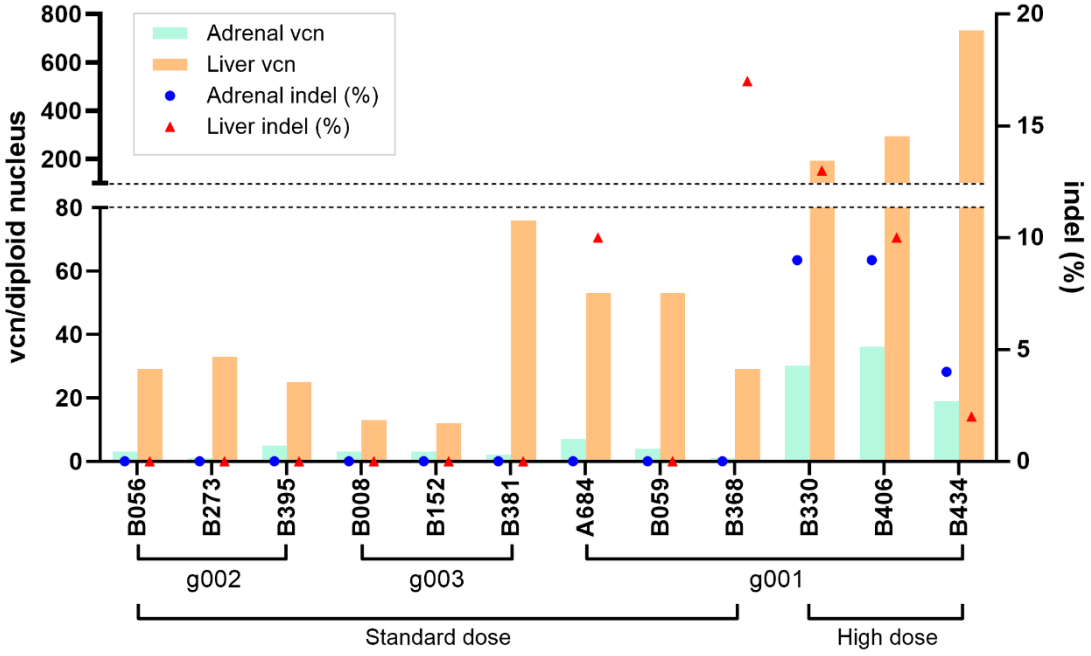

Figure 6-8 Vector copy number per cell vs indel rate in adrenal and liver DNA.
Data from individual mice are shown. The bar graph uses the left y axis and shows vector copy number for the Cas9/guide vector per diploid nucleus. The dot graph uses the right y axis and shows the percent of insertions/deletions (indels). Standard dose was 5×10^{11} vg/mouse and high dose was 2.5×10^{12} vg/mouse. Abbreviations: vg, vector genomes; vcn, vector copy number; indel, insertions or deletions; g001, Guide 1; g002, Guide 2; g003, Guide 3.

6.3.2 *In vivo* gene editing conferred editing events and phenotypic change

6.3.2.1 Delivery of SaCas9 and donor template

Delivery of the vectors to the liver and adrenal gland was quantified with dPCR. The vector copy number (vcn) per diploid nucleus for the SaCas9 vector and donor vector are shown (Figure 6-9). There was no relationship in vector copy between the two vectors (Figure 6-10).

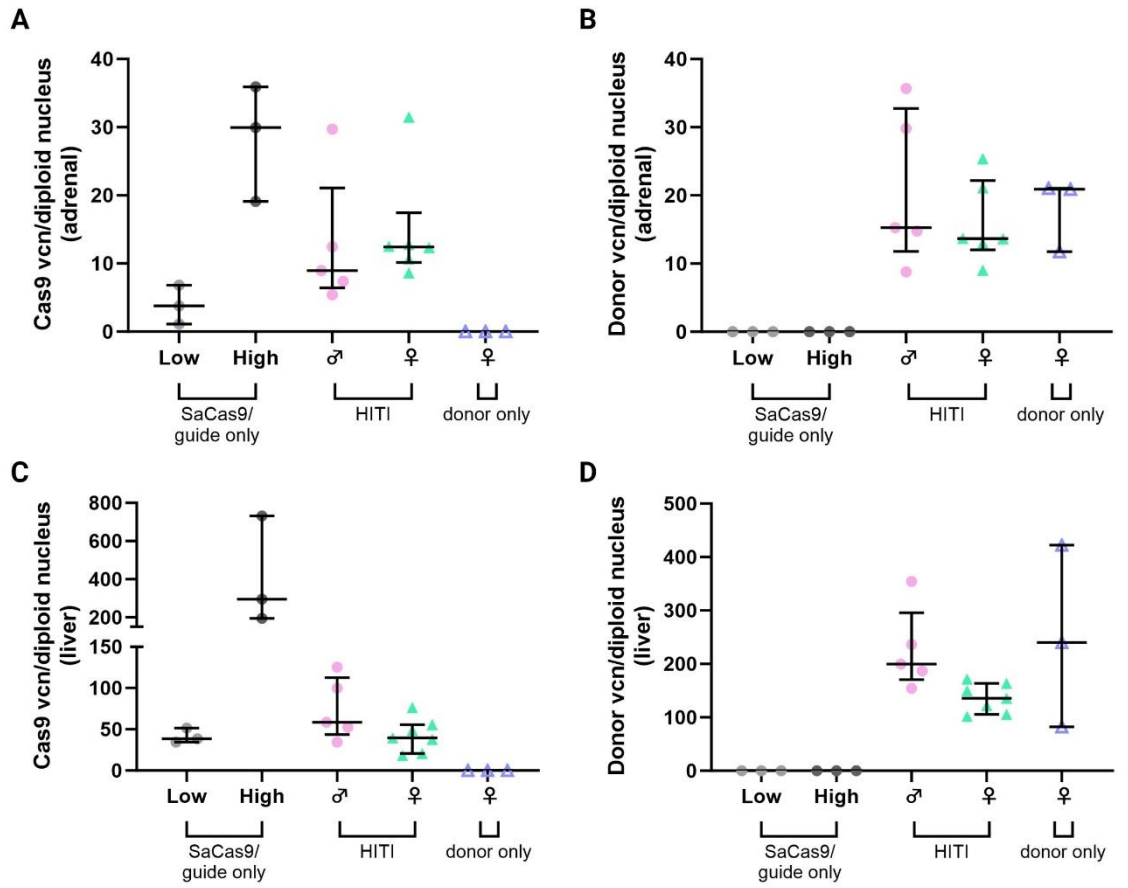

Figure 6-9 Vector copy number per cell in adrenal gland and liver genomic DNA. **A.** Cas9 vector copy number (vcn) per diploid nucleus in adrenal genomic DNA. **B.** Donor vcn per diploid nucleus in adrenal genomic DNA. **C.** Cas9 vcn per diploid nucleus in liver genomic DNA. **D.** Donor vcn per diploid nucleus in liver genomic DNA. Abbreviations: Low, 5×10^{11} vg/mouse; High, 2.5×10^{12} vg/mouse; vg, vector genomes; vcn, vector copy number; HITI, homozygous 21-hydroxylase deficient mice that were treated with both the SaCas9/guide and donor vectors; ♀, female; ♂, male. Individual data points are shown, and error bars represent median and interquartile range.

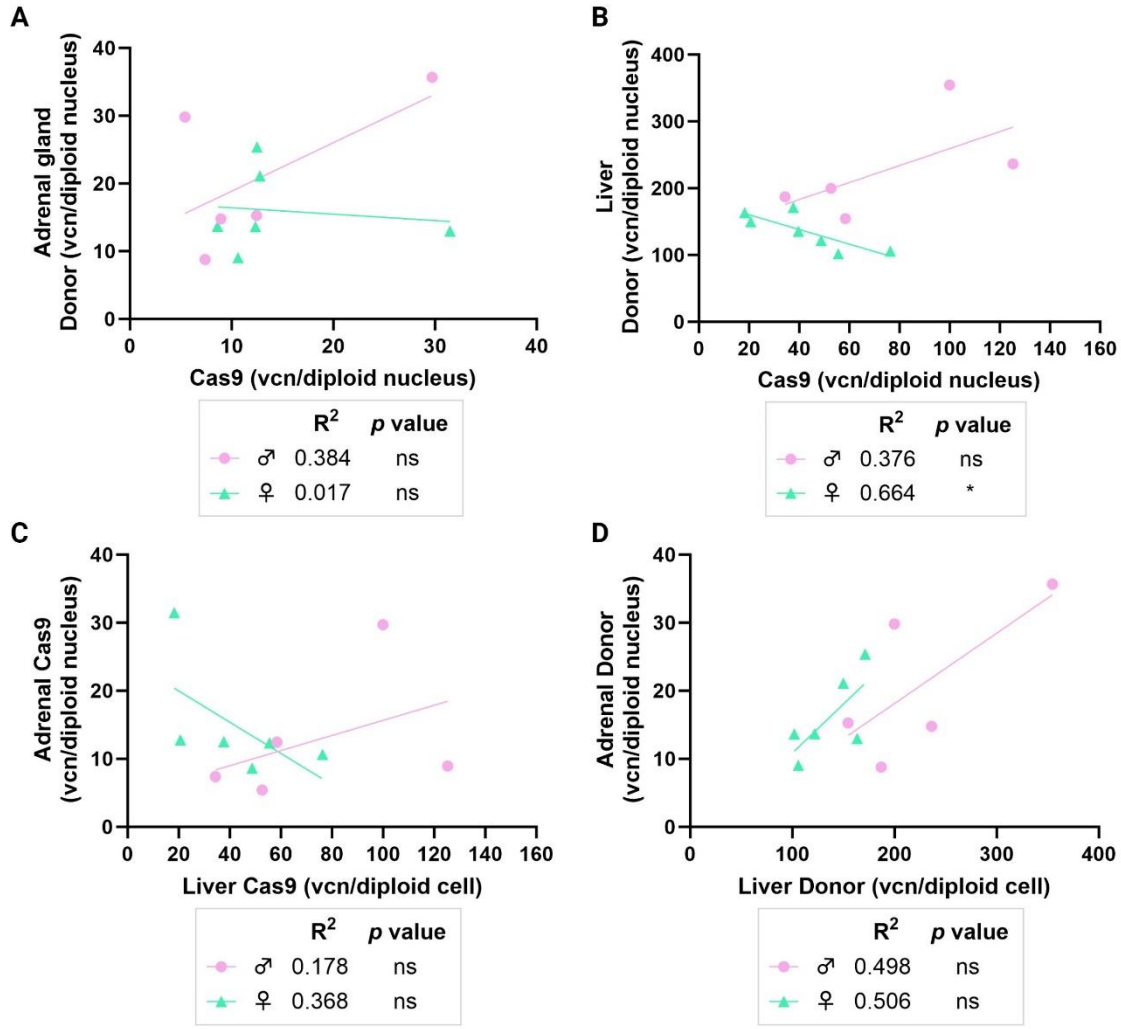

Figure 6-10 No relationship between SaCas9/guide and donor vcn/diploid cell.

A. Donor vector vs SaCas9 vector in adrenal genomic DNA. **B.** Donor vector vs SaCas9 vector in liver genomic DNA. **C.** Adrenal SaCas9 vs liver Cas9 vector. **D.** Adrenal donor vector vs liver donor vector. Abbreviations: vcn, vector copy number; ♀, female; ♂, male; ns, not significant. Individual data points are shown. * $p<0.05$ on linear regression modelling.

6.3.2.2 Evidence of DNA editing events

Following treatment with the SaCas9/guide vector and donor cassette vector there were specific editing events detected in the *Cyp21a1* locus. Sanger sequencing confirmed the insertion of the donor segment at the target site (Figure 6-11). Digital PCR was used to quantify correctly oriented donor insertion with primers spanning the 5' junction and 3' junction, reverse oriented donor insertion at the 5' and 3' junctions, and unedited alleles (Figure 6-12A). Correctly oriented donor cassette insertion determined by 5' junctional dPCR was present in 4.6 to 12.4% of alleles in the adrenal gland (Figure 6-12B) and 11-24% alleles in the liver (Figure 6-12C). The correctly oriented inserted donor (5' junction) contributed to a median of 7.8% of total alleles in female adrenal glands and 6.7% alleles in male adrenal glands. There were fewer 3' junctions detected than 5' junctions with median 3' junctions detected as 6.5% of total alleles in females and 4.8% total alleles in males. The reverse orientation insertion was detected in 2.6 to 7.3% of alleles in the adrenal gland and 4.4 to 14.4% alleles in the liver. In the adrenal gland, the ratio of correctly oriented insertions to reverse orientated insertions ranged from 1.5:1 to 2.5:1 (median 1.8:1). The proportion of correct 5' junctions, reverse 5' junctions and unedited alleles are shown and do not add up to 100%, indicating the presence of unknown/undetected events (Figures 6-12D-E).

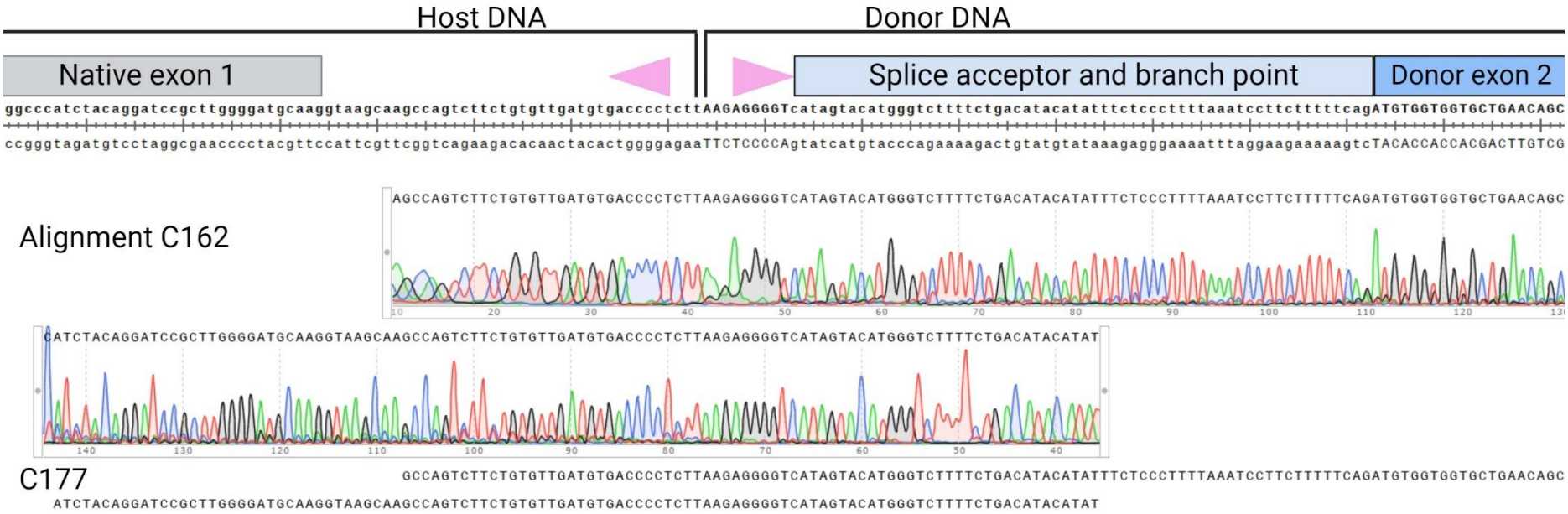

Figure 6-11 Sequencing alignment demonstrating genomic editing.

Sequencing alignment from representative mice (C162 and C177) demonstrating 5' junction. Insertions and deletions (indels) are seen in the traces around the cut sites. PAM sites are shown (pink).

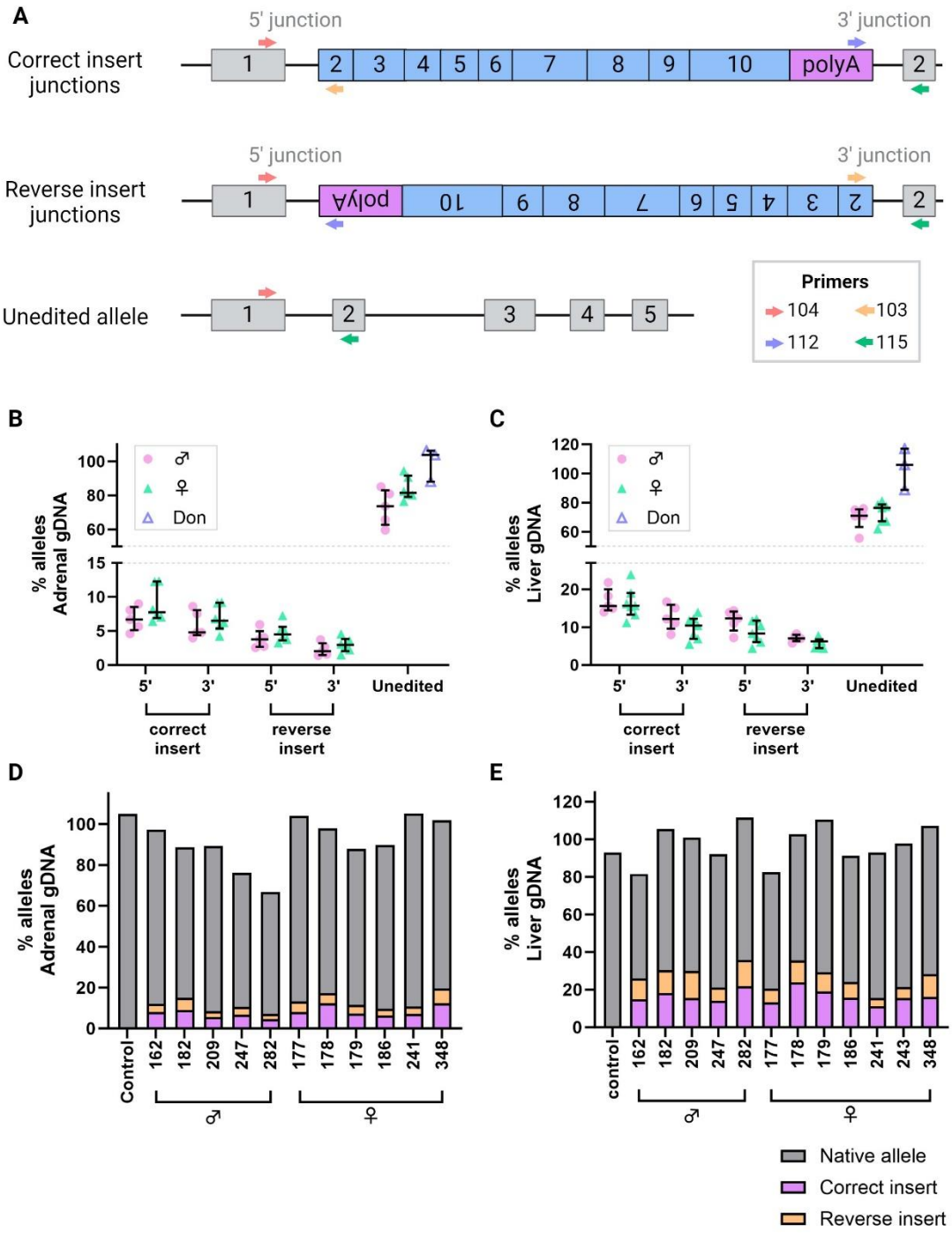

Figure 6-12 Quantification of editing events.

A. Editing events tested by digital PCR: HITI junctions (5' and 3' junctions) with correctly oriented donor insert or reverse inserted donor and unedited allele. **B.** Editing events expressed as a percentage of copies of the murine albumin allele in adrenal genomic DNA. **C.** Editing events expressed as a percentage of copies of the murine albumin allele in liver genomic DNA. **D.** Total detected events in individuals in adrenal gDNA. **E.** Total detected events in individuals in liver gDNA. Abbreviations: Don, homozygous 21-hydroxylase deficient mice that were only treated with the donor vector; ♀, female mice treated with SaCas9/guide and donor vectors; ♂, male mice treated with SaCas9/guide and donor vectors; 5', event at 5' junction of expected cut site, ie 3' to native exon 1; 3', event at 3' junction of expected cut site, i.e. 5' to native exon 2. Individual data points are shown, and error bars represent median and interquartile range.

6.3.2.3 Specific expression of edited *Cyp21a1* in the adrenal gland

cDNA was synthesised from adrenal RNA and *Cyp21a1* expression was quantified using dPCR (Figure 6-13A). There was a negligible amount of expression in the liver after editing (median 0.07 5' junctional transcripts per *Tbp* transcript). Edited *Cyp21a1* transcripts were normalised to *Tbp* and accounted for 25-77% of the total *Cyp21a1* transcripts detected, with a median of 34% in males and 43% in females (Figure 6-13B). The ratio of edited transcripts to native transcripts in each individual mouse ranged from 0.34 – 3.27 edited 5' junctional transcript to one native transcript (Figure 6-13C). There was a weak correlation between 5' junctions in genomic DNA and edited transcripts in males but there was no correlation in females (Figure 6-13D). Immunohistochemical staining demonstrated protein translation of 21-hydroxylase in the adrenal cortex of a representative treated mouse (Figure 6-14).

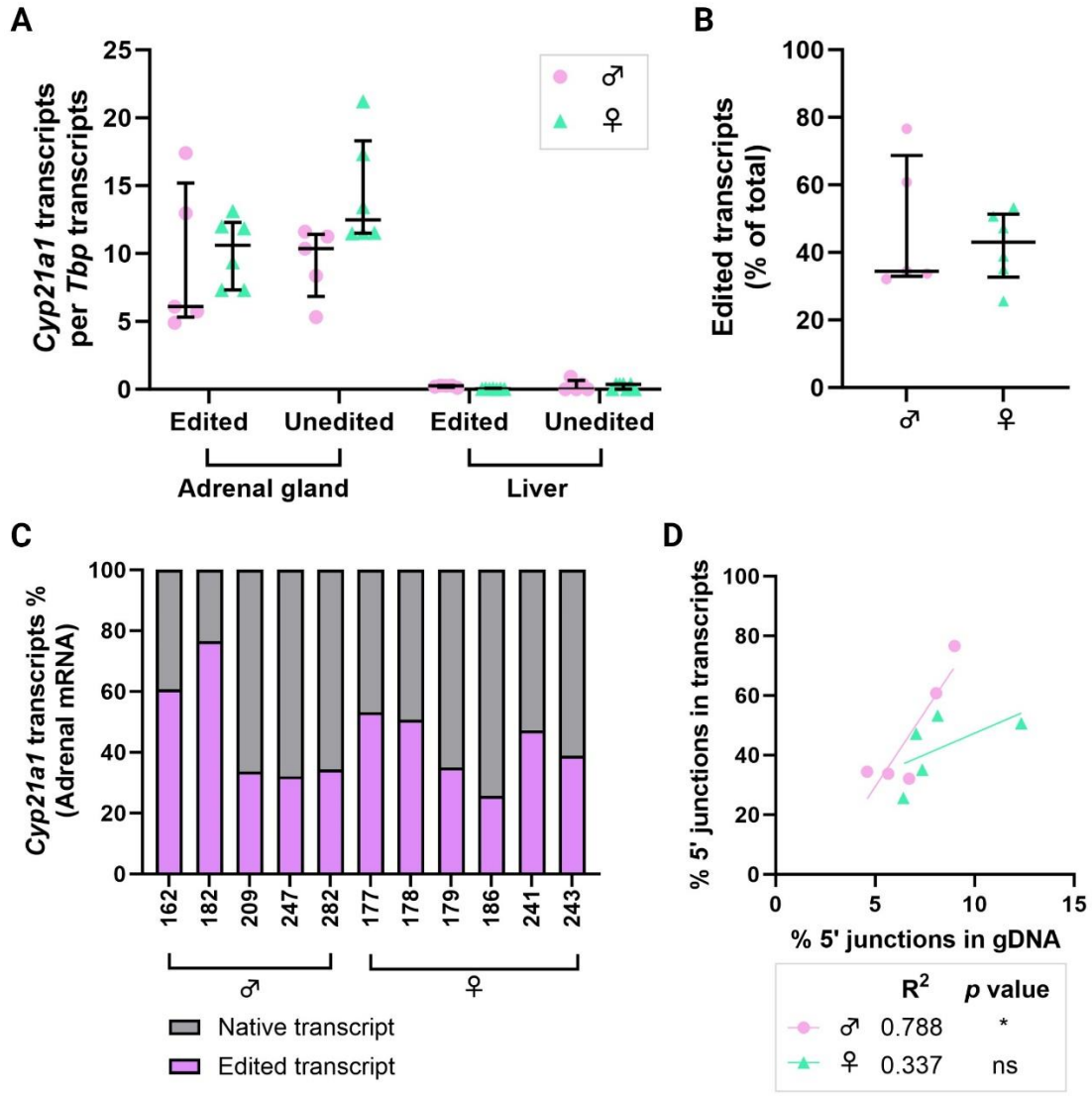

Figure 6-13 Edited *Cyp21a1* transcripts were detected.

A. *Cyp21a1* transcripts were detected as either 5' edited junctions or unedited alleles and normalised to *Tbp*. **B.** Edited transcripts as a percentage of the total transcripts detected in the adrenal mRNA (5' junction transcripts and unedited transcripts). **C.** Ratio of detected edited transcripts to unedited transcripts in individual mice adrenal glands, demonstrated as a percentage of total transcripts. **D.** 5' junctional allele genomic DNA versus 5' junctional transcripts. Abbreviations: ♀, female; ♂, male; *Tbp*, TATA-box binding protein; ns, not significant. Individual data points are shown, and error bars represent median and interquartile range. * $p<0.05$ on linear regression modelling.

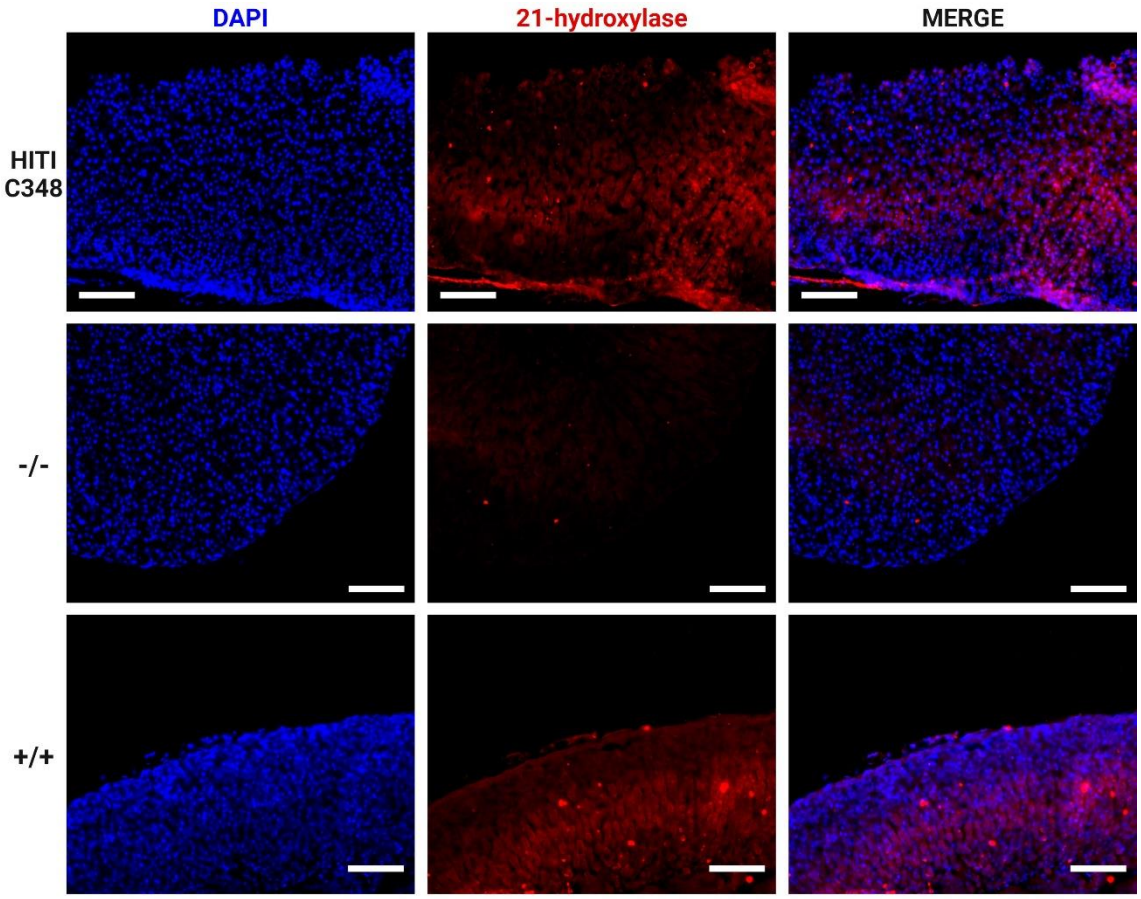

Figure 6-14 Immunohistochemistry slides from a treated mouse, and homozygous and wild-type controls.

IHC staining demonstrated 21-hydroxylase protein (red) in the adrenal cortex of treated mouse C348. 21-hydroxylase was not expressed as consistently across the adrenal cortex as in the wild-type mouse. DAPI nuclear staining in blue. Abbreviations: +/+, wild-type 21-hydroxylase sufficiency; -/-, homozygous 21-hydroxylase deficiency; HITI, homozygous 21-hydroxylase deficient mouse (C348) that was treated with both the Cas9/guide and donor vectors. Scale bar represents 100µm.

6.3.2.4 Improved adrenal steroidogenesis following gene editing

With successful editing, there was improvement in adrenal steroidogenesis. Serum corticosterone improved 6.7-fold in males and 9-fold in females after treatment (Figure 6-15A). In the treated males, serum corticosterone was 60% that of wild-type and was restored to that of wild-type male levels in the treated females. Treated females had serum and whole blood corticosterone that was half that of wild-type females. All mice had improvement in dried whole blood corticosterone from baseline (Figure 6-15B). Aldosterone increased 4-fold above wild-type levels in the treated mice (Figure 6-16A). Renin (*Ren1*) expression normalised (Figure 6-16B); therefore, this increased aldosterone production was not renin-driven. Chronic upregulation of aldosterone synthase (*Cyp11b2*) could account for the increased serum aldosterone above wild-type levels. Although *Cyp11b2* expression reduced 6.6 and 8-fold in the treated male and female mice compared with the untreated, it remained 10 and 7-fold elevated above male and female wild-type expression levels (Figure 6-16C). While the 25% reduction in progesterone in the females was statistically significant, it remained 19-fold elevated above wild-type female levels, and there was no reduction in progesterone in the males (Figure 6-16D).

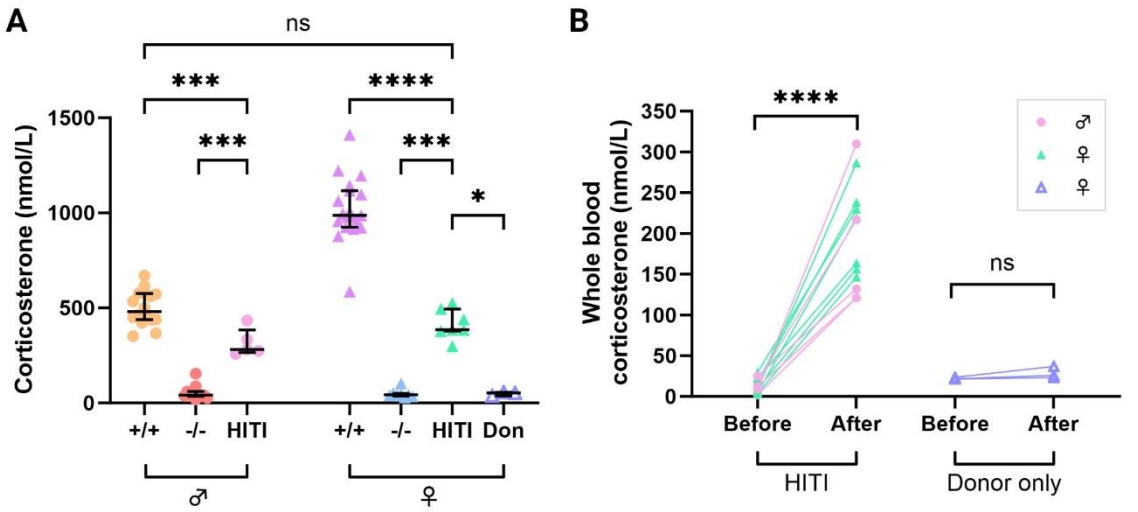

Figure 6-15 Improved corticosterone production after genomic editing.

A. Serum corticosterone. **B.** Whole blood corticosterone, before and after treatment. Abbreviations: +/+, wild-type 21-hydroxylase sufficiency; -/-, homozygous 21-hydroxylase deficiency; HITI, homozygous 21-hydroxylase deficient mice that were treated with both the Cas9/guide and donor vectors; Don, homozygous 21-hydroxylase deficient mice that were only treated with the donor vector; ♀, female; ♂, male; ns not significant. Individual data points are shown, and error bars represent median and interquartile range. * $p<0.05$, ** $p<0.01$, *** $p<0.001$, **** $p<0.0001$ on Mann Whitney *U* test (Panel A) or ANOVA (Panel B).

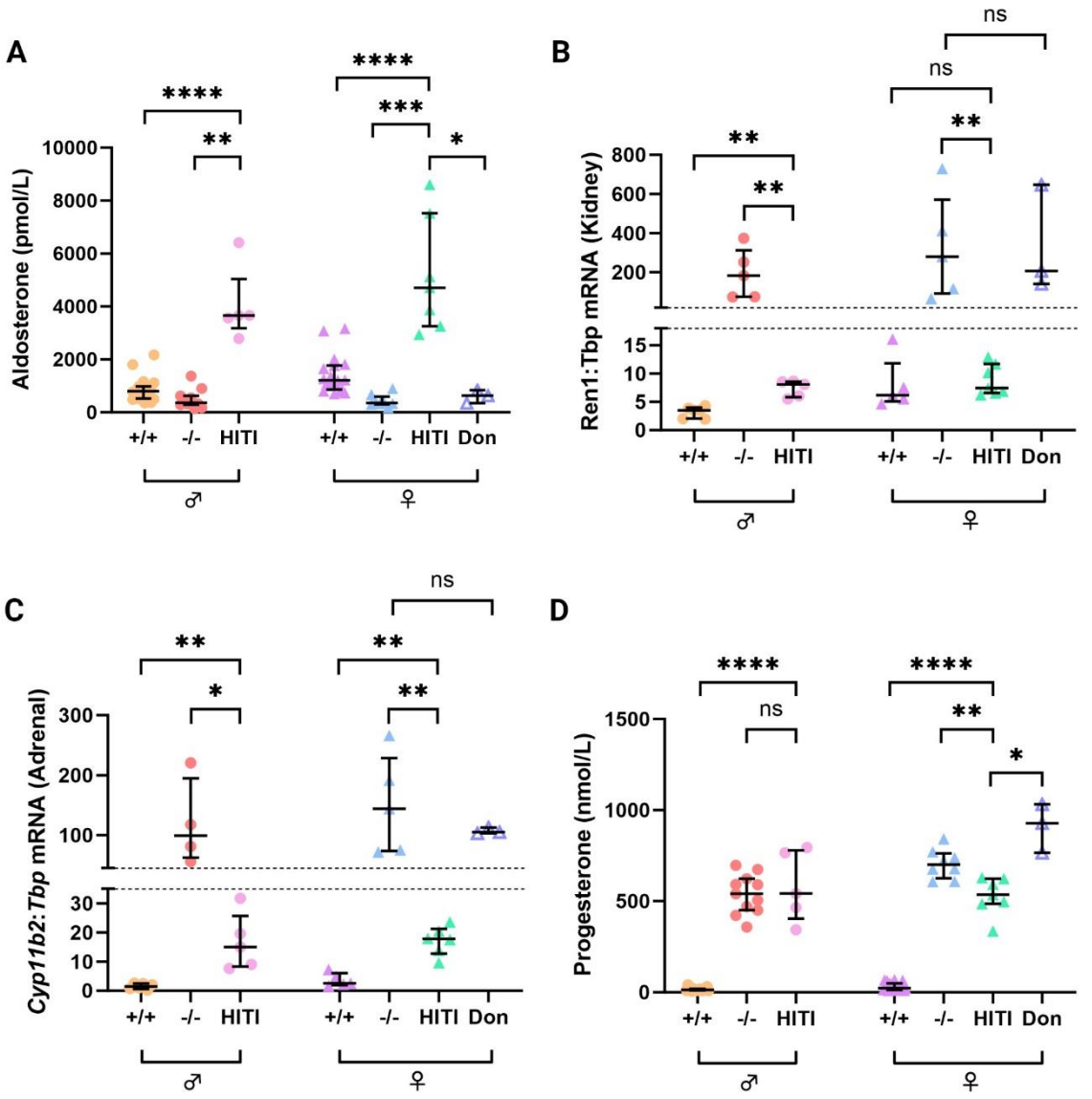

Figure 6-16 Aldosterone and progesterone after genomic editing.

A. Serum aldosterone. **B.** Renin expression demonstrated as the ratio of renal renin (*Ren1*) mRNA transcripts to *Tbp* transcripts. **C.** Aldosterone synthase expression demonstrated as the ratio of adrenal *Cyp11b2* mRNA transcripts to *Tbp* transcripts. **D.** Serum progesterone. Abbreviations: +/+, wild-type 21-hydroxylase sufficiency; -/-, homozygous 21-hydroxylase deficiency; HITI, homozygous 21-hydroxylase deficient mice that were treated with both the Cas9/guide and donor vectors; Don, homozygous 21-hydroxylase deficient mice that were only treated with the donor vector; ♀, female; ♂, male; *Ren1*, renin; *Tbp*, TATA-box binding protein; *Cyp11b2*, aldosterone synthase; ns not significant. Individual data points are shown, and error bars represent median and interquartile range. * $p<0.05$, ** $p<0.01$, *** $p<0.001$, **** $p<0.0001$ on Mann Whitney *U* test.

6.3.2.5 Reduction in adrenal hyperplasia following gene editing

Adrenal gland hyperplasia improved after treatment with the Cas9 and donor vectors, with the reduction in size macroscopically visible (Figure 6-17). Prior to treatment, the donor-only homozygous mice had lower body mass than the untreated homozygous controls. There was a relationship between body size and adrenal mass in the untreated homozygous and treated female mice, but not in the male mice (Figure 6-18A and B). A correlation between body size and adrenal mass was not statistically significant in the donor-only female mice ($r^2 = 0.97$) but the small sample size limited the statistical power of the comparison. The few numbers were due to the low fertility rate of the colony. Therefore, both absolute and relative adrenal mass is shown (Figure 6-18C and D). The smaller adrenal mass in donor-only females was due to their lower body weight and when adjusted for body weight was not significant. The absolute adrenal mass was reduced 1.9-fold in the females and 1.4-fold in the males (Figure 6-18C). Adrenal mass relative to body size improved 1.6-fold in females and 1.1-fold in males (Figure 6-18D).

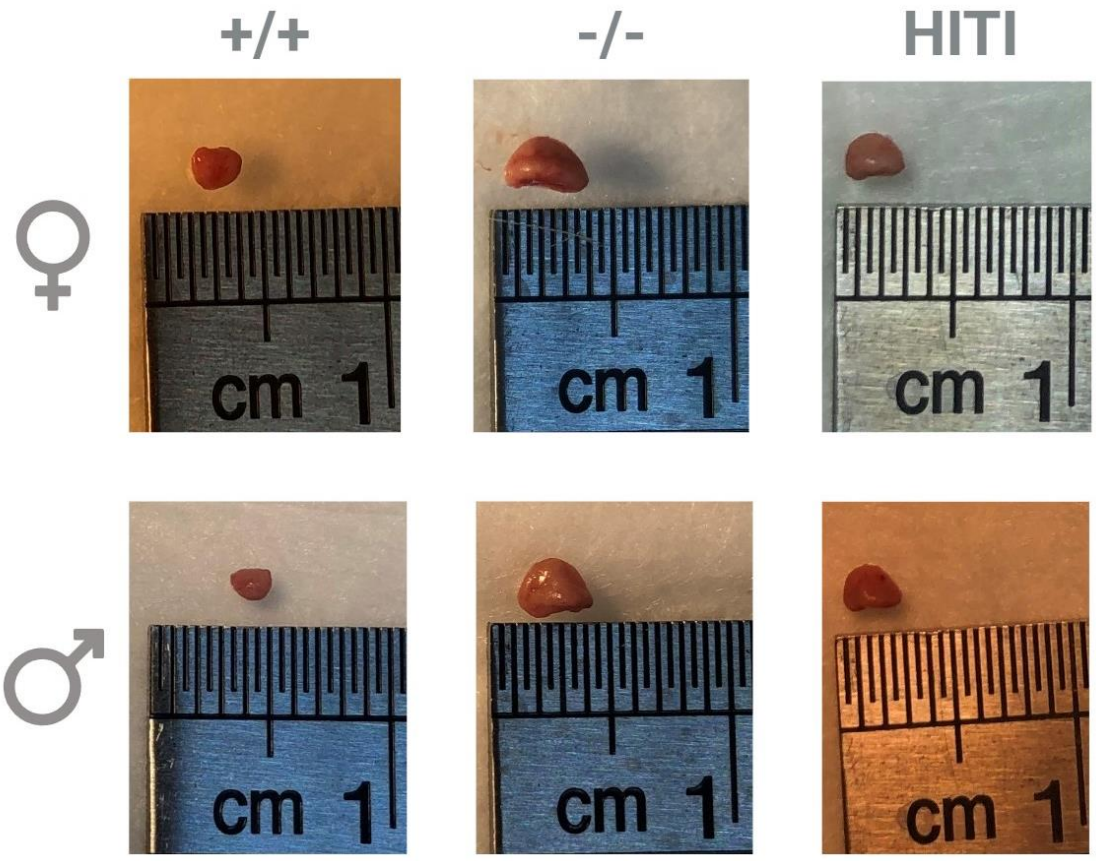

Figure 6-17 Photographs comparing untreated and treated adrenal gland size.
Photographs of representative adrenal glands after fat dissection. Abbreviations: +/+, wild-type 21-hydroxylase sufficiency; -/-, homozygous 21-hydroxylase deficiency; ♂, male; ♀, female; HITI, homozygous 21-hydroxylase deficient mice that were treated with the Cas9/guide and donor vectors.

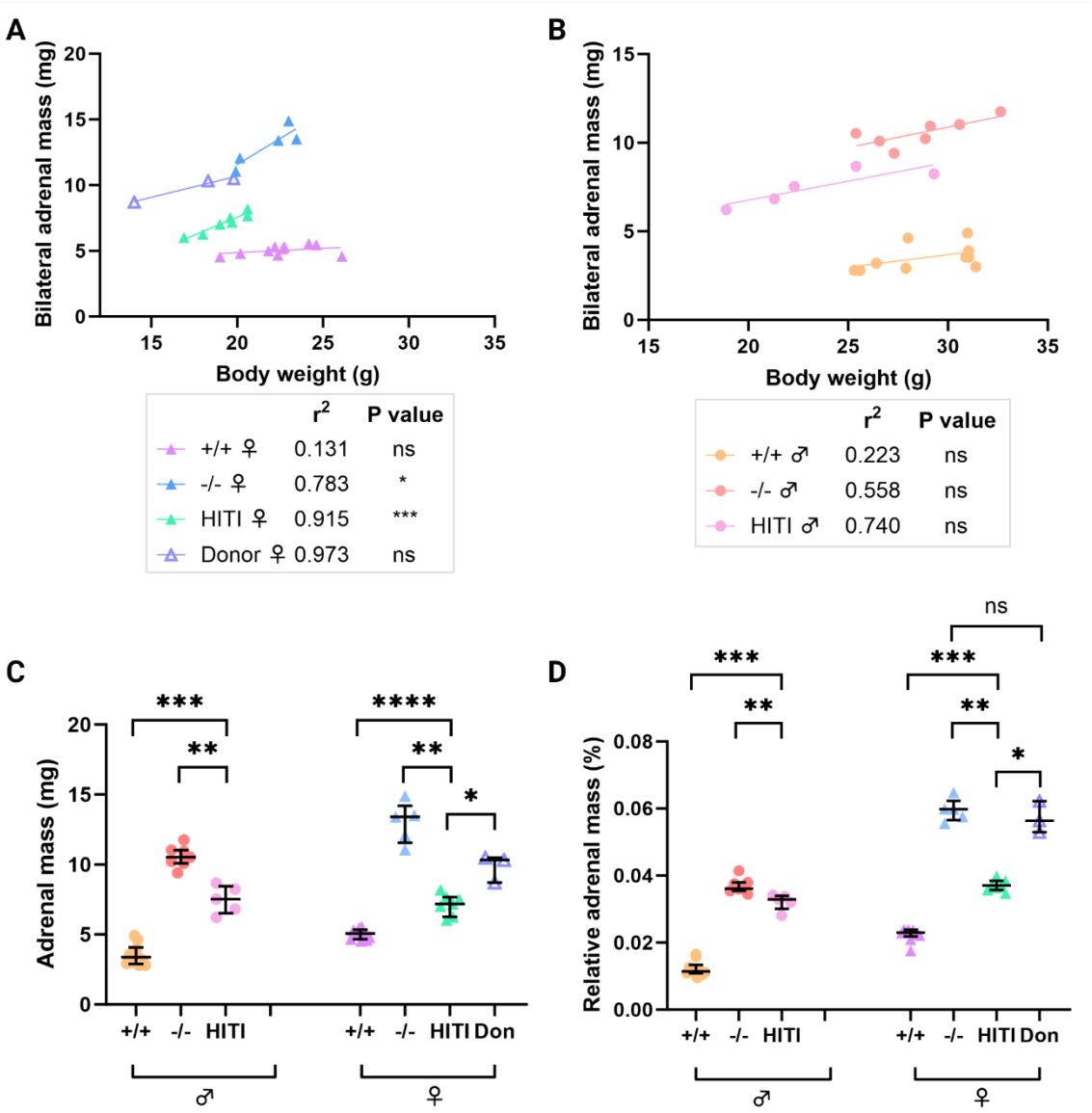

Figure 6-18 Adrenal gland size reduced after gene editing.

A. Relationship between body weight and adrenal mass in female mice. **B.** Relationship between body weight and adrenal mass in male mice. **C.** Absolute bilateral adrenal mass. **D.** Bilateral adrenal mass represented as a percentage of total body mass. Abbreviations: +/+, wild-type 21-hydroxylase sufficiency; -/-, homozygous 21-hydroxylase deficiency; ♂, male; ♀, female; HITI, homozygous 21-hydroxylase deficient mice that were treated with the Cas9/guide and donor vectors; Don, homozygous 21-hydroxylase deficient mice that were treated with the donor vector only, without the Cas9 vector; ns, not significant. Individual data points are shown, and error bars represent as median and interquartile range. * $p<0.05$, ** $p<0.01$, *** $p<0.001$, **** $p<0.0001$ on Mann-Whitney *U* test or linear regression modelling.

6.4 Discussion

The adrenal cortex constantly renews itself from populations of stem and progenitor cells located in the capsule and outer cortex, with differentiated cells undergoing very minimal cellular replication as they pass down the cortex towards the medulla. As a result, standard rAAV-based gene therapy cannot provide a durable effect. Genomic editing has the potential to overcome this as it provides site-specific modifications that are passed on to daughter cells. This is the first known successful editing of the 21-hydroxylase locus *in vivo*. Not only was there successful genomic editing, but this editing event conferred phenotypic benefit in reducing pathological adrenal hypertrophy and improving steroidogenesis. As the specific capsid serotypes that transduce adrenocortical progenitor and mature cells have not yet been determined, it is likely this study targeted the differentiated adrenocortical cells. As such, it proves that the locus is amenable to effective gene editing and the reagents used could be repackaged into a suitable capsid once that is determined.

Homology-independent targeted integration was the chosen strategy as it permits editing in both dividing and non-dividing cells. This accommodates potentially quiescent progenitor cells. Methods such as homology-directed repair (HDR),[28] single homology arm donor mediated intron-targeting integration (SATI)[4] or microhomology-mediated end-joining mediated gene insertion known as precise integration into target chromosome (PITCh),[29] would not be appropriate as they require specific homology sequences that must be adapted to an individual's single nucleotide polymorphisms flanking the target site. Other editing strategies such as base editing[30] or prime editing[25] would also have limited utility in 21-hydroxylase deficient CAH as they can only create single nucleotide

changes and the majority of CAH mutations are caused by large genetic recombination events between two *CYP21* genes.[31, 32]

The 21-hydroxylase locus is challenging, due to the presence of a pseudogene. In humans, there is 98% exonic and 96% intronic homology between the active 21-hydroxylase gene (*CYP21A2*) and the inactive pseudogene (*CYP21A1P*).[12] This homology is an important consideration when choosing the target site for site-specific modification. The *CYP21A2* and *CYP21A1P* genes are 30 kb apart, and similarly 80 kb apart in the mouse. The target sequence must not be present in both the active and pseudogene or it risks cutting out a large segment of genome, including the complement *C4B* gene. Furthermore, it is preferable to design guides that target deep in non-coding regions of the locus, as a double stranded break and subsequent indels in a coding sequence of a hypomorphic allele could completely knock out any residual function. Thus, targeting introns is desirable. The *Cyp21a1* gene is challenging as the introns are very small, meaning there are very few appropriate target sequences and PAM sites. Indeed intron 1 in murine *Cyp21a1* is only 64 bp (97 bp in the human), compared to other genes that have been the target of genomic editing by our team such as the murine *Otc* gene which has a first intron of over 14 kb. Therefore, the homology between the active and pseudogenes coupled with tiny introns severely limited the options for target sites, therefore in this study we only found three suitable guides to test. There are more than 10 different CRISPR/Cas systems that have been discovered and each Cas endonuclease recognises a different PAM sequence.[33] Therefore, alternate Cas protein choices have the potential to increase the number of target sites available for utilisation with HITI. An additional challenge in our study that was not anticipated was the difficulty in sequencing across the second intron due to 16

cytosine nucleotide repeats. This meant we could not reliably determine the presence of indels when the guide close to this site was used.

Guide 1 was chosen as it was the only guide of the three tested that demonstrated indels in the liver and then at high doses was able to demonstrate indels in the adrenal gland as well. However, in our lab we have shown that Cas9-induced double stranded DNA breaks in some target sequences repair more faithfully than others and that indels may not be the most effective way to determine guide efficiency. It is plausible that a double-stranded break induced at the target site for Guide 3 may not have resulted in indels due to the DNA repairing faithfully. In the future this could be analysed using a strategy that also supplies a repair template and sequencing for the insertion of the donor cassette. However, this was not pursued as Guide 1 was able to demonstrate proof of concept.

Due to the small size of the *Cyp21a1* introns limiting target site choice, the chosen guide site disrupted the splice acceptor region of the second exon. Therefore, the native splice site could not be included in the donor vector and an alternative splice acceptor sequence was included in the donor vector. This ensured that the native exon 1 would splice together with the donor exon 2 to create functional mature mRNA once the donor cassette was properly integrated into the genome.

Co-delivery of the Cas9/guide vector and donor template vector was able to deliver site-specific modification in the *Cyp21a1* locus in both the liver and adrenal glands. The editing efficiency was 2-fold higher in the liver than the adrenal gland. Higher editing efficiency in the liver was expected as more vector reached the liver than adrenal. However, it was not as high as expected given the Cas9/guide and donor vector

vcn/diploid cell in the liver was 4-fold and 11-fold higher than the adrenal gland, respectively. We postulate that given *Cyp21a1* is not expressed in the liver, the locus may have been compacted and methylated rendering it less accessible to the editing reagents.

Theoretically, when a HITI strategy is utilised, if the donor template is inserted in the reverse orientation the target sequence and PAM sites are reconstituted, allowing re-cleavage by Cas9, providing an opportunity for the donor segment to be reinserted in the correct orientation. However, reverse oriented insertions were detected with the ratio to correct orientation to reverse orientation insertions in the adrenal gland approximately 1.8:1. A similar ratio of correctly orientated to reverse oriented inserts (2:1) has been previously detected when AAV6 was used to deliver HITI-mediated editing of haematopoetic stem cells *ex vivo*, with correctly inserted editing rates of approximately 4% of total alleles, and reverse oriented inserts approximately 2% or total alleles on ddPCR.[5] The process of repairing double-stranded DNA cleavage can also induce indels, which means that even with the target sequence and PAM site realigning, indels may render the sequence unrecognisable by the guide strand and therefore Cas9 cannot make further DNA cuts. Partial or reverse insertion of a donor cassette is non-therapeutic so the strategy needs to be optimised to maximise the number of correctly inserted fragments, such as through the use of alternative Cas proteins that rely on microhomology, for example Cas12a.[34]

Despite a low number of alleles detected as having the 5' junctional insertion (median 6.7% in males and 7.8% in females) and therefore assumed to have been correctly edited, there were proportionally more detected edited transcripts (median 34% in males and 43% in females). This could be explained by several possibilities. A large number of non-

steroidogenic cells that do not express the native transcript may have remained unedited (such as medullary cells) and the steroidogenic cells that had an allele successfully edited had high expression of this edited transcript. However, as 21-hydroxylase is transported from the nucleus to the endoplasmic reticulum and not released extra-cellularly, this high rate of functional transcript production would be isolated to the low number of individual cells that had been successfully edited. Furthermore, non-functional mRNA transcripts may be actively degraded, such as via nonsense mediated decay.[35] Additionally, there may have been alleles that underwent editing events that were not detectable by the dPCR methodology used, but nevertheless reconstituted 21-hydroxylase expression.

A limitation of the use of PCR to determine and quantify on-target events is that unintended events may not be detected. These events could include subgenomic integration of vector DNA from the Cas9/guide or donor vectors. On-target unintended events will compete with the complete donor segment and reduce the editing efficiency. Deletions that result in destruction of the PCR primer binding site or large insertions that separate the primer binding sites to produce a PCR amplicon beyond the size limit of the technology will be missed. Additionally, smaller insertions and deletions will not be detected if the PCR amplicon remains the same size. Unintended on-target recombination must be considered and technology such as long read DNA sequencing could be utilised to determine the presence of these events.[6]

Despite the detected editing events in the adrenal gland being low our experiments conferred a phenotypic benefit. Serum corticosterone increased in both sexes, but the treated mice did not reach wild-type corticosterone levels for their sex. The treated females produced corticosterone levels that were comparable to the wild-type males.

Female wild-type mice have a higher corticosterone level than males, a phenomenon that occurs in the reverse in humans.[36, 37] Less than 1 in 10 alleles were demonstrated to be corrected in the adrenal gland: it is postulated that improved editing efficiency may improve the corticosterone production. This could be achieved by using a more highly adrenal-tropic rAAV serotype such as Anc80 (Chapter 5). There was subsequent improvement in adrenal hyperplasia, likely due to the improved corticosterone production allowing negative feedback on the pituitary and reducing ACTH release. The study period was completed 4 weeks after treatment; however, it is postulated that if the study interval was longer there may have been further reduction in adrenal size, particularly in the males who had near normal corticosterone production. A limitation of this study was that the recently born homozygous mice had smaller adult body weights than those homozygous used as controls. This was likely due to environmental noise from local construction work that had also reduced the fertility rate. Due to the scarcity of the model (low survival rates of 21-hydroxylase deficient animals and reduced fertility) priority was given to the dual Cas9/guide and donor vector treatment groups. Data to complete the donor-only and guide-only treatment groups will be accrued beyond the timeline of this thesis. Similarly, long term dual vector treated mice will be set up to determine durability of effect using the Rh10 capsid or other capsids.

Aldosterone production was markedly elevated in the treated mice. Aldosterone is only produced in picomolar concentrations whereas corticosterone is produced in nanomolar concentrations. Therefore, a smaller amount of aldosterone is needed to be produced to completely normalise the axis, and renin (*Ren1*) expression normalised. The over-production of aldosterone was due to upregulation of aldosterone synthase (*Cyp11b2*) due to chronic hypoaldosteronism. It has been shown that *Cyp11b2* is markedly upregulated

18 weeks after treatment with a gene addition strategy that normalised urine progesterone.[38] Our study was less than a quarter of the duration of this previously published study so the persistent elevation in *Cyp11b2* that was found was expected. However, the level of *Cyp11b2* expression following gene editing was reduced more than following *CYP21A2* delivery to the liver (Chapter 4.1), both of which had a 4-week study duration. The improved aldosterone production suppressed *Ren1* expression in the kidneys despite not completely normalising *Cyp11b2* expression in the adrenal glands. It is unclear why aldosterone synthase over-expression is more persistent than renin expression.

Despite recovery of corticosterone production, progesterone did not reduce. Studies using a gene addition strategy reduced urinary progesterone by 75% at 5 weeks[38] or reduced serum progesterone 10-fold by 2 weeks.[39] When using a gene addition strategy, every cell that is transduced may express 1 or more copies of 21-hydroxylase to utilise the progesterone substrate. However, with our editing approach, we successfully edited less than 10% of alleles in the adrenal cortex. While this was enough to confer improvement in corticosterone, the progesterone remained elevated. A similar situation is seen in non-classical CAH where serum cortisol response to ACTH stimulation is normal, however there is elevated 17OHP and androgens. In non-classical CAH, there is approximately 10-50% residual function in the mutant 21-hydroxylase enzyme, which although corticosterone can be produced it cannot do so efficiently enough to reduce ACTH stimulation and subsequent androgen production.[40] While 100% activity in 10% of cells and 10-50% activity in 100% of cells is not directly comparable, it is plausible that normalisation of progesterone requires the greatest 21-hydroxylase activity. Nevertheless,

our strategy has the potential to improve a clinical phenotype from severe salt-wasting to the much milder non-classical CAH.

One major challenge that has not been addressed by this study is the delivery of the editing reagents to the correct target cells. The adrenal cortex undergoes constant cellular renewal and differentiated adrenocortical cells undergo very minimal replication. Thus, for a robust, durable effect, the stem/progenitor pool must be edited, rather than just the differentiated cells.[41] This study did not attempt to determine whether the progenitor cells had been edited: if this study was to extend beyond the turnover period and a durable effect was seen, it could be inferred that the progenitor pool was transduced, without isolating this unknown cellular population. Indeed, further studies are planned to elucidate this.

To our knowledge, targeted editing events have taken place in the adrenal cortex in one previous study, and this team also used a HITI approach. In this study, the capsid serotype AAV9 was chosen for widespread targeting, particularly the liver, brain and spinal cord. Sequencing results revealed editing events in the liver and adrenal cortex with expression of edited transcript in corpus callosum of the brain, brain stem, spinal cord, liver, kidney, testis, and adrenal cortex.[42] However, the adrenal cortex was not a target organ, and there was no attempt to quantify the editing events or to determine the durability of expression in the adrenal cortex. Most studies that examine editing events outside of the target organ do not include the adrenal gland in their analysis, and it is likely that due to the affinity for AAV for the adrenal cortex that other studies have edited the adrenal gland in the past but went unrecognised.

One of the major concerns with gene editing, is the avoidance of inadvertent editing of germ cells in the gonads, prior to completion of reproduction choices. The adrenal cortex and gonads share embryological origins, so that it is feasible that a capsid that targets the adrenal cortex could potentially also target cells of the gonads. Indeed, edited gene was expressed in the testis and adrenal gland when the brain was targeted.[42] To clarify, analysis of the biodistribution of viral vectors to the gonads and their ability to transduce and edit germ cell genomes would be required. The first step for this study would be to sequence DNA from the gonads to determine the presence of editing events, and then follow this in the longer term to determine if there is sustainment of these editing events or if the edited cells are lost. A suggested methodology to determine the transmissibility of editing events in the gonads is to determine the presence of the editing event in offspring of the edited animal.[43] However, mice with CAH are infertile, due to the high progesterone levels, so in this particular model it would be difficult to ascertain.

This study utilised rAAV vectors to deliver both CRISPR/Cas9 and the donor template. Expression of transgene delivered by rAAV has been documented to persist up to 8 to 10 years after treatment in humans.[44, 45] Long-term expression of Cas9 may result in prolonged editing events and increased risk of off-target events. Furthermore, the Cas9 vector requires the inclusion of promoter-enhancer elements, which risk inadvertent integration into the host genome. Therefore, the gene editing field is moving towards the delivery of editing reagents as mRNA via lipid nanoparticles (LNP).[46-50] There is mounting evidence that LNP can deliver CRISPR/Cas9 to the adrenal gland[48]; however, this has not yet been exploited for genetic adrenal disorders. LNP are currently unable to effectively deliver large DNA cassettes to the nucleus,[51] therefore rAAV is still required to deliver the donor cassette. However, if the native promoter is captured by the editing

strategy, the donor cassette has no requirement for a strong promoter-enhancer element and thus the use of a combined LNP/rAAV strategy could improve safety.

This study demonstrated that rAAV-mediated delivery of CRISPR/Cas9 and a donor template to the adrenal gland via systemic delivery can induce targeted integrative editing events that conferred clinical benefit through phenotype correction. Repairing the murine native mutant locus restored 21-hydroxylase function under physiological control. While this study provides proof-of-concept that the locus is amenable to editing with phenotypic effect, future work is required to determine durability, safety and to translate into humans. Targeting the adrenocortical progenitor cells is required to ensure there is a robust effect despite adrenocortical cellular turnover. Moreover, the utilisation of lipid nanoparticles to deliver CRISPR/Cas9 as mRNA should be the focus of future work to improve safety by limiting prolonged expression of Cas9 and to remove the delivery of strong promoter-enhancer elements that risk integration in an off-target site.

6.5 References

1. Wilson RC and Gilbert LA. The Promise and Challenge of In Vivo Delivery for Genome Therapeutics. *ACS Chem Biol* 2018; 13: 376-382. 2017/10/12. DOI: 10.1021/acschembio.7b00680.
2. Rouet P, Smih F and Jasin M. Introduction of double-strand breaks into the genome of mouse cells by expression of a rare-cutting endonuclease. *Mol Cell Biol* 1994; 14: 8096-8106. 1994/12/01. DOI: 10.1128/mcb.14.12.8096-8106.1994.
3. Suzuki K, Tsunekawa Y, Hernandez-Benitez R, et al. In vivo genome editing via CRISPR/Cas9 mediated homology-independent targeted integration. *Nature* 2016; 540: 144-149. 2016/11/17. DOI: 10.1038/nature20565.
4. Suzuki K, Yamamoto M, Hernandez-Benitez R, et al. Precise in vivo genome editing via single homology arm donor mediated intron-targeting gene integration for genetic disease correction. *Cell Res* 2019; 29: 804-819. 2019/08/25. DOI: 10.1038/s41422-019-0213-0.
5. Bloomer H, Smith RH, Hakami W, et al. Genome editing in human hematopoietic stem and progenitor cells via CRISPR-Cas9-mediated homology-independent targeted integration. *Mol Ther* 2021; 29: 1611-1624. 2020/12/15. DOI: 10.1016/j.ymthe.2020.12.010.
6. Higashitani Y and Horie K. Long-read sequence analysis of MMEJ-mediated CRISPR genome editing reveals complex on-target vector insertions that may escape standard PCR-based quality control. *Sci Rep* 2023; 13: 11652. 2023/07/20. DOI: 10.1038/s41598-023-38397-y.
7. Stephenson AA, Nicolau S, Vetter TA, et al. CRISPR-Cas9 homology-independent targeted integration of exons 1-19 restores full-length dystrophin in mice. *Mol Ther Methods Clin Dev* 2023; 30: 486-499. 2023/09/14. DOI: 10.1016/j.omtm.2023.08.009.

8. Gitelman SE, Bristow J and Miller WL. Mechanism and consequences of the duplication of the human C4/P450c21/gene X locus. *Mol Cell Biol* 1992; 12: 2124-2134. 1992/05/01. DOI: 10.1128/mcb.12.5.2124-2134.1992.
9. Yu CY. Molecular genetics of the human MHC complement gene cluster. *Exp Clin Immunogenet* 1998; 15: 213-230. 1999/03/11. DOI: 10.1159/000019075.
10. Shen L, Wu LC, Sanlioglu S, et al. Structure and genetics of the partially duplicated gene RP located immediately upstream of the complement C4A and the C4B genes in the HLA class III region. Molecular cloning, exon-intron structure, composite retroposon, and breakpoint of gene duplication. *J Biol Chem* 1994; 269: 8466-8476. 1994/03/18.
11. Tee MK, Babalola GO, Aza-Blanc P, et al. A promoter within intron 35 of the human C4A gene initiates abundant adrenal-specific transcription of a 1 kb RNA: location of a cryptic CYP21 promoter element? *Hum Mol Genet* 1995; 4: 2109-2116. 1995/11/01. DOI: 10.1093/hmg/4.11.2109.
12. White PC, New MI and Dupont B. Structure of human steroid 21-hydroxylase genes. *Proc Natl Acad Sci U S A* 1986; 83: 5111-5115. 1986/07/01. DOI: 10.1073/pnas.83.14.5111.
13. Narasimhan ML and Khattab A. Genetics of congenital adrenal hyperplasia and genotype-phenotype correlation. *Fertil Steril* 2019; 111: 24-29. 2019/01/07. DOI: 10.1016/j.fertnstert.2018.11.007.
14. White PC, Vitek A, Dupont B, et al. Characterization of frequent deletions causing steroid 21-hydroxylase deficiency. *Proc Natl Acad Sci U S A* 1988; 85: 4436-4440. 1988/06/01. DOI: 10.1073/pnas.85.12.4436.
15. Higashi Y, Yoshioka H, Yamane M, et al. Complete nucleotide sequence of two steroid 21-hydroxylase genes tandemly arranged in human chromosome: a pseudogene and a genuine gene. *Proc Natl Acad Sci U S A* 1986; 83: 2841-2845. 1986/05/01. DOI: 10.1073/pnas.83.9.2841.
16. Finkielstain GP, Chen W, Mehta SP, et al. Comprehensive genetic analysis of 182 unrelated families with congenital adrenal hyperplasia due to 21-hydroxylase deficiency. *J Clin Endocrinol Metab* 2011; 96: E161-172. 2010/10/12. DOI: 10.1210/jc.2010-0319.
17. Carroll MC, Campbell RD and Porter RR. Mapping of steroid 21-hydroxylase genes adjacent to complement component C4 genes in HLA, the major histocompatibility complex in man. *Proc Natl Acad Sci U S A* 1985; 82: 521-525. 1985/01/01. DOI: 10.1073/pnas.82.2.521.
18. Miller WL and Auchus RJ. The molecular biology, biochemistry, and physiology of human steroidogenesis and its disorders. *Endocr Rev* 2011; 32: 81-151. 2010/11/06. DOI: 10.1210/er.2010-0013.
19. Higashi Y, Tanae A, Inoue H, et al. Evidence for frequent gene conversion in the steroid 21-hydroxylase P-450(C21) gene: implications for steroid 21-hydroxylase deficiency. *Am J Hum Genet* 1988; 42: 17-25. 1988/01/01.
20. Wedell A and Luthman H. Steroid 21-hydroxylase (P450c21): a new allele and spread of mutations through the pseudogene. *Hum Genet* 1993; 91: 236-240. 1993/04/01. DOI: 10.1007/BF00218263.
21. Werkmeister JW, New MI, Dupont B, et al. Frequent deletion and duplication of the steroid 21-hydroxylase genes. *Am J Hum Genet* 1986; 39: 461-469. 1986/10/01.
22. New M, Yau M, Lekarev O, et al. Congenital Adrenal Hyperplasia. In: Feingold KR, Anawalt B, Boyce A, et al. (eds) *Endotext*. South Dartmouth (MA), 2000.
23. Riepe FG, Tatzel S, Sippell WG, et al. Congenital adrenal hyperplasia: the molecular basis of 21-hydroxylase deficiency in H-2(aw18) mice. *Endocrinology* 2005; 146: 2563-2574. 2005/02/26. DOI: 10.1210/en.2004-1563.
24. Stenson PD, Mort M, Ball EV, et al. The Human Gene Mutation Database (HGMD((R))): optimizing its use in a clinical diagnostic or research setting. *Hum Genet* 2020; 139: 1197-1207. 2020/07/01. DOI: 10.1007/s00439-020-02199-3.
25. Anzalone AV, Randolph PB, Davis JR, et al. Search-and-replace genome editing without double-strand breaks or donor DNA. *Nature* 2019; 576: 149-157. 2019/10/22. DOI: 10.1038/s41586-019-1711-4.
26. Ran FA, Cong L, Yan WX, et al. In vivo genome editing using Staphylococcus aureus Cas9. *Nature* 2015; 520: 186-191. 2015/04/02. DOI: 10.1038/nature14299.
27. Conant D, Hsiau T, Rossi N, et al. Inference of CRISPR Edits from Sanger Trace Data. *CRISPR J* 2022; 5: 123-130. 2022/02/05. DOI: 10.1089/crispr.2021.0113.
28. Bibikova M, Carroll D, Segal DJ, et al. Stimulation of homologous recombination through targeted cleavage by chimeric nucleases. *Mol Cell Biol* 2001; 21: 289-297. 2000/12/13. DOI: 10.1128/MCB.21.1.289-297.2001.
29. Nakade S, Tsubota T, Sakane Y, et al. Microhomology-mediated end-joining-dependent integration of donor DNA in cells and animals using TALENs and CRISPR/Cas9. *Nat Commun* 2014; 5: 5560. 2014/11/21. DOI: 10.1038/ncomms6560.
30. Anzalone AV, Koblan LW and Liu DR. Genome editing with CRISPR-Cas nucleases, base editors, transposases and prime editors. *Nat Biotechnol* 2020; 38: 824-844. 2020/06/24. DOI: 10.1038/s41587-020-0561-9.

31. White PC and Speiser PW. Congenital adrenal hyperplasia due to 21-hydroxylase deficiency. *Endocr Rev* 2000; 21: 245-291. 2000/06/17. DOI: 10.1210/edrv.21.3.0398.
32. Tajima T, Fujieda K, Nakayama K, et al. Molecular analysis of patient and carrier genes with congenital steroid 21-hydroxylase deficiency by using polymerase chain reaction and single strand conformation polymorphism. *J Clin Invest* 1993; 92: 2182-2190. 1993/11/01. DOI: 10.1172/JCI116820.
33. Xu Y and Li Z. CRISPR-Cas systems: Overview, innovations and applications in human disease research and gene therapy. *Comput Struct Biotechnol J* 2020; 18: 2401-2415. 2020/10/03. DOI: 10.1016/j.csbj.2020.08.031.
34. Li P, Zhang L, Li Z, et al. Cas12a mediates efficient and precise endogenous gene tagging via MITI: microhomology-dependent targeted integrations. *Cell Mol Life Sci* 2020; 77: 3875-3884. 2019/12/19. DOI: 10.1007/s00018-019-03396-8.
35. Morse DE and Yanofsky C. Polarity and the degradation of mRNA. *Nature* 1969; 224: 329-331. 1969/10/25. DOI: 10.1038/224329a0.
36. Sofer Y, Osher E, Limor R, et al. Gender Determines Serum Free Cortisol: Higher Levels in Men. *Endocr Pract* 2016; 22: 1415-1421. 2016/08/20. DOI: 10.4158/EP161370.OR.
37. Bielohuby M, Herbach N, Wanke R, et al. Growth analysis of the mouse adrenal gland from weaning to adulthood: time- and gender-dependent alterations of cell size and number in the cortical compartment. *Am J Physiol Endocrinol Metab* 2007; 293: E139-146. 2007/03/22. DOI: 10.1152/ajpendo.00705.2006.
38. Perdomini M, Dos Santos C, Goumeaux C, et al. An AAVrh10-CAG-CYP21-HA vector allows persistent correction of 21-hydroxylase deficiency in a Cyp21(-/-) mouse model. *Gene Ther* 2017; 24: 275-281. 2017/02/07. DOI: 10.1038/gt.2017.10.
39. Markmann S, De BP, Reid J, et al. Biology of the Adrenal Gland Cortex Obviates Effective Use of Adeno-Associated Virus Vectors to Treat Hereditary Adrenal Disorders. *Hum Gene Ther* 2018; 29: 403-412. 2018/01/11. DOI: 10.1089/hum.2017.203.
40. New MI, Abraham M, Gonzalez B, et al. Genotype-phenotype correlation in 1,507 families with congenital adrenal hyperplasia owing to 21-hydroxylase deficiency. *Proc Natl Acad Sci U S A* 2013; 110: 2611-2616. 2013/01/30. DOI: 10.1073/pnas.1300057110.
41. Graves LE, Torpy DJ, Coates PT, et al. Future Directions for Adrenal Insufficiency: Cellular Transplantation and Genetic Therapies. *J Clin Endocrinol Metab* 2023; 108: 1273-1289. 2023/01/08. DOI: 10.1210/clinem/dgac751.
42. Hong SA, Seo JH, Wi S, et al. In vivo gene editing via homology-independent targeted integration for adrenoleukodystrophy treatment. *Mol Ther* 2022; 30: 119-129. 2021/06/01. DOI: 10.1016/j.ymthe.2021.05.022.
43. National Academies of Sciences Engineering and Medicine. . Chapter 4. Somatic Genome Editing. *Human Genome Editing: Science, Ethics, and Governance*. Washington (DC), 2017.
44. Buchlis G, Podsakoff GM, Radu A, et al. Factor IX expression in skeletal muscle of a severe hemophilia B patient 10 years after AAV-mediated gene transfer. *Blood* 2012; 119: 3038-3041. 2012/01/25. DOI: 10.1182/blood-2011-09-382317.
45. Nathwani AC, Tuddenham EG, Rangarajan S, et al. Adenovirus-associated virus vector-mediated gene transfer in hemophilia B. *N Engl J Med* 2011; 365: 2357-2365. 2011/12/14. DOI: 10.1056/NEJMoa1108046.
46. Finn JD, Smith AR, Patel MC, et al. A Single Administration of CRISPR/Cas9 Lipid Nanoparticles Achieves Robust and Persistent In Vivo Genome Editing. *Cell Rep* 2018; 22: 2227-2235. 2018/03/01. DOI: 10.1016/j.celrep.2018.02.014.
47. Liu J, Chang J, Jiang Y, et al. Fast and Efficient CRISPR/Cas9 Genome Editing In Vivo Enabled by Bioreducible Lipid and Messenger RNA Nanoparticles. *Adv Mater* 2019; 31: e1902575. 2019/06/20. DOI: 10.1002/adma.201902575.
48. Musunuru K, Chadwick AC, Mizoguchi T, et al. In vivo CRISPR base editing of PCSK9 durably lowers cholesterol in primates. *Nature* 2021; 593: 429-434. 2021/05/21. DOI: 10.1038/s41586-021-03534-y.
49. Gillmore JD, Gane E, Taubel J, et al. CRISPR-Cas9 In Vivo Gene Editing for Transthyretin Amyloidosis. *N Engl J Med* 2021; 385: 493-502. 2021/07/03. DOI: 10.1056/NEJMoa2107454.
50. Qiu M, Glass Z, Chen J, et al. Lipid nanoparticle-mediated codelivery of Cas9 mRNA and single-guide RNA achieves liver-specific in vivo genome editing of Angptl3. *Proc Natl Acad Sci U S A* 2021; 118: e2020401118. 2021/03/03. DOI: 10.1073/pnas.2020401118.
51. Durymanov M and Reineke J. Non-viral Delivery of Nucleic Acids: Insight Into Mechanisms of Overcoming Intracellular Barriers. *Front Pharmacol* 2018; 9: 971. 2018/09/07. DOI: 10.3389/fphar.2018.00971.

Chapter 7

Towards genomic editing as a therapeutic approach to congenital adrenal hyperplasia

7.1 General discussion

Congenital adrenal hyperplasia due to 21-hydroxylase deficiency is a life-threatening condition where cortisol and aldosterone cannot be synthesised in adequate quantities. Untreated, the severe, classical salt-wasting form can result in neonatal death however there is increased risk of mortality in all forms.[1] Steroids were first utilised as therapy for CAH in the 1950s and remain the foundation for treatment.[2-4] While exogenous steroids are life-saving, they cannot mimic the physiological secretion of cortisol, and a number of complications arise in CAH from both over-and under-treatment. New treatments are sought. The gene therapy field will revolutionise the modern medical management of many monogenic diseases and this thesis addresses the application of rAAV-based gene therapy to CAH. Recombinant AAV is the leading viral vector for *in vivo* gene delivery, and the prospect of a "one and done" treatment for monogenic adrenal disorders such as CAH with rAAV gene therapy is enticing. The culmination of this thesis lays the foundation for the utilization of recombinant AAV vectors for the treatment of CAH.

There are some challenges that must be surmounted to apply rAAV gene therapy to the adrenal cortex. Despite this, a clinical trial is underway that utilises the serotype AAV5 to deliver *CYP21A2* cDNA systemically to humans with CAH at four dose rates (ClinicalTrials.gov: NCT04783181). By January 2024, seven adults had been treated with the vector, with one participant's serum cortisol improving from 105 nmol/L at baseline to 235 nmol/L at week 12.[5] However, this trial does not address the challenges of applying standard gene addition-based rAAV gene therapy to the adrenal cortex, nor does it take into account the effect of systemically expressed vector,[6, 7] and has been criticised as premature.[8] AAV genomes are predominantly episomal and will be lost during cellular replication.[9, 10] This has implications for the adrenal cortex as it undergoes constant cellular renewal from populations of stem and progenitor cells in the periphery of the cortex, and no previous work on gene therapy for CAH has been able to address this issue with a statistically significant phenotypic effect.[9, 11-13]

One strategy that could overcome the limitations imposed by the biology of the adrenal cortex is to deliver the 21-hydroxylase gene to a readily targetable organ outside of the adrenal cortex.[6] This theoretical possibility was explored in Chapter 4 by delivering rAAV vectors encoding human 21-hydroxylase (*CYP21A2*), with or without human 11ß-hydroxylase (*CYP11B1*), for specific hepatic expression in a mouse model for CAH. The liver was chosen for several reasons:

- the use of rAAV for gene delivery to the liver is well established,[14-16]
- it is a relatively stable organ in adults, with durable rAAV-delivered transgene expression for life,[17] and
- there are already hepatically expressed cytochrome P450 enzymes that 21-hydroxylate progesterone.[18]

Therefore, the liver was the logical site for ectopic adrenal enzyme delivery. Hepatically-expressed adrenal enzymes were shown to co-operatively reconstitute adrenal steroidogenesis, with increases in aldosterone and corticosterone production and resultant normalisation of renin expression and reduction in adrenal gland size.[6] While corticosterone did not reach wild-type levels, aldosterone was normalised and this strategy could also be considered for mineralocorticoid defects such as aldosterone synthase deficiency. Additionally, this showed that extra-adrenal enzyme expression can have a meaningful clinical effect, therefore a biochemical effect seen when utilising systemically delivered rAAV encoding adrenal enzyme genes with a ubiquitous promoter-enhancer cannot be definitively attributed to adrenal transgene expression alone. Ectopic adrenal enzyme delivery could be directly applied to an adult population with completed liver growth; however, this strategy would need to be adapted to a gene editing approach for a durable effect in the paediatric CAH population due to hepatocyte replication during organ growth.

As the glucocorticoid production was not completely normalised and the delivery of standard rAAV gene therapy to the paediatric population would not provide a durable effect, designing a durable gene therapy that targets the adrenal cortex was warranted. There has been no published attempt to optimise rAAV capsid serotype choice for targeting the adrenal cortex. It is plausible that rAAV could efficiently transduce adrenocortical cells due the biological properties it shares with the liver: high blood flow relative to organ size[19] and fenestrated endothelium.[20] In Chapter 5, a comprehensive panel for 67 known rAAV capsid serotypes were tested for efficiency of adrenal gland transduction and multiple serotypes were found that delivered gene expression more efficiently than the commonly used Rh10. While transduction efficiency is important for

efficacy of the treatment, packaging efficiency must also be considered. This was not specifically examined in this thesis, however virus production when using the Anc80 capsid had a reduced yield compared with other serotypes and therefore may not be the ideal serotype with which to pursue a commercial product. Nevertheless, the biology of the adrenal cortex obviates the use of standard rAAV gene addition,[9, 21] and thus targeting the adrenocortical progenitor cell population is warranted. Therefore, single nuclei RNA sequencing was used to develop transcriptomic atlases for the wild-type and 21-hydroxylase deficient murine adrenal glands, and to identify adrenocortical progenitor cells. This was the first time that potential adrenocortical progenitor cells were identified on single cell transcriptomic analysis and could be used in future studies to confirm transduction with rAAV. In future work, the top rAAV capsid serotypes that were determined in Chapter 5 will be used to construct a customised AAV testing kit that is compatible with single cell transcriptomics to identify which of these top candidates can transduce murine adrenocortical progenitor cells.

For a durable effect, gene therapy for CAH must edit the genome of the adrenocortical progenitor cells to ensure subsequent daughter cells maintain the correction. As the optimal rAAV serotype for gene delivery and expression to the adrenocortical progenitor cells has not yet been determined, the gene editing approach that was developed was pseudo-serotyped with Rh10 which was known to deliver gene expression to the differentiated cells of the adrenal cortex. This study commenced prior to the identification of rAAV capsid serotypes with functional transduction efficiency greater than Rh10 in Chapter 5. Homology-independent targeted integration was the chosen strategy as it permits editing in both dividing and non-dividing cells which accommodates potentially quiescent progenitor cells, and methods that utilise homology such as HDR[22], SATI[23] or

PITCh[24] would require specific homology sequences that cater for an individual's single nucleotide polymorphisms. Other editing strategies such as base editing[25] or prime editing[26] have limited utility in 21-hydroxylase deficiency as they can only cause single nucleotide or short sequence changes and the majority of pathogenic mutations in *CYP21A2* are caused by large genetic recombination events between two *CYP21* genes.[27, 28] Prime editing is a new technology which causes less off-target events than standard CRISPR/Cas9 systems,[26] and despite its current limited applicability to 21-hydroxylase deficiency, work is underway to develop strategies which may allow the introduction of larger genetic changes.[29] However these developments are in their early stages and prime editing has low editing efficiency and limited safety data.[30] Furthermore, the system is too large to be packaged into rAAV which limits *in vivo* delivery,[30] however, non-viral delivery methods such as LNP have a larger packaging capacity than AAV and LNP could facilitate *in vivo* prime editing for 21-hydroxylase deficiency.[31] In Chapter 6, the 21-hydroxylase locus was shown to be amenable to HITI-based editing, despite challenges with targeting the *Cyp21a1* locus due to small introns resulting in limited non-coding regions from which to safely choose target sites, and the presence of a highly homologous pseudogene, limiting the target sites to only those that are unique to *Cyp21a1*. Despite these challenges, locus-specific genomic modification was achieved, and this had a phenotypic effect. Using a HITI strategy, there was evidence of correction of the *Cyp21a1* gene in less than 10% of alleles. This was determined using digital PCR to quantify the presence of 5' junctions between the host genome and the donor cassette. Despite the apparent small rate of correction there was a phenotypic effect with increased mineralocorticoid and glucocorticoid production, reduction in renin and aldosterone synthase expression and reduction in adrenal size. A phenotypic benefit was considered possible despite a low editing efficiency. A small increase in enzymatic function can have

a profound effect on the phenotype with only 2% residual activity required for a simple-virilising phenotype which is more mild than classical salt-wasting CAH, with the caveat that 2-10% enzyme activity in 100% of cells is not directly comparable to 50-100% activity in 10% of cells. This strategy could be repackaged in an appropriate capsid serotype that targets the adrenocortical progenitor cells once it has been determined.

When utilising HITI, the process of targeted DNA cleavage mediated by Cas9 should repair via NHEJ with indels, or, in the presence of a donor template, integration of the provided template sequence. However, emerging evidence suggests the existence of additional outcomes beyond these expected events.[32-36] These phenomena are often overlooked, primarily due to the prevalent use of PCR for the detection of editing events.[36] The reliance on PCR introduces bias as it necessitates assumptions regarding potential outcomes. Integration of subgenomic fragments sourced from either the Cas9/guide vector or donor vector may occur, and these events compete with integration of the correctly oriented donor cassette. Additionally, when utilising homology-directed repair (HDR), the donor template has the potential to form concatemers with chimeric ITRs and these large sequences may integrate at the cut site.[36] During HDR, the frequency of this occurrence is reduced when ITRs are removed after transduction.[36] AAV concatemer integration at the cut site has not been reported when utilising HITI, and ITRs are routinely removed from the donor cassette when a HITI strategy is employed. However, it is plausible that concatemers of Cas9 vector genomes could integrate at the cut site in a similar way, although the absence of homology arms may reduce this effect. Nevertheless, unintended on-target recombination must be considered and advanced sequencing technology such as PCR-free long-read DNA sequencing could present a viable approach to determine the occurrence of these events.[37]

Recombinant AAV serotype tropism for cell populations in one species is not necessarily translatable to other species including humans. Therefore, both gene therapy strategies discussed in Chapters 4 and 6 of this thesis would need to be repackaged for human clinical translation. Using rAAV to deliver adrenal enzymes to the liver in humans could be achieved using a high human liver-tropic capsid serotype such as the AAV-SYDs,[53] AAV-NP59[38] or AAV-LK03,[54] rather than the murine liver-tropic AAV8 serotype. A method to test rAAV capsid tropism for human adrenocortical cells needs to be developed. This is complicated by the difficulty in identifying adrenocortical progenitor cell populations, which would need to be targeted for an adrenal-directed gene editing approach to have a durable effect. Chimeric human/mouse liver models have been used to establish AAV capsid tropism for human hepatocytes,[53] but a similar method has not been established for the human adrenal cortex. Donated human livers that were not suitable for organ transplantation were maintained on a perfusion circuit to facilitate rAAV capsid testing[39]; perhaps cadaveric adrenal glands could be similarly maintained for pre-clinical capsid investigation. Organoids are three-dimensional cell cultures with cell organisational structure and function that resembles the original organ,[40] and have been utilised for pre-clinical rAAV capsid selection in human-derived tissue, including liver, retinal, cerebral, cardiac, intestinal, lung and renal.[38, 41-46] It is plausible that organoids could be used to study rAAV capsid tropism for the human adrenal gland. However, adrenal organoids are not well established, and differentiating the cells beyond a foetal-like adrenal state remains challenging.[47] Adrenocortical tumour organoids, foetal-like adrenal organoids and adrenal organoids derived from animal cells have been produced,[47-49] but organoids with post-natal human adrenocortical cell properties remain elusive.

Assuming an appropriate rAAV capsid serotype for human adrenal cortex is determined separately, testing the editing reagents could be achieved using a humanised mouse model, where the human *CYP21A2* locus has replaced the murine *Cyp21a1* locus.[50] This would allow editing reagents to be tested that target the human *CYP21A2* locus, however it would require an rAAV capsid that was murine tropic so could not assess the complete gene therapy product. The limitations of this model are that it does not have a human *CYP21A1P* pseudogene, and other unexpected off-target sites would be murine not human. As previously discussed, chimeric mouse/human liver models have been developed, and could be utilised to develop reagents that edit the native human locus. However, as *CYP21A2* is not expressed in the liver, the locus may be methylated and more difficult to target, resulting in a lower editing efficiency rate. Nevertheless, the model would allow for the analysis of off-target events in the human genome. In addition to the limitations imposed by the *CYP21A1P* pseudogene, discussed in Chapter 6, when adapting the editing strategy to the human locus, it will be important to ensure that the chosen guide site or sites are not affected by single nucleotide polymorphisms as this could render the product non-functional in people with polymorphisms at that site.

If both the gene therapy techniques described in this thesis were applied to humans, women and children with CAH would require strategies to manage ongoing elevation of androgens and related sequelae. This is less of an issue in men, and most men with non-classical CAH do not require therapy once they have reached their final height. The requirement for fludrocortisone can be assessed with measuring plasma renin activity or absolute serum renin levels and with serum aldosterone. Additionally, patients treated with the either strategy will need their adrenal axis challenged with an ACTH stimulation

test to determine the peak cortisol production. The glucocorticoid treatment regimen is dictated by intrinsic cortisol production. If baseline cortisol is adequate but stimulated peak cortisol is suboptimal, only stress precautions may be required. However, if the peak stimulated cortisol is adequate, there is the potential that no additional glucocorticoid supplementation is required.

Thirty years after AAV was first used for *in vivo* gene delivery,[51] one of the major challenges that remains is liver toxicity. By December 2023, there were six rAAV-based gene therapies that were approved for use in the clinic in the world, targeting retinal, neurological, liver and neuromuscular diseases.[52] A seventh, Glybera, the first rAAV-based therapy to be approved, was taken off the market due to lack of demand and cost of manufacture.[53] Two of these rAAV therapies were approved for use in Australia: Luxturna for RPE65 associated retinal dystrophy and Zolgensma for spinal muscular atrophy.[52] Zolgensma is delivered intravenously for central nervous system treatment. Two human subjects that died from complications of their disease who had received treatment with the gene therapy had vector detected 300-1000 times higher in the liver than the central nervous system.[54] Furthermore, two participants died due to acute liver failure following treatment with Zolgensma, and four patients died following during the ASPIRO clinical trial (NCT03199469) to treat X-linked myotubular myopathy, although those four subjects had pre-existing liver disease.[55] The liver is the major target for most rAAV serotypes, and liver-detargeting should be considered when delivering systemic vector with the aim of targeting extra-hepatic organs, in order to minimise the risk of hepatotoxicity.[55] Reduced liver targeting has been achieved with capsid manipulation, which reduces the viral load on the liver while maintaining dose efficacy for the target tissue.[56, 57] Reducing gene expression through the use of promoters that are specific to

extra-hepatic organs or the use of microRNA to degrade mRNA in the liver can reduce immunogenicity to the transgene and potential off-target effects in the liver, however it does not reduce the risk of hepatotoxicity due to the vector itself.[55] Therefore, consideration should be given to liver-detargeting when optimising a capsid to target the adrenocortical progenitor cells.

The first CRISPR-based gene therapy has been approved for use in the clinic for treatment of the haemoglobinopathies sickle cell disease and transfusion-dependent ß-thalassaemia.[58] This strategy is a non-viral cell therapy and works by disrupting expression of *BCL11A* which is required for the suppression of foetal haemoglobin expression. By increasing foetal haemoglobin expression, which is biologically functional, this reduces anaemia and painful sickling attacks. While this approval, which comes only 11 years after the discovery of the CRISPR/Cas system,[59] paves the way for other CRISPR based therapies, knocking out a gene's function is much simpler than repairing a gene. With the HITI approach described in this thesis, a double-hit is required: the correct location in the genome must be cut, and the entire donor segment must be integrated in the correct orientation.

An increasingly recognised risk of genomic editing is on-target unexpected events such as integration of sub-genomic fragments from either the Cas9 or donor vector, in addition to off-target editing events.[32-36] When DNA is delivered by AAV it may be retained in a non-dividing cell for years[60, 61] and Cas9 delivered as DNA will require promoter sequences to facilitate expression. Long-term expression of Cas9 may cause prolonged editing events. Furthermore, there is a risk that these strong promoter-enhancer sequences may be unexpectedly integrated. Therefore, the field is moving towards delivering Cas9

as mRNA, which is transiently expressed and eliminates the requirement for strong promoter-enhancer elements, limiting editing events.[62-65] Additionally, as Cas9 is provided as mRNA, it cannot be integrated into the cut site, limiting the opportunity for unproductive editing events at the target locus. LNP have been successfully used to deliver editing reagents (mRNA encoding Cas9 and a sgRNA) to the liver in humans to knock out *TTR* and *KLKB1* for the treatment of transthyretin amyloidosis and hereditary angioedema, respectively.[64, 65] These treatments target the liver, however there is emerging evidence that lipid nanoparticles (LNP) could be used to deliver mRNA to the adrenal gland. Onpattro™ (patisiran) is an approved LNP therapy for the treatment of hereditary transthyretin-mediated amyloidosis which delivers the therapeutic siRNA to the liver, and pre-clinical studies demonstrated LNP accumulation in the adrenal gland of rats.[66] Additionally, a LNP gene therapy that utilised base editing in the treatment of familial hypercholesterolaemia demonstrated editing events in the adrenal glands of NHP.[62] The liver and adrenal cortex share some features that may make the adrenal cortex is amenable to vector and LNP-mediated delivery of editing machinery in order to cure CAH including high blood flow relative to organ size[19], fenestrated endothelium[20], and high expression of the LDL receptor.[67, 68] Ideally, genomic editing of the adrenal gland will move towards utilising LNP to deliver Cas9, however LNP is inefficient in the delivery of DNA to the nucleus and therefore there is an ongoing requirement for the donor cassette to be delivered by rAAV. However, if the native promoter is captured, the donor cassette can be developed without the need for strong promoter-enhancer elements and the combination of LNP/rAAV to deliver the editing machinery will be safer than dual rAAV vectors.

The immediate future directions for this work include determining the durability of the editing strategy by following mice long term (up to 12 months), past the adrenocortical turnover period. Additionally, using a highly adrenal-tropic capsid serotype found in Chapter 5 (such as NP22 in female mice or Anc80 in either sex) or the utilisation of LNP could be used to determine if the editing efficiency can be improved. The next direction for the capsid tropism work is to determine if any of the top capsids found in Chapter 5 can transduce the adrenocortical progenitors through either scRNA Seq to directly identify cells expressing markers for adrenocortical progenitor cells that are co-expressing barcodes from AAV genomes, or through indirect identification with durable expression of a reporter gene in a reporter mouse model. Additionally, the delivery of editing reagents by LNP to the adrenal gland should also be explored, to improve the safety and efficacy of the editing strategy.

While there are challenges yet to be surmounted, including improving on-target editing efficiency, determining tropism for human adrenocortical progenitor cells, and safety analysis including gonadal off-target effects, this thesis provides the foundation on which future work can build towards a goal of treating CAH with AAV-based gene therapy in the clinic.

7.2 References

1. Claahsen-van der Grinten HL, Speiser PW, Ahmed SF, et al. Congenital Adrenal Hyperplasia-Current Insights in Pathophysiology, Diagnostics, and Management. *Endocr Rev* 2022; 43: 91-159. 2021/05/08. DOI: 10.1210/endrev/bnab016.
2. Wilkins L, Lewis RA, Klein R, et al. The suppression of androgen secretion by cortisone in a case of congenital adrenal hyperplasia. *Bull Johns Hopkins Hosp* 1950; 86: 249-252. 1950/04/01.
3. Wilkins L, Lewis RA, Klein R, et al. Treatment of congenital adrenal hyperplasia with cortisone. *J Clin Endocrinol Metab* 1951; 11: 1-25. 1951/01/01. DOI: 10.1210/jcem-11-1-1.
4. Bartter FC, Albright F, Forbes AP, et al. The effects of adrenocorticotropic hormone and cortisone in the adrenogenital syndrome associated with congenital adrenal hyperplasia: an attempt to explain and

correct its disordered hormonal pattern. *J Clin Invest* 1951; 30: 237-251. 1951/03/01. DOI: 10.1172/JCI102438.
5. Adrenas. Trial Update from Adrenas Therapeutics, https://cahgenetherapy.com/news/jan24 (2024, accessed 31st March 2024).
6. Graves LE, van Dijk EB, Zhu E, et al. AAV-delivered hepato-adrenal cooperativity in steroidogenesis: Implications for gene therapy for congenital adrenal hyperplasia. *Mol Ther Methods Clin Dev* 2024; 32: 101232. 2024/04/01. DOI: 10.1016/j.omtm.2024.101232.
7. Pontoizeau C, Simon-Sola M, Gaborit C, et al. Neonatal gene therapy achieves sustained disease rescue of maple syrup urine disease in mice. *Nat Commun* 2022; 13: 3278. 2022/06/08. DOI: 10.1038/s41467-022-30880-w.
8. White PC. Emerging treatment for congenital adrenal hyperplasia. *Curr Opin Endocrinol Diabetes Obes* 2022; 29: 271-276. 2022/03/15. DOI: 10.1097/MED.0000000000000723.
9. Markmann S, De BP, Reid J, et al. Biology of the Adrenal Gland Cortex Obviates Effective Use of Adeno-Associated Virus Vectors to Treat Hereditary Adrenal Disorders. *Hum Gene Ther* 2018; 29: 403-412. 2018/01/11. DOI: 10.1089/hum.2017.203.
10. Cunningham SC, Dane AP, Spinoulas A, et al. Gene delivery to the juvenile mouse liver using AAV2/8 vectors. *Mol Ther* 2008; 16: 1081-1088. 2008/04/17. DOI: 10.1038/mt.2008.72.
11. Tajima T, Okada T, Ma XM, et al. Restoration of adrenal steroidogenesis by adenovirus-mediated transfer of human cytochromeP450 21-hydroxylase into the adrenal gland of21-hydroxylase-deficient mice. *Gene Ther* 1999; 6: 1898-1903. 1999/12/22. DOI: 10.1038/sj.gt.3301018.
12. Naiki Y, Miyado M, Horikawa R, et al. Extra-adrenal induction of Cyp21a1 ameliorates systemic steroid metabolism in a mouse model of congenital adrenal hyperplasia. *Endocr J* 2016; 63: 897-904. 2016/11/01. DOI: 10.1507/endocrj.EJ16-0112.
13. Perdomini M, Dos Santos C, Goumeaux C, et al. An AAVrh10-CAG-CYP21-HA vector allows persistent correction of 21-hydroxylase deficiency in a Cyp21(-/-) mouse model. *Gene Ther* 2017; 24: 275-281. 2017/02/07. DOI: 10.1038/gt.2017.10.
14. Cabanes-Creus M, Navarro RG, Zhu E, et al. Novel human liver-tropic AAV variants define transferable domains that markedly enhance the human tropism of AAV7 and AAV8. *Mol Ther Methods Clin Dev* 2022; 24: 88-101. 2022/01/04. DOI: 10.1016/j.omtm.2021.11.011.
15. Lisowski L, Dane AP, Chu K, et al. Selection and evaluation of clinically relevant AAV variants in a xenograft liver model. *Nature* 2014; 506: 382-386. 2014/01/07. DOI: 10.1038/nature12875.
16. Pekrun K, De Alencastro G, Luo QJ, et al. Using a barcoded AAV capsid library to select for clinically relevant gene therapy vectors. *JCI Insight* 2019; 4 2019/11/15. DOI: 10.1172/jci.insight.131610.
17. Cunningham SC, Spinoulas A, Carpenter KH, et al. AAV2/8-mediated correction of OTC deficiency is robust in adult but not neonatal Spf(ash) mice. *Mol Ther* 2009; 17: 1340-1346. 2009/04/23. DOI: 10.1038/mt.2009.88.
18. Gomes LG, Huang N, Agrawal V, et al. Extraadrenal 21-hydroxylation by CYP2C19 and CYP3A4: effect on 21-hydroxylase deficiency. *J Clin Endocrinol Metab* 2009; 94: 89-95. 2008/10/30. DOI: 10.1210/jc.2008-1174.
19. Sapirstein LA and Goldman H. Adrenal blood flow in the albino rat. *Am J Physiol* 1959; 196: 159-162. 1959/01/01. DOI: 10.1152/ajplegacy.1958.196.1.159.
20. Ryan US, Ryan JW, Smith DS, et al. Fenestrated endothelium of the adrenal gland: freeze-fracture studies. *Tissue Cell* 1975; 7: 181-190. 1975/01/01. DOI: 10.1016/s0040-8166(75)80015-2.
21. Graves LE, Torpy DJ, Coates PT, et al. Future Directions for Adrenal Insufficiency: Cellular Transplantation and Genetic Therapies. *J Clin Endocrinol Metab* 2023; 108: 1273-1289. 2023/01/08. DOI: 10.1210/clinem/dgac751.
22. Bibikova M, Carroll D, Segal DJ, et al. Stimulation of homologous recombination through targeted cleavage by chimeric nucleases. *Mol Cell Biol* 2001; 21: 289-297. 2000/12/13. DOI: 10.1128/MCB.21.1.289-297.2001.
23. Suzuki K, Yamamoto M, Hernandez-Benitez R, et al. Precise in vivo genome editing via single homology arm donor mediated intron-targeting gene integration for genetic disease correction. *Cell Research* 2019; 29: 804-819. DOI: 10.1038/s41422-019-0213-0.
24. Nakade S, Tsubota T, Sakane Y, et al. Microhomology-mediated end-joining-dependent integration of donor DNA in cells and animals using TALENs and CRISPR/Cas9. *Nat Commun* 2014; 5: 5560. 2014/11/21. DOI: 10.1038/ncomms6560.
25. Anzalone AV, Koblan LW and Liu DR. Genome editing with CRISPR-Cas nucleases, base editors, transposases and prime editors. *Nat Biotechnol* 2020; 38: 824-844. 2020/06/24. DOI: 10.1038/s41587-020-0561-9.
26. Anzalone AV, Randolph PB, Davis JR, et al. Search-and-replace genome editing without double-strand breaks or donor DNA. *Nature* 2019; 576: 149-157. 2019/10/22. DOI: 10.1038/s41586-019-1711-4.

27. White PC and Speiser PW. Congenital adrenal hyperplasia due to 21-hydroxylase deficiency. *Endocr Rev* 2000; 21: 245-291. 2000/06/17. DOI: 10.1210/edrv.21.3.0398.
28. Tajima T, Fujieda K, Nakayama K, et al. Molecular analysis of patient and carrier genes with congenital steroid 21-hydroxylase deficiency by using polymerase chain reaction and single strand conformation polymorphism. *J Clin Invest* 1993; 92: 2182-2190. 1993/11/01. DOI: 10.1172/JCI116820.
29. Anzalone AV, Gao XD, Podracky CJ, et al. Programmable deletion, replacement, integration and inversion of large DNA sequences with twin prime editing. *Nat Biotechnol* 2022; 40: 731-740. 2021/12/11. DOI: 10.1038/s41587-021-01133-w.
30. Zhao Z, Shang P, Mohanraju P, et al. Prime editing: advances and therapeutic applications. *Trends Biotechnol* 2023; 41: 1000-1012. 2023/04/01. DOI: 10.1016/j.tibtech.2023.03.004.
31. Chen Z, Kelly K, Cheng H, et al. In Vivo Prime Editing by Lipid Nanoparticle Co-Delivery of Chemically Modified pegRNA and Prime Editor mRNA. *GEN Biotechnology* 2023; 2: 490-502. DOI: 10.1089/genbio.2023.0045.
32. Miller DG, Petek LM and Russell DW. Adeno-associated virus vectors integrate at chromosome breakage sites. *Nat Genet* 2004; 36: 767-773. 2004/06/23. DOI: 10.1038/ng1380.
33. Kosicki M, Tomberg K and Bradley A. Repair of double-strand breaks induced by CRISPR-Cas9 leads to large deletions and complex rearrangements. *Nat Biotechnol* 2018; 36: 765-771. 2018/07/17. DOI: 10.1038/nbt.4192.
34. Cullot G, Boutin J, Toutain J, et al. CRISPR-Cas9 genome editing induces megabase-scale chromosomal truncations. *Nat Commun* 2019; 10: 1136. 2019/03/10. DOI: 10.1038/s41467-019-09006-2.
35. Leibowitz ML, Papathanasiou S, Doerfler PA, et al. Chromothripsis as an on-target consequence of CRISPR-Cas9 genome editing. *Nat Genet* 2021; 53: 895-905. 2021/04/14. DOI: 10.1038/s41588-021-00838-7.
36. Suchy FP, Karigane D, Nakauchi Y, et al. Genome engineering with Cas9 and AAV repair templates generates frequent concatemeric insertions of viral vectors. *Nat Biotechnol* 2024 2024/04/09. DOI: 10.1038/s41587-024-02171-w.
37. Higashitani Y and Horie K. Long-read sequence analysis of MMEJ-mediated CRISPR genome editing reveals complex on-target vector insertions that may escape standard PCR-based quality control. *Sci Rep* 2023; 13: 11652. 2023/07/20. DOI: 10.1038/s41598-023-38397-y.
38. Paulk NK, Pekrun K, Zhu E, et al. Bioengineered AAV Capsids with Combined High Human Liver Transduction In Vivo and Unique Humoral Seroreactivity. *Mol Ther* 2018; 26: 289-303. 2017/10/23. DOI: 10.1016/j.ymthe.2017.09.021.
39. Cabanes-Creus M, Liao SHY, Gale Navarro R, et al. Harnessing whole human liver ex situ normothermic perfusion for preclinical AAV vector evaluation. *Nat Commun* 2024; 15: 1876. 2024/03/15. DOI: 10.1038/s41467-024-46194-y.
40. Hofer M and Lutolf MP. Engineering organoids. *Nat Rev Mater* 2021; 6: 402-420. 2021/02/25. DOI: 10.1038/s41578-021-00279-y.
41. Westhaus A, Eamegdool SS, Fernando M, et al. AAV capsid bioengineering in primary human retina models. *Sci Rep* 2023; 13: 21946. 2023/12/12. DOI: 10.1038/s41598-023-49112-2.
42. Depla JA, Sogorb-Gonzalez M, Mulder LA, et al. Cerebral Organoids: A Human Model for AAV Capsid Selection and Therapeutic Transgene Efficacy in the Brain. *Mol Ther Methods Clin Dev* 2020; 18: 167-175. 2020/07/09. DOI: 10.1016/j.omtm.2020.05.028.
43. Kok CY, Tsurusaki S, Cabanes-Creus M, et al. Development of new adeno-associated virus capsid variants for targeted gene delivery to human cardiomyocytes. *Mol Ther Methods Clin Dev* 2023; 30: 459-473. 2023/09/07. DOI: 10.1016/j.omtm.2023.08.010.
44. Vidovic D, Carlon MS, da Cunha MF, et al. rAAV-CFTRDeltaR Rescues the Cystic Fibrosis Phenotype in Human Intestinal Organoids and Cystic Fibrosis Mice. *Am J Respir Crit Care Med* 2016; 193: 288-298. 2015/10/29. DOI: 10.1164/rccm.201505-0914OC.
45. Meyer-Berg H, Zhou Yang L, Pilar de Lucas M, et al. Identification of AAV serotypes for lung gene therapy in human embryonic stem cell-derived lung organoids. *Stem Cell Res Ther* 2020; 11: 448. 2020/10/25. DOI: 10.1186/s13287-020-01950-x.
46. Ikeda Y, Sun Z, Ru X, et al. Efficient Gene Transfer to Kidney Mesenchymal Cells Using a Synthetic Adeno-Associated Viral Vector. *J Am Soc Nephrol* 2018; 29: 2287-2297. 2018/07/07. DOI: 10.1681/ASN.2018040426.
47. Sakata Y, Cheng K, Mayama M, et al. Reconstitution of human adrenocortical specification and steroidogenesis using induced pluripotent stem cells. *Dev Cell* 2022; 57: 2566-2583 e2568. 2022/11/23. DOI: 10.1016/j.devcel.2022.10.010.
48. Bornstein S, Shapiro I, Malyukov M, et al. Innovative multidimensional models in a high-throughput-format for different cell types of endocrine origin. *Cell Death Dis* 2022; 13: 648. 2022/07/26. DOI: 10.1038/s41419-022-05096-x.

49. Steenblock C, Fliedner S, Spinas GA, et al. Development of adrenal 3-dimensional spheroid cultures: potential for the treatment of adrenal insufficiency and neurodegenerative diseases. *Explor Endocr Metab Dis* 2024; 1: 27-38. DOI: 10.37349/eemd.2023.00005.
50. Schubert T, Reisch N, Naumann R, et al. CYP21A2 Gene Expression in a Humanized 21-Hydroxylase Mouse Model Does Not Affect Adrenocortical Morphology and Function. *J Endocr Soc* 2022; 6: bvac062. 2022/05/21. DOI: 10.1210/jendso/bvac062.
51. Flotte TR, Afione SA, Conrad C, et al. Stable in vivo expression of the cystic fibrosis transmembrane conductance regulator with an adeno-associated virus vector. *Proc Natl Acad Sci U S A* 1993; 90: 10613-10617. 1993/11/15. DOI: 10.1073/pnas.90.22.10613.
52. ASGCT and Citeline. *Gene, Cell, + RNA Therapy Landscape Report: Q4 2023 Quarterly Data Report*. 2023.
53. Chiesi Farmaceutici Glybera (alipogene tiparvovec) in Europe, https://www.chiesi.com/en/glybera-alipogene-tiparvovec-in-europe/ (2017, accessed 5th April 2024).
54. Thomsen G, Burghes AHM, Hsieh C, et al. Biodistribution of onasemnogene abeparvovec DNA, mRNA and SMN protein in human tissue. *Nat Med* 2021; 27: 1701-1711. 2021/10/06. DOI: 10.1038/s41591-021-01483-7.
55. Asokan A and Shen S. Redirecting AAV vectors to extrahepatic tissues. *Mol Ther* 2023; 31: 3371-3375. 2023/10/08. DOI: 10.1016/j.ymthe.2023.10.005.
56. Seo JW, Ajenjo J, Wu B, et al. Multimodal imaging of capsid and cargo reveals differential brain targeting and liver detargeting of systemically-administered AAVs. *Biomaterials* 2022; 288: 121701. 2022/08/20. DOI: 10.1016/j.biomaterials.2022.121701.
57. Sellier P, Vidal P, Bertin B, et al. Muscle-specific, liver-detargeted adeno-associated virus gene therapy rescues Pompe phenotype in adult and neonate Gaa(-/-) mice. *J Inherit Metab Dis* 2024; 47: 119-134. 2023/05/19. DOI: 10.1002/jimd.12625.
58. Sheridan C. The world's first CRISPR therapy is approved: who will receive it? *Nat Biotechnol* 2024; 42: 3-4. 2023/11/22. DOI: 10.1038/d41587-023-00016-6.
59. Jinek M, Chylinski K, Fonfara I, et al. A Programmable Dual-RNA-Guided DNA Endonuclease in Adaptive Bacterial Immunity. *Science* 2012; 337: 816-821. DOI: 10.1126/science.1225829.
60. Buchlis G, Podsakoff GM, Radu A, et al. Factor IX expression in skeletal muscle of a severe hemophilia B patient 10 years after AAV-mediated gene transfer. *Blood* 2012; 119: 3038-3041. 2012/01/25. DOI: 10.1182/blood-2011-09-382317.
61. Nathwani AC, Tuddenham EG, Rangarajan S, et al. Adenovirus-associated virus vector-mediated gene transfer in hemophilia B. *N Engl J Med* 2011; 365: 2357-2365. 2011/12/14. DOI: 10.1056/NEJMoa1108046.
62. Musunuru K, Chadwick AC, Mizoguchi T, et al. In vivo CRISPR base editing of PCSK9 durably lowers cholesterol in primates. *Nature* 2021; 593: 429-434. 2021/05/21. DOI: 10.1038/s41586-021-03534-y.
63. Qiu M, Glass Z, Chen J, et al. Lipid nanoparticle-mediated codelivery of Cas9 mRNA and single-guide RNA achieves liver-specific in vivo genome editing of Angptl3. *Proc Natl Acad Sci U S A* 2021; 118: e2020401118. 2021/03/03. DOI: 10.1073/pnas.2020401118.
64. Gillmore JD, Gane E, Taubel J, et al. CRISPR-Cas9 In Vivo Gene Editing for Transthyretin Amyloidosis. *N Engl J Med* 2021; 385: 493-502. 2021/07/03. DOI: 10.1056/NEJMoa2107454.
65. Longhurst HJ, Lindsay K, Petersen RS, et al. CRISPR-Cas9 In Vivo Gene Editing of KLKB1 for Hereditary Angioedema. *N Engl J Med* 2024; 390: 432-441. 2024/01/31. DOI: 10.1056/NEJMoa2309149.
66. Akinc A, Maier MA, Manoharan M, et al. The Onpattro story and the clinical translation of nanomedicines containing nucleic acid-based drugs. *Nat Nanotechnol* 2019; 14: 1084-1087. 2019/12/06. DOI: 10.1038/s41565-019-0591-y.
67. Werbin H and Chaikoff IL. Utilization of adrenal gland cholesterol for synthesis of cortisol by the intact normal and the ACTH-treated guinea pig. *Arch Biochem Biophys* 1961; 93: 476-482. 1961/06/01. DOI: 10.1016/s0003-9861(61)80039-8.
68. Kraemer FB. Adrenal cholesterol utilization. *Mol Cell Endocrinol* 2007; 265-266: 42-45. 2007/01/09. DOI: 10.1016/j.mce.2006.12.001.

Appendix

8.1 Publications

8.1.1 Future directions for adrenal insufficiency: cellular transplantation and genetic therapies

Graves, LE, Torpy, DJ, Coates, PT, Alexander, IE, Bornstein, S and Clarke, B, Future directions for adrenal insufficiency: cellular transplantation and genetic therapies, *The Journal of Clinical Endocrinology and Metabolism*. 2023;108(6):1273-1289. Doi: 10.1210/clinem/dgac751

The Journal of Clinical Endocrinology & Metabolism, 2023, **108**, 1273–1289
https://doi.org/10.1210/clinem/dgac751
Advance access publication 6 January 2023
Invited Mini-Review

Future Directions for Adrenal Insufficiency: Cellular Transplantation and Genetic Therapies

Lara E. Graves,[1,2,3] David J. Torpy,[4,5] P. Toby Coates,[5,6] Ian E. Alexander,[2,3] Stefan R. Bornstein,[7] and Brigette Clarke[4,5]

[1]Institute of Endocrinology and Diabetes, Children's Hospital at Westmead, Westmead, New South Wales 2145, Australia
[2]Gene Therapy Research Unit, Children's Medical Research Institute, Faculty of Medicine and Health, The University of Sydney and Sydney Children's Hospitals Network, Westmead, New South Wales 2145, Australia
[3]Discipline of Child and Adolescent Health, Sydney Medical School, Faculty of Medicine and Health, The University of Sydney, Westmead, New South Wales 2145, Australia
[4]Endocrine and Metabolic Unit, Royal Adelaide Hospital, 5000 Adelaide, South Australia, Australia
[5]Adelaide Medical School, Faculty of Health and Medical Sciences, University of Adelaide, Adelaide, South Australia 5005, Australia
[6]Central Northern Adelaide Renal and Transplantation Service, Royal Adelaide Hospital, Adelaide, South Australia 5000, Australia
[7]Department of Medicine III, Universitätsklinikum Carl Gustav Carus an der Technischen Universität Dresden, 01307 Dresden, Germany

Correspondence: Lara E. Graves, BVSc, MBBS, FRACP, Institute of Endocrinology and Diabetes, The Children's Hospital at Westmead, Hawkesbury Rd, Locked Bag 4001, Westmead, NSW 2145, Australia. Email: Lara.graves@health.nsw.gov.au.

Abstract

Primary adrenal insufficiency (PAI) occurs in 1 in 5 to 7000 adults. Leading etiologies are autoimmune adrenalitis in adults and congenital adrenal hyperplasia (CAH) in children. Oral replacement of cortisol is lifesaving, but poor quality of life, repeated adrenal crises, and dosing uncertainty related to lack of a validated biomarker for glucocorticoid sufficiency persists. Adrenocortical cell therapy and gene therapy may obviate many of the shortcomings of adrenal hormone replacement. Physiological cortisol secretion regulated by pituitary adrenocorticotropin could be achieved through allogeneic adrenocortical cell transplantation, production of adrenal-like steroidogenic cells from either stem cells or lineage conversion of differentiated cells, or for CAH, gene therapy to replace or repair a defective gene. The adrenal cortex is a high-turnover organ and thus failure to incorporate progenitor cells within a transplant will ultimately result in graft exhaustion. Identification of adrenocortical progenitor cells is equally important in gene therapy, for which new genetic material must be specifically integrated into the genome of progenitors to ensure a durable effect. Delivery of gene-editing machinery and a donor template, allowing targeted correction of the 21-hydroxylase gene, has the potential to achieve this. This review describes advances in adrenal cell transplants and gene therapy that may allow physiological cortisol production for children and adults with PAI.

Key Words: adrenal insufficiency, Addison disease, congenital adrenal hyperplasia, adrenal cortex, cell therapy, gene therapy

Abbreviations: 3T3, fibroblast growth factor–secreting cell line; ACT, adrenal cell transplant; ACTH, adrenocorticotropin; AD, Addison disease; Adx, adrenalectomy; βAir, oxygenating and immunoisolating βAir device; BAC, bovine adrenocortical cells; CAH, congenital adrenal hyperplasia; cAMP, cyclic adenosine monophosphate; cDNA, complementary DNA; ECM, extracellular matrix; enBACs, alginate-encapsulated bovine adrenocortical cells; GLI1, glioma-associated oncogene homolog 1; HAC, human adrenocortical cells; HITI, homology-independent targeted integration; ICAM-1, intercellular-adhesion molecule-1; iPSCs, induced pluripotent stem cells; MAC, murine adrenocortical cells; mADSC, mouse adipose tissue stem cells; MC, mineralocorticoid; MHC, major histocompatibility complex ; mRNA, messenger RNA; MSC, mesenchymal stem cell; NHP, nonhuman primate; PAI, primary adrenal insufficiency; rAAV, recombinant adeno-associated virus; SCID, severe combined immunodeficiency; SF-1, steroidogenic factor-1; SHH, sonic hedgehog; vgc, vector genome copies; Wnt, wingless-type MMTV integration; WT1, Wilms tumor 1.

Excess mortality and morbidity remain for people with primary adrenal insufficiency (PAI), despite adrenal steroid replacement (1, 2). PAI, including Addison disease (AD) and congenital adrenal hyperplasia (CAH), are characterized by insufficient production of the key adrenocortical hormones. AD is commonly due to autoimmune adrenal destruction with sequential loss of aldosterone and then cortisol secretion (3). CAH is the most common form of PAI in children and includes 7 monogenic adrenal disorders, caused by mutations in genes coding for various enzymes in the adrenal steroidogenic pathway: *CYP21A2*, *CYP11B1*, *CYP17A1*, *3BHSD*, *STAR*, *CYP11A1*, and *POR* (4). In approximately 95% of cases, CAH is due to autosomal recessive pathogenic variants in the *CYP21A2* gene. Loss of activity of the adrenal biosynthetic enzyme 21-hydroxylase results in varying degrees of adrenal insufficiency and concomitant adrenocorticotropin (ACTH)-driven overproduction of adrenal-derived androgens (4). Phenotypically, 21-hydroxylase–deficient CAH can be divided into classic and nonclassic forms, with the classic form further divided into salt-wasting and simple virilizing. Although the phenotypes are defined as such, the phenotype seen in 21-hydroxylase deficiency is a continuous spectrum based on residual enzyme activity. While aldosterone deficiency is not generally clinically significant in simple virilizing

Received: 19 July 2022. **Editorial Decision:** 23 December 2022. **Corrected and Typeset:** 10 January 2023

and nonclassic CAH, there is some degree of aldosterone deficiency in all phenotypes (5). Most patients have compound heterozygosity, and the phenotype tends to correlate with the less severe allele (6, 7). Pathogenic variants in the *CYP11B1* gene are the second most common cause of CAH and result in CAH with elevated deoxycorticosterone and 11-deoxycortisol, virilization, and hypertension due to the mineralocorticoid effect of deoxycorticosterone (4).

The isolation and synthesis of adrenal steroids in the mid-20th century provided effective replacement of cortisol with hydrocortisone, cortisone acetate, or synthetic steroids and aldosterone with fludrocortisone, ensuring prolonged survival (3, 8, 9). Ongoing clinical difficulties in PAI include a 2-fold increased mortality largely due to cardiovascular, malignant, and infectious causes with higher mortality in women (1); impaired quality of life in a substantial minority of treated cases (10); and potential overtreatment or undertreatment with glucocorticoids, given the lack of a practically validated biomarker to allow dose individualization (1). Adrenal crises also remain a substantial issue in treated AD, with an annual incidence of 6% to 8% (11, 12). Nearly half of all affected individuals with AD experience at least one adrenal crisis in their lifetime (12). The mortality rate associated with each adrenal crisis event may be as high as 6% in individuals with AD optimally educated in crisis management (13). A detailed review of adrenal crisis has recently been published elsewhere and is beyond the scope of this review (14).

Children with CAH have the burden of androgen excess with virilization of the genitalia, premature pubarche, central precocious puberty, rapid skeletal growth and maturation, menstrual irregularity, short stature, and hirsutism. In adulthood health risks include reduced fertility due to disturbance of hypothalamic-pituitary gonadal function, adrenal rest tissue within testes (or ovaries) that may cause infertility, obesity, hypertension, low bone density, reduced stature, and neurocognitive effects such as attention-deficit/hyperactivity disorder, anxiety, and depression (15-21). There is reduced life expectancy by almost 2 decades, and adrenal crisis remains the major cause of death for individuals with CAH (2, 21, 22). For most people with CAH, hormone replacement rarely achieves simultaneous optimal adrenal hormone replacement and androgen suppression, to the extent that bilateral adrenalectomy is occasionally considered (23).

In skeletally immature children with adrenal insufficiency, standard maintenance therapy is thrice-daily oral hydrocortisone, with fludrocortisone if biochemically indicated. Adults should be treated with twice- or thrice-daily hydrocortisone or other long-acting glucocorticoids with or without fludrocortisone (3, 24). However, the balance between overtreatment and undertreatment, and quality of life, is challenging. Attempts to mitigate the shortcomings of conventional oral glucocorticoid tablets, attributed in part to a lack of normal circadian cortisol concentrations, have included multidosing diurnal regimens, long-acting hydrocortisone preparations including once-daily Plenadren (suitable for adults with AD) (25) and twice-daily Efmody (suitable for people aged > 12 years with CAH) (26) and experimentally, subcutaneous hydrocortisone infusions (27, 28). Plenadren combines immediate- and delayed-release hydrocortisone (29). Efmody is a modified-release hydrocortisone that attempts to mimic the circadian rhythm through delayed release and sustained absorption with a twice-daily dosing regimen marketed for individuals with CAH older than 12 years (30). However, when compared to standard therapy, there was no difference in the 24-hour 17-hydroxyprogesterone (17OHP) profile (31). Pulsatile glucocorticoid signals are required for regulatory systems within the hypothalamic-pituitary-adrenal axis and long-acting synthetic glucocorticoids cannot mimic this (32). While quality of life may be improved with these long-acting preparations, this has not been subject to double-blinded clinical trials. None of these approaches offer the panoply of features needed to recapitulate physiology, including individualized glucocorticoid replacement in accord with circadian, ultradian, and stress requirements. Recovery of native adrenocortical function has been achieved in a minority of individuals with autoimmune AD, using immunosuppression and/or ACTH stimulation (33-35). This implies a population of potentially hormonally viable adrenocytes that may recover with appropriate stimulus and protection from autoimmune attack and remains an area of ongoing investigation as has been extensively and recently reviewed (36).

There is precedent for endocrine cell therapy in place of pharmacologic hormone replacement, with allogeneic pancreatic β-cell transplantation for type 1 diabetes already in clinical use. It is evident from the islet cell experience that heterotopic cell transplantation is feasible and that in appropriately selected patients, the risks of immunosuppression are outweighed by the restoration of physiological regulated hormone secretion (37-40). Provision of self-sustaining adrenal cell therapy regulated by physiologic stimuli for people with PAI and/or durable installation of a functioning gene in CAH offers the potential for restoration of normal physiology without the requirement for constant patient intervention (Fig. 1). Recent work has moved cell and gene therapies closer to realization and is the subject of this review.

Adrenal Ontogeny and Regeneration

The adrenal cortex originates from the adrenogonadal primordium, a cluster of cells in the coelomic epithelium that give rise to adrenal and gonadal anlagen (41). The adrenal anlagen are invaded by neural crest cells to form the medulla and fibroblasts to form the adrenal capsule (42). The molecular signals driving differentiation toward either the adrenocortical or gonadal phenotype remain to be fully defined, but GATA binding protein 4 activation appears critical in gonadal differentiation (43, 44). In fetal life there is an initial development of the adrenal cortex as the large central fetal zone, followed by the peripheral definitive zone and later the transitional zone. The inner fetal zone involutes postnatally via apoptosis, and the definitive zone gives rise to the adult zona glomerulosa and zona fasciculata (45). The zona reticularis (present in humans and nonhuman primates [NHPs]) begins to form in humans from age 4 to 6 years and by 6 to 8 years produces adrenal androgens including dehydroepiandrostenedione, testosterone, 11-β hydroxytestosterone, and 11-ketotestosterone, a process known as adrenarche (46-48).

The capacity of the rat adrenal to regenerate from remaining capsular cells after enucleation was described in 1938 (49). Cell-lineage tracing has confirmed long-held notions of centripetal migration and lineage conversion of adrenocortical cells across adrenal zones until apoptosis at the corticomedullary junction (50-53). In addition to cell-programmed death, steroidogenesis results in accumulation of reactive oxygen species and as a result of this adrenocortical cells are sensitive to an iron-dependent mechanism of cell death known as

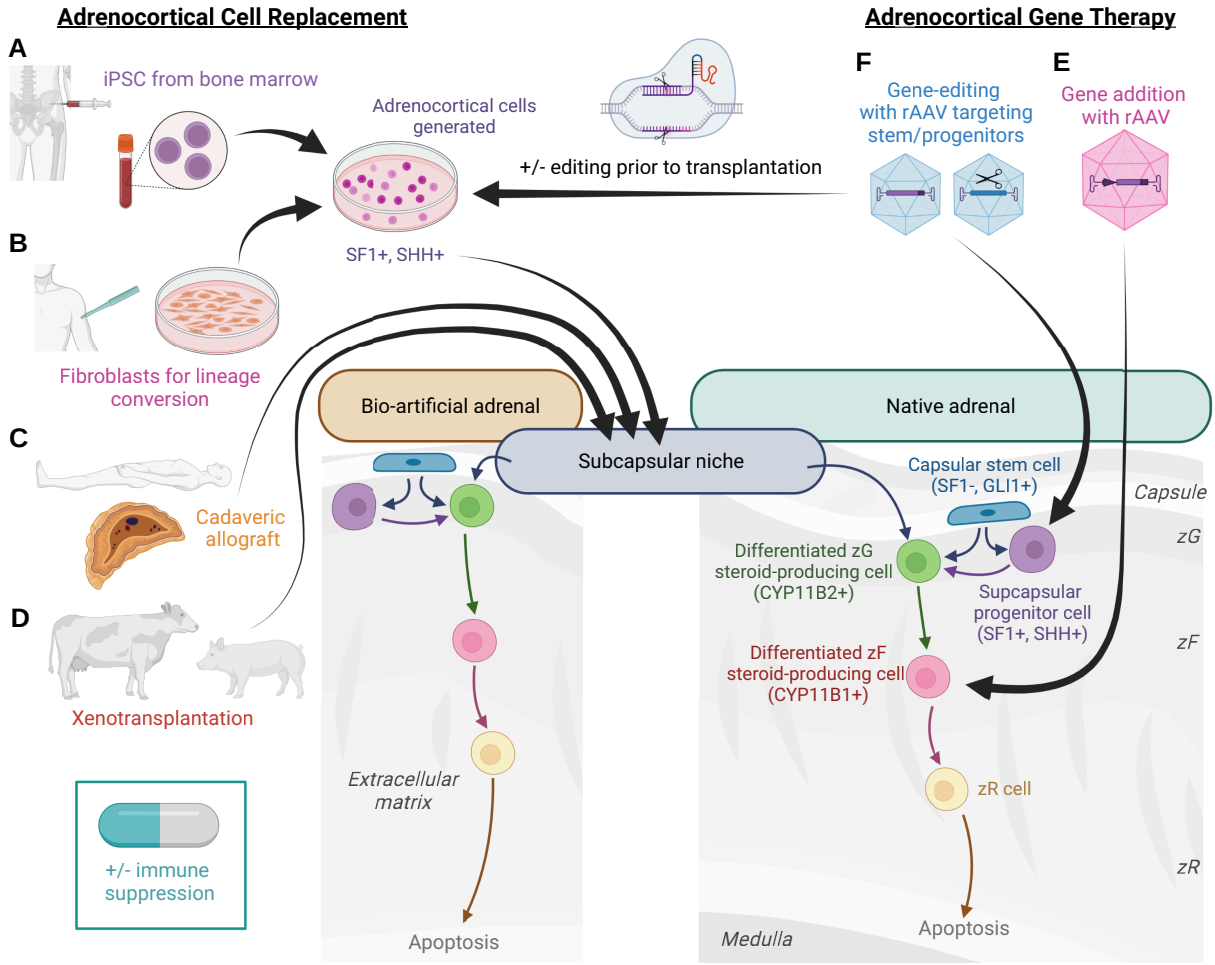

Figure 1. Proposed cell transplant and gene therapy approaches. Adrenocortical cellular replacement could occur in the form of A, induced pluripotent stem cells harvested from bone marrow, or B, cells such as fibroblasts that are forced to undergo lineage conversion. Both of these cell populations could be used to generate adrenocortical cells including SF1+/SHH + adrenal progenitor cells before implantation in either an artificial niche, or directly into the extracellular matrix of the adrenal cortex. C, Cadaveric allografts or D, xenotransplants are potential sources of primary adrenocortical cells. Immune suppression may be required for allografts and xenografts or for suppression of autoimmunity. E, Gene therapy using gene addition has been attempted whereby differentiated steroid producing cells were transduced with recombinant adeno-associated virus (rAAV). However, this tactic is limited by cellular turnover. F, For gene therapy to be durable, the adrenocortical progenitor or stem cells must be targeted with gene editing technology whereby the new genetic material is stably integrated into the host cell genome to allow the therapy to be passed on to daughter cells. Cells destined for transplantation may also be treated with gene editing before transplant, if necessary for example in other monogenic adrenal insufficiencies. Created with BioRender.com.

ferroptosis (54, 55). With the high rate of cell turnover, adrenocortical cells are relatively short-lived (56). This has important implications for the application of cellular therapies, particularly when compared to the characteristics of islet cells, which are long-lived cells with low turnover (57).

Paracrine factors crucial in adrenocortical cell development include those of the sonic hedgehog (SHH) and wingless-type MMTV integration pathway (Wnt) pathways (Fig. 2). Glioma-associated oncogene homolog (GLI1) expressing capsular cells respond to paracrine effectors of the SHH pathway and are important in cell differentiation and adult tissue regeneration through proliferation. Wilms tumor 1 (WT1)-expressing cells produce WT1, which initiates synthesis of steroidogenesis factor 1 (SF-1, encoded by the gene *NR5A1*), a transcription factor essential for adrenal development and an initiator of steroidogenic gene expression through binding to their response elements (58, 59).

GLI1+/SF-1–capsular cells appear to behave as adrenocortical stem cells, giving rise to SF-1 + cells and the SF-1+/SHH + progenitor cell pool (60). Canonical β-catenin–dependent Wnt signaling (Wnt 4 and 5) is essential for adrenal development and maintenance of the subcapsular progenitor cell population. β-catenin expression is present in the progenitor cells and the differentiated zona glomerulosa cells but absent in the zona fasciculata cells as ACTH dependence develops (50, 61, 62). As cells migrate away from Wnt influence, they become receptive to ACTH, which enforces differentiation into a steroid-producing cell of the zona fasciculata (62). Dosage-sensitive sex reversal, adrenal hypoplasia critical region, on chromosome X, gene 1 (*DAX1*) is a repressor of SF-1–mediated transcription maintaining a lack of steroidogenesis in SF1 + adrenocortical progenitors (63, 64). Hence, the SHH pathway is important in cell differentiation and the Wnt4 pathway is key to adrenal cell proliferation in the zona glomerulosa with SF-1 acting to initiate steroidogenesis, requiring the cyclic adenosine monophosphate (cAMP) pathway. Adrenal cell specialization occurs through lineage conversion of cells with activation of the *CYP11B2* gene leading

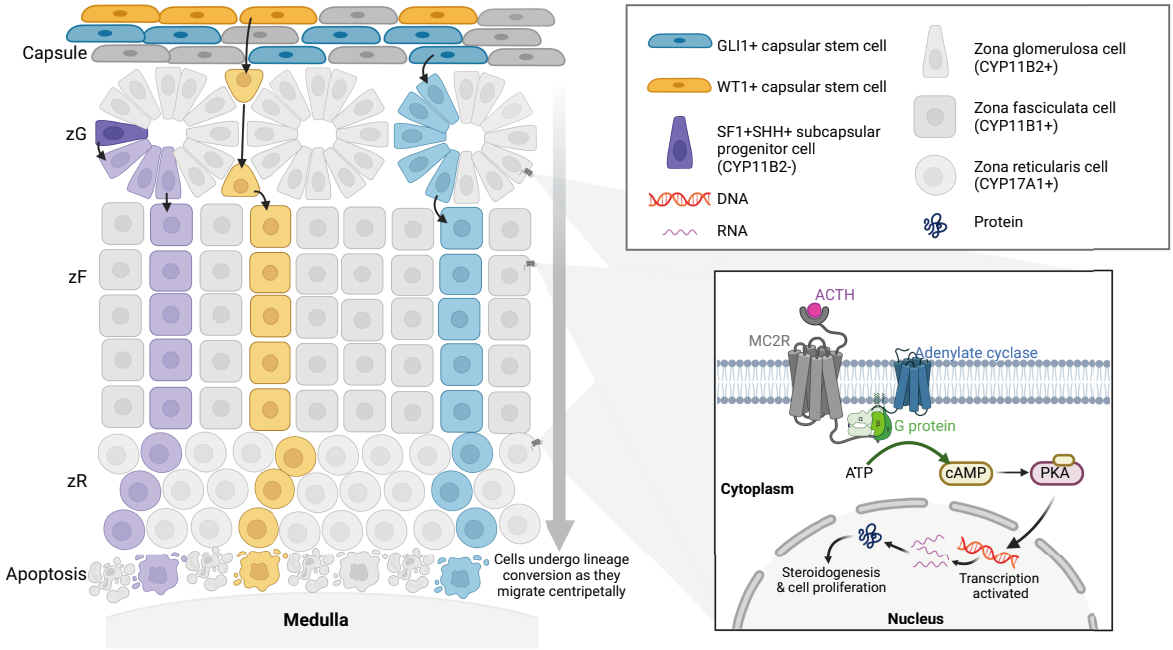

Figure 2. The subcapsular adrenal cortex contains stem cells expressing GLI1, which respond to paracrine signals of the hedgehog pathway, crucial in adrenal differentiation. WT1-expressing cells produce WT1 to initiate SF1 expression to initiate the adrenal cell steroidogenic pathway, requiring activation of the cyclic AMP (cAMP) pathway stimulated by circulating pituitary ACTH for effective steroidogenesis and negatively regulate the Wnt-β-catenin pathway. High Wnt pathway activity keeps adrenal cells in a zG state, reducing Wnt activity has a mitogenic effect. The MC2R (ACTH) receptor is expressed following SF-1 action as are steroidogenic genes; ACTH stimulates expression of most adrenal transcription factors and acts through the cAMP/protein kinase A (PKA) pathway. The 3 adrenal layers differentially express steroidogenic pathways to produce a predominance of aldosterone (zG, CYP11B2+), cortisol (zF, CYP11B1+), and adrenal androgens, DHEA, and androstenedione (zR, CYP17A1+). Adrenal cells migrate centripetally to reach an apoptotic state at the corticomedullary junction.
Abbreviations: ACTH, adrenocorticotropin; DHEA, dehydroepiandrostenedione; GLI1, glioma-associated oncogene homolog; SF1, steroidogenic factor 1; WT1, Wilms tumor 1; zF, zona fasciculata; zG, zona glomerulosa; zR, zona reticularis. Created with BioRender.com.

to aldosterone secretion and, with further centripetal migration, expression of *CYP11B1* and glucocorticoid secretion (62). Subsequent activation of *CYP17A1* is required for zona reticularis function.

ACTH sustains the adrenal cortex via the cell surface receptor ACTH receptor, melanocortin 2 receptor (MC2R), which requires the melanocortin receptor accessory protein (MRAP) for action (65). While ACTH acts on both zona glomerulosa and zona fasciculata cells, maintenance of the zona fasciculata cell-type and stimulation of glucocorticoid steroidogenesis is paramount (62). ACTH increases cytoplasmic cAMP production and hence protein kinase A activity, a process regulated by its regulatory subunits (PRKAR1A, PRKAR1B, PRKAR2A, PRKAR2B) and phosphodiesterases in steroidogenesis. ACTH stimulates the growth of the adrenal cortex through cellular proliferation in stress and disease, as well as the growth of vascular endothelial cells in the adrenal cortex (66-68). Angiotensin II sustains and regulates the zona glomerulosa, stimulating aldosterone production by zona glomerulosa cells as part of the renin-angiotensin-aldosterone system (50, 69). The extracellular matrix is also thought to modulate the cellular response to ACTH, angiotensin II, and growth factors (50).

Adrenocortical regeneration is sexually dimorphic with male mice regenerating from SHH+/SF-1 + progenitor cells in the zona glomerulosa and females additionally from GLI + capsular stem cells (56). The speed of tissue renewal also depends on sex: The adrenal cortex turns over every 3 months in female mice and every 9 months in males (56). Capsular stem cell recruitment and proliferation is suppressed by androgens, leading to a 3-fold higher tissue turnover in females (56). Adrenal sex differences in postpubertal rats are also dependent on liver-produced plasma corticosteroid-binding globulin (70). The relevance of these sex-dependent findings in mice is uncertain in humans: Adrenocortical volume is greater in female mice but less in women as compared to men when measured at autopsy, but centripetal cell migration is present in humans (62, 71). Whether human adrenal cortices undergo the same rapid cellular turnover of other species or whether the adrenal is more stable with slow turnover is not known. An effect of androgens on adrenocortical cell turnover has not been demonstrated in humans; however, speculatively, adrenal androgen excess in CAH may reduce cell turnover and exacerbate glucocorticoid and mineralocorticoid deficiency. ACTH stimulation of humans with PAI has shown greater residual secretory function among men (35, 72).

Stem and progenitor cells are generally imbedded in a specialized environment of extracellular matrix (ECM) with cell localization and growth factors known as a niche; the precise composition of the adrenocortical cell niche is not established (50). Adrenal cell cultures in vitro indicate that specific components of the ECM affect cellular responses to ACTH and growth factors (50). The provision of adrenocortical stem and/or progenitor cells and an appropriate niche is likely to be of critical importance in adrenal replacement therapies. Incorporation of progenitor cells in primary cell isolates for transplantation would ensure graft longevity, facilitating a self-sustaining transplant cell population as mature functioning

cells reach senescence and apoptose. In addition, for genomic therapy to be durable, the adrenal stem or progenitor cells must be targeted as immune responses preclude repeated doses of vector-based therapies. Residual adrenocortical function has also been identified in a significant minority of individuals with autoimmune AD (73-76) and it may be hypothesized that there is persistence of adrenocortical progenitor and or stem cells to explain this finding. Exploration of therapeutics to promote proliferation and differentiation of these cells, while protecting them from autoimmune-mediated destruction to regenerate the native adrenal, remains an area for further investigation (36). Complete isolation and characterization of adrenocortical stem and progenitor cells has not been achieved and remains an important priority.

Adrenal Cell Transplantation

Requirements for Adrenal Cell Transplantation

Successful adrenal cell transplantation (ACT) has several prerequisites:

- Cortisol secretion from transplanted cells in response to ACTH under basal, circadian, and ultradian and physiological stress conditions.
- Aldosterone secretion in accord with the major physiological drivers, especially angiotensin II and potassium.
- Transplant site with provision of cell requirements and ideally protection of transplanted cells from immune attack, both rejection in the case of allogenic cells and from autoimmunity in AD.
- Provision of adrenocortical progenitor cells for long-term maintenance of functional adrenal tissue after senescence of transplanted differentiated cells.

Procuring Adrenal Cells for Transplantation

Potential sources of cells to replace adrenocortical cell function by transplantation include cadaveric human donors, either as allogenic whole-gland transplants or primary cellular isolates, xenografts from animal donors, adrenal-like steroidogenic cells produced from stem cells, or by altering adult cells through reprogramming or lineage conversion (see Fig. 1A-1D). Use of mature adrenal organs or cells offers the benefit of immediate function. Whole-gland as compared to cell transplantation is limited by the technical challenges of primary revascularization (77) and likely increased immunologic load due to incorporation of multiple cell types (78), although it retains the benefit of a natural cell environment and incorporation of progenitor cells within the niche. As demonstrated with islet cell transplantation, the intact adrenal structure may not be necessary to restore hormonal function. ACT has the additional benefits of being less invasive and may facilitate the use of immune-isolating devices to prevent immune-mediated cellular destruction (79). A central problem is that transplanted cells may already be or ultimately become terminally differentiated. Since adrenal cell turnover is likely to be as high within the transplant as in the native gland (56), the durability of adrenal cell function may be limited without the presence of adrenocortical progenitor cells. Ensuring primary adrenocortical cell isolates include progenitors is of critical importance, though in the absence of well-defined markers for identification (50), there are currently no existing mechanisms to objectively evaluate this. Adrenocortical cell isolation processes for the purpose of clinical transplantation also requires further optimization, including determining the role of additional constituents such as cotransplanted nonsteroidogenic cells or ECM components, and maximizing cellular yield to achieve a cell mass capable of delivering clinically significant hormonal production.

Availability of allogenic human donor organs is a major limitation in transplantation; xenografts have the benefit of reliable supply, though are more immunogenic and thus carry a considerably higher risk of immunologic rejection. Risk of xenozoonosis also exists (80). Fetal organ and cell transplants have long been considered desirable because of the perceived lower immunogenicity, due to reduced major histocompatibility complex (MHC) class I and II antigen expression, though experimental data specific to transplantation of fetal adrenal cells do not necessarily support this theory (81). In experimental pancreatic islet xenotransplantation, the use of neonatal islet clusters as a cellular source has been studied by several groups (82-85). While these sources are efficacious in preclinical models, they have the disadvantage of requiring in vivo maturation before full function (82, 86). Experience with transplantation of fetal adrenocortical cells is limited, though a similar delay to function seems apparent; xenotransplantation of human fetal ACT resulted in negligible cortisol and aldosterone secretion after 20 days compared with mature adrenocytes (87). Comparison of fetal and mature grafts has not been evaluated head to head over a longer period of observation, though in comparable animal models, corticosterone levels reached only 70% of normal controls at 6 months with murine fetal grafts (88) and were restored to near normal levels within 4 to 5 weeks with adult murine ACT (89, 90).

Cellular reprogramming is the transformation of differentiated cells into a mature cell of a different type. This may involve de-differentiation: initial studies involved the production of induced pluripotent stem cells (iPSCs) from mature murine cells (91). Alternatively, lineage conversion from differentiated cells to another cell type using forced gene expression does not require dedifferentiation to stem cells and may reduce mutation frequencies (92). Adrenal-like steroidogenic cells have been produced from embryonic stem cells, iPSCs from skin fibroblasts (93), mouse bone marrow cells (94), mouse adipose mesenchymal cells (95, 96), human bone marrow mesenchymal stem cells (MSCs) (97), urine-derived stem cells (98), umbilical cord blood (UCB-MSCs), and Wharton jelly–derived MSCs (UC-MSCs) (99).

Generating steroidogenic cells from autologous sources may expand the applicability of cell transplantation therapy by obviating allograft rejection. Induced steroidogenesis nonetheless risks incomplete reproduction of the adrenal cell steroid secretory repertoire or production of a steroid output comparable to gonadal or trophoblast cells. The molecular signals critical for directing cell differentiation toward an adrenal-like as compared to gonadal-like steroidogenic cell are incompletely defined. Over expression of SF-1, desert hedgehog, human choriogonadotropin, and cAMP is required for production both of adrenocortical-like steroidogenic cells and Leydig-like cells in culture of human iPSC-derived early mesenchymal progenitors, though inclusion of type 1 collagen is essential for the latter (100). Ensuring appropriate responsiveness to physiologic stimuli controlling steroidogenesis, including ACTH, is also critical for the success of transplanted induced steroidogenic cells (96). The longevity of generated steroidogenic cells in vivo also remains uncertain, with only short-term experimental data to 30 days reported to date (96).

Outcomes of Reported Adrenal Cell Transplantation Experiments

There are a small number of case reports of successful adult human adrenal allotransplants for primary adrenal insufficiency, facilitated by en bloc engraftment with the kidney (101, 102), or intramuscular implantation of piecemeal tissue (103); cotransplantation of another solid organ and standard immunosuppressive therapy occurred in all cases. Restoration of adrenal function was successfully reported by demonstration of normalization of basal cortisol and aldosterone levels, the absence of requirement of mineralocorticoid and/or glucocorticoid supplementation, or a cortisol response to synthetic ACTH, with or without the continuation of immunosuppressive glucocorticoid. A series of human fetal adrenal allografts with primary anastomosis has also reported normalization of serum cortisol and urine 17-hydroxycorticosterone and 17-ketosteroid levels and cessation of glucocorticoid support in 9 of 13 individuals at follow-up between 3 and 21 months' duration (104). Immunosuppression with either cyclosporine A or azathioprine was administered to all patients in this series.

Experience with ACT for primary adrenal insufficiency is, at present, predominantly preclinical, and centered on murine studies; immunodeficient or syngeneic recipients have been widely employed in these models to obviate rejection.

Transplant success has been evidenced by on one or more of production of corticosterone (murine donor) (89, 90, 105) or cortisol (bovine or human donor) (79, 87, 106-109), adrenal responsiveness to exogenous ACTH (79), or confirmation of adrenal-specific gene expression more than 8 weeks after ACT (110). Circulating aldosterone, where measured, was inconsistently present (107, 108). Experience with transplantation of induced steroidogenic cells in an adrenalectomized model is limited to a single published study. Systemic glucocorticoid production by transplanted cells was evident, though ACTH responsiveness was absent due to low expression of the ACTH receptor and cells failed to form a tissue structure as seen with primary cell transplantation (96). The outcomes of the published murine ACT models to date are summarized in Table 1.

In addition to biochemical evidence of ACT function, ACT in the setting of bilateral adrenalectomy significantly improves short-term (3-8 weeks) survival rates in rodents to between 80% and 100% (68, 79, 87, 89, 105, 106, 108, 109, 113). Long-term survival over 300 days with persistent adrenocortical hormone production is also described (77, 90). Survival following ACT in adrenalectomized models is enhanced by early glucocorticoid support post adrenalectomy (68), a greater transplanted cellular dose (105), and cotransplantation with fibroblast growth factor–producing fibroblast growth factor–secreting cells (3T3) cells (68).

Practical Issues for Clinical Translation of Adrenal Cell Transplantation

The renal subcapsular site has been the favored approach for cell transplantation in murine ACT studies, chosen for its vascularity (115). It is possible that this site may provide MSCs capable of differentiation, but this has not been explored as a factor in ACT success. Free cells, or devices such as polycarbonate cylinders, collagen sponges, or gels have variously been employed for cell delivery (see Table 1), with the latter techniques having the benefit of containing the transplanted cells. In the native gland, adrenocortical ECM, and its associated proteins collagen IV, laminin, and fibronectin provide structural support and regulate cell signaling and cell-to-cell interactions, with differences in composition exhibited across the adrenocortical zones (50). Whether these components are required for cell transplant success has not been determined.

An optimal site for clinical ACT would require good vascularization and ideally, access for graft monitoring. Islet cell transplantation to the liver via the portal circulation has been successful; the site has high vascularity, is exposed to dietary nutrients and only a modest number of cells is sufficient (116). Encapsulation of cells is appealing as it allows reduced or no immunosuppression and may allow the use of xenogeneic cells (79). However, alginate capsules elicit a strong fibrotic foreign-body response with cell necrosis in humans (117). Other mechanical barriers such as Theracyte and Beta-air devices may have insufficient space for the cell numbers required for adrenal cell grafts. Decellularized porcine adrenal ECM as an in vitro scaffold improved adrenal cell proliferation (118); the capability to produce a 3-dimensional adrenal tissue structure, and contributions of specific ECM components in adrenocortical cell proliferation, differentiation, and function may be important for ACT success. Advanced 3-dimensional bioprinting of biomaterials acting as a scaffold and a vascularized space containing cells grouped as organoids are being developed for islet transplants and may be ideal for adrenal transplantation (119).

Alternative sites for endocrine cell transplantation have been trialed both experimentally and clinically for islet cells and may inform ACT. Implanted rods to create a dense vascular network in the subcutaneous tissue for cell transplant has been studied by the Edmonton group (120). An alternative approach, using a fully biodegradable temporizing matrix, a clinically approved artificial dermal scaffold for the treatment of wounds and severe burns, has recently begun a phase 1 clinical trial for islet cell transplantation (anzctr.org.au ACTRN12621001573842). Porous scaffolds made from novel biocompatible polymers have also been extensively studied in small-animal models and show promise for translation for cell therapy to the clinic (121).

In translation to a clinical setting, ACT recipients will require initial glucocorticoid support to avoid adrenal crisis during engraftment. However, glucocorticoid support will reduce circulating ACTH. Graft production of cortisol is reduced in animal experiments in which adrenalectomized animals are transiently supported with corticosteroids after transplantation (106, 108, 109). ACTH promotes the differentiation of adrenal progenitors into steroidogenic cells (122) and stimulates proliferation of the transplanted adrenal cell mass (123). Exogenous ACTH stimulation using long-acting depot preparations, as has been used in adrenal cell regeneration studies in patients with adrenal insufficiency (34, 35), may be required to expedite adrenocortical function of transplanted cells.

Glucocorticoids are immunomodulatory, inhibiting proliferation of antigen-presenting cells, tumor necrosis factor-α secretion, and T-cell stimulatory responses—a net result is inhibition of local inflammation and fibrosis formation within biocompatible polymer scaffolds (124, 125). Glucocorticoid production from allogeneic ACTs may reduce immunosuppressive requirements as compared to other allografts; studies suggest that adrenal cells are less prone to rejection than other endocrine cells such as those of the adrenal medulla or

Table 1. Summary of adrenal cell transplantation experiment outcomes in bilaterally adrenalectomized animal models

Year	Cell type and recipient species	Transplant site and method	Outcomes		
			Structural	Hormonal	Survival and duration following Adx
1987 (111)	MAC, syngeneic Wistar rats Allogenic MAC, Lewis rats	KC, enucleated adrenal capsule ± 2 wk immunosuppression (CyA) ± 7 d cell culture pre transplant	Normal adrenal morphology and regeneration Lymphocytic infiltration evident in + CyA group, but absent in all grafts treated both with CyA and culture	CS levels lower than control (non-Adx) animals CS levels in surviving animals lower compared to syngeneic transplants at 28 d	100% survival, all conditions, 30 d No culture/CyA: 0%; +culture and CyA: 100%; +CyA only: 66%; +culture only: < 10%, 30 d
1989 (89)	MAC, syngeneic Lewis rats	KC, cell suspension Transplant 2 wk before Adx	Viable adrenocortical cells without cortical architectural arrangement	Basal CS levels comparable to wild-type controls at 5 wk	100%, 8 wk
1997 (106)	BAC clone + 3T3, SCID mice	KC, cell suspension 7 d of GC and MC after Adx	Viable, well-vascularized adrenal tissue. Evidence of continued cell proliferation	Detectable blood cortisol levels at 30 d	81%, 36-41 d
1999 (87)	Primary BAC + 3T3, SCID mice Primary HAC + 3T3, SCID mice Primary fetal HAC + 3T3, SCID mice	Subcutaneous in type 1 collagen gel	Viable, well-vascularized adrenal tissue. Cell proliferation evident. Variable nodule size. Cells vascularized and arranged in cord-like structures within larger nodules. Low cell proliferation. High cell proliferation. Histologic features less well developed, including absence of sinusoidal capillaries	Cortisol and aldosterone levels significantly higher with BAC compared with adult HAC transplants at d 20. Minimal hormone production with fetal HAC grafts. Preserved circadian rhythm of cortisol production with BAC transplant	77%, > 20 d 83%, > 20 d 31%, > 20 d
1999 (68)	Primary BAC, SCID mice	KC, cell suspension. ± 3T3 ± 7 d GC/MC support ± saline drinking water	Viable, well-vascularized adrenal tissue	Detectable cortisol and detectable but low-level aldosterone and CS in surviving animals (all groups) at 36 d	BAC alone: 65% ; +3T3: ~ 75% ; +GC/MC: 80%; +3T3 and GC/MC: 100%; +3T3 and saline: 100%, 36 d
1999 (112)	MAC, Immune-competent Wistar rats	Omental sac, allogenic fetal adrenal without primary vascular anastomosis Staged Adx at 1 y No immune suppression	At 1 y, persistence of viable adrenal tissue in 35% Rejection with lymphocytic infiltrate in 50% and technical failure (no detectable tissue) in 15%	Rapid decline in measured CS within 6 h of completion Adx, regardless of presence/absence of viable adrenal graft	0% (irrespective of presence/absence of viable adrenal graft), 48 h
2000 (107)	Primary BAC + 3T3, SCID mice Primary BAC + 3T3, SCID mice Primary BAC + 3T3, SCID mice	Subcutaneous fascial pocket Intradermal, as cell suspension Intradermal, in injectable collagen	Viable, well-vascularized adrenal tissue	Comparable results for all transplantation methods Detectable cortisol levels at ≥ 14 d in all surviving animals, though high variability Inconsistent aldosterone production	Survival rates not described
2000 (113)	GM BAC, SCID mice	KC, cell suspension	Normal-appearing adrenocortical tissue similar to that formed by non-GM transplanted cells. Low proliferation	Cortisol production similar to non-GM transplants	100%, 36 d
2000 (90)	MAC, syngeneic Lewis rats	KC, cell suspension	Viable, well-vascularized adrenal tissue out to 360 d. Rare proliferating cells	Near normalization of CS levels by d 30, persisting to study end in ZG and ZF ACTs. Normalization of aldosterone levels by d 120 in transplants containing ZG cells. Subnormal levels in ZF only ACT	100%, > 120 d

(*continued*)

Table 1. Continued

Year	Cell type and recipient species	Transplant site and method	Outcomes		
			Structural	Hormonal	Survival and duration following Adx
2000 (78)	MAC, B10.Br (H-2k) mice	KC, cell suspension Syngeneic MAC, MHC-I (Kb) incompatible MAC or fully MHC-incompatible MAC grafts No immune suppression	Syngeneic and MHC-I incompatible: Viable, well-vascularized adrenal tissue with no evidence of lymphocytic infiltration. MHC mismatch: Evidence of acute graft rejection.	Syngeneic and MHC-I incompatible: Normalization of CS levels to pretransplant levels by 20 d and maintained to 100 d with normal ACTH responsiveness. MHC mismatch: significantly reduced CS	Syngeneic and MHC-I incompatible: 100%; MHC mismatch: 43%, 20 d
2002 (114)	MAC, B10.br mice	KC, adrenal fragments. Syngeneic MAC, Allogenic complete MHC mismatch MAC or Allogenic ICAM-1 deficient MHC mismatch	Evidence of graft rejection in nonsurviving animals	CS detectable, with similar basal and stimulated CS levels in all surviving transplanted animals at d 70, though significantly lower compared to controls	Syngeneic: 100%; Allogenic MHC mismatch 8%; Allogenic ICAM-1 deficient: 55%, 70 d
2002 (108)	Primary HAC + 3T3, SCID mice	KC, cell suspension 7 d of GC and MC after Adx	Viable, well-vascularized adrenal tissue Very low cell proliferation Low intracellular lipid content. No clear evidence of zonation	Detectable blood cortisol, with plateau by 30-40 d post transplant Detectable aldosterone in 46%	92%, > 16 d
2002 (109)	Primary BAC + 3T3, SCID mice	Intradermal, cell suspension, or cells in soluble collagen 7 d of GC and MC after Adx	Viable, well-vascularized, adrenal tissue similar to findings following KC ACT Difficult to control size and shape of transplant with dissociated cells	Detectable blood cortisol levels, higher with collagen than without Aldosterone levels not reported	100%, 35 d
2011 (105)	Primary MAC, syngeneic C57/BL6 mice	KC, collagen sponge Simultaneous (Si) bilateral vs staged (St) Adx ± laparotomy ± double-cell dose	Viable MAC at 3 wk post transplantation without formation of glandular structure	Plasma CS comparable to normal untreated levels. Sf1, Cyp11b1, and Cyp11b2 RNA detected at 3 weeks—lower expression compared to native adrenal gland	Si only: 69% Si + laparotomy: 0% St + laparotomy: 42% St + laparotomy + double cell dose: 100%, 14 d
2015 (79)	BAC, athymic Rowett Nude rats	KC, cell suspension KC, enBAC	enBAC: viable adrenal cells at 25 d	Cortisol levels 2.5 × higher with enBAC compared with free cells; EnBAC: progressive rise in cortisol during observation Cell suspension: Peak cortisol d 11 then decline; EnBAC: ACTH response evident at 25 d	100%, 25 d
	BAC, immune competent Wistar rats	Intraperitoneal, enBAC or subcutaneous, βAir	enBAC and βAir: high levels of cell viability at 21 d	Detectable cortisol levels with ACTH responsiveness, though measured levels higher with enBAC compared with B-air	enBAC and B-air: 100%, 21 d
2020 (96)	SF-1 induced mADSC, syngeneic C57/BL6 mice	KC, cell suspension	Absence of well-defined macroscopic tissue structure at 30 d. SF-1–positive cell clusters within KC space, but absence of typical adrenal histological architecture	Detectable plasma CS at levels comparable to KC murine adrenal gland transplantation. Absence of ACTH responsiveness	44%, 30 d

Abbreviations: 3T3, fibroblast growth factor–secreting cells; ACT, adrenal cell transplant; ACTH, adrenocorticotropin; Adx, adrenalectomy; βAir, designates use of the oxygenating and immunoisolating βAir device; BAC, bovine adrenocortical cells; CS, corticosterone; CyA, cyclosporin A; enBACs, alginate-encapsulated bovine adrenocortical cells; GC, glucocorticoid; GM, genetically modified; HAC, human adrenocortical cells; ICAM-1, intercellular-adhesion molecule-1; KC, into kidney subcapsular space; MAC, murine adrenocortical cells; mADSC, mouse adipose tissue stem cells; MC, mineralocorticoid; MHC, major histocompatibility complex; SCID, severe combined immunodeficiency; SF-1, steroidogenic factor-1; ZG, zona glomerulosa; ZF, zona fasciculata; ZR, zona reticularis.

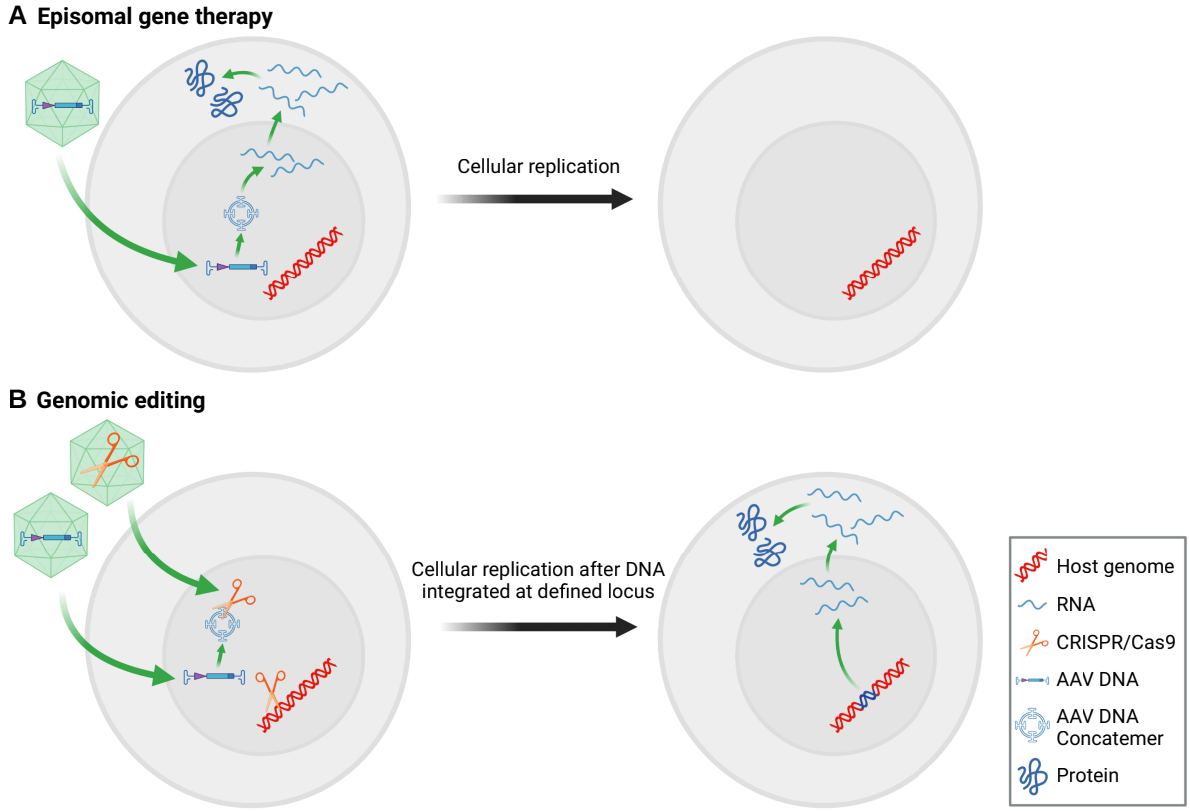

Figure 3. A, Adeno-associated virus (AAV) gene therapy will enter the cell then nucleus, and undergo structural change to become a concatemer. When a gene addition strategy is used with rAAV, the transgene will be transcribed into messenger RNA (mRNA) directly from the vector DNA transgene without integration into the host genome. If the cell replicates, the episomal DNA will not be passed on to any daughter cells. B, With gene editing, a targeted double-stranded break is induced both in the donor cassette and the host genome by Cas9. The donor template is integrated into the host genome at a defined locus using cellular DNA repair mechanisms and transcribed into mRNA from the host genome. The transgene will be passed on to daughter cells during cell replication. Created with BioRender.com.

parathyroid (126, 127). In vitro mixed lymphocyte reactions suggest that glucocorticoid production and nonglucocorticoid-related effects of adrenal cells may directly limit lymphocyte activation and proliferation, with results unaffected by the coadministration of the glucocorticoid receptor antagonist mifepristone (128). Nonetheless, in the absence of intervention, adrenocortical allografts undergo acute rejection (78, 111, 112, 114, 129). A combination of pretransplant adrenal cell culture and transient immunosuppression prevents acute allogeneic graft rejection (111, 126), although in isolation these measures have little effect (111, 129). In the absence of transplantation to an immune-privileged site, some degree of immunosuppressive treatment would be anticipated to be required for adrenocortical allografts or in autoimmune PAI.

The role of immunosuppression is a critical issue for the field of allogeneic adrenal transplantation. Like islet cell transplantation, adrenal allografts will have to contend both with recurrent autoimmunity and alloimmunity. The success of the Edmonton protocol, which allowed clinical islet transplantation to progress from experimental therapy to clinical therapy, followed advances in immunosuppression (130). To this end, it is likely that adrenal allografts will need therapy that targets both the T-cell immunity (via depletion) and blocked production of both de novo alloantibody as well as adrenal-specific autoantibody. Induction therapy with T-cell depletion antibody such as antithymocyte globulin will be needed (103). Newer therapies that target costimulation molecule expression such as CTLAg (Belatacept/Abatacept) have the distinct advantage of providing effective immunosuppression, but exquisitely blocking the ability to form de novo alloantibody. Critical to the development of these translational strategies will be robust models of adrenal allotransplantation that will allow detailed study of both the cellular immune response and critically the alloantibody response to the grafted tissues.

Genetic Therapies

Gene therapy technology has advanced to a point where potential curative treatments are realistic and enticing possibilities for monogenic adrenal disorders such as CAH. Gene therapy approaches correct, prevent, or alleviate disease by replacing (gene addition) or repairing (gene editing) genes carrying pathogenic variants. Potential gene therapy complications include acute toxicity from infusion of foreign material (eg, viral particles), cellular and humoral immune responses against the transduced cells and the therapeutic gene product respectively, and insertional mutagenesis (131). The major challenge for gene therapy is delivery. Ex vivo gene therapy has been explored in tissues that can be genetically manipulated in culture and then engrafted into the patient, but this approach has limited application in the adrenal cortex (132). For in vivo gene delivery, viral vectors are currently the most capable delivery approach: By 2021, 89% of genetic therapeutics in development used viral vectors, and recombinant adeno-associated

virus (rAAV) was the leading viral vector for gene delivery (133, 134). Nonviral approaches involving lipid nanoparticle and RNA technology are developing rapidly and will increasingly complement the power of viral vector–mediated gene transfer.

Vectorology

Vectorology exploits the natural ability of a virus to introduce its own genome into a host cell, where the viral genes are removed and replaced with therapeutic genetic cargo, eliminating the ability for viral replication and infection: Only the ability to deliver genetic cargo to cells remains. A crucial advantage of rAAV over other vector types is that the rAAV2 genome can be cross-packaged into the capsid (protein shell) of numerous types of AAV, known as pseudo-serotyping. The capsid serotype determines the type of cells the vector enters and the efficiency with which the genetic material is delivered (efficiency of transduction) (135, 136). With appropriate capsid selection, parenteral administration of targeted treatment is possible.

A limitation of rAAV-facilitated gene delivery is that the vector DNA is predominantly episomal (extrachromosomal) and is not reliably integrated into the host cell's genome. Thus, the introduced genetic material is expressed predominantly from the episomal vector DNA, which is progressively lost in concert with cellular replication, such as during pediatric organ growth or in organs with rapid cellular turnover such as the adrenal cortex (Fig. 3A) (137, 138). As current immunomodulatory technology stands, rAAV treatment can currently be administered only once as subsequent development of neutralizing antibodies renders further doses ineffective; preexisting naturally acquired wild-type AAV antibodies also preclude treatment (139, 140). Due to these durability and readministration limitations, genomic editing is poised to supplant gene addition, and rapidly progressing clustered regularly interspaced short palindromic repeat-associated nuclease Cas (CRISPR/Cas)-based technology is leading this field (132). The CRISPR/Cas system facilitates RNA-guided double-stranded DNA cleavage and evolved as a bacterial immune-defense mechanism against viruses (141-143). By using locus-specific RNA guides, this targeted DNA cleavage can be used for knockdown or knockout of the function of a selected target gene. In genomic editing, this can be exploited further by providing a repair template, from which a site-specific modification or entire cDNA sequence can be integrated into the host genome through native DNA repair mechanisms (144). A modification that is integrated into the host genome will be passed on to daughter cells following cellular replication (Fig. 3B). Moreover, if appropriate stem or progenitor cells are modified in this manner, durable life-long correction after a single treatment is possible.

Gene Therapy and the Adrenal Cortex

Gene therapy for CAH is conceptually appealing; however, there is a paucity of adrenocortical gene therapy studies (Table 2). All studies thus far have used a gene-addition strategy, and none has proven durability beyond the adrenocortical cellular turnover period.

Murine studies

The 21-hydroxylase–deficient mouse model (C57BL/10SnSlc-H-2 <AW18>; *Cyp21a1*$^{-/-}$) used in preclinical adrenocortical gene therapy studies, has elevated progesterone levels rather than 17-hydroxyprogesterone, due to lack of 17-hydroxylase expression in the murine adrenal (150, 151). The first attempt at gene therapy for CAH was in 1999, when an adenovirus vector containing human *CYP21A2* was directly injected into the adrenal glands of *Cyp21a1*$^{-/-}$ mice and resulted in improvement in adrenal morphology and increased plasma corticosterone. The effect was brief, and corticosterone concentrations declined over 40 days (145). Wild-type adenovirus infection and adenoviral-mediated gene transfer may interfere with adrenocortical function as adenoviral vectors are more proinflammatory than rAAV, with vigorous stimulation of the innate immune response (152). Furthermore, intra-adrenal injections are invasive, with a high mortality rate in the mouse model (153), and less-invasive parenteral injection is desirable.

Transduction of adrenocortical cells using a systemic intravenous injection of human *CYP21A2* packaged in an AAVrh10 capsid in male and female *Cyp21a1*$^{-/-}$ mice reduced urine progesterone for at least 15 weeks, and improved the expression of *Mc2r*, *Sf1*, *Star*, *Cyp17a1*, and *Cyp11b2* in the adrenal and *Ren1* in the kidney (147). Despite very low vector genome copies (vgc), a measurement of vector-derived DNA in the host tissue, in the mouse adrenals at 15 weeks (0.13 ± 0.09 vgc per cell), the therapeutic effect was still present (147). A subsequent rAAV gene therapy study used female mice alone, which have a more rapid adrenocortical cellular turnover than males (56). It was demonstrated that the effect from intravenous administration of their AAVRh10-*CYP21A2* vector on serum progesterone was transient, lasting only 8 weeks (148). Perhaps the durability of effect seen in some studies is due to the use of male animal subjects with slower adrenocortical turnover or transduction of stable cells outside the adrenal cortex. The use of a ubiquitous promoter means that it is plausible the transgene could be expressed by any cell that is transduced including in extra-adrenal sites, such as liver and muscle, hence it is difficult to ascertain if the study results were exclusively due to adrenal 21-hydroxylase expression.

One way to overcome rapid adrenocortical cellular turnover is the use of stable extra-adrenal tissue to gain 21-hydroxylation function (154). Two strategies have been tested using *Cyp21a1*$^{-/-}$ mice: The first strategy was to autotransplant primary tail fibroblasts transduced in vitro with an AAV2 vector containing murine *Cyp21a1* into subcutaneous tissue, and the second strategy was to inject rAAV2-*Cyp21a1* vector directly into thigh muscle. Due to small numbers of mice used, neither strategy produced statistically significant results; however, in both there was a trend toward reduced progesterone levels during the 4-week study period, indicating extra-adrenal 21-hydroxylation may be possible (146). A single mouse was studied for 7 months, and there was a durable effect after intramuscular vector administration (146). Although the vector was injected intramuscularly, vector DNA was detected in liver and cardiac muscle indicating that the extra-adrenal 21-hydroxylation may not have been from the thigh muscles alone. Despite initial indicators of success with ectopic expression, in a later study by the same group, they moved away from intramuscular administration. A mouse model for 11-β hydroxylase deficiency was created using CRISPR/Cas9 to knock down *Cyp11b1* function, and these mice were subsequently treated with unilateral intra-adrenal injection of an rAAV vector containing human *CYP11B1* with a ubiquitous promoter packaged in either AAV2 or AAV9 (149). Statistically

Table 2. Published adrenocortical gene therapy studies to date

Year	Species	Vector and delivery	Outcome—phenotype	Outcome—molecular
1999 (145)	Mouse	Adenovirus with human *CYP21A2* cDNA Intra-adrenal	Improvement in adrenal cortex ultrastructure 7 d after treatment. Plasma corticosterone increased to wild-type levels by d 7-14, but declining over next 40 d	Highest mRNA expression d 2-7 then gradual decline In vitro 21-hydroxylase activity in adrenals harvested from treated mice increased from undetectable to levels found in wild-type mice 2-7 d after treatment
2016 (146)	Mouse	Retrovirus with murine *Cyp21a1* cDNA Tail fibroblasts transduced in vitro then implanted subcutaneously	Statistically insignificant reduction of serum progesterone/deoxycorticosterone ratio at 4 wk in 4/6 mice (increase in 2/6) 4 wk after treatment	
2016 (146)	Mouse	AAV2 with murine *Cyp21a1* cDNA intramuscular	Statistically insignificant reduction in serum progesterone/deoxycorticosterone ratio 4 wk after treatment Single mouse monitored to 7 mo; serum progesterone/deoxycorticosterone remained low	*Cyp21a1* weak expression in thigh muscle, heart, and liver
2017 (147)	Mouse	AAVrh10 with human *CYP21A2* cDNA Intravenous	Increased body mass after treatment. Reduced urine progesterone by 5 wk, for at least 15 wk	*CYP21A2* expression detected in adrenals and weakly in heart Improved expression of *renin*, *Mc2r*, *Prkar2a*, *Sf1*, *Star*, *Cyp17a1*, and *Cyp11b2* genes
2018 (148)	Mouse	AAVrh10 with human *CYP21A2* cDNA Intravenous	Serum progesterone and ACTH normalized to wild-type levels from 2 to 8 wk, then increased to preinjection levels by 32 wk	*CYP21A2* expression was highest at 2 wk then waned over time to 32 wks Liver had substantial *CYP21A2* expression at 32 wk *CYP21A2* expression also waned over similar time period in immunodeficient mice, indicating loss of transgene not due to immune responses to vector/transgene
2022 (149)	Mouse	AAV9 with human *CYP11B1* cDNA Intra-adrenal	Statistically significant improvement but not normalization in serum deoxycorticosterone-to-corticosterone ratio, 4 wk after treatment. Two mice were monitored to 4 and 5 mo post treatment with persistence of effect, although ratio started to increase again from 2 mo post treatment	*Cyp11a1* expression in adrenal increased in vector-treated *Cyp11b1* knockout mice compared to wild-type. Even with vector treatment, *Cyp11b1* expression in adrenal markedly lower than wild-type

Studies published 1999 to 2018 used the same 21-hydroxylase deficient mouse model C57BL/10SnSlc-H-2aw18, which develops elevated progesterone rather than 17-hydroxyprogesterone (17OHP) as the murine adrenal lacks *Cyp17a1* expression (151). The 2022 study created a mouse model for 11-β hydroxylase deficiency by knocking down *Cyp11b1* function using CRISPR/Cas9, which developed elevated deoxycorticosterone (149). The 21-hydroxylase gene is represented as *CYP21A2* for human origin, *Cyp21a1* for murine. The 11-β hydroxylase gene is represented as *CYP11B1* for human and *Cyp11b1* for murine. Abbreviations: AAV, adeno-associated virus; ACTH, adrenocorticotropin; cDNA, complementary DNA; mRNA, messenger RNA.

significant reduction in the serum deoxycorticosterone-to-corticosterone was achieved using the AAV9 capsid serotype from 4 weeks post treatment (n = 4) and persisted up to 5 months after treatment (n = 1). There was no effect using the AAV2 serotype (149). Why AAV9 and AAV2 serotypes were chosen is unclear, as the AAVRh10 serotype transduces adrenocortical cells more efficiently than AAV9 (148). Moreover, the applicability to the human clinical context is unclear, as an invasive delivery strategy that is undesirable was used despite previous studies showing effective delivery of vector to the adrenal using intravenous administration (147, 148).

Nonhuman primate studies

While there are no published studies using NHPs for adrenocortical gene therapy, preliminary data have been presented at scientific meetings. To determine the most effective rAAV capsid serotype for gene delivery, NHPs were administered *CYP21A2* cDNA packaged in AAV1, AAV5, or AAV6, and these were given intra-adrenally or intravenously (155). *CYP21A2* cDNA packaged in capsid serotype AAV5 resulted in the highest vector presence (determined by vgc) in the adrenals from both administration methods, and subsequent studies used this capsid serotype. Why these 3 specific serotypes were initially chosen is unclear, as capsid technology has evolved so that unique capsid serotypes have been developed that can target relatively specific cell populations with high tropism and there are now innumerable capsids available with the rapid expansion of the capsid engineering field (156-158). NHPs (21-hydroxylase–sufficient) received rAAV5-*CYP21A2* with a ubiquitous promoter (159). Vector DNA in the adrenal tissue waned over

time. Two animals were studied to 24 weeks, 1 male and 1 female. While the sex of these animals was not specified, 1 had a low vector copy count at 24 weeks (3 vgc/cell) and 1 had a relatively higher count (13 vgc/cell). There was more vector DNA and higher transgene expression in the liver than the adrenal, which is expected when using rAAV5 with a ubiquitous promoter, as most AAV serotypes target hepatocytes. The adult liver is a relatively stable organ and episomal gene therapy will persist, unlike the growing pediatric liver (138, 160, 161).

Human clinical trial activity

A phase 1/2 human clinical trial is now under way in which adults with 21-hydroxylase deficiency are administered an intravenous infusion of a rAAV5-*CYP21A2* with a ubiquitous promoter (NCT04783181). The first human was treated in early 2022. Results of this study are not yet available. While it is expected that this rAAV therapy will have some effect, the duration of effect is uncertain, and there is some hesitancy regarding the potential prematurity of this trial (162). If a durable effect is seen, it could be related to extra-adrenal transduction and expression of 21-hydroxylase, and it will be difficult to ascertain the source of 21-hydroxylation in human participants.

Limitations of episomal gene therapy and the adrenal cortex

Thus far, no adrenocortical targeting gene therapy has shown durability of effect beyond the cellular turnover period. Episomal gene therapy used in the adrenal cortex will be transient because of the adrenocortical cellular turnover as the vector DNA will not replicate during cell division. Furthermore, differentiated adrenocortical cells apoptose without significant cellular replication and thus even if the *CYP21A2* locus were directly repaired in differentiated cells, this would provide a only transient effect. To overcome this, the genome of the adrenal progenitor cells must be repaired to ensure daughter cells maintain the correction. CRISPR/Cas is one technological platform that could achieve this (143, 163). There are several editing techniques with various applications including homology-directed repair (164), homology-independent targeted integration (HITI) (165), single homology arm donor-mediated intro-targeting integration (166), precise integration into target chromosome (167, 168), and non-CRISPR–based strategies including base editing (169) and prime editing (170). The major limitation is that the progenitor cells have not yet been adequately defined and without accurate methods to identify these cell populations, it is difficult to establish which rAAV serotypes (if any) can deliver editing machinery to adrenal progenitor cells with any certainty.

The 21-hydroxylase pseudogene (*CYP21A1P* in the human and *Cyp21a2-ps* in the mouse) creates an added complication due to high homology with the active gene, with 98% exonic and 96% intronic homology (171). As a result, the target protospacer adjacent motif sequence chosen as the cut site in a CRISPR/Cas strategy must not also cause a double-stranded break in the pseudogene. As the *CYP21A2* gene at 6p21.3 is within 30Kb of *CYP21A1P* (21), a cut in both sites could induce a large deletion and/or genomic rearrangements. Therefore, potential protospacer adjacent motif sites are limited to those that are unique to *CYP21A2*. There are more than 300 known variants in *CYP21A2* listed in the Human Gene Mutation Database (HGMD, http://www.hgmd.cf.ac.uk) spanning all 10 exons. Therefore, the editing strategy chosen is important: Homology-directed repair is limited to actively dividing cells, has relatively low editing efficiency, and requires a unique set of reagents for each group of variants (164, 172). Furthermore, not all double-stranded breaks induced will undergo repair and risks eliminating any residual function of a hypomorphic allele if the strand break is exonic. These limitations can be overcome by using the HITI strategy, which is dependent on DNA repair by NHEJ (165). The *CYP21A2* open-reading frame is approximately 1.5 kb (173), compatible with packaging into the rAAV genome backbone, which has a capacity of 4.7 kb. With HITI, a strategy could be developed whereby a double-stranded DNA break is induced deep in a noncoding sequence such as an intron and the entire wild-type *CYP21A2* open-reading frame is integrated downstream of the endogenous *CYP21A2* promoter, treating all pathogenic variants that occur distal to the insertion site. Alternatively, mutations upstream of the insertion site could also be treated by introducing termination of the upstream cistron and expressing the entire wild-type *CYP21A2* cDNA, for example, from a downstream cistron using an internal ribosome entry site.

Although the adrenal cortex shares properties such as high relative blood flow and fenestrated vascular endothelium with the liver that make it highly amenable to gene delivery (174-176), the predilection of rAAV to transduce hepatocytes is a challenge in adrenal-targeting gene therapy. Without liver detargeting, much higher doses of vector may be required to ensure adequate amounts reach the adrenal cortex. This entails a greater risk of AAV-associated adverse events such as liver toxicity (177, 178), thrombotic microangiopathy (179), and dorsal root ganglion toxicity (180).

Conclusion

Adrenocortical cell or gene therapies are clinically appealing for treatment of PAI as they offer the promise of restoration of homeostatic cortisol secretion, overcoming the residual morbidity and mortality of current treatment. Current technologies make cell therapy possible but require refinement such as cell isolation for allogeneic transplant, cell production from adult cells using reprogramming or lineage conversion to allow a suitable adrenal-like steroidogenesis profile, correction of genomic deficits, and use of devices to provide a suitable environment for cell growth and function. The isolation and transplantation of adrenocortical cell stem cells needs further work to ensure transplant durability. While simple gene addition therapy is possible, this will result in only a transient effect. Gene therapy as a treatment option is limited by the necessity to delivery editing reagents to the adrenal progenitor cells, and the tools for targeting these cells also require further technological development and refinement. The current rate of knowledge of adrenal regeneration and trial development in this field suggests that cellular and genetic adrenocortical therapies will come to fruition in a reasonable time frame.

Acknowledgments

Figures were created using Biorender.com.

Financial Support

B.C. is supported by the Royal Adelaide Hospital (Research Committee Dawes Scholarship). S.B. receives funding from Adrenal Research (No. DFG CRC/TRR 205) and the Transcampus International Research Training Group 2251.

Disclosures

The authors have no to declare.

Data Availability

Data sharing is not applicable to this article as no data sets were generated or analyzed during the present study.

References

1. Bergthorsdottir R, Leonsson-Zachrisson M, Odén A, Johannsson G. Premature mortality in patients with Addison's disease: a population-based study. *J Clin Endocrinol Metab*. 2006;91(12):4849-4853.
2. Falhammar H, Frisén L, Norrby C, *et al*. Increased mortality in patients with congenital adrenal hyperplasia due to 21-hydroxylase deficiency. *J Clin Endocrinol Metab*. 2014;99(12):E2715-E2721.
3. Bornstein SR, Allolio B, Arlt W, *et al*. Diagnosis and treatment of primary adrenal insufficiency: an Endocrine Society clinical practice guideline. *J Clin Endocrinol Metab*. 2016;101(2):364-389.
4. El-Maouche D, Arlt W, Merke DP. Congenital adrenal hyperplasia. *Lancet*. 2017;390(10108):2194-2210.
5. Nimkarn S, Lin-Su K, Berglind N, Wilson RC, New MI. Aldosterone-to-renin ratio as a marker for disease severity in 21-hydroxylase deficiency congenital adrenal hyperplasia. *J Clin Endocrinol Metab*. 2007;92(1):137-142.
6. Krone N, Braun A, Roscher AA, Knorr D, Schwarz HP. Predicting phenotype in steroid 21-hydroxylase deficiency? Comprehensive genotyping in 155 unrelated, well defined patients from southern Germany. *J Clin Endocrinol Metab*. 2000;85(3):1059-1065.
7. Finkielstain GP, Chen W, Mehta SP, *et al*. Comprehensive genetic analysis of 182 unrelated families with congenital adrenal hyperplasia due to 21-hydroxylase deficiency. *J Clin Endocrinol Metab*. 2011;96(1):E161-E172.
8. Wilkins L, Lewis RA, Klein R, *et al*. Treatment of congenital adrenal hyperplasia with cortisone. *J Clin Endocrinol Metab*. 1951;11(1):1-25.
9. Bartter FC, Albright F, Forbes AP, Leaf A, Dempsey E, Carroll E. The effects of adrenocorticotropic hormone and cortisone in the adrenogenital syndrome associated with congenital adrenal hyperplasia: an attempt to explain and correct its disordered hormonal pattern. *J Clin Invest*. 1951;30(3):237-251.
10. Løvås K, Loge JH, Husebye ES. Subjective health status in Norwegian patients with Addison's disease. *Clin Endocrinol (Oxf)*. 2002;56(5):581-588.
11. Rushworth RL, Torpy DJ, Falhammar H. Adrenal crises: perspectives and research directions. *Endocrine*. 2017;55(2):336-345.
12. Hahner S, Loeffler M, Bleicken B, *et al*. Epidemiology of adrenal crisis in chronic adrenal insufficiency: the need for new prevention strategies. *Eur J Endocrinol*. 2010;162(3):597-602.
13. Hahner S, Spinnler C, Fassnacht M, *et al*. High incidence of adrenal crisis in educated patients with chronic adrenal insufficiency: a prospective study. *J Clin Endocrinol Metab*. 2015;100(2):407-416.
14. Rushworth RL, Torpy DJ, Falhammar H. Adrenal crisis. *N Engl J Med*. 2019;381(9):852-861.
15. Gilban DL, Alves Junior PA, Beserra IC. Health related quality of life of children and adolescents with congenital adrenal hyperplasia in Brazil. *Health Qual Life Outcomes*. 2014;12(1):107.
16. Yau M, Vogiatzi M, Lewkowitz-Shpuntoff A, Nimkarn S, Lin-Su K. Health-related quality of life in children with congenital adrenal hyperplasia. *Horm Res Paediatr*. 2015;84(3):165-171.
17. Fleming L, Van Riper M, Knafl K. Management of childhood congenital adrenal hyperplasia—an integrative review of the literature. *J Pediatr Health Care*. 2017;31(5):560-577.
18. Bachelot A, Plu-Bureau G, Thibaud E, *et al*. Long-term outcome of patients with congenital adrenal hyperplasia due to 21-hydroxylase deficiency. *Horm Res*. 2007;67(6):268-276.
19. Idris AN, Chandran V, Syed Zakaria SZ, Rasat R. Behavioural outcome in children with congenital adrenal hyperplasia: experience of a single centre. *Int J Endocrinol*. 2014;2014:483718.
20. Engberg H, Butwicka A, Nordenström A, *et al*. Congenital adrenal hyperplasia and risk for psychiatric disorders in girls and women born between 1915 and 2010: a total population study. *Psychoneuroendocrinology*. 2015;60:195-205.
21. Claahsen-van der Grinten HL, Speiser PW, Ahmed SF, *et al*. Congenital adrenal hyperplasia-current insights in pathophysiology, diagnostics, and management. *Endocr Rev*. 2022;43(1):91-159.
22. Jenkins-Jones S, Parviainen L, Porter J, *et al*. Poor compliance and increased mortality, depression and healthcare costs in patients with congenital adrenal hyperplasia. *Eur J Endocrinol*. 2018;178(4):309-320.
23. MacKay D, Nordenström A, Falhammar H. Bilateral adrenalectomy in congenital adrenal hyperplasia: a systematic review and meta-analysis. *J Clin Endocrinol Metab*. 2018;103(5):1767-1778.
24. Speiser PW, Arlt W, Auchus RJ, *et al*. Congenital adrenal hyperplasia due to steroid 21-hydroxylase deficiency: an Endocrine Society clinical practice guideline. *J Clin Endocrinol Metab*. 2018;103(11):4043-4088.
25. Isidori AM, Venneri MA, Graziadio C, *et al*. Effect of once-daily, modified-release hydrocortisone versus standard glucocorticoid therapy on metabolism and innate immunity in patients with adrenal insufficiency (DREAM): a single-blind, randomised controlled trial. *Lancet Diabetes Endocrinol*. 2018;6(3):173-185.
26. Mallappa A, Sinaii N, Kumar P, *et al*. A phase 2 study of Chronocort, a modified-release formulation of hydrocortisone, in the treatment of adults with classic congenital adrenal hyperplasia. *J Clin Endocrinol Metab*. 2015;100(3):1137-1145.
27. Nella AA, Mallappa A, Perritt AF, *et al*. A phase 2 study of continuous subcutaneous hydrocortisone infusion in adults with congenital adrenal hyperplasia. *J Clin Endocrinol Metab*. 2016;101(12):4690-4698.
28. Gagliardi L, Nenke MA, Thynne TRJ, *et al*. Continuous subcutaneous hydrocortisone infusion therapy in Addison's disease: a randomized, placebo-controlled clinical trial. *J Clin Endocrinol Metab*. 2014;99(11):4149-4157.
29. Johannsson G, Nilsson AG, Bergthorsdottir R, *et al*. Improved cortisol exposure-time profile and outcome in patients with adrenal insufficiency: a prospective randomized trial of a novel hydrocortisone dual-release formulation. *J Clin Endocrinol Metab*. 2012;97(2):473-481.
30. Whitaker M, Debono M, Huatan H, Merke D, Arlt W, Ross RJ. An oral multiparticulate, modified-release, hydrocortisone replacement therapy that provides physiological cortisol exposure. *Clin Endocrinol (Oxf)*. 2014;80(4):554-561.
31. Merke DP, Mallappa A, Arlt W, *et al*. Modified-release hydrocortisone in congenital adrenal hyperplasia. *J Clin Endocrinol Metab*. 2021;106(5):e2063-e2077.
32. Lightman SL, Birnie MT, Conway-Campbell BL. Dynamics of ACTH and cortisol secretion and implications for disease. *Endocr Rev*. 2020;41(3):470-490.
33. Pearce SH, Mitchell AL, Bennett S, *et al*. Adrenal steroidogenesis after B lymphocyte depletion therapy in new-onset Addison's disease. *J Clin Endocrinol Metab*. 2012;97(10):E1927-E1932.
34. Napier C, Gan EH, Mitchell AL, *et al*. Residual adrenal function in autoimmune Addison's disease-effect of dual therapy with

rituximab and depot tetracosactide. *J Clin Endocrinol Metab*. 2020;105(4):e1250-e1259.
35. Gan EH, MacArthur K, Mitchell AL, *et al*. Residual adrenal function in autoimmune Addison's disease: improvement after tetracosactide (ACTH1-24) treatment. *J Clin Endocrinol Metab*. 2014;99(1):111-118.
36. Pearce SHS, Gan EH, Napier C. Management of endocrine disease: residual adrenal function in Addison's disease. *Eur J Endocrinol*. 2021;184(2):R61-R67.
37. Hering BJ, Clarke WR, Bridges ND, *et al*; Clinical Islet Transplantation Consortium. Phase 3 trial of transplantation of human islets in type 1 diabetes complicated by severe hypoglycemia. *Diabetes Care*. 2016;39(7):1230-1240.
38. Foster ED, Bridges ND, Feurer ID, Eggerman TL, Hunsicker LG, Alejandro R, Clinical Islet Transplantation Consortium. Improved health-related quality of life in a phase 3 islet transplantation trial in type 1 diabetes complicated by severe hypoglycemia. *Diabetes Care*. 2018;41(5):1001-1008.
39. Lablanche S, Vantyghem MC, Kessler L, *et al*; TRIMECO Trial Investigators. Islet transplantation versus insulin therapy in patients with type 1 diabetes with severe hypoglycaemia or poorly controlled glycaemia after kidney transplantation (TRIMECO): a multicentre, randomised controlled trial. *Lancet Diabetes Endocrinol*. 2018;6(7):527-537.
40. Fensom B, Harris C, Thompson SE, Al Mehthel M, Thompson DM. Islet cell transplantation improves nerve conduction velocity in type 1 diabetes compared with intensive medical therapy over six years. *Diabetes Res Clin Pract*. 2016;122:101-105.
41. Yates R, Katugampola H, Cavlan D, *et al*. Adrenocortical development, maintenance, and disease. *Curr Top Dev Biol*. 2013;106:239-312.
42. Mariniello K, Ruiz-Babot G, McGaugh EC, *et al*. Stem cells, self-renewal, and lineage commitment in the endocrine system. *Front Endocrinol (Lausanne)*. 2019;10:772.
43. Cheng K, Seita Y, Moriwaki T, *et al*. The developmental origin and the specification of the adrenal cortex in humans and cynomolgus monkeys. *Sci Adv*. 2022;8(16):eabn8485.
44. Röhrig T, Pihlajoki M, Ziegler R, *et al*. Toying with fate: redirecting the differentiation of adrenocortical progenitor cells into gonadal-like tissue. *Mol Cell Endocrinol*. 2015;408:165-177.
45. Spencer SJ, Mesiano S, Lee JY, Jaffe RB. Proliferation and apoptosis in the human adrenal cortex during the fetal and perinatal periods: implications for growth and remodeling. *J Clin Endocrinol Metab*. 1999;84(3):1110-1115.
46. Rege J, Turcu AF, Kasa-Vubu JZ, *et al*. 11-Ketotestosterone is the dominant circulating bioactive androgen during normal and premature adrenarche. *J Clin Endocrinol Metab*. 2018;103(12):4589-4598.
47. Dumontet T, Martinez A. Adrenal androgens, adrenarche, and zona reticularis: a human affair? *Mol Cell Endocrinol*. 2021;528:111239.
48. Rosenfield RL. Normal and premature adrenarche. *Endocr Rev*. 2021;42(6):783-814.
49. Ingle DJ, Higgins GM. Autotransplantation and regeneration of the adrenal gland. *Endocrinology*. 1938;22(4):458-464.
50. Lerario AM, Finco I, LaPensee C, Hammer GD. Molecular mechanisms of stem/progenitor cell maintenance in the adrenal cortex. *Front Endocrinol (Lausanne)*. 2017;8:52.
51. Freedman BD, Kempna PB, Carlone DL, *et al*. Adrenocortical zonation results from lineage conversion of differentiated zona glomerulosa cells. *Dev Cell*. 2013;26(6):666-673.
52. Chang SP, Morrison HD, Nilsson F, Kenyon CJ, West JD, Morley SD. Cell proliferation, movement and differentiation during maintenance of the adult mouse adrenal cortex. *PLoS One*. 2013;8(12):e81865.
53. Hammer GD, Basham KJ. Stem cell function and plasticity in the normal physiology of the adrenal cortex. *Mol Cell Endocrinol*. 2021;519:111043.
54. Belavgeni A, Bornstein SR, von Massenhausen A, *et al*. Exquisite sensitivity of adrenocortical carcinomas to induction of ferroptosis. *Proc Natl Acad Sci U S A*. 2019;116(44):22269-22274.
55. Weigand I, Schreiner J, Röhrig F, *et al*. Active steroid hormone synthesis renders adrenocortical cells highly susceptible to type II ferroptosis induction. *Cell Death Dis*. 2020;11(3):192.
56. Grabek A, Dolfi B, Klein B, Jian-Motamedi F, Chaboissier MC, Schedl A. The adult adrenal cortex undergoes rapid tissue renewal in a sex-specific manner. *Cell Stem Cell*. 2019;25(2):290-296.e2.
57. Cnop M, Hughes SJ, Igoillo-Esteve M, *et al*. The long lifespan and low turnover of human islet beta cells estimated by mathematical modelling of lipofuscin accumulation. *Diabetologia*. 2010;53(2):321-330.
58. Buaas FW, Gardiner JR, Clayton S, Val P, Swain A. In vivo evidence for the crucial role of SF1 in steroid-producing cells of the testis, ovary and adrenal gland. *Development*. 2012;139(24):4561-4570.
59. Wong M, Ikeda Y, Luo X, *et al*. Steroidogenic factor 1 plays multiple roles in endocrine development and function. *Recent Prog Horm Res*. 1997;52:167-184.
60. King P, Paul A, Laufer E. Shh signaling regulates adrenocortical development and identifies progenitors of steroidogenic lineages. *Proc Natl Acad Sci U S A*. 2009;106(50):21185-21190.
61. Little DW III, Dumontet T, Lapensee CR, Hammer GD. β-Catenin in adrenal zonation and disease. *Mol Cell Endocrinol*. 2021;522:111120.
62. Lyraki R, Schedl A. Adrenal cortex renewal in health and disease. *Nat Rev Endocrinol*. 2021;17(7):421-434.
63. El-Khairi R, Martinez-Aguayo A, Ferraz-de-Souza B, Lin L, Achermann JC. Role of DAX-1 (NR0B1) and steroidogenic factor-1 (NR5A1) in human adrenal function. *Endocr Dev*. 2011;20:38-46.
64. Ito M, Yu R, Jameson JL. DAX-1 inhibits SF-1-mediated transactivation via a carboxy-terminal domain that is deleted in adrenal hypoplasia congenita. *Mol Cell Biol*. 1997;17(3):1476-1483.
65. Fridmanis D, Roga A, Klovins J. ACTH receptor (MC2R) specificity: what do we know about underlying molecular mechanisms? *Front Endocrinol (Lausanne)*. 2017;8:13.
66. Smith PE. Hypophysectomy and a replacement therapy in the rat. *Am J Anatomy*. 1930;45(2):205-273.
67. Gaillard I, Keramidas M, Liakos P, Vilgrain I, Feige JJ, Vittet D. ACTH-regulated expression of vascular endothelial growth factor in the adult bovine adrenal cortex: a possible role in the maintenance of the microvasculature. *J Cell Physiol*. 2000;185(2):226-234.
68. Thomas M, Hornsby PJ. Transplantation of primary bovine adrenocortical cells into SCID mice. *Mol Cell Endocrinol*. 1999;153(1-2):125-136.
69. Guagliardo NA, Klein PM, Gancayco CA, *et al*. Angiotensin II induces coordinated calcium bursts in aldosterone-producing adrenal rosettes. *Nat Commun*. 2020;11(1):1679.
70. Toews JNC, Philippe TJ, Hill LA, *et al*. Corticosteroid-binding globulin (SERPINA6) establishes postpubertal sex differences in rat adrenal development. *Endocrinology*. 2022;163(11):bqac152.
71. Lam KY, Chan AC, Lo CY. Morphological analysis of adrenal glands: a prospective analysis. *Endocr Pathol*. 2001;12(1):33-38.
72. Gan EH, Pearce SH. Management of endocrine disease: regenerative therapies in autoimmune Addison's disease. *Eur J Endocrinol*. 2017;176(3):R123-R135.
73. Smans LCCJ, Zelissen PMJ. Partial recovery of adrenal function in a patient with autoimmune Addison's disease. *J Endocrinol Invest*. 2008;31(7):672-674.
74. Vulto A, Bergthorsdottir R, van Faassen M, Kema IP, Johannsson G, van Beek AP. Residual endogenous corticosteroid production in patients with adrenal insufficiency. *Clin Endocrinol (Oxf)*. 2019;91(3):383-390.
75. Napier C, Allinson K, Gan EH, *et al*. Natural history of adrenal steroidogenesis in autoimmune Addison's disease following

diagnosis and treatment. *J Clin Endocrinol Metab*. 2020;105(7):2322-2330.
76. Sævik ÅB, Åkerman AK, Methlie P, *et al*. Residual corticosteroid production in autoimmune Addison disease. *J Clin Endocrinol Metab*. 2020;105(7):2430-2441.
77. Hornsby PJ, Thomas M, Northrup SR, *et al*. Cell transplantation: a tool to study adrenocortical cell biology, physiology, and senescence. *Endocr Res*. 1998;24(3-4):909-918.
78. Seeliger H, Hoffmann MW, Behrend M, *et al*. Transplantation of H-2Kb-transgenic adrenocortical cells in the mouse having undergone an adrenalectomy: functional and morphological aspects. *Transplantation*. 2000;69(8):1561-1566.
79. Balyura M, Gelfgat E, Ehrhart-Bornstein M, *et al*. Transplantation of bovine adrenocortical cells encapsulated in alginate. *Proc Natl Acad Sci U S A*. 2015;112(8):2527-2532.
80. Lu T, Yang B, Wang R, Qin C. Xenotransplantation: current status in preclinical research. *Front Immunol*. 2019;10:3060.
81. Metzger R, Parasta A, Joppich I, Till H. Does the transplantation process modify the immunogenicity of fetal adrenal grafts in rat? *Pediatr Transplant*. 2003;7(3):209-216.
82. Korbutt GS, Elliott JF, Ao Z, Smith DK, Warnock GL, Rajotte RV. Large scale isolation, growth, and function of porcine neonatal islet cells. *J Clin Invest*. 1996;97(9):2119-2129.
83. Hawthorne WJ, Salvaris EJ, Chew YV, *et al*. Xenotransplantation of genetically modified neonatal pig islets cures diabetes in baboons. *Front Immunol*. 2022;13:898948.
84. Shin JS, Kim JM, Min BH, *et al*. Pre-clinical results in pig-to-non-human primate islet xenotransplantation using anti-CD40 antibody (2C10R4)-based immunosuppression. *Xenotransplantation*. 2018;25(1):e12356.
85. Bottino R, Wijkstrom M, van der Windt DJ, *et al*. Pig-to-monkey islet xenotransplantation using multi-transgenic pigs. *Am J Transplant*. 2014;14(10):2275-2287.
86. O'Connell PJ, Hawthorne WJ, Simond D, *et al*. Genetic and functional evaluation of the level of inbreeding of the Westran pig: a herd with potential for use in xenotransplantation. *Xenotransplantation*. 2005;12(4):308-315.
87. Popnikolov NK, Hornsby PJ. Subcutaneous transplantation of bovine and human adrenocortical cells in collagen gel in SCID mice. *Cell Transplant*. 1999;8(6):617-625.
88. Till H, Metzger R, Mempel T, Boehm R, Joppich I. Proliferation, zonal maturation, and steroid production of fetal adrenal transplants in adrenalectomized rats. *Pediatr Surg Int*. 2000;16(4):293-296.
89. Scheumann GF, Hiller WF, Schroder S, Schurmeyer T, Klempnauer J, Dralle H. Adrenal cortex transplantation after bilateral total adrenalectomy in the rat. *Henry Ford Hosp Med J*. 1989;37(3-4):154-156.
90. Teebken OE, Scheumann GF. Differentiated corticosteroid production and regeneration after selective transplantation of cultured and noncultured adrenocortical cells in the adrenalectomized rat. *Transplantation*. 2000;70(5):836-843.
91. Takahashi K, Yamanaka S. Induction of pluripotent stem cells from mouse embryonic and adult fibroblast cultures by defined factors. *Cell*. 2006;126(4):663-676.
92. Ahlenius H. Past, present, and future of direct cell reprogramming. *Cell Reprogram*. 2022;24(5):205-211.
93. Sonoyama T, Sone M, Honda K, *et al*. Differentiation of human embryonic stem cells and human induced pluripotent stem cells into steroid-producing cells. *Endocrinology*. 2012;153(9):4336-4345.
94. Gondo S, Yanase T, Okabe T, *et al*. SF-1/Ad4BP transforms primary long-term cultured bone marrow cells into ACTH-responsive steroidogenic cells. *Genes Cells*. 2004;9(12):1239-1247.
95. Gondo S, Okabe T, Tanaka T, *et al*. Adipose tissue-derived and bone marrow-derived mesenchymal cells develop into different lineage of steroidogenic cells by forced expression of steroidogenic factor 1. *Endocrinology*. 2008;149(9):4717-4725.
96. Tanaka T, Aoyagi C, Mukai K, Nishimoto K, Kodama S, Yanase T. Extension of survival in bilaterally adrenalectomized mice by implantation of SF-1/Ad4BP-induced steroidogenic cells. *Endocrinology*. 2020;161(3):bqaa007.
97. Tanaka T, Gondo S, Okabe T, *et al*. Steroidogenic factor 1/adrenal 4 binding protein transforms human bone marrow mesenchymal cells into steroidogenic cells. *J Mol Endocrinol*. 2007;39(5):343-350.
98. Ruiz-Babot G, Balyura M, Hadjidemetriou I, *et al*. Modeling congenital adrenal hyperplasia and testing interventions for adrenal insufficiency using donor-specific reprogrammed cells. *Cell Rep*. 2018;22(5):1236-1249.
99. Wei X, Peng G, Zheng S, Wu X. Differentiation of umbilical cord mesenchymal stem cells into steroidogenic cells in comparison to bone marrow mesenchymal stem cells. *Cell Prolif*. 2012;45(2):101-110.
100. Li L, Li Y, Sottas C, *et al*. Directing differentiation of human induced pluripotent stem cells toward androgen-producing Leydig cells rather than adrenal cells. *Proc Natl Acad Sci U S A*. 2019;116(46):23274-23283.
101. Dubernard JM, Cloix P, Tajra LC, *et al*. Simultaneous adrenal gland and kidney allotransplantation after synchronous bilateral renal cell carcinoma: a case report. *Transplant Proc*. 1995;27(1):1320-1321.
102. Vouillarmet J, Buron F, Houzard C, *et al*. The first simultaneous kidney-adrenal gland-pancreas transplantation: outcome at 1 year. *Am J Transplant*. 2013;13(7):1905-1909.
103. Grodstein E, Hardy MA, Goldstein MJ. A case of human intramuscular adrenal gland transplantation as a cure for chronic adrenal insufficiency. *Am J Transplant*. 2010;10(2):431-433.
104. Yan ZB, Bing ZX, Yang WR, Long WL. A study of cadaveric fetal adrenal used for adrenal transplantation to treat Addison's disease: thirteen cases reported. *Transplant Proc*. 1990;22(1):280-282.
105. Zupekan T, Dunn JCY. Adrenocortical cell transplantation reverses a murine model of adrenal failure. *J Pediatr Surg*. 2011;46(6):1208-1213.
106. Thomas M, Northrup SR, Hornsby PJ. Adrenocortical tissue formed by transplantation of normal clones of bovine adrenocortical cells in SCID mice replaces the essential functions of the animals' adrenal glands. *Nat Med*. 1997;3(9):978-983.
107. Ciancio SJ, King SR, Suwa T, *et al*. Transplantation of normal and genetically modified adrenocortical cells. *Endocr Res*. 2000;26(4):931-939.
108. Thomas M, Wang X, Hornsby PJ. Human adrenocortical cell xenotransplantation: model of cotransplantation of human adrenocortical cells and 3T3 cells in SCID mice to form vascularized functional tissue and prevent adrenal insufficiency. *Xenotransplantation*. 2002;9(1):58-67.
109. Zhang H, Hornsby PJ. Intradermal cell transplantation in soluble collagen. *Cell Transplant*. 2002;11(2):139-145.
110. Dunn JCY, Chu Y, Lam MM, Wu BM, Atkinson JB, McCabe ER. Adrenal cortical cell transplantation. *J Pediatr Surg*. 2004;39(12):1856-1858.
111. Ricordi C, Santiago JV, Lacy PE. Use of culture and temporary immunosuppression to prolong adrenal cortical allograft survival. *Endocrinology*. 1987;121(2):745-748.
112. Kiriştioglu I, Dogruyol H, Cavuşoglu I. Long-term outcome of the fetal adrenal gland transplantation in rats. *Eur J Pediatr Surg*. 1999;9(6):400-405.
113. Thomas M, Yang L, Hornsby PJ. Formation of functional tissue from transplanted adrenocortical cells expressing telomerase reverse transcriptase. *Nat Biotechnol*. 2000;18(1):39-42.
114. Musholt TJ, Klebs SHG, Musholt PB, Ellerkamp V, Klempnauer J, Hoffmann MW. Transplantation of adrenal tissue fragments in a murine model: functional capacities of syngeneic and allogeneic grafts. *World J Surg*. 2002;26(8):950-957.
115. Hornsby PJ. Transplantation of adrenocortical cells. *Rev Endocr Metab Disord*. 2001;2(3):313-321.

116. Delaune V, Berney T, Lacotte S, Toso C. Intraportal islet transplantation: the impact of the liver microenvironment. *Transpl Int*. 2017;30(3):227-238.
117. David A, Day J, Shikanov A. Immunoisolation to prevent tissue graft rejection: current knowledge and future use. *Exp Biol Med (Maywood)*. 2016;241(9):955-961.
118. Allen RA, Seltz LM, Jiang H, *et al.* Adrenal extracellular matrix scaffolds support adrenocortical cell proliferation and function in vitro. *Tissue Eng Part A*. 2010;16(11):3363-3374.
119. Jiang L, Shen Y, Liu Y, Zhang L, Jiang W. Making human pancreatic islet organoids: progresses on the cell origins, biomaterials and three-dimensional technologies. *Theranostics*. 2022;12(4):1537-1556.
120. Pepper AR, Gala-Lopez B, Pawlick R, Merani S, Kin T, Shapiro AMJ. A prevascularized subcutaneous device-less site for islet and cellular transplantation. *Nat Biotechnol*. 2015;33(5):518-523.
121. Gibly RF, Zhang X, Lowe WL Jr, Shea LD. Porous scaffolds support extrahepatic human islet transplantation, engraftment, and function in mice. *Cell Transplant*. 2013;22(5):811-819.
122. Balyura M, Gelfgat E, Steenblock C, *et al.* Expression of progenitor markers is associated with the functionality of a bioartificial adrenal cortex. *PLoS One*. 2018;13(3):e0194643.
123. Thomas M, Hawks CL, Hornsby PJ. Adrenocortical cell transplantation in scid mice: the role of the host animals' adrenal glands. *J Steroid Biochem Mol Biol*. 2003;85(2-5):285-290.
124. Cadic C, Vitiello S, Gin H, Neveu PJ, Dupuy B. Embedded adrenal cells graft reduced local and early nonspecific inflammatory phenomena which follow agarose beads implantation. *Cell Transplant*. 1992;1(5):349-354.
125. Acarregui A, Herrán E, Igartua M, *et al.* Multifunctional hydrogel-based scaffold for improving the functionality of encapsulated therapeutic cells and reducing inflammatory response. *Acta Biomater*. 2014;10(10):4206-4216.
126. Ricordi C, Lacy PE, Santiago JV, Cryer PE, Di Carlo V. Transplantation of parathyroid, adrenal cortex and adrenal medulla using procedures which successfully prolonged islet allograft survival. *Horm Metab Res Suppl*. 1990;25:132-135.
127. Ricordi C, Cryer PE, Lacy PE. Effect of in vitro culture and cyclosporine A treatment on adrenal medulla allograft survival. *J Surg Res*. 1989;47(1):20-23.
128. Ellerkamp V, Musholt TJ, Klebs SH, *et al.* A murine model of allogeneic adrenocortical cell transplantation: perspectives for the treatment of Addison's disease in humans. *Surgery*. 2000;128(6):999-1006.
129. Liu D, Qi S, Xu D, Zhu S, Chen H. A new vascularized adrenal transplantation model in the rat. *Microsurgery*. 2001;21(4):124-126.
130. Barton FB, Rickels MR, Alejandro R, *et al.* Improvement in outcomes of clinical islet transplantation: 1999-2010. *Diabetes Care*. 2012;35(7):1436-1445.
131. Kay MA, Glorioso JC, Naldini L. Viral vectors for gene therapy: the art of turning infectious agents into vehicles of therapeutics. *Nat Med*. 2001;7(1):33-40.
132. Wilson RC, Gilbert LA. The promise and challenge of in vivo delivery for genome therapeutics. *ACS Chem Biol*. 2018;13(2):376-382.
133. Barrett D, Nguyen-Jatkoe L, Foss-Campbell B, Micklus A, Wendland A, Millington S. Gene, cell, & RNA therapy landscape, Q2 2021 quarterly data report. 2021. American Society for Gene and Cell Therapy. Available at https://asgct.org/global/documents/asgct-pharma-intelligence-quarterly-report-july-20.aspx [Accessed 28th November 2022]
134. Wang D, Tai PWL, Gao G. Adeno-associated virus vector as a platform for gene therapy delivery. *Nat Rev Drug Discov*. 2019;18(5):358-378.
135. Rabinowitz JE, Rolling F, Li C, *et al.* Cross-packaging of a single adeno-associated virus (AAV) type 2 vector genome into multiple AAV serotypes enables transduction with broad specificity. *J Virol*. 2002;76(2):791-801.
136. Zhong L, Li B, Mah CS, *et al.* Next generation of adeno-associated virus 2 vectors: point mutations in tyrosines lead to high-efficiency transduction at lower doses. *Proc Natl Acad Sci U S A*. 2008;105(22):7827-7832.
137. Alexander IE, Cunningham SC, Logan GJ, Christodoulou J. Potential of AAV vectors in the treatment of metabolic disease. *Gene Ther*. 2008;15(11):831-839.
138. Cunningham SC, Dane AP, Spinoulas A, Alexander IE. Gene delivery to the juvenile mouse liver using AAV2/8 vectors. *Mol Ther*. 2008;16(6):1081-1088.
139. Boutin S, Monteilhet V, Veron P, *et al.* Prevalence of serum IgG and neutralizing factors against adeno-associated virus (AAV) types 1, 2, 5, 6, 8, and 9 in the healthy population: implications for gene therapy using AAV vectors. *Hum Gene Ther*. 2010;21(6):704-712.
140. Li A, Tanner MR, Lee CM, *et al.* AAV-CRISPR gene editing is negated by pre-existing immunity to Cas9. *Mol Ther*. 2020;28(6):1432-1441.
141. Wiedenheft B, Sternberg SH, Doudna JA. RNA-guided genetic silencing systems in bacteria and archaea. *Nature*. 2012;482(7385):331-338.
142. Sorek R, Lawrence CM, Wiedenheft B. CRISPR-mediated adaptive immune systems in bacteria and archaea. *Annu Rev Biochem*. 2013;82(1):237-266.
143. Jinek M, Chylinski K, Fonfara I, Hauer M, Doudna JA, Charpentier E. A programmable dual-RNA-guided DNA endonuclease in adaptive bacterial immunity. *Science*. 2012;337(6096):816-821.
144. Rouet P, Smih F, Jasin M. Introduction of double-strand breaks into the genome of mouse cells by expression of a rare-cutting endonuclease. *Mol Cell Biol*. 1994;14(12):8096-8106.
145. Tajima T, Okada T, Ma XM, Ramsey W, Bornstein S, Aguilera G. Restoration of adrenal steroidogenesis by adenovirus-mediated transfer of human cytochrome P450 21-hydroxylase into the adrenal gland of 21-hydroxylase-deficient mice. *Gene Ther*. 1999;6(11):1898-1903.
146. Naiki Y, Miyado M, Horikawa R, *et al.* Extra-adrenal induction of Cyp21a1 ameliorates systemic steroid metabolism in a mouse model of congenital adrenal hyperplasia. *Endocr J*. 2016;63(10):897-904.
147. Perdomini M, Dos Santos C, Goumeaux C, Blouin V, Bougnères P. An AAVrh10-CAG-CYP21-HA vector allows persistent correction of 21-hydroxylase deficiency in a Cyp21$^{-/-}$ mouse model. *Gene Ther*. 2017;24(5):275-281.
148. Markmann S, De BP, Reid J, *et al.* Biology of the adrenal gland cortex obviates effective use of adeno-associated virus vectors to treat hereditary adrenal disorders. *Hum Gene Ther*. 2018;29(4):403-412.
149. Naiki Y, Miyado M, Shindo M, *et al.* Adeno-associated virus-mediated gene therapy for patients' fibroblasts, induced pluripotent stem cells, and a mouse model of congenital adrenal hyperplasia. *Hum Gene Ther*. 2022;33(15-16):801-809.
150. Vinson GP. Functional zonation of the adult mammalian adrenal cortex. *Front Neurosci*. 2016;10:238.
151. Gotoh H, Sagai T, Hata J, Shiroishi T, Moriwaki K. Steroid 21-hydroxylase deficiency in mice. *Endocrinology*. 1988;123(4):1923-1927.
152. Alesci S, Ramsey WJ, Bornstein SR, *et al.* Adenoviral vectors can impair adrenocortical steroidogenesis: clinical implications for natural infections and gene therapy. *Proc Natl Acad Sci U S A*. 2002;99(11):7484-7489.
153. Macapagal MC, Slowinska BS, Nimkarn S, *et al.* Gene therapy of 21-hydroxylase deficient mice utilizing an adeno-associated virus vector. ENDO 2002: The Endocrine Society's 84th Annual Meeting; San Francisco, 2002, Abstract 1-503.
154. Naiki Y, Fukami M. Letter to the Editor: "Congenital adrenal hyperplasia due to steroid 21-hydroxylase deficiency: an

Endocrine Society clinical practice guideline". *J Clin Endocrinol Metab*. 2019;104(6):1926-1927.
155. Bougnères P, Gao G, inventors; Adrenas Therapeutics Inc, assignee. Adeno-associated virus gene therapy for 21-hydroxylase deficiency. International Patent WO 2019/143803 A1. July 25, 2019.
156. Cabanes-Creus M, Navarro RG, Zhu E, *et al.* Novel human liver-tropic AAV variants define transferable domains that markedly enhance the human tropism of AAV7 and AAV8. *Mol Ther Methods Clin Dev*. 2022;24:88-101.
157. Westhaus A, Cabanes-Creus M, Jonker T, *et al.* AAV-p40 bioengineering platform for variant selection based on transgene expression. *Hum Gene Ther*. 2022;33(11-12):664-682.
158. Westhaus A, Cabanes-Creus M, Rybicki A, *et al.* High-throughput in vitro, ex vivo, and in vivo screen of adeno-associated virus vectors based on physical and functional transduction. *Hum Gene Ther*. 2020;31(9-10):575-589.
159. Eclov RJ, Lewis TEW, Kapandia M, *et al.* Durable CYP21A2 gene therapy in non-human primates for treatment of congenital adrenal hyperplasia. ESGCT 27th Annual Congress in collaboration with SETGyc; Barcelona, Spain, 2019, Abstract A1-A221.
160. Nakai H, Yant SR, Storm TA, Fuess S, Meuse L, Kay MA. Extrachromosomal recombinant adeno-associated virus vector genomes are primarily responsible for stable liver transduction in vivo. *J Virol*. 2001;75(15):6969-6976.
161. Miao CH, Snyder RO, Schowalter DB, *et al.* The kinetics of rAAV integration in the liver. *Nat Genet*. 1998;19(1):13-15.
162. White PC. Emerging treatment for congenital adrenal hyperplasia. *Curr Opin Endocrinol Diabetes Obes*. 2022;29(3):271-276.
163. Ran FA, Hsu PD, Wright J, Agarwala V, Scott DA, Zhang F. Genome engineering using the CRISPR-Cas9 system. *Nat Protoc*. 2013;8(11):2281-2308.
164. Sadelain M, Papapetrou EP, Bushman FD. Safe harbours for the integration of new DNA in the human genome. *Nat Rev Cancer*. 2012;12(1):51-58.
165. Suzuki K, Tsunekawa Y, Hernandez-Benitez R, *et al.* In vivo genome editing via CRISPR/Cas9 mediated homology-independent targeted integration. *Nature*. 2016;540(7631):144-149.
166. Suzuki K, Yamamoto M, Hernandez-Benitez R, *et al.* Precise in vivo genome editing via single homology arm donor mediated intron-targeting gene integration for genetic disease correction. *Cell Res*. 2019;29(10):804-819.
167. Nakade S, Tsubota T, Sakane Y, *et al.* Microhomology-mediated end-joining-dependent integration of donor DNA in cells and animals using TALENs and CRISPR/Cas9. *Nat Commun*. 2014;5(1):5560.
168. Taleei R, Nikjoo H. Biochemical DSB-repair model for mammalian cells in G1 and early S phases of the cell cycle. *Mutat Res*. 2013;756(1-2):206-212.
169. Anzalone AV, Koblan LW, Liu DR. Genome editing with CRISPR-Cas nucleases, base editors, transposases and prime editors. *Nat Biotechnol*. 2020;38(7):824-844.
170. Anzalone AV, Randolph PB, Davis JR, *et al.* Search-and-replace genome editing without double-strand breaks or donor DNA. *Nature*. 2019;576(7785):149-157.
171. White PC, New MI, Dupont B. Structure of human steroid 21-hydroxylase genes. *Proc Natl Acad Sci U S A*. 1986;83(14):5111-5115.
172. Orthwein A, Noordermeer SM, Wilson MD, *et al.* A mechanism for the suppression of homologous recombination in G1 cells. *Nature*. 2015;528(7582):422-426.
173. Higashi Y, Yoshioka H, Yamane M, Gotoh O, Fujii-Kuriyama Y. Complete nucleotide sequence of two steroid 21-hydroxylase genes tandemly arranged in human chromosome: a pseudogene and a genuine gene. *Proc Natl Acad Sci U S A*. 1986;83(9):2841-2845.
174. Sapirstein LA, Goldman H. Adrenal blood flow in the albino rat. *Am J Physiol*. 1958;196(1):159-162.
175. Greenway CV, Stark RD. Hepatic vascular bed. *Physiol Rev*. 1971;51(1):23-65.
176. Ryan US, Ryan JW, Smith DS, Winkler H. Fenestrated endothelium of the adrenal gland: freeze-fracture studies. *Tissue Cell*. 1975;7(1):181-190.
177. Hinderer C, Katz N, Buza EL, *et al.* Severe toxicity in nonhuman primates and piglets following high-dose intravenous administration of an adeno-associated virus vector expressing human SMN. *Hum Gene Ther*. 2018;29(3):285-298.
178. Taha EA, Lee J, Hotta A. Delivery of CRISPR-Cas tools for in vivo genome editing therapy: trends and challenges. *J Control Release*. 2022;342:345-361.
179. Chand DH, Zaidman C, Arya K, *et al.* Thrombotic microangiopathy following onasemnogene abeparvovec for spinal muscular atrophy: a case series. *J Pediatr*. 2021;231:265-268.
180. Mullard A. Gene therapy community grapples with toxicity issues, as pipeline matures. *Nat Rev Drug Discov*. 2021;20(11):804-805.

8.1.2 Gene therapy for paediatric homozygous familial hypercholesterolaemia

Graves LE, Horton A, Alexander IE, and Srinivasan, S. Gene therapy for paediatric homozygous familial hypercholesterolaemia. *Heart Lung and Circulation* 2023;32(7):769-779. DOI: 10.1016/j.hlc.2023.01.017.

Heart, Lung and Circulation (2023) **32**, 769–779
1443-9506/23/$36.00
https://doi.org/10.1016/j.hlc.2023.01.017

REVIEW

Gene Therapy for Paediatric Homozygous Familial Hypercholesterolaemia

Lara E. Graves, MBBS, FRACP [a,b,c,*],
Ari Horton, MBBS, FRACP, FCSANZ [d,e,f,g,h],
Ian E. Alexander, MBBS, PhD, FRACP, FAHMS [b,c],
Shubha Srinivasan, MBBS, PhD, FRACP [a,b]

[a]Institute of Endocrinology and Diabetes, The Children's Hospital at Westmead, Sydney, NSW, Australia
[b]Children's Hospital at Westmead Clinical School, University of Sydney, Sydney, NSW, Australia
[c]Gene Therapy Research Unit, Children's Medical Research Institute, Sydney, NSW, Australia
[d]Monash Heart and Monash Children's Hospital, Monash Health, Melbourne, Vic, Australia
[e]Monash Cardiovascular Research Centre, Victorian Heart Institute, Melbourne, Vic, Australia
[f]Monash Genetics, Monash Health, Melbourne, Vic, Australia
[g]Department of Genomic Medicine, The Royal Melbourne Hospital, Parkville, Vic, Australia
[h]Department of Paediatrics, Monash University Clayton, Vic, Australia

Received 14 July 2022; received in revised form 26 November 2022; accepted 4 January 2023; online published-ahead-of-print 1 April 2023

The clinical outcome for children and adolescents with homozygous familial hypercholesterolaemia (HoFH) can be devastating, and treatment options are limited in the presence of a null variant. In HoFH, atherosclerotic risk accumulates from birth. Gene therapy is an appealing treatment option as restoration of low-density lipoprotein receptor (*LDLR*) gene function could provide a cure for HoFH. A clinical trial using a recombinant adeno-associated vector (rAAV) to deliver *LDLR* DNA to adult patients with HoFH was recently completed; results have not yet been reported. However, this treatment strategy may face challenges when translating to the paediatric population. The paediatric liver undergoes substantial growth which is significant as rAAV vector DNA persists primarily as episomes (extra-chromosomal DNA) and are not replicated during cell division. Therefore, rAAV-based gene addition treatment administered in childhood would likely only have a transient effect. With over 2,000 unique variants in *LDLR*, a goal of genomic editing-based therapy development would be to treat most (if not all) mutations with a single set of reagents. For a robust, durable effect, *LDLR* must be repaired in the genome of hepatocytes, which could be achieved using genomic editing technology such as clustered regularly interspaced short palindromic repeats (CRISPR)/Cas9 and a DNA repair strategy such as homology-independent targeted integration. This review discusses this issue in the context of the paediatric patient group with severe compound heterozygous or homozygous null variants which are associated with aggressive early-onset atherosclerosis and myocardial infarction, together with the important pre-clinical studies that use genomic editing strategies to treat HoFH in place of apheresis and liver transplantation.

Keywords Homozygous familial hypercholesterolaemia • Gene therapy • Genomic editing

Introduction

Familial hypercholesterolaemia (FH) is an autosomal dominant condition with a heterozygous prevalence estimated at 1:250 [1,2]. Homozygous or compound heterozygous states also exist, and the cardiovascular consequences in children and adolescents with homozygous familial hypercholesterolaemia (HoFH) resulting from biallelic null variants can be devastating. With limited treatment options, children often present with advanced coronary artery disease

*Corresponding author at: Dr Lara E. Graves, Institute of Endocrinology and Diabetes, The Children's Hospital at Westmead, Locked Bag 4001, Westmead, 2145, NSW, Australia; Email: lara.graves@health.nsw.gov.au

and myocardial ischaemia or stroke before the age of 20 years [3]. HoFH prevalence is estimated between 1:160,000–1:300,000 [4,5]. Over 2,190 unique variants in the *LDLR* gene have been reported as of 1 November 2022, spanning all 18 exons, with around 80% considered pathogenic or likely pathogenic [6,7]. FH is associated with marked elevation in low density lipoprotein (LDL) due to impaired hepatic clearance of LDLs from the circulation. Normally, the LDL receptor (LDLR) binds to LDL, removing it from circulation and delivering it to lysosomes, where it undergoes degradation (Figure 1) [3]. Over 90% of patients with FH have pathogenic variants in the *LDLR* gene, but FH may also be caused by variants in *APOB* and *PCSK9* or combinations of changes in multiple genes with small effect changes resulting in polygenic FH. When LDLR function is reduced, the removal of LDL from plasma is reduced and the plasma LDL level increases. *LDLR* mutations are divided into classes based on the effect on LDL metabolism. Class 1 mutations are considered null alleles and there is no residual LDLR protein produced. Class 2 mutations affect intracellular transport; Class 3 mutations affect the binding of LDL with the receptor; Class 4 mutations result in an inability to internalise bound LDL; and, Class 5 mutations are unable to release LDL from the endosome and cannot recycle the LDLR back to the surface for further use [3]. Proprotein convertase subtilisin/kexin type 9 (PCSK9) enhances LDLR degradation along with the LDL molecule and LDLR recycling is increased with loss of PCSK9 function [8]. *APOB* encodes for apolipoprotein B (ApoB) which forms a structural component of very low-density lipoproteins (VLDL) and chylomicrons [9]. Gene therapy promises to be an appealing treatment option in homozygous familial hypercholesterolaemia with restoration of normal cholesterol pathways and potential reversal of cardiovascular disease.

Cardiovascular Outcomes

The cardiovascular risk associated with FH is present from birth and is related to the cumulative burden of LDL exposure [4,10]. LDL levels are much higher in HoFH than heterozygous FH. In FH, coronary artery disease is accelerated with premature atherosclerosis: onset is 15–20 years earlier than the general population in people with heterozygous FH, and 30–40 years earlier in HoFH [4]. The natural history of HoFH is devastating, with the mean first cardiac event occurring at 12.8 years of age, and the mean age of death being 18.4 years [11].

Standard Therapeutic Options

In the paediatric population, statin therapy is recommended to commence from 8–10 years of age for severe heterozygous FH [12,13]; however, in children with HoFH, statin therapy is used from diagnosis [5,11] ideally commenced prior to 2 years of age [13,14]. Statins work by upregulating the LDLR and therefore require residual LDLR function and thus may have a reduced or limited effect in those with biallelic null mutations. On average, statins may only reduce LDL by 32% [12] and in children with HoFH their LDL could be as high as 20–30 mmol/L [15] and thus even a 30% reduction results in the LDL remaining significantly elevated, well above therapeutic targets. Other treatment options include plasmapheresis, which can be effective in children with severe HoFH [16]; however, this may be associated with significant morbidity from vascular access and burdens related to hospital attendance. Liver transplant may be required; however, will not reverse atherosclerosis that has already developed, can be associated with significant lifelong morbidity and will have associated peri- and post-transplantation risks [16]. Accessing organ transplant for children prior to the onset of atherosclerosis is also challenging, as it involves transplantation into an essentially "healthy" child.

New and Emerging Therapeutic Options

PCSK9 inhibitors such as evolocumab can work for some genotypes but will have minimal effect with biallelic null *LDLR* variants as residual LDLR function is required [17,18]. Angiopoietin-like 3 (ANGPTL3) is an inhibitor of lipoprotein lipase and plays a role in increasing lipid levels and is required for VLDL production. Evinacumab is a monoclonal antibody that blocks the ANGPTL3 protein, thereby reducing VLDL, independently of LDLR [19]. This treatment has been shown to reduce LDL levels by almost 50% in adults, independent of LDL receptor function [19] and is currently undergoing clinical trial for paediatric HoFH (ClinicalTrials.gov Identifier: NCT04233918). In children aged 5–11, LDL was reduced by 48% on average at 24 weeks post-evinacumab treatment [20]. However, evinacumab also reduces high density lipoprotein levels (HDL), which is disadvantageous [19].

Small interfering RNA (siRNA) are used to silence genes by specifically binding with mRNA causing degradation, limiting protein translation. Inclisiran is a siRNA which interferes with the translation of PCSK9 protein from mRNA. It has an advantage over PCSK9 antibodies as treatment is only required every 3–6 months, compared with every few weeks [21]. It has been used in adults with hypercholesterolaemia due to various aetiologies with good effect, lowering the LDL by 52% [22]. It has recently been approved for use in adults with heterozygous FH by the Australian Therapeutic Goods Administration and the US Food and Drug Administration. A pilot study administered inclisiran to four adult patients with HoFH and there was a lipid lowering effect in three of the four [23]. The patient in which LDL reduction was not observed had a history of poor response to PCSK9 antibody therapies. Following this pilot, a trial in adults with HoFH was recently completed but not yet reported (ClinicalTrials.gov Identifier: NCT03851705). A further trial in adolescents aged 12–17 years with HoFH is underway (ClinicalTrials.gov Identifier: NCT04659863). While this treatment shows promise, interfering with PCSK9 function to treat hypercholesterolaemia

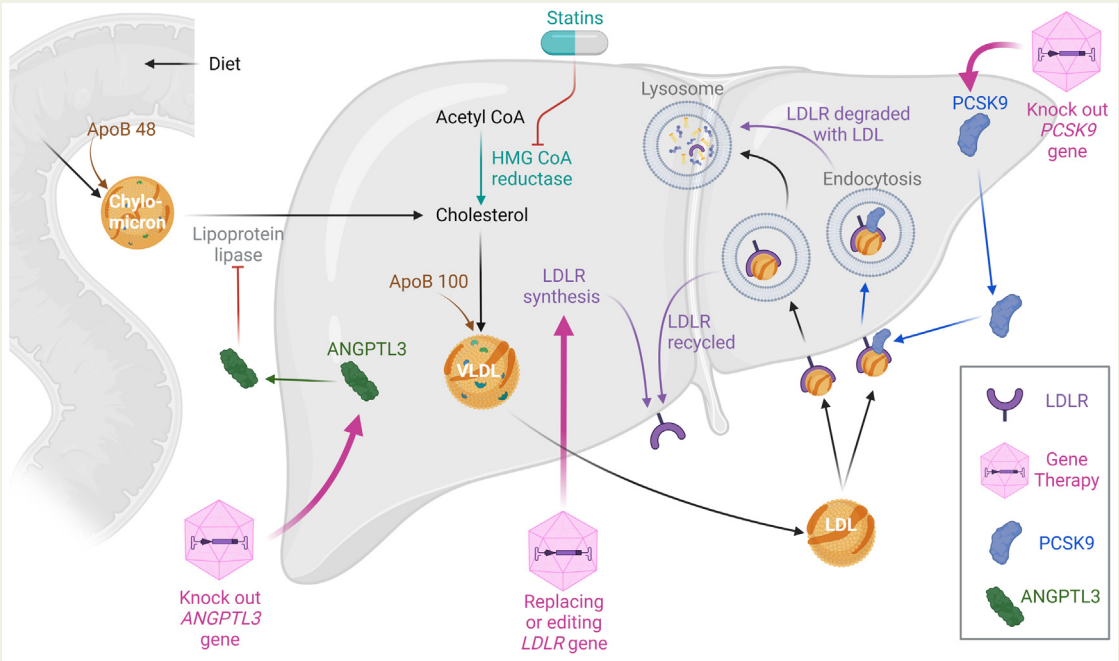

Figure 1 Gene therapy targets in the cholesterol pathway.
Cholesterol is either synthesised from acetyl CoA or absorbed from the diet. Statins work by inhibiting the conversion of acetyl CoA to cholesterol. ApoB is formed by the intestine (ApoB 48) or the liver (ApoB 100) and is required for the formation of chylomicrons and very low-density lipoproteins (VLDL). VLDL are subsequently converted to low-density lipoproteins (LDL) which circulate in the blood stream. LDL is removed from the blood by binding with LDL receptors (LDLR), which are then endocytosed and degraded. In the presence of PCSK9, LDLR degradation is enhanced and, in its absence, the LDLR is recycled back to the hepatocyte surface which results in more removal of LDL from the blood stream. Gene therapy may target the LDLR production by replacing or editing the defective *LDLR* gene. Another strategy is to introduce loss-of-function mutations into the *PCSK9*. Introducing loss-of-function mutations in *ANGPTL3* will allow lipoprotein lipase to breakdown fats, reducing VLDL in dependently of the LDLR. Created with BioRender.com
Abbreviations: ApoB, apolipoprotein B; LDLR, low-density lipoprotein receptor; LDL, low-density lipoprotein; PCSK9, Proprotein convertase subtilisin/kexin type 9; ANGPTL3, angiopoietin-like 3.

requires residual LDLR function to be effective; therefore patients with null variants in *LDLR* are unlikely to respond to this treatment and have been excluded from this clinical trial. Clinical trials using a siRNA targeting *ANGPTL3* are also underway and preliminary data show effectiveness in reducing LDL in patients with heterozygous FH [24] (ClinicalTrials.gov Identifiers: NCT03747224, NCT05217667 and NCT04832971).

Early Detection

Treatment for HoFH should commence as soon as possible and routine screening during late infancy/early childhood has been proposed [25,26]. In these studies, toddlers were screened for FH at routine medical visits for immunisations by measuring lipid profiles on heel prick samples, and subsequently genetic testing was undertaken if appropriate. Families were screened following the diagnosis of FH in a child and a new diagnosis of FH was detected for every 56–125 children screened, with on average four family members being diagnosed by reverse cascade screening for each proband [25,26]. With advances in next-generation sequencing, newborn screening may also be feasible, and a pilot study in Queensland, Australia detected 15 cases of FH among 2,552 screened newborns (Glenn Bennett, Founder and Chief Medical Officer, Genepath Laboratories, personal communication, 29th June 2022). Pre-conception screening is also possible as part of commercially available comprehensive carrier screening, and may result in diagnoses of FH for prospective parents. The Australian Reproductive Carrier Screening Project (Mackenzie's Mission) aims to screen partners for risk of autosomal recessive and X-linked conditions to allow informed pre-conception planning and *LDLR* is included in the panel [27].

Despite the imminent opportunity for early detection, current medical therapy is inadequate for many paediatric patients with HoFH, particularly those that carry null mutations. Gene therapy is an enticing treatment option as it may offer cure with a single treatment, however it must be considered in the context of paediatric organ growth. With future progress in the gene therapy field, ideally patients will

be identified at newborn screening, prior to the development of any atherosclerotic sequelae and be treated with a single therapy with robust, lifelong efficacy.

Gene Therapy

Gene therapy techniques have reached an inflection point in technological advancement whereby potentially curative treatments are within realistic reach and are an appealing option for monogenic liver disorders [29] such as HoFH. Gene therapy approaches correct, prevent, or alleviate disease by replacing (gene addition) or repairing (genomic editing) genes carrying pathogenic variants in the human genome. By early 2022, there were 1,986 gene therapies in development [30]. The major challenge for gene therapy is delivery. *Ex vivo* gene therapy has been explored in tissues that can be cultured and then engrafted into the patient, but this technique has limited application [31]. For *in vivo* gene delivery, viral vectors appear to be the most immediately promising delivery approach. Vectorology exploits the natural ability of a virus to introduce its own genome into a host cell. There has been a decline in the use of retroviral and adenovirus vectors in favour of recombinant adeno-associated viral (rAAV) and lentiviral vector-based therapy [32]. Viral vectors were used in 89% of gene therapies in development, and of these, rAAV was the leading vector used for *in vivo* gene delivery [33]. Adeno-associated virus (AAV) is a small dependent parvovirus [34] that has not been proven to cause disease in humans and in non-dividing cells is a stable vector for gene transfer *in vivo* [35,36]. Risk of adverse events increases with very high doses of rAAV, which are often utilised when targeting organs outside of the liver, and in 2020, four children who received some of the highest human doses of rAAV as part of a trial for treatment of X-linked myotubular myopathy passed away after developing severe hepatobiliary disease as a result of the rAAV treatment [37,38]. Adverse events that have been associated with rAAV therapy include liver toxicity [39,40], thrombotic microangiopathy [41] and dorsal root ganglion toxicity [38]. In addition to risk/benefit and safety considerations, other ethical aspects such as goals of treatment and ensuring equitable access to therapies must be considered in the development and delivery of genetic therapies [42].

Recombinant AAV vectors have had most of their native genetic sequence removed, leaving only inverted terminal repeats (ITRs) which contain the *cis*-acting elements critical for rescue and replication from proviral plasmids and packaging of the recombinant genomic during vector production [32,43,44]. Instead, the therapeutic cassette which, depending on the specific application, commonly includes the gene of interest and various regulatory genes such as promoter-enhancers and polyadenylation signals may be cloned in its place. By removing the wild-type genome, the packaging capacity is maximised, and reduces the immunogenicity and cytotoxicity [32]. A critical advantage of AAV is that the recombinant AAV2 genome can be cross-packaged into the protein coat (capsid) of multiple types of AAV, known as pseudo-serotyping. The capsid serotype determines the efficiency of vector transduction depending on the target cell type and tissue [45,46], allowing parenteral administration of treatment with targeted effect. Specific tissues may be targeted by naturally occurring AAV or AAV capsids that have been optimised or engineered [46]. Most naturally occurring capsid serotypes target hepatocytes with various efficiency. One caveat with the use of rAAV is that the vector genomes are predominantly extra-chromosomal (episomal) and are lost in actively dividing cells such as during paediatric organ growth or in organs with rapid cellular turnover throughout life (Figure 2) [36,47]. A further limitation of the use of rAAV may be the presence of pre-existing neutralising antibodies to AAV which preclude the use of AAV-based therapy, and this can occur following natural exposure to wild-type AAV or from previous AAV vector-based treatment [48,49]. As immunomodulating technology currently stands, rAAV may only be administered once in a lifetime.

Clinical Trials for HoFH Gene Therapy

Liver-directed gene therapy, whereby a new functional copy of the *LDLR* gene is provided or the native *LDLR* gene is repaired, is a tempting therapeutic option for HoFH, particularly when LDL targets are not able to be met by conventional therapies [50]. The first attempt to treat HoFH in humans using gene therapy was published in 1994, where a 29-year-old woman was treated with *ex vivo* gene therapy [51]. She underwent a 25% hepatectomy and the harvested hepatocytes were transduced *ex vivo* with a recombinant retrovirus that carried wild-type *LDLR* cDNA. The autologous hepatocytes were then engrafted back into the liver via the portal vein. Due to improvement in this patient's LDL level following treatment, four subsequent patients underwent the same treatment [52]. However, there was only a modest improvement in three of the five total treated patients (LDL level reduced 6%–25%), and no improvement in two of the five. The effect seen declined over time and, due to this, the low efficiency of treatment and the significant morbidity associated with the procedure, this approach was not pursued. It would be difficult to improve the efficiency of this approach as infusing cells into the liver via the portal vein is limited by the number of cells that can be reinfused without causing embolism.

Despite this early attempt, there were no gene therapy trials in humans for HoFH for more than two decades. A phase 1/2 human clinical trial commenced in 2016 (ClinicalTrials.gov Identifier: NCT02651675) whereby human *LDLR* cDNA was packaged into rAAV8 and used to treat patients with HoFH [53]. The trial was completed in November 2020, but the result of this trial is yet to be published, and in a press release in 2020 it was announced that the sponsor company, Regenxbio, was discontinuing internal clinical development for this product [54]. Nine participants were treated and there were no symptomatic adverse events.

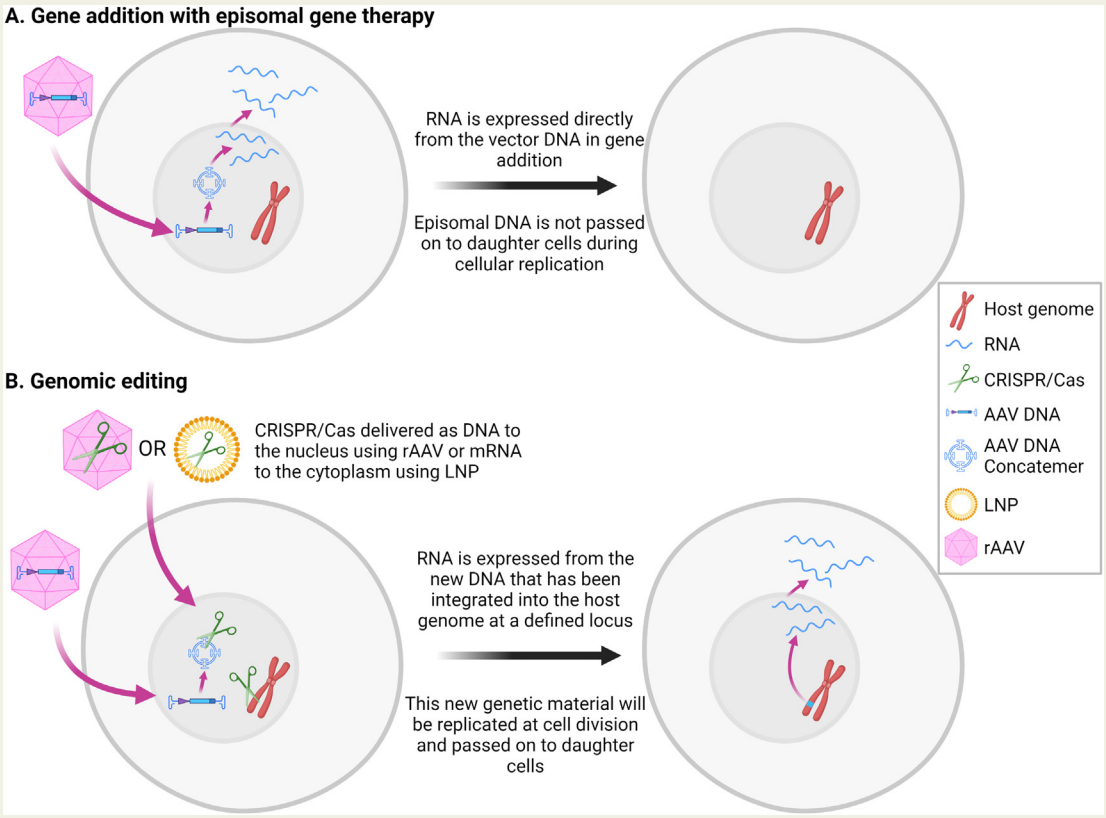

Figure 2 Gene addition versus genomic editing.
A. RNA is expressed directly from the vector DNA with episomal gene therapy such as with recombinant adeno-associated viral vectors. The viral DNA undergoes a conformational change to become a concatemer and RNA is expressed. Episomal DNA is not replicated during cell division and the therapy will be lost in actively dividing cells.
B. CRISPR/Cas may be delivered as DNA or RNA, whereas the repair template must be delivered as DNA in order to reach the nucleus. With genomic editing, new DNA is stably integrated into the genomic DNA at a defined locus and RNA is expressed directly from the genomic DNA. This new genetic material will be replicated during cell division.
Created with BioRender.com
Abbreviation: CRISPR/Cas, clustered regularly interspaced short palindromic repeat-associated nuclease Cas.

The patients developed elevated liver transaminases at 4 weeks post treatment, which was treated with steroids with improvement [55]. This is a common side effect of rAAV-based gene therapy [56,57]. Further optimisation of the vector is warranted, and capsid choice is imperative. Despite the importance of capsid choice, codon optimisation is underway using the same capsid [58]. Capsid tropism that is robust in the mouse or other preclinical animal model may fail in the human. The serotype AAV8 is trophic to the murine liver, however in chimeric mouse–human livers it transduces human hepatocytes markedly less efficiently than it does murine hepatocytes [59]. Modern capsids such as AAV-LK03, which transduces human hepatocytes *in vivo* far more efficiently than AAV8 when compared in chimeric mouse-human livers, give hope for robust clinical success in the future [59]. With recent adverse events associated with high-dose rAAV, research is being directed towards optimising vectors to minimise the dose required. Vector optimisation can involve: capsid engineering to target specific tissues or to de-target commonly transduced tissue such as the liver; safe manufacturing and purification methods; increased understanding of AAV biology; strategies to avoid immunogenicity; and, new methods of administration, among others [37].

Limitation of Gene Therapy in the Paediatric Population

A limitation of gene addition with AAV vectors is that the transgene is not reliably integrated into the host cell's genome and may be lost in concert with cellular replication [36,60]. This is particularly important in the paediatric population where rapid growth through cell division is taking place [47,61]. At birth, the liver weighs approximately 80 g, doubling to 160 g by 4 months of age, and then over 400 g by 3 years of age. By age 12 years, the liver weighs over 900 g: a

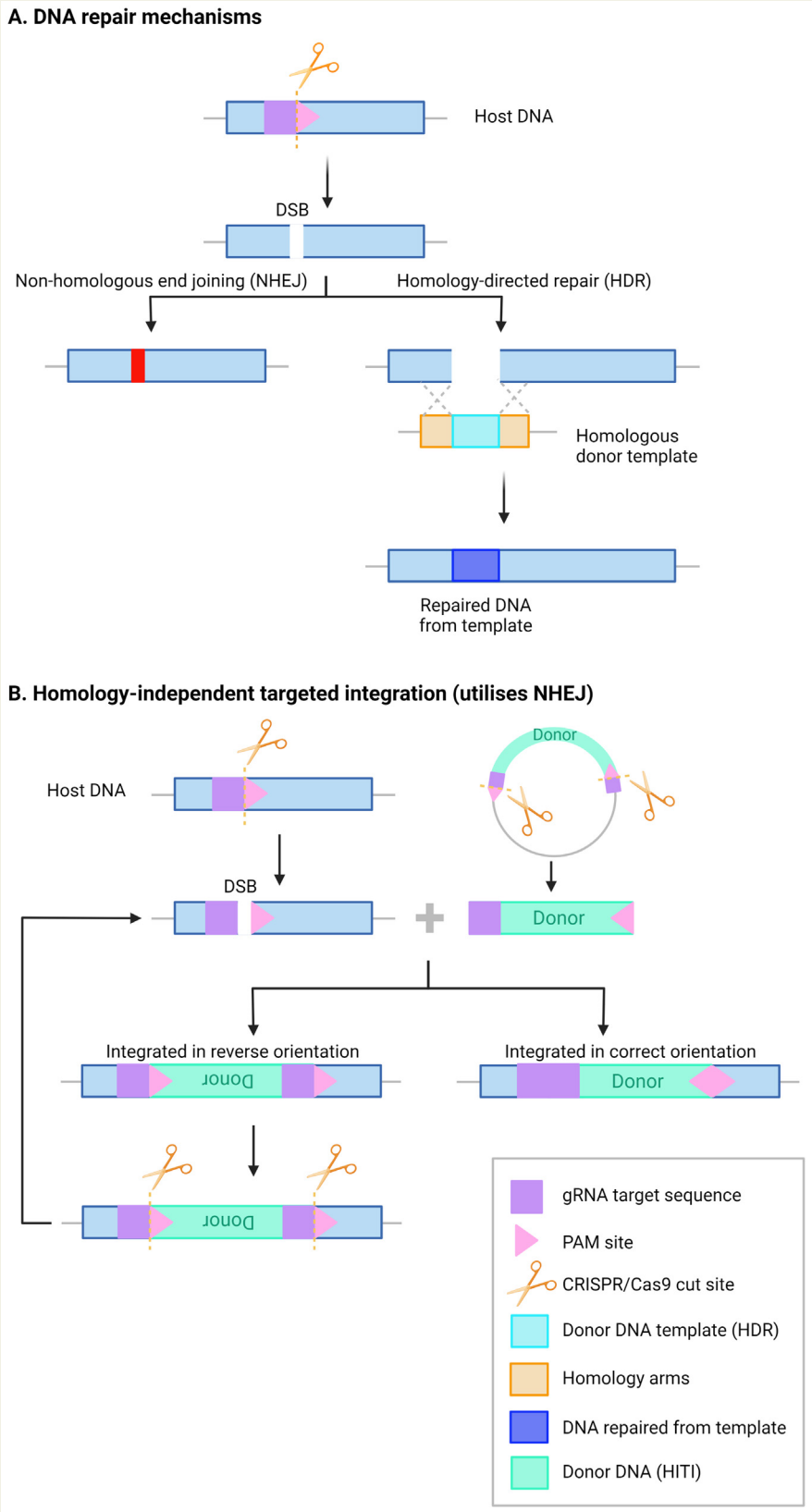

Figure 3 DNA repair mechanisms.
A. CRISPR/Cas9 introduces a double-stranded break in DNA at a protospacer adjacent motif (PAM) site and is directed there using guide RNA. Repairing the cut with non-homologous end-joining (NHEJ) is error prone and can result in small insertions and deletions (indels). Homology-directed repair (HDR) is more reliable as the cut site is repaired using a

12-fold increase in size from birth [28]. This increase in liver mass could be considered a surrogate for hepatocellular proliferation. This has technology-related implications for the delivery of durable liver-directed gene therapy in the paediatric population. Thus, the recent clinical trial for AAV-based HoFH gene therapy has limited applicability to the paediatric population. For the growing organ, modification or repair of the host genome must be undertaken such that it will be passed on to daughter cells during cell division to ensure durability of treatment effect.

Genomic Editing

Genomic editing offers the potential to repair a native locus, retaining physiological gene expression with minimal risk of mutagenesis as the native endogenous enhancer-promoter elements are utilised. Various technological platforms based on programmable nucleases have been employed in order to enable loci-specific genomic editing including meganucleases, zinc-finger nucleases, and transcription activator-like effector nucleases [62]. These strategies have largely been superseded by the clustered regularly interspaced short palindromic repeat-associated nuclease Cas (CRISPR/Cas). The CRISPR/Cas system and its potential in programmable genome editing was described by Doudna and Charpentier in 2012 [63] resulting in a Nobel Prize for the authors in 2020 [64]. The CRISPR/Cas system facilitates RNA-guided double-stranded DNA cleavage with Cas proteins and originates as an immune defence mechanism for bacteria against viruses and plasmids [63,65,66]. Shortly after its potential in genome editing was considered, the CRISPR/Cas ability to facilitate genome engineering in mammalian cells was demonstrated [67]. To repair the native locus, a DNA repair template is provided and is used by the host's DNA repair mechanisms to repair the cut site and simultaneously introduce a site-specific modification into the host genome [68].

DNA repair mechanisms include non-homologous end joining (NHEJ) or homology-directed repair (HDR) where the donor template has homology to the target site (Figure 3A) [67,69,70]. Ligation of DNA ends through NHEJ is error-prone and may cause small insertions or deletions (indels) at the break site which can be exploited to disrupt pathogenic sequences [71]. In the absence of a donor template, NHEJ can be used to introduce indels which disrupt the function of a gene resulting in gene silencing. HDR can be used to repair a pathogenic variant at either the endogenous locus or another region of the genome that is considered safe from insertional mutagenesis or disruption of resident gene function [72]. HDR repair is limited to actively dividing cells [73]. Other editing strategies include single homology arm donor mediated intron-targeting integration (SATI) which is a combination of HDR and NHEJ [75], precise integration into target chromosome (PITCh) which can be used in non-dividing cells using micro-homology-mediated end-joining [76,77]. The efficiency of an editing technique is dependent on the DNA repair process used. Editing techniques which do not induce a break in the DNA include base editing which introduces precise point mutations [78] and prime editing which allows targeted insertion, deletion, or replacement of a single nucleotide through the delivery of RNA reagents, without the need for a repair template [79]. There are too many *LDLR* variants for prime editing to be a logistically useful tool in HoFH. NHEJ is the major repair pathway in mammalian cells and therefore editing using this technique will occur at a relatively high frequency [71]. However, this may be limited by the formation of undesirable indels. HDR strategies are precise; however, they are reliant on the target cell undergoing mitosis and occurs at lower frequencies than NHEJ.

The chosen editing strategy is important and depends on the goal. HDR requires a unique set of reagents for each group of variants and risks eliminating residual function in a hypomorphic allele as not all double stranded DNA breaks will undergo repair [72,73]. Homology-independent targeted integration (HITI) overcomes the limitations of HDR by using NHEJ and allows robust DNA modification in both dividing and non-dividing cells (Figure 3B) [74]. With a HITI strategy, potentially all *LDLR* mutation types could be treated with a single set of reagents, which would also be effective in compound heterozygous states. Editing efficiency is relatively high in hepatocytes [29,80], which makes HoFH an ideal candidate for liver-directed genomic editing.

The packaging capacity of rAAV is small, at only 4.7 kb, and thus the donor template and CRISPR/Cas9 must be packaged separately either as DNA in a second rAAV or encoded as RNA in lipid nanoparticles (LNP). The

template with homology arms, however it is limited to actively dividing cells, risks knocking down a hypomorphic allele if repair does not occur, and a separate set of reagents is required for each group of variants.
B. Homology-independent targeted integration (HITI) is not limited to the cell cycle as it utilises NHEJ, and the entire wild-type cDNA can be integrated under a native promoter, refunctioning the locus with a single cassette. The donor sequence is integrated into the host DNA at the cut site. If the donor sequence is integrated in the reverse orientation, the guide sequence and PAM sites realign, and further double stranded breaks occur until the template is integrated in the correct orientation. Figure adapted from Ginn et al, 2021 [29].Created with BioRender.com
Abbreviations: CRISPR/Cas, clustered regularly interspaced short palindromic repeat-associated nuclease Cas.

limitations of AAV-based genomic editing include immunogenicity to the virus, liver toxicity, prolonged Cas9 expression and random integration of the viral genome [56,60]. Transgene expression from AAV vector can persist up to 10 years or more, and prolonged expression of Cas9 is unnecessary and may increase the potentially mutagenic risk [81,82]. The first human clinical trial that delivered CRISPR/Cas9 editing machinery *in vivo* shows promise for the treatment of transthyretin amyloidosis [83]. CRISPR/Cas9 was delivered as RNA in LNP. LNP have gained recent attention following the widespread use of severe acute respiratory syndrome coronavirus 2 (SARS-CoV-2) vaccinations [84,85]. While CRISPR/Cas9 may be delivered as DNA by rAAV, DNA is relatively stable and sustained expression of Cas9 may result in prolonged editing events and associated safety risks [82]. LNP-delivered RNA has a distinct advantage as the RNA coding the editing reagents is expressed only transiently [86]. LNP can only deliver RNA to the cytoplasm, which is translated into protein, and without rAAV can only be used to silence a gene. Expression of LNP-delivered RNA peaks at 4 hours–8 hours and is only expressed for a total of 1 day–4 days [87,88] and therefore cannot be used as a gene delivery system alone. When LNP is utilised to deliver editing reagents, rAAV must still be used to efficiently deliver the repair template as DNA to the nucleus. When the repair template is designed such that the host enhancer-promoter of the target gene is utilised and the DNA template has no enhancer-promoter of its own, the risk of insertional mutagenesis is greatly reduced.

Pre-Clinical Genomic Editing Studies

It was recently demonstrated that *LDLR* expression can be rescued in a mouse model for HoFH using a dual rAAV CRISPR/Cas9/repair template HDR *in vivo* strategy [89]. Notably, the mice were treated shortly after birth and analysed as adults at 8 weeks of age. Following treatment, the mice had significantly lower plasma LDL levels and reduced burden of atherosclerotic plaque on the aorta when compared to the untreated controls. The study was limited by low editing efficiency (6.7%) and editing events in off-target sites. While this strategy did not cure the mice to wild-type levels, the introduction of functional LDLR will render the ability to respond to statin treatment where previously a null mutation limited any effect from statins. Editing efficiency could be improved by using a HITI editing strategy combined with a highly human-tropic rAAV capsid, which has been shown to have an editing efficiency in primary human hepatocytes in a chimeric mouse–human liver of >30% [80]. Nevertheless, this study is significant for the paediatric HoFH population as it demonstrated durability of effect throughout the paediatric organ growth period; however, it would not be directly translatable to the human clinical context. HDR was used in this strategy, which is suitable in a mouse model where all study animals have the same pathogenic variant in the *LDLR* gene. However, the *LDLR* gene spans 18 exons and there are over 2,000 pathogenic variants [6,7]. If HDR was to be applied to the human clinical context, a new strategy would need to be developed for each group of mutations. Furthermore, inducing a double-stranded break in the coding region risks completely knocking out function in a hypomorphic allele if repair does not take place, potentially worsening the phenotype. HDR is also limited to actively dividing cells. HITI overcomes these limitations. The *LDLR* cDNA is approximately 2.5 kb, which is easily packaged into the 4.7 kb capacity rAAV backbone. As such, the entire wild-type *LDLR* gene could be inserted downstream of the endogenous *LDLR* enhancer-promoter region, leaving the *LDLR* gene under physiological control. Alternatively, mutations in exons upstream of the insertion site could also be treated, such as by introducing termination of the upstream cistron and expressing the entire wild-type *LDLR* cDNA from a downstream cistron using an internal ribosome entry site. This would allow robust correction of all pathogenic variants with a single mutation-independent strategy.

Capsid choice can affect efficiency of cellular transduction, and serotypes that are efficient in murine hepatocytes are not necessarily efficient in human hepatocytes. Therefore, choice of capsid and pre-clinical model can affect how applicable the findings are to human patients. One of the best model systems employs patient-derived hepatocytes engrafted into a chimeric mouse liver [90]. This model has been successfully engrafted with human hepatocytes from a donor affected by FH [91]. The mice developed a "human" lipid profile and were successfully rescued using gene addition. This model system would be a useful pre-clinical tool for future genomic editing exploration.

There has been recent interest in introducing loss-of-function mutations in the *PCSK9* gene as a potential treatment option for hypercholesterolaemia. Gain-of-function mutations result in familial hypercholesterolaemia [92], and naturally occurring loss-of-function *PCSK9* mutations are associated with lower LDL levels and reduced cardiovascular risk and do not appear to be associated with adverse health risks [93]. Recently, multiple teams have published successful introduction of a loss-of-function mutation into *PCSK9* using either dual rAAV or LNP/rAAV strategies in non-human primates [94–96]. A human clinical trial is underway where LNP is used to deliver gene editing technology to disrupt the *PCSK9* gene and the first three participants with heterozygous FH have been treated [97] (ClinicalTrials.gov Identifier: NCT05398029). This strategy would not be effective in people with no residual LDLR function and is more applicable to those with HoFH due to mild variants or heterozygous FH. Similarly, loss-of-function mutations in *ANGPTL3* are associated with reduced risk of coronary heart disease, with no associated adverse health consequences. Using rAAV CRISPR/Cas9 base-editing to introduce a mutation in *Angpltl3* of LDLR knockout mice successfully improved the lipid profile of

these mice, even when knocking out *Pcsk9* had little effect [98]. LNP has also been used to deliver knockdown of *Angptl3* in mice [99]. These alternative strategies are more relevant to patients with heterozygous FH or even multifactorial hypercholesterolaemia.

Conclusion

HoFH is a devastating disease with high morbidity and mortality rate starting in early childhood. Gene therapy to treat homozygous familial hypercholesterolaemia was one of the earliest human trials of gene therapy, however almost 30 years has passed, and this early enthusiasm has not translated into the clinic or changed patient outcomes. A recently completed clinical trial using rAAV (ClinicalTrials.gov Identifier: NCT02651675) may have limited translation to children as during paediatric organ growth the newly introduced genetic material will be lost during cell division. There have been dramatic improvements in gene transfer and genomic editing technology since this trial was commenced, and thus future trials with newer technology are anticipated. There is great potential in genomic editing technology for use in the paediatric population and the trajectory of further research should be directed towards this technology. Further studies and strategies are required to optimise the editing efficiency and minimise off-target effects. The future of HoFH is early diagnosis (such as with newborn screening and universal screening programs) followed by a robust, permanent modification of the affected gene prior to the development of atherosclerotic sequelae, combined with multidisciplinary management.

Acknowledgements

Figures were created using Biorender.com

Declarations of Interest

None.

Funding

Nil.

References

[1] Sjouke B, Kusters DM, Kindt I, Besseling J, Defesche JC, Sijbrands EJ, et al. Homozygous autosomal dominant hypercholesterolaemia in the Netherlands: prevalence, genotype–phenotype relationship, and clinical outcome. Eur Heart J. 2015;36:560–5.

[2] Beheshti SO, Madsen CM, Varbo A, Nordestgaard BG. Worldwide prevalence of familial hypercholesterolemia: meta-analyses of 11 million subjects. J Am Coll Cardiol. 2020;75:2553–66.

[3] Goldstein JL, Hobbs HH, Brown MS. Familial hypercholesterolemia. In: Valle DL, Antonarakis S, Ballabio A, Beaudet AL, Mitchell GA, editors. The Online Metabolic and Molecular Bases of Inherited Disease. New York, NY: McGraw-Hill Education; 2019.

[4] Nordestgaard BG, Chapman MJ, Humphries SE, Ginsberg HN, Masana L, Descamps OS, et al. Familial hypercholesterolaemia is underdiagnosed and undertreated in the general population: guidance for clinicians to prevent coronary heart disease: consensus statement of the European Atherosclerosis Society. Eur Heart J. 2013;34:3478–3490a.

[5] Cuchel M, Bruckert E, Ginsberg HN, Raal FJ, Santos RD, Hegele RA, et al. Homozygous familial hypercholesterolaemia: new insights and guidance for clinicians to improve detection and clinical management. A position paper from the Consensus Panel on Familial Hypercholesterolaemia of the European Atherosclerosis Society. Eur Heart J. 2014;35:2146–57.

[6] Leigh S. The LDLR gene homepage, Leiden Open Variation Database. 2022. https://databases.lovd.nl/shared/genes/LDLR. [accessed 27.11. 2022].

[7] Leigh S, Futema M, Whittall R, Taylor-Beadling A, Williams M, Den Dunnen JT, et al. The UCL low-density lipoprotein receptor gene variant database: pathogenicity update. J Med Genet. 2017;54:217–23.

[8] Lambert G, Sjouke B, Choque B, Kastelein JJ, Hovingh GK. The PCSK9 decade. J Lipid Res. 2012;53:2515–24.

[9] Elovson J, Chatterton JE, Bell GT, Schumaker VN, Reuben MA, Puppione DL, et al. Plasma very low density lipoproteins contain a single molecule of apolipoprotein B. J Lipid Res. 1988;29:1461–73.

[10] Korneva V, Kuznetsova T, Julius U. The role of cumulative LDL cholesterol in cardiovascular disease development in patients with familial hypercholesterolemia. J Pers Med. 2022;12:71.

[11] Raal FJ, Pilcher GJ, Panz VR, van Deventer HE, Brice BC, Blom DJ, et al. Reduction in mortality in subjects with homozygous familial hypercholesterolemia associated with advances in lipid-lowering therapy. Circulation. 2011;124:2202–7.

[12] Vuorio A, Kuoppala J, Kovanen PT, Humphries SE, Tonstad S, Wiegman A, et al. Statins for children with familial hypercholesterolemia. Cochrane Database Syst Rev. 2019;2019(11):CD006401.

[13] Horton AE, Martin AC, Srinivasan S, Justo RN, Poplawski NK, Sullivan D, et al. Integrated guidance to enhance the care of children and adolescents with familial hypercholesterolaemia: practical advice for the community clinician. J Paediatr Child Health. 2022;58:1297–312.

[14] Watts GF, Sullivan DR, Hare DL, Kostner KM, Horton AE, Bell DA, et al. Integrated guidance for enhancing the care of familial hypercholesterolaemia in Australia. Heart Lung Circ. 2021;30:324–49.

[15] Kolansky DM, Cuchel M, Clark BJ, Paridon S, McCrindle BW, Wiegers SE, et al. Longitudinal evaluation and assessment of cardiovascular disease in patients with homozygous familial hypercholesterolemia. Am J Cardiol. 2008;102:1438–43.

[16] Cohen H, Stefanutti C. The Mighty Medic Satellite Research Group for Pediatric Dyslipidemia. Current approach to the diagnosis and treatment of heterozygote and homozygous FH children and adolescents. Curr Atheroscler Rep. 2021;23(6):30.

[17] Watts GF, Sullivan DR, Poplawski N, van Bockxmeer F, Hamilton-Craig I, Clifton PM, et al. Familial hypercholesterolaemia: a model of care for Australasia. Atheroscler Suppl. 2011;12:221–63.

[18] Santos RD, Stein EA, Hovingh GK, Blom DJ, Soran H, Watts GF, et al. Long-term evolocumab in patients with familial hypercholesterolemia. J Am Coll Cardiol. 2020;75:565–74.

[19] Raal FJ, Rosenson RS, Reeskamp LF, Hovingh GK, Kastelein JJP, Rubba P, et al. ELIPSE HoFH Investigators. Evinacumab for homozygous familial hypercholesterolemia. N Engl J Med. 2020;383:711–20.

[20] Reijman D. The clinical utility of CTA in determining treatment effects in children with homozygous FH (if possible evinacumab paediatric trial data). Milan, Italy: 5th European Atherosclerosis Society (EAS) Paediatric Familial Hypercholesterolemia symposium; 21 May 2022.

[21] Marais AD, Blom DJ, Raal FJ. Homozygous familial hypercholesterolemia and its treatment by inclisiran. Expert Opin Orphan Drugs. 2020;8:197–208.

[22] Ray KK, Wright RS, Kallend D, Koenig W, Leiter LA, Raal FJ, et al. Two phase 3 trials of inclisiran in patients with elevated LDL cholesterol. N Engl J Med. 2020;382:1507–19.

[23] Hovingh GK, Lepor NE, Kallend D, Stoekenbroek RM, Wijngaard PLJ, Raal FJ. Inclisiran durably lowers low-density lipoprotein cholesterol and proprotein convertase subtilisin/kexin type 9 expression in homozygous familial hypercholesterolemia: The ORION-2 Pilot Study. Circulation. 2020;141:1829–31.

[24] Watts GF, Schwabe C, Scott R, Gladding P, Sullivan D, Baker J, et al. Abstract 15751: Pharmacodynamic effect of ARO-ANG3, an investigational RNA interference targeting hepatic angiopoietin-like protein 3, in patients with hypercholesterolemia. Circulation. 2020;142: A15751.

[25] Martin AC, Hooper AJ, Norman R, Nguyen LT, Burnett JR, Bell DA, et al. Pilot study of universal screening of children and child-parent cascade testing for familial hypercholesterolaemia in Australia. J Paediatr Child Health. 2022;58:281–7.
[26] Wald DS, Bestwick JP, Morris JK, Whyte K, Jenkins L, Wald NJ. Child-parent familial hypercholesterolemia screening in primary care. N Engl J Med. 2016;375:1628–37.
[27] Kirk EP, Ong R, Boggs K, Hardy T, Righetti S, Kamien B, et al. Gene selection for the Australian Reproductive Genetic Carrier Screening Project ("Mackenzie's Mission"). Eur J Hum Genet. 2021;29:79–87.
[28] Coppoletta JM, Wolbach SB. Body length and organ weights of infants and children: a study of the body length and normal weights of the more important vital organs of the body between birth and twelve years of age. Am J Pathol. 1933;9:55–70.
[29] Ginn SL, Christina S, Alexander IE. Genome editing in the human liver: progress and translational considerations. Prog Mol Biol Transl Sci. 2021;182:257–88.
[30] Barrett D, Millington S, Wendland A, Micklus A, Rose D, Nguyen-Jatkoe L. Gene, Cell & RNA Therapy Landscape, ASGCT/Pharma Intelligence Quarterly Report: Q1 2022. 2022.
[31] Wilson RC, Gilbert LA. The promise and challenge of in vivo delivery for genome therapeutics. ACS Chem Biol. 2018;13:376–82.
[32] Wang D, Tai PWL, Gao G. Adeno-associated virus vector as a platform for gene therapy delivery. Nat Rev Drug Discov. 2019;18:358–78.
[33] Barrett D, Nguyen-Jatkoe L, Foss-Campbell B, Micklus A, Wendland A, Shin D. Gene, Cell, & RNA Therapy Landscape, Q2 2021 Quarterly Data Report. 2021.
[34] Berns KI, Parrish CR. Parvoviridae. In: Fields BN, Knipe DM, Howley PM, editors. Fields Virology. 6th ed. Philadelphia: Wolters Kluwer Health/Lippincott Williams & Wilkins; 2013.
[35] Buning H, Srivastava A. Capsid modifications for targeting and improving the efficacy of AAV vectors. Mol Ther Methods Clin Dev. 2019;12:248–65.
[36] Alexander IE, Cunningham SC, Logan GJ, Christodoulou J. Potential of AAV vectors in the treatment of metabolic disease. Gene Ther. 2008;15:831–9.
[37] Paulk NK. Gene therapy: it's time to talk about high-dose AAV. Genet Eng Biotechnol News. 2020;40:14–6.
[38] Mullard A. Gene therapy community grapples with toxicity issues, as pipeline matures. Nat Rev Drug Discov. 2021;20:804–5.
[39] Hinderer C, Katz N, Buza EL, Dyer C, Goode T, Bell P, et al. Severe toxicity in nonhuman primates and piglets following high-dose intravenous administration of an adeno-associated virus vector expressing human SMN. Hum Gene Ther. 2018;29:285–98.
[40] Taha EA, Lee J, Hotta A. Delivery of CRISPR-Cas tools for in vivo genome editing therapy: trends and challenges. J Control Release. 2022;342:345–61.
[41] Chand DH, Zaidman C, Arya K, Millner R, Farrar MA, Mackie FE, et al. Thrombotic microangiopathy following onasemnogene abeparvovec for spinal muscular atrophy: a case series. J Pediatr. 2021;231:265–8.
[42] Howard HC, Van El CG, Forzano F, Radojkovic D, Rial-Sebbag E, De Wert G, et al. One small edit for humans, one giant edit for humankind? Points and questions to consider for a responsible way forward for gene editing in humans. Eur J Hum Genet. 2018;26:1–11.
[43] Wilmott P, Lisowski L, Alexander IE, Logan GJ. A user's guide to the inverted terminal repeats of adeno-associated virus. Hum Gene Ther Methods. 2019;30:206–13.
[44] Samulski RJ, Berns KI, Tan M, Muzyczka N. Cloning of adeno-associated virus into pBR322: rescue of intact virus from the recombinant plasmid in human cells. Proc Natl Acad Sci USA. 1982;79:2077–81.
[45] Rabinowitz JE, Rolling F, Li C, Conrath H, Xiao W, Xiao X, et al. Cross-packaging of a single adeno-associated virus (AAV) type 2 vector genome into multiple AAV serotypes enables transduction with broad specificity. J Virol. 2002;76:791–801.
[46] Zhong L, Li B, Mah CS, Govindasamy L, Agbandje-McKenna M, Cooper M, et al. Next generation of adeno-associated virus 2 vectors: point mutations in tyrosines lead to high-efficiency transduction at lower doses. Proc Natl Acad Sci U S A. 2008;105:7827–32.
[47] Cunningham SC, Spinoulas A, Carpenter KH, Wilcken B, Kuchel PW, Alexander IE. AAV2/8-mediated correction of OTC deficiency is robust in adult but not neonatal Spf(ash) mice. Mol Ther. 2009;17:1340–6.
[48] Boutin S, Monteilhet V, Veron P, Leborgne C, Benveniste O, Montus MF, et al. Prevalence of serum IgG and neutralizing factors against adeno-associated virus (AAV) types 1, 2, 5, 6, 8, and 9 in the healthy population: implications for gene therapy using AAV vectors. Hum Gene Ther. 2010;21:704–12.
[49] Li A, Tanner MR, Lee CM, Hurley AE, De Giorgi M, Jarrett KE, et al. AAV-CRISPR gene editing is negated by pre-existing immunity to Cas9. Mol Ther. 2020;28:1432–41.
[50] Taheri F, Taghizadeh E, Baniamerian F, Rostami D, Rozeian A, Mohammad Gheibi Hayat S, et al. Cellular and molecular aspects of managing familial hypercholesterolemia: recent and emerging therapeutic approaches. Endocr Metab Immune Disord Drug Targets. 2022;22:1018–28.
[51] Grossman M, Raper SE, Kozarsky K, Stein EA, Engelhardt JF, Muller D, et al. Successful ex vivo gene therapy directed to liver in a patient with familial hypercholesterolaemia. Nat Genet. 1994;6:335–41.
[52] Grossman M, Rader DJ, Muller DW, Kolansky DM, Kozarsky K, Clark BJ 3rd, et al. A pilot study of ex vivo gene therapy for homozygous familial hypercholesterolaemia. Nat Med. 1995;1:1148–54.
[53] Bajaj A, Cuchel M. Homozygous familial hypercholesterolemia: what treatments are on the horizon? Curr Opin Lipidol. 2020;31:119–24.
[54] REGENXBIO Reports Second Quarter 2020 Financial Results and Operational Highlights. 2020. http://ir.regenxbio.com/news-releases/news-release-details/regenxbio-reports-second-quarter-2020-financial-results-and. [accessed 8.7.22].
[55] Cuchel M, Bajaj A, Carr R, Sikora T, Duell PB, Tardif J-C, et al. 612. Use of prophylactic steroids to mitigate potential T-Cell response in AAV8-mediated hLDLR gene transfer in subjects with homozygous familial hypercholesterolemia. 23rd Annual Meeting of the American Society for Gene and Cell Therapy. Virtual Meeting. 2020:270. asgct.org/global/documents/asgct20_abstracts_may8.aspx. [accessed 28.5.22].
[56] Mingozzi F, High KA. Immune responses to AAV vectors: overcoming barriers to successful gene therapy. Blood. 2013;122:23–36.
[57] George LA, Ragni MV, Rasko JEJ, Raffini LJ, Samelson-Jones BJ, Ozelo M, et al. Long-term follow-up of the first in human intravascular delivery of AAV for gene transfer: AAV2-hFIX16 for severe hemophilia B. Mol Ther. 2020;28:2073–82.
[58] Wang L, Muthuramu I, Somanathan S, Zhang H, Bell P, He Z, et al. Developing a second-generation clinical candidate AAV vector for gene therapy of familial hypercholesterolemia. Mol Ther Methods Clin Dev. 2021;22:1–10.
[59] Lisowski L, Dane AP, Chu K, Zhang Y, Cunningham SC, Wilson EM, et al. Selection and evaluation of clinically relevant AAV variants in a xenograft liver model. Nature. 2014;506:382–6.
[60] Sabatino DE, Bushman CFD, Chandler RJ, Crystal RG, Davidson BL, Dolmetsch R, et al. Evaluating the state of the science for adeno-associated virus (AAV) integration:an integrated perspective. Mol Ther. 2022;30:2646–63.
[61] Cunningham SC, Dane AP, Spinoulas A, Alexander IE. Gene delivery to the juvenile mouse liver using AAV2/8 vectors. Mol Ther. 2008;16:1081–8.
[62] Cox DBT, Platt RJ, Zhang F. Therapeutic genome editing: prospects and challenges. Nat Med. 2015;21:121–31.
[63] Jinek M, Chylinski K, Fonfara I, Hauer M, Doudna JA, Charpentier E. A programmable dual-RNA-guided DNA endonuclease in adaptive bacterial immunity. Science. 2012;337:816–21.
[64] Cohen J. A cut above: pair that developed CRISPR earns historic award. Science. 2020;370:271–2.
[65] Wiedenheft B, Sternberg SH, Doudna JA. RNA-guided genetic silencing systems in bacteria and archaea. Nature. 2012;482:331–8.
[66] Sorek R, Lawrence CM, Wiedenheft B. CRISPR-mediated adaptive immune systems in bacteria and archaea. Annu Rev Biochem. 2013;82:237–66.
[67] Ran FA, Hsu PD, Wright J, Agarwala V, Scott DA, Zhang F. Genome engineering using the CRISPR-Cas9 system. Nat Protoc. 2013;8:2281–308.
[68] Rouet P, Smih F, Jasin M. Introduction of double-strand breaks into the genome of mouse cells by expression of a rare-cutting endonuclease. Mol Cell Biol. 1994;14:8096–106.
[69] Bibikova M, Carroll D, Segal DJ, Trautman JK, Smith J, Kim YG, et al. Stimulation of homologous recombination through targeted cleavage by chimeric nucleases. Mol Cell Biol. 2001;21:289–97.
[70] Bibikova M, Golic M, Golic KG, Carroll D. Targeted chromosomal cleavage and mutagenesis in Drosophila using zinc-finger nucleases. Genetics. 2002;161:1169–75.
[71] Prakash V, Moore M, Yanez-Munoz RJ. Current progress in therapeutic gene editing for monogenic diseases. Mol Ther. 2016;24:465–74.
[72] Sadelain M, Papapetrou EP, Bushman FD. Safe harbours for the integration of new DNA in the human genome. Nat Rev Cancer. 2011;12:51–8.

[73] Orthwein A, Noordermeer SM, Wilson MD, Landry S, Enchev RI, Sherker A, et al. A mechanism for the suppression of homologous recombination in G1 cells. Nature. 2015;528:422–6.
[74] Suzuki K, Tsunekawa Y, Hernandez-Benitez R, Wu J, Zhu J, Kim EJ, et al. In vivo genome editing via CRISPR/Cas9 mediated homology-independent targeted integration. Nature. 2016;540:144–9.
[75] Suzuki K, Yamamoto M, Hernandez-Benitez R, Li Z, Wei C, Soligalla RD, et al. Precise in vivo genome editing via single homology arm donor mediated intron-targeting gene integration for genetic disease correction. Cell Research. 2019;29:804–19.
[76] Nakade S, Tsubota T, Sakane Y, Kume S, Sakamoto N, Obara M, et al. Microhomology-mediated end-joining-dependent integration of donor DNA in cells and animals using TALENs and CRISPR/Cas9. Nat Commun. 2014;5:5560.
[77] Taleei R, Nikjoo H. Biochemical DSB-repair model for mammalian cells in G1 and early S phases of the cell cycle. Mutat Res. 2013;756:206–12.
[78] Anzalone AV, Koblan LW, Liu DR. Genome editing with CRISPR–Cas nucleases, base editors, transposases and prime editors. Nat Biotechnol. 2020;38:824–44.
[79] Anzalone AV, Randolph PB, Davis JR, Sousa AA, Koblan LW, Levy JM, et al. Search-and-replace genome editing without double-strand breaks or donor DNA. Nature. 2019;576:149–57.
[80] Ginn SL, Amaya AK, Liao SHY, Zhu E, Cunningham SC, Lee M, et al. Efficient *in vivo* editing of OTC-deficient patient-derived primary human hepatocytes. JHEP Rep. 2020;2:100065.
[81] Buchlis G, Podsakoff GM, Radu A, Hawk SM, Flake AW, Mingozzi F, et al. Factor IX expression in skeletal muscle of a severe hemophilia B patient 10 years after AAV-mediated gene transfer. Blood. 2012;119:3038–41.
[82] Ishida K, Gee P, Hotta A. Minimizing off-target mutagenesis risks caused by programmable nucleases. Int J Mol Sci. 2015;16:24751–71.
[83] Gillmore JD, Gane E, Taubel J, Kao J, Fontana M, Maitland ML, et al. CRISPR-Cas9 in vivo gene editing for transthyretin amyloidosis. N Engl J Med. 2021;385:493–502.
[84] Polack FP, Thomas SJ, Kitchin N, Absalon J, Gurtman A, Lockhart S, et al. Safety and efficacy of the BNT162b2 mRNA Covid-19 vaccine. N Engl J Med. 2020;383:2603–15.
[85] Baden LR, El Sahly HM, Essink B, Kotloff K, Frey S, Novak R, et al. Efficacy and safety of the mRNA-1273 SARS-CoV-2 vaccine. N Engl J Med. 2021;384:403–16.
[86] Finn JD, Smith AR, Patel MC, Shaw L, Youniss MR, van Heteren J, et al. A single administration of CRISPR/Cas9 lipid nanoparticles achieves robust and persistent in vivo genome editing. Cell Rep. 2018;22:2227–35.
[87] Pardi N, Tuyishime S, Muramatsu H, Kariko K, Mui BL, Tam YK, et al. Expression kinetics of nucleoside-modified mRNA delivered in lipid nanoparticles to mice by various routes. J Control Release. 2015;217:345–51.
[88] Di J, Du Z, Wu K, Jin S, Wang X, Li T, et al. Biodistribution and non-linear gene expression of mRNA LNPs affected by delivery route and particle size. Pharm Res. 2022;39:105–14.
[89] Zhao H, Li Y, He L, Pu W, Yu W, Li Y, et al. In vivo AAV-CRISPR/Cas9-mediated gene editing ameliorates atherosclerosis in familial hypercholesterolemia. Circulation. 2020;141:67–79.
[90] Azuma H, Paulk N, Ranade A, Dorrell C, Al-Dhalimy M, Ellis E, et al. Robust expansion of human hepatocytes in Fah-/-/Rag2-/-/Il2rg-/- mice. Nat Biotechnol. 2007;25:903–10.
[91] Bissig-Choisat B, Wang L, Legras X, Saha PK, Chen L, Bell P, et al. Development and rescue of human familial hypercholesterolaemia in a xenograft mouse model. Nat Commun. 2015;6:7339.
[92] Abifadel M, Varret M, Rabes JP, Allard D, Ouguerram K, Devillers M, et al. Mutations in PCSK9 cause autosomal dominant hypercholesterolemia. Nat Genet. 2003;34:154–6.
[93] Cohen JC, Boerwinkle E, Mosley TH Jr, Hobbs HH. Sequence variations in PCSK9, low LDL, and protection against coronary heart disease. N Engl J Med. 2006;354:1264–72.
[94] Wang L, Breton C, Warzecha CC, Bell P, Yan H, He Z, et al. Long-term stable reduction of low-density lipoprotein in nonhuman primates following in vivo genome editing of PCSK9. Mol Ther. 2021;29:2019–29.
[95] Rothgangl T, Dennis MK, Lin PJC, Oka R, Witzigmann D, Villiger L, et al. In vivo adenine base editing of PCSK9 in macaques reduces LDL cholesterol levels. Nat Biotechnol. 2021;39:949–57.
[96] Musunuru K, Chadwick AC, Mizoguchi T, Garcia SP, DeNizio JE, Reiss CW, et al. In vivo CRISPR base editing of PCSK9 durably lowers cholesterol in primates. Nature. 2021;593:429–34.
[97] Therapeutics Verve. Verve Therapeutics Provides Regulatory Update on VERVE-101 Investigational New Drug Application and Reports Third Quarter 2022 Financial Results. 2022. https://ir.vervetx.com/news-releases/news-release-details/verve-therapeutics-provides-regulatory-update-verve-101. [accessed 27.11.2022].
[98] Chadwick AC, Evitt NH, Lv W, Musunuru K. Reduced blood lipid levels with in vivo CRISPR-Cas9 base editing of ANGPTL3. Circulation. 2018;137:975–7.
[99] Qiu M, Glass Z, Chen J, Haas M, Jin X, Zhao X, et al. Lipid nanoparticle-mediated codelivery of Cas9 mRNA and single-guide RNA achieves liver-specific in vivo genome editing of *Angptl3*. Proc Natl Acad Sci U S A. 2021;118(10):e2020401118.

8.1.3 AAV-delivered hepato-adrenal cooperativity in steroidogenesis: implications for gene therapy for congenital adrenal hyperplasia

Graves, LE, van Dijk, EB, Zhu, E, Koyyalamudi, S, Wotton, T, Sung, D, Srinivasan, S, Ginn, SL, and Alexander, IE. AAV-delivered hepato-adrenal cooperativity in steroidogenesis: implications for gene therapy for congenital adrenal hyperplasia. *Molecular Therapies Methods & Clinical Development.* 2024;32(2): 101232. DOI: 10.1016/j.omtm.2024.101232

Molecular Therapy
Methods & Clinical Development
Original Article

AAV-delivered hepato-adrenal cooperativity in steroidogenesis: Implications for gene therapy for congenital adrenal hyperplasia

Lara E. Graves,[1,2,3] Eva B. van Dijk,[1] Erhua Zhu,[1] Sundar Koyyalamudi,[2,3] Tiffany Wotton,[4] Dinah Sung,[4] Shubha Srinivasan,[2,3] Samantha L. Ginn,[1,5] and Ian E. Alexander[1,2,5]

[1]Gene Therapy Research Unit, Children's Medical Research Institute, Faculty of Medicine and Health, The University of Sydney and Sydney Children's Hospitals Network, Westmead, NSW 2145, Australia; [2]Discipline of Child and Adolescent Health, Sydney Medical School, Faculty of Medicine and Health, The University of Sydney, Westmead, NSW 2145, Australia; [3]Institute of Endocrinology and Diabetes, The Children's Hospital at Westmead, Westmead, NSW 2145, Australia; [4]NSW Newborn Screening Program, The Children's Hospital at Westmead, Westmead, NSW 2145, Australia

Despite the availability of life-saving corticosteroids for 70 years, treatment for adrenal insufficiency is not able to recapitulate physiological diurnal cortisol secretion and results in numerous complications. Gene therapy is an attractive possibility for monogenic adrenocortical disorders such as congenital adrenal hyperplasia; however, requires further development of gene transfer/editing technologies and knowledge of the target progenitor cell populations. Vectors based on adeno-associated virus are the leading system for direct *in vivo* gene delivery but have limitations in targeting replicating cell populations such as in the adrenal cortex. One strategy to overcome this technological limitation is to deliver the relevant adrenocortical gene to a currently targetable organ outside of the adrenal cortex. To explore this possibility, we developed a vector encoding human 21-hydroxylase and directed expression to the liver in a mouse model of congenital adrenal hyperplasia. This extra-adrenal expression resulted in reconstitution of the steroidogenic pathway. Aldosterone and renin levels normalized, and corticosterone levels improved sufficiently to reduce adrenal hyperplasia. This strategy could provide an alternative treatment option for monogenic adrenal disorders, particularly for mineralocorticoid defects. These findings also demonstrate, when targeting the adrenal gland, that inadvertent liver transduction should be precluded as it may confound data interpretation.

INTRODUCTION

Little has changed in the treatment for congenital adrenal hyperplasia (CAH) since exogenous steroids were first introduced 70 years ago.[1–3] CAH encompasses seven monogenic disorders of the adrenal that disrupt enzymatic function and result in a deficiency of one or more adrenal steroids with compensatory adrenal hyperplasia secondary to adrenocorticotropic hormone (ACTH) stimulation.[4] Deficiency of 21-hydroxylase is the most common cause of CAH with a global incidence of classical salt-wasting CAH estimated to be between 1 in 10,000 to 1 in 22,000.[5–7] There is resultant deficiency of cortisol and aldosterone, and upstream precursor steroids are shunted along the 17-hydroxylase-facilitated pathway to form adrenal androgens in excess causing pre- and postnatal virilization.[4] While exogenous corticosteroids are life-saving, treatment is far from perfect and cannot mimic the diurnal rhythm and physiological control of cortisol secretion, resulting in intervals of over- and undertreatment within a 24-h period. Adrenal crisis remains the most common cause of death and there is shorter life expectancy in those with CAH than the general population.[8]

Superior treatment options are needed to overcome the burden of disease in CAH.[9] As current standard management is imperfect, alternative and adjunctive treatment options have been explored, including subcutaneous hydrocortisone pumps[10,11] and modified-release once-daily hydrocortisone.[12,13] Neither of these alternatives is ideal, as pump management is complex and the modified-release hydrocortisone has not been shown to be superior to standard management.[14] Recent success with gene therapy for conditions such as spinal muscular atrophy has paved the way for other genetic treatments.[15] There is a paucity of gene therapy studies targeting the adrenal cortex, despite publication of the first pre-clinical gene therapy study for CAH over 20 years ago.[9] The murine adrenal cortex lacks 17-hydroxylase expression so does not produce adrenal androgens, and the major glucocorticoid in the mouse is corticosterone[16]: thus in the 21-hydroxylase-deficient mouse model, serum progesterone levels are elevated rather than 17-hydroxyprogesterone (17OHP).[17] While there is no hyperandrogenism, the model otherwise appropriately recapitulates the human classical salt-wasting CAH phenotype with inadequate glucocorticoid and mineralocorticoid production

Received 13 October 2023; accepted 8 March 2024;
https://doi.org/10.1016/j.omtm.2024.101232.

[5]These authors contributed equally

Correspondence: Lara E. Graves, Gene Therapy Research Unit, Children's Medical Research Institute, Faculty of Medicine and Health, The University of Sydney and Sydney Children's Hospitals Network, Westmead, NSW 2145, Australia.
E-mail: lara.graves@health.nsw.gov.au

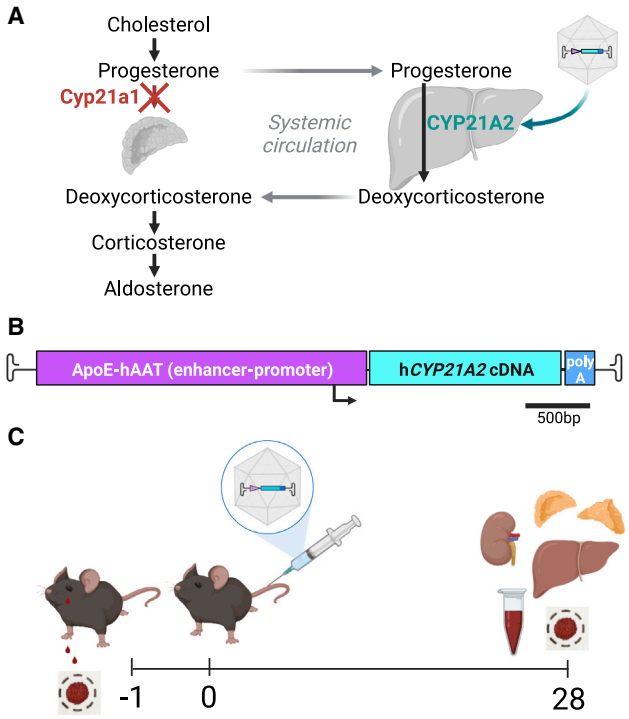

Figure 1. Study set up to assess hepato-adrenal cooperativity in steroidogenesis

(A) Hypothesis: in 21-hydroxylase deficiency, the precursor steroid (progesterone in the mouse, 17-hydroxyprogesterone in the human) accumulates and enters the systemic circulation where it will circulate to the liver. Recombinant AAV-derived human 21-hydroxylase expressed in the liver will convert progesterone to deoxycorticosterone, which will then enter the systemic circulation, reaching the adrenal gland. Enzymes downstream of 21-hydroxylase will be unaffected and will be able to complete steroidogenesis. (B) Recombinant AAV vector genome; liver-specific enhancer-promoter (ApoE-hAAT), human 21-hydroxylase cDNA (h*CYP21A2*), and bovine growth hormone poly-adenylated tail (polyA). The scale bar represents 500 base pairs. (C) Prior to treatment, dried whole blood was collected on to filter paper. Mice (n = 5 male, n = 5 female) were administered the purified vector intravenously via the tail vein and harvested 4 weeks later. AAV, adeno-associated virus.

to sustain neonatal life. Murine studies using intra-adrenal or intravenous delivery of a viral vector with 21-hydroxylase cDNA has demonstrated short-term improvement in progesterone.[18–20] Based on these pre-clinical studies a human clinical trial is now under way using a gene addition strategy with rAAV5-CYP21A2 (ClinicalTrials.gov: NCT04783181).

However, these studies do not address the rapid cellular turnover in the adrenal cortex. The recombinant adeno-associated virus (rAAV) genome is maintained predominantly as extra-chromosomal episomes that are lost during cellular replication. Therefore, a gene addition strategy using rAAV will not provide a lasting effect.[20,21] Furthermore, the development of neutralizing antibodies currently limits the use of rAAV therapy to a single treatment.[22,23] For durable adrenal-directed gene therapy, the new genetic material must be integrated into the genome of adrenocortical progenitor cells, a feat that is beyond current technology due to difficulties in targeting this cell population.[9] One strategy that could overcome this technological limitation is to deliver ectopic expression of 21-hydroxylase in a readily targetable organ outside of the adrenal cortex. We explored this theoretical possibility by developing an rAAV encoding human 21-hydroxylase (*CYP21A2*) and directing expression specifically to the liver in a mouse model of CAH. We hypothesized that hepatically expressed human *CYP21A2* could participate in steroidogenesis and facilitate downstream adrenal production of corticosterone and aldosterone (Figure 1A). We found that extra-adrenal expression of a deficient adrenocortical enzyme could indeed co-operatively reconstitute adrenal steroidogenesis.

RESULTS

Expression of human *CYP21A2* in murine liver following rAAV-mediated delivery

An rAAV2/8 vector utilizing a liver-specific promoter with the human *CYP21A2* cDNA (Figure 1B) was intravenously delivered to 21-hydroxylase-deficient (C57BL/10SnSlc-H-2^{aw18}; *Cyp21a1*$^{-/-}$) adult mice, homozygous for a pathogenic variant in *Cyp21a1*, at a dose of 5×10^{11} vector genomes per mouse (Figure 1C). Four weeks after administration, liver transduction was confirmed by vector copy number (vcn) per diploid nucleus and vector encoded mRNA detected in the livers of treated *Cyp21a1*$^{-/-}$ mice (Figures 2A and 2B, respectively; Table S1). The median vcn/diploid nucleus was similar in males and females; however, there was 3-fold higher vector transcription into mRNA in males than females, as expected.[24] In both sexes, the mouse with the lowest vcn/diploid nucleus had the lowest mRNA transcription (Figure 2C). Protein translation was demonstrated by immunohistochemical staining for CYP21A2 (Figure 2D). While human *CYP21A2* mRNA was detectable in the treated *Cyp21a1*$^{-/-}$ mouse adrenals, levels were 300- to 800-fold lower than native *Cyp21a1* mRNA in wild-type (*Cyp21a1*$^{+/+}$) adrenals (Figure S1A).

Human *CYP21A2* expression in the liver co-operatively improved adrenal steroidogenesis

Serum aldosterone in the vector-treated *Cyp21a1*$^{-/-}$ mice was restored to *Cyp21a1*$^{+/+}$ levels (Figure 3A; Table S1). Serum corticosterone in the treated *Cyp21a1*$^{-/-}$ mice was increased 4- to 5-fold compared with untreated *Cyp21a1*$^{-/-}$ controls; however, *Cyp21a1*$^{+/+}$ serum corticosterone levels were not achieved following vector administration (Figure 3B; Table S1). *Cyp21a1*$^{+/+}$ females had 2-fold higher serum corticosterone than their *Cyp21a1*$^{+/+}$ male counterparts, as has been previously demonstrated by other researchers.[25] The change in individual dried whole blood corticosterone improved in all but one *Cyp21a1*$^{-/-}$ mouse (Figure 3C). Although this mouse had the lowest vcn/diploid nucleus, lowest vector expression among the males, and lowest serum corticosterone (69.8 nmol/L), vcn/diploid nucleus did not always correlate with steroidogenic effect in other treated mice. Progesterone improved in the treated *Cyp21a1*$^{-/-}$ female mice but there was no change in the *Cyp21a1*$^{-/-}$ male progesterone levels (Figure 3D; Table S1). The progesterone remained 17- and 35-fold higher in *Cyp21a1*$^{-/-}$ females and males than *Cyp21a1*$^{+/+}$ levels, respectively.

Renin expression normalized and adrenal hyperplasia reduced following human *CYP21A2* expression in the liver

Given that renin increases in response to reduced renal perfusion and reduced tubular sodium content to activate the renin-angiotensin-aldosterone system,[26,27] renin (*Ren1*) expression was measured as a marker of mineralocorticoid function. *Ren1* mRNA expression in the kidneys was normalized to TATA-box binding protein (*Tbp*) mRNA as the chosen reference housekeeping transcript.[19,28–30] Renin expression was 25- to 30-fold higher in untreated $Cyp21a1^{-/-}$ mice compared with $Cyp21a1^{+/+}$. Renin expression in $Cyp21a1^{-/-}$ mice was restored to $Cyp21a1^{+/+}$ levels following treatment with the vector (Figure 3E; Table S1).

Female mice are known to have larger adrenal glands than males.[25] This pattern remained consistent in the $Cyp21a1^{-/-}$ mice with the bilateral adrenal mass 20% higher in $Cyp21a1^{-/-}$ females than $Cyp21a1^{-/-}$ males. $Cyp21a1^{-/-}$ females had adrenal mass 2.6-fold larger than $Cyp21a^{+/+}$ females and $Cyp21a1^{-/-}$ male adrenal mass was 3.2-fold larger than $Cyp21a1^{+/+}$ male adrenal mass. While the effect on corticosterone was partial, there was a reduction in size of the bilateral adrenal mass by one-third following treatment in both $Cyp21a1^{-/-}$ males and females (Figure 4A; Table S1). The bilateral adrenal mass was also measured as a percentage of the total body mass to account for any variation in body size and the reduction in adrenal size persisted (Figure S1B). Upon direct macroscopic examination, the adrenal glands from the treated $Cyp21a1^{-/-}$ animals were collapsed and flat, consistent with a reduction in volume, compared with the round untreated $Cyp21a1^{-/-}$ glands. The difference was visible macroscopically (Figure 4B). There was no change in the histological architecture of the adrenal cortex following treatment (data not shown).

Blood was collected during exsanguination causing physiological stress. The difference in maximal ACTH secretion in the treated $Cyp21a1^{-/-}$ mice was not statistically significant compared with the untreated $Cyp21a1^{-/-}$ mice (Figure S1C). Due to the short half-life of ACTH, expression of the ACTH receptor (*Mc2r*) was also examined. Although the expression of *Mc2r* did not change in the female mice following treatment, expression was reduced by 28% in treated $Cyp21a1^{-/-}$ male mice compared with untreated $Cyp21a1^{-/-}$(Figure S1D).

DISCUSSION

The adrenal cortex is an attractive gene therapy target, but its challenging biological properties have yet to be surmounted by contemporary gene delivery technology. Adeno-associated virus has natural tropism for the liver and is a logical target for gene therapies. Our approach exploits this characteristic with good clinical effect. This study demonstrated that extra-adrenal expression of human *CYP21A2* facilitated by rAAV gene delivery to the liver successfully conferred hepato-adrenal co-operativity in steroidogenesis resulting in significant phenotypic correction in a 21-hydroxylase-deficient mouse. In adults with completed liver growth, this strategy overcomes the limitations imposed by adrenocortical cellular turnover, rAAV gene delivery, and targeting stem/progenitor cell populations that are not fully characterized.[9,20] Mineralocorticoid function was restored and glucocorticoid production improved. This is the first study that has looked at the effect of rAAV-mediated adrenocortical gene delivery to the liver. Based on these data, this strategy could provide a treatment option for mineralocorticoid disorders such as aldosterone synthase deficiency; however, requires further development for use in disorders that impact glucocorticoid production. This study also highlights a need for caution in the interpretation of the effects of systemically administered therapies that may result from inadvertent liver transduction.

The clinically relevant outcomes of our strategy include improved steroidogenesis with subsequent phenotypic benefit. Restoration of aldosterone production would likely result in resolution of the salt-wasting component of the phenotype and therefore could improve the clinical phenotype from severe salt-wasting to simple virilizing CAH. This is important as the most severe form, salt-wasting CAH, has a higher mortality rate than milder phenotypes.[31] While blood pressure and urine sodium were unable to be measured, renin expression was considered an appropriate surrogate marker for mineralocorticoid function. Following normalization of aldosterone production, renin expression in the kidney also normalized. The aldosterone likely allowed appropriate salt retention, which removed stimulation on the renin-angiotensin-aldosterone system and thus increased renin expression was no longer required.

Aldosterone is produced in picomolar serum concentrations, whereas corticosterone is produced in nanomolar concentrations. This means the amount of aldosterone required for physiological normalization is 1,000-fold less than corticosterone and is therefore more achievable. Corticosterone production improved 4- to 5-fold in the treated $Cyp21a1^{-/-}$ mice compared with untreated $Cyp21a1^{-/-}$ mice. However, it was still only 40% of wild-type level in males and 22% of wild-type level in females. Despite the corticosterone production not reaching wild-type levels, the increased corticosterone production was sufficient to reduce the hypothalamic-pituitary-adrenal axis stimulation, demonstrated by a reduction in adrenal size. As the serum was collected during a terminal procedure, the ACTH level detected was the maximum secretory capacity. When the pituitary is subject to chronic corticotropic releasing hormone stimulation from the hypothalamus, the pituitary ACTH-producing corticotrophic cells undergo hyperplasia.[32] ACTH secretion is biphasic with the immediate release of stored ACTH followed by sustained release of newly synthesized ACTH.[33] Untreated $Cyp21a1^{-/-}$ mice had a greater maximal ACTH secretory capacity than the treated $Cyp21a1^{-/-}$ mice. This indicates that either the storage or secretory capacity of ACTH by pituitary corticotrophs reduced following the vector treatment, likely due to reduced hypothalamic stimulation upon the pituitary as a direct result of increased corticosterone production by the adrenal cortex. Improvement in expression of the ACTH receptor in our $Cyp21a1^{-/-}$ male treatment group was similar to that of a previous study in which males and females were combined into a single treatment group, although the proportion of males and females in that study was not described.[19] The finding was not detected in our treated $Cyp21a1^{-/-}$ female group

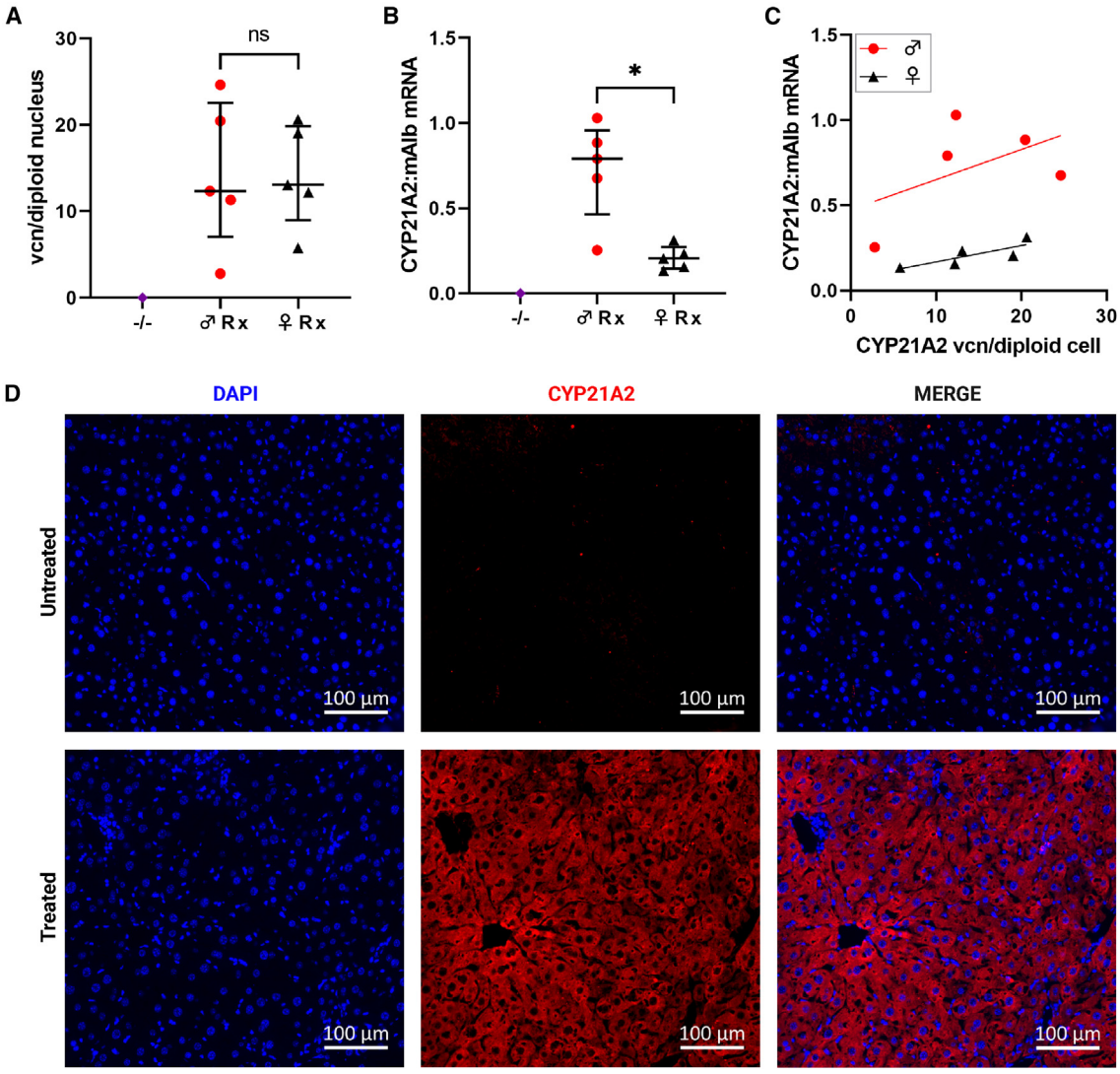

Figure 2. Robust delivery to and expression of human *CYP21A2* in the murine liver

(A) Vector DNA detected in the livers of treated mice. (B) The ratio of vector-derived mRNA transcripts to murine albumin transcripts. (C) Vector copy number vs. vector expression in males (red) and females (black). (D) IHC staining demonstrated CYP21A2 protein (red) in the liver from a representative treated male −/− mouse with 20.5 vcn/diploid nucleus and transcript mRNA ratio 0.88. Scale bar represents 100 µm. DAPI nuclear staining in blue. vcn, vector copy number; IHC, immunohistochemistry; −/−, homozygous 21-hydroxylase deficiency; ♂, male; ♀, female; Rx, homozygous 21-hydroxylase deficient mice that were treated with vector; *CYP21A2*, human 21-hydroxylase; mAlb, murine albumin; ns, not significant. Individual data points are shown, and error bars represent median and interquartile range. *p < 0.05 on Mann-Whitney *U* test.

demonstrating the importance of documenting both sexes separately as results are not generalizable between the sexes.

Despite these improvements, and some reduction in progesterone in the treated *Cyp21a1*$^{-/-}$ females, progesterone remained elevated and if recapitulated in humans would be associated with persistent androgen elevation. This could contribute to morbidity, particularly in women with CAH, and anti-androgen treatment may be required. Elevated progesterone may be required for the continual corticosterone production as increased progesterone production by the adrenal cortex allows spill-over into the systemic circulation, allowing the precursor to reach the newly expressed 21-hydroxylase in the liver, and therefore conversion to corticosterone. Should progesterone normalize, it is unclear whether that would still provide enough circulating substrate for hepatic 21-hydroxylation.

To our knowledge, this is the first study that has examined the effect of rAAV-mediated adrenocortical gene delivery to the liver. This could provide an alternative treatment option for CAH. The adrenal cortex can regenerate itself when only the capsule remains,[34] from populations of cells located in the capsule and subcapsular region.[35] Cells from the peripheral layers differentiate into zona glomerulosa

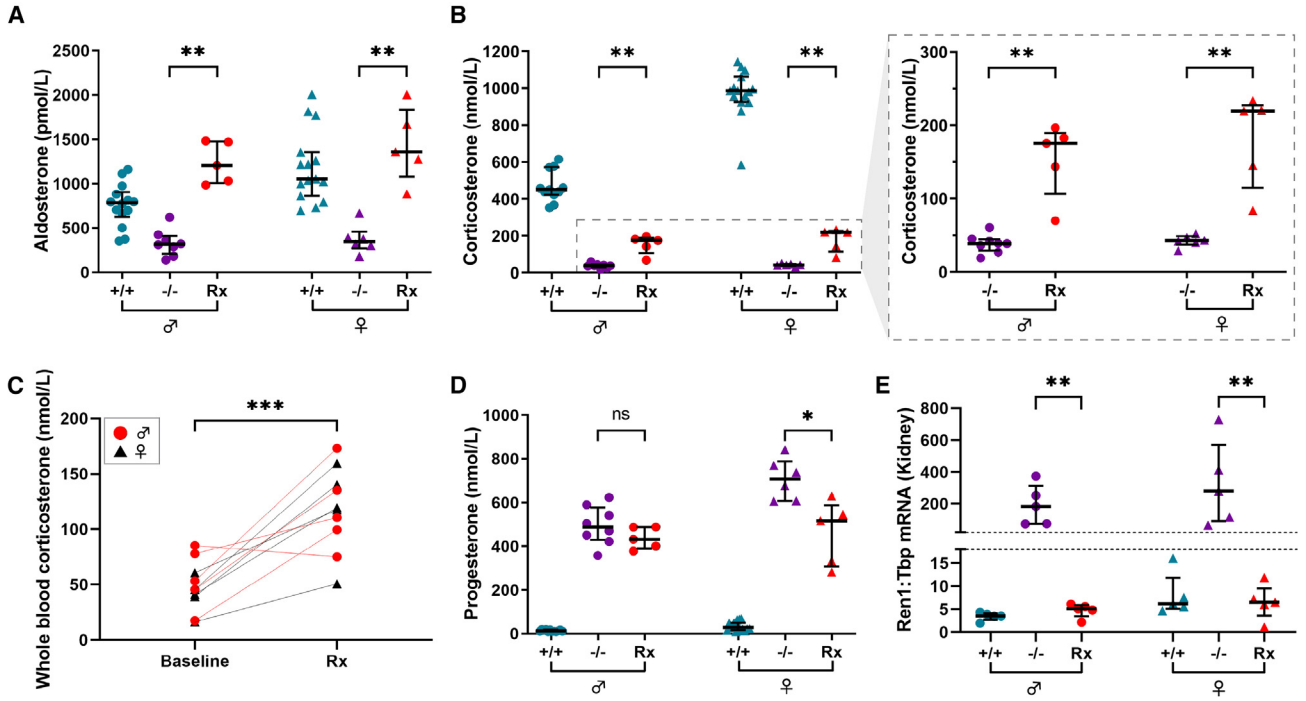

Figure 3. Improvement in steroidogenesis following hepatic *CYP21A2* expression

(A) Serum aldosterone. (B) Serum corticosterone. In the call-out box, +/+ controls were removed to demonstrate more clearly the change in serum corticosterone levels in −/− treated vs. −/− untreated. (C) Dried whole blood corticosterone before treatment and at harvest in males (red) and females (black). (D) Serum progesterone. (E) Renin expression demonstrated as the ratio of renal renin (*Ren1*) mRNA transcripts to *Tbp* transcripts. +/+, wild-type 21-hydroxylase sufficiency; −/−, homozygous 21-hydroxylase deficiency; ♂, male; ♀, female; Rx, homozygous 21-hydroxylase deficient mice that were treated with vector; *Ren1*, renin; *Tbp*, TATA-box binding protein; ns, not significant. Individual data points are shown, and error bars represent median and interquartile range. *p < 0.05; **p < 0.01 on Mann-Whitney *U* test. ***p < 0.001 on two-way ANOVA.

cells and then undergo lineage conversion as they migrate centripetally to populate the deeper zones until they reach the cortico-medullary junction where they apoptose.[36–38] While rAAV is the most popular vector-based gene delivery system *in vivo*,[39,40] and has shown long-term durability of expression in the liver of adults,[41] one caveat is that it is predominantly episomal. Thus, during pediatric organ growth or in organs with life-long cellular turnover such as the adrenal cortex, the effect of gene therapy will be transient as the episomal vector genomes will be lost during cellular division.[20,21,42] Moreover, repeated doses of rAAV therapy are not currently feasible due to the development of neutralizing antibodies and immunomodulatory technology has not yet been clinically validated.[22,23] Thus, effective treatment must be durable after a single dose. We have demonstrated that hepatically expressed adrenal enzymes are able to contribute to adrenal steroidogenesis, and this gene addition approach is directly applicable to adults with monogenic adrenocortical disorders. Conventional gene addition strategies using rAAV do not address hepatocellular proliferation, which is a particular challenge in the pediatric liver.[21,43] However, this could be surmounted in the pediatric CAH population, by use of a gene editing approach whereby the newly introduced genetic material is stably integrated into the host genome, which has been shown to be an effective method to provide durable hepatic transgene expression in the growing liver.[44]

Our study also provides evidence supporting the possibility that enzyme activity from inadvertent extra-adrenal organ transduction could contribute to the biochemical effects seen when rAAV is used to deliver adrenocortical genes systemically, particularly when ubiquitously expressing enhancer-promoters are used. This unrecognized effect may lead to misinterpretation of results, attributing delivery of vector to the adrenal cortex as the cause of the phenotypic effect rather than vector expressed outside the adrenal gland. A persistent effect may be seen despite anticipated adrenal turnover. Despite this, a phase I/II clinical trial is under way whereby rAAV5 is used to deliver *CYP21A2* with a ubiquitous promoter to adults with 21-hydroxylase deficiency (ClinicalTrials.org: NCT04783181), and at least four adults with CAH have been treated thus far.[45] Use of the rAAV5 capsid serotype and a ubiquitous promoter means that the *CYP21A2* will be expressed extensively throughout the body, including the liver, and not just in the adrenal cortex. Indeed the rAAV5 capsid is used for liver-targeted delivery of factor IX in the approved product Hemgenix.[46] There is some caution regarding the potential prematurity of this clinical trial in CAH, given concerns about safety and durability, particularly when traditional inexpensive steroid treatment (although not perfect) can suffice.[47]

rAAV-delivered extra-adrenal 21-hydroxylase has been previously attempted; however, did not achieve statistically significant results.[48] To

date, most of the pre-clinical gene therapy studies for CAH have focused on gene delivery to the adrenal cortex and none has proven durability beyond the adrenocortical cellular turnover period.[18–20,49] While one group demonstrated a positive effect on the *Cyp21a1*$^{-/-}$ phenotype for at least 15 weeks despite very low levels of residual vector DNA in the adrenal glands,[19] another demonstrated the effect was transient, lasting only 8 weeks in female *Cyp21a1*$^{-/-}$ mice.[20] Use of a ubiquitous promoter can allow persistent expression of vector-derived DNA delivered to stable organs such as liver and muscle, implicating expression of vector from sites external to the target organ.[50] In non-human primates that were treated with rAAV5-CYP21A2, the vector DNA in adrenal glands waned with time and there was more vector DNA and transgene expression in the liver than adrenal glands.[51] While our *CYP21A2* vector had a liver-specific promoter, a very small amount of *CYP21A2* mRNA was expressed in the adrenal gland at detectable levels. However, it was up to 800-fold lower than native *Cyp21a1* expression in wild-type adrenal glands and therefore unlikely to have exerted a clinical effect. Our study demonstrated that *CYP21A2* specifically expressed in the liver can exert a steroidogenic effect, implying that some of the effect seen in other studies may have been due to 21-hydroxylase expressed extra-adrenally. Female mice have a more rapid adrenocortical cellular turnover rate than males (3 months vs. 9 months).[52] Use of predominantly male mice may also prolong the duration of effect of rAAV gene delivery to the adrenal cortex. Ours is the first pre-clinical adrenocortical gene therapy study to report male and female data separately. It is known that female mice have larger adrenal cortices due to a larger zona fasciculata and as such, have higher corticosterone levels at baseline.[25] Therefore, we considered it important to demonstrate the changes following gene therapy in both sexes.

While human clinical translation is plausible, the approach described would require refinement. From a gene delivery perspective, this would include pseudo-serotyping the rAAV vector with a highly human liver tropic capsid such as the AAV-SYDs[53] or AAV-LK03,[54] rather than the murine liver tropic AAV8 capsid serotype. This in turn would facilitate the use of lower vector doses with an associated reduction in unwanted immune-mediated adverse events currently being observed in high-dose rAAV trials, such as thrombotic microangiopathy. These are being increasingly well managed with short courses of glucocorticoids and other immune-modulating drugs.[55,56] No other changes to the vector construct are likely to be required, such as inclusion of an inducible promoter-enhancer, given that upstream and downstream glucocorticoid production remains under physiological control. In women with CAH, as already discussed, the only other refinement would be inclusion of strategies to manage ongoing elevation of androgens and related sequelae with or without stress precautions in both sexes.

With current technology, simple gene delivery to the adrenal cortex using rAAV will not have a durable effect. We have demonstrated an alternative whereby adrenocortical genes can be delivered to a stable organ outside of the adrenal cortex using contemporary technology. The future of adrenal-directed gene therapy is to stably integrate new genetic material into the genome of adrenocortical progenitor cells such that the daughter cells maintain the correction.[9] This method is impeded by the difficulty in identifying adrenocortical progenitor cells, which is required for the development or discovery of rAAV capsids that can transduce this cell population. Alternatively, a method that allows rAAV to evade the immune system would allow repeated administration of rAAV without the need to target the elusive progenitor population.

We have demonstrated that specifically expressing human *CYP21A2* in the livers of 21-hydroxylase-deficient mice can correct the CAH phenotype through hepato-adrenal cooperativity in steroidogenesis with resultant normalization of aldosterone production and renin expression, and sufficient improvement in corticosterone production to allow reduction in adrenal gland hyperplasia. This strategy has the potential to overcome the current technological limitations of direct adrenal cortex targeting with rAAV. While this could be directly applied to an adult population with completed liver growth, it would need to be adapted to a gene editing approach for a durable effect in the pediatric CAH population. This work also demonstrates that extra-adrenal 21-hydroxylation has a meaningful clinical effect and any biochemical effect seen when utilizing systemically delivered rAAV with a ubiquitous promoter-enhancer cannot be definitively attributed to adrenal 21-hydroxylase expression.

MATERIALS AND METHODS

Animal procedures

All animal care and experimental procedures were evaluated and approved by the joint Children's Medical Research Institute and The Children's Hospital at Westmead Animal Care and Ethics Committee (Project C381). The C57BL/10SnSlc-H-2^{aw18} mouse model was kindly provided by Toshihiko Shiroishi (National Institute of Genetics) and the RIKEN BRC through the National BioResource Project of the Ministry of Education, Culture, Sports, Science and Technology, Japan. The H-2^{aw18} mouse model has 21-hydroxylase deficiency, which is neonatally lethal.[57] Heterozygous (H-2$^{b/aw18}$; *Cyp21a1*$^{+/-}$) mice were bred to produce homozygous (H-2^{aw18}, *Cyp21a1*$^{-/-}$) offspring. Exogenous steroid rescue was required for survival of the homozygous offspring. Dams were examined daily to determine the presence of a vaginal plug, indicating E0.5. All dams received 5 μg of dexamethasone (Ilium Dexason, Troy Animal Healthcare) subcutaneously daily from gestational day 18 until the birth. Day 19 was the most common day of delivery in this colony. All pups received 10 μg corticosterone and 0.05 μg fludrocortisone subcutaneously from birth second daily until 3 weeks of age. Once genotype was available, steroid treatment was ceased prior to 3 weeks of age in non-homozygous pups. Genotype was determined using a PCR-based assay with genomic DNA from toe removal during identification at 9 days of age. Dams, pups, and weaned *Cyp21a1*$^{-/-}$ mice were provided with table rock salt thrice weekly. *Cyp21a1*$^{-/-}$ pups were weaned to small groups with other *Cyp21a1*$^{-/-}$ animals from the same litter or a single non-homozygous littermate to avoid resource competition. Animals were maintained with 12-h light/dark cycles with free access to standard mouse chow and water.

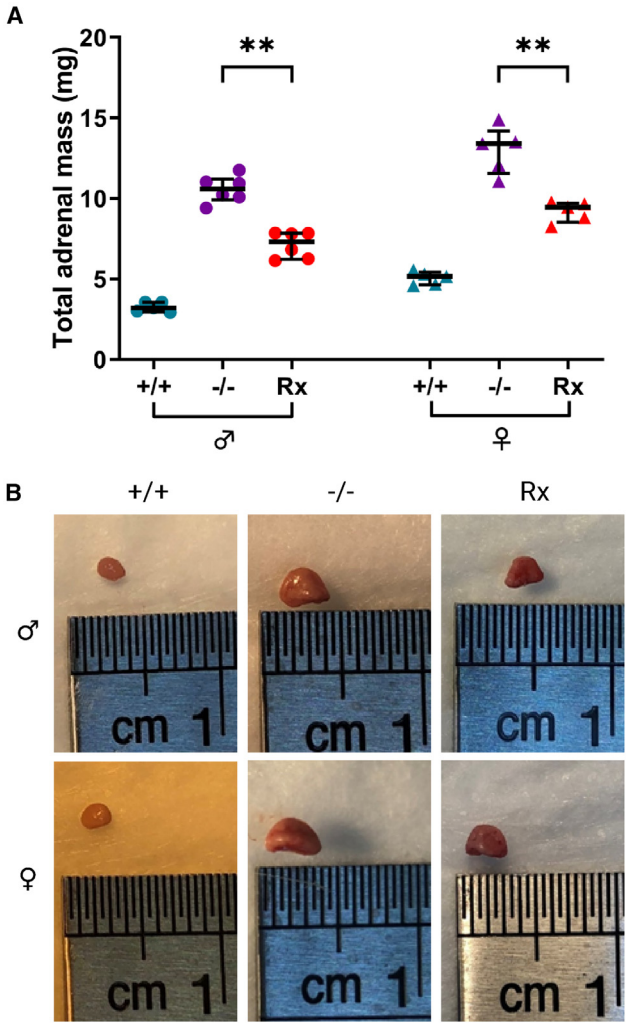

Figure 4. Reduction in adrenal hyperplasia after hepatic *CYP21A2* expression

(A) Absolute bilateral adrenal mass. (B) Macroscopic photographs of representative adrenal glands after fat dissection. +/+, wild-type 2-hydroxylase sufficiency; −/−, homozygous 21-hydroxylase deficiency; ♂, male; ♀, female; Rx, homozygous 21-hydroxylase-deficient mice that were treated with vector. Individual data points are shown, and error bars represent as median and interquartile range. **$p < 0.01$ on Mann-Whitney *U* test.

With exogenous steroid rescue, 35%–50% of *Cyp21a1*$^{-/-}$ offspring survived the neonatal period with the higher survival rate seen with experienced dams. This is higher than the previously published 12% survival rate.[19] *Cyp21a1*$^{-/-}$ males outnumbered *Cyp21a1*$^{-/-}$ females in the surviving offspring approximately 2:1, implying a survival advantage in males or disadvantage in females. Female mice are known to have higher serum corticosterone levels than males[25] so the corticosterone deficiency may have had a more profound effect on female mice due to an increased absolute requirement. The median bilateral adrenal mass was 2.6 times greater in *Cyp21a1*$^{-/-}$ females and 3.4 times greater in *Cyp21a1*$^{-/-}$ males compared with wild-type adrenals.

Prior to injection, a whole blood spot was collected on filter paper between 2 and 4 p.m. from a conscious submandibular bleed. Adult *Cyp21a1*$^{-/-}$ mice received the rAAV8-CYP21A2 vector at a dose of 5×10^{11} vgc/mouse intravenously via the tail vein. Four weeks later the treated *Cyp21a1*$^{-/-}$ animals were harvested between 2 and 4 p.m. The same method was used to harvest untreated *Cyp21a1*$^{-/-}$ and wild-type (H-2^{b}, *Cyp21a1*$^{+/+}$) controls. The mice were anesthetized using isoflurane (3%–5%) to facilitate open cardiac puncture for blood collection. Blood was collected on filter paper and the remaining spun down to collect serum that was stored at −80°C until analysis. Following exsanguination, the animal was terminated with cervical dislocation and tissues harvested. Tissues for biochemical and molecular analysis were snap frozen in liquid nitrogen and stored at −80°C. Samples for immunohistochemistry were fixed in 4% (w/v) PFA overnight at 4°C and then underwent a sucrose gradient until embedding in optimal cutting temperature compound and snap frozen in isopentane chilled in liquid nitrogen.

Vector construction and production

The human *CYP21A2* cDNA (GenBank: NM_000500.9) was cloned into an AAV2 backbone that had an ApoE-hAAT enhancer-promoter (liver-specific) that was provided by S. Cunningham[21] (Figure 1B). A Kozak sequence was included immediately upstream of the h*CYP21A2* cDNA. The vector was packaged by triple transfection of human embryonic kidney 293 cells, as previously described,[21] and was pseudo-serotyped with the AAV8 capsid (rAAV2/8). Vector particles were purified from cell lysate using standard cesium chloride gradient centrifugation. Titer was assigned using digital droplet PCR (C1000 Touch Thermal Cycler #1851196 and QX200 Droplet Reader #1864003, BioRad) using primers specific for the bovine growth hormone polyadenylation tail signal (Table S2) with QX200 ddPCR EvaGreen Supermix (BioRad 1864034). The conditions were 95°C for 5 min, 40 cycles of 95°C for 30 s and 60°C for 1 min, followed by 4°C for 5 min, 90°C for 5 min.

Immunohistochemistry

Frozen liver sections (5 μm) were permeabilized in methanol and then 0.1% (v/v) Triton X-100. They were then blocked with 10% (v/v) donkey serum and 10% (v/v) fetal bovine serum in phosphate buffered saline without magnesium or calcium (PBS). After washing with 0.1% (v/v) Tween 20, the sections were incubated overnight with the rabbit primary CYP21A2 antibody (Abcam ab230327) diluted 1:50. After washing with 0.1% (v/v) Tween 20, the sections were incubated with the secondary antibody (AlexaFluor Donkey anti-rabbit 594, Invitrogen A32754) diluted 1:500, and then counterstained with DAPI, diluted to 0.03 μg/mL.

Vector copy number determination

Genomic DNA was extracted from frozen liver using a standard phenol-chloroform extraction method. It was digested with restriction enzyme HindIII-HF (New England BioLabs R3104L).

Vector copy number (vcn) was determined using digital droplet PCR (C1000 Touch Thermal Cycler #1851196 and QX200 Droplet Reader

#1864003, BioRad) using primers specific for human *CYP21A2* and murine albumin (Table S2) with QX200 ddPCR EvaGreen Supermix (BioRad 1864034). The conditions were 95°C for 5 min, 40 cycles of 95°C for 30 s and 60°C for 1 min, followed by 4°C for 5 min, 90°C for 5 min. The *CYP21A2* count was normalized to two copies of murine albumin to determine vcn/diploid nucleus.

Quantitative real-time PCR

RNA was extracted using the Purelink RNA Mini Kit (Invitrogen 12183018A) and stored at −80°C. cDNA was generated from extracted RNA using the SuperScript IV First-Strand Synthesis System (Invitrogen 18091050) using the Oligo $d(T)_{20}$ primer and stored at −20°C. Primers were used to detect gene expression for *CYP21A2* (normalized to murine albumin as the reference transcript) in liver, *Ren1* (normalized to *Tbp* as the reference transcript) in kidney and *Mc2r*, the ACTH receptor (normalized to *Tbp*) in adrenal cDNA, (Table S2). TB Green Premix Ex Taq II (Takara RR82WR) was used in the reaction with conditions as follows: 95°C for 30 s, 40 cycles of 95°C for 5 s, 60°C for 20 s, and 76°C for 10 s followed by melt 60°C–95°C (Qiagen Rotor-Gene Q).

Steroid profiles

Serum aldosterone, corticosterone, and progesterone

The steroid calibrators, controls, and isotopically labeled internal standard mix were obtained from Chromsystems Instruments & Chemicals Gmbh, Germany. The Optima LC-MS grade solvents including water, methanol, methyl t-butyl ether, acetonitrile, and formic acid were obtained from Fisher Chemicals, UK. Internal standard solution was added to calibrators, controls, and test samples and organic solvents were used for extraction. The extract supernatants were evaporated to dryness under nitrogen in a 37°C water bath. After evaporation, the extracted steroids were reconstituted in 50% methanol. Steroids were analyzed by ultra performance liquid chromatography-tandem mass spectrometry (UPLC-MSMS) using validated in-house developed methods (Waters Acquity UPLC and Xevo TQ-S mass spectrometer).

Whole blood corticosterone

The dried blood spot samples were collected onto filter paper and were extracted using an organic solvent (95% methanol) containing deuterated internal standards for each steroid. Whole blood corticosterone was measured using liquid chromatography-tandem mass spectrometry (Waters Xevo TQ-S with Acquity UPLC system).

ACTH ELISA

ACTH was measured after thawing snap frozen serum using the Mouse/Rat ACTH SimpleStep ELISA Kit as per manufacturer instructions (Ab263880, Abcam).

Statistical analysis

GraphPad Prism 9 was used for statistical analysis and graph production. Non-parametric statistical methods including the Mann-Whitney *U* test were used.

DATA AND CODE AVAILABILITY

All relevant data are included in the manuscript or supplementary materials. Any additional details of the studies not clearly described can be obtained by contacting Lara E. Graves.

SUPPLEMENTAL INFORMATION

Supplemental information can be found online at https://doi.org/10.1016/j.omtm.2024.101232.

ACKNOWLEDGMENTS

The authors would like to acknowledge and thank Sharon C Cunningham for providing the liver-specific vector backbone, and Sharntie Christina for assistance with some laboratory techniques.
L.E.G. was supported by the University of Sydney Post-Graduate Award (UPA) scholarship and the Yass Memorial Scholarship from the Children's Medical Research Institute. This research was supported by the Australasian Paediatric Endocrine Group (APEG)/Pfizer Industry Research Grant 2019. The APEG Research Grants, supported by industry, are funded through an unsolicited institutional research grant. Companies outside of APEG are not involved in the program design and selection of awardees.
Figures were created with BioRender.com.

AUTHOR CONTRIBUTIONS

L.E.G. contributed to conceptualization, data curation and analysis, funding acquisition, investigation, project administration, visualization, and writing – original draft, reviewing and editing. E.B.v.D. and C.Z. contributed to investigation and writing – reviewing and editing. S.K. and T.W. contributed to investigation, resources and writing the relevant methodology. S.S. contributed to resources, supervision, and writing – reviewing and editing. S.G. contributed to conceptualization, methodology, project administration, supervision, and writing – reviewing and editing. I.E.A. contributed to conceptualization, methodology, project administration, resources, supervision, and writing – reviewing and editing.

DECLARATION OF INTERESTS

The authors declare no competing interests.

REFERENCES

1. Wilkins, L., Lewis, R.A., Klein, R., and Rosemberg, E. (1950). The suppression of androgen secretion by cortisone in a case of congenital adrenal hyperplasia. Bull. Johns Hopkins Hosp. *86*, 249–252.
2. Wilkins, L., Lewis, R.A., Klein, R., Gardner, L.I., Crigler, J.F., Jr., Rosemberg, E., and Migeon, C.J. (1951). Treatment of congenital adrenal hyperplasia with cortisone. J. Clin. Endocrinol. Metab. *11*, 1–25. https://doi.org/10.1210/jcem-11-1-1.
3. Bartter, F.C., Albright, F., Forbes, A.P., Leaf, A., Dempsey, E., and Carroll, E. (1951). The effects of adrenocorticotropic hormone and cortisone in the adrenogenital syndrome associated with congenital adrenal hyperplasia: an attempt to explain and correct its disordered hormonal pattern. J. Clin. Invest. *30*, 237–251. https://doi.org/10.1172/JCI102438.
4. El-Maouche, D., Arlt, W., and Merke, D.P. (2017). Congenital adrenal hyperplasia. Lancet *390*, 2194–2210. https://doi.org/10.1016/S0140-6736(17)31431-9.
5. Lai, F., Srinivasan, S., and Wiley, V. (2020). Evaluation of a Two-Tier Screening Pathway for Congenital Adrenal Hyperplasia in the New South Wales Newborn

Screening Programme. Int. J. Neonatal Screen. *6*, 63. https://doi.org/10.3390/ijns6030063.

6. Navarro-Zambrana, A.N., and Sheets, L.R. (2023). Ethnic and National Differences in Congenital Adrenal Hyperplasia Incidence: A Systematic Review and Meta-Analysis. Horm. Res. Paediatr. *96*, 249–258. https://doi.org/10.1159/000526401.

7. Berglund, A., Ornstrup, M.J., Lind-Holst, M., Dunø, M., Bækvad-Hansen, M., Juul, A., Borch, L., Jørgensen, N., Rasmussen, Å.K., Andersen, M., et al. (2023). Epidemiology and diagnostic trends of congenital adrenal hyperplasia in Denmark: a retrospective, population-based study. Lancet Reg. Health. Eur. *28*, 100598. https://doi.org/10.1016/j.lanepe.2023.100598.

8. Claahsen-van der Grinten, H.L., Speiser, P.W., Ahmed, S.F., Arlt, W., Auchus, R.J., Falhammar, H., Flück, C.E., Guasti, L., Huebner, A., Kortmann, B.B.M., et al. (2022). Congenital Adrenal Hyperplasia-Current Insights in Pathophysiology, Diagnostics, and Management. Endocr. Rev. *43*, 91–159. https://doi.org/10.1210/endrev/bnab016.

9. Graves, L.E., Torpy, D.J., Coates, P.T., Alexander, I.E., Bornstein, S.R., and Clarke, B. (2023). Future Directions for Adrenal Insufficiency: Cellular Transplantation and Genetic Therapies. J. Clin. Endocrinol. Metab. *108*, 1273–1289. https://doi.org/10.1210/clinem/dgac751.

10. Nella, A.A., Mallappa, A., Perritt, A.F., Gounden, V., Kumar, P., Sinaii, N., Daley, L.A., Ling, A., Liu, C.Y., Soldin, S.J., and Merke, D.P. (2016). A Phase 2 Study of Continuous Subcutaneous Hydrocortisone Infusion in Adults With Congenital Adrenal Hyperplasia. J. Clin. Endocrinol. Metab. *101*, 4690–4698. https://doi.org/10.1210/jc.2016-1916.

11. Mallappa, A., Nella, A.A., Sinaii, N., Rao, H., Gounden, V., Perritt, A.F., Kumar, P., Ling, A., Liu, C.Y., Soldin, S.J., and Merke, D.P. (2018). Long-term use of continuous subcutaneous hydrocortisone infusion therapy in patients with congenital adrenal hyperplasia. Clin. Endocrinol. *89*, 399–407. https://doi.org/10.1111/cen.13813.

12. Mallappa, A., Sinaii, N., Kumar, P., Whitaker, M.J., Daley, L.A., Digweed, D., Eckland, D.J.A., Van Ryzin, C., Nieman, L.K., Arlt, W., et al. (2015). A phase 2 study of Chronocort, a modified-release formulation of hydrocortisone, in the treatment of adults with classic congenital adrenal hyperplasia. J. Clin. Endocrinol. Metab. *100*, 1137–1145. https://doi.org/10.1210/jc.2014-3809.

13. Jones, C.M., Mallappa, A., Reisch, N., Nikolaou, N., Krone, N., Hughes, B.A., O'Neil, D.M., Whitaker, M.J., Tomlinson, J.W., Storbeck, K.H., et al. (2017). Modified-Release and Conventional Glucocorticoids and Diurnal Androgen Excretion in Congenital Adrenal Hyperplasia. J. Clin. Endocrinol. Metab. *102*, 1797–1806. https://doi.org/10.1210/jc.2016-2855.

14. Speiser, P.W. (2019). Emerging medical therapies for congenital adrenal hyperplasia. F1000Res. *8*, 363. https://doi.org/10.12688/f1000research.17778.1.

15. Pascual-Morena, C., Cavero-Redondo, I., Lucerón-Lucas-Torres, M., Martínez-García, I., Rodríguez-Gutiérrez, E., and Martínez-Vizcaíno, V. (2023). Onasemnogene Abeparvovec in Type 1 Spinal Muscular Atrophy: A Systematic Review and Meta-Analysis. Hum. Gene Ther. *34*, 129–138. https://doi.org/10.1089/hum.2022.161.

16. Vinson, G.P. (2016). Functional Zonation of the Adult Mammalian Adrenal Cortex. Front. Neurosci. *10*, 238. https://doi.org/10.3389/fnins.2016.00238.

17. Gotoh, H., Sagai, T., Hata, J., Shiroishi, T., and Moriwaki, K. (1988). Steroid 21-hydroxylase deficiency in mice. Endocrinology *123*, 1923–1927. https://doi.org/10.1210/endo-123-4-1923.

18. Tajima, T., Okada, T., Ma, X.M., Ramsey, W., Bornstein, S., and Aguilera, G. (1999). Restoration of adrenal steroidogenesis by adenovirus-mediated transfer of human cytochrome P450 21-hydroxylase into the adrenal gland of 21-hydroxylase-deficient mice. Gene Ther. *6*, 1898–1903. https://doi.org/10.1038/sj.gt.3301018.

19. Perdomini, M., Dos Santos, C., Goumeaux, C., Blouin, V., and Bougnères, P. (2017). An AAVrh10-CAG-CYP21-HA vector allows persistent correction of 21-hydroxylase deficiency in a Cyp21(-/-) mouse model. Gene Ther. *24*, 275–281. https://doi.org/10.1038/gt.2017.10.

20. Markmann, S., De, B.P., Reid, J., Jose, C.L., Rosenberg, J.B., Leopold, P.L., Kaminsky, S.M., Sondhi, D., Pagovich, O., and Crystal, R.G. (2018). Biology of the Adrenal Gland Cortex Obviates Effective Use of Adeno-Associated Virus Vectors to Treat Hereditary Adrenal Disorders. Hum. Gene Ther. *29*, 403–412. https://doi.org/10.1089/hum.2017.203.

21. Cunningham, S.C., Dane, A.P., Spinoulas, A., Alexander, I.E., and Alexander, I.E. (2008). Gene delivery to the juvenile mouse liver using AAV2/8 vectors. Mol. Ther. *16*, 1081–1088. https://doi.org/10.1038/mt.2008.72.

22. Boutin, S., Monteilhet, V., Veron, P., Leborgne, C., Benveniste, O., Montus, M.F., and Masurier, C. (2010). Prevalence of Serum IgG and Neutralizing Factors Against Adeno-Associated Virus (AAV) Types 1, 2, 5, 6, 8, and 9 in the Healthy Population: Implications for Gene Therapy Using AAV Vectors. Hum. Gene Ther. *21*, 704–712. https://doi.org/10.1089/hum.2009.182.

23. Li, A., Tanner, M.R., Lee, C.M., Hurley, A.E., De Giorgi, M., Jarrett, K.E., Davis, T.H., Doerfler, A.M., Bao, G., Beeton, C., and Lagor, W.R. (2020). AAV-CRISPR gene editing is negated by pre-existing immunity to Cas9. Mol. Ther. *28*, 1432–1441. https://doi.org/10.1016/j.ymthe.2020.04.017.

24. Dane, A.P., Cunningham, S.C., Graf, N.S., and Alexander, I.E. (2009). Sexually dimorphic patterns of episomal rAAV genome persistence in the adult mouse liver and correlation with hepatocellular proliferation. Mol. Ther. *17*, 1548–1554. https://doi.org/10.1038/mt.2009.139.

25. Bielohuby, M., Herbach, N., Wanke, R., Maser-Gluth, C., Beuschlein, F., Wolf, E., and Hoeflich, A. (2007). Growth analysis of the mouse adrenal gland from weaning to adulthood: time- and gender-dependent alterations of cell size and number in the cortical compartment. Am. J. Physiol. Endocrinol. Metab. *293*, E139–E146. https://doi.org/10.1152/ajpendo.00705.2006.

26. Page, I.H., and Helmer, O.M. (1940). A Crystalline Pressor Substance (Angiotonin) Resulting from the Reaction between Renin and Renin-Activator. J. Exp. Med. *71*, 29–42. https://doi.org/10.1084/jem.71.1.29.

27. Braun-Menendez, E., Fasciolo, J.C., Leloir, L.F., and Muñoz, J.M. (1940). The substance causing renal hypertension. J. Physiol. *98*, 283–298. https://doi.org/10.1113/jphysiol.1940.sp003850.

28. Radonić, A., Thulke, S., Mackay, I.M., Landt, O., Siegert, W., and Nitsche, A. (2004). Guideline to reference gene selection for quantitative real-time PCR. Biochem. Biophys. Res. Commun. *313*, 856–862. https://doi.org/10.1016/j.bbrc.2003.11.177.

29. Costello, H.M., Krilis, G., Grenier, C., Severs, D., Czopek, A., Ivy, J.R., Nixon, M., Holmes, M.C., Livingstone, D.E.W., Hoorn, E.J., et al. (2023). High salt intake activates the hypothalamic-pituitary-adrenal axis, amplifies the stress response, and alters tissue glucocorticoid exposure in mice. Cardiovasc. Res. *119*, 1740–1750. https://doi.org/10.1093/cvr/cvac160.

30. Witt, A., Mateska, I., Palladini, A., Sinha, A., Wölk, M., Harauma, A., Bechmann, N., Pamporaki, C., Dahl, A., Rothe, M., et al. (2023). Fatty acid desaturase 2 determines the lipidomic landscape and steroidogenic function of the adrenal gland. Sci. Adv. *9*, eadf6710. https://doi.org/10.1126/sciadv.adf6710.

31. Falhammar, H., Frisén, L., Norrby, C., Hirschberg, A.L., Almqvist, C., Nordenskjöld, A., and Nordenström, A. (2014). Increased mortality in patients with congenital adrenal hyperplasia due to 21-hydroxylase deficiency. J. Clin. Endocrinol. Metab. *99*, E2715–E2721. https://doi.org/10.1210/jc.2014-2957.

32. Scheithauer, B.W., Kovacs, K., and Randall, R.V. (1983). The pituitary gland in untreated Addison's disease. A histologic and immunocytologic study of 18 adenohypophyses. Arch. Pathol. Lab Med. *107*, 484–487.

33. DeBold, C.R., DeCherney, G.S., Jackson, R.V., Sheldon, W.R., Alexander, A.N., Island, D.P., Rivier, J., Vale, W., and Orth, D.N. (1983). Effect of synthetic ovine corticotropin-releasing factor: prolonged duration of action and biphasic response of plasma adrenocorticotropin and cortisol. J. Clin. Endocrinol. Metab. *57*, 294–298. https://doi.org/10.1210/jcem-57-2-294.

34. Ingle, D.J., and Higgins, G.M. (1938). Autotransplantation and Regeneration of the Adrenal Gland. Endocrinology *22*, 458–464. https://doi.org/10.1210/endo-22-4-458.

35. Zwemer, R.L., Wotton, R.M., and Norkus, M.G. (1938). A study of corticoadrenal cells. Anat. Rec. *72*, 249–263. https://doi.org/10.1002/ar.1090720210.

36. Chang, S.P., Morrison, H.D., Nilsson, F., Kenyon, C.J., West, J.D., and Morley, S.D. (2013). Cell proliferation, movement and differentiation during maintenance of the adult mouse adrenal cortex. PLoS One *8*, e81865. https://doi.org/10.1371/journal.pone.0081865.

37. Freedman, B.D., Kempna, P.B., Carlone, D.L., Shah, M., Guagliardo, N.A., Barrett, P.Q., Gomez-Sanchez, C.E., Majzoub, J.A., and Breault, D.T. (2013). Adrenocortical zonation results from lineage conversion of differentiated zona glomerulosa cells. Dev. Cell *26*, 666–673. https://doi.org/10.1016/j.devcel.2013.07.016.

38. Zwemer, R.L. (1936). A study of adrenal cortex morphology. Am. J. Pathol. *12*, 107–114.1. https://doi.org/10.1097/00005053-193607000-00010.

39. Wang, D., Tai, P.W.L., and Gao, G. (2019). Adeno-associated virus vector as a platform for gene therapy delivery. Nat. Rev. Drug Discov. *18*, 358–378. https://doi.org/10.1038/s41573-019-0012-9.

40. Barrett, D., Nguyen-Jatkoe, L., Foss-Campbell, B., Micklus, A., and Wendland, A. (2021). Gene, Cell, & RNA Therapy Landscape, Q2 2021 Quarterly Data Report. https://asgct.org/global/documents/asgct-pharma-intelligence-quarterly-report-july-20.aspx.

41. Nathwani, A.C., Reiss, U.M., Tuddenham, E.G.D., Rosales, C., Chowdary, P., McIntosh, J., Della Peruta, M., Lheriteau, E., Patel, N., Raj, D., et al. (2014). Long-Term Safety and Efficacy of Factor IX Gene Therapy in Hemophilia B. N. Engl. J. Med. *371*, 1994–2004. https://doi.org/10.1056/nejmoa1407309.

42. Alexander, I.E., Cunningham, S.C., Logan, G.J., and Christodoulou, J. (2008). Potential of AAV vectors in the treatment of metabolic disease. Gene Ther. *15*, 831–839. https://doi.org/10.1038/gt.2008.64.

43. Cunningham, S.C., Spinoulas, A., Carpenter, K.H., Wilcken, B., Kuchel, P.W., and Alexander, I.E. (2009). AAV2/8-mediated correction of OTC deficiency is robust in adult but not neonatal Spf(ash) mice. Mol. Ther. *17*, 1340–1346. https://doi.org/10.1038/mt.2009.88.

44. Ginn, S.L., Amaya, A.K., Liao, S.H.Y., Zhu, E., Cunningham, S.C., Lee, M., Hallwirth, C.V., Logan, G.J., Tay, S.S., Cesare, A.J., et al. (2020). Efficient in vivo editing of OTC-deficient patient-derived primary human hepatocytes. JHEP Rep. *2*, 100065. https://doi.org/10.1016/j.jhepr.2019.100065.

45. Adrenas. (2023). Trial Update from Adrenas Therapeutics. https://adrenastx.com/wp-content/uploads/CAH-Letter-to-Community-Q1-2023-Update-FINAL.pdf.

46. Heo, Y.A. (2023). Etranacogene Dezaparvovec: First Approval. Drugs *83*, 347–352. https://doi.org/10.1007/s40265-023-01845-0.

47. White, P.C. (2022). Emerging treatment for congenital adrenal hyperplasia. Curr. Opin. Endocrinol. Diabetes Obes. *29*, 271–276. https://doi.org/10.1097/MED.0000000000000723.

48. Naiki, Y., Miyado, M., Horikawa, R., Katsumata, N., Onodera, M., Pang, S., Ogata, T., and Fukami, M. (2016). Extra-adrenal induction of Cyp21a1 ameliorates systemic steroid metabolism in a mouse model of congenital adrenal hyperplasia. Endocr. J. *63*, 897–904. https://doi.org/10.1507/endocrj.EJ16-0112.

49. Naiki, Y., Miyado, M., Shindo, M., Horikawa, R., Hasegawa, Y., Katsumata, N., Takada, S., Akutsu, H., Onodera, M., and Fukami, M. (2022). AAV-mediated gene therapy for patients' fibroblasts, iPS cells, and a mouse model of congenital adrenal hyperplasia. Hum. Gene Ther. *33*, 801–809. https://doi.org/10.1089/hum.2022.005.

50. Pontoizeau, C., Simon-Sola, M., Gaborit, C., Nguyen, V., Rotaru, I., Tual, N., Colella, P., Girard, M., Biferi, M.-G., Arnoux, J.-B., et al. (2022). Neonatal gene therapy achieves sustained disease rescue of maple syrup urine disease in mice. Nat. Commun. *13*, 3278. https://doi.org/10.1038/s41467-022-30880-w.

51. Eclov, R.J., Lewis, T.E.W., Kapandia, M., Scott, D.W., Rouse, J.L., Romero, K.B., Mansfield, G., and Beard, C.W. (2019). Durable CYP21A2 gene therapy in non-human primates for treatment of congenital adrenal hyperplasia. ESGCT 27th Annual Congress In collaboration with SETGyc Barcelona, Spain October 22-25, 2019 Abstracts. Hum. Gene Ther. A93–A94. https://doi.org/10.1089/hum.2019.29095.abstracts.

52. Grabek, A., Dolfi, B., Klein, B., Jian-Motamedi, F., Chaboissier, M.C., and Schedl, A. (2019). The Adult Adrenal Cortex Undergoes Rapid Tissue Renewal in a Sex-Specific Manner. Cell Stem Cell *25*, 290–296.e2. https://doi.org/10.1016/j.stem.2019.04.012.

53. Cabanes-Creus, M., Navarro, R.G., Zhu, E., Baltazar, G., Liao, S.H.Y., Drouyer, M., Amaya, A.K., Scott, S., Nguyen, L.H., Westhaus, A., et al. (2022). Novel human liver-tropic AAV variants define transferable domains that markedly enhance the human tropism of AAV7 and AAV8. Mol. Ther. Methods Clin. Dev. *24*, 88–101. https://doi.org/10.1016/j.omtm.2021.11.011.

54. Lisowski, L., Dane, A.P., Chu, K., Zhang, Y., Cunningham, S.C., Wilson, E.M., Nygaard, S., Grompe, M., Alexander, I.E., and Kay, M.A. (2014). Selection and evaluation of clinically relevant AAV variants in a xenograft liver model. Nature *506*, 382–386. https://doi.org/10.1038/nature12875.

55. Au, H.K.E., Isalan, M., and Mielcarek, M. (2021). Gene Therapy Advances: A Meta-Analysis of AAV Usage in Clinical Settings. Front. Med. *8*, 809118. https://doi.org/10.3389/fmed.2021.809118.

56. Merke, D.P., Auchus, R.J., Sarafoglou, K., Geffner, M.E., Kim, M.S., Escandon, R.D., Bharucha, K.N., Shaywitz, A.J., Eclov, R., Beard, C.W., et al. (2021). Design of a Phase 1/2 Open-Label, Dose-Escalation Study of the Safety and Efficacy of Gene Therapy in Adults With Classic Congenital Adrenal Hyperplasia (CAH) Due to 21-hydroxylase Deficiency Through Administration of an Adeno-Associated Virus (AAV) Serotype 5-Based Recombinant Vector Encoding the Human CYP21A2 Gene. J. Endocr. Soc. *5*, A82. https://doi.org/10.1210/jendso/bvab048.165.

57. Shiroishi, T., Sagai, T., Natsuume-Sakai, S., and Moriwaki, K. (1987). Lethal deletion of the complement component C4 and steroid 21-hydroxylase genes in the mouse H-2 class III region, caused by meiotic recombination. Proc. Natl. Acad. Sci. USA *84*, 2819–2823. https://doi.org/10.1073/pnas.84.9.2819.

OMTM, Volume *32*

Supplemental information

AAV-delivered hepato-adrenal cooperativity in steroidogenesis: Implications for gene therapy for congenital adrenal hyperplasia

Lara E. Graves, Eva B. van Dijk, Erhua Zhu, Sundar Koyyalamudi, Tiffany Wotton, Dinah Sung, Shubha Srinivasan, Samantha L. Ginn, and Ian E. Alexander

Table S1: Median values for results presented in figures

Measurement	Genotype	Treated	Male	Female
Vector DNA (vcn/diploid nucleus)	-/-	Yes	13.1	12.3
Vector RNA (ratio of *CYP21A2* mRNA transcripts to albumin transcripts)	-/-	Yes	0.79	0.20
Serum aldosterone (pmol/L)	+/+	No	784	1056
	-/-	No	341	390
	-/-	Yes	1206	1360
Serum corticosterone (nmol/L)	+/+	No	436	987
	-/-	No	39	43
	-/-	Yes	175	220
Serum progesterone (nmol/L)	+/+	No	12.1	28.6
	-/-	No	506	723
	-/-	Yes	443	517
Renal renin expression (ratio of *Ren1* mRNA transcripts to *Tbp* transcripts)	+/+	No	3.5	6.2
	-/-	No	129	197
	-/-	Yes	5.1	6.5
Bilateral adrenal mass (mg)	+/+	No	3.2	5.1
	-/-	No	10.9	13.4
	-/-	Yes	7.3	9.5

Abbreviations: vcn, vector copy number; *Tbp*, TATA-box binding protein; +/+, wild-type 21-hydroxylase sufficiency; -/-, homozygous 21-hydroxylase deficiency

Table S2: Primers

Purpose	Target	Sequence (5'-3')
Genotyping (PCR)	Wild-type *Cyp21a1* allele	ACCACCCTGAGGTGCACT
		GGGAGATTGATGCCAGCATAAG
	Mutant *Cyp21a1* allele	TCCTTGGGGATGTCATAGCCA
		TCACCATCCTGAAGTGCACC
Vector genome titre (ddPCR)	Bovine growth hormone polyA	GCCTTCCTTGACCCTGGA
		ACTCAGACAATGCGATGCAA
Vector genome copies (ddPCR) and *CYP21A2* expression (qPCR)	Human *CYP21A2*	TACCTCACCTTCGGAGACAA
		CCACGATGTGATCCCTCTTC
Vector copy number normalisation (ddPCR)	Albumin	AACTGCTACTCCCCTCCTAC
		TTTACCCCAGTGCAGGAAAG
Albumin expression (qPCR)	Albumin	TACAGCGGAGCAACTGAAGA
		TTGCAGCACAGAGACAAGAA
Renin expression (qPCR)	*Ren1*	CTCTGGGCACTCTTGTTGCT
		AGAAGGCATTTTCTTGAGCG
ACTH receptor expression (qPCR)	*Mc2r*	TTTCTCAGTCATCTTGCCGA
		ATGCTCCTCTCCTTGGCTTT
Cyp21a1 expression (qPCR)	Murine wild-type *Cyp21a1*	ACAGGAACCGAATGCAGCTG
		CTTAGGGATGTCATAGCCGG
TATA-box binding protein expression for normalisation (qPCR)	*Tbp*	CCCTTGTACCCTTCACCAATGAC
		TCACGGTAGATACAATATTTTGAAGCTG

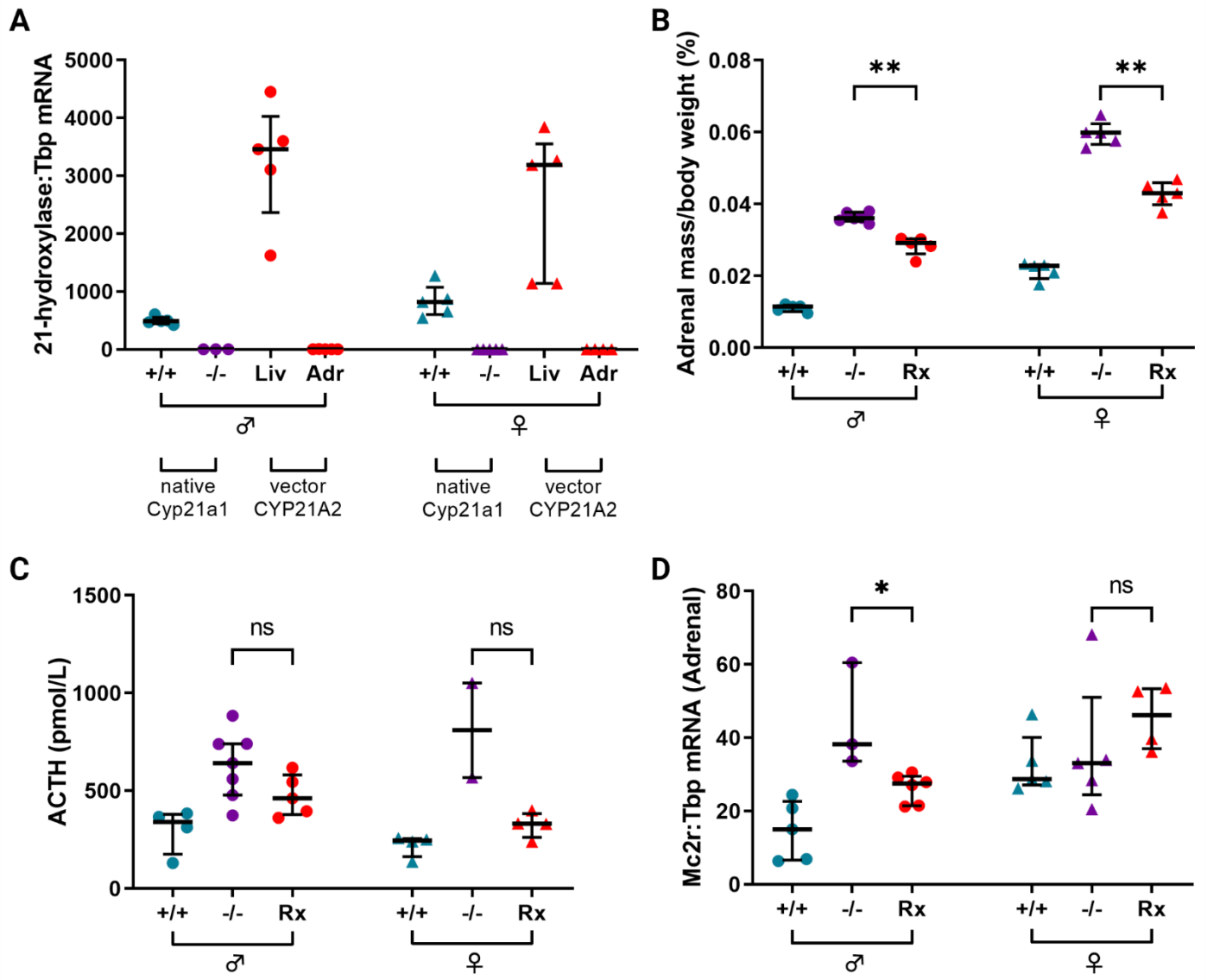

Figure S1.

A. 21-hydroxylase mRNA transcripts. Native murine *Cyp21a1* transcripts in the adrenal gland or vector-derived human *CYP21A2* transcripts in the liver or adrenal gland of vector-treated mice are shown as a ratio to *Tbp* transcripts. **B.** Relative bilateral adrenal mass as a ratio to body weight as a percentage to account for any variation in body size. **C.** Serum ACTH. **D.** ACTH receptor (*Mc2r*) transcripts normalised to *Tbp*. Abbreviations: +/+, wild-type 21-hydroxylase sufficient controls; -/-, homozygous 21-hydroxylase deficient controls; ♂, male; ♀, female; Rx, homozygous 21-hydroxylase deficient mice that were treated with vector; Liv, liver; Adr, adrenal; ACTH, adrenocorticotropic hormone; *Tbp*, TATA-box binding protein; *Cyp21a1*, murine 21-hydroxylase; *CYP21A2*, vector-derived human 21-hydroxylase. Individual data points are shown, and error bars represent as median and interquartile range. * $p<0.05$ and ** $p<0.01$ on Mann-Whitney U test.